LACTIC ACID BACTERIA: MICROBIAL METABOLISM AND EXPANDING APPLICATIONS

EDITED BY: Jian-Ming Liu, Fuping Lu, Csaba Fehér, Mingfeng Cao and Peter Ruhdal Jensen

PUBLISHED IN: Frontiers in Bioengineering and Biotechnology

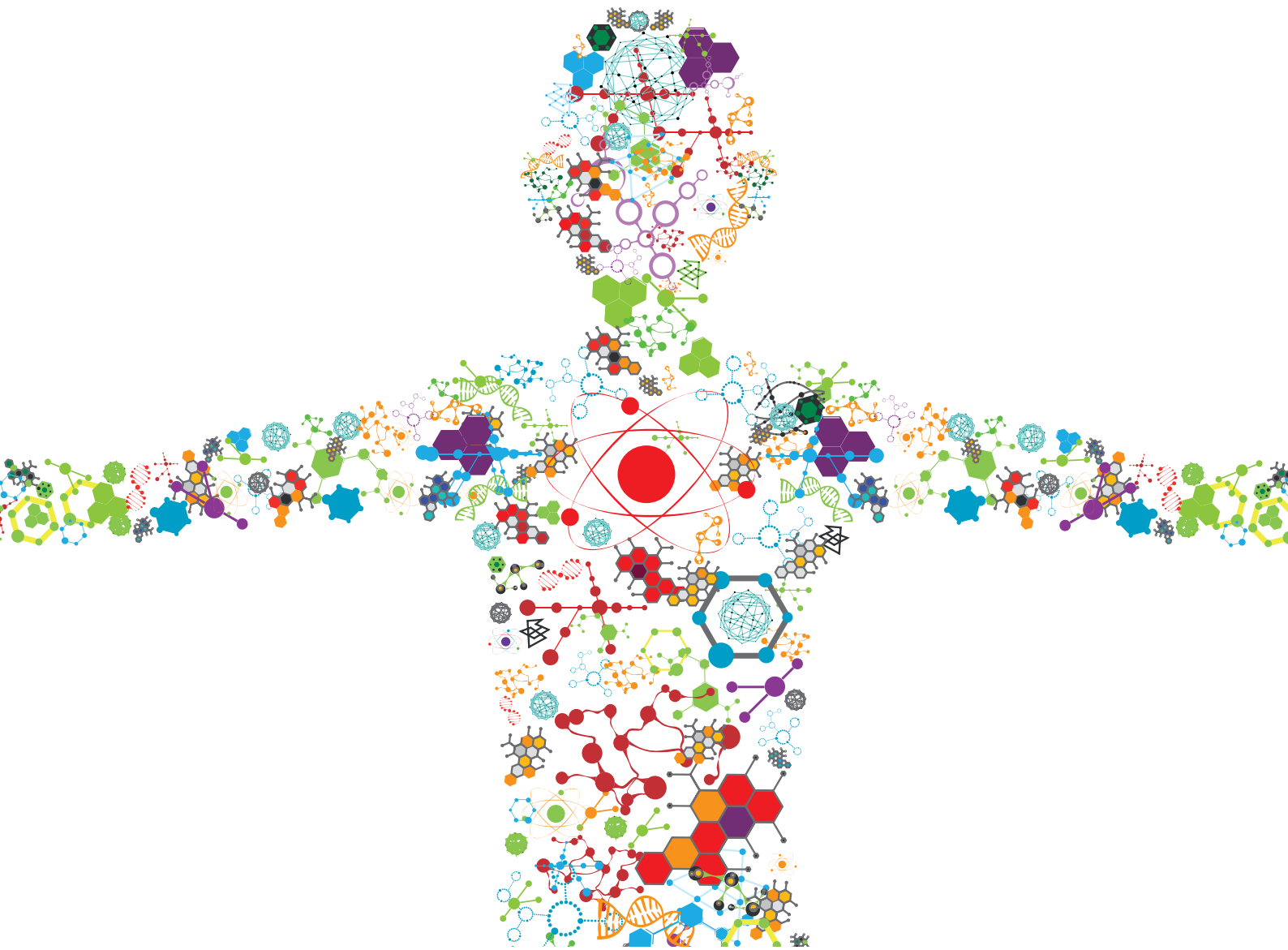

frontiers Research Topics

frontiers

ISSN 1664-8714
ISBN 978-2-88971-982-2
DOI 10.3389/978-2-88971-982-2

About Frontiers

Frontiers is more than just an open-access publisher of scholarly articles: it is a pioneering approach to the world of academia, radically improving the way scholarly research is managed. The grand vision of Frontiers is a world where all people have an equal opportunity to seek, share and generate knowledge. Frontiers provides immediate and permanent online open access to all its publications, but this alone is not enough to realize our grand goals.

Frontiers Journal Series

The Frontiers Journal Series is a multi-tier and interdisciplinary set of open-access, online journals, promising a paradigm shift from the current review, selection and dissemination processes in academic publishing. All Frontiers journals are driven by researchers for researchers; therefore, they constitute a service to the scholarly community. At the same time, the Frontiers Journal Series operates on a revolutionary invention, the tiered publishing system, initially addressing specific communities of scholars, and gradually climbing up to broader public understanding, thus serving the interests of the lay society, too.

Dedication to Quality

Each Frontiers article is a landmark of the highest quality, thanks to genuinely collaborative interactions between authors and review editors, who include some of the world's best academicians. Research must be certified by peers before entering a stream of knowledge that may eventually reach the public - and shape society; therefore, Frontiers only applies the most rigorous and unbiased reviews.
Frontiers revolutionizes research publishing by freely delivering the most outstanding research, evaluated with no bias from both the academic and social point of view. By applying the most advanced information technologies, Frontiers is catapulting scholarly publishing into a new generation.

What are Frontiers Research Topics?

Frontiers Research Topics are very popular trademarks of the Frontiers Journals Series: they are collections of at least ten articles, all centered on a particular subject. With their unique mix of varied contributions from Original Research to Review Articles, Frontiers Research Topics unify the most influential researchers, the latest key findings and historical advances in a hot research area! Find out more on how to host your own Frontiers Research Topic or contribute to one as an author by contacting the Frontiers Editorial Office: frontiersin.org/about/contact

LACTIC ACID BACTERIA: MICROBIAL METABOLISM AND EXPANDING APPLICATIONS

Topic Editors:
Jian-Ming Liu, South China University of Technology, China
Fuping Lu, Tianjin University of Science and Technology, China
Csaba Fehér, Budapest University of Technology and Economics, Hungary
Mingfeng Cao, Xiamen University, China
Peter Ruhdal Jensen, Technical University of Denmark, Denmark

Citation: Liu, J.-M., Lu, F., Fehér, C., Cao, M., Jensen, P. R., eds. (2021). Lactic Acid Bacteria: Microbial Metabolism and Expanding Applications.
Lausanne: Frontiers Media SA. doi: 10.3389/978-2-88971-982-2

Table of Contents

frontiers in Bioengineering and Biotechnology

EDITORIAL
published: 12 November 2021
doi: 10.3389/fbioe.2021.794164

Editorial: Lactic Acid Bacteria: Microbial Metabolism and Expanding Applications

Jian-Ming Liu[1], Csaba Fehér[2], Mingfeng Cao[3], Fuping Lu[4] and Peter Ruhdal Jensen[5]*

[1]School of Biology and Biological Engineering, South China University of Technology, Guangzhou, China, [2]Department of Applied Biotechnology and Food Science, Budapest University of Technology and Economics, Budapest, Hungary, [3]College of Chemistry and Chemical Engineering, Xiamen University, Xiamen, China, [4]College of Biotechnology, Tianjin University of Science and Technology, Tianjin, China, [5]The National Food Institute, Technical University of Denmark, Kongens Lyngby, Denmark

Keywords: metabolic engineering, fermentation, plant food, gut microbiome, bacteriocins, lactic acid bacteria, traditional mutagenesis

Editorial on the Research Topic

Lactic Acid Bacteria: Microbial Metabolism and Expanding Applications

INTRODUCTION

Lactic acid bacteria (LAB) are a group of lactic acid-forming bacteria that are generally recognized as safe (GRAS), facultatively anaerobic, non-respiring and non-sporulating. They are ubiquitous in nature, present from plant materials, milk and meat to the intestine of mammals. The metabolism of LAB is diverse and in this collection, Wang et al. reviewed LAB metabolism with a particular focus on carbon (polysaccharide) and nitrogen (protein) degradation as well as their metabolic activities to produce a large number of valuable metabolites, including organic acids, flavors, vitamins, exopolysaccharides, antimicrobial and antioxidant compounds.

DIVERSE METABOLISM

In LAB metabolism, one of the major features is that they produce predominantly lactic acid (LA). The LA formed as well as the drop in pH can inhibit the growth of other microorganisms and increase the shelf-life of the fermented foods (Liu et al., 2019). But the overproduction of LA, especially in non-growing conditions, might negatively affect the product flavor and quality. To measure the long-term LA production, Nugroho et al. developed a high-throughput approach to determine the metabolic pathway activities of non-growing cells, including LA production and the arginine deiminase pathway, over prolonged periods. The method was based on the real-time monitoring of pH change through the use of fluorescent pH indicators, which enabled the study of different strains and different growth conditions efficiently.

Another important feature of LAB is their bacteriocins production. Bacteriocins are ribosomally synthesized antimicrobial peptides. Many bacteriocins have been used or show great potential for use in the food and clinical industry. For example, nisin is a well-established preservative against some gram-positive bacteria in foods and its production is established by a conservative biosynthetic gene cluster comprised of *nisABTCIPRK* and *nisFEG* (Kuipers et al., 1993). NisI, a membrane-associated lipoprotein, and NisFEG, an ABC transporter, confer nisin immunity. To investigate the distribution of nisin immunity not only on the producing cells but overall on dairy *Lactococcus lactis*, van Gijtenbeek et al. examined nisin tolerance on more than 700 *L. lactis* in both phenotype and genotype. They found nisin

OPEN ACCESS

Edited and reviewed by:
Jean Marie François, Institut Biotechnologique de Toulouse (INSA), France

****Correspondence:***
Jian-Ming Liu
jial@dtu.dk

Specialty section:
This article was submitted to Synthetic Biology, a section of the journal Frontiers in Bioengineering and Biotechnology

Received: *13 October 2021*
Accepted: *26 October 2021*
Published: *12 November 2021*

Citation:
Liu J-M, Fehér C, Cao M, Lu F and Jensen PR (2021) Editorial: Lactic Acid Bacteria: Microbial Metabolism and Expanding Applications. Front. Bioeng. Biotechnol. 9:794164. doi: 10.3389/fbioe.2021.794164

Nisin tolerance systems in *Lactococcus lactis*

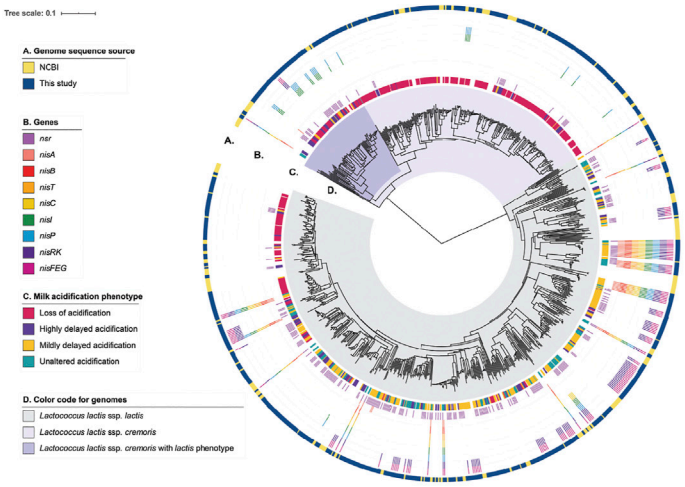

Gijtenbeek et al.

Predicted structure of Proteinase (CEP)

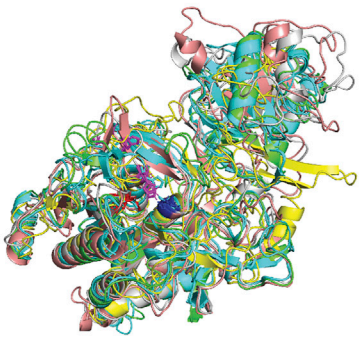

Hansen et al.

Biosynthetic pathway for menaquinone

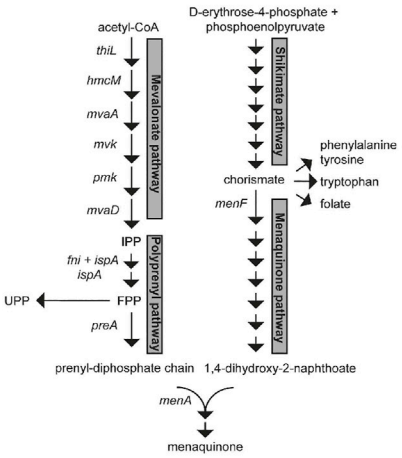

Arnason Bøe et al.

SEM of selenized cells

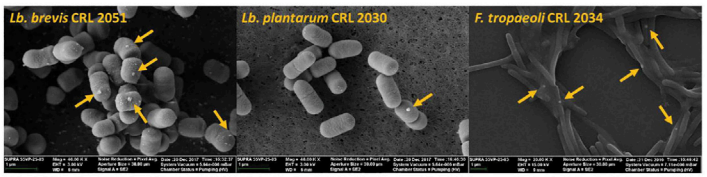

Martinez et al.

Nisin and PLA co-production

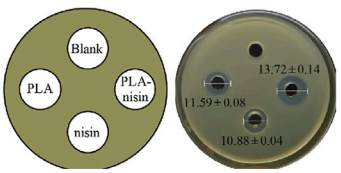

Liu et al.

Wheat bran fermentation

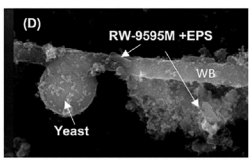

Bertsch et al.

Non-GMO derivatives of *L. rhamnosus* GG

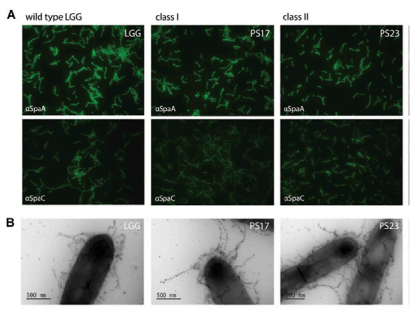

Rasinkangas et al.

A leaderless two-peptide bacteriocin

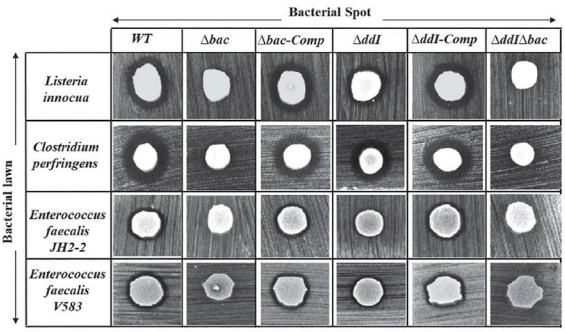

Ladjouzi et al.

FIGURE 1 | Some representative works in this collection.

tolerance was widely distributed in non-nisin-producing *L. lactis*, contributed mainly by NSR (a nisin degradation enzyme). This work facilitates the selection of strains that do not produce nisin but have immunity for designing nisin-compatible starter cultures in food fermentations.

Nisin production is initiated by its pre-peptide synthesis with an N-terminal leader peptide, followed by the leader peptide cleavage and a typical post-translational modification step. It is different for leaderless bacteriocins that do not have any N-terminal leader sequence and can become immediately active after their translations. Enterocin DD14 is such a leaderless bacteriocin produced by *Enterococcus faecalis* 14. It shows antagonistic activities against many pathogens, such as *Staphylococcus aureus* and *Listeria monocytogenes*. It remains largely elusive how the bacteriocinogenic strain can develop the immunity for its own bacteriocin that has activities immediately after translation. Ladjouzi et al. investigated the immunity system of EntDD14 at the molecular level and demonstrated that intracellular EntDD14 is involved in self-immunity.

Bacteriocins show great potential to fight various pathogens. Todorov et al. discussed the potential to harness bacteriocins widely produced by different LAB species as promising biotherapeutic agents for controlling *Clostridium* and *Clostridiodes* infections. The pathogenic *Clostridium* and *Clostridiodes* spp. are difficult to tackle because of their ability to form highly resistant endospores and antibiotic resistance and they are directly related to food poisoning and human gastrointestinal problems. A number of bacteriocins are effective against *Clostridium* and *Clostridiodes* species.

EXPANDING APPLICATIONS

Some LAB are widely used in the dairy industry for yogurt and cheese (Liu et al., 2019). One important reason that these LAB can grow efficiently in the milk-derived matrix is due to their excellent proteolytic system, including proteinase, peptide transporter and peptidase, to metabolize milk proteins. Hansen and Marcatili presented a molecular model of the cell envelope proteinase (CEP) of *L. lactis*. The *L. lactis* CEP has multi-domains and this simulation work predicts functions to the domains in the context of degradation of caseins. It makes an important contribution to our understanding of dairy protein metabolism as well as LAB growth in dairy fermentations. In dairies, many researchers focus on developing better starter cultures to improve food qualities and functionalities. Sørensen et al. investigated antimicrobial agents that target the cell envelope to improve LAB texturizing abilities in milk fermentation. They created pressure for strain mutagenesis using ampicillin, vancomycin or triclosan, and selected some mutants with improved phenotypic traits in a high-throughput manner based on the liquid handling pressure (Poulsen et al., 2019). The identified genetic changes in the mutants were distributed in genes encoding sugar transporter, ATPase, cell membranes and others.

In addition to the dairy industry, LAB play important roles in plant-food diversification with different functions. As one example, LAB fermentation can improve the bioavailability and bioaccessibility of phenolic compounds that have antioxidant activities. It can add value to the production of newly fermented plant-based foods. Bertsch et al. studied three LAB strains to produce functional bioingredients by single or co-fermentation with yeast. They found LAB fermentation could improve the extraction and production efficiency of both free and bound phenolic compounds. In monoculture, the total and bound phenolic compounds were higher than co-culture. But in co-culture, it had a higher content of water-soluble polysaccharides. LAB fermentation can also increase the bioavailability of micronutrients. Selenium (Se) is an essential micronutrient for most living organisms and Se deficiency is associate with many diseases. Martinez et al. explored the transformation of selenite into selenium-nanoparticles and Se-amino acids using LAB. Some *Lactobacillus* show great potential for the enrichment of fermented foods with selenium.

Due to the GRAS status and their metabolic functions, some LAB exhibit promising health-promoting applications as probiotics or therapeutic agents. Rasinkangas et al. worked on the well-characterized probiotic *L. rhamnosus* GG and generated its non-GMO (genetically modified organisms) mutants using Ethyl methanesulphonate mutagenesis. 13 mutant strains that showed increased mucus-adherent phenotypes were characterized and their whole genomes were sequenced. The identified gene mutations in either pili-encoding genes *spaCBA* or other genes open a window on understanding the synthesis and regulation of pill formation as well as the mucus binding properties. The developed non-GMO derivatives show direct potential in the pharmaceutical industries. Since many *Lactobacillus* can colonize mucosa in humans and animals, the surface display of functional proteins on them could have biomedical applications. Tay et al. tested a new cell-anchoring domain CAD4a bound to peptidoglycan in LAB cell wall and optimized the conditions for its optimal anchoring. They demonstrated that the surface-displayed superoxide dismutase using CAD4a could be protected from gastric digestion in a polymer matrix.

Last but not least, many LAB have been metabolically engineered as cell factories. Bøe and Holo engineered *L. lactis* MG1363 to produce menaquinone (MK, vitamin K2). They found that the key enzymes, including *menF* (isochorismate synthase), *menA* (DHNA polyprenyltransferase), *mvk (*mevalonate kinase) and *preA* (prenyl diphosphate synthase), were able to control the MK flux. The combined overexpression of *preA*, *menA* and *mvk* gave rise to a higher level of MK7-9 (680 nmol/L) than individual overexpression. This work elucidated metabolic bottlenecks in the biosynthetic MK pathway and provided a foundation for further engineering to increase MK production or develop food-grade strains with high vitamin K2 content. In another work, Suo et al. worked on the same strain *L. lactis* MG1363 and rewired the metabolic flux for producing pyruvate through knocking out all the competitive pathways leading to the formation of lactate, acetate, acetoin and ethanol. They further optimized the fermentation medium and achieved a high titer (40 g/L) and high yield (close to 80% of the theoretical maximum) of pyruvate by using dairy waste as substrate. These results demonstrate the economic feasibility of using *L. lactis* for producing valuable products on waste streams.

Additionally, Liu et al. showed the co-production of nisin and phenylacetic acid (PLA) that displayed enhanced antibacterial activities against pathogenic microorganisms, such as *S. xylosus* and *Micrococcus luteus*. They constructed a new *L. lactis* strain based on a nisin-producing strain F44 by knocking out two main

L-lactate dehydrogenases (LDH) and expressing a D-LDH mutant. The new strain delivered high antimicrobial activities.

Overall, we believe this collection presents benchmark work in the LAB field. It will benefit the readers to gain the recent developments and the LAB community to move forward for the next achievements.

REFERENCES

Kuipers, O. P., Beerthuyzen, M. M., Siezen, R. J., and Vos, W. M. (1993). Characterization of the Nisin Gene Cluster nisABTCIPR of Lactococcus Lactis. Requirement of Expression of the nisA and nisIgenes for Development of Immunity. *Eur. J. Biochem.* 216, 281–291. doi:10.1111/j.1432-1033.1993.tb18143.x

Liu, J., Chan, S. H. J., Chen, J., Solem, C., and Jensen, P. R. (2019). Systems Biology - A Guide for Understanding and Developing Improved Strains of Lactic Acid Bacteria. *Front. Microbiol.* 10, 876. doi:10.3389/fmicb.2019.00876

Poulsen, V. K., Derkx, P., and Oregaard, G. (2019). High-throughput Screening for texturingLactococcusstrains. *FEMS Microbiol. Lett.* 366, fnz001. doi:10.1093/femsle/fnz001

AUTHOR CONTRIBUTIONS

All authors listed have made a substantial, direct, and intellectual contribution to the work and approved it for publication.

Conflict of Interest: The authors declare that the research was conducted in the absence of any commercial or financial relationships that could be construed as a potential conflict of interest.

Publisher's Note: All claims expressed in this article are solely those of the authors and do not necessarily represent those of their affiliated organizations, or those of the publisher, the editors and the reviewers. Any product that may be evaluated in this article, or claim that may be made by its manufacturer, is not guaranteed or endorsed by the publisher.

frontiers in Bioengineering and Biotechnology

ORIGINAL RESEARCH
published: 18 March 2020
doi: 10.3389/fbioe.2020.00191

Engineering *Lactococcus lactis* for Increased Vitamin K2 Production

Cathrine Arnason Bøe[1] *and Helge Holo*[1,2]*

[1] *Laboratory of Microbial Gene Technology, Faculty of Chemistry, Biotechnology and Food Science, Norwegian University of Life Sciences, Ås, Norway,* [2] *Tine SA, Oslo, Norway*

Cheese produced with *Lactococcus lactis* is the main source of vitamin K2 in the Western diet. Subclinical vitamin K2 deficiency is common, calling for foods with enhanced vitamin K2 content. In this study we describe analyses of vitamin K2 (menaquinone) production in the lactic acid bacterium *L. lactis* ssp. *cremoris* strain MG1363. By cloning and expression from strong promoters we have identified genes and bottlenecks in the biosynthetic pathways leading to the long-chained menaquinones, MK-8 and MK-9. Key genes of the biosynthetic menaquinone pathway were overexpressed, singly or combined, to examine how vitamin K2 production can be enhanced. We observed that the production of the long menaquinone polyprenyl side chain, rather than production of the napthoate ring (1,4-dihydroxy-2-naphtoic acid), limits total menaquinone synthesis. Overexpression of genes causing increased ring formation (*menF* and *menA*) led to overproduction of short chained MK-3, while overexpression of other key genes (*mvk* and *llmg_0196*) resulted in enhanced full-length MK-9 production. Of two putatively annotated prenyl diphosphate synthases we pinpoint *llmg_0196* (*preA*) to be important for menaquinone production in *L. lactis*. The genes *mvk*, *preA, menF,* and *menA* were found to be important contributors to menaquinone levels as single overexpression of these genes double and more than triple the total menaquinone content in culture. Combined overexpression of *mvk*, *preA,* and *menA* increased menaquinone levels to a higher level than obtained individually. When the overproducing strains were applied for milk fermentations vitamin K2 content was effectively increased 3-fold compared to the wild type. The results provide a foundation for development of strains to ferment foods with increased functional value i.e., higher vitamin K2 content.

Keywords: *Lactococcus lactis*, menaquinone, vitamin K2, mevalonate kinase, prenyl diphosphate synthase, MK-8, MK-9, MK-3

OPEN ACCESS

Edited by:
Jian-Ming Liu, Technical University of Denmark, Denmark

Reviewed by:
Lin Chen, Hamburg University of Technology, Germany
Jie Zhao, Inner Mongolia Agricultural University, China
Joshua Chan, Colorado State University, United States

***Correspondence:**
Helge Holo
helge.holo@nmbu.no

Specialty section:
This article was submitted to Synthetic Biology, a section of the journal Frontiers in Bioengineering and Biotechnology

Received: *20 December 2019*
Accepted: *27 February 2020*
Published: *18 March 2020*

Citation:
Bøe CA and Holo H (2020) Engineering Lactococcus lactis for Increased Vitamin K2 Production. Front. Bioeng. Biotechnol. 8:191. doi: 10.3389/fbioe.2020.00191

MATERIALS AND METHODS

Bacterial Strains, Plasmids, and Culture Conditions

Strains and plasmids used in this study are listed in **Table 1**. *Lactococcus lactis* ssp. *cremoris* MG1363 or NZ9000 were used as hosts for expression studies. *E. coli* NEB10 beta (NEB, Ipswich, MA, USA) electrocompetent cells were used for routine cloning and One Shot™ Mach1™ T1R (Invitrogen, Carlsbad, CA, USA) chemically competent cells were used for subcloning. Unless otherwise stated lactococci were inoculated into M17 medium (Formedium, Norfolk, UK) supplemented with 0.5% glucose and antibiotics required for selection (erythromycin 10 μg/ml, tetracyclin 12.5 μg/ml, chloramphenicol 10 μg/ml), and grown over night at 30°C under static conditions. Nisin (Sigma,

St. Louis, MO, USA) was added from a 1 mg/ml (w/v) stock in 0.05% (v/v) acetic acid when the OD600 in the cultures reached 0.2 to induce expression from the *nisA* promoter. For milk fermentations 10% dry skimmed milk supplemented with 0.5% (w/v) glucose and 1% (w/v) tryptone was heat sterilized at 90°C for 45 min. Tubes with five ml milk was inoculated from a GM17 preculture and fermented for 20 h at 30°C. Nisin was added 1 h after start of the milk fermentations at a concentration of 2 ng/ml.

Construction of Plasmids

A shuttle vector, pHH145, with capacity to carry large DNA fragments in *L. lactis* was made by ligating EcoRI restricted pSMART and the high DNA capacity vector for Gram positive bacteria, pIL252 (Simon and Chopin, 1988) and propagated in *E. coli* (**Supplementary Figure 2**).

All genes were amplified from MG1363 chromosomal DNA except the tetracycline resistance gene (*tetM*) that was amplified from pAS222. The P32 promoter was amplified from pMG36e. Primers used in this study are listed in **Table 2**. The *menF* and *menA* genes were cloned into the XbaI/HindIII sites of pMG36e using the appropriate restriction enzymes. The genes of the mevalonate and polyprenyl pathways, except *hmcM*, were cloned into the SmaI site of pMG36e by blunt-end cloning. Gibson assembly (Gibson et al., 2009) was employed to clone *hmcM* into the SmaI site of pMG36e, to clone *preA-menA* into pNZ8037 and for construction of pMEV-PP, pMEV-PP-2, and pCTR.

HiFi DNA Assembly Master Mix (NEB, Ipswich, MA, USA) was employed for the Gibson assemblies. Overlap extension PCR (Horton et al., 1989) was used to combine the P32 promoter, *hmcM*, *thiL-mvaA,* and *mvk* into one fragment and *mvaD-pmk*, *fni*, *ispA,* and *tetM* to a second fragment before Gibson assembly with the *preA* and pHH145 fragments (4-component assembly). For pMEV-PP-2 a 3-component assembly was performed as described for pMEV-PP, but *preA* was left out of the reaction mix and primers were adjusted accordingly to amplify the mevalonate and polyprenyl pathway fragments. The tetracycline resistance gene (*tetM*) was positioned at the end, after all MEV and PP genes, to ensure transcription through the whole construct when transformed cells were cultured with tetracycline (pMEV-PP and pMEV-PP-2 **Supplementary Figure 2**). As a control, the *tetM* gene was assembled in a similar way into pHH145 behind the P32 promoter (pCTR, **Supplementary Figure 2**).

The *preA* and *gerCA-ispB* genes were cloned into the NcoI/XhoI site of pNZ8037 using appropriate restriction enzymes. Difficult fragments were subcloned into pCR™Blunt II-TOPO® vector (Invitrogen, St. Louis, MO, USA) and all inserts were routinely confirmed by DNA sequencing. Plasmids were transformed by electroporation into MG1363 or NZ9000 (Holo and Nes, 1989).

Menaquinone Extraction and Analyses

The menaquinones of cells in culture were extracted essentially as described by others (Koivu-Tikkanen et al., 2000; Manoury et al., 2013) using a heptane:2-propanol mix (1:2, v/v) as extraction agent (2-propanol mix; 2-propanol:HCl (37%):MeOH 8.25:1:1 v/v/v). Phylloquinone (vitamin K1) at 40 ng/ml was included in the MeOH fraction and used as an internal standard. The extracts were analyzed by reverse phase HPLC on an UltiMate 3000 UHPLC system equipped with a Shiseido C18 (2.0 × 100 mm) column followed by a Shiseido CQ-R (2.0 × 20 mm) reduction column (Shiseido, Tokyo, Japan) and an RS FL fluorescence detector (Thermo Fisher Scientific, Rockford, IL, USA) set at 248 nm for emission and detection at 436 nm. The mobile phase was methanol:2-propanol (1:1, v/v), flow rate 200 µl/min, the injection volume was 0.5 µl and the column temperature 50°C. A sample containing standards MK-4, MK-7, MK-9, and K1 was employed for determination of retention times (**Supplementary Figure 1A**). The fluorescence response per mol was the same for all vitamin K standards. The molar concentrations of menaquinones were quantified using MK-7 as external standard (standard curve for MK-7 ranging from 10 to 1,000 ng/ml is shown in **Supplementary Figure 1B**). All reagents used for menaquinone extraction were of HPLC grade and standards K1 (95271), MK-4 (V-9378), and MK-7 (1381119) were purchased at Sigma (St. Louis, MO, USA). Standard MK-9 (M213610) was purchased at Toronto Research Chemicals (Toronto, ON, Canada). *P*-values were calculated using two-tailed *T*-tests.

INTRODUCTION

Vitamin K is a family of essential, fat-soluble vitamins required for blood coagulation, but also involved in deposition and removal of calcium in various tissues (Flore et al., 2013; Schwalfenberg, 2017). The family comprises two naturally active vitamers: vitamin K1 (phylloquinone) produced by plants, and vitamin K2 (menaquinone, MK-n where n represents the number of isoprene units). Menaquinones are principally of bacterial origin, but MK-4 can be formed in mammals through conversion of phylloquinone (Okano et al., 2008). In humans and other mammals vitamin K is essential for its role as a cofactor for the enzyme γ-glutamyl carboxylase (Furie et al., 1999). This enzyme carboxylates glutamine residues on certain proteins into γ-carboxyglutamic acid (Gla) residues. Gla-proteins have increased affinity for calcium and are involved in protein-protein interactions (through Ca^{2+}), cell membrane interactions and processes that promote correct deposition of calcium in bone and prevents deposition in soft tissues like arteries, cartilage, and heart valves (Wen et al., 2018).

A daily consumption of 0.75–1 µg vitamin K per kg body weight is regarded as the minimum adequate daily intake since it reinstates normal coagulation in elderly male patients with vitamin K deficiency (Frick et al., 1967). Life-threatening (primary) vitamin K deficiency, caused by excessive bleeding due to insufficient carboxylation of coagulation factors, is rare except in newborns (Vermeer, 2012; Schwalfenberg, 2017). The Western diet is thus sufficient to prevent acute disease. However, to fully carboxylate Gla-proteins other than the coagulation factors and thus prevent secondary (sub-clinical) vitamin K deficiency Western diets appear insufficient (Vermeer, 2012; Bruno, 2016). A long-lasting secondary vitamin K deficiency can lead to development of cardiovascular disease and osteoporosis (Szulc

TABLE 1 | Strains and plasmids used in this study.

Strain or plasmid	Relevant characteristic(s)	Reference or source
Strains		
L. lactis		
MG1363	*Lactococcus lactis* ssp. *cremoris*	Gasson, 1983
NZ9000	MG1363; *pepN*::*nisRK*	Kuipers et al., 1998
E. coli		
NEB 10 beta	Commercial cloning host	NEB
One Shot^{TM} Mach1^{TM}- T1R	Commercial cloning host used for pCR^{TM}Blunt II	Invitrogen
Plasmids		
pMG36e	Em^r, *L.lactis* expression vector, P32 promoter	van de Guchte et al., 1989
pMenF	pMG36e constitutively expressing *menF*	This study
pMenA	pMG36e constitutively expressing *menA*	This study
pHmcM	pMG36e constitutively expressing *hmcM*	This study
pThiL-MvaA	pMG36e constitutively expressing *thiL* and *mvaA*	This study
pMvk	pMG36e constitutively expressing *mvk*	This study
pMvaD-Pmk	pMG36e constitutively expressing *mvaD* and *pmk*	This study
pFni	pMG36e constitutively expressing *fni*	This study
pIspA	pMG36e constitutively expressing *ispA*	This study
pAS-222	Tet^r, *L. lactis* vector, derivate of pG$^+$host4 and pBluescript SK	Jonsson et al., 2009
pCR^{TM}Blunt II	Kan^r, Zeo^r, TOPO vector for subcloning in *E. coli*, derivative of pUC	Invitrogen
pNZ8037	Cm^r, inducible expression vector, P_{nisA} promoter	de Ruyter et al., 1996
pPreA	pNZ8037 expressing *preA* upon induction with nisin	This study
pGerCA-IspB	pNZ8037 expressing *gerCA* and *ispB* upon induction with nisin	This study
pPreA-MenA	pNZ8037 expressing *preA* and *menA* upon induction with nisin	This study
pSMART	Amp^r, cloning vector, low copy, derivative of pUC	Lucigen
pIL252	Em^r, *L. lactis* low copy vector, derivative of pAMb1	Simon and Chopin, 1988
pHH145	Em^r Amp^r, pSMART, and pIL252 combined, high DNA capacity shuttle vector for *E. coli* and *L.lactis*	This study
pCTR	pHH145 constitutively expressing *tetM* from P32	This study
pMEV-PP	pHH145 constitutively expressing *hmcM*, *thiL*, *mvaA*, *mvk*, *preA*, *mvaD*, *pmk*, *fni*, *ispA* and *tetM* from P32	This study
pMEV-PP-2	pHH145 constitutively expressing *hmcM*, *thiL*, *mvaA*, *mvk*, *mvaD*, *pmk*, *fni*, *ispA,* and *tetM* from P32	This study

et al., 1993; Luukinen et al., 2000; Schurgers et al., 2005; Cranenburg et al., 2010; Shea et al., 2011; Vermeer, 2012; Schwalfenberg, 2017). Increased vitamin K intake appears to be beneficial and important for public health. The advantage of increasing the consumption of menaquinone compared to phylloquinone has been stressed significantly over the years. Firstly, menaquinone intake, but not phylloquinone has been shown to be inversely correlated to all-cause mortality, cardiovascular disease and certain cancers in large population-based studies (Geleijnse et al., 2004; Gast et al., 2009; Nimptsch et al., 2010). In addition, the longer menaquinones appear to have extended stability (days, compared to hours) and better bioavailability after ingestion compared to phylloquinone (Vermeer, 2012).

Our most important dietary sources of vitamin K2 are fermented foods like cheese and natto (fermented soybean). Fermentation of soybean by the bacterium *Bacillus subtilis* var. *natto* yield very high MK-7 amounts as levels up to 1,100 μg/100 g can be achieved (Schurgers and Vermeer, 2000). Regular consumption of natto could fulfill our requirement for vitamin K2, but unfortunately natto has a rather sharp taste and is not enjoyed much outside of Japan. In Europe and Northern America lactic acid bacteria (LAB) are the most important vitamin K2-producers for our diet as they ferment milk into dairy products such as cheese rich in vitamin K2 (up to 110 μg/100 g) (Manoury et al., 2013; Vermeer et al., 2018). LAB are highly valued and exploited in food fermentations and have potential to be used as cell factories for production of various metabolites for industry (Sauer et al., 2017). An extensive set of genetic tools has been developed for LABs over the years and this can enable efficient metabolic engineering of industrially important strains. Efforts have been made to enhance production of vitamins like riboflavin (Burgess et al., 2004; Chen et al., 2017; Juarez Del Valle et al., 2017), folate (Albuquerque et al., 2017; Saubade et al., 2017; Meucci et al., 2018) and cobalamin (Bhushan et al., 2017; Li et al., 2017) in LAB and thereby increase the functional value of fermented food, but until very recently there were no reports on optimization of dairy production or metabolic engineering of LAB strains to achieve higher menaquinone levels. Several genomes of the dominating vitamin K2 producing LAB, *L. lactis* have been sequenced, and putative genes encoding the enzymes for the individual

TABLE 2 | Primers used in this study.

Primers	Sequence 5′-3′
Construction of pMenF, pMenA, pHmcM, pThiL-MvaA, pMvk, pMvaD-Pmk, pFni, and pIspA:	
Fw MenF	TATGTCTAGAGTTATAATTTCTATGGTAGAAAAAATG
Rev MenF	ATAGAAGCTTTCATAAGGCTTCTAAAATCGTTTTTAA
Fw MenA	TATGTCTAGAATCACATTAAAAGAGGAAATAATG
Rev MenA	ATAGAAGCTTTTAAAATCTAATCAAACTAATAAAGAGC
Fw HmcM ol pMG36e GC	AATTCGAGCTCGCCCATGAAAGTCGGTATTGATAAAC
Rev HmcM ol pMG36e GC	GAGGATCGATCCCCCAGAAAAGCTGTCAGTATTTTTTTATATTTTTTTATATTTAC
Fw pMG36e ol HmcM GC	AATTCGAGCTCGCCCATGAAAGTCGGTATTGATAAAC
Rev pMG36e ol HmcM GC	AGAGGATCGATCCCCCAGAAAAGCTGTCAGTATTTTTTTATATTTTTTTATATTTAC
Fw ThiL	CTTTCGGAGGTTCATTCGTGAAAG
Rev MvaA	TTATTTTCTCAAATTTTTTAGTAAATTTTGG
Fw Mvk	GCAGGAGAATTGTTAAAAATGAC
Rev Mvk	TTAAAAGGAGTAAATCCACGTG
Fw MvaD	TTTGATATAATAGTTTCATGAAAAATATTG
Rev Pmk	TCAGTTATTTTTTTGAGCAATCTTAAAC
Fw Fni	GAATTGAGAAATAAATGATGAAAAG
Rev Fni	TTATTTTTTTCTTTGTTGGATAAAATCG
Fw IspA	TGGTATAATTAGGGTAATGGATAC
Rev IspA	TTATTCCACTTCCAGTTGTTCAATT
Construction of pMEV-PP, pMEV-PP-2, and pCTR:	
Fw TetM ol P32 prom GC	CGTAATTCGAGCTCGCCCCGGCTTGTCTAGATTTGAATGG
Rev TetM ol pHH145 GC	GACTTTCTGCTATGGAGGTCAGGTATGATTTAAATGGTCACTAAGTTATTTTATTGAACATATATCGTAC
Fw P32 prom ol pHH145 GC	CAAAGTGATTAAATAGAATTCTCTAGATATCGCTCAATACATGGGTCGATCGAATTCG
Rev P32 prom	GGGCGAGCTCGAATTACG
Fw hmcM ol P32 prom	CGTAATTCGAGCTCGCCCGATAAGGAAATTTTTAAAATATGAAAGTC
Rev hmcM	TTATATTTTTTTTATATTTACGATGGTTATCAAC
Fw thiL ol hmcM	GTTGATAACCATCGTAAATATAAAAAAATATAACTTTCGGAGGTTCATTCGTGAAAG
Rev mvaA	TTATTTTCTCAAATTTTTTAGTAAATTTTGG
Fw mvk ol mvaA	CCAAAATTTACTAAAAAATTTGAGAAAATAAGCAGGAGAATTGTTAAAAATGAC
Rev mvk ol preA GC	CTTTCCTCTCGATAATTAAAAGGAGTAAATCCACGTG
Fw preA ol mvk GC	ATTTACTCCTTTTAATTATCGAGAGGAAAGAGAAAAAC
Rev preA ol mvaD GC	AACTATTATATCAAACTTTTAATAATTTCGCTCTAATAAAATC
Fw mvaD ol preA GC	CGAAATTATTAAAAGTTTGATATAATAGTTTCATGAAAAATATTG
Rev pmk	TCAGTTATTTTTTTGAGCAATCTTAAAC
Fw fni ol pmk	GTTTAAGATTGCTCAAAAAAATAACTGAGAATTGAGAAATAAATGATGAAAAG
Rev fni	TTATTTTTTTCTTTGTTGGATAAAATCG
Fw ispA ol fni	CGATTTTATCCAACAAAGAAAAAAATAATGGTATAATTAGGGTAATGGATAC
Rev ispA	TTATTCCACTTCCAGTTGTTCAATT
Fw TetM ol ispA	AATTGAACAACTGGAAGTGGAATAACGGCTTGTCTAGATTTGAATGG
Rev TetM ol pHH145 GC	GACTTTCTGCTATGGAGGTCAGGTATGATTTAAATGGTCACTAAGTTATTTTATTGAACATATATCGTAC
Fw pHH145 GC	TGACCATTTAAATCATACCTGACC
Rev pHH145 GC	GTATTGAGCGATATCTAGAGAATTCTATTTAATC
Rev mvk ol mvaD GC	CATGAAACTATTATATCAAATTAAAAGGAGTAAATCCACGTG
Fw mvaD ol mvk GC	CGTGGATTTACTCCTTTTAATTTGATATAATAGTTTCATGAAAAATATTG
Construction of pPreA, pGerCA-IspB and pPreA-MenA:	
Fw preA BsaI	TTGAGGTCTCACATGCTCACATTTTGGCAGGATTATCCC
Rev preA XhoI	TGTCAACTCGAGCCTATCGGTGACAGGCTTTTAATAATTTC
Fw gerCA/ispB BsaI	TTGAGGTCTCACATGAATATCAAAGAATACGTTTATGTTTCCTTATTAAC
Rev gerCA/ispB XhoI	TGTCAACTCGAGAAAATTCATCAGGGGTCATAAAGTTCGCT
Fw preA menA GC	TACAAAATAAATTATAAGGAGGCACTCACCTTGCTCACATTTTGGCAG
Rev preA menA GC	TGCAGCCCGGGATCCATGTGCAGTACCCATTATTTAAAATCTAATCAAACTAATAAAGAG
Fw pNZ8037 GC	ATGGGTACTGCACATGGATC
Rev pNZ8037 GC	GGTGAGTGCCTCCTTATAATTTATTTTG

ol, overlap; GC, primers used for amplification of fragments for Gibson cloning.

steps of menaquinone biosynthesis annotated (Wegmann et al., 2007).

In *L. lactis* menaquinones are synthesized from acetyl-CoA, phosphoenolpyruvate and D-erythrose-4-phosphate. The precursors are converted step by step to a hydrophobic polyprenyl diphosphate (PP) chain (mevalonate and polyprenyl pathways) and a hydrophilic naphtoquinone ring; 1,4-dihydroxy-2-napthoate (DHNA) (shikimate and menaquinone pathways). Finally, MenA, a DHNA polyprenyltransferase, joins the prenyl diphosphate and DHNA to form demethylmenaquinone (**Figure 1**). The product of the shikimate pathway, chorismate, is also a substrate for synthesis of the essential aromatic amino acids (AAA) and folate and its production and further conversion is highly regulated (Dosselaere and Vanderleyden, 2001). For instance, the first enzyme of the shikimate pathway, 3-Deoxy-D-arabinoheptulosonate 7-phosphate synthase (DAHPS), is known to be feedback inhibited by AAA in diverse microorganisms (Mir et al., 2015) and similar regulatory events are likely to exist in lactococci. Chorismate is converted to DHNA through 7 enzymatic steps starting with isochorismate synthase (encoded by *menF*). The polyprenyl diphosphate chain is synthesized from isopentenyl pyrophosphate (IPP) units formed through the mevalonate pathway. Six enzymatic steps, catalyzed by 3-ketoacyl-CoA thiolase (*thiL*), hydroxymethylglutaryl-CoA synthase (*hmcM*), hydroxymethylglutaryl-CoA reductase (*mvaA*), mevalonate kinase (*mvk*), phosphomevalonate kinase (*pmk*), and diphosphomevalonate decarboxylase (*mvaD*) are required to convert acetyl-CoA into IPP (C5). These reactions constitute the most energy- and substrate-consuming part of menaquinone synthesis as they require 3 acetyl-CoA, 3 ATP, and 1 NADPH per IPP formed. The geranyltranstransferase (*ispA*) and isopentenyl-diphosphate delta-isomerase (*fni*) then combine IPP units into FPP (farnesyl diphosphate, C15). FPP is a scaffold for further lengthening of the prenyl diphosphate chain by consecutive addition of IPP units to make the all-trans polyprenyl diphosphate (for MK-n production) or di-trans, poly-cis-undecaprenyl pyrophosphate (UPP, C55). UPP is essential for lactococci as it is a substrate for synthesis of peptidoglycan (Bouhss et al., 2008). In *L. lactis* 2 genomic loci encode possible prenyl diphosphate synthases. The *gerCA* (*llmg_1111*) and *ispB* (*llmg_1110*) locus encodes proteins with homology to 2-component heptaprenyl diphosphate synthases. The gene *llmg_0196* is in an operon with *menA* (DHNA polyprenyltransferase) and encodes a putative geranylgeranyl pyrophosphate synthase. In *L. lactis* ssp. *lactis* the gene and gene product of *llmg_0196* are called *preA* and PreA and we will hereafter employ these names also for *L. lactis* ssp. *cremoris* MG1363.

Menaquinones play an essential role in electron transport but are not essential for fermentative growth in *L. lactis* (Rezaiki et al., 2008). However, in the presence of heme *L. lactis* can produce cytochrome and a functional electron transport chain enabling respiratory growth resulting in improved growth and survival in stationary phase (Sijpesteijn, 1970; Duwat et al., 2001; Gaudu et al., 2002; Rezaiki et al., 2008; Brooijmans et al., 2009). In addition, menaquinones can reduce both Fe and Cu and might be important for assimilation of metals (Rezaiki et al., 2008). The levels of menaquinone found in *L. lactis* are strain-dependent and vary in response to aerobic vs. anaerobic conditions as well as culture medium, carbon source and temperature. In *L. lactis* MK-9 is produced as the dominating menaquinone species, but minor amounts of MK-3, MK-7, MK-8 and MK-10 are also formed (Morishita et al., 1999; Rezaiki et al., 2008; Brooijmans et al., 2009). One recent study show that adjusting fermentation parameters like preculture conditions, carbon source and temperature result in up to 50% increase of vitamin K2 in fermented milk (Liu et al., 2019). However, there are no other reports available describing how to increase strain performance or optimize conditions to elevate menaquinone content during food fermentations, neither is information on the contribution of each enzyme to the biosynthetic pathway of menaquinones in lactococci. Such knowledge could be helpful in selecting the optimal lactococci for fermentation of milk into a product with higher functional value regarding vitamin K2. Therefore, in the present study several genes of the biosynthetic pathway of menaquinones in *L. lactis* ssp. *cremoris* MG1363 were overexpressed singly or in combination to investigate their potential to raise menaquinone levels. We identify bottle-necks and key genes for biosynthesis of menaquinones in MG1363 and thereby provide a foundation for development of strains capable of higher K2-production during food fermentations.

RESULTS

Overexpression of *menF* or *menA* Increase Menaquinone Levels in *L. lactis*

We have employed "pull and push engineering" in our efforts to increase vitamin K2 production in MG163. Overexpression of isochorismate synthase (encoded by *menF)* was chosen in order to enhance flow through the shikimate pathway. More isochorismate synthase activity could create a metabolic pull through this pathway and increase flux into the menaquinone pathway (**Figure 1**). Overexpression of *menF* from the P32 promoter in pMG36e resulted in increased production (p-value 0.03) of the long-chained menaquinones MK-7, MK-8, and MK-9 (MK7-9) compared to the control strain (**Figure 2A**). The second gene chosen for overexpression, *menA*, encodes the DHNA polyprenyltransferase catalyzing the joining of the prenyl diphosphate chain and DHNA resulting in demethylated menaquinone. The content of MK7-9 in *L. lactis* expressing this gene from P32 on pMG36e was also higher (p-value 0.006) than the control strain (**Figure 2A**). Moreover, a dramatic increase of a short-chained menaquinone with retention time (RT) 2.75 min was observed (**Figure 2A**). A comparable increase in short chained MK content was seen for the *menF* overproducer. The presence of menaquinones with 3 prenyl units (MK-3) has been reported in lactococci (Rezaiki et al., 2008; Brooijmans et al., 2009). To determine the isoprenyl unit number of the short-chained menaquinone we employed the reported strategy by Rezaiki et al. (2008) and made a plot of the $\log_{10}$ (net RT in minutes) of standards MK-4 and MK-7 against their number of isoprenyl units (**Figure 2B**). The linear function of the graph was

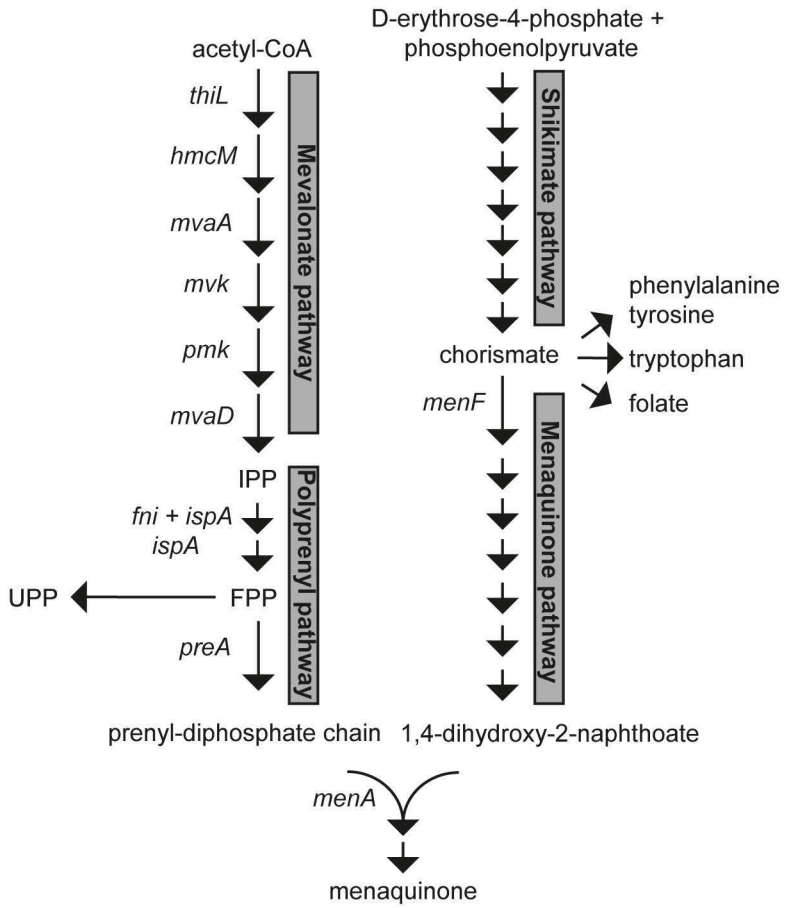

FIGURE 1 | The lactococcal biosynthetic pathways for menaquinone(s). Intermediates that are substrates for competing essential pathways are shown as branched points (chorismate and FPP). IPP, isopentenyl pyrophosphate; FPP, farnesyl pyrophosphate; UPP, undecaprenyl pyrophosphate.

used to calculate the number of isoprenyl units for the short-chained menaquinone (MK-X). We determined the number of isoprenyl units for MK-X to be 3. From here onwards, we assume that the species with RT 2.75 min is MK-3.

The MK7-9 levels nearly doubled by overexpression of *menA* and increased by 60% when overexpressing *menF* (**Figure 2C** and **Table 3**). The concentrations of total menaquinones (MK-3 + MK7-9) in the cultures with the strain overexpressing *menF* or *menA* (**Figure 2C**) were both around 400 nmol/L on average, which is almost 3 times that of the control strain (140 nmol/L). Most of the increase was attributed to MK-3. The MK-3/MK-9 ratio was markedly lower for MG1363 (0.6) than the strains overexpressing *menF* (1.7) or *menA* (1.3) as seen in **Table 3**. We also observed that the ratio of MK-3/MK-9 in MG1363 could vary from 0.2 to 0.7 between experiments possibly reflecting growth medium variation.

llmg_0196 Encodes the Prenyl Diphosphate Synthase in *L. lactis*

Although we achieved a 3-fold increase in total MK production in *L. lactis* by overproducing either *menF* or *menA*, the isoprenoid chain length of the menaquinones produced was not optimal. Long-chained MKs are more desirable in foods than short-chained MKs since longer MKs have a longer half-life and stability in the blood and are also reported to have a stronger protective effect on the risk of coronary heart disease than shorter menaquinones (Gast et al., 2009; Sato et al., 2012; Vermeer, 2012; Bruno, 2016). There was considerably more MK-3 than MK7-9 made by the overproducers of MenF and MenA (**Figure 2C**). This indicates that DHNA is in surplus and the production of the isoprenoid chain appears to be limiting. We therefore reasoned that the high levels of MK-3 represents a potential for higher MK7-9 production and focused on enhancing the mevalonate and polyprenyl pathways to stimulate production of longer isoprenoid chains.

To analyze the impact of mevalonate or polyprenyl pathway genes we first determined the involvement of the genes encoding the two putative prenyl diphosphate synthases; *gerCA+ispB* and *preA*. The coding sequences of either *gerCA+ispB* or *preA* was cloned into pNZ8037 and expressed using the inducible NICE expression system (de Ruyter et al., 1996) in strain NZ9000. Induction of the P_{nisA} promoter was regulated by addition of nisin at increasing concentrations (**Figure 3A**). We found that *preA*, but not *gerCA+ispB*, appear to encode a functional prenyl

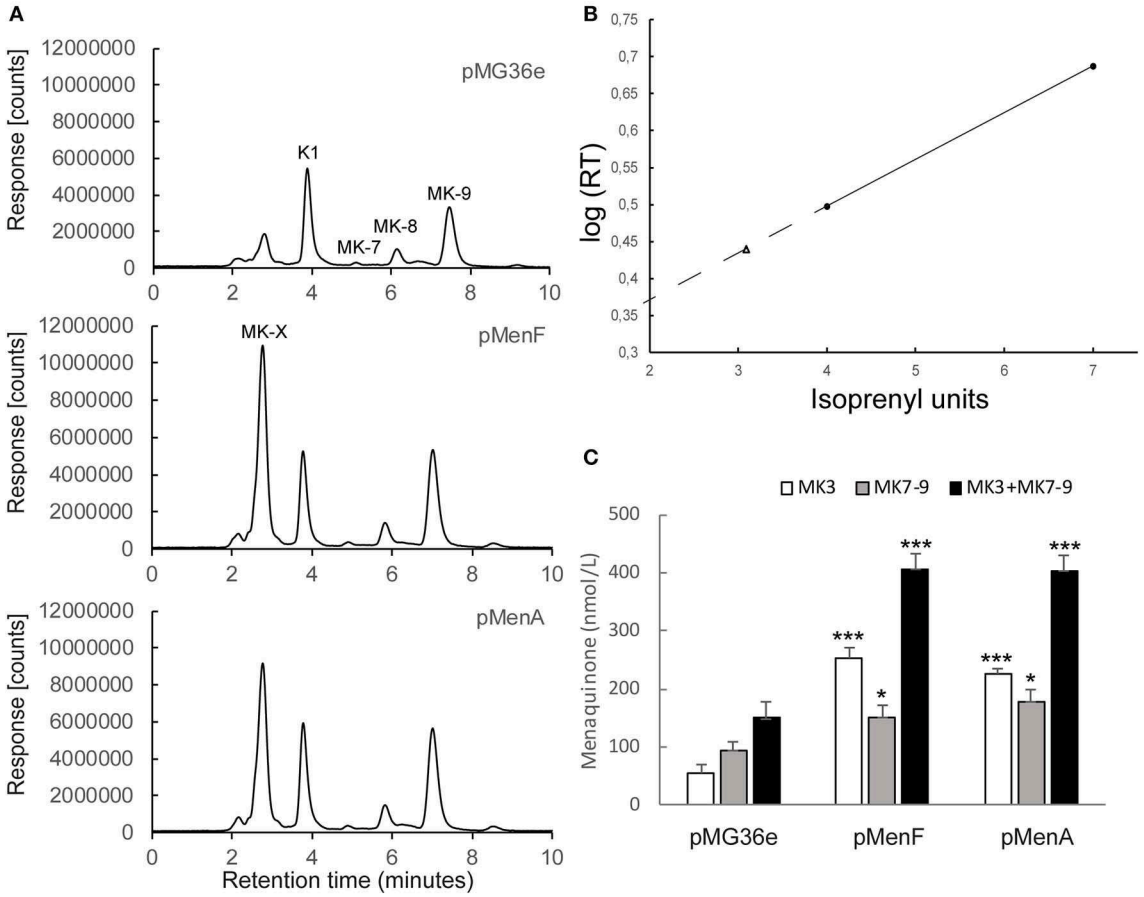

FIGURE 2 | (A) Analytical HPLC chromatograms of quinones from recombinant *L. lactis* MG1363 cultures expressing additional lactococcal isochorismate synthase (encoded by *menF*) or DHNA polyprenyltransferase (encoded by *menA*) from P32 promoter of pMG36e. *L. lactis* containing empty vector (pMG36e) is shown in the upper panel for comparison. Peaks K1, MK-7 to MK-9 were identified based on retention times (RTs) compared to RTs of standards. **(B)** Plot of isoprenyl unit lengths vs. $\log_{10}$ (net RT in min) for standards MK-4 and MK-7. The linear function of the graph between 4 and 7 isoprenyl units was used to calculate the isoprenyl unit number of MK-X. The dashed line represents extrapolation of the graph. MK-X (RT = 2.75) is designated using a triangle and corresponds to 3 isoprenyl units (MK-3). **(C)** Quantification of MK levels from (a). Average and standard error of the means are shown from at least 3 independent experiments. The * and *** represent a *p*-value below 0.05 and 0.0005 respectively. The *p*-values were obtained using a two-tailed *T*-test where the strains overexpressing *menF* or *menA* were compared to the control strain carrying empty pMG36e.

diphosphate synthase for MK production in *L. lactis*. When expression of *preA* was induced with nisin the levels of MK7-9 increased in a dose dependent manner reaching 480 nmol/L (**Figure 3A** and **Table 3**). This represented a fourfold increase in MK7-9 levels compared to control the strain pNZ8037. In contrast, menaquinone levels showed a slight, dose-dependedent decline upon induction of *gerCA+ispB* with nisin. There was no noticeable change in MK-3 levels as either prenyl diphosphate synthase was expressed.

Increasing the Substrate Pool for Prenyl Diphosphate Synthase: Overexpression of Mevalonate and Polyprenyl (MEV-PP) Pathway Genes

Overexpression of *preA* was sufficient to increase MK levels close to 500 nmol/L. We reasoned that increasing the amounts of FPP and IPP, the substrates of PreA, could stimulate menaquinone production in the PreA strain even more. To this end we used Gibson cloning (Gibson et al., 2009) to construct a plasmid where all the genes of the MEV-PP pathways (**Figure 1**) could be expressed from the same promoter and possibly ensure an increased supply of IPP and FPP. The genes *hmcM*, *thiL*, *mvaA*, *mvk*, *preA*, *mvaD, pmk*, *fni*, *ispA* were cloned in pHH145 with the P32 promoter up front (**Supplementary Figure 2**). In *L. lactis* ssp. *cremoris* MG1363 transformed with pMEV-PP MK production increased 3-fold compared to MG1363 transformed with pCTR (from 172 to 520 nmol/L on average) (**Figure 3B** and **Table 3**).

In *L. lactis* total enzyme activity of the MEV and PP pathways is dependent on the amount of transcription from seven transcriptional start sites. It is likely that increased expression of all mevalonate and PP genes not necessarily infers the correct balance of each intermediate for optimal

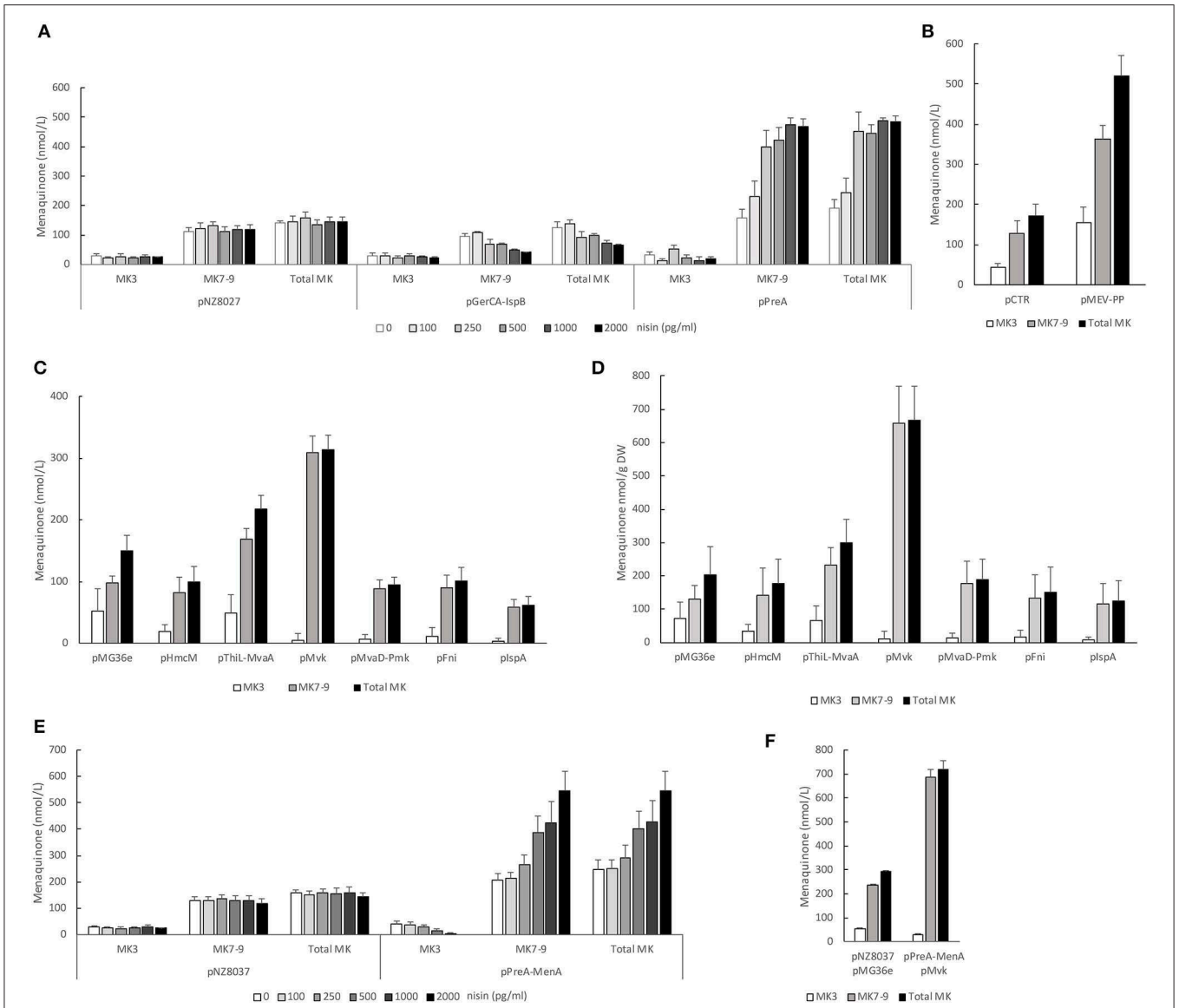

FIGURE 3 | (A) PreA is a functional polyprenyl PP synthase in *L. lactis* ssp. *cremoris*. Strain NZ9000 containing empty pNZ8037 or expressing either *gerCA+ispB* or *preA* after induction of P_{nisA} using increasing concentrations of nisin. **(B)** Combined overexpression of all mevalonate and polyprenyl pathway genes in one transcript [genes were cloned in cis after the constitutive P32 promoter and inserted into pHH145 (pMEV-PP)]. Strain *L. lactis* ssp. *cremoris* MG1363 transformed with pMEV-PP or pCTR. **(C)** Overexpression of mevalonate and polyprenyl pathway genes from the P32 promoter of pMG36e. Strain *L. lactis* ssp. *cremoris* MG1363 transformed with pHmcM, pThiL-MvaA, pMvk, pMvaD-Pmk, pFni or pIspA. **(D)** Specific concentrations of vitamin K2 (nmol MK/g DW) when overexpressing mevalonate or polyprenyl pathway genes from the P32 promoter of pMG36e. **(E)** Combined overexpression of *preA* and *menA* and its effect on menaquinone production. Strain *L.lactis* NZ9000 containing empty pNZ8037 or transformed with pPreA-MenA after induction of P_{nisA} with increasing concentrations of nisin. **(F)** Combined overexpression of *preA*, *menA,* and *mvk* and its effect on menaquinone production. Strain *L. lactis* NZ9000 containing empty pNZ8037 and empty pMG36e or transformed with pMvk and pPreA-MenA. Induction of P_{nisA} with 2 ng/ml nisin. All strains were cultivated in GM17 and statically incubated at 30°C over night. Quantification of MK-3, MK7-9 and MK-3+MK7-9 levels from average of at least 3 independent experiments. Error bars represent standard error of the means.

prenyl diphosphate chain production. To clarify this issue and determine whether any of the mevalonate or PP genes are more important for increasing the MK production than others they were overexpressed individually or in pairs (for genes where endogenous location is together in cis: *thiL+mvaA* and *mvaD+pmk*) from the P32 promoter on plasmid pMG36e (**Figure 3C**). Of all the genes overexpressed only *mvk* significantly increased total MK levels (p-value 0.002) which doubled compared to the control strain. The overexpression of *ispA* was the only gene that significantly reduced total MK levels compared to the control strain (p-value 0.02).

As several of these clones grew to lower cell density than the control strain, we included a measurement of the MK content on dry weight basis. As shown in **Figure 3D** most clones contained

TABLE 3 | Summary of overexpression studies.

L. lactis host	Plasmid	MK^*_{Total} (nmol/L)	MK7-9* (nmol/L)	MK-3/MK-9
MG1363	pMG36e	150 ± 12.2	97 ± 25.4	0.6
MG1363	pMenF	406 ± 18.2	152 ± 27.3	1.7
MG1363	pMenA	404 ± 19.6	179 ± 26.1	1.3
MG1363	pHmcM	100 ± 26.6	81 ± 24.3	0.2
MG1363	pThiL-MvaA	218 ± 17.1	169 ± 22.4	0.3
MG1363	pMvk	314 ± 26.2	309 ± 23.6	<0.1
MG1363	pMvaD-Pmk	94 ± 14.8	88 ± 13.4	0.1
MG1363	pFni	100 ± 20.3	90 ± 22.5	0.1
MG1363	pIspA	61 ± 13.4	58 ± 13.8	0.1
MG1363	pCtr	172 ± 32.6	128 ± 28.1	0.3
MG1363	pMEV-PP	520 ± 33.7	364 ± 51.1	0.4
NZ9000	pNZ8037	143 ± 16.5	119 ± 16.3	0.2
NZ9000	pPreA	485 ± 28.7	467 ± 20.2	<0.1
NZ9000	pGerCA-IspB	66 ± 0.6	43 ± 4.0	0.5
NZ9000	pPreA-MenA	544 ± 75.1	544 ± 75.1	<0.1
NZ9000	pNZ8037 pMG36e	292 ± 3.4	238 ± 6.9	0.2
NZ9000	pPreA-MenA pMvk	719 ± 33.0	687 ± 35.6	<0.1
NZ9000	pNZ8037 pCtr	127 ± 1.5	114 ± 3.2	0.1
NZ9000	pMEV-PP-2 pPreA-MenA	657 ± 32.6	651 ± 30.2	<0.1

Numbers for NZ9000 strains are from experiments using 2 ng/ml for induction of the nisA promoter.
**Average and standard error of the means of at least 3 experiments.*

less MK-3/g DW than the control, while MK7-9 was the same or slightly elevated. However, overexpression of *mvk* led to more than 3-fold higher specific concentration of MK7-9, while MK-3 was reduced.

Combined Overexpression of Key Genes

Increased expression of either *preA*, *menA*, *menF,* or *mvk* all led to at least doubled levels of MK and appear to be key genes for MK synthesis. Combined overexpression of several of these genes could have an additive effect on MK production, and this possibility was explored. As *preA* and *menA* are located after one another in an operon they were cloned together and overexpressed using the NICE expression system (**Figure 3E**). At maximal induction of cells transformed with pPreA-MenA we obtained an average concentration of 540 nmol/L MK7-9 (**Table 3**), the highest concentration obtained through our genetic engineering approach thus far. Next, we transformed this clone with pMvk (**Figure 3F**). In this strain the gene encoding mevalonate kinase is expressed constitutively and *preA* + *menA* upon induction with nisin. This led to another slight increase of MK production, reaching 680 nmol/L MK7-9 (**Table 3**). We note that the MK level in the control strain harboring the two empty plasmids is higher than what we have observed for other control strains. We also analyzed the MK production in a strain overexpressing all mevalonate and PP genes in addition to MenA (pMEV-PP-2 and pPreA-MenA). This strain produced an average of 651 nmol/L MK7-9 (**Table 3**), comparable to the strain overexpressing *mvk*, *preA,* and *menA*. All results obtained through overexpression studies are summarized in **Table 3**.

Fermentation of Milk by Vitamin K2 Overproducing Strains

Finally, we tested whether overexpression of the key genes identified earlier affect MK content also during fermentation of milk (**Figure 4**). All strains except the overproducer of mevalonate kinase acidified the milk to a pH below 5.0 and caused coagulation, and this strain also produced less MK than the control strain in milk. Overexpression of *preA* alone or together with *menA* or *menA*+*mvk* caused elevated production of vitamin K2. The total vitamin K2 levels reached close to 700 nmol/L (500 ng/g fermented milk) using any of the 3 strains, and MK7-9 constituted more than 93% of the total menaquinone content.

DISCUSSION

Subclinical vitamin K deficiency, not uncommon in the Western world, is associated with increased risks of diseases including osteoporosis and cardiovascular disease (Geleijnse et al., 2004; Gast et al., 2009; Schwalfenberg, 2017). Being more effective than vitamin K1, increasing the intake of long-chained vitamin K2 would be the best way to improve vitamin K status. In this study, we have analyzed MK biosynthesis in the most important menaquinone-producer for our diets; *L. lactis*. Our results demonstrate that it is possible to increase MK production by *L. lactis* by enhancing transcription of key genes like *menF*, *menA*, *preA,* or *mvk*.

Metabolic pathway engineering for increased product formation often involve increasing the substrate pools. Chorismate represents a critical branch-point in menaquinone biosynthesis since it is also a substrate for production of the essential AAA and folate. A good strategic starting point for metabolic engineering of *L. lactis* could be to ensure increased chorismate levels and thereby elevate the supply of substrate for isochorismate synthase. However, efforts to increase chorismate levels by manipulating the shikimate pathway have proven unsuccessful in *B. subtilis*, probably due to increased feedback inhibition of the shikimate pathway caused by a concomitant rise in AAA levels (Tsukamoto et al., 2001; Yang et al., 2019). Moreover, by overexpressing enzymes involved in conversion of chorismate to folate Wegkamp et al. (2007) obtained considerable increases in folate production in *L. lactis*. Basic levels of folate production were in the same range as MK production, indicating that flux through the shikimate pathway would not be a bottleneck in our work. Our first targeted genetic approach was consequently aimed at steps outside of the shikimate pathway by trying to push carbon flux into the menaquinone pathway or pull flux through both pathways by cloning and expression of *menF* and *menA,* respectively. Overexpression of either *menF* or *menA* increased total menaquinone levels and MK-3 was the main menaquinone generated. The increase in MK-3 levels can be explained by a shortage of long-chained polyprenyl diphosphates

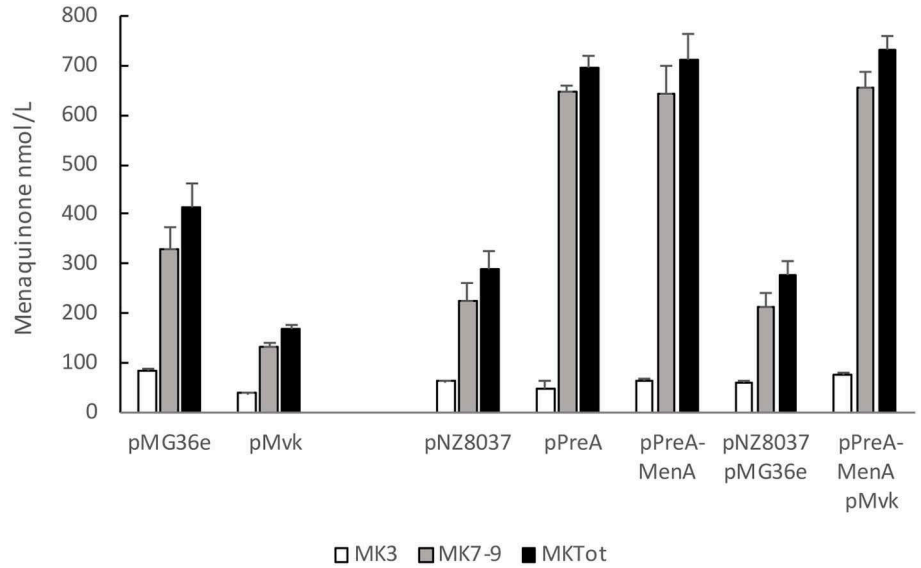

FIGURE 4 | Vitamin K2 content in milk fermented by strains overexpressing key genes of the biosynthetic menaquinone pathway. Fermentation was carried out for 20 h at 30°C in heat-sterilized skimmed milk supplemented with 0.5% glucose and 1% tryptone. Nisin (2 ng/ml) was added to NZ9000 strains 1 h after inoculation. Quantification of MK-3, MK7-9 and MK-3+MK7-9 levels from average of at least 3 independent experiments. Error bars represent standard error of the means.

compared to the amount of DHNA present and pinpoint prenyl diphosphate chain synthesis as rate-limiting for MK synthesis. As DHNA prenyltransferases are highly specific for DHNA, but unspecific for the prenyl diphosphate chain, MenA will join DHNA with any prenyl diphosphate chain available (Saito and Ogura, 1981). Therefore, in the overproducers of MenA and MenF FPP (C15) appears to be in excess as MK-3 is formed in large quanta. Longer prenyl diphosphate chains (C40-C50) form by sequential condensation of FPP with 5-7 IPP units in a reaction catalyzed by prenyl diphosphate synthase (Ogura and Koyama, 1998; Koyama, 1999). The mevalonate pathway, which is required for formation of IPP (C5), or prenyl diphosphate synthase activity consequently appear limiting in the MenF and MenA overproducers. MK-3 can be a major contributor to the total menaquinone content in lactococci (Brooijmans et al., 2009) in agreement with our data. The presence of MK-3 indicate that the mevalonate and polyprenyl pathways are also limiting in the wild type. Cells overexpressing PreA produced long chained MK instead of MK3 showing that prenyl diphosphate chain elongation activity and not IPP supply limits MK synthesis. MK-3 was reduced when the mevalonate or polyprenyl pathway genes were overexpressed, likely to be caused by the metabolic pull created by the increased enzymatic activity.

In late growth energy supply is reduced and the production of MK-3 relative to MK-9 has been shown to increase in *L. lactis* (Rezaiki et al., 2008). Interestingly, *menF* transcription was found to increase by aerobic conditions (Cretenet et al., 2014), but the MK-3/MK-9 ratio decreased (Brooijmans et al., 2009). Aeration alters metabolism, and improves energy and redox status in *L. lactis*, and this may favor enhanced synthesis of IPP.

From the *menF* and *menA* overexpression studies it is apparent that there is a lack of prenyl diphosphate synthase activity to create longer isoprenoid chains so that the more valuable longer menaquinones can form. The genome of *L. lactis* ssp. *cremoris* MG1363 contains ORFs encoding 2 different putative prenyl diphosphate synthetases. When overexpressing *llmg_0196* (*preA*) MK7-9 production increased 3-fold. The length of the isoprenoid side chains of menaquinones is defined by the prenyl diphosphate synthases and these enzymes are classified as short-, medium-, or long-chained prenyl diphosphate synthases accordingly (Ogura and Koyama, 1998; Koyama, 1999). Long-chain prenyl diphosphate synthases are homodimers that add IPP units to allylic diphosphates generating C40 and longer prenyl diphosphate chains. Our results indicate that PreA is a functional long-chain (C45) prenyl diphosphate synthase as the levels of longer menaquinones are increased when transcription of *preA* is induced.

The second putative prenyl diphosphate synthase of MG1363 is encoded by 2 overlapping ORFs annotated as *gerCA* and *ispB*. Heterodimeric prenyl diphosphate synthases generate medium chain prenyl diphosphates (C30 and C35) (Ogura and Koyama, 1998; Koyama, 1999). However, we did not observe an increase in the amount of medium length MKs when overexpressing *gerCA+ispB*. This implies that the *gerCA+ispB* locus could either contain a non-functional prenyl diphosphate synthase or that GerCA+IspB generates a polyprenyl diphosphate chain used for something different than MK production. Since MK7-9 levels were reduced by increased expression of *gerCA+ispB* we assume that less substrate (FPP, IPP) became available to maintain normal PreA activity and MK production.

Mevalonate kinase was identified as a key gene for MK production in MG1363 as overexpression of *mvk* doubled the amount of MK produced. This result is in accordance with Song et al. (2014) who identified *mvk* to be a metabolic bottleneck

of the mevalonate pathway. Overexpression of other mevalonate genes did not result in greatly increased MK levels. We observed that overexpression of several mevalonate or polyprenyl pathway genes, especially *mvk*, inhibited growth as seen by the lower OD600 reached after overnight cultivation. Alterations of the mevalonate or polyprenyl pathway enzyme activity could result in a build-up of mevalonic or isoprenoid intermediates. An abundance of isoprenoid precursors is cytotoxic (Martin et al., 2003; Sivy et al., 2011), likely true also for *L. lactis*. When *mvk* was overexpressed together with *preA* and *menA* the growth defect was abrogated. In this strain increased mevalonate kinase activity is accompanied with increased PreA and MenA activity withdrawing possible toxic isoprenoid precursors.

To increase menaquinone production by bacteria several approaches has been explored. They include optimization of the fermentation process, increasing menaquinone secretion, improving bioreactor design, directed mutagenesis of strains or genetic engineering of strains (Ren et al., 2019). To enhance strain performance genomic changes has been made in order to maximize substrate pools, limit the production of by-products, overexpress key genes, express novel pathways, or combinations of the aforementioned strategies (Kong and Lee, 2011; Liu et al., 2017, 2018; Xu et al., 2017; Ma et al., 2019; Yang et al., 2019). Most of these studies have been performed using *B. subtilis*, *B. amyloliquefaciens*, *E. meningoseptica,* or *E. coli* and seek to produce menaquinone on an industrial scale for use as a nutritional supplement or food additive. The present study is the first to genetically engineer menaquinone synthesis in *L. lactis* and in a proof-of-principle manner use these GMO strains for vitamin K2 fortification of milk. We employed several of the strategies mentioned above to increase menaquinone production: limiting the production of by-products by committing substrates to menaquinone production (*menF*, *preA*), identification and overexpression of key genes (*menA*, *preA*, *mvk*) and increasing substrate pools (pMEV-PP). Based on our results and others there appear to be some general approaches that are successful when aiming to overproduce MK among diverse bacteria including *L. lactis* ssp. *cremoris*. Firstly, enhanced expression of *menA* result in around 2-fold higher MK production in *E. coli*, *B. amyloliquefaciens*, *E. meningoseptica,* and *B.subtilis* (Kong and Lee, 2011; Liu et al., 2017, 2018; Xu et al., 2017; Ma et al., 2019; Yang et al., 2019) and we found that this also applies for *L. lactis*. More MenA activity will pull out products of both the menaquinone and MEV+PP pathways possibly leading to an increased flux through both pathways. Secondly, optimizing the precursor pool for prenyl diphosphate synthase appears to be a fruitful strategy to increase MK production. In most bacterial species IPP form through the mevalonate-independent pathway called the MEP pathway (Frank and Groll, 2017). Overexpression of MEP and/or PP pathway genes increase MK production in *B. subtilis*, *E. coli* and *E. meningoseptica* (Kong and Lee, 2011; Ma et al., 2019; Yang et al., 2019). In line with these studies we achieved a doubling of the menaquinone content by overexpression of the *mvk* gene of the IPP-producing mevalonate pathway in *L. lactis*.

By cloning all genes of the MEV and PP pathways and expressing them from the P32 promoter we expected to increase MK production compared to single expression of *mvk* or *preA*. However, we achieved only slightly higher MK levels than by overexpressing *preA* alone using the NICE system. The difference in promoter strength between the constitutive P32 and the strong P_{nisA}, might be a reason why combined expression of all MEV+PP genes did not evoke a higher MK production than *preA* alone.

We achieved a maximum MK7-9 titer of 687 nmol/L when combining overexpression of *menA*, *preA* and *mvk*. An additive effect on MK production when increasing the precursor pool for the prenyl diphosphate synthase combined with increased MenA activity has also been reported by others. In *E. menigoseptica* a 2.5-fold increase was achieved by combining overexpression of *menA* and a single MEP pathway gene (Liu et al., 2018). In *B. subtilis* a recent study reported 11-fold increase by overexpressing *menA* and three genes of the MEP pathway (Ma et al., 2019).

Five times increased MK production has been achieved by overexpression in *E. coli* and *B. subtilis* (Kong and Lee, 2011; Yang et al., 2019) similar to the fourfold increase reported here. Except from the clones overexpressing single mevalonate genes there was no change in growth yield in *L. lactis* overproducing vitamin K2. The highest specific vitamin K2 content was 0.67mg/g DW, slightly lower than the 290 μg MK/g wet cell weight (=1.26 mg/m DCW) (Glazyrina et al., 2010) in the *E. coli* overproducer (Kong and Lee, 2011). However, the specific menaquinone content in *B. subtilis* can get much higher, and Yang et al. (2019) reported 12.0 mg/g DCW after optimization of culture conditions of their overproducing clone.

As a proof-of-principle, we employed several of the MK overproducing strains to verify whether these strains would increase menaquinone content of fermented milk to a beneficial level. Fermented milk is a dairy product mostly consumed in Nordic countries and contains vitamin K2 levels up to 80 ng/g (Koivu-Tikkanen et al., 2000; Liu et al., 2019). We achieved a significantly higher level using our overproducers as we obtained more than 5 times higher MK7-9 levels (450 ng/g). We also found that MK levels in general were higher after milk fermentation than by culturing in M17. The daily requirement for vitamin K is set at 1 μg/kg body weight (Frick et al., 1967). A serving of 200 ml fermented milk produced by our genetically engineered menaquinone overproducers would contain 90 μg long chained vitamin K2 and fulfill the daily requirement for most people. Hard cheese contains an average of 30–40 μg MK/100 g (Manoury et al., 2013; Vermeer et al., 2018). The average pro capita cheese consumption in Western countries is in the range of 41–82 g cheese/day (IDF, 2016) corresponding to a daily vitamin K2 intake of 12–32 μg. In this work we have shown by cloning that the bacterial specific vitamin K2 content can be increased fourfold, suggesting that a similar stimulation can be achieved in a cheese. With a vitamin K2 content of 120–160 μg MK/100 g such cheese could be a main contributor to meet the daily requirement of vitamin K even in people with a moderate cheese intake.

We have pinpointed the mevalonate and polyprenyl pathways as rate-limiting for MK synthesis and increasing the pool size of the precursor acetyl-CoA could be a strategy for further improvement of vitamin K2 production. Possibly this could be

achieved by redirecting carbon flow from homolactic to more mixed acid fermentation. However, increasing flux from pyruvate to acetyl-CoA would also affect the taste of the dairy product in a negative manner (Gaspar et al., 2011).

CONCLUSION

Biosynthesis of menaquinones require over 20 enzymatic reactions and it is reasonable to expect that an elevated level of a single enzyme is insufficient to dramatically increase the amount of pathway product. However, when it comes to vitamin K2, just doubling or tripling the amount in our food could play a vital role for public health. Here, we have shown that overexpression of key genes is enough to double (*mvk*), triple (*menA*) and even quadruple (*preA*, *preA* + *menA*) vitamin K2 levels produced by the important vitamin K2 producer *L. lactis* ssp. *cremoris* MG1363 under laboratory conditions. We further demonstrate how these strains can ferment milk and increase the vitamin K2 content 3-fold in the resulting fermented milk. A minimal step to achieve 3 times higher levels of the long-chained MKs could therefore be to modify the endogenous promoter of the *preA-menA* operon to enhance transcription. The use of genetically-modified organisms (GMOs) for food production is under heavy jurisdiction in most countries, nevertheless over 100 GMOs are approved worldwide for use in commercial food or feed so far (Kamle et al., 2017). The rise of CRISPR-technology, to make precise genetic alterations in organisms ranging from bacteria like *L. lactis* (Guo et al., 2019) to human beings, is also believed to impact the legislation around GMO's and food production possibly enabling the use of such GMO's in a near future.

DATA AVAILABILITY STATEMENT

The datasets generated for this study are available on request to the corresponding author.

AUTHOR CONTRIBUTIONS

CB performed all the experiments except construction of pHH145 which was carried out by HH. CB and HH designed, analyzed, and interpreted all experiments and wrote the paper.

FUNDING

This work was funded by the Norwegian Research Council, project number 256331, and Tine SA.

SUPPLEMENTARY MATERIAL

The Supplementary Material for this article can be found online at: https://www.frontiersin.org/articles/10.3389/fbioe.2020.00191/full#supplementary-material

REFERENCES

Albuquerque, M. A. C., Bedani, R., LeBlanc, J. G., and Saad, S. M. I. (2017). Passion fruit by-product and fructooligosaccharides stimulate the growth and folate production by starter and probiotic cultures in fermented soymilk. *Int. J. Food Microbiol.* 261, 35–41. doi: 10.1016/j.ijfoodmicro.2017.09.001

Bhushan, B., Tomar, S. K., and Chauhan, A. (2017). Techno-functional differentiation of two vitamin B_{12} producing Lactobacillus plantarum strains: an elucidation for diverse future use. *Appl. Microbiol. Biotechnol.* 101, 697–709. doi: 10.1007/s00253-016-7903-z

Bouhss, A., Trunkfield, A. E., Bugg, T. D., and Mengin-Lecreulx, D. (2008). The biosynthesis of peptidoglycan lipid-linked intermediates. *FEMS Microbiol. Rev.* 32, 208–233. doi: 10.1111/j.1574-6976.2007.00089.x

Brooijmans, R., Smit, B., Santos, F., van Riel, J., de Vos, W. M., and Hugenholtz, J. (2009). Heme and menaquinone induced electron transport in lactic acid bacteria. *Microb. Cell Fact.* 8:28. doi: 10.1186/1475-2859-8-28

Bruno, E. J. (2016). The prevalence of vitamin k deficiency / insufficiency, and recommendations for increased intake. *J. Hum. Nutr. Food Sci.* 4:1077.

Burgess, C., O'Connell-Motherway, M., Sybesma, W., Hugenholtz, J., and van Sinderen, D. (2004). Riboflavin production in *Lactococcus lactis*: potential for *in situ* production of vitamin-enriched foods. *Appl. Environ. Microbiol.* 70, 5769–5777. doi: 10.1128/AEM.70.10.5769-5777.2004

Chen, J., Vestergaard, M., Jensen, T. G., Shen, J., Dufva, M., Solem, C., et al. (2017). Finding the needle in the haystack–the use of microfluidic droplet technology to identify vitamin-secreting lactic acid bacteria. *MBio* 8, e00526–17. doi: 10.1128/mBio.00526-17

Cranenburg, E. C., Koos, R., Schurgers, L. J., Magdeleyns, E. J., Schoonbrood, T. H., Landewe, R. B., et al. (2010). Characterisation and potential diagnostic value of circulating matrix Gla protein (MGP) species. *Thromb. Haemost.* 104, 811–822. doi: 10.1160/TH09-11-0786

Cretenet, M., Le Gall, G., Wegmann, U., Even, S., Shearman, C., Stentz, R., et al. (2014). Early adaptation to oxygen is key to the industrially important traits of *Lactococcus lactis* ssp. cremoris during milk fermentation. *BMC Genomics* 15:1054. doi: 10.1186/1471-2164-15-1054

de Ruyter, P. G., Kuipers, O. P., and de Vos, W. M. (1996). Controlled gene expression systems for *Lactococcus lactis* with the food-grade inducer nisin. *Appl. Environ. Microbiol.* 62, 3662–3667. doi: 10.1128/AEM.62.10.3662-3667.1996

Dosselaere, F., and Vanderleyden, J. (2001). A metabolic node in action: chorismate-utilizing enzymes in microorganisms. *Crit. Rev. Microbiol.* 27, 75–131. doi: 10.1080/20014091096710

Duwat, P., Sourice, S., Cesselin, B., Lamberet, G., Vido, K., Gaudu, P., et al. (2001). Respiration capacity of the fermenting bacterium *Lactococcus lactis* and its positive effects on growth and survival. *J. Bacteriol.* 183, 4509–4516. doi: 10.1128/JB.183.15.4509-4516.2001

Flore, R., Ponziani, F. R., Di Rienzo, T. A., Zocco, M. A., Flex, A., Gerardino, L., et al. (2013). Something more to say about calcium homeostasis: the role of vitamin K2 in vascular calcification and osteoporosis. *Eur. Rev. Med. Pharmacol. Sci.* 17, 2433–2440.

Frank, A., and Groll, M. (2017). The methylerythritol phosphate pathway to isoprenoids. *Chem. Rev.* 117, 5675–5703. doi: 10.1021/acs.chemrev.6b00537

Frick, P. G., Riedler, G., and Brogli, H. (1967). Dose response and minimal daily requirement for vitamin K in man. *J. Appl. Physiol.* 23, 387–389. doi: 10.1152/jappl.1967.23.3.387

Furie, B., Bouchard, B. A., and Furie, B. C. (1999). Vitamin K-dependent biosynthesis of gamma-carboxyglutamic acid. *Blood* 93, 1798–1808. doi: 10.1182/blood.V93.6.1798.406k22_1798_1808

Gaspar, P., Neves, A. R., Gasson, M. J., Shearman, C. A., and Santos, H. (2011). High yields of 2,3-butanediol and mannitol in *Lactococcus lactis* through engineering of NAD^+ cofactor recycling. *Appl. Environ. Microbiol.* 77, 6826–6835. doi: 10.1128/AEM.05544-11

Gasson, M. J. (1983). Plasmid complements of Streptococcus lactis NCDO 712 and other lactic streptococci after protoplast-induced curing. *J. Bacteriol.* 154, 1–9. doi: 10.1128/JB.154.1.1-9.1983

Gast, G. C., de Roos, N. M., Sluijs, I., Bots, M. L., Beulens, J. W., Geleijnse, J. M., et al. (2009). A high menaquinone intake reduces the incidence of coronary heart disease. *Nutr. Metab. Cardiovasc. Dis.* 19, 504–510. doi: 10.1016/j.numecd.2008.10.004

Gaudu, P., Vido, K., Cesselin, B., Kulakauskas, S., Tremblay, J., Rezaiki, L., et al. (2002). Respiration capacity and consequences in *Lactococcus lactis*. *Antonie. Leeuwenhoek* 82, 263–269. doi: 10.1023/A:1020635600343

Geleijnse, J. M., Vermeer, C., Grobbee, D. E., Schurgers, L. J., Knapen, M. H., van der Meer, I. M., et al. (2004). Dietary intake of menaquinone is associated with a reduced risk of coronary heart disease: the Rotterdam Study. *J. Nutr.* 134, 3100–3105. doi: 10.1093/jn/134.11.3100

Gibson, D. G., Young, L., Chuang, R. Y., Venter, J. C., Hutchison, C. A. III., and Smith, H. O. (2009). Enzymatic assembly of DNA molecules up to several hundred kilobases. *Nat. Methods* 6, 343–345. doi: 10.1038/nmeth.1318

Glazyrina, J., Materne, E. M., Dreher, T., Storm, D., Junne, S., Adams, T., et al. (2010). High cell density cultivation and recombinant protein production with *Escherichia coli* in a rocking-motion-type bioreactor. *Microb. Cell Fact.* 9:42. doi: 10.1186/1475-2859-9-42

Guo, T., Xin, Y., Zhang, Y., Gu, X., and Kong, J. (2019). A rapid and versatile tool for genomic engineering in *Lactococcus lactis*. *Microb. Cell Fact.* 18:22. doi: 10.1186/s12934-019-1075-3

Holo, H., and Nes, I. F. (1989). High-Frequency transformation, by electroporation, of *Lactococcus lactis* subsp. cremoris grown with glycine in osmotically stabilized media. *Appl. Environ. Microbiol.* 55, 3119–3123. doi: 10.1128/AEM.55.12.3119-3123.1989

Horton, R. M., Hunt, H. D., Ho, S. N., Pullen, J. K., and Pease, L. R. (1989). Engineering hybrid genes without the use of restriction enzymes: gene splicing by overlap extension. *Gene* 77, 61–68. doi: 10.1016/0378-1119(89)90359-4

IDF (2016). *2016 World Dairy Situation Report*. International Dairy Federation.

Jonsson, M., Saleihan, Z., Nes, I. F., and Holo, H. (2009). Construction and characterization of three lactate dehydrogenase-negative *Enterococcus faecalis* V583 mutants. *Appl. Environ. Microbiol.* 75, 4901–4903. doi: 10.1128/AEM.00344-09

Juarez Del Valle, M., Laino, J. E., Savoy de Giori, G., and LeBlanc, J. G. (2017). Factors stimulating riboflavin produced by Lactobacillus plantarum CRL 725 grown in a semi-defined medium. *J. Basic Microbiol.* 57, 245–252. doi: 10.1002/jobm.201600573

Kamle, M., Kumar, P., Patra, J. K., and Bajpai, V. K. (2017). Current perspectives on genetically modified crops and detection methods. *3 Biotech.* 7:219. doi: 10.1007/s13205-017-0809-3

Koivu-Tikkanen, T. J., Ollilainen, V., and Piironen, V. I. (2000). Determination of phylloquinone and menaquinones in animal products with fluorescence detection after postcolumn reduction with metallic zinc. *J. Agric. Food Chem.* 48, 6325–6331. doi: 10.1021/jf000638u

Kong, M. K., and Lee, P. C. (2011). Metabolic engineering of menaquinone-8 pathway of *Escherichia coli* as a microbial platform for vitamin K production. *Biotechnol. Bioeng.* 108, 1997–2002. doi: 10.1002/bit.23142

Koyama, T. (1999). Molecular analysis of prenyl chain elongating enzymes. *Biosci. Biotechnol. Biochem.* 63, 1671–1676. doi: 10.1271/bbb.63.1671

Kuipers, O. P., de Ruyter, P. G. G. A., Kleerebezem, M., and de Vos, W. M. (1998). Quorum sensing-controlled gene expression in lactic acid bacteria. *J. Biotechnol.* 64, 15–21. doi: 10.1016/S0168-1656(98)00100-X

Li, P., Gu, Q., Yang, L., Yu, Y., and Wang, Y. (2017). Characterization of extracellular vitamin B_{12} producing Lactobacillus plantarum strains and assessment of the probiotic potentials. *Food Chem.* 234, 494–501. doi: 10.1016/j.foodchem.2017.05.037

Liu, Y., Ding, X.-,m., Xue, Z.-,l., Hu, L.-,x., Cheng, Q., and Chen, M.-,h., et al. (2017). Site-directed mutagenesis of UbiA to promote menaquinone biosynthesis in *Elizabethkingia meningoseptica*. *Process Biochem.* 58, 186–192. doi: 10.1016/j.procbio.2017.05.002

Liu, Y., van Bennekom, E. O., Zhang, Y., Abee, T., and Smid, E. J. (2019). Long-chain vitamin K2 production in *Lactococcus lactis* is influenced by temperature, carbon source, aeration and mode of energy metabolism. *Microb. Cell Fact.* 18:129. doi: 10.1186/s12934-019-1179-9

Liu, Y., Yang, Z., Xue, Z., Qian, S., Wang, Z., Hu, L., et al. (2018). Influence of site-directed mutagenesis of UbiA, overexpression of dxr, menA and ubiE, and supplementation with precursors on menaquinone production in *Elizabethkingia meningoseptica*. *Process Biochem.* 68, 64–72. doi: 10.1016/j.procbio.2018.01.022

Luukinen, H., Kakonen, S. M., Pettersson, K., Koski, K., Laippala, P., Lovgren, T., et al. (2000). Strong prediction of fractures among older adults by the ratio of carboxylated to total serum osteocalcin. *J. Bone Miner. Res.* 15, 2473–2478. doi: 10.1359/jbmr.2000.15.12.2473

Ma, Y., McClure, D. D., Somerville, M. V., Proschogo, N. W., Dehghani, F., Kavanagh, J. M., et al. (2019). Metabolic engineering of the MEP pathway in *Bacillus subtilis* for increased biosynthesis of menaquinone-7. *ACS Synth. Biol.* 8, 1620–1630. doi: 10.1021/acssynbio.9b00077

Manoury, E., Jourdon, K., Boyaval, P., and Fourcassie, P. (2013). Quantitative measurement of vitamin K_2 (menaquinones) in various fermented dairy products using a reliable high-performance liquid chromatography method. *J. Dairy Sci.* 96, 1335–1346. doi: 10.3168/jds.2012-5494

Martin, V. J., Pitera, D. J., Withers, S. T., Newman, J. D., and Keasling, J. D. (2003). Engineering a mevalonate pathway in *Escherichia coli* for production of terpenoids. *Nat. Biotechnol.* 21, 796–802. doi: 10.1038/nbt833

Meucci, A., Rossetti, L., Zago, M., Monti, L., Giraffa, G., Carminati, D., et al. (2018). Folates biosynthesis by *Streptococcus thermophilus* during growth in milk. *Food Microbiol.* 69, 116–122. doi: 10.1016/j.fm.2017.08.001

Mir, R., Jallu, S., and Singh, T. P. (2015). The shikimate pathway: review of amino acid sequence, function and three-dimensional structures of the enzymes. *Crit. Rev. Microbiol.* 41, 172–189. doi: 10.3109/1040841X.2013.813901

Morishita, T., Tamura, N., Makino, T., and Kudo, S. (1999). Production of menaquinones by lactic acid bacteria. *J. Dairy Sci.* 82, 1897–1903. doi: 10.3168/jds.S0022-0302(99)75424-X

Nimptsch, K., Rohrmann, S., Kaaks, R., and Linseisen, J. (2010). Dietary vitamin K intake in relation to cancer incidence and mortality: results from the heidelberg cohort of the european prospective investigation into cancer and nutrition (EPIC-Heidelberg). *Am. J. Clin. Nutr.* 91, 1348–1358. doi: 10.3945/ajcn.2009.28691

Ogura, K., and Koyama, T. (1998). Enzymatic Aspects of isoprenoid chain elongation. *Chem. Rev.* 98, 1263–1276. doi: 10.1021/cr9600464

Okano, T., Shimomura, Y., Yamane, M., Suhara, Y., Kamao, M., Sugiura, M., et al. (2008). Conversion of phylloquinone (Vitamin K1) into menaquinone-4 (Vitamin K2) in mice: two possible routes for menaquinone-4 accumulation in cerebra of mice. *J. Biol. Chem.* 283, 11270–11279. doi: 10.1074/jbc.M702971200

Ren, L., Peng, C., Hu, X., Han, Y., and Huang, H. (2019). Microbial production of vitamin K2: current status and future prospects. *Biotechnol. Adv.* 39:107453. doi: 10.1016/j.biotechadv.2019.107453

Rezaiki, L., Lamberet, G., Derre, A., Gruss, A., and Gaudu, P. (2008). *Lactococcus lactis* produces short-chain quinones that cross-feed Group B *Streptococcus* to activate respiration growth. *Mol. Microbiol.* 67, 947–957. doi: 10.1111/j.1365-2958.2007.06083.x

Saito, Y., and Ogura, K. (1981). Biosynthesis of menaquinones. enzymatic prenylation of 1,4-dihydroxy-2-naphthoate by micrococcus luteus membrane fractions. *J. Biochem.* 89, 1445-1452. doi: 10.1093/oxfordjournals.jbchem.a133337

Sato, T., Schurgers, L. J., and Uenishi, K. (2012). Comparison of menaquinone-4 and menaquinone-7 bioavailability in healthy women. *Nutr. J.* 11:93. doi: 10.1186/1475-2891-11-93

Saubade, F., Hemery, Y. M., Guyot, J. P., and Humblot, C. (2017). Lactic acid fermentation as a tool for increasing the folate content of foods. *Crit. Rev. Food Sci. Nutr.* 57, 3894–3910. doi: 10.1080/10408398.2016.1192986

Sauer, M., Russmayer, H., Grabherr, R., Peterbauer, C. K., and Marx, H. (2017). The efficient clade: lactic acid bacteria for industrial chemical production. *Trends Biotechnol.* 35, 756–769. doi: 10.1016/j.tibtech.2017.05.002

Schurgers, L. J., Teunissen, K. J., Knapen, M. H., Kwaijtaal, M., van Diest, R., Appels, A., et al. (2005). Novel conformation-specific antibodies against matrix gamma-carboxyglutamic acid (Gla) protein: undercarboxylated matrix Gla protein as marker for vascular calcification. *Arterioscler. Thromb. Vasc. Biol.* 25, 1629–1633. doi: 10.1161/01.ATV.0000173313.46222.43

Schurgers, L. J., and Vermeer, C. (2000). Determination of phylloquinone and menaquinones in food. Effect of food matrix on circulating vitamin K concentrations. *Haemostasis* 30, 298–307. doi: 10.1159/000054147

Schwalfenberg, G. K. (2017). Vitamins K1 and K2: the emerging group of vitamins required for human health. *J. Nutr. Metab.* 2017:6254836. doi: 10.1155/2017/6254836

Shea, M. K., O'Donnell, C. J., Vermeer, C., Magdeleyns, E. J., Crosier, M. D., Gundberg, C. M., et al. (2011). Circulating uncarboxylated matrix gla protein is associated with vitamin K nutritional status, but not coronary artery calcium, in older adults. *J. Nutr.* 141, 1529–1534. doi: 10.3945/jn.111.139634

Sijpesteijn, A. K. (1970). Induction of cytochrome formation and stimulation of oxidative dissimilation by hemin in *Streptococcus lactis* and *Leuconostoc mesenteroides*. *Antonie. Leeuwenhoek* 36, 335–348. doi: 10.1007/BF02069035

Simon, D., and Chopin, A. (1988). Construction of a vector plasmid family and its use for molecular cloning in *Streptococcus lactis*. *Biochimie* 70, 559–566. doi: 10.1016/0300-9084(88)90093-4

Sivy, T. L., Fall, R., and Rosenstiel, T. N. (2011). Evidence of isoprenoid precursor toxicity in *Bacillus subtilis*. *Biosci. Biotechnol. Biochem.* 75, 2376–2383. doi: 10.1271/bbb.110572

Song, A. A., Abdullah, J. O., Abdullah, M. P., Shafee, N., Othman, R., Noor, N. M., et al. (2014). Engineering the lactococcal mevalonate pathway for increased sesquiterpene production. *FEMS Microbiol. Lett.* 355, 177–184. doi: 10.1111/1574-6968.12469

Szulc, P., Chapuy, M. C., Meunier, P. J., and Delmas, P. D. (1993). Serum undercarboxylated osteocalcin is a marker of the risk of hip fracture in elderly women. *J. Clin. Invest.* 91, 1769–1774. doi: 10.1172/JCI116387

Tsukamoto, Y., Kasai, M., and Kakuda, H. (2001). Construction of a *Bacillus subtilis* (natto) with high productivity of vitamin K2 (menaquinone-7) by analog resistance. *Biosci. Biotechnol. Biochem.* 65, 2007–2015. doi: 10.1271/bbb.65.2007

van de Guchte, M., van der Vossen, J. M., Kok, J., and Venema, G. (1989). Construction of a lactococcal expression vector: expression of hen egg white lysozyme in *Lactococcus lactis* subsp. *lactis*. *Appl Environ Microbiol* 55, 224–228. doi: 10.1128/AEM.55.1.224-228.1989

Vermeer, C., Raes, J., van 't Hoofd, C., Knapen, M. H. J., and Xanthoulea, S. (2018). Menaquinone content of cheese. *Nutrients* 10:446. doi: 10.3390/nu10040446

Vermeer, C. (2012). Vitamin K: the effect on health beyond coagulation - an overview. *Food Nutr. Res.* 56:5329. doi: 10.3402/fnr.v56i0.5329

Wegkamp, A., van Oorschot, W., de Vos, W. M., and Smid, E. J. (2007). Characterization of the role of para-aminobenzoic acid biosynthesis in folate production by *Lactococcus lactis*. *Appl. Environ. Microbiol.* 73, 2673–2681. doi: 10.1128/AEM.02174-06

Wegmann, U., O'Connell-Motherway, M., Zomer, A., Buist, G., Shearman, C., Canchaya, C., et al. (2007). Complete genome sequence of the prototype lactic acid bacterium *Lactococcus lactis* subsp. cremoris MG1363. *J. Bacteriol.* 189, 3256–3270. doi: 10.1128/JB.01768-06

Wen, L., Chen, J., Duan, L., and Li, S. (2018). Vitamin Kdependent proteins involved in bone and cardiovascular health (Review). *Mol. Med. Rep.* 18, 3–15. doi: 10.3892/mmr.2018.8940

Xu, J.-Z., Yan, W.-L., and Zhang, W.-G. (2017). Enhancing menaquinone-7 production in recombinant *Bacillus amyloliquefaciens* by metabolic pathway engineering. *RSC Adv.* 7, 28527–28534. doi: 10.1039/C7RA03388E

Yang, S., Cao, Y., Sun, L., Li, C., Lin, X., Cai, Z., et al. (2019). Modular pathway engineering of *Bacillus subtilis* to promote *de novo* biosynthesis of menaquinone-7. *ACS Synth. Biol.* 8, 70–81. doi: 10.1021/acssynbio.8b00258

Conflict of Interest: The authors declare that the research was conducted in the absence of any commercial or financial relationships that could be construed as a potential conflict of interest.

frontiers in Bioengineering and Biotechnology

ORIGINAL RESEARCH
published: 12 June 2020
doi: 10.3389/fbioe.2020.00506

Biotransformation of Selenium by Lactic Acid Bacteria: Formation of Seleno-Nanoparticles and Seleno-Amino Acids

Fernando Gabriel Martínez[1,2], *Gustavo Moreno-Martin*[2], *Micaela Pescuma*[1], *Yolanda Madrid-Albarrán*[2] *and Fernanda Mozzi*[1]*

[1] Centro de Referencia para Lactobacilos (CERELA-CONICET), Tucumán, Argentina, [2] Departamento de Química Analítica, Facultad de Ciencias Químicas, Universidad Complutense de Madrid, Madrid, España

Selenium (Se) is an essential micronutrient for the majority of living organisms, and it has been identified as selenocysteine in the active site of several selenoproteins such as glutathione peroxidase, thioredoxin reductase, and deiodinases. Se deficiency in humans is associated with viral infections, thyroid dysfunction, different types of cancer, and aging. In several European countries as well as in Argentina, Se intake is below the recommended dietary Intake (RDI). Some lactic acid bacteria (LAB) can accumulate and bio-transform selenite (toxic) into Se-nanoparticles (SeNPs) and Se-amino acids (non-toxic). The microbial growth, Se metabolite distribution, and the glutathione reductase (involved in selenite reduction) activity of Se-enriched LAB were studied in this work. The ninety-six assayed strains, belonging to the genera *Lactococcus*, *Weissella*, *Leuconostoc*, *Lactobacillus*, *Enterococcus*, and *Fructobacillus* could grow in the presence of 5 ppm sodium selenite. From the total, eight strains could remove more than 80% of the added Se from the culture medium. These bacteria accumulated intracellularly between 1.2 and 2.5 ppm of the added Se, from which *F. tropaeoli* CRL 2034 contained the highest intracellular amount. These strains produced only the seleno-amino acid SeCys as observed by LC-ICP-MS and confirmed by LC-ESI-MS/MS. The intracellular SeCys concentrations were between 0.015 and 0.880 ppm; *Lb. brevis* CRL 2051 (0.873 ppm), *Lb. plantarum* CRL 2030 (0.867 ppm), and *F. tropaeoli* CRL 2034 (0.625 ppm) were the strains that showed the highest concentrations. Glutathione reductase activity values were higher when the strains were grown in the presence of Se except for the *F. tropaeoli* CRL 2034 strain, which showed an opposite behavior. The cellular morphology of the strains was not affected by the presence of Se in the culture medium; interestingly, all the strains were able to form spherical SeNPs as determined by transmission electron microscopy (TEM). Only two *Enterococcus* strains produced the volatile Se compounds dimethyl-diselenide identified by GC-MS. Our results show that *Lb. brevis* CRL 2051, *Lb. plantarum* CRL 2030, and *F. tropaeoli* CRL 2034 could be used for the development of nutraceuticals or as starter cultures for the bio-enrichment of fermented fruit beverages with SeCys and SeNPs.

Keywords: lactic acid bacteria, selenium metabolism, probiotic, starter culture, selenocysteine, microbial cell factory, nutraceuticals

OPEN ACCESS

Edited by:
Jian-Ming Liu, Technical University of Denmark, Denmark

Reviewed by:
Gisele LaPointe, University of Guelph, Canada
Vijayalakshmi Kandasamy, Technical University of Denmark, Denmark

***Correspondence:**
Fernanda Mozzi
fmozzi@cerela.org.ar

Specialty section:
This article was submitted to Synthetic Biology, a section of the journal Frontiers in Bioengineering and Biotechnology

Received: *24 March 2020*
Accepted: *29 April 2020*
Published: *12 June 2020*

Citation:
Martínez FG, Moreno-Martin G, Pescuma M, Madrid-Albarrán Y and Mozzi F (2020) Biotransformation of Selenium by Lactic Acid Bacteria: Formation of Seleno-Nanoparticles and Seleno-Amino Acids. Front. Bioeng. Biotechnol. 8:506. doi: 10.3389/fbioe.2020.00506

INTRODUCTION

Selenium (Se) is a metalloid considered a vital micronutrient in the human diet. Se replaces sulfur in cysteine and is incorporated as selenocysteine (SeCys) in selenoproteins (Mounicou et al., 2006). The main selenoenzymes are glutathione peroxidase, iodothyronine deiodinase, and thioredoxin reductase, which are involved in antioxidant defense, detoxification, and thyroid functions (Palomo-Siguero and Madrid, 2017).

Se incorporation into the body is possible through food consumption; fish and vegetables are the main sources of Se. The amount of Se intake worldwide depends on the amount present in the soil of each country and the capacity of vegetables to accumulate Se, the type of crop grown and consumed, Se speciation, soil pH, organic matter content, etc. (Rayman, 2012). Although Se has been considered a toxic element before 1973, a narrow concentration difference between Se essentiality and toxicity exists, which is dependent on its speciation (Zhang et al., 2009). Se deficiency in humans is associated with hypothyroidism, cardiovascular disease, and immune system wickedness (Pedrero et al., 2006). In nature, Se is found as selenide (Se^{2-}), as elemental Se (Se^0), and as the soluble salts selenite (SeO_3^{2-}) and selenate (SeO_4^{2-}), which are the most toxic forms. Some bacteria can biotransform Se salts into the seleno-amino acids selenomethionine (SeMet) and SeCys; volatile Se compounds (diethylselenide, DESe; dimethylselenide, DMSe, and dimethyldiselenide, DMDSe); and seleno-nanoparticles (SeNPs) containing mainly Se^0 (Javed et al., 2015).

Lactic acid bacteria (LAB) inhabit a large diversity of niches such as dairy products, fermented foods, plants, soil, and the gastrointestinal and urogenital tracts, and oral cavities of humans and animals. LAB have acquired specific physiological and biochemical properties (i.e., proteolytic and lipolytic activities, tolerance to acidic conditions, etc.) to be able to survive in a wide variety of environments. These microorganisms are often suitable to be used as starter cultures for food fermentations and as probiotics for humans and animals due to their fermentative capacity, which contributes positively to food safety and the sensorial characteristics of the raw material in addition to their health-beneficial effects (Endo et al., 2018).

Some LAB can accumulate and biotransform Se salts into seleno-amino acids and SeNPs (Moreno-Martin et al., 2017; Pescuma et al., 2017); however, the metabolic pathways by which LAB bio-convert selenite remain unclear. It has been established that selenite may react with glutathione producing selenotrisulfide derivatives, which are intermediates in the conversion of inorganic Se into bioactive selenocompounds. In this reaction, reduced glutathione (GSH) is oxidized to Se diglutathione (GSSeSG) that in turn is reduced back to GSH by glutathione reductase (GR). Unstable GSSeSG is decomposed to form elemental Se [Se^0, (Ogasawara et al., 2005)] or used as substrate for selenophosphate synthetase. The enzyme GR is a flavoprotein disulfide oxidoreductase, which catalyzes NADPH-dependent reduction of glutathione and is involved in cell defense against oxidative stress by maintaining a high intracellular GSH/GSSG (glutathione disulfide) level (Jänsch et al., 2007). On the other hand, selenocysteine lyase (SCL) is able to decompose SeCys to Se^0 and to mobilize Se into SeCys for selenophosphate synthesis necessary for producing SeCys $_t$RNA, the precursor of SeCys and selenoproteins (Lamberti et al., 2011). Both GR and SCL have been detected in some LAB (Lamberti et al., 2011; Pusztahelyi et al., 2015); however, Se metabolism has been studied mainly in dairy- or human gut-origin strains (Zhang et al., 2009; Mangiapane et al., 2014; Palomo et al., 2014; Saini et al., 2014; Deng et al., 2015; Pescuma et al., 2017; Gomez-Gomez et al., 2019).

LAB are present in vegetables and fruits in a range between 10^2 and 10^4 cfu/g, and although they represent a small percentage of the total microbial population represented mainly by yeasts, a broad genera and species diversity has been found in these niches (Endo et al., 2009; Di Cagno et al., 2010; Ruiz Rodriguez et al., 2019). Fruits contain high carbohydrate concentrations and low pH and protein content; environmental conditions that these bacteria have adapted to by modifying their metabolism. Within different fruit-origin LAB, fructophilic bacteria constitute a unique group, which prefers fructose over glucose consumption due to their inability to regenerate NAD^+ through the conversion of acetaldehyde to ethanol; thus, pyruvate, fructose, or oxygen can be used as electron acceptors for NAD^+ regeneration (Endo et al., 2018). Since selenite produces an oxidant stress response in LAB, which are mostly micro-aerophilic, the elucidation of Se metabolism in fructophilic LAB (FLAB) becomes an interesting feature (Gomez-Gomez et al., 2019). In this work, we aimed to determine the capacity of fruit-origin LAB to grow in the presence of selenite and to biotransform Se into SeNPs and Se-amino acids. Moreover, the presence of genes related to Se metabolism and the activity of GR in the presence of this metalloid in LAB were analyzed.

MATERIALS AND METHODS

Bacterial Strains and Growth Media

Ninety-six LAB strains, belonging to the genera *Lactococcus*, *Weissella*, *Leuconostoc*, *Lactobacillus*, *Enterococcus,* and *Fructobacillus* and to twenty-one species were previously isolated from wild fruits and flowers from Northern Argentina (Ruiz Rodríguez et al., 2017; Ruiz Rodriguez et al., 2019). The cultures were stored at −20°C in MRS broth with 20% (v/v) glycerol. MRS was supplemented with 2% (w/v) fructose (MRSf) for fructophilic species (i.e., those belonging to the genus *Fructobacillus*). Before experiments, cells were transferred in fresh MRS/MRSf for LAB and FLAB, respectively, and cultured overnight (16 h) at 30°C.

Microbial Growth in the Presence of Se

Active cultures of the studied LAB strains previously grown in MRS or MRSf were inoculated at 2% (v/v) in MRS or MRSf supplemented or not (control) with 5 ppm of Se as Na_2SeO_3 (Sigma-Aldrich Chemical Co., MO, USA) and incubated at 30°C for 24 h. Microbial growth was determined by following the optical density at 600 nm (OD_{600}). Differences in OD_{600} at 8 and 24 h compared with initial OD were evaluated; in addition, maximum growth rates (μ_{max}) were calculated as: $\mu\mathbf{max} = \frac{\ln OD2 - \ln OD1}{t2 - t1}$.

TABLE 1 | Operating conditions for LC-ICP-MS.

Operating Conditions	
ICP-MS parameters for Se determination	
RF power (W)	1,550
Plasma gas flow rate (L/min)	15.0
Ar auxiliary flow rate (L/min)	0.30
Carrier gas flow rate (L/min)	0.75
Nebulizer	Slurry
Spray chamber	Scott
Acquisition mode	Continuous
Isotopes monitored	^{76}Se, ^{77}Se, ^{78}Se, ^{80}Se
Replicates	3
Reaction gas	H_2
Reaction gas flow rate (ml H_2/min)	6
AEX chromatographic parameters	
Column	Hamilton PRP-X100 (150 mm × 4.6 mm, 10 μm)
Mobile phases	Ammonium citrate 10 mM, 2% MeOH (pH 5.0)
Mode	Isocratic
Flow rate (ml/min)	1
Injection volume (μl)	100
RP chromatographic parameters	
Column	Kinetex EVO C18 (150 mm × 3.0 mm, 5 μm)
Mobile phases	0.1% Formic acid, 0.5% MeOH
Mode	Isocratic
Flow rate (ml/min)	0.5
Injection volume (μl)	20

To evaluate microbial colony phenotypes, strains were spread onto MRS or MRSf agar (MRS/MRSf with 2%, w/v, agar) with and without (control) 5 ppm Se. Plates were incubated at 30°C for 48 h and the color and shape of colonies were visualized.

Biotransformation of Sodium Selenite

The capability of the assayed LAB to reduce selenite was analyzed by growing the strains in 5 ml MRS or MRSf supplemented with 20 ppm Se, as Na_2SeO_3 at 30°C for 24 h. Grown cultures were centrifuged at 5,600 × *g* for 5 min and the remaining SeO_3^{2-} concentration in the supernatants was determined spectrophotometrically by the modified method of Brown and Watkinson (Kessi et al., 1999) using a microplate assay. Briefly, 160 μl of 0.5 M HCl, 80 μl of 0.1 M EDTA, 40 μl of 0.1 M NaF, and 40 μl of 0.1 M dipotassium oxalate were mixed in a 1.5-ml microtube. Then, 500 μl of each culture supernatant and 200 μl of 0.1% 2,3-diaminonaphthalene in 0.1 M HCl were added. After mixing, the microtubes were incubated at 40°C for 40 min and then cooled in ice bath. A volume of 500 μl of cyclohexane was utilized for extracting the Se-2,3-diaminonaphthalene complex by shaking the microtubes placed horizontally in an orbital shaker for 10 min at 850 × g. Then, samples were centrifuged at 3000 × g for 10 min. Aliquots of 150 μl of the organic phase were placed in a 96-well microplate and the absorbance at 377 nm was determined with a Versamax Microplate reader (Molecular Devices, CA, USA). The whole reaction procedure was done in the dark. Calibration curves were obtained by adding 0, 2.5, 5.0, 10, 20, and 30 ppm Se in MRS broth. All measurements were done in triplicate.

Intracellular Se Accumulation as Determined by Inductively Coupled Plasma Mass Spectrometry (ICP-MS)

Cells were grown in MRS or MRSf at 30°C for 24 h in the absence or presence of 5 ppm Se and then centrifuged at 4,600 × g for 5 min. For this purpose, supernatants and bacterial cell pellets (0.1 g obtained from 10 ml culture) were submitted to acid digestion in a 1000-W microwave oven (MSP microwave oven, CEM, Matthews, NC, USA) using closed vessels containing 1 ml of concentrated HNO_3 and 0.5 ml of 30% (v/v) H_2O_2 (Pescuma et al., 2017). The resulting solutions were cooled, diluted to a 25-ml final volume with MilliQ water and analyzed for the Se concentration with an Agilent 7700-collision/reaction cell ICP-MS (Agilent Technologies, Santa Clara, CA, USA). Hydrogen gas was employed as collision gas for Se determination. Optimal operating conditions are included in **Table 1**. A control group of each bacterial species unexposed to Se was performed in parallel. Three independent replicates were made; the reaction mixture without the addition of cell pellets was used as a blank and considered in the final results.

Selenium Species Determination by Liquid Chromatography-ICP-MS (LC-ICP-MS)

Selenium species were determined in enzymatically hydrolyzed bacterial cell pellets previously grown in 5 ppm Se MRS/MRSf by LC-ICP-MS (Pescuma et al., 2017). Cell pellets (0.1 g obtained from 10 ml culture) were mixed with 600 μl of 10 mg/ml lysozyme (Sigma-Aldrich Chemical Co.) in Tris–HCl buffer, pH 7.0, and incubated at 37°C for 3 h. Then, cell suspensions were sonicated with an ultrasonic probe (Sonoplus ultrasonic homogenizer, Bandenlin, Berlin, Germany) using 6 cycles of 50 s at 60% of ultrasound amplitude. Afterwards, 400 μl of 2 mg/ml protease type XIV (Sigma-Aldrich Chemical Co.) in Tris–HCl buffer was added and incubated overnight at 37°C. Finally, mixtures were centrifuged at 7,000 × g for 15 min and the supernatants were collected, filtered through 0.22 μm nylon membrane filters, and analyzed by LC-ICP-MS by using an anion exchange column (Hamilton PRP-X100, 250 × 4.1 mm, 10 μm) following the experimental conditions given in **Table 1**. The following five Se species: the seleno-amino acids, selenomethionine (SeMet), selenomethylcysteine (SeMetCys), and selenocystine ($SeCys_2$), as well as two inorganic salts, sodium selenite (Na_2SeO_3) and sodium selenate (Na_2SeO_4), were analyzed in this study. Identification of Se species was carried out by matching retention times and by spiking experiments. A calibration curve was performed for each standard species. Three independent replicates were made for each sample; the enzymatic mixture without the addition of bacterial cell pellets was used as a blank and considered in the final results.

Confirmation of the SeCys Species by LC-Tandem Mass Spectrometry (LC-ESI-MS/MS)

Carbamidomethylation was used for preserving SeCys integrity according to Palomo-Siguero et al. (2016) with slight modifications. The procedure was applied before enzymatic digestion. *F. tropaeoli* CRL 2034 was grown in MRSf with 5 ppm Se at 30°C for 24 h and then the culture was centrifuged at 4600 × g for 5 min. Pellets were washed twice with MilliQ water and suspended in 1 ml of 0.1 M Tris–HCl buffer, pH 7.5. A reduction of S–S, Se–S, and Se–Se bridges of the proteins was performed by incubating at 37°C with 60 μl of 0.2 M dithiothreitol (DTT) in the dark followed by alkylation with 100 μl of 0.5 M iodoacetamide in the same conditions for 1.5 h in each step. To remove the excess of iodoacetamide, 400 μl of DTT was added and shaken at 200 × g for 1 h. After carbamidomethylation, samples were submitted to enzymatic digestion as described above. The extracts were centrifuged at 7,000 × *g* for 15 min; supernatants were filtered using 0.22-μm nylon membrane filters and stored at −80°C until analysis. To evaluate the correct formation of carbamidomethyl-SeCys (CAM-SeCys), Se species were analyzed by LC-ICP-MS using a Phenomenex Kinetex EVO C18 column following the experimental conditions given in **Table 1**. Confirmation of CAM-SeCys was done with LC-ESI-MS/MS using the same reversed-phase chromatographic column and conditions as for LC-ICP-MS. Analyses were carried out with a Shimadzu LC-MS-8030 triple quadrupole system (Shimadzu Scientific Instrument, Columbia, MD, USA) supplied with a Nexera LC-30AD solvent delivery unit, a Nexera SIL 30AC autosampler with a temperature-controlled tray, and a CTO- 20AC column oven. The equipment was operated in positive electrospray ionization (ESI) mode. Nitrogen was used as nebulizing (1.5 $L \cdot min^{-1}$) and drying (15.0 $L \cdot min^{-1}$) gas. Collision-induced dissociation was done using argon as collision gas at a pressure of 230 kPa in the collision cell with a collision energy voltage of 25 eV. Ionization voltage for ESI was set at 4.5 kV; the interface current was fixed at 4.4 μA, and the detector voltage was fixed at 2.10 kV. Due to lack of standard for CAM-SeCys species, a bibliographical search was made with the aim of selecting the most common transitions. As precursor ion $[M + H]^+$, was selected and the detection was carried out in multiple reaction monitoring (MRM) mode, with a dwell time of 100 ms, by monitoring three or four selective transitions for each species.

Extraction and Determination of Volatile Se Compounds by HS-SPME-GC-MS

The volatile Se compound production by eight selected strains was evaluated following the method described by Moreno-Martin et al. (2019). Cells were cultured in 50 ml of MRS or MRSf supplemented with 5 ppm Se at 30°C for 24 h in 250-ml Erlenmeyer flasks sealed with a silicone septum. The analytical procedure for volatile Se compound determination consisted of two steps: extraction by headspace solid-phase microextraction (HS-SPME) followed by separation and analysis by gas chromatography coupled to mass spectrometry (GC-MS). In the extraction step, a 75-μm fiber coated with Carboxen/PDMS (Supelco, Bellefonte, PA, USA) was inserted into each Erlenmeyer flask through the septum and placed statically in an incubator at 30°C. Analyte extraction was carried out in the headspace for 26 min. Immediately after the extraction, separation and analysis of the resulting extracts were performed in an Agilent 7890A/5975C GC-MS (Agilent Technologies S.A., Madrid, Spain) instrument. High-purity helium (>99.999%) was used as carrier gas at a flow rate of 0.5 ml/min. A 0.75 mm ID SPME Inlet Liner (Supelco, Bellefonte, PA, USA) was used with splitless mode injections. The inlet temperature was set at 300°C and desorption was done at a purge flow of 60 ml/min for 0.25 min, and the septum purge flow was 3 ml/min. A polydimethylsiloxane (95%) cross-linked ZB5MS (Zebron, Phenomenex, Madrid, Spain) capillary column was used (30 m × 0.25 mm ID, 0.25 μm d_f); the oven temperature program was as follows: from 40°C (3 min) to 180°C (5 min) at 10°C/min and from 180°C to 200°C (1 min) at 30°C/min. The mass spectrometer conditions were as follow: 150°C of quadrupole temperature, 280°C of transfer line temperature, and 230°C of ion source temperature. SCAN mode with an acquisition range of 25–300 m/z was selected for the identification of the Se volatile compounds based on the retention times as well as the fragmentations of standard solutions. Three volatile Se compounds were analyzed: dimethyl selenide (DMSe), dimethyl diselenide (DMDSe), and diethyl selenide (DESe) (Sigma-Aldrich Chemical Co.). These compounds were dissolved in H_2O:MeOH (50:50, v/v) with pure water (18 MΩ/cm) from a Milli-Q system (Millipore, Bedford, MA, USA) and MeOH (HPLC grade, Scharlab, Barcelona, Spain). The following fragments, referred to the mass to charge ratio (m/z), were selected in SIM mode for the identification of volatile Se compounds: m/z 80, 95 and 110 for DMSe, m/z 80, 95, 110 and 138 for DESe, and m/z 95, 160, 175, and 190 for DMDSe. Data were acquired using MSD ChemStation software and analyzed in an MSD ChemStation Data Analysis Application (Agilent Technologies S.A., Madrid, Spain). Identification of Se volatile compounds was done based on the 2011 NIST library and supported by corrected retention times and fragmentation standard (Moreno-Martin et al., 2019).

GR Activity

Strains were grown in MRS/MRSf in the absence or presence of 5 ppm Se at 30°C for 24 h; cells were harvested by centrifugation and washed with 0.1 M sodium phosphate buffer (pH 7.5) with 1 mM EDTA. Then, microbial cells were mixed with the same buffer and glass beads (150–212 μm diameter; Sigma-Aldrich Chemical Co.) in a 1:2:1 ratio (cells:buffer:glass beads, w/v/w). Cells were lysed by mechanical beating after loading the vials in a Mini-Bead Beater-8 cellular disruptor (Biospec Products Inc., Bartlesville, OK, USA) with intermittent cooling on ice-bath (6 cycles of 1.5 min). The cell debris were removed by centrifugation and lysates were used for GR activity assay (Pophaly et al., 2017). The assay depends upon the transformation of GSSG to GSH with concomitant oxidation of 5,5′-Dithiobis(2-nitrobenzoic acid) (DTNB, Sigma-Aldrich Chemical Co.) to a colored compound. Briefly, the reaction

mixture contained 150 μl of 0.6 mg/ml DTNB, 10 μl of 10 mg/ml NADPH (Sigma-Aldrich Chemical Co.), and 20 μl of cell-free extract. The reaction was initiated by adding 10 μl of 1 mg/ml GSSG (Sigma-Aldrich Chemical Co.). All solutions were made in 0.1 M sodium phosphate buffer (pH 7.5) with 1 mM EDTA. Absorbance was monitored at 405 nm over a period of 4 min in a 15-s time interval in a microplate reader (Versamax, Molecular Devices, USA).

Genes Involved in Se Metabolism

PCR assay was used to investigate the presence of genes involved in Se metabolism. Genes coding for GR (*GshR*/*gor*) and selenocysteine lyase (*Scl*) were sought in the genome of eight strains in this work. Genomic DNA was extracted from selected strains according to Ruiz Rodriguez et al. (2019). Five milliliters of stationary phase cultures were centrifuged at 7000 × *g* for 5 min. Cells were washed with 500 μl of TE buffer [10 mM Tris–HCl (pH 7.5), 10 mM EDTA] and resuspended in 1.7 ml of lysozyme (15 mg/ml) and dissolved in SET buffer [20 mM Tris–HCl (pH 7.5), 25 mM EDTA, 75 mM NaCl]. After holding at 37°C for 2 h, 170 μl of 10% (w/v) sodium dodecyl sulfate (SDS) and 50 μl of proteinase K (15 mg/ml) were added, and the mixture was incubated at 55°C for 2 h. Then, 700 μl of 5 M NaCl and 2.7 ml of chloroform:isoamyl alcohol (24:1) were added to the mixture, maintaining it at room temperature for 30 min. After centrifugation at 11,200 × *g* for 10 min, the aqueous phase was transferred to another tube, and the DNA was precipitated with 2.5 ml of isopropanol. The precipitate was washed with 1 ml of 70% (v/v) ethanol and centrifuged for 10 min at 11,200 × *g*. DNA was dried by evaporating the alcohol and then resuspended in 30 μl of MilliQ water. DNA concentration and purity were spectrophotometrically determined by measuring the OD at 260 and 280 nm and determining the OD_{260}/OD_{280} ratio (Brown, 1995).

The PCR assay mixture (25 μl) consisted of 5 μl of 5× Green GoTaq® Reaction Buffer (Promega, Madison, WI, USA), 1 μl of a mixture of dNTPs (dATP, dTTP, dCTP, and dGTP, 5 mM), 0.2 μl of 5 U/μl GoTaq® DNA Polymerase (Promega), 2.5 μl of 10 μM each primer, 9.8 μl of nuclease-free water, and 4 μl of the purified chromosomal DNA (50 ng/μl) as template. Primers were designed by searching each gene sequence for the corresponding bacterial species in the National Center for Biotechnology Information (NCBI) nucleotide database; the sequences found were aligned and compared, and the conserved region of the gene sequences were used to design the primers. PCR amplifications were performed with a My Cycler™ thermal cycler (Bio-Rad Laboratories, Inc., Hercules, CA, USA) using the following program: 94°C for 4 min, 30 cycles of 94°C for 30 s, accurate annealing temperature for 30 s, and 72°C for 45 s, and a final extension step at 72°C for 5 min. Primers and their corresponding melting temperatures used in this work are listed in **Table 2**. PCR products were electrophoresed in a 0.8% (w/v) agarose gel at 80 V for 45 min in 1× TAE buffer and then, were visualized after staining with GelRed™ Nucleic Acid Gel Stain (Biotium, Hayward, CA, USA) under a UV trans-illuminator and digital image documentation using a CCD camera (ChemiDoc™ XRS+ System, Bio-Rad Laboratories, Inc., CA, USA), and images were recorded using Image Lab™ Software. The size of DNA fragments was estimated using a standard 1-kb DNA ladder (1Kb Plus DNA Ladder, Invitrogen™, Carlsbad, CA, USA). Amplicons were purified by polyethylene glycol precipitation (protocol available at http://gator.biol.sc.edu/; http://labs.mcdb.lsa.umich.edu/labs/olsen/files/PCR.pdf). Nucleotide sequences of purified PCR products were determined at the CERELA sequencing facility with an ABI 3130 DNA sequencer (Applied Biosystems, Foster, CA, USA).

Detection of Se Nanoparticles by Transmission Electron Microscopy

The presence, composition, and size of Se nanoparticles (SeNPs) were assessed by TEM. The studied strains were grown in MRS or MRSf supplemented with 5 ppm Se at 30°C for 24 h. Samples were prepared by placing a drop of culture onto a 300-mesh lacey carbon copper TEM grids. The film on the TEM grids was allowed to dry for 5 min at room temperature before analysis. Transmission electron micrographs were recorded using a high-resolution transmission electron microscope (JEM-2100, JEOL USA, CA, USA) equipped with an X-ray energy dispersive spectroscopy (XEDS) microanalysis composition system (Oxford Inc.). Analysis of SeNP composition was carried out by XEDS microanalysis (Dhanjal and Cameotra, 2010). The diameter of SeNPs ($n = 100$) was measured from the obtained images by using the free image-processing software, ImageJ (version 1.52a, Java 1.8.0_112, Wayne Rasband, National Institutes of Health, USA; website: https://imagej.nih.gov/ij/).

Visualization of LAB Cells and SeNPs by Scanning Electron Microscopy

The cell morphology of *Lactobacillus brevis* CRL 2051, *Lb. plantarum* CRL 2030, and *Fructobacillus tropaeoli* CRL 2034 (which accumulated the highest amounts of SeCys) and the formation of SeNPs by these strains were visualized by scanning electron microscopy (SEM) with a Zeiss Supra 55VP instrument (Oberkochen, Germany) in the CISME-CCT-CONICET electron microscopy facility, San Miguel de Tucumán, Argentina. For this purpose, LAB strains were grown in MRS or MRSf with 5 ppm Se at 30°C for 24 h, centrifuged, and washed three times with saline solution. Fixation was done by suspending the cells with 4% (v/v) glutaraldehyde solution, and then suspensions were layered onto solid agar-coated SEM coverslips. Fixed cells were dehydrated through a series of alcohol dehydration steps (30, 50, 70, 90, and 100%). Finally, the samples were coated with gold and visualized under SEM.

Statistics

Assays were carried out in triplicate and results were expressed as the mean ± SD. TEM and SEM images were selected from independent assays for each strain. One-way analysis of variance (ANOVA) and Tukey's post comparison test using MINITAB 16 Statistical Software (Minitab, State College, PA, USA) was applied for statistical analysis.

TABLE 2 | Primer sequences for genes coding for glutathione reductase and selenocysteine lyase genes.

	Name	Sequence (5′ → 3′)	Annealing temperature	Amplicon length (bp)
Glutathione reductase	GRL-FW	GGGAGGAACTTGTCCAAACTAT	50	663
	GRL-RV	CCTACTCCCGCAATCACTAAAT		
	GRW-FW	CAACAAGCCAGCCACATAAC	50	673
	GRW-RV	CTTGGACGATGCGGGTATTA		
	GRW2-FW	CTCAATGGCTGGCAACAAAG	50	819
	GRW2-RV	ACGATACCAGGTGCAGATTTAG		
	GRE-FW	GCGAGGCGTAGAAGTCAAA	50	575
	GRE-RV	ATGCTTGTGTCTGGATCGTATAG		
	GRP-FW	AATGACGGCTGATGGGATTAC	50	324
	GRP-RV	GTCAACTCACCGACCAGATAAC		
	GRF-FW	CCAAGAACATGGCCCGTAAA	50	776
	GRF-RV	TGTGGTACCGATAGCTGGATAG		
Selenocysteine lyase	LyaseL-FW	ACAAGACAACAGGAGCAGTATC	50	486
	LyaseL-RV	ACGGTGTCGCAAAGGTATTAT		
	LyaseW-FW	GGATAGAGACACCGTCAAACC	50	453
	LyaseW-RV	CCTCCGCTAAGTAGAACGAAAT		
	LyaseE-FW	CAGCTATCATGAGGCCCTAATAC	50	602
	LyaseE-RV	CTTGGTCAGCCAAAGCAATATG		
	LyaseB-FW	CTTGGCAAACCCACGATAGA	40	678
	LyaseB-RV	GTACAACCCTTGGCTGAAATTG		
	LyaseF-FW	TGAACACCCGCTAGGTTAAAG	50	454
	LyaseF-RV	GGGCAACGGTTATTGTTGATG		

GR, glutathione reductase; Lyase, selenocysteine lyase; -FW, forward; -RV, reverse; L, Lactococcus; W, Weissella; E, Enterococcus; P, Lb. plantarum; F, Fructobacillus; B, Lb. brevis.

RESULTS

Microbial Growth in the Presence of Se

We studied the growth behavior of ninety-six fruit- and flower-origin LAB strains belonging to 6 genera and 21 different species in MRS or MRSf (for FLAB) in the absence or the presence of 5 ppm Se. All strains were able to grow in the presence of Se at the evaluated concentration although different growth behaviors were noticed depending on the assayed strains (**Table S1**). The presence of Se did not significantly affect the growth of 41 strains, which included those belonging to the species *Weissella minor* (9), *Leuc. pseudomesenteroides* (18 out of 28), and *F. tropaeoli* (6). In general, all fructobacilli strains, including the four studied species, showed the highest cell growth rates in the presence of Se, while the highest cell growth values after 24 h corresponded to both the fructobacilli and the majority of the *Leuc. pseudomesenteroides* strains. From the total, the growth parameters of only 10 strains were significantly affected in the presence of Se, among which the four *Ec. hirae* strains were included. The most negatively affected strains by Se were *Lc. lactis* subsp. *lactis* CRL 2009, *Leuc. mesenteroides* CRL 2059, *Leuc. pseudomesenteroides* CRL 1997, and *Lb. rhamnosus* CRL 2031, which showed a deleterious effect (more than 50% alteration) in at least one of the growth parameters evaluated.

LAB colonies showed their typical translucent white color in MRS and MRSf agar, while in the presence of 5 ppm Se, all the evaluated strains showed a reddish color indicating their ability to reduce the colorless Na_2SeO_3 salt to elementary Se (Se^0, orange-reddish); examples of reddish colonies are shown in **Figure S1**. Colonies changed from white to red color after 24 h of incubation, increasing the intensity of the reddish color over time. After 48 h of incubation, no color change was further observed.

Biotransformation of Sodium Selenite

To evaluate the ability of the assayed 96 LAB strains to biotransform and intracellularly accumulate Se, the remaining selenite concentration in 24-h culture supernatants was determined spectrophotometrically. The ability of the strains to remove Se from the culture medium was variable (between 8 and 100% of the added selenite) and strain- and species-dependent (**Table 3**). The species *Lc. lactis*, *W. cibaria*, *Ec. casseliflavus*, and *F. tropaeoli* removed the greater Se amounts (>70%) from the culture medium compared to the other species within each genus. Interestingly, while several strains of *Ec. casseliflavus* showed 100% Se removal, the strains of *Ec. durans* and *Ec. faecium* showed an opposite behavior by scarcely removing Se in amounts lower than 27%. Regarding the *Leuconostoc* genus, all species removed low to moderate amounts (between 14 and 71%). In general, the *Lactobacillus* strains removed low amounts (<45%) of selenite from the culture medium, except for *Lb. brevis* CRL 2051 and *Lb. plantarum* CRL 2030, which removed both more than 95% of the added Se.

TABLE 3 | Percentage of selenite removal from the culture medium by the studied LAB strains.

Bacterial strains		Percentage removal of selenite by each strain				
Lactococcus	*lactis subsp. lactis*	76 ± 11	93 ± 1	104 ± 5		
	lactis subsp. cremoris	81 ± 5				
	lactis	34 ± 1				
Weissella	*cibaria*	85 ± 4	84 ± 8	74 ± 4	84 ± 3	
	fabalis	57 ± 1				
	minor	31 ± 4	24 ± 3	15 ± 2	24 ± 3	28 ± 4
		23 ± 2	49 ± 3	22 ± 3	30 ± 4	
Leuconostoc	*mesenteroides subsp. mesenteroides*	39 ± 2	56 ± 6	28 ± 4	46 ± 2	43 ± 2
	mesenteroides	37 ± 4	42 ± 3	28 ± 4	28 ± 4	30 ± 2
	pseudomesenteroides	42 ± 6	43 ± 2	40 ± 6	32 ± 4	39 ± 6
		46 ± 3	54 ± 5	57 ± 8	28 ± 2	38 ± 1
		46 ± 3	19 ± 2	50 ± 4	42 ± 3	52 ± 2
		45 ± 3	44 ± 3	49 ± 2	14 ± 2	58 ± 2
		52 ± 2	44 ± 4	64 ± 2	71 ± 11	43 ± 2
		60 ± 8	49 ± 3	68 ± 10		
	citreum	62 ± 3	59 ± 5			
Lactobacillus	*brevis*	37 ± 5	95 ± 3	33 ± 5	46 ± 1	43 ± 3
		40 ± 3	43 ± 2			
	plantarum	98 ± 6				
	rhamnosus	24 ± 3	26 ± 4			
Enterococcus	*casseliflavus*	102 ± 4	101 ± 1	101 ± 1	100 ± 1	104 ± 2
		58 ± 2	84 ± 3	101 ± 4		
	faecalis	86 ± 13				
	hirae	62 ± 4	72 ± 4	47 ± 4	47 ± 7	
	mundtii	39 ± 2				
	faecium	22 ± 3	27 ± 4	26 ± 3		
	durans	8 ± 1				
Fructobacillus	*durionis*	41 ± 3				
	fructosus	52 ± 6				
	pseudoficulneus	57 ± 3				
	tropaeoli	75 ± 6	71 ± 3	79 ± 4	63 ± 2	80 ± 4
		3 ± 2				

Each value corresponds to a different strain. Results are mean values with standard deviations. Color scale represents different values, red meaning higher and green lower ones.

Intracellular Se Accumulation as Determined by ICP-MS

From the total assayed LAB, eight strains, namely, *Lc. lactis* CRL 2011, *W. cibaria* 10 and 25, *Ec. casseliflavus* 47 and 82, *Lb. brevis* CRL 2051, *Lb. plantarum* CRL 2030, and *F. tropaeoli* CRL 2034, were selected for further experiments due to their capacity to grow in the presence of Se and to reduce more than 80% of the added selenite in the culture medium. The strains grew similarly (8.5–9.1 log CFU/ml) and could intracellularly accumulate between 1.2 and 2.5 ppm Se (red bars, **Figure 1**) after 24-h incubation as revealed by ICP-MS. Considering the cell pellet weights, the assayed strains accumulated between 126 and 580 μg Se/g cell; the highest amount corresponded to *F. tropaeoli* CRL 2034 while the lowest corresponded to *Lb. brevis* CRL 2051. The remaining Se content in the cell-free supernatants was greater in samples of *Lb. plantarum* CRL 2030 and *W. cibaria* 25. Whereas, the two enterococci samples showed similar values, those of the two *W. cibaria* strains showed a strain-dependent behavior.

Determination of Se Species in Cell Pellets of LAB Strains by LC-ICP-MS

Selenium species in the enzymatic extracts were determined by LC-ICP-MS using a PRP-X100 anion exchange column. Identification of Se species was done by comparing the retention times and spiking experiments with Se standard species (**Figure 2A**); Se species concentration was calculated with the obtained calibration curve performed for each standard species. For all the assayed strains, $SeCys_2$ was detected at 2.4 min as the main Se species with concentration values between 0.01 and 0.87 ppm (**Figure 2B**). Traces of selenite (Se IV) from the culture medium were also detected at 3.3 min in the majority of the cell pellets, although in very low concentrations (<0.05 ppm). Only for the strain *Ec. casseliflavus* 82, selenite

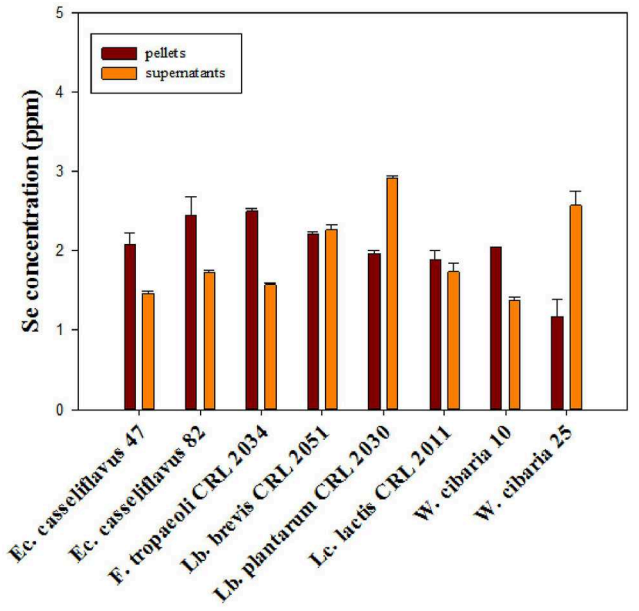

FIGURE 1 | Total Se content in cell pellets and supernatants of selected LAB strains grown in MRS and MRSf with sodium selenite at 30°C for 24 h, as revealed by ICP-MS.

was not detected. *Lb. brevis* CRL 2051, *Lb. plantarum* CRL 2030, and *F. tropaeoli* CRL 2034 accumulated the highest intracellular $SeCys_2$ values (39, 44, and 25%, respectively), highlighting the ability of these strains to incorporate Se as $SeCys_2$. Similar $SeCys_2$ concentrations were observed for the enterococci while different values were noticed for the *Weissella* strains.

Confirmation of the Presence of SeCys Species as Revealed by LC-ESI-MS/MS

To corroborate that the detected Se species $SeCys_2$ by LC-ICP-MS effectively corresponded to SeCys, carbamidomethylation of this compound (CAM-SeCys) was done using the cell pellet of the strain *F. tropaeoli* CRL 2034. Comparison of CAM-SeCys retention time to that of the carbamidomethylated standard was carried out using a reversed-phase C_{18} column coupled to ICP-MS since its mobile phase is compatible with the LC-ESI-MS/MS analysis used for identifying CAM-SeCys. Only one intense peak at 4.9 min corresponding to CAM-SeCys (**Figure 3A**) was observed. Further, CAM-SeCys was confirmed by comparing the fragmentation ions of the sample obtained by LC-MS/MS (**Figure 3B**) with those theoretical ion fragments reported for CAM-SeCys by Dernovics and Lobinski (2008). All theoretical peaks corresponding to CAM-SeCys were detected in the sample and listed in **Table 4**; confirming that the peak obtained at 4.9 min corresponded to the presence of CAM-SeCys (and consequently confirming SeCys as the major Se species found in Se-treated bacteria).

Production of Volatile Se Compounds by LAB Strains

Identification of volatile Se species produced by selected LAB strains grown in presence of selenite was determined by HS-SPME-GC-MS. Only the two enterococci strains produced volatile Se compounds; DMDSe and DMSe were formed by *Ec. casseliflavus* 47 and 82, respectively, albeit at very scarce amounts, which were under the limit of quantification (LOQ) of the technique. These volatile Se compounds were identified based on retention times and m/z ratios by comparing them with their respective standards. It should be noted that, for these compounds, two out of three fragments were found. The production of DMSe (2.64 min) could be identified by the increase in the signal in m/z 110 and 95 fragment ions, while no signal was found at this time for the ionic fragment m/z 80, whereas for DMDSe (7.90 min), m/z 160 was not found in the chromatograms while a slight signal was detected for fragments m/z 190 and 175 (**Figure 4**). The presence of the species DESe was not detected in anyone of the assayed strains.

GR Activity

GR activity was determined in the eight selected LAB strains; the GR activity values were higher (between 7 and 14 U/g protein) in the absence of Se for the *Enterococcus* strains. In general, a two-fold increase in the presence of Se was detected except for *Ec. casseliflavus* 47, which showed a six-fold increase (from 7 to 45 U/g protein) compared to non-selenized cells (**Figure 5**). An opposite behavior was observed for *F. tropaeoli* CRL 2034 as a three-fold higher GR activity was detected in the absence of Se than when cells were selenized.

Detection of Genes Involved in Se Metabolism

In this work, the presence of two important genes involved in Se metabolism was studied by PCR reactions, i.e., genes coding for GR, *GshR*/*gor* and for selenocysteine lyase, *Scl*. Primers used are listed in **Table 2**. Amplification fragments for *GshR*/*gor* were detected in all studied strains (**Figure 6**). Two different *GshR*/*gor* bands of 673 and 819 bp were detected for the *W. cibaria* species, which were amplified by using different primers (GRW and GRW2). The *Scl* genes coding for the enzyme SCL were detected in all strains (amplicon length from 453 to 678 bp), except for the two studied *Lactobacillus* (**Figure 6**), which were not amplified with the primers used (LyaseB). In all cases, the identity of the obtained PCR amplicons was further confirmed by sequence analysis. The size of DNA fragments was estimated using a standard 1-kb DNA ladder and was accurate with the expected length of the amplicons (**Table 2**).

Detection of SeNPs by TEM

The eight studied strains formed spherical SeNPs (indicated with arrows) when grown in MRS/MRSf with 5 ppm Se (**Figure 7A**). Additionally, XEDS elementary microanalysis confirmed the presence of Se [Lα (1.4 keV), Kα (11.22 keV), and Kβ (12.49 keV)] in the visualized nanoparticles (**Figure 7B**). The crystalline nature of SeNPs was evidenced in the images (**Figure 7C**), which showed typical electron diffraction patterns for microcrystalline

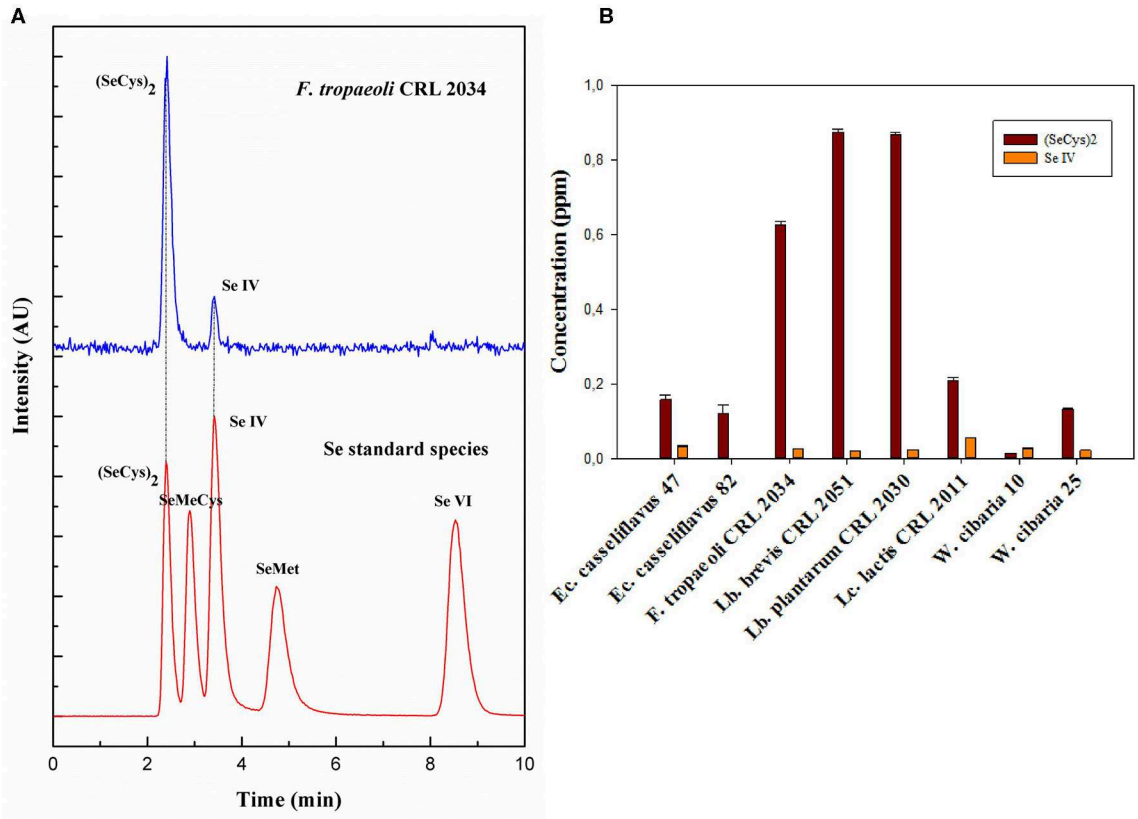

FIGURE 2 | Se species in enzymatically hydrolyzed LAB cell pellets. **(A)** Anion exchange ICP-MS chromatograms of standard Se species, and Se species formed by *F. tropaeoli* CRL 2034 (as example) are represented in red and blue, respectively. **(B)** Se species concentration for the assayed LAB. AU, arbitrary units.

structures. The size distribution of the SeNPs was strain-dependent (**Figure 7D**). Interestingly, the two enterococci strains showed different nanoparticle sizes, whereas the size of the SeNPs of the two *W. cibaria* strains was similar. *Lc. lactis* CRL 2011 and *Ec. casseliflavus* 47 produced SeNPs with the largest diameters (125–155 nm and 110–140 nm, respectively), while the size of SeNPs of the remaining strains was between 50 and 90 nm.

Visualization of LAB Cells and SeNPs by SEM

The effect of the presence of Se on cell morphology of the three strains that showed the highest SeCys concentrations (namely, *Lb. brevis* CRL 2051, *Lb. plantarum* CRL 2030, and *F. tropaeoli* CRL 2034) was analyzed by SEM. Neither detrimental effects on the bacterial shapes nor alterations in the cell surface were observed (**Figure 8**). Interestingly, the formation of SeNPs as white spheres in selenized cells was clearly noticed in the three assayed LAB.

DISCUSSION

Selenium is an essential trace element for human health with a recommended daily intake (RDI) of 25 to 34 μg for adults depending on age and gender according to Argentinean Food Codex (ANMAT, 2018), which is based on values established by the World Health Organization (FAO/WHO, 2004). Furthermore, it has been stated that higher Se intakes (up to 200 μg per day) can have a positive effect against free radicals, which cause age-related diseases and cancer (Alzate et al., 2010). Health benefits of Se depend on the species consumed; organic Se compounds are the least toxic and most bio-available forms for human body (Alzate et al., 2010; Palomo et al., 2014).

LAB are commonly used in the food industry worldwide due to their capacity to improve the food safety, nutritional value, flavor, and texture of fermented food products (Hugenholtz et al., 2002). In addition, functional LAB are able to increase the bioavailability of nutrients and to reduce toxic components and anti-nutritive factors present in raw materials (Tamang et al., 2016). Interestingly, some LAB can transform inorganic Se into seleno-amino acids (i.e., SeMet, SeCys, and SeMeCys), SeNPs, and/or volatile Se compounds (Pophaly et al., 2014; Javed et al., 2015; Moreno-Martin et al., 2017; Pescuma et al., 2017). Se-enrichment of bacterial cells with non-toxic Se forms could be an interesting alternative for formulating Se dietary supplements or Se enriched-containing foods.

In this work, we exhaustively studied the Se metabolism by ninety-six fruit- and flower-origin LAB strains. The bacterial capacity to grow in the presence of 5 ppm Se

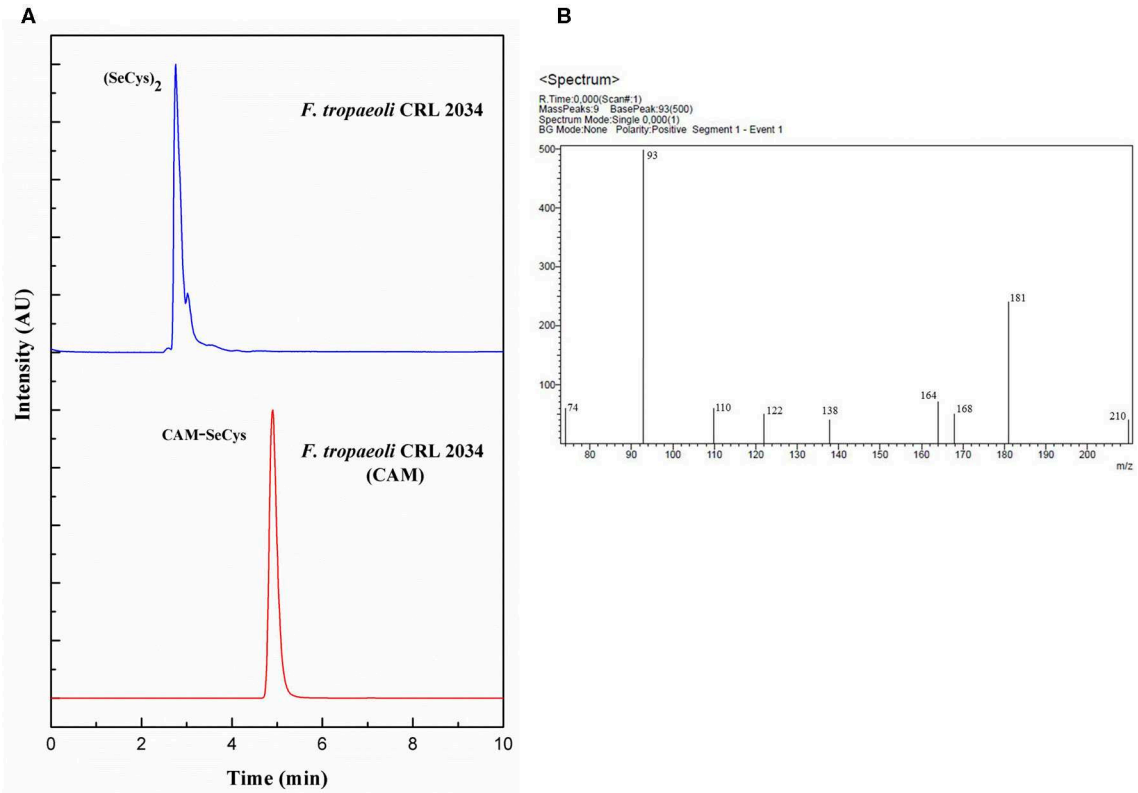

FIGURE 3 | Detection of CAM-SeCys in the cell pellet of *F. tropaeoli* CRL 2034: **(A)** Chromatograms obtained from reversed-phase column coupled to ICP-MS, *F. tropaeoli* CRL 2034 with and without applying the carbamidomethylation procedure are represented in red and blue, respectively; **(B)** Fragmentation of CAM-SeCys by LC-ESI-MS/MS. AU, arbitrary units; CAM, carbamidomethylated.

TABLE 4 | Description of the proposed fragment ions formed during the fragmentation of cabamidomethyl-SeCys, *m/z* 226.9 ($[M + H]^+$).

No.	Elemental composition	Theoretical mass/Th[a]	Measured mass/Th[a]	Notes on losses and fragments
1	$C_5H_8NO_3Se^+$	209.9664	209.9	NH_3
2	$C_4H_9N_2OSe^+$	180.9875	180.9	Formic acid
3	$C_3H_6NO_2Se^+$	167.9564	167.9	Alkylating group
4	$C_4H_6NOSe^+$	163.9609	163.9	Formic acid and NH_3
5	$C_2H_4NOSe^+$	137.9453	137.9	-
6	$C_2H_4NSe^+$	121.9503	121.9	Formic acid and alkylating group
7	CH_4NSe^+	109.9503	109.9	NH_3 addition to fragment No. 8
8	$CHSe^+$	92.9238	92.9	-
9	$C_2H_4NO_2^+$	74.0237	74.0	-

[a]*Th, Thomson, where 1 Th, 1 m/z. All the indicated losses are related to the intact Se species.*

and to accumulate and reduce selenite producing either seleno-amino acids, volatile Se compounds, and/or SeNPs were evaluated. Furthermore, the GR enzyme activity as well as the presence of genes involved in Se metabolism were also analyzed.

When the assayed strains were grown in solid medium, all colonies displayed a time-dependent color change from white to orange-reddish. A similar behavior was observed in a *Pseudomonas alcaliphila* strain by Zhang et al. (2011). This characteristic red color is due to the excitation of the surface plasmon vibrations of the monoclinic Se particles (Lin and Wang, 2005).

As a first approach to study Se metabolism, we quantified the remaining sodium selenite in bacterial culture supernatants to indirectly measure the reductive activity on selenite oxyanion by the studied microorganisms. The 96 assayed bacteria resisted and biotransformed Se as a mechanism of cellular detoxification, as previously proposed by Lampis et al. (2014). Using this method, eight strains belonging to different genera achieved 80% selenite removal; this capacity was species- and strain-dependent. In this work, the ability of a wide diversity of LAB isolated from fruits and fruit flowers to reduce sodium selenite is shown in contrast to previous reports that were performed using strains of dairy or human origin.

Considering the Se RDI and in view of future applications of selenized cells as starter cultures for the preparation of Se-enriched functional foods, amounts of 5 ppm Se were used in our studies. All strains could grow in MRS or MRSf medium supplemented with Se although growth alteration due to the presence of this micronutrient was strain-dependent. Within

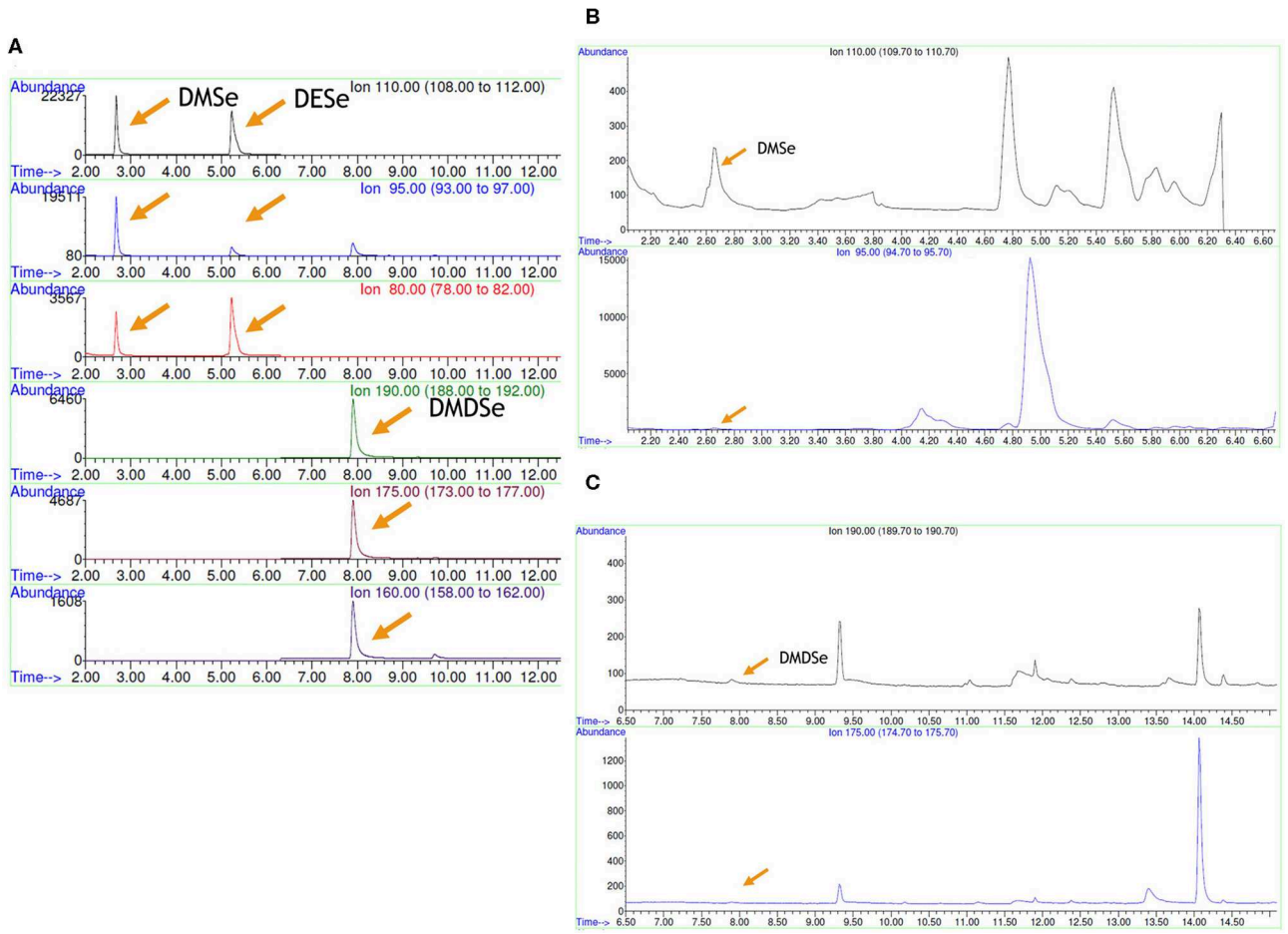

FIGURE 4 | Volatile Se compounds determined by HS-SPME-GC-MS. **(A)** Standard solutions, **(B)** strain *Ec. casseliflavus* 82, and **(C)** *Ec. casseliflavus* 47. DMSe, dimethyl selenide; DESe, diethyl selenide; DMDSe, dimethyl diselenide.

the *Fructobacillus* genus, the strains belonging to the *tropaeoli* species were not affected by the presence of Se, highlighting the capability of this particular species to resist to its presence. The concentration of 5 ppm Se was used in other studies with different LAB strains. Pescuma et al. (2017) reported that *Lb. reuteri* CRL 1101 and *Lb. acidophilus* CRL 636 could grow and resist the presence of 5 ppm Se, and that the former strain was the most resistant one showing only 1 log CFU/ml decrease in cell viability after 24 h of incubation. Similar results were obtained by Lamberti et al. (2011) who reported that 4.38 ppm Se were needed to observe the same decrease in the cell viability of *Lb. reuteri* Lb2 BM. The viability of LAB in the presence of Se was studied in several works and it resulted to be dependent on the LAB used. Interestingly, the selected strains in our work were able to accumulate intracellularly between 24 and 50% of the added Se (5 ppm) after 24 h of incubation. Similarly, Palomo-Siguero et al. (2016) showed that a *Lb. bulgaricus* strain could accumulate 60% of the added Se (10 ppm) after 24 h of incubation, while Pescuma et al. (2017) found that *Lb. acidophilus* CRL 636 and *Lb. reuteri* CRL 1101 accumulated Se intracellularly, noting that the amounts increased with the incubation time; the *Lb. reuteri* strain accumulated 78% of added Se after 24 h. Chen et al. (2019) reported a 2 ppm Se accumulation by a *Lb. plantarum* strain, a similar value obtained by our strain *Lb. plantarum* CRL 2030, which showed a Se accumulation of 1.96 ± 0.05 ppm.

Noteworthy, SeCys (the most bio-available Se form) was the only Se amino acid found in the LAB cells analyzed in this work. Other authors reported that *Lactobacillus* strains could biotransform selenite into SeCys and SeMet (Palomo-Siguero et al., 2016; Pescuma et al., 2017), while only SeMet was observed for a *Bifidobacteium animalis* strain (Zhang et al., 2009) and yeast, such as *Saccharomyces cerevisiae* (Ruiz Encinar et al., 2003). The incorporation of SeCys into selenoproteins in animals and bacteria is done through a process directed by a UGA codon while SeMet is non-specifically incorporated into proteins in place of methionine during protein synthesis. Hence, SeMet is not as readily accessible as SeCys for further metabolism (Alzate et al., 2008). This fact should be considered when nutraceuticals or fermented foods are formulated using microorganisms since SeCys is the main seleno-amino acid for man and animal metabolism (Zhu et al., 2000).

As $SeCys_2$ and SeMetO (Selenomethionine–Se-oxide) co-elute when a PRP-X100 anion exchange HPLC column is used, their clear discrimination is not possible (Palomo-Siguero et al., 2016); thus, the use of a second chromatographic procedure is mandatory to accurately identify Se species. Palomo-Siguero et al. (2016) and Pescuma et al. (2017) successfully used a reversed-phase Zorbax C8 column for the correct separation of Se species and proper identification of $SeCys_2$. Nevertheless, one of the main problems related to the identification of the SeCys amino acid, is its high instability after extraction as it is expected to be oxidized to form S–Se or Se–Se bond, bridging Cys- or SeCys-containing peptides. Moreover, $SeCys_2$ (the available commercial standard for SeCys detection by chromatographic methods) can co-elute with other non-retained Se species in some chromatographic procedures. The synthesis of carbamidomethyl-SeCys is thus a requisite for SeCys identification and the correct separation of SeCys from other species by chromatographic methods (Dernovics and Lobinski, 2008). In our work, a carbamidomethylation process to protect the SeCys structure was carried out prior to the enzymatic step. The carbamidomethylated derivates were separated by a reversed-phase EVO-C18 column coupled to ICP-MS and LC-ESI-MS/MS. The chromatogram obtained by LC-ICP-MS for the carbamidomethylated and enzymatically digested pellet of *F. tropaeoli* CRL 2034 showed a single peak eluting in the same retention time as CAM-SeCys. In order to identify this compound, a LC-MS/MS approach was carried out; the ionic fragmentation pattern obtained corresponded to the ionized fragments of the CAM-SeCys molecule.

Some bacteria can reduce Se salts into elemental Se (Se^0) for cellular detoxification (Narasingarao and Häggblom, 2007; Lampis et al., 2014). SeNPs are formed as Se^0 aggregates alone or in combination with exopolysaccharides and proteins. Formation of SeNPs by the eight studied LAB was confirmed by TEM images. Since surface area-to-volume ratio increases when decreasing particle size, smaller SeNPs have greater biological activity, including anti-hydroxyl radical property and protective effect against DNA oxidation (Zhang et al., 2011). On the other hand, the absorption of NPs smaller than 100 nm in the gastrointestinal tract is 15 to 250 times higher than that of larger-sized NPs (Hosnedlova et al., 2018). Interestingly, the size of SeNPs of the studied strains were between 50 and 90 nm except for the strains *Lc. lactis* CRL 2011 and *Ec. casseliflavus* 47, which produced SeNPs with larger diameters (125–155 nm and 110–140 nm, respectively). The production of SeNPs by LAB

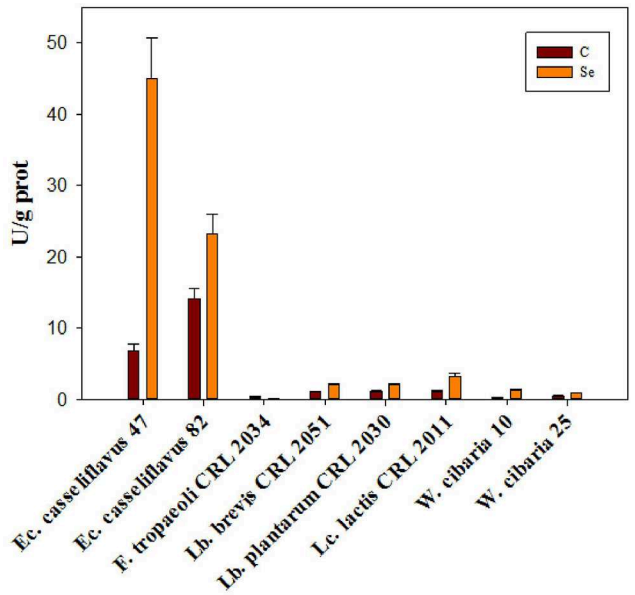

FIGURE 5 | Glutathione reductase activity of eight selected LAB strains grown in MRS and MRSf with and without 5 ppm Se at 30°C for 24 h.

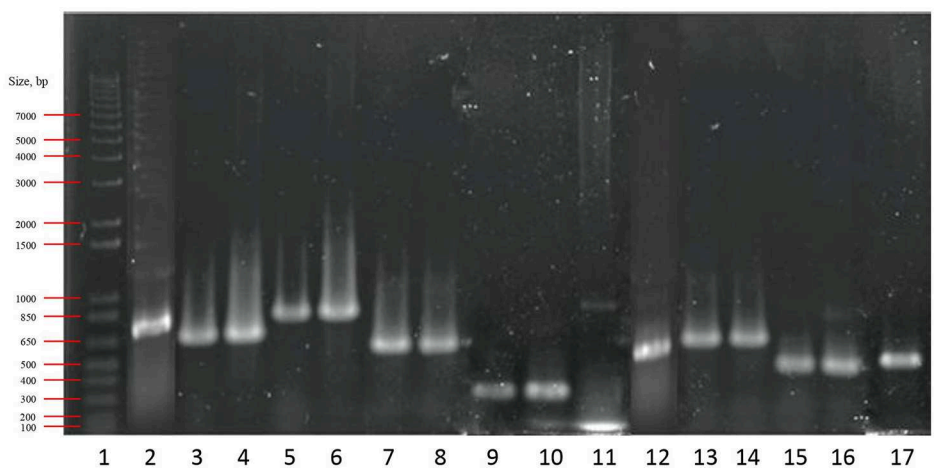

FIGURE 6 | PCR products of the glutathione reductase and selenocysteine lyase genes. Lanes: 1, molecular weight marker (1 Kb Plus DNA Ladder; Invitrogen™, CA, USA); 2, 3, 4, 5, 6, 7, 8, 9, 10, and 11, glutathione reductase; 12, 13, 14, 15, 16, and 17, selenocysteine lyase. Lanes 2 and 12 correspond to *Lc lactis* CRL 2011; 3, 5, and 15, *W. cibaria* 10; 4, 6, and 16 *W. cibaria* 25; 7 and 13, *Ec. casseliflavus* 47; 8 and 14, *Ec. casseliflavus* 82; 9, *Lb. brevis* CRL 2051; 10, *Lb. plantarum* CRL 2030; while lanes 11 and 17 correspond to *F. tropaeoli* CRL 2034.

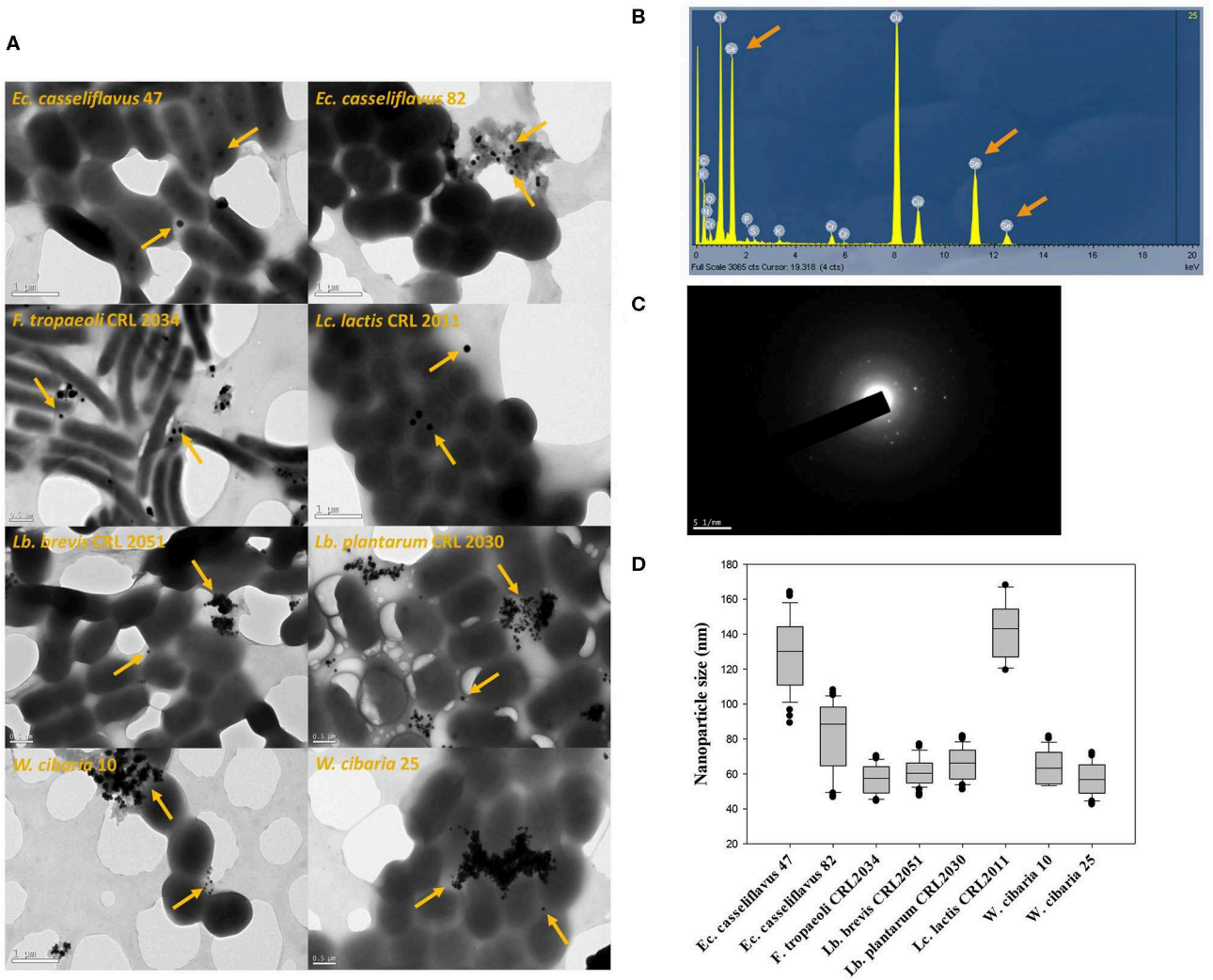

FIGURE 7 | TEM images and XEDS analysis obtained for samples of eight selected strains grown in MRS/MRSf supplemented with 5 ppm Se at 30°C for 24 h. **(A)** TEM images of eight LAB strains; orange arrows indicate the presence of isolated or gathered nanoparticles. **(B)** X-Ray Energy Dispersive Spectroscopy (XEDS) analysis graph depicting energy on *X*-axis and number of counts on *Y*-axis representing elemental composition derived from selenium nanoparticles. Arrows in XEDS spectra indicate the Se emission peaks consisting of SeLα, SeKα, and SeKβ at 1.4, 11.22, and 12.49 keV, respectively. **(C)** Diffraction pattern of nanoparticles. **(D)** Nanoparticle size distribution ($n = 100$) of eight selected strains.

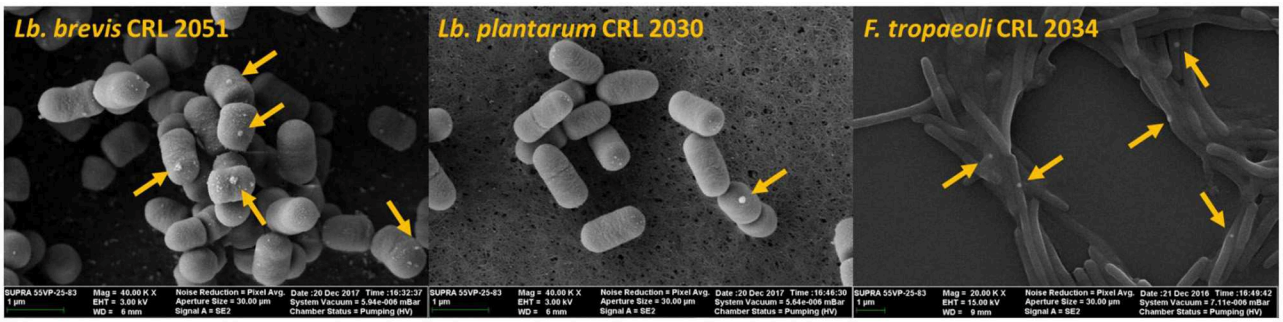

FIGURE 8 | SEM microphotographs of selenized cells after 24-h incubation at 30°C in MRS or MRSf.

has been studied elsewhere (Eszenyi et al., 2011; Sasidharan and Balakrishnaraja, 2014; Visha et al., 2015; Moreno-Martin et al., 2017; Pescuma et al., 2017) showing also NP sizes between 40 and 500 nm depending on the strain used. Contrary to the majority of biosynthetic SeNPs like those reported by Moreno-Martin et al. (2017), the nanoparticles produced by our strains were microcrystalline. Also, Visha et al. (2015) reported a crystalline structure for the SeNPs produced by a *Lb. acidophilus* strain; these differences demonstrate the particle diversity produced by LAB. SeNPs are less toxic than inorganic Se; moreover, their capacity to diminish cancer has been studied *in vivo* and *in vitro* (Yazdi et al., 2013; Lopez-Heras et al., 2014). Yazdi et al. (2012) reported that a *Lb. plantarum* strain enriched with SeNPs could elevate INF-γ, TNF-α, and IL-2 levels as well as natural killer cell activity in a murine model. Moreover, a SeNP-enriched *Lb. brevis* strain inhibited liver metastasis in metastatic mouse breast cancer (Yazdi et al., 2013). Interestingly, it has been reported that biogenic SeNPs possessed antimicrobial properties and that, when administered alone or in combination with antibiotics, they inhibit growth of multi-resistant bacteria and can disaggregate biofilms produced by these pathogens (Cremonini et al., 2016). Furthermore, Se-enriched probiotics improved lipid metabolism, antioxidant status, and histopathological lesions induced by a fat-rich diet in an obesity model in mice (Nido et al., 2016).

Some microorganisms can reduce Se oxyanions (Yee et al., 2014), playing a fundamental role in the recycling and transformation of Se through redox and methylation reactions. Microorganisms living in Se-rich environments are usually able to convert inorganic Se compounds into volatile compounds. These microorganisms can secrete methyltransferases stimulating the emission of DMSe (Javed et al., 2015). Volatile Se compounds have a strong odor and can contribute to unpleasant flavors in foods; thus, bacteria producing these compounds may be unsuitable for their use in the food industry (Michalke et al., 2000). Our results showed that among the eight selected strains, only *Ec. casseliflavus* 47 and 82 were able to form DMDSe and DMSe, respectively, although in scarce amounts. Pophaly et al. (2014) reported the formation of the same compounds by the strains *Streptococcus salivarius* K12, *Lb. rhamnosus* 67B, *Lb. acidophilus* L10, and *B. lactis* LAFTI B94 when the cultures were previously enriched with SeMet, while formation of DMSe, DMDSe, and Se^0 was observed when selenite enrichment was done.

In many bacteria and eukaryotes, reduced glutathione (GSH) is a prime candidate as thiol compound source because GSH is the most abundant low-molecular-weight thiol in these organisms. Selenite can react with several thiols producing seleno-trisulfide derivatives. When GSH reacts with selenite, selenodiglutathione (GSSeSG) is produced; this compound is a key intermediate in the Se metabolic pathway, leading to the conversion of inorganic Se into bioactive selenocompounds such as Se^0 (SeNPs) (Ogasawara et al., 2005) or selenophosphate through the selenophosphate synthetase enzyme activity (Seale, 2019). The enzyme GR catalyzes NADPH-dependent reduction of glutathione and has an important role in cell defense against oxygen stress by maintaining a high intracellular GSH/GSSG level (Jänsch et al., 2007). Chung and Maines (1981) reported that Se could increase the activities of γ-glutamyl cysteine synthetase, the first and rate-limiting enzyme in GSH biosynthesis, and GR, which catalyzes the reduction of GSSG to GSH. The increase in the activities of these enzymes was observed 24 h after Se (10 and 20 pmol/kg) administration. This finding coincides with our results in which the GR activity presented a two- to six-fold increase when the strains were grown in the presence of Se after 24 h of incubation, indicating an active Se metabolism; an opposite behavior was seen for the *F. tropaeoli* strain.

On the other hand, the enzyme SCL is able to decompose SeCys into Se^0 and alanine; this enzyme can also mobilize Se into SeCys for selenophosphate synthesis necessary for producing SeCys-tRNA, the precursor of SeCys and selenoproteins (Ogasawara et al., 2005; Lamberti et al., 2011). The SCL activity was detected in several bacterial species, such as *Pseudomonas alkanolytica*, *Alcaligenes viscolactis*, and *Escherichia freundii* (Chocat et al., 1983). In bacteria, SCL activity has been related to three enzymes, the *Azobacter vinelandii* Nifs-like protein, and the *E. coli* CsdA and CsdB cysteine desulfurases (Lacourciere et al., 2000). Moreover, a SCL/cysteine desulfurase regulated by selenite levels was identified in a probiotic *Lb. reuteri* strain by Lamberti et al. (2011). These enzymes can decompose L-cysteine and L-SeCys into alanine and elemental sulfur and selenium, respectively (Seale, 2019). Both enzymes GR and SCL have been detected in some LAB strains (Lamberti et al., 2011; Pusztahelyi et al., 2015); however, Se metabolism has been studied mainly in dairy- or human gut-origin LAB (Zhang et al., 2009; Mangiapane et al., 2014; Palomo et al., 2014; Saini et al., 2014; Deng et al., 2015; Pescuma et al., 2017; Gomez-Gomez et al., 2019). The gene *GshR* coding for GR was detected in the eight analyzed strains, while *Scl* could be amplified in all strains except for the *Lactobacillus* strains with the primers used. The presence of these genes supports the capability of these strains to metabolize Se and to produce SeNPs and SeCys.

In this work, we studied nine *Fructobacillus* strains that belong to a particular group of bacteria called FLAB. This group, which was described a decade ago and consists of five species of *Fructobacillus* and a few *Lactobacillus* species, shares some unique characteristics including poor growth on glucose, the preference of oxygen, and the need of an external electron acceptor to grow, such as fructose, which is the optimum substrate for growth (Endo et al., 2009). It is thus not surprising to find FLAB in fructose-rich environments, including flowers, fruits, fermented foods derived from fruits and even guts of insects that feed on plants rich in fructose (Endo and Salminen, 2013). The genomic level of FLAB changed to adapt to these different types of environments; further studies are required to explore their beneficial properties in animals and humans and their applications in the food industry (Endo et al., 2018). Among the nine *Fructobacillus* strains isolated from fig (7 strains), custard apple (1), and khaki (1) studied in this work, we selected the fig-isolate *F. tropaeoli* CRL 2034, which presented the largest selenite percentage removal from the culture medium. This strain could accumulate Se intracellularly and produce SeNPs and SeCys in large amounts, while the genes encoding for GR and SCL enzymes were found in the genome; nevertheless, the GR activity decreased when the strain was grown in the presence of Se. This could be due to differences in the requirements and metabolism of this group of LAB. The unusual growth characteristics of

FLAB are a consequence of the incomplete gene *adhE* encoding a bi-functional alcohol/acetaldehyde dehydrogenase, which results in the imbalance of NAD/NADH and the requirement of additional electron acceptors to metabolize glucose such as oxygen, fructose, and pyruvate (Endo et al., 2018). It is likely that the NAD/NADH imbalance could alter the normal Se metabolism. Also, FLAB could use Se as an electron acceptor in a GSH/GR-independent manner reflecting on the reduction of GR activity; however, further studies need to be done to better understand Se metabolism in this bacterial group.

Interestingly, LAB able to biotransform Se could be established in the intestine and biotransform the inorganic Se ingested by the diet or supplements into organic Se (i.e., seleno-amino acids); this fact is feasible if the strains survive the human gastrointestinal conditions. Martinez et al. (2019) showed that the fruit-origin strains *Lb. brevis* CRL 2051 and *F. tropaeoli* CRL 2034 could survive the *in vitro* gastrointestinal tract conditions when present in a fermented fruit juice-milk beverage. The *Fructobacillus* strain preferred fructose to glucose to grow and produced the low calorie sugar mannitol in an equal amount of that of fructose consumed; mannitol may provide health beneficial effects by acting as antioxidant and low-calorie sweetener applicable for diabetic patients (Ortiz et al., 2015). In this study, the presence of selenite did not affect cell survival of *Lb. brevis* CRL 2051 but improved the *Fructobacillus* strain viability after a 28-day storage period (Martinez et al., 2019). Remarkably, selenized cells of the *Fructobacillus* strain were more resistant to the incubation with digestive enzymes than non-selenized bacteria, indicating that Se accumulation may confer a selective advantage to tolerate digestion. In contrast, no effect was detected with the *Lb. brevis* strain. These results demonstrate that *Lb. brevis* CRL 2051 and *F. tropaeoli* CRL 2034 may be used as Se-enriched strains in the industry of functional foods. Also, Pescuma et al. (2017) reported that the growth of a selenized *Lb. reuteri* strain was not affected by the presence of bile salts in the culture medium while a negative effect on the growth of non-selenized strain was noticed. Similar results were reported for *Lb. reuteri* Lb2BM by Mangiapane et al. (2014).

Nowadays, a worldwide tendency to consume fruit and vegetable fermented products exists due to the high incidence of milk allergy/intolerance, the search for cholesterol-free foods, and vegan habits (Di Cagno et al., 2010), among others. In this context, the ability of the studied strains to biotransform and accumulate Se is highly relevant since they can better grow in fruit matrixes than bacteria coming from different niches. Moreover, the selected strains produced only the Se amino acid SeCys, which is more bioavailable and has no toxic effect as it has been observed for SeMet, when consumed in high concentrations. In addition, these strains produced small-size SeNPs, which may be better absorbed in the gastrointestinal tract than bigger size ones.

CONCLUSIONS

Eight LAB strains were selected for their ability to grow, resist, and biotransform inorganic Se into organic forms. These microorganisms could accumulate Se intracellularly, produce SeNPs and incorporate SeCys, which is the most bioavailable Se form. In this work, the Se metabolism was extensively studied in selected strains. Furthermore, the ability of two *Enterococcus* strains to produce volatile Se compounds is reported in this study. Moreover, differences in Se metabolism were observed for a *Fructobacillus* strain for which GR activity was inhibited in the presence of Se, indicating that other mechanisms in selenite reduction are involved. Our findings suggest that *Lb brevis* CRL 2051, *Lb. plantarum* CRL 2030, and *F. tropaeoli* CRL 2034 could be used for the development of nutraceuticals or be used as starter cultures for the bio-enrichment of fermented (fruit) beverages with SeCys and SeNPs.

DATA AVAILABILITY STATEMENT

The raw data supporting the conclusions of this article will be made available by the authors, without undue reservation.

AUTHOR CONTRIBUTIONS

FGM conducted the experimental work, analyzed the results, and wrote the manuscript. GM-M conducted with FGM some experimental determinations and analyzed some of the results. MP directed and designed the work, and wrote and revised the manuscript. YM-A directed part of the work and revised the manuscript. FM directed the work and revised the manuscript. All authors read and approved the submitted version.

FUNDING

We acknowledge the financial support of PIP 003-CONICET and FONCyT (PICT 2014-0312 and PICT 2015-2330) from Argentina. FGM is recipient of a doctoral fellowship from CONICET. The UCM group thanks the Spanish Commission of Science and Technology (CTQ2017-83569-C2-1-R), the Comunidad of Madrid, and the European funding from FSE and FEDER programs for financial support (project S2018/BAA-4393, AVANSECAL-II-CM); and the Complutense University through a pre-doctoral grant (CT42/18-CT43/18).

ACKNOWLEDGMENTS

FGM acknowledges ICFMH Mobility Grants 2018 from the International Committee on Food Microbiology and Hygiene (ICFMH) for an external internship at Departamento de Química Analítica, Facultad de Ciencias Químicas, Universidad Complutense de Madrid, Ciudad Universitaria, 28040 Madrid, Spain.

SUPPLEMENTARY MATERIAL

The Supplementary Material for this article can be found online at: https://www.frontiersin.org/articles/10.3389/fbioe.2020.00506/full#supplementary-material

REFERENCES

Alzate, A., Fernández-Fernández, A., Pérez-Conde, M., Gutiérrez, A., and Cámara, C. (2008). Comparison of biotransformation of inorganic selenium by Lactobacillus and Saccharomyces in lactic fermentation process of yogurt and kefir. *J. Agric. Food Chem.* 56, 8728–8736. doi: 10.1021/jf8013519

Alzate, A., Pérez-Conde, M., Gutiérrez, A., and Cámara, C. (2010). Selenium-enriched fermented milk: a suitable dairy product to improve selenium intake in humans. *Int. Dairy J.* 20, 761–769. doi: 10.1016/j.idairyj.2010.05.007

ANMAT (2018). *Codigo Alimentario Argentino. Capítulo XVII: Alimentos de régimen o dietéticos*. Available online at: https://www.argentina.gob.ar/anmat/codigoalimentario (accessed February 20, 2020).

Brown, T. A. (1995). *Purification of DNA from Living Cells, in Gene Cloning: An Introduction*. Manchester: Stanley Thornes, Chapman & Hall, 27–51.

Chen, Y., Li, Q., Xia, C., Yang, F., Xu, N., Wu, Q., et al. (2019). Effect of selenium supplements on the antioxidant activity and nitrite degradation of lactic acid bacteria. *World J. Microbiol. Biotechnol.* 35:61. doi: 10.1007/s11274-019-2609-x

Chocat, P., Esaki, N., Nakamura, T., Tanaka, H., and Soda, K. (1983). Microbial distribution of selenocysteine lyase. *J. Bacteriol.* 156, 455–457. doi: 10.1128/JB.156.1.455-457.1983

Chung, A-S., and Maines, M. D. (1981). Effect of selenium on glutathione metabolism. Induction of γ-glutamylcysteine synthetase and glutathione reductase in the rat liver. *Biochem. Pharmacol.* 30, 3217–3223. doi: 10.1016/0006-2952(81)90521-9

Cremonini, E., Zonaro, E., Donini, M., Lampis, S., Boaretti, M., Dusi, S., et al. (2016). Biogenic selenium nanoparticles: characterization, antimicrobial activity and effects on human dendritic cells and fibroblasts. *Microb. Biotechnol.* 9, 758–771. doi: 10.1111/1751-7915.12374

Deng, Y., Man, C., Fan, Y., Wang, Z., Li, L., Ren, H., et al. (2015). Preparation of elemental selenium-enriched fermented milk by newly isolated *Lactobacillus brevis* from kefir grains. *Int. Dairy J.* 44, 31–36. doi: 10.1016/j.idairyj.2014.12.008

Dernovics, M., and Lobinski, R. (2008). Characterization of the selenocysteine-containing metabolome in selenium-rich yeast Part II. on the reliability of the quantitative determination of selenocysteine. *J. Anal. At. Spectrom.* 23, 744–751. doi: 10.1039/b716140a

Dhanjal, S., and Cameotra, S. S. (2010). Aerobic biogenesis of selenium nanospheres by *Bacillus cereus* isolated from coalmine soil. *Microb. Cell Fact.* 9:52. doi: 10.1186/1475-2859-9-52

Di Cagno, R., Cardinali, G., Minervini, G., Antonielli, L., Rizzello, C. G., Ricciuti, P., et al. (2010). Taxonomic structure of the yeasts and lactic acid bacteria microbiota of pineapple (*Ananas comosus L. Merr.)* and use of autochthonous starters for minimally processing. *Food Microbiol.* 27, 381–389. doi: 10.1016/j.fm.2009.11.012

Endo, A., Futagawa-Endo, Y., and Dicks, L. M. (2009). Isolation and characterization of fructophilic lactic acid bacteria from fructose-rich niches. *Syst. Appl. Microbiol.* 32, 593–600. doi: 10.1016/j.syapm.2009.08.002

Endo, A., Maeno, S., Tanizawa, Y., Kneifel, W., Arita, M., Dicks, L., et al. (2018). Fructophilic lactic acid bacteria, a unique group of fructose-fermenting microbes. *Appl. Environ. Microbiol.* 84, e01290–e01218. doi: 10.1128/AEM.01290-18

Endo, A., and Salminen, S. (2013). Honeybees and beehives are rich sources for fructophilic lactic acid bacteria. *Syst. Appl. Microbiol.* 36, 444–448. doi: 10.1016/j.syapm.2013.06.002

Eszenyi, P., Sztrik, A., Babka, B., and Prokisch, J. (2011). Elemental, nano-sized (100-500 nm) selenium production by probiotic lactic acid bacteria. *Int. J. Biosci. Biochem. Bioinform.* 1:148. doi: 10.7763/IJBBB.2011.V1.27

FAO/WHO, (2004). *Vitamin and Mineral Requirements in Human Nutrition. Chapter 10, Selenium*. Bangkok: World Health Organization Second edition, 194–216

Gomez-Gomez, B., Perez-Corona, T., Mozzi, F., Pescuma, M., and Madrid, Y. (2019). Silac-based quantitative proteomic analysis of *Lactobacillus reuteri* CRL 1101 response to the presence of selenite and selenium nanoparticles. *J. Proteomics* 195, 53–65. doi: 10.1016/j.jprot.2018.12.025

Hosnedlova, B., Kepinska, M., Skalickova, S., Fernandez, C., Ruttkay-Nedecky, B., Peng, Q., et al. (2018). Nano-selenium and its nanomedicine applications: a critical review. *Int. J. Nanomed.* 13, 2107–2128. doi: 10.2147/IJN.S157541

Hugenholtz, J., Sybesma, W., Groot, M. N., Wisselink, W., Ladero, V., Burgess, K., et al. (2002). Metabolic engineering of lactic acid bacteria for the production of nutraceuticals. *Antonie Van Leeuwenhoek.* 82, 217–235. doi: 10.1007/978-94-017-2029-8_13

Jänsch, A., Korakli, M., Vogel, R. F., and Gänzle, M. G. (2007). Glutathione reductase from *Lactobacillus sanfranciscensis* DSM20451T: contribution to oxygen tolerance and thiol exchange reactions in wheat sourdoughs. *Appl. Environ. Microbiol.* 73, 4469–4476. doi: 10.1128/AEM.02322-06

Javed, S., Sarwar, A., Tassawar, M., and Faisal, M. (2015). Conversion of selenite to elemental selenium by indigenous bacteria isolated from polluted areas. *Chem. Spec. Bioavailab.* 27, 162–168. doi: 10.1080/09542299.2015.1112751

Kessi, J., Ramuz, M., Wehrli, E., Spycher, M., and Bachofen, R. (1999). Reduction of selenite and detoxification of elemental selenium by the phototrophic bacterium *Rhodospirillum rubrum*. *Appl. Environ. Microbiol.* 65, 4734–4740. doi: 10.1128/AEM.65.11.4734-4740.1999

Lacourciere, G. M., Mihara, H., Kurihara, T., Esaki, N., and Stadtman, T. C. (2000). *Escherichia coli* NifS-like proteins provide selenium in the pathway for the biosynthesis of selenophosphate. *J. Biol. Chem.* 275, 23769–23773. doi: 10.1074/jbc.M000926200

Lamberti, C., Mangiapane, E., Pessione, A., Mazzoli, R., Giunta, C., and Pessione, E. (2011). Proteomic characterization of a selenium-metabolizing probiotic *Lactobacillus reuteri* Lb2 BM for nutraceutical applications. *Proteomics* 11, 2212–2221. doi: 10.1002/pmic.201000747

Lampis, S., Zonaro, E., Bertolini, C., Bernardi, P., Butler, C. S., and Vallini, G. (2014). Delayed formation of zero-valent selenium nanoparticles by *Bacillus mycoides* SeITE01 as a consequence of selenite reduction under aerobic conditions. *Microb. Cell Fact.* 13:35. doi: 10.1186/1475-2859-13-35

Lin, Z-H., and Wang, C. C. (2005). Evidence on the size-dependent absorption spectral evolution of selenium nanoparticles. *Mater. Chem. Phys.* 92, 591–594. doi: 10.1016/j.matchemphys.2005.02.023

Lopez-Heras, I., Sanchez-Diaz, R., Anunciação, D. S., Madrid, Y., Luque-Garcia, J. L., and Camara, C. (2014). Effect of chitosan-stabilized selenium nanoparticles on cell cycle arrest and invasiveness in hepatocarcinoma cells revealed by quantitative proteomics. *J. Nanomed. Nanotechnol.* 5:1. doi: 10.4172/2157-7439.1000226

Mangiapane, E., Lamberti, C., Pessione, A., Galano, E., Amoresano, A., and Pessione, E. (2014). Selenium effects on the metabolism of a Se-metabolizing *Lactobacillus reuteri*: analysis of envelope-enriched and extracellular proteomes. *Mol. Biosyst.* 10, 1272–1280. doi: 10.1039/C3MB70557A

Martinez, F. G., Cuencas Barrientos, M. E., Mozzi, F., and Pescuma, M. (2019). Survival of selenium-enriched lactic acid bacteria in a fermented drink under storage and simulated gastro-intestinal digestion. *Food Res. Int.* 123, 115–124. doi: 10.1016/j.foodres.2019.04.057

Michalke, K., Wickenheiser, E., Mehring, M., Hirner, A., and Hensel, R. (2000). Production of volatile derivatives of metal (loid) s by microflora involved in anaerobic digestion of sewage sludge. *Appl. Environ. Microbiol.* 66, 2791–2796. doi: 10.1128/AEM.66.7.2791-2796.2000

Moreno-Martin, G., Pescuma, M., Pérez-Corona, T., Mozzi, F., and Madrid, Y. (2017). Determination of size and mass-and number-based concentration of biogenic SeNPs synthesized by lactic acid bacteria by using a multimethod approach. *Anal. Chim. Acta* 992, 34–41. doi: 10.1016/j.aca.2017.09.033

Moreno-Martin, G., Sanz-Landaluze, J., León-Gonzalez, M. E., and Madrid, Y. (2019). *In-vivo* solid phase microextraction for quantitative analysis of volatile organoselenium compounds in plants. *Anal. Chim. Acta* 1081, 72–80. doi: 10.1016/j.aca.2019.06.061

Mounicou, S., Vonderheide, A. P., Shann, J. R., and Caruso, J. A. (2006). Comparing a selenium accumulator plant (*Brassica juncea*) to a nonaccumulator plant (*Helianthus annuus*) to investigate selenium-containing proteins. *Anal. Bioanal. Chem.* 386, 1367–1378. doi: 10.1007/s00216-006-0707-8

Narasingarao, P., and Häggblom, M. M. (2007). Identification of anaerobic selenate-respiring bacteria from aquatic sediments. *Appl. Environ. Microbiol.* 73, 3519–3527. doi: 10.1128/AEM.02737-06

Nido, S. A., Shituleni, S. A., Mengistu, B. M., Liu, Y., Khan, A. Z., Gan, F., et al. (2016). Effects of selenium-enriched probiotics on lipid metabolism, antioxidative status, histopathological lesions, and related gene

expression in mice fed a high-fat diet. *Biol. Trace Elem. Res.* 171, 399–409. doi: 10.1007/s12011-015-0552-8

Ogasawara, Y., Lacourciere, G. M., Ishii, K., and Stadtman, T. C. (2005). Characterization of potential selenium-binding proteins in the selenophosphate synthetase system. *Proc. Natl. Acad. Sci.U.S.A.* 102, 1012–1016. doi: 10.1073/pnas.0409042102

Ortiz, M. E., Raya, R. R., and Mozzi, F. (2015). Efficient mannitol production by wild-type *Lactobacillus reuteri* CRL 1101 is attained at constant pH using a simplified culture medium. *Appl. Microbiol. Biotechnol.* 99, 8717–8729. doi: 10.1007/s00253-015-6730-y

Palomo, M., Gutiérrez, A. M., Pérez-Conde, M. C., Cámara, C., and Madrid, Y. (2014). Se metallomics during lactic fermentation of Se-enriched yogurt. *Food Chem.* 164, 371–379. doi: 10.1016/j.foodchem.2014.05.007

Palomo-Siguero, M., Gutiérrez, A. M. A., Pérez-Conde, C., and Madrid, Y. (2016). Effect of selenite and selenium nanoparticles on lactic bacteria: a multi-analytical study. *Microchem. J.* 126, 488–495. doi: 10.1016/j.microc.2016.01.010

Palomo-Siguero, M., and Madrid, Y. (2017). Exploring the behavior and metabolic transformations of SeNPs in exposed lactic acid bacteria. Effect of nanoparticles coating agent. *Int. J. Mol. Sci.* 18:1712. doi: 10.3390/ijms18081712

Pedrero, Z., Madrid, Y., and Cámara, C. (2006). *Selenium species* bioaccessibility in enriched radish (*Raphanus sativus*): a potential dietary source of selenium. *J. Agric. Food Chem.* 54, 2412–2417. doi: 10.1021/jf052500n

Pescuma, M., Gomez-Gomez, B., Perez-Corona, T., Font, G., Madrid, Y., and Mozzi, F. (2017). Food prospects of selenium enriched-*Lactobacillus acidophilus* CRL 636 and *Lactobacillus reuteri* CRL 1101. *J. Funct. Foods* 35, 466–473. doi: 10.1016/j.jff.2017.06.009

Pophaly, S., Poonam, S., Pophaly, S., Kapila, S., Nanda, D., Tomar, S., et al. (2017). Glutathione biosynthesis and activity of dependent enzymes in food-grade lactic acid bacteria harbouring multidomain bifunctional fusion gene (gshF). *J. Appl. Microbiol.* 123, 194–203. doi: 10.1111/jam.13471

Pophaly, S. D., Singh, P., Kumar, H., Tomar, S. K., and Singh, R. (2014). Selenium enrichment of lactic acid bacteria and bifidobacteria: a functional food perspective. *Trends Food Sci. Technol.* 39, 135–145. doi: 10.1016/j.tifs.2014.07.006

Pusztahelyi, T., Kovács, S., Pócsi, I., and Prokisch, J. (2015). Selenite-stress selected mutant strains of probiotic bacteria for Se source production. *J. Trace Elem. Med. Biol.* 30, 96–101. doi: 10.1016/j.jtemb.2014.11.003

Rayman, M. P. (2012). Selenium and human health. *Lancet* 379, 1256–1268. doi: 10.1016/S0140-6736(11)61452-9

Ruiz Encinar, J., Ouerdane, L., Buchmann, W., Tortajada, J., Lobinski, R., and Szpunar, J. (2003). Identification of water-soluble selenium-containing proteins in selenized yeast by size-exclusion-reversed-phase HPLC/ICPMS followed by MALDI-TOF and electrospray Q-TOF mass spectrometry. *Anal. Chem.* 75, 3765–3774. doi: 10.1021/ac034103m

Ruiz Rodríguez, L. G., Aller, K., Bru, E., De Vuyst, L., Hébert, E. M., and Mozzi, F. (2017). Enhanced mannitol biosynthesis by the fruit origin strain *Fructobacillus tropaeoli* CRL 2034. *Appl. Microbiol. Biotechnol.* 101, 6165–6177. doi: 10.1007/s00253-017-8395-1

Ruiz Rodriguez, L. G., Mohamed, F., Bleckwedel, J., Medina, R. B., De Vuyst, L., Hebert, E. M., et al. (2019). Diversity and functional properties of lactic acid bacteria isolated from wild fruits and flowers present in Northern Argentina. *Front. Microbiol.* 10:1091. doi: 10.3389/fmicb.2019.01091

Saini, K., Tomar, S. K., Sangwan, V., and Bhushan, B. (2014). Evaluation of lactobacilli from human sources for uptake and accumulation of selenium. *Biol. Trace Elem. Res.* 160, 433–436. doi: 10.1007/s12011-014-0065-x

Sasidharan, S., and Balakrishnaraja, R. (2014). Comparison studies on the synthesis of selenium nanoparticles by various microorganisms. *Int. J. Pure Appl. Biosci.* 2, 112–117.

Seale, L. A. (2019). Selenocysteine β-Lyase: biochemistry, regulation and physiological role of the selenocysteine decomposition enzyme. *Antioxidants* 8:357. doi: 10.3390/antiox8090357

Tamang, J. P., Shin, D.-H., Jung, S.-J., and Chae, S.-W. (2016). Functional properties of microorganisms in fermented foods. *Front. Microbiol.* 7:578. doi: 10.3389/fmicb.2016.00578

Visha, P., Nanjappan, K., Selvaraj, P., Jayachandran, S., Elango, A., and Kumaresan, G. (2015). Biosynthesis and structural characteristics of selenium nanoparticles using *Lactobacillus acidophilus* bacteria by wet sterilization process. *Int. J. Adv. Vet. Sci. Technol.* 4, 178–183. doi: 10.23953/cloud.ijavst.183

Yazdi, M., Mahdavi, M., Kheradmand, E., and Shahverdi, A. (2012). The preventive oral supplementation of a selenium nanoparticle-enriched probiotic increases the immune response and lifespan of 4T1 breast cancer bearing mice. *Arzneimittelforschung* 62, 525–531. doi: 10.1055/s-0032-1323700

Yazdi, M. H., Mahdavi, M., Setayesh, N., Esfandyar, M., and Shahverdi, A. R. (2013). Selenium nanoparticle-enriched *Lactobacillus brevis* causes more efficient immune responses *in vivo* and reduces the liver metastasis in metastatic form of mouse breast cancer. *DARU J.Pharm. Sci.* 21:33. doi: 10.1186/2008-2231-21-33

Yee, N., Choi, J., Porter, A. W., Carey, S., Rauschenbach, I., and Harel, A. (2014). Selenate reductase activity in *Escherichia coli* requires Isc iron–sulfur cluster biosynthesis genes. *FEMS Microbiol. Lett.* 361, 138–143. doi: 10.1111/1574-6968.12623

Zhang, B., Zhou, K., Zhang, J., Chen, Q., Liu, G., Shang, N., et al. (2009). Accumulation and species distribution of selenium in Se-enriched bacterial cells of the *Bifidobacterium animalis* 01. *Food Chem.* 115, 727–734. doi: 10.1016/j.foodchem.2008.12.006

Zhang, W., Chen, Z., Liu, H., Zhang, L., Gao, P., and Li, D. (2011). Biosynthesis and structural characteristics of selenium nanoparticles by *Pseudomonas alcaliphila*. *Colloids Surf. B Biointerfaces* 88, 196–201. doi: 10.1016/j.colsurfb.2011.06.031

Zhu, Z., Jiang, W., Ganther, H. E., Ip, C., and Thompson, H. J. (2000). Activity of Se-allylselenocysteine in the presence of methionine γ-lyase on cell growth, DNA integrity, apoptosis, and cell-cycle regulatory molecules. *Mol. Carcinog.* 29, 191–197. doi: 10.1002/1098-2744(200012)29:4<191::aid-mc1000>3.0.co;2-7

Conflict of Interest: The authors declare that the research was conducted in the absence of any commercial or financial relationships that could be construed as a potential conflict of interest.

frontiers in Bioengineering and Biotechnology

ORIGINAL RESEARCH
published: 26 June 2020
doi: 10.3389/fbioe.2020.00644

A Leaderless Two-Peptide Bacteriocin, Enterocin DD14, Is Involved in Its Own Self-Immunity: Evidence and Insights

Rabia Ladjouzi[1], *Anca Lucau-Danila*[1], *Abdellah Benachour*[2] *and Djamel Drider*[1]*

[1] UMR Transfrontalière BioEcoAgro N° 1158, Univ. Lille, INRAE, Univ. Liège, UPJV, YNCREA, Univ. Artois, Univ. Littoral Côte d'Opale, ICV – Institut Charles Viollette, Lille, France, [2] UR Risques Microbiens, Normandie Univ, UNICAEN, U2RM, Caen, France

Enterocin DD14 (EntDD14) is a two-peptide leaderless bacteriocin produced by *Enterococcus faecalis* 14, a strain previously isolated from meconium. EntDD14 has a strong antibacterial activity against Gram-positive bacteria. Leaderless bacteriocins, unlike bacteriocins with leader peptides, are immediately active after their translation, and a producing strain has then to develop specific mechanisms to protect both intra and extracellular compartments. The *in silico* analysis of *Ent. faecalis* 14 genome allowed to locate downstream of structural *ddAB* genes, 8 other adjacent genes, designed *ddCDEFGHIJ*, which collectively may form three operons. To gain insights on immunity mechanisms of *Ent. faecalis* 14, mutant strains knocked out in *ddAB* genes encoding bacteriocin precursor peptides (Δ*bac*) and/or ABC transporter (Δ*ddI*) of EntDD14 were constructed and characterized. Importantly, Δ*bac* mutant strains, from which structural *ddAB* genes were deleted, resulted unable to produce EntDD14 and sensitive to exogenous EntDD14 showing their involvement in the *Ent. faecalis* 14 immunity system. Moreover, the sensitivity of Δ*bac* mutants appeared not to be associated with the down-regulation of *ddCDEFGHIJ* gene expression since they were similarly expressed in both Δ*bac* and wild-type strains during the log phase while they were found significantly down-regulated in the Δ*bac* mutant strain after 24 h of growth. Data gathered from this study suggest also the implication of the ABC transporter (*ddHIJ*) in the active export of EntDD14 but ruled-out its involvement in the primary self-immunity system. Interestingly, non-bacteriocin producing *Ent. faecalis* JH2-2 cells transformed with *ddAB,* or *ddAB* plus genes encoding the ABC transporter (*ddAB-HIJ*) did not produce EntDD14 and remained sensitive to its action. Of note, trans-complementation of the Δ*bac* mutant strain with these constructions allowed to recover the WT phenotype. To the best of our knowledge, this is the first study delineating the role of the intracellular two-peptide leaderless bacteriocins in their self-immunity.

Keywords: leaderless peptides, two-peptide enterocin DD14, bacterial self-immunity, regulation, antimicrobial peptide, ABC transporter

OPEN ACCESS

Edited by:
Csaba Fehér, Budapest University of Technology and Economics, Hungary

Reviewed by:
Sylvie Françoise Rebuffat, Muséum National d'Histoire Naturelle, France
Thomas Dandekar, Julius Maximilian University of Würzburg, Germany

***Correspondence:**
Djamel Drider
djamel.drider@univ-lille.fr

Specialty section:
This article was submitted to Synthetic Biology, a section of the journal Frontiers in Bioengineering and Biotechnology

Received: *01 April 2020*
Accepted: *26 May 2020*
Published: *26 June 2020*

Citation:
Ladjouzi R, Lucau-Danila A, Benachour A and Drider D (2020) A Leaderless Two-Peptide Bacteriocin, Enterocin DD14, Is Involved in Its Own Self-Immunity: Evidence and Insights. Front. Bioeng. Biotechnol. 8:644. doi: 10.3389/fbioe.2020.00644

INTRODUCTION

Enterococci are members of the lactic acid bacteria (LAB) group that are known to produce potent bacteriocins, named enterocins. Bacteriocins are ribosomally synthesized, antimicrobial peptides active against a group of closely related species (Klaenhammer, 1993; Nes et al., 1996). Many studies have reported the promising potential of bacteriocins for use in in different areas like food industry (Perez et al., 2014; Juturu and Wu, 2018), and both clinical and veterinary applications (Papo and Shai, 2005; Diez-Gonzalez, 2007; van Heel et al., 2011; Hu et al., 2018). According to their physicochemical properties, bacteriocins can cause perturbations of cell membranes (pore formation, followed by efflux of metabolites and ions), depolarization of membranes, inhibition of cell wall synthesis or septum formation, disruption of DNA replication and transcription, or interference at the ribosomal level preventing protein synthesis (Cotter et al., 2013; Verma et al., 2014; Johnson et al., 2018).

Different classifications of bacteriocins have been proposed. Cotter et al. (2013) subdivided bacteriocins into two main classes. Class I contains bacteriocins that undergo significant post-translational modifications and class II contains unmodified peptides but that can undergo only slight modification such as the formation of disulphide bridges or circularization. Recently, Alvarez-Sieiro et al. proposed a classification constituted of three classes, with emphasis on modified bacteriocins (Alvarez-Sieiro et al., 2016). Class I contains small post-translationally modified peptides, designed RiPPs (ribosomally synthesized, post-translationally modified peptides), and are <10 kDa; class II contains unmodified bacteriocins smaller than 10 KDa; and class III contains unmodified bacteriocins larger than 10 KDa and endowed with bacteriolytic or non-lytic mechanisms.

Class II bacteriocins of the lactic acid bacteria can be divided into four groups; Class IIa pediocin-like bacteriocins are peptides that containing a YGNGV motif; Class IIb contain two-peptide bacteriocins whose antimicrobial activity depends on the complementarity of the two peptide partners; Class IIc are circular bacteriocins; and class IId groups unmodified linear peptides, non-pediocin-like, single-peptide bacteriocins that do not fit into the three other groups (Cotter et al., 2013). This latter group is relatively diverse and includes a leaderless bacteriocin subgroup whose members are different from other bacteriocins. While most bacteriocins are synthesized with an N-terminal leader peptide, leaderless bacteriocins do not involve any N-terminal leader sequence for their export outside of the cell (Cotter et al., 2013).

Many leaderless bacteriocins with different characteristics have been recently described in the literature, overall constituting a large group. Leaderless bacteriocins can be composed of from one to four peptides. The leaderless single peptide bacteriocins include enterocin Q, aureocin A53, BHT-B, LsbB, lacticin Q, lacticin Z, weisselicin Y, weissellicin M, enterocin EJ97, enterocin K1, epidermicin NI01, lactolisterin BU, for review see Perez et al. (2018). The leaderless two-peptide bacteriocins group enterocin L50 (A, B), enterocin MR10 (A, B), enterocin DD14 (A, B), enterocin Ent7 (A, B) and enterocin A5-11 (A, B) (Cintas et al., 1998; Batdorj et al., 2006; Martín-Platero et al., 2006; Liu et al., 2011; Caly et al., 2017). The leaderless multi-peptide bacteriocins include aureocin A70 (A, B, C, D) (Netz et al., 2001) and garvicin KS (A, B, C), cereucin X (A, B, C), cereucin V (A, B, C), and cereucin H (A, B, C, D) (Ovchinnikov et al., 2016).

Enterocin DD14 is a two-peptide leaderless bacteriocin produced by *Ent. faecalis* 14 isolated from meconium at the Roubaix Hospital, in the north of France (Al Atya et al., 2015). The antagonistic activity of EntDD14 was reported against a panel of Gram-positive bacteria such as Staphylococcus aureus, Listeria monocytogenes, *Ent. faecalis*, Bacillus subtilis and *Clostridium perfringens*.

The scale-up production of bacteriocins requires an understanding of their genetic regulation and expression. Thus, it would be pertinent to identify the mechanisms involved in the secretion of EntDD14, a bacteriocin which lacks a transport signal domain. It has been reported that bacteriocin production is generally associated with the expression of specific immunity proteins, allowing protection of the bacteriocinogenic strain from the toxicity of its own bacteriocin (Bierbaum and Sahl, 2009; Nissen-Meyer et al., 2009). The leaderless bacteriocins are active immediately after their translation process (Perez et al., 2018). Their intracellular toxicity has been reported for lacticin Q (Iwatani et al., 2012), but many questions related to this topic remain to be solved. The self-immunity system would have to protect the bacteriocinogenic strain from both intra- and extracellular bacteriocins. To date there are little data in the literature reporting biosynthetic pathways of leaderless bacteriocins. Genes implicated in the secretion and immunity of aureocin A70 (Netz et al., 2001; Coelho et al., 2014), aureocin A53 (Nascimento et al., 2012) and lacticins Q and Z (Iwatani et al., 2012, 2013) have been experimentally confirmed. Interestingly, the protein LmrB, an ABC-type multi-drug transporter, has been reported to play a role in secretion and immunity of the leaderless bacteriocin, LsbB, and that of a non-leaderless bacteriocin, LsbA (Gajic et al., 2003). Here, the two-peptide leaderless bacteriocin EntDD14 has been investigated at the molecular level to decipher and better understand its role in the self-immunity system.

MATERIALS AND METHODS

Bacterial Strains, Plasmids, and Growth Conditions

Bacterial strains, plasmids and oligonucleotides used in this study are listed in **Tables 1**, **2**. Cultures of *Ent. faecalis, Listeria innocua* and *C. perfringens* strains were performed in M17 medium supplemented with 0.5% (w/v) of glucose (GM17) or in brain heart infusion (BHI) at 37°C under semi-aerobic or anaerobic conditions. Where necessary, media were supplemented with erythromycin (Em) (150 μg/mL) or chloramphenicol (Cm) (15 μg/mL). Growth of the cultures was followed by measuring the optical density at a wavelength of 600 nm (OD_{600}) with a spectrophotometer (Aquoalabo, France) and by determining cfu counts on agar plates. *Escherichia coli* strains were cultivated at 37°C in Luria-Bertani (LB) broth with vigorous shaking (160 rpm) or on LB agar medium. Where appropriate, ampicillin

TABLE 1 | Bacterial strains and plasmids used in this study.

Designation	Relevant characteristics	Reference
Strain		
Enterococcus faecalis		
14	Wild-type strain isolated from meconium	Al Atya et al., 2015
14 Δ*bac*	*Ent. faecalis* 14 *ddA* and *ddB* deletion mutant	This study
14 Δ*bac-Comp*	*Ent. faecalis* 14Δ*ddA/ddB* harboring pAT18:*ddA/ddB*	This study
14 Δ*ddl*	*Ent. faecalis* 14 Δ*ddl gene* deletion mutant	This study
14 Δ*ddl-Comp*	*Ent. faecalis* 14 Δ*ddl* harboring pAT18:*ddl*	This study
14 Δ*ddl*Δ*bac*	*Ent. faecalis* 14 Δ*ddl,* Δ*ddA* and Δ*ddB* deletion mutant	This study
14 Δ*ddl*Δ*bac-Comp*	*Ent. faecalis* 14Δ*ddl* Δ*ddA/ddB* harboring pAT18:*ddAB-HlJ*	This study
JH2-2	Fus^R Rif^R plasmid-free wild-type strain	Yagi and Clewell, 1980
JH2-2-*ddAB*	*Ent. faecalis* JH2-2 harboring pAT18:*ddA/ddB* of *Ent. faecalis* 14	This study
JH2-2-*ddAB-HlJ*	*Ent. faecalis* JH2-2 harboring pAT18:*ddAB-HlJ* of *Ent. faecalis* 14	This study
V583	Clinical isolate from blood. Van^R, Em^R	Sahm et al., 1989
Listeria innocua	*Listeria innocua* ATCC 33090	Bougherra et al., 2017
Clostridium perfringens	DSM756 corresponds to the type strainATCC®13124™ (type A, α+)	DSM
E. coli		
XL-1 Blue	*recA1 endA1 gyrA96 thi-1 hsdR17 supE44 relA1 Lac* [F' *proAB lacI* ^{q}ZΔM15Tn*10* (Tet^R)]	Stratagene
JM109	*recA1. endAl, gyrA96, thi. hsdR17, supE44, relA1, l-, A(iac-proAB), [F', traD36, proAB, iacl^{q}ZAM15]*	Yanisch-Perron et al., 1985
Plasmids		
pLT06	*lacZ*, P-*pheS* from pCJK47, *Cm* from pGB354, *orfB*, *orfC*, *repA* (*Ts*), *orfD* from pCASPER	Thurlow et al., 2009
pLT06Δ*ddAB*	pLT06 derivative carrying a 2.7 kb DNA fragment from *Ent. faecalis 14* harboring mutated *ddA* and *ddB* gene	This study
pLT06Δ*ddl*	pLT06 derivative carrying a 2.139 kb DNA fragment from *Ent. faecalis 14* harboring mutated *ddl* gene	This study
pAT18	Em^R, Tra $^-$, Mob $^+$, *lac*Za$^+$, *ori*R pUC, *ori*R pAMβI, MCS pUCl8	Trieu-Cuot et al., 1991
pAT18:*ddAB*	pAT18 derivative carrying a 0.64 kb DNA fragment from *Ent. faecalis* 14 with *ddA and ddB genes*	This study
pAT18:*ddl*	pAT18 derivative carrying a 0.765 kb DNA fragment from *Ent. faecalis* 14 with *ddl genes*	This study
pAT18:*ddAB-HlJ*	pAT18 derivative carrying a 1.43 kb DNA fragment from *Ent. faecalis* 14 with *ddAB* and *ddHlJ genes*	This study

Amp, ampicillin; Em, erythromycin; Fus, fusidic acid; Rif, rifampin; Str, streptomycin; Kan, kanamycin; Tet, tetracycline; Cm, chloramphenicol; bgaB, Beta-galactosidase; R, resistant; S, sensitive; Ts, thermosensitive.

(100 μg/mL), erythromycin (150 μg/mL) or chloramphenicol (10 μg/mL) was added to the medium. Bacterial stocks were stored at −80°C in GM17, BHI or LB broth supplemented with 50% (v/v) glycerol.

General Molecular Methods

Molecular cloning and other standard techniques were performed essentially as previously described (Sambrook and Russell, 2001). Antibiotics, chemicals, and enzymes were of reagent grade. Restriction endonucleases and T4 ligase were obtained from ThermoFicher Scientific and used in accordance with the manufacturer's instructions. Plasmids and PCR products were purified using NucleoSpin kits (Macherey-Nagel, Dünen, Germany) and the final plasmid constructions and the resulting deletion mutants were verified by PCR and sequencing (Eurofins, Ebersberg, Germany). The resulting sequences were analyzed using the SnapGenes tool (GSL Biotech LLC, CA). The strains were transformed by heat shock for *E. coli* and by electroporation for *Ent. faecalis* using Gene Pulser Apparatus (Bio-Rad Laboratories).

Antibacterial Activity Assays

The screening of antimicrobial activity of WT *Ent. faecalis* 14 and its isogenic mutant strains against the target bacteria was performed using well-diffusion and the spot-on-lawn methods (Caly et al., 2017). Briefly, BHI plates (1% agar) were inoculated with *L. innocua*, *C. perfringens*, *Ent. faecalis* JH2-2 and *Ent. faecalis* V583 strains and were allowed to dry. Then, 4 μL of a bacterial culture or 50 μL of culture supernatant/pure EntDD14 of the tested strain was spotted on the plate and incubated overnight at 37°C in appropriate conditions. The radius of the inhibition zone was measured from the edge of the well/spot to the edge of the inhibition halo. Antibacterial activity was quantified using the Arbitrary Units (AU) method (Cintas et al., 2000).

EntDD14 Purification and Quantification

A volume of 200 mL culture of *Ent. faecalis* 14 was grown for 24 h in GM17 medium at 37°C without shaking. The culture supernatant was harvested by centrifugation (8,000 rpm) and was incubated for 24 h at 4°C with CM Sephadex® C-25 (GE Healthcare Life Sciences, Milwaukee, WI). The resin was then washed with 5 bed volumes (BV) of 50 mM sodium phosphate (pH 6.3) and 5 BV of 0.5 M NaCl. The resin-bound bacteriocin was then eluted with 2 BV of 1.5 M NaCl. The EntDD14 was then further purified by gel filtration using PD MidiTrap G-10 columns (GE Healthcare Life Sciences) in Milli-Q water. The eluted solution was dried by miVac

TABLE 2 | Oligonucleotides used in this study.

Name	Sequence 5′→3′	Use
Construction of *Ent. faecalis* 14 Δ*bac mutant* and complementation		
Bac1F -PstI	AAAAAACTGCAGGAGGAACCCTTATTTTAAAGGATTC	Amplification of *ddA/ddB* up-stream fragment
Bac2R-Stop	CATTCACTAGGATCCTTAGACTTACTCCCATAATATATCTCCTCC	
Bac3F-Stop	TAAGTCTAAGGATCCTAGTGAATGGGTTAAAAAGACATTGATTTT	Amplification of *ddA/ddB* down-stream fragment
Bac4R -NcoI	AAAAAACCATGGCCGTGTATACTTTAGCCTTAGG	
Bac5F	CGGTGGATTATGAGACTGGAAC	Outer primer; verification of the plasmid integration
Bac6R	GCTCGATTTTTTTCCAATATTT	
BacF-screen	GTCTAAGGATCCTAGTGAATG	Screening of the mutants
Bac-compF-KpnI	AAAAGGTACCATCATGTTGATGACTAGAATCC	Complementation of Δ*bac* mutant
Bac-compR-BamHI	AAAAGGATCCAAGGATATACTTATTATTTCACAG	
ORIf	CAATAATCGCATCCGATTGC	Cloning verification in pLT06 plasmid
KS05seqR	CCTATTATACCATATTTTGGAC	
Construction of *Ent. faecalis* 14 Δ*ddl* mutant and complementation		
ddl 1F-PstI	ATTAAACTGCAGCGCCACTGAGCCAAAAGAAG	Amplification of *ddl* up-stream fragment
ddl 2R-Stop	CATTCACTAGGATCCTTAGACTTAGAGTTTAATCATTGTTTCACCG	
ddl 3F-Stop	TAAGTCTAAGGATCCTAGTGAATGGAATCTTTATGTAAACATGCG	Amplification of *ddl* down-stream fragment
ddl 4R-NcoI	ATTAAACCATGGCCTTCTAAAAGGAATTGTAAC	
ddl 5F	GGCGCGACCCTTATTTATAAG	Outer primer; verification of the plasmid integration
ddl 6R	GTGAACCTTTATCAAGGAGCC	
ddl -compF-BamHI	ATTAAAGGATCCGACTGGACTTAAAGAAAATGATTC	Complementation of Δ*ddl* mutant
ddl -compR-PstI	ATTAAACTGCAGCCTATCATGGTTAATACACTACG	
Construction of pAT18:*ddAB-HIJ*		
Op AF-KpnI	AAAAGGTACCATCATGTTGATGACTAGAATCC	Amplification of *ddA* and *ddB*
Op BR	ACCGACCTGCAGTAAACCGACAAC AAGGATATACTTATTATTTCACAG	
Op HF	GTTGTCGGTTTACTGCAGGTCGGTGATATAGGAGAAGATAATGAGTAA	Amplification of ABC transporter *ddHIJ*
Op JR-BamHI	AAAAGGATCCATGTGACAGCCTGTCTAATTC	
PU	GTAAAACGACGGCCAGT	Cloning verification in pAT18 plasmid
PR	CAGGAAACAGCTATGAC	

Underlined sequences correspond to the recognition sites of the restriction endonucleases mentioned in the primer name. The sequences underlined by a discontinuous line represent complementary sequences.

Sample Concentrators (SP Scientific NY-USA) and the dried samples were then resuspended in appropriate volumes of Milli-Q water to give the desired concentration. After each purification step, protein concentration was measured using a bicinchoninic acid assay (Sigma-Aldrich). The purity of the EntDD14 was verified by MALDI-TOF/MS analyses (Bruker Daltonics, Bremen, Germany) according to the recommendations of the manufacturer.

Sensitivity Assays to Pure EntDD14

To analyze the sensitivity of the *Ent. faecalis* 14 mutant strains, and other targets to the purified EntDD14, kinetics at 37°C in GM17 medium, supplemented with purified EntDD14 at a final concentration of 10 μg/mL, were performed in a 96-well microplate using a SpectraMax i3 spectrophotometer (Molecular Devices, CA, USA). The cultures were inoculated with the same bacterial charge thus giving the same initial OD_{600} of 0.2. Measurements were taken every 30 min at OD_{600} for 12 H. In parallel, the activity of EntDD14 (60 μg/mL) or serial dilutions of culture supernatant was also tested using the well-diffusion assay and the bacteriocin activity was expressed in AU/mL, which corresponds to the inverse of the last active dilution multiplied by 100 (Batdorj et al., 2006).

Construction of the Double Mutant Strain Δ*bac*

The double mutant strain Δ*bac* was constructed by allelic exchange using a method based on the conditional replication of the pLT06 vector (Thurlow et al., 2009). For this purpose, we used the *Ent. faecalis* 14 strain (Al Atya et al., 2015) to prepare the DNA template for PCR amplification using the Phusion™ High-Fidelity DNA Polymerase Mix (Thermo Fisher Scientific, Strasbourg, France). First, we amplified separately the upstream (900 bp) and downstream (1,057 bp) regions of the *ddA/ddB* genes using the primer pairs Bac1F-PstI/Bac2R-Stop and Bac3F-Stop/ Bac4R-NcoI, respectively (**Table 2**). The Bac3F-Stop and Bac2R-Stop primers share a complementary sequence of 24 bp, where four stop codons and the BamHI restriction site were inserted (**Figure S1**). To generate the entire DNA fragment harboring the mutated *ddA* and *ddB* genes, a second PCR was performed using the primer pair Bac1F-PstI/Bac4R-NcoI and the mix of the two previous amplified fragments as template DNA.

The resulting DNA fragment of 1,981 bp was excised from the electrophoresis agarose gel and purified. After digestion with appropriate restriction enzymes (*Pst*I and *Nco*I), this fragment was cloned into the pLT06 plasmid to generate pLT06Δ*ddAB* using the *E. coli* JM109 strain. This recombinant plasmid was used to transform *Ent. faecalis* 14 and clones were obtained on GM17 with 15 μg/mL of Cm at 30°C (the permissive temperature of the plasmid). To trigger the first cross-over (CO), cultures were grown for 2½ h at 30°C then shifted to 42°C for an additional 4 h in the presence of Cm. After serial dilutions, agar plates supplemented with 15 μg/mL Cm and X-Gal 80 μg/ml were inoculated. The larger blue colonies were verified by PCR using the outer primers Bac5F with one of the primers located on the plasmid (ORIf or KS05seqR). A colony from the 1st CO was cultured in the absence of selection pressure until the culture had reached stationary phase (∼2×10^9 cfu/mL). Serial dilutions were prepared and a new culture of ∼100 cfu/mL was inoculated and subsequently grown to stationary phase overnight. At this step, the chloramphenicol-susceptible clones underwent the 2nd CO and were screened for the deletion of the *ddA* and *ddB* genes. The BacFscreen primer (**Table 2**) was designed on the basis of the introduced modified sequence in place of the *ddA* and *ddB* sequence (**Figure S1**) thereby allowing the screening by PCR of the chloramphenicol-susceptible clones obtained after the second crossing-over event. When BacFscreen primer was used in combination with the Bac6R primer (located outside of the construct; **Figure S1**), only the double mutant strain Δ*bac* clones were able to produce a 1,132 pb DNA product. Moreover, PCR with Bac5F/Bac6R amplified a shorter fragment than that amplified in the wild-type, confirming that the deletion occurred in the structure of the *ddA* and *ddB* genes. Finally, the EntDD14 genetic environment of the obtained mutant clones was also verified by sequencing.

Construction of the Δ*ddI* Mutant Strain

To delete the gene *ddI* of *Ent. faecalis*14 corresponding to an ATP-binding protein of the ABC transporter, a strategy identical to that used to generate the Δ*bac* mutant strain was followed. Briefly, the upstream (1,128 bp) and downstream (987 bp) regions of the *ddI* gene were amplified using the primer pairs ddI 1F-PstI/ddI 2R-Stop and ddI 3F-Stop/ddI 4R-NcoI, respectively (**Table 2**). A second PCR using the primer pair *ddI* 1F-PstI/*ddI* 4R-NcoI was performed using the mix of the two previous amplified fragments as DNA template in order to obtain the entire DNA fragment harboring the mutated *ddI* gene. After that, the resulting DNA fragment was cloned into the pLT06 vector and the resulting plasmid pLT06Δ*ddI* was transformed into *E. coli* JM109 then into *Ent. faecalis* 14. After the 1st and 2nd CO events, the chloramphenicol-susceptible clones were screened for the deletion of *ddI* gene by PCR using BacFscreen/ddI 6R and ddI 5F/ddI 6R primer pairs. Finally, the genetic environment of the resulting mutant strains was verified by sequencing.

Construction of the Triple Mutant Strain Δ*I*Δ*bac*

The Δ*ddI* mutant strain was used to generate the *Ent. faecalis* 14 Δ*I*Δ*bac* triple mutant strain by using a double homologous recombination as described above. Competent *Ent. faecalis* 14 Δ*ddI* cells were transformed by the recombinant pLT06Δ*ddAB* plasmid and the same method was then used to obtain the triple mutant strain Δ*I*Δ*bac.* All these mutant strains and their required genetic correctness were checked by PCR and sequencing.

Complementation of *Ent. Faecalis* 14 Mutant Strains and Construction of *Ent. Faecalis* JH2-2 Harboring Structural and ABC Transporter Genes

For the complementation assays, a DNA fragment containing the entire *ddA, ddB* and the promoter region was obtained by PCR using Bac-compF-KpnI and Bac-compR-BamHI primers and cloned into pAT18 (**Table 1**). The recombinant plasmid pAT18:*ddAB* was used to transform competent cells of the Ent. faecalis 14 Δ*bac* mutant and Ent. faecalis JH2-2 after passing through *E. coli* XL-1 blue selected on LB, Em (150 μg/mL), X-gal (40 μg/mL) and IPTG (40 μg/mL). The colonies obtained on GM17 agar Em (150 μg/mL) after 48 h at 37°C, (Ent. faecalis 14Δ*bac comp* and JH2-2 pAT18:*ddAB*) were analyzed by PCR and sequencing for the presence of the recombinant plasmid. In the same way we complemented the Δ*ddI* mutant strain using the primers *ddI*-compF-BamHI and *ddI*-compR-PstI. To complement the Δ*I*Δ*bac* triple mutant strain, we constructed a pAT18:*ddAB-HIJ* containing the structural genes *ddA* and *ddB* and the *ABC* transporter module *ddH, ddI,* and *ddJ* intact genes. For this, a first PCR with the OpAF-KpnI/OpBR primer pair was used to amplify the *ddAB* genes including the promoter region. A second PCR with the Op HF/Op JR-BamHI primers amplified the *ddHIJ* genes of the ABC transporter. As the Op BR and Op HF primers share a complemented sequence of 24 bp (see **Table 2**), a PCR using the AF-*Kpn*I/Op JR-*Bam*HI primers was able to amplify the *ddAB-HIJ* genes. After digestion by *Bam*HI/*Kpn*I, the obtained fragment was cloned into the pAT18 vector to obtain pAT18:*ddAB-HIJ* (3,7 kb). This construction was used to transform the Δ*I*Δ*bac* mutant and *Ent. faecalis* JH2-2 strains leading to Δ*I*Δ*bac-Comp* and *Ent. faecalis* JH2-2-*ddAB-HIJ* strains, respectively.

RNA Isolation and Microarrays Analysis

For microarray analysis, three distinct cultures of *Ent. faecalis* 14Δ*bac* were used (Δ*bac1*, Δ*bac2* and Δ*bac3*) in order to compare with the *Ent. faecalis* 14 wild-type strain (WT1, WT2 and WT3), after 6 and 24 h of growth in GM17 medium. Analyses were performed with total RNA isolated using NucleoSpin™ RNA Plus columns (Macherey-Nagel, Hoerdt, France). RNA quality was verified with Nanodrop and absorbance ratios A260/280 and A260/230 were between 2.0 and 2.2. RNA quality was also examined with Bioanalyzer 2100 (Agilent, Les Ulis, France) and a minimal RNA integrity number (RIN) of 0.8 was required for all samples.

Agilent G2509F *Ent. faecalis* custom oligo-based DNA microarray (8 × 15 K) containing spots of 60-mer oligonucleotide probes (in duplicate) were used to study the gene expression profile. RNA amplification, staining, hybridization

TABLE 3 | The probes designed for microarray experiments.

Target gene	Probe sequence
ddA	GCAATTTATTGGAGAAGGATGGGCAATTAACAAAATTATTGATTG GATCAAAAAACATAT
ddB	ACAAACAAATTATGCAGTTTATCGGACAAGGATGGACAATAG ATCAAATTGAAAAATGGT
ddC	AAAGCAAGGTATTCACAAGATTCTTTAAAAGAGTATTTAGATATT CTTGTTTCTGAGGAT
ddD	TGAGTTTGAATGTAATTGTGTTGTTAGCGCTATTAGCTGTGCAAA CGTGGCTGATACCAA
ddE	AGGTTCAATTCTAGTTATAGGCATTGCAGGTTTGGTTCAAAC CATTATTGATCAAAAATT
ddF	ACGTGGGGTTACTGAGACACAAGTATCAAAAGTTTTTAAGGA GTTAAATAATAAAGAGAA
ddG	ACCCGGATCGCTCAATCCAGATAAAACTTTTTATCAAAAACT TGGCAATGATGGAATGGA
ddH	AAAAGCAACAGACGGAATAATTACTGAAATTAACGCACTGCC TGAAGAGATGGCTGTCAG
ddI	TAACGCTTATTATGGTTACGCACAACCCTGAAGTCGTTCCTTATT GTCACCGGTTGATTA
ddJ	TTATTAGCAGTTGGCGTCTCTTCAGTTATTGGCCTAGTTTTCTCT GTAATGCCTGCATCA

and washing were conducted according to the manufacturer's instructions. Slides were scanned at 5 μm/pixel resolution using the GenePix 4000B scanner (Molecular Devices Corporation, Sunnyvale, CA, USA). Images were used for grid alignment and expression data digitization with GenePix Pro 6.0 software. Expression data were normalized by Quantile algorithm. To ascertain the quality of normalized data, filtering of data was mandatory for flagged signals. Expression data from the 3 wild-type samples were filtered for $p < 0.05$ and the average was calculated for each gene. Genes of interest were selected for this study (*ddABCDEFGHIJ*) and the log2 ratio from individual Δ*bac* samples and the mean of WT samples was calculated. The corresponding probes designed for these genes are shown in **Table 3**.

Bioinformatics Analysis

The *Ent. faecalis* 14 genome sequence was obtained from GenBank under accession number CP021161. Here, different databases and bioinformatics tools were used to analyze the DNA sequences and predict the EntDD14 operon organization, with location of putative promoters and terminators. This analysis included the Basic Local Alignment Search Tool of the National Center for Biotechnology Information (BLAST-NCBI: https://blast.ncbi.nlm.nih.gov/Blast.cgi), the SnapGene®4.3.7 tool, the Softberry software for analysis of bacterial genomes (http://www.softberry.com), the ARNold program (http://rssf.i2bc.paris-saclay.fr/toolbox/arnold/index.php#Results) and the RibEx program (Abreu-Goodger and Merino, 2005)

Statistical Analysis

Differences between samples were calculated using the Student test. $P \leq 0.05$ were considered to be significant.

RESULTS

Genetic Environment of EntDD14 Encoding DNA

Previous sequencing of the *Ent. faecalis* 14 genome showed that the EntDD14 encoding genes are chromosomal determinants (Belguesmia et al., 2017). *In silico* analysis of the genetic neighborhood of the EntDD14 structural genes revealed a cluster of 10 open reading frames (ORFs) *ddABCDEFGHIJ* (**Figure 1**). This cluster encodes two-peptide leaderless bacteriocins (DdA and DdB), five unknown proteins (DdC, D, E, F, and G) and a putative ABC transporter (DdH, I and J) (**Table 4**). The sequence alignment of this 6.5kb region with the BLAST-NCBI showed a high homology with the translated two-peptide leaderless bacteriocin regions of other known enterococci such as *Ent. faecalis* DBH18 (GenBank ID: EF502034.2) (Arbulu et al., 2016), *Ent. faecalis* KB1 (GenBank ID: CP022712.1), Ent. faecalis plasmid Efsorialis-p1 (GenBank ID: CP015884.1), *Ent. faecium* SRCM103341 plasmid (GenBank ID: CP035137.1), *Ent. faecium* strain FA3 plasmid (GenBank ID: CP042833.1), *Ent. faecium* strain 6T1a plasmid pEF1 (GenBank ID: DQ198088.1), *Ent. faecium* strain HB-1 plasmid (GenBank ID: CP040877.1), *Ent. faecium* strain SRCM103470 plasmid (GenBank ID: CP035221.1), *Ent. faecium* strain Gr17 plasmid pGR17 (GenBank ID: CP033377.1) and *Ent. faecium* strain 4928STDY7387800 (GenBank ID: LR607382.1). Noteworthy, the sequence analysis by the *Bacterial Operon and Gene Prediction* (http://www.softberry.com) predicted three operons. The first operon consisted of the *ddAB* genes, the second contained the *ddCDEFGH* genes and the third consisted of the two *ddIJ* genes (**Figure 1**). The structural genes *ddA* and *ddB* are expected to be co-transcribed as only one promoter has been detected upstream of the *ddA* gene and a clear processing site motif of 48 bp was detected between the *ddB* and *ddC* genes (**Figure 2**). The alignment of the DdA and DdB peptides with all other known two-peptide leaderless bacteriocins displayed a very high degree of identity. In this sense, EntDD14 was identical to MR-10 and Ent7 produced by *Ent. faecalis* MRR 10-3 (Martín-Platero et al., 2006) and *Ent. faecalis* 710C (Liu et al., 2011), respectively (**Figure 3**). Moreover, DdA and DdB were 98 and 95% identical to the corresponding peptide of L50 and A5-11 bacteriocins produced, respectively, by *Ent. faecium* L50 (Cintas et al., 2000) and *Ent. durans* (Batdorj et al., 2006; Belguesmia et al., 2013). Interestingly, all the bacteriocinogenic strains above-cited share at least a set of 3 genes, which are highly homologous to the second ABC transport system (As-48FGH) described for the cyclic bacteriocin AS-48 (Diaz et al., 2003) (**Figure 1**).

Antimicrobial Activity of *Ent. Faecalis* 14 Is Solely Due to EntDD14

The antibacterial activity of *Ent. faecalis* 14 against *L. innocua, C. perfringens*, *Ent. faecalis* JH2-2 and *Ent. faecalis* V583 was solely attributable to EntDD14, and not to any other potential antibacterial agent, which could be produced by the WT strain. Indeed, the Δ*bac* mutant strain, deleted in *ddA* and *ddB* genes, was completely devoid of any antibacterial activity despite the comparable pH values of the supernatants

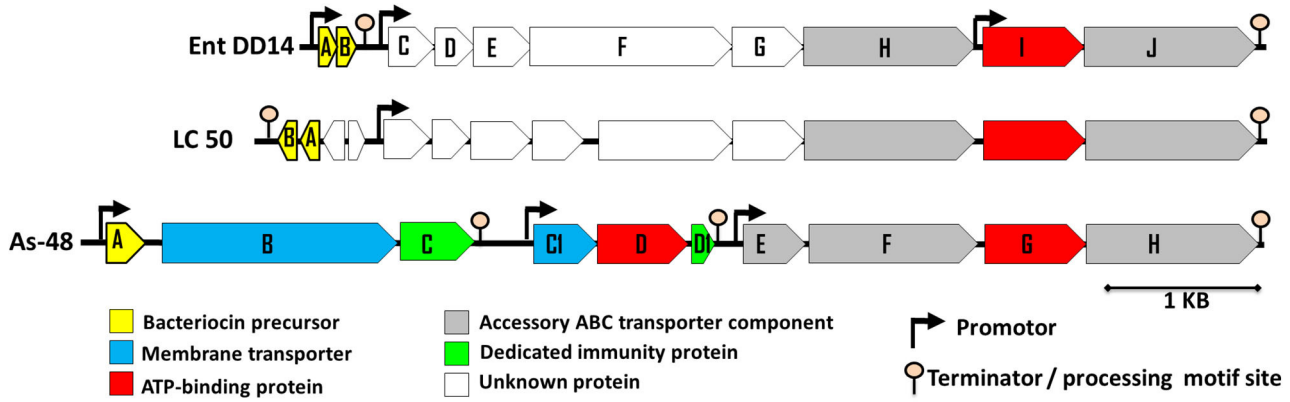

FIGURE 1 | Genetic organization of *Ent. faecalis* 14 predicted ORFs. The genetic organization of *Ent. faecalis* 14 is compared to that of *Ent. faecalis* LC50 and to that of *Ent. faecalis* AS48 that are shown on the figure and produce enterocins L50AB and AS-48, respectively. The predicted promoters and ORFs were obtained using *Softberry* software.

TABLE 4 | Characteristics of the predicted ORF products of DD14 gene *locus*.

ORF	Size (aa)	PI	MW	TM	Average of hydrophobicity	Characteristics of encoded protein
ORF A	44	10	5176.35	0	0.202273	Peptide A of two-peptide leaderless bacteriocin
ORF B	43	10.22	5182.27	0	−0.109302	Peptide B of two-peptide leaderless bacteriocin
ORF C	89	8.57	10578.27	0	−0.555056	DUF2089 family protein. Soluble. Unknown function
ORF D	90	9.70	0702.05	2/3*	0.748889	Membrane protein. Unknown function
ORF E	135	9.54	15998.46	2	0.548148	Membrane protein YdbT. contains bPH2 domain
ORF F	458	9.43	54950.64	7/6*	0.281441	Membrane protein. PH domain-containing protein
ORF G	163	8.95	18588.34	4	0.668712	Membrane protein. Unknown function
ORF H	406	5.88	45035.10	1	−0.547044	Periplasmic component of efflux system
ORF I	227	6.10	25716.70	0	−0.192952	ABC transporter ATP-binding protein. ATPase
ORF J	399	9.15	44043.23	4	0.044361	ABC transporter. FtsX-like permease family protein

**Result obtained using TMHMM program (http://www.cbs.dtu.dk/services/TMHMM/).*

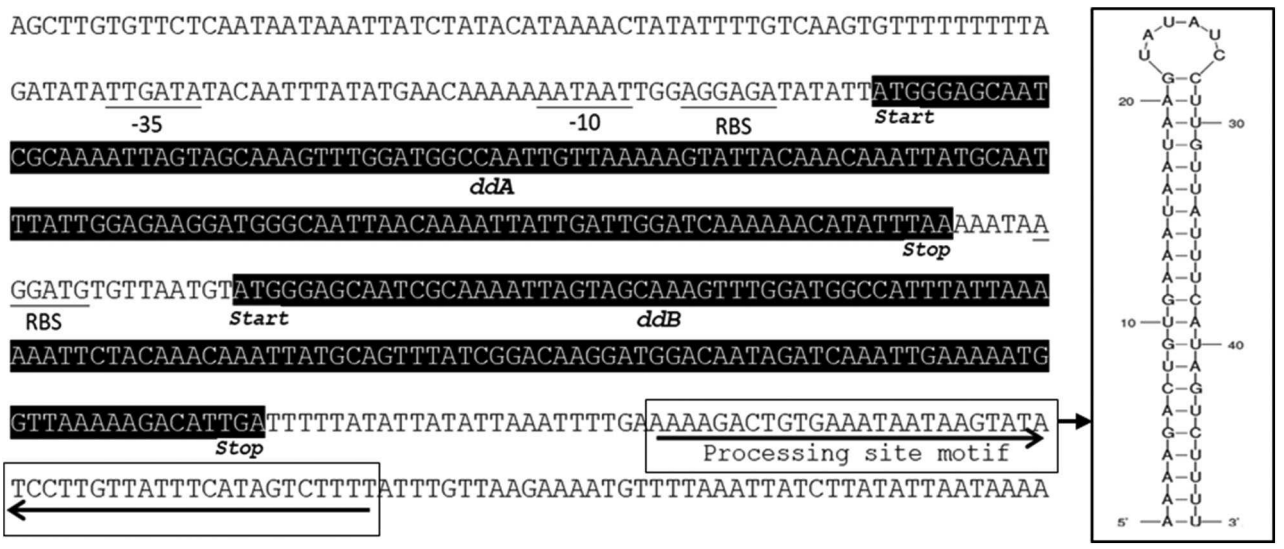

FIGURE 2 | Genetic characterization of the *ddA* and *ddB* structural genes. The processing site motif has been detected by using both ARNold and RibEX programs.

Peptide	Sequence	Identities	Positives
DdA	MGAIAKLVAKFGWPIVKKYYKQIMQFIGEGWAINKIIDWIKKHI		
Ent7A	MGAIAKLVAKFGWPIVKKYYKQIMQFIGEGWAINKIIDWIKKHI	100%	100%
MR10A	MGAIAKLVAKFGWPIVKKYYKQIMQFIGEGWAINKIIDWIKKHI		
L50A	MGAIAKLVAKFGWPIVKKYYKQIMQFIGEGWAINKIIEWIKKHI	98%	100%
A5-11A	MGAIAKLVAKFGWPIVKKYYKQIMQFIGEGWAINKIIEWIKKHI		
DdB	MGAIAKLVAKFGWPFIKKFYKQIMQFIGQGWTIDQIEKWLKRH		
Ent7B	MGAIAKLVAKFGWPFIKKFYKQIMQFIGQGWTIDQIEKWLKRH	100%	100%
MR10B	MGAIAKLVAKFGWPFIKKFYKQIMQFIGQGWTIDQIEKWLKRH		
L50B	MGAIAKLVTKFGWPFLKKFYKQIMQFIGQGWTIDQIEKWLKRH	95%	95%
A5-11B	MGAIAKLVTKFGWPLIKKFYKQIMQFIGQGWTIDQIEKWLKRH	95%	95%

Yellow: homologous residues in all peptides
Red: Different residues in peptides A and B separately

FIGURE 3 | Alignment of the EntDD14 peptides with other leaderless two-peptide bacteriocins. The EntDD14 peptides (A and B) are aligned with the corresponding peptides of Ent 7, MR-10, L50, and A5-11 produced by *Ent. faecalis* 710C, *Ent. faecalis* MRR 10-3, *Ent. faecium* L50, and *Ent. Durans,* respectively.

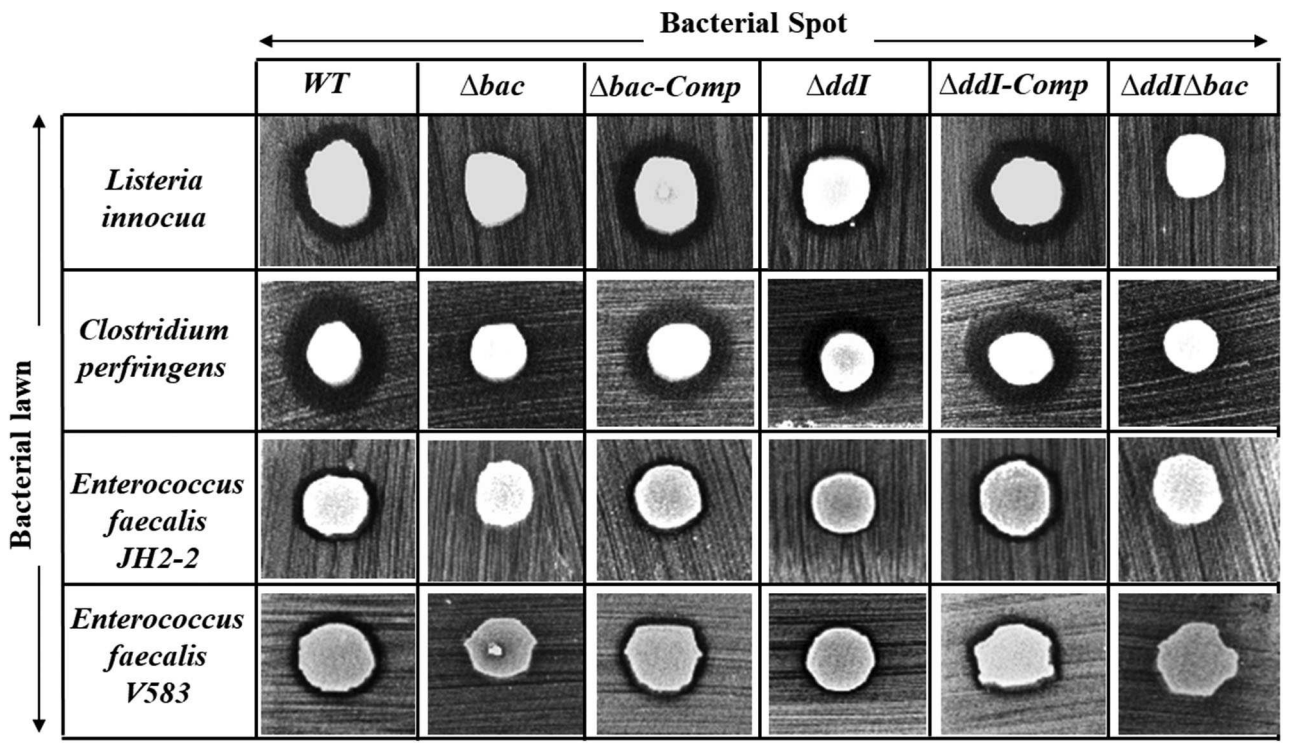

FIGURE 4 | Antimicrobial activity of *Ent. faecalis* 14 wild-type, its null and complemented mutant strains against *Listeria innocua*, *Clostridium perfringens*, *Enterococcus faecalis* JH2-2 and *Enterococcus faecalis* V583. Δ*bac*: *Ent. faecalis* 14 mutant deleted in *ddA* and *ddB* bacteriocin structural genes, Δ*bac*-Comp: the Δ*bac* complemented strain, Δ*ddI*: *Ent. faecalis* 14 mutant deleted in *ddI* gene, Δ*ddI-Comp*: the Δ*ddI* complemented strain, Δ*ddI*Δ*bac*: *Ent. faecalis* 14 mutant deleted in *ddI*, *ddA,* and *ddB* genes. If present, the inhibition zone indicated the susceptibility of the bacterial lawn (target bacteria) to the produced EntDD14 bacteriocin. The data are representative of at least three independent experiments.

obtained from the mutant and the WT strains. Noteworthy, after 24 h of culture, the supernatant final pH measured was 5.12 for the WT strain and 4.87 for the Δ*bac* mutant strain. This slight difference in pH values could be explained by the basic nature of the two peptides of EntDD14 produced by the WT strain. Similar data were obtained with the WT vs. the Δ*ddI*Δ*bac* triple mutant strain (**Figure 4**), which strengthens this argument. Trans-complementation assays conducted upon cloning the *ddA* and *ddB* genes into the Gram-positive replicative plasmid pAT18 recovered the WT phenotype in the Δ*bac* mutant

strain as shown by the complemented strain *Ent. faecalis 14* Δ*bac-Comp* phenotype. Therefore, production of EntDD14 was comparable between the WT and the *Ent. faecalis 14* Δ*bac-Comp* complemented strains (**Figure 4**). Thus, the inhibition potency of *Ent. faecalis* 14 was exclusively due to EntDD14 production, and not to any other factor such as pH decrease or organic acid production, which occur in LAB during glucose metabolism.

The Role of the ABC Transporter in the Transport of EntDD14

Bacterial ABC transporters are often composed of an ATP-binding protein and one or more accessory proteins (Beis and Rebuffat, 2019). In the EntDD14 locus, the ABC transporter is located downstream of the structural genes encoding for the EntDD14 enterocin. As shown in **Figure 1** and **Table 4**, the ABC transporter associated with EntDD14 production contained at least three genes named *dd-H, I,* and *J*. The gene *ddH* encodes a putative efflux system protein YvrP. The *ddI* gene encodes an ABC transporter ATP-binding protein of the ATPase family, and the *ddJ* gene encodes a putative macrolide export ATP-binding/permease protein (MacB). Our results show that this ABC transporter is involved in the active transport of intracellular EntDD14 peptides to the outside of the membrane. Indeed, the mutant deleted in the *ddI* gene encoding an ATP binding cassette of the ABC transporter has considerably reduced the production of EntDD14, comparative to the WT strain (**Figure 4**). Indeed, the Δ*ddI* mutant strain produced only 25% of the EntDD14 produced by the WT strain. This rate was based on the anti-*Listeria* activity of the Δ*ddI* mutant strain (200 AU/mL) compared to the WT (800 AU/mL). The levels of EntDD14 production were restored when the Δ*ddI* mutant strain was complemented with a functional *ddI* gene cloned into pAT18 vector (*Ent. faecalis* Δ*ddI-Comp*) (**Figure 4**), arguing the role of this putative transporter in the active export of EntDD14. Nevertheless, this result suggested that additional systems are also exporting EntDD14 outside of the cell, as this mutant strain, was still producing about 25% of EntDD14 compared to the WT strain. To check whether other non-specific enterococcal transporters were involved in EntDD14 export, we transformed the non-bacteriocinogenic and sensitive *Ent. faecalis* JH2-2 strain with the EntDD14 precursor including its promoter region and structural *ddA* and *ddB* genes cloned into the pAT18 vector. No production of EntDD14 was observed in the resulting strains (data not shown).

The Contribution of the ABC Transporter to the Immunity System Against Exogenous EntDD14

ABC transporters can contribute to bacteriocin immunity by pumping bacteriocins to the outside of the cell membrane (Diaz et al., 2003; Sánchez-Hidalgo et al., 2003; Beis and Rebuffat, 2019). To better understand the role of the ABC transporter in immunity to EntDD14, we performed sensitivity tests to EntDD14 by the well-diffusion method and also by growth kinetics in the presence of purified EntDD14 (10 μg/mL). Unexpectedly, the Δ*ddI* mutant strain did not exhibit any sensitivity to EntDD14 even at highest concentration (60 μg/ml) nor to the cell-free supernatant (CFS) obtained from the WT strain (**Figure 5**). Notably, EntDD14's MIC values were similar to those obtained for the WT (resistant phenotype). Growth kinetics in the presence of EntDD14 at 10 μg/mL showed no significant differences between the WT strain, the Δ*ddI* mutant strain and the complemented *ddI-Comp* strain (**Figure 6A**). These results refuted therefore the involvement of an ATP-binding protein/ATPase transporter in the self-immunity system of EntDD14. In order to unravel the role of the entire ABC transporter (*ddHIJ*) in the mechanism of immunity, we constructed a recombinant plasmid pAT18:*ddAB-HIJ* which we used to transform the sensitive *Ent. faecalis* JH2-2 strain. In this case, if the ABC transporter played a dual transport and immunity function, then this construction would be sufficient to produce EntDD14 and to immunize the host strain against the inhibitory action of EntDD14. Unexpectedly, the obtained clones of *Ent. faecalis* JH2-2-*ddAB-HIJ* were unable to produce EntDD14. In addition, growth kinetics in the presence of 10 μg/mL of EntDD14 showed the sensitive phenotype of *Ent. faecalis* JH2-2 compared to the WT strain. Overall, no significant difference was observed between *Ent. faecalis* JH2-2 and the transformed strain, JH2-2-*ddAB-HIJ* (**Figure 6B**). To verify the integrity of the pAT18:*ddAB-HIJ* construction, we used it in order to complement the Δ*bac* double mutant strain, which is deleted in both *ddA* and *ddB,* and also to transform the Δ*ddI*Δ*bac* triple mutant strain, which is deleted in genes *ddA, ddB* and *ddI* of the ABC transporter. Remarkably, the WT phenotype was restored in both cases. Indeed, the pAT18:*ddAB-HIJ* construction transformed the Δ*bac* mutant strain to a producer strain and the resulting transformed strain Δ*ddI*Δ*bac* produced as much EntDD14 as the WT (data not shown).

All these data ruled out the involvement of the ABC transporter in the primary self-immunity system of the two peptides leaderless bacteriocin EntDD14. Moreover, the precursor genes *ddAB* and ABC transporter genes *ddHIJ* in themselves seem to be insufficient to produce EntDD14.

Intracellular EntDD14 Is Involved in the Self-Immunity System

Mutants obtained during this study were screened for their susceptibility to bacteriocin EntDD14. Of importance, the Δ*bac* mutant strain appeared to be sensitive to its own bacteriocin. This was observed not only when the mutant strain was treated with pure EntDD14 at 60 μg/mL but also when it was exposed to the supernatant of the WT strain, or to that of the less producing strain Δ*ddI* (**Figure 5**). During growth in the presence of 10 μg/ml of EntDD14, the Δ*bac* mutant strain extended its lag phase and entered the exponential growth phase only after 5 h of incubation (**Figure 6C**). The OD_{600} values obtained after 12 h of growth were significantly different between the WT strain and the Δ*bac* mutant strain ($P = 0.0001$). The trans-complementation experiment using the pAT18-*ddAB* construction allowed the Δ*bac* mutant strain to recover its resistance to EntDD14 (**Figures 5**, **6C**). To confirm this result, we constructed a Δ*bac* mutant in a host strain other than *Ent. faecalis* 14, and thus

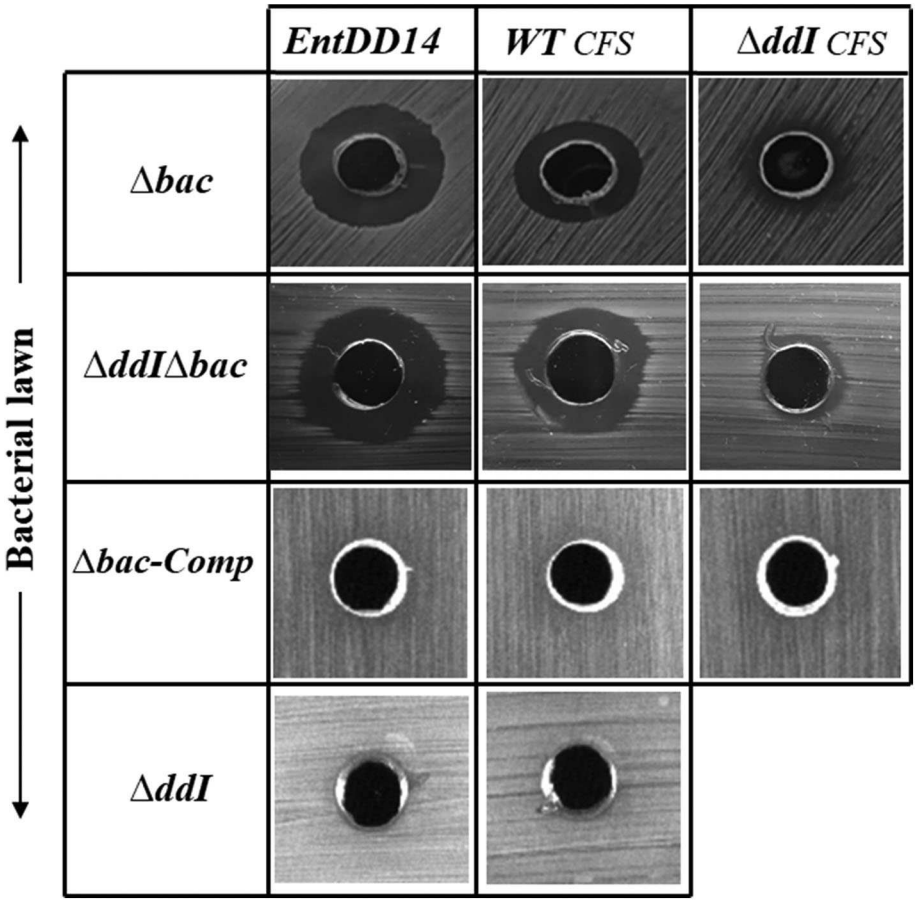

FIGURE 5 | Sensitivity of the *Ent. faecalis* 14 mutant and complemented strains to pure EntDD14 at 60 μg/mL, cell free supernatant (CFS) of the wild-type strain and that of the Δ*ddI* mutant. Δ*bac*: *Ent. faecalis* 14 mutant deleted in *ddA* and *ddB* bacteriocin structural genes, Δ*ddI*Δ*bac*: *Ent. faecalis* 14 mutant deleted in *ddI*, *ddA,* and *ddB* genes, Δ*bac*-Comp: the Δ*bac* complemented strain and Δ*ddI*: *Ent. faecalis* 14 mutant deleted in *ddI* gene. If present, the inhibition zone indicates the susceptibility of the bacterial lawn (target bacteria) to EntDD14. The data are representative of at least three independent experiments.

selected the *Ent. faecalis* 14 Δ*ddI* mutant strain. This strain was resistant to EntDD14 and produced about 25% of this bacteriocin compared to the WT strain. As expected, Δ*ddI*Δ*bac* did not produce EntDD14 and was found to be sensitive to this bacteriocin, like the Δ*bac* mutant strain (**Figures 5**, **6D**). The complementation of this triple mutant with the pAT18:*ddAB-HIJ* construction fully restored the phenotype of the WT strain, which displayed almost identical kinetics in the presence of EntDD14 at 10 μg/mL (**Figure 6C**). Taken together, these results highlight the clear role of intracellular EntDD14 in the mechanism of its own immunity.

Gene Expression Analysis of EntDD14 Cluster

To explain the sensitive phenotype of the Δ*bac* mutant strain to EntDD14, we checked whether the genes *ddCDEFGHIJ* were expressed in this strain. To this end, we used data generated from a comparative transcriptomic analysis of the Δ*bac* mutant strain vs. the WT, after 6 and 24 h of growth in GM17 medium. The gene expression analysis did not reveal any significant differences between these strains after 6 h of growth except for the *ddF* gene which was slightly down-regulated, as the log2 ratio Δ*bac*/WT ranged from −1 to 1 (**Figure 7** and **Table S1**). Interestingly, all analyzed *ddCDEFGHIJ* genes were found to be significantly down-regulated in the Δ*bac* mutant strain after 24 h of growth in GM17 (**Figure 7** and **Table S1**). Moreover, mean gene expression showed that *ddI*, *ddE* and *ddJ* genes were the most deregulated with log2 Δ*bac*/WT ratios of − 2.86, − 1.78, and − 1.70, respectively (**Table S1**). Finally, as expected, *ddA* and *ddB* encoding the structural genes were highly down-regulated in the Δ*bac* mutant strain at both 6 and 24 h since they were deleted in this host (**Figure 7** and **Table S1**).

DISCUSSION

Bacteriocins are known for their effectiveness in fighting and eradicating microbial pathogens (Quintana et al., 2014; Graham et al., 2017; Johnson et al., 2018). Interactions of these charged antimicrobial peptides with cell membrane leads to the formation of ion-permeable channels, resulting in perturbation of ion

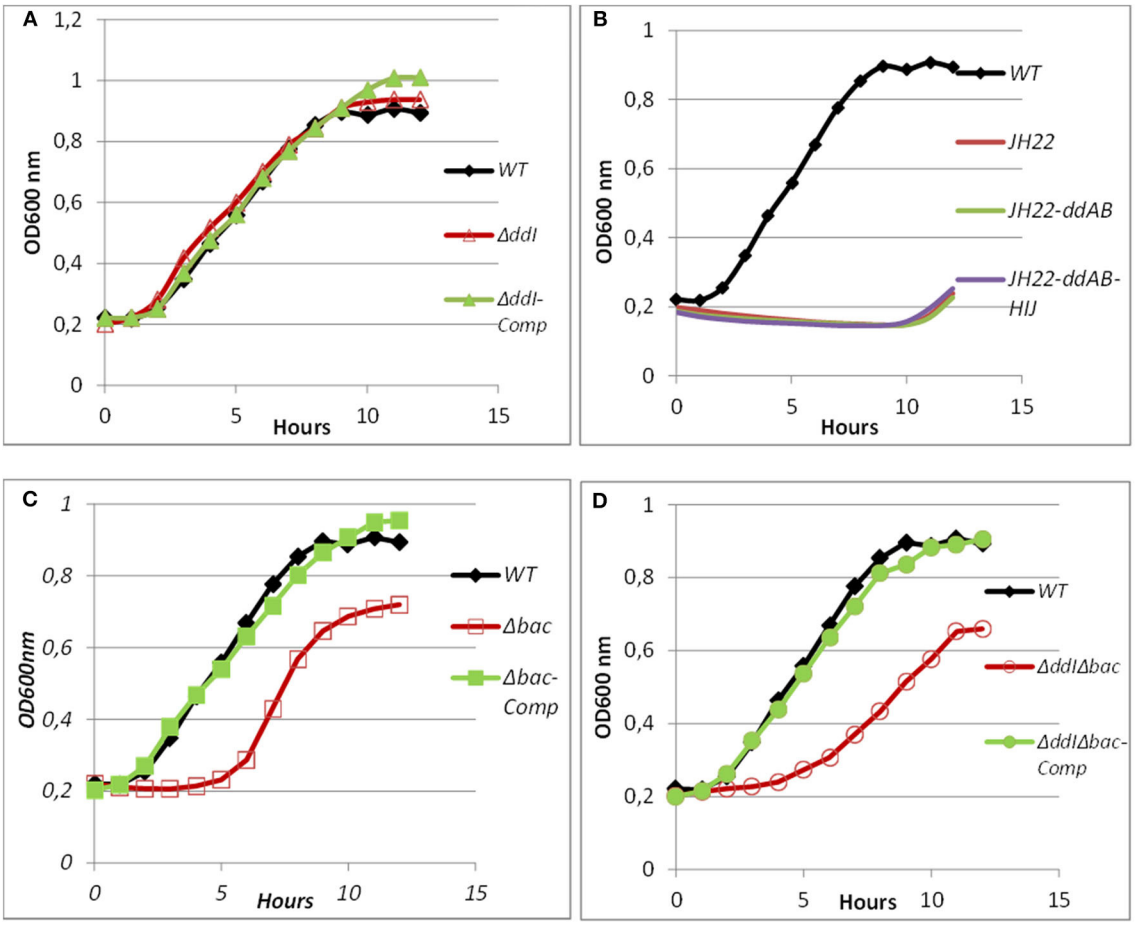

FIGURE 6 | Growth curves of WT, mutated and complemented *Ent. faecalis* 14 strains in the presence of pure EntDD14 at 10 μg/mL. *Ent. faecalis* 14 WT (♦) **(A)**: Δ*ddI* mutant (△) and the Δ*ddI* complemented strain (▲); **(B)**: *Ent. faecalis JH2-2* (red line) *Ent. faecalis* JH2-2-*ddAB* (green line) and *Ent. faecalis JH2-2-ddAB-HIJ* (purple line); **(C)**: Δ*bac* mutant (□) and the Δ*bac* complemented strain (■); and **(D)**: Δ*ddI*Δ*bac* mutant (○) and the Δ*ddI*Δ*bac* complemented strain (•).The data are the means of at least three independent experiments.

gradients by passive efflux of vital intracellular metabolites, such as ions, amino acids and ATP, which causes serious metabolic disruption and finally cell death (Karpinski et al., 2016). At the molecular level, bacteriocin production requires complex machinery consisting of the transcription-translation processes, transport out of the cell, and also immunity mechanisms to protect the strain from the toxicity of its own products (Bastos et al., 2015; Bountra et al., 2017).

Leaderless bacteriocins are active after their translation, and do not undergo significant post-translational modifications or processing. Therefore, bacteria producing such bacteriocins have certainly specific immunity systems that ensure their protection from the toxicity of their own peptides. This protection is expected to be ascertained from the translation step until their export outside of the cell. Of note, no-dedicated immunity proteins have been reported for leaderless two-peptide bacteriocins. Only the role of export and immunity of the ABC transporter has been described. Several mechanisms of self-immunity have been described for many bacteriocins. These involve for the well-known nisin, a lipoprotein, designed NisI, which is able to bind and thereby prevent nisin to access its predicted target lipid II through direct interactions (Hacker et al., 2015). In direct line, Abi proteins, which are putative membrane-bound metalloproteases, have been reported to play a role in the self-immunity of bacteriocins (Kjos et al., 2010). Using EntDD14 as a representative model of this category of bacteriocins, based on its high homology with other known leaderless two peptides bacteriocins (**Figure 3**), we have undertaken a genetic study to obtain relevant information on the immunity system of two-peptide leaderless bacteriocin-producers. First, an *in silico* genetic analysis of the EntDD14 bacteriocin region predicted a least 10 ORFs (*ddABCDEFGHIJ*), which could be organized into three closed operons. As shown in **Figure 2**, predictions of mRNA folding, using ARNold and RibEX algorithms permitted the location of a potential secondary structure between *ddB and ddC,* suggesting a possible post-transcriptional regulation, in which the synthesis of peptides A and B can be dissociated from the translation of other genes. To the best of our

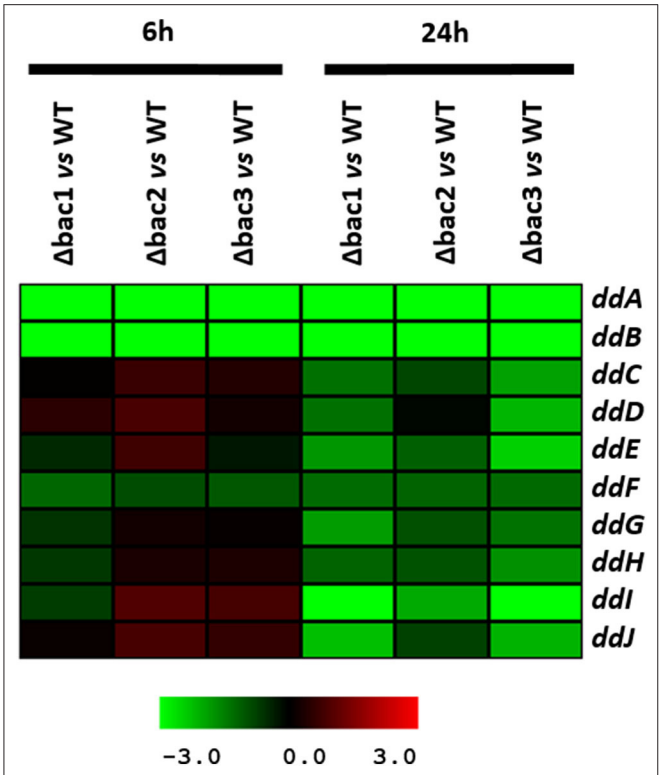

FIGURE 7 | Profile of the EntDD14 predicted ORFs in Δ*bac vs.* WT strain. Log2 ratios were registered for three biological repetitions after 6 and 24 h of growth in GM17 medium.

knowledge regulation and expression of bacteriocins at the post-transcriptional level has been reported only for the cyclic Enterocin AS-48 (Fernández et al., 2008).

Here, a BLAST analysis of the proteins encoded by the EntDD14 gene cluster did not reveal any significant homology with other known dedicated immunity proteins. However, sequence alignment established that the *ddHIJ* genes share significant similarities with several of the ABC transporters found in most leaderless, and cyclic bacteriocins, despite the absence of sequence similarities for the structural genes encoding these bacteriocins (Cintas et al., 2000; Diaz et al., 2003; Iwatani et al., 2012; Nascimento et al., 2012). These data support a potential relationship in the mediated mechanisms (production and/or immunity) and a close structural feature between leaderless and cyclic bacteriocins (Towle and Vederas, 2017; Perez et al., 2018). In the case of EntDD14, the ABC transporter was found to be involved in bacteriocin export, as a Δ*ddI* mutant strain, affected in an ATP-binding protein of the ATPase family, could produce only 25% of bacteriocin compared to the wild-type strain. Similar results were reported for the leaderless single peptide aureocin 53. Indeed, the aureocin 53 bacteriocinogenic strain could produce only 24% of this bacteriocin when the ABC transporter *aucEFG* was affected in the first gene *aucE* (Nascimento et al., 2012). Here, we established that in the Δ*ddI* mutant, production of EntDD14 was not completely abolished, indicating that another export pathway is also used by the bacteriocinogenic strain. Unexpectedly, the susceptible *Ent. faecalis* JH2-2 strain was unable to produce EntDD14 when transformed by the *ddAB* genes. In terms of the bacteriocin export pathways, it was established that enterocin L50 can be successfully expressed heterologously in two yeast expression systems through the general secretory pathways (Basanta et al., 2009, 2010), suggesting a possible use of another transport pathway. Here, the *ddF* gene, which encodes a putative pH domain protein, was found to be down-regulated after 6 h and 24 h of growth in the Δ*bac* mutant but not in the wild-type strain (**Figure 7**, **Table S1**). The *ddF* gene displayed 23% identity (and 42% of positive residue) with *orf8* of the pRJ9 plasmid of *S. aureus* (Netz et al., 2002). Remarkably, in *S. aureus*, the disruption of this gene abolished bacteriocin production (Nascimento et al., 2012). Therefore, we can hypothesize that *ddF* gene might play a role in the export of EntDD14.

The three-component ABC transporters, which are similar to those of *ddHIJ,* were previously shown to contribute to bacteriocin immunity by active extrusion of the peptide, most likely by reducing the concentration of the bacteriocin in direct contact with the cytoplasmic membrane (Klein and Entian, 1994; Siegers and Entian, 1995; Yarmus et al., 2000). Similarly, Rincé et al. (1997) reported that the self-immunity to the lantibiotic lacticin 481 was abolished when any *lctE*, *lctF*, or *lctG* gene was deleted (Rincé et al., 1997).

Taking into consideration all these published data, and in order to gain novel insights into the immunity systems of two-peptide leaderless bacteriocins, we looked at the role of the ABC transporter in the synthesis and immunity of EntDD14. To this end, we tested the sensitivity of the Δ*ddI* mutant strain to EntDD14, and also by cloning *ddAB-HIJ* genes and studying their effects in the sensitive *Ent. faecalis* JH2-2 strain. Consequently our data were in discordance with those formerly reported. Indeed, the Δ*ddI* mutant strain, as well as the WT strain were resistant to EntDD14 (up to 60 μg/mL) (**Figures 5**, **6A**). Furthermore, cloning and expression of the full ABC transporter in *Ent. faecalis* JH2-2 strain did not grant any resistance to EntDD14 even at low concentrations (**Figure 6B**). Although cloning of the entire ABC transporter did not allow the *Ent. faecalis* JH2-2 strain to gain resistance to exogenous EntDD14, this does not necessarily rule out the role of this ABC transporter in the detoxification of intracellular EntDD14. This has already been attributed to the ABC transporter for aureocin 53, which contains two other immunity proteins named AucIA and AucIB (Nascimento et al., 2012). AucIA and AuIB exhibited, respectively, 28 and 29% identity with the proteins encoded by *ddD* and *ddC.* These homologies were even higher, 52 and 60%, when compared to the products of DdC and DdD, and their aureocin counterparts AucIA and AucIB, suggesting therefore that the DdC and DdD proteins could be good candidates for studying the immunity of bacteriocinogenic *Ent. faecalis* 14.

Considering the different genetic constructions, their expression and phenotypes, we assume that intracellular EntDD14 plays a role in its own immunity system. This original finding was strengthened by the phenotypes of the Δ*bac* and Δ*ddI*Δ*bac* mutant strains, which exhibited sensitivity

to EntDD14, as opposed to the WT and the complemented strains (**Figure 5**). At low EntDD14 concentration, the Δ*bac* and Δ*ddI*Δ*bac* mutant strains showed an extended lag phase and a final OD_{600} significantly below that of the WT strain (**Figures 6C,D**), pointing again to the role of the intracellular EntDD14 in its own immunity system. The sensitivity of null-mutant strains was not ascribed to shut-down of expression of the *ddCDEFGHIJ* genes, as mostly these genes were expressed during the log phase of the Δ*bac* mutant strain (**Figure 7**, **Table S1**).

The comparative study of the gene expression of the Δ*bac* mutant strain vs. WT strain underpinned the role of EntDD14 in the positive regulation of the *ddCDEFGHIJ* genes since all of them were significantly down-regulated in the Δ*bac* mutant strain, mainly after 24 h of growth (**Figure 7**, **Table S1**). Recent studies have reported the implication of transcriptional regulators in the synthesis of lacticin Q and aureocin A70 (Coelho et al., 2016; Iwatani et al., 2016). Environmental factors such as temperature or nutrition-adaptation were reported to control biosynthesis of enterocin L50 and enterocin Q in the multiple bacteriocin producing strains *Ent. faecium* L50 (Criado et al., 2006) and *Weissella hellenica* QU 13 (Masuda et al., 2016). In the case of non-leaderless bacteriocins, regulation by quorum sensing and leader peptide seemed to be involved (Kleerebezem, 2004; Kuipers et al., 2004; Rink et al., 2007; Abts et al., 2013). Related to that, Perez et al. (2017) reported that mutations in the leader peptide altered the overall conformation of the precursor peptide, which reduced, or enhanced its ability to fit and interact with the substrate-binding cleft of its processing enzyme(s).

As a conclusion, we report that to the best of our knowledge, an intracellular two-peptide leaderless bacteriocin plays a role in its own self-immunity system. The characterization of other genes of the EntDD14 operon (*ddCDEFG*) and their role in overall EntDD14 expression and immunity constitutes our next goal.

DATA AVAILABILITY STATEMENT

The datasets presented in this study can be found in online repositories. The names of the repository/repositories and accession number(s) can be found in the article/ **Supplementary Material**.

AUTHOR CONTRIBUTIONS

DD, AB, and RL conceived the ideas, designed the experiments, discussed the data throughout the project, and wrote the article. RL performed the experiments and AL-D did the transcriptomic analysis. DD, RL, AB, and AL-D revised and approved the manuscript dissertation. All authors contributed to the article and approved the submitted version.

FUNDING

This work has been supported by the CPER/FEDER grant awarded by la Région des Hauts-de-France (2016-2021).

ACKNOWLEDGMENTS

The MALDI-TOF/MS profiling experiments to verify the purity of EntDD14 were performed on the REALCAT platform issued from French governmental subvention administrated by the French National Research Agency (ANR) program [ANR-11-EQPX-0037]. The authors are grateful to Nacim Barache for his assistance in some experiments of this work. The authors would like to thank Prof. Leon Dicks and Dr. Steve W. Elson for their critical reading of the manuscript.

SUPPLEMENTARY MATERIAL

The Supplementary Material for this article can be found online at: https://www.frontiersin.org/articles/10.3389/fbioe.2020.00644/full#supplementary-material

REFERENCES

Abreu-Goodger, C., and Merino, E. (2005). RibEx: a web server for locating riboswitches and other conserved bacterial regulatory elements. *Nucleic Acids Res* 33, W690–W692. doi: 10.1093/nar/gki445

Abts, A., Montalban-Lopez, M., Kuipers, O. P., Smits, S. H., and Schmitt, L. (2013). NisC binds the FxLx motif of the nisin leader peptide. *Biochemistry* 52, 5387–5395. doi: 10.1021/bi4008116

Al Atya, A. K., Drider-Hadiouche, K., Ravallec, R., Silvain, A., Vachee, A., and Drider, D. (2015). Probiotic potential of *Enterococcus faecalis* strains isolated from meconium. *Front. Microbiol.* 6:227. doi: 10.3389/fmicb.2015.00227

Alvarez-Sieiro, P., Montalbán-López, M., Mu, D., and Kuipers, O. P. (2016). Bacteriocins of lactic acid bacteria: extending the family. *Appl. Microbiol. Biotechnol.* 100, 2939–2951. doi: 10.1007/s00253-016-7343-9

Arbulu, S., Jimenez, J. J., Borrero, J., Sánchez, J., Frantzen, C., Herranz, C., et al. (2016). Draft genome sequence of the bacteriocinogenic strain *Enterococcus faecalis* DBH18, isolated from mallard ducks (Anas platyrhynchos). *Genome Announc.* 4:e00663-16. doi: 10.1128/genomeA.00663-16

Basanta, A., Gómez-Sala, B., Sánchez, J., Diep, D. B., Herranz, C., Hernández, P. E., et al. (2010). Use of the yeast Pichia pastoris as an expression host for secretion of enterocin L50, a leaderless two-peptide (L50A and L50B) bacteriocin from *Enterococcus faecium* L50. *Appl. Environ. Microbiol.* 76, 3314–3324. doi: 10.1128/AEM.02206-09

Basanta, A., Herranz, C., Gutiérrez, J., Criado, R., Hernández, P. E., and Cintas, L. M. (2009). Development of bacteriocinogenic strains of *Saccharomyces cerevisiae* heterologously expressing and secreting the leaderless enterocin L50 peptides L50A and L50B from *Enterococcus faecium* L50. *Appl. Environ. Microbiol.* 75, 2382–2392. doi: 10.1128/AEM.01476-08

Bastos, M. do. C. de. F., Coelho, M. L. V., and Santos, O. C. da S. (2015). Resistance to bacteriocins produced by gram-positive bacteria. *Microbiology* 161, 683–700. doi: 10.1099/mic.0.082289-0

Batdorj, B., Dalgalarrondo, M., Choiset, Y., Pedroche, J., Métro, F., Prévost, H., et al. (2006). Purification and characterization of two bacteriocins produced by lactic acid bacteria isolated from Mongolian airag. *J. Appl. Microbiol.* 101, 837–848. doi: 10.1111/j.1365-2672.2006.02966.x

Beis, K., and Rebuffat, S. (2019). Multifaceted ABC transporters associated to microcin and bacteriocin export. *Res. Microbiol.* 170, 399–406. doi: 10.1016/j.resmic.2019.07.002

Belguesmia, Y., Choiset, Y., Rabesona, H., Baudy-Floc'h, M., Le Blay, G., Haertlé, T., et al. (2013). Antifungal properties of durancins isolated from *Enterococcus durans* A5-11 and of its synthetic fragments. *Lett. Appl. Microbiol.* 56, 237–244. doi: 10.1111/lam.12037

Belguesmia, Y., Leclère, V., Duban, M., Auclair, E., and Drider, D. (2017). Draft genome sequence of *Enterococcus faecalis* DD14, a bacteriocinogenic lactic acid bacterium with anti-clostridium activity. *Genome Announc.* 5, e00695-17. doi: 10.1128/genomeA.00695-17

Bierbaum, G., and Sahl, H.-G. (2009). Lantibiotics: mode of action, biosynthesis and bioengineering. *Curr. Pharm. Biotechnol.* 10, 2–18. doi: 10.2174/138920109787048616

Bougherra, F., Dilmi-Bouras, A., Balti, R., Przybylski, R., Adoui, F., Elhameur, H., et al. (2017). Antibacterial activity of new peptide from bovine casein hydrolyzed by a serine metalloprotease of *Lactococcus lactis* subsp lactis BR16. *J. Funct. Foods* 32, 112–122. doi: 10.1016/j.jff.2017.02.026

Bountra, K., Hagelueken, G., Choudhury, H. G., Corradi, V., El Omari, K., Wagner, A., et al. (2017). Structural basis for antibacterial peptide self-immunity by the bacterial ABC transporter McjD. *EMBO J.* 36, 3062–3079. doi: 10.15252/embj.201797278

Caly, D. L., Chevalier, M., Flahaut, C., Cudennec, B., Al Atya, A. K., Chataigné, G., et al. (2017). The safe enterocin DD14 is a leaderless two-peptide bacteriocin with anti-Clostridium perfringens activity. *Int. J. Antimicrob. Agents* 49, 282–289. doi: 10.1016/j.ijantimicag.2016.11.016

Cintas, L. M., Casaus, P., Herranz, C., Håvarstein, L. S., Holo, H., Hernández, P. E., et al. (2000). Biochemical and genetic evidence that *Enterococcus faecium* L50 produces enterocins L50A and L50B, the sec-dependent enterocin P, and a novel bacteriocin secreted without an N-terminal extension termed enterocin Q. *J. Bacteriol.* 182, 6806–6814. doi: 10.1128/jb.182.23.6806-6814.2000

Cintas, L. M., Casaus, P., Holo, H., Hernandez, P. E., Nes, I. F., and Håvarstein, L. S. (1998). Enterocins L50A and L50B, Two novel bacteriocins from *Enterococcus faecium* L50, are related to staphylococcal hemolysins. *J. Bacteriol.* 180, 1988–1994.

Coelho, M. L. V., Coutinho, B. G., Cabral da Silva Santos, O., Nes, I. F., and Bastos, M. do. C. de. F. (2014). Immunity to the *Staphylococcus aureus* leaderless four-peptide bacteriocin aureocin A70 is conferred by AurI, an integral membrane protein. *Res. Microbiol.* 165, 50–59. doi: 10.1016/j.resmic.2013.11.001

Coelho, M. L. V., Fleming, L. R., and Bastos, M. do. C. de. F. (2016). Insights into aureocin A70 regulation: participation of regulator AurR, alternative transcription factor σ(B) and phage φ11 regulator cI. *Res. Microbiol.* 167, 90–102. doi: 10.1016/j.resmic.2015.10.004

Cotter, P. D., Ross, R. P., and Hill, C. (2013). Bacteriocins - a viable alternative to antibiotics? *Nat. Rev. Microbiol.* 11, 95–105. doi: 10.1038/nrmicro2937

Criado, R., Gutiérrez, J., Martín, M., Herranz, C., Hernández, P. E., and Cintas, L. M. (2006). Immunochemical characterization of temperature-regulated production of enterocin L50 (EntL50A and EntL50B), enterocin P, and enterocin Q by *Enterococcus faecium* L50. *Appl. Environ. Microbiol.* 72, 7634–7643. doi: 10.1128/AEM.00983-06

Diaz, M., Valdivia, E., Martínez-Bueno, M., Fernández, M., Soler-González, A. S., Ramírez-Rodrigo, H., et al. (2003). Characterization of a new operon, as-48EFGH, from the as-48 gene cluster involved in immunity to enterocin AS-48. *Appl. Environ. Microbiol.* 69, 1229–1236. doi: 10.1128/aem.69.2.1229-1236.2003

Diez-Gonzalez, F. (2007). Applications of bacteriocins in livestock. *Curr. Issues Intest. Microbiol.* 8, 15–23

Fernández, M., Sánchez-Hidalgo, M., García-Quintáns, N., Martínez-Bueno, M., Valdivia, E., López, P., et al. (2008). Processing of as-48ABC RNA in AS-48 enterocin production by *Enterococcus faecalis*. *J. Bacteriol.* 190, 240–250. doi: 10.1128/JB.01528-07

Gajic, O., Buist, G., Kojic, M., Topisirovic, L., Kuipers, O. P., and Kok, J. (2003). Novel mechanism of bacteriocin secretion and immunity carried out by lactococcal multidrug resistance proteins. *J. Biol. Chem.* 278, 34291–34298. doi: 10.1074/jbc.M211100200

Graham, C. E., Cruz, M. R., Garsin, D. A., and Lorenz, M. C. (2017). *Enterococcus faecalis* bacteriocin EntV inhibits hyphal morphogenesis, biofilm formation, and virulence of Candida albicans. *Proc. Natl. Acad. Sci. U.S.A.* 114, 4507–4512. doi: 10.1073/pnas.1620432114

Hacker, C., Christ, N. A., Duchardt-Ferner, E., Korn, S., Göbl, C., Berninger, L., et al. (2015). The solution structure of the lantibiotic immunity protein NisI and its interactions with nisin. *J. Biol. Chem.* 290, 28869–28886. doi: 10.1074/jbc.M115.679969

Hu, J., Ma, L., Nie, Y., Chen, J., Zheng, W., Wang, X., et al. (2018). A Microbiota-derived bacteriocin targets the host to confer diarrhea resistance in early-weaned piglets. *Cell Host Microbe.* 24, 817–832.e8. doi: 10.1016/j.chom.2018.11.006

Iwatani, S., Horikiri, Y., Zendo, T., Nakayama, J., and Sonomoto, K. (2013). Bifunctional gene cluster lnqBCDEF mediates bacteriocin production and immunity with differential genetic requirements. *Appl. Environ. Microbiol.* 79, 2446–2449. doi: 10.1128/AEM.03783-12

Iwatani, S., Ishibashi, N., Flores, F. P., Zendo, T., Nakayama, J., and Sonomoto, K. (2016). LnqR, a TetR-family transcriptional regulator, positively regulates lacticin Q production in *Lactococcus lactis* QU 5. *FEMS Microbiol. Lett.* 363:fnw200. doi: 10.1093/femsle/fnw200

Iwatani, S., Yoneyama, F., Miyashita, S., Zendo, T., Nakayama, J., and Sonomoto, K. (2012). Identification of the genes involved in the secretion and self-immunity of lacticin Q, an unmodified leaderless bacteriocin from *Lactococcus lactis* QU 5. *Microbiology* 158, 2927–2935. doi: 10.1099/mic.0.062943-0

Johnson, M. E. M., Jung, D. Y.-G., Jin, D. Y.-Y., Jayabalan, D. R., Yang, D. S. H., and Suh, P. J. W. (2018). Bacteriocins as food preservatives: challenges and emerging horizons. *Crit. Rev. Food Sci. Nutr.* 58, 2743–2767. doi: 10.1080/10408398.2017.1340870

Juturu, V., and Wu, J. C. (2018). Microbial production of bacteriocins: latest research development and applications. *Biotechnol. Adv.* 36, 2187–2200. doi: 10.1016/j.biotechadv.2018.10.007

Karpinski, T., Szkaradkiewicz, A., Caballero, B., Finglas, P. M., and Toldrá, F. (2016). "Bacteriocins," in *Encyclopedia of Food and Health*, eds B. Caballero, P. M. Finglas, and F. Toldrá (Amsterdam: Academic Press), 312–419.

Kjos, M., Snipen, L., Salehian, Z., Nes, I. F., and Diep, D. B. (2010). The abi proteins and their involvement in bacteriocin self-immunity. *J. Bacteriol.* 192, 2068–2076. doi: 10.1128/JB.01553-09

Klaenhammer, T. R. (1993). Genetics of bacteriocins produced by lactic acid bacteria. *FEMS Microbiol. Rev.* 12, 39–85. doi: 10.1111/j.1574-6976.1993.tb00012.x

Kleerebezem, M. (2004). Quorum sensing control of lantibiotic production; nisin and subtilin autoregulate their own biosynthesis. *Peptides* 25, 1405–1414. doi: 10.1016/j.peptides.2003.10.021

Klein, C., and Entian, K. D. (1994). Genes involved in self-protection against the lantibiotic subtilin produced by *Bacillus subtilis* ATCC 6633. *Appl. Environ. Microbiol.* 60, 2793–2801.

Kuipers, A., Boef, E., de Rink, R., Fekken, S., Kluskens, L. D., Driessen, A. J. M., et al. (2004). NisT, the transporter of the lantibiotic nisin, can transport fully modified, dehydrated, and unmodified prenisin and fusions of the leader peptide with non-lantibiotic peptides. *J. Biol. Chem.* 279, 22176–22182. doi: 10.1074/jbc.M312789200

Liu, X., Vederas, J. C., Whittal, R. M., Zheng, J., Stiles, M. E., Carlson, D., et al. (2011). Identification of an N-terminal formylated, two-peptide bacteriocin from *Enterococcus faecalis* 710C. *J. Agric. Food Chem.* 59, 5602–5608. doi: 10.1021/jf104751v

Martín-Platero, A. M., Valdivia, E., Ruíz-Rodríguez, M., Soler, J. J., Martín-Vivaldi, M., Maqueda, M., et al. (2006). Characterization of antimicrobial substances produced by *Enterococcus faecalis* MRR 10-3, isolated from the uropygial gland of the hoopoe (upupa epops). *Appl. Environ. Microbiol.* 72, 4245–4249. doi: 10.1128/AEM.02940-05

Masuda, Y., Perez, R. H., Zendo, T., and Sonomoto, K. (2016). Nutrition-adaptive control of multiple-bacteriocin production by Weissella hellenica QU 13. *J. Appl. Microbiol.* 120, 70–79. doi: 10.1111/jam.12997

Nascimento, J., dos, S., Coelho, M. L. V., Ceotto, H., Potter, A., Fleming, L. R., et al. (2012). Genes involved in immunity to and secretion of aureocin A53, an atypical class II bacteriocin produced by *Staphylococcus aureus* A53. *J. Bacteriol.* 194, 875–883. doi: 10.1128/JB.06203-11

Nes, I. F., Diep, D. B., Håvarstein, L. S., Brurberg, M. B., Eijsink, V., and Holo, H. (1996). Biosynthesis of bacteriocins in lactic acid bacteria. *Antonie Van Leeuwenhoek* 70, 113–128. doi: 10.1007/BF00395929

Netz, D. J., Sahl, H. G., Marcelino, R., dos Santos Nascimento, J., de Oliveira, S. S., Soares, M. B., et al. (2001). Molecular characterisation of aureocin A70, a multi-peptide bacteriocin isolated from *Staphylococcus aureus*. *J. Mol. Biol.* 311, 939–949. doi: 10.1006/jmbi.2001.4885

Netz, D. J. A., Pohl, R., Beck-Sickinger, A. G., Selmer, T., Pierik, A. J., Bastos, M., et al. (2002). Biochemical characterisation and genetic analysis of aureocin A53, a new, atypical bacteriocin from *Staphylococcus aureus*. *J. Mol. Biol.* 319, 745–756. doi: 10.1016/S0022-2836(02)00368-6

Nissen-Meyer, J., Rogne, P., Oppegard, C., Haugen, H., and Kristiansen, P. (2009). Structure-function relationships of the non-lanthionine-containing peptide (class II) bacteriocins produced by gram-positive bacteria. *CPB* 10, 19–37. doi: 10.2174/138920109787048661

Ovchinnikov, K. V., Chi, H., Mehmeti, I., Holo, H., Nes, I. F., and Diep, D. B. (2016). Novel group of leaderless multipeptide bacteriocins from gram-positive bacteria. *Appl. Environ. Microbiol.* 82, 5216–5224. doi: 10.1128/AEM.01094-16

Papo, N., and Shai, Y. (2005). Host defense peptides as new weapons in cancer treatment. *Cell. Mol. Life Sci.* 62, 784–790. doi: 10.1007/s00018-005-4560-2

Perez, R. H., Sugino, H., Ishibashi, N., Zendo, T., Wilaipun, P., Leelawatcharamas, V., et al. (2017). Mutations near the cleavage site of enterocin NKR-5-3B prepeptide reveal new insights into its biosynthesis. *Microbiology* 163, 431–441. doi: 10.1099/mic.0.000435

Perez, R. H., Zendo, T., and Sonomoto, K. (2014). Novel bacteriocins from lactic acid bacteria (LAB): various structures and applications. *Microb. Cell Fact.* 13:S3. doi: 10.1186/1475-2859-13-S1-S3

Perez, R. H., Zendo, T., and Sonomoto, K. (2018). Circular and leaderless bacteriocins: biosynthesis, mode of action, applications, and prospects. *Front. Microbiol.* 9:2085. doi: 10.3389/fmicb.2018.02085

Quintana, V. M., Torres, N. I., Wachsman, M. B., Sinko, P. J., Castilla, V., and Chikindas, M. (2014). Antiherpes simplex virus type 2 activity of the antimicrobial peptide subtilosin. *J. Appl. Microbiol.* 117, 1253–1259. doi: 10.1111/jam.12618

Rincé, A., Dufour, A., Uguen, P., Le Pennec, J. P., and Haras, D. (1997). Characterization of the lacticin 481 operon: the *Lactococcus lactis* genes lctF, lctE, and lctG encode a putative ABC transporter involved in bacteriocin immunity. *Appl. Environ. Microbiol.* 63, 4252–4260. doi: 10.1128/AEM.63.11.4252-4260.1997

Rink, R., Kluskens, L. D., Kuipers, A., Driessen, A. J. M., Kuipers, O. P., and Moll, G. N. (2007). NisC, the cyclase of the lantibiotic nisin, can catalyze cyclization of designed nonlantibiotic peptides. *Biochemistry* 46, 13179–13189. doi: 10.1021/bi700106z

Sahm, D. F., Kissinger, J., Gilmore, M. S., Murray, P. R., Mulder, R., Solliday, J., et al. (1989). *In vitro* susceptibility studies of vancomycin-resistant *Enterococcus faecalis*. *Antimicrob. Agents Chemother.* 33, 1588–1591. doi: 10.1128/AAC.33.9.1588

Sambrook, J., and Russell, D. W. (2001). *Molecular Cloning*: *A Laboratory Manual*. New York, NY: Cold Spring Harbor Laboratory Press.

Sánchez-Hidalgo, M., Maqueda, M., Gálvez, A., Abriouel, H., Valdivia, E., and Martínez-Bueno, M. (2003). The genes coding for enterocin EJ97 production by *enterococcus faecalis* EJ97 are located on a conjugative plasmid. *Appl. Environ. Microbiol.* 69, 1633–1641. doi: 10.1128/AEM.69.3.1633-1641.2003

Siegers, K., and Entian, K. D. (1995). Genes involved in immunity to the lantibiotic nisin produced by *Lactococcus lactis* 6F3. *Appl. Environ. Microbiol.* 61, 1082–1089. doi: 10.1128/AEM.61.3.1082-1089.1995

Thurlow, L. R., Thomas, V. C., and Hancock, L. E. (2009). Capsular polysaccharide production in *Enterococcus faecalis* and contribution of CpsF to capsule serospecificity. *J. Bacteriol.* 191, 6203–6210. doi: 10.1128/JB.00592-09

Towle, K. M., and Vederas, J. C. (2017). Structural features of many circular and leaderless bacteriocins are similar to those in saposins and saposin-like peptides. *Medchemcomm* 8, 276–285. doi: 10.1039/C6MD00607H

Trieu-Cuot, P., Carlier, C., Poyart-Salmeron, C., and Courvalin, P. (1991). Shuttle vectors containing a multiple cloning site and a lacZ alpha gene for conjugal transfer of DNA from *Escherichia coli* to gram-positive bacteria. *Gene* 102, 99–104. doi: 10.1016/0378-1119(91)90546-N

van Heel, A. J., Montalban-Lopez, M., and Kuipers, O. P. (2011). Evaluating the feasibility of lantibiotics as an alternative therapy against bacterial infections in humans. *Expert. Opin. Drug Metab. Toxicol.* 7, 675–680. doi: 10.1517/17425255.2011.573478

Verma, A. K., Banerjee, R., Dwivedi, H. P., Juneja, V. K., and Carl, A. B. (2014). "BACTERIOCINS | potential in food preservation," in *Encyclopedia of Food Microbiology*, eds C. A. Batt and M. L. Tortorello (Cambridge, MA: Elsivier Ltd, Academic Press), 180–206. doi: 10.1016/B978-0-12-384730-0.00029-X

Yagi, Y., and Clewell, D. B. (1980). Recombination-deficient mutant of *Streptococcus faecalis*. *J. Bacteriol.* 143, 966–970. doi: 10.1128/JB.143.2.966-970.1980

Yanisch-Perron, C., Vieira, J., and Messing, J. (1985). Improved M13 phage cloning vectors and host strains: nucleotide sequences of the M13mpl8 and pUC19 vectors. *Gene* 33, 103–119. doi: 10.1016/0378-1119(85)90120-9

Yarmus, M., Mett, A., and Shapira, R. (2000). Cloning and expression of the genes involved in the production of and immunity against the bacteriocin lacticin RM. *Biochim. Biophys. Acta* 1490, 279–290. doi: 10.1016/S0167-4781(00)00012-9

Conflict of Interest: The authors declare that the research was conducted in the absence of any commercial or financial relationships that could be construed as a potential conflict of interest.

frontiers in Bioengineering and Biotechnology

ORIGINAL RESEARCH
published: 07 August 2020
doi: 10.3389/fbioe.2020.00956

Fermentation of Wheat Bran and Whey Permeate by Mono-Cultures of *Lacticaseibacillus rhamnosus* Strains and Co-culture With Yeast Enhances Bioactive Properties

Annalisse Bertsch[1,2†], *Denis Roy*[1,2] *and Gisèle LaPointe*[3*]

[1] Department of Food Science, Laval University, Quebec City, QC, Canada, [2] Institute of Nutrition and Functional Foods (INAF), Laval University, Quebec City, QC, Canada, [3] Department of Food Science, University of Guelph, Guelph, ON, Canada

OPEN ACCESS

Edited by:
Jian-Ming Liu,
Technical University of Denmark, Denmark

Reviewed by:
Limin Cao,
Capital Normal University, China
Jingyu Chen,
China Agricultural University, China

***Correspondence:**
Gisèle LaPointe
glapoint@uoguelph.ca

†Present address:
Annalisse Bertsch,
Biena, Saint-Hyacinthe, QC, Canada

Specialty section:
This article was submitted to Synthetic Biology, a section of the journal Frontiers in Bioengineering and Biotechnology

Received: 27 March 2020
Accepted: 23 July 2020
Published: 07 August 2020

Citation:
Bertsch A, Roy D and LaPointe G (2020) Fermentation of Wheat Bran and Whey Permeate by Mono-Cultures of Lacticaseibacillus rhamnosus Strains and Co-culture With Yeast Enhances Bioactive Properties. Front. Bioeng. Biotechnol. 8:956. doi: 10.3389/fbioe.2020.00956

The aim of this work was to obtain a bioingredient (BI) with bioactive properties through the solid fermentation of a wheat bran-whey permeate (WB/WP) mixture with three strains of *Lacticaseibacillus rhamnosus* (R0011, ATCC 9595, and RW-9595M) in mono or co-culture with *Saccharomyces cerevisiae*. The choice of these strains was based on their capacity to produce the same exopolysaccharide (EPS), but at different yields. The solid fermentation of WB/WP revealed a similar growth pattern, sugar utilization and metabolite production between strains and types of culture. Lactic acid, soluble protein, free amino acid and phenolic compound content in BI were compared to NFWB. Water soluble polysaccharides (including EPS) were significantly increased in co-culture for (44%) ATCC 9595, (40%) R0011 and (27%) RW-9595M. The amount of bound Total Phenolic Content (TPC) as well as the antioxidant activity in BI were higher after fermentation. The free phenolic acid content was higher after fermentation with ATCC 9595 (53–59%), RW-9595M (45–46%), and R0011 (29–39%) compared to non-fermented NFWB. Fermentation by these strains increased the amounts of free caffeic acid and 4-hydroxybenzoic acid in both types of culture. The bound phenolic acid content was enhanced in co-culture for the BI obtained from the highest EPS producer strain RW-9595M which was 30% higher than NFWB. After *in vitro* digestion, bioaccessibility of free total phenolic acids was improved by more than 40% in BI compared to NFWB. The co-culture increased recovery of TPC (%) and antioxidant activity compared to monoculture for the strains in digested product. In contrast, the recovery of bound total phenolic acids in co-culture was 33 and 38% lower when compared to monoculture for R0011 and RW-9595M. Our findings provide new insights into the impact of LAB/yeast co-culture on the bioactive properties of fermented wheat bran.

Keywords: coculture, lactic acid bacteria, yeast, wheat bran, bioaccessibility, phenolic compounds

INTRODUCTION

Cereals have increasingly been used in fermentation to produce fiber-enhanced beverages, as well as potential prebiotic sources in probiotic dairy products and bakery products (Stevenson et al., 2012; Onipe et al., 2015; Russo et al., 2016). Wheat bran (WB) has attracted much interest because it represents the most important milling by-product of grain cereals with a production of approximately 150 million tons per year. Wheat bran is a complex substrate composed mainly of dietary fiber, proteins and starch (Anson et al., 2011; Onipe et al., 2015). It contains vitamins, minerals and bioactive molecules, such as low-molecular weight phenolic acid compounds including p-coumaric and mainly ferulic acid (FA), which have shown antioxidant activity (Anson et al., 2011, Anson et al., 2012; Laddomada et al., 2015). In wheat bran, the phenolic compounds can be found in free form or linked to the structural components of plants (cellulose, arabinoxylan, and proteins) through ester bonds or covalently bound (Anson et al., 2012). Fermentation can improve the nutritional, functional, and sensorial properties of wheat bran (Poutanen et al., 2009; Katina et al., 2012). Yeast fermentation of wheat bran increased the level of folates (1.62-fold), free ferulic acid (5.5-fold), and soluble arabinoxylan (1.54-fold) (Katina et al., 2012). Bio-processing causes hydrolysis and solubilization of proteins and fibers allowing the delivery of bioactive and potentially protective compounds when consumed (Coda et al., 2014; Verni et al., 2019).

During fermentation, changes in temperature and pH of the medium can influence the action of both endogenous and bacterial enzymes. Grain constituents are modified by hydrolysis of water insoluble arabinoxylan causing cleavage in the backbone structure generating arabinoxylan-oligosaccharide (AXOS), which enhances total phenolic content and antioxidant activities principally by releasing free ferulic acid (Anson et al., 2012; Coda et al., 2014). However, the bioavailability of the wheat bran fractions depends on the proportion of the compounds in the food matrix, as well as their release and possible absorption by the intestine (bioaccessibility). The free phenolic compounds are mainly hydrolyzed and a small portion is absorbed in the upper intestinal tract of humans. Conversely, the insoluble, bound compounds represent the main fraction (83%) of phenolic compounds that pass through the small intestine without absorption (Cömert and Gökmen, 2017). Thus, they can undergo fermentation by the colon microbiota, which may result in metabolites with greater biological activity (Valdés et al., 2015).

Lactic acid bacteria (LAB) have been co-cultured with yeast for fermentation of bran (Coda et al., 2014; Zhao et al., 2017). Strains of *Lacticaseibacillus rhamnosus* or *Saccharomyces cerevisiae* in monoculture were able to enhance levels of antioxidant activity in cereals (Dordevic et al., 2010). The total phenolic content (TPC) was increased in wheat bran fermented by these two microorganism in co-culture more than in monoculture (Zhao et al., 2017). To promote microbial growth, several authors reported the supplementation of cereal-based medium with sucrose, raffinose or glucose (Kajala et al., 2016; Xu et al., 2017). Similarly, whey permeate (WP) has been used as a carbon source (lactose) in LAB fermentations (Macedo et al., 2002; Bergmaier et al., 2003). Therefore, the combination of both cereal and WP represents a promising source for the creation of innovative fermented bioproducts (Slukovà et al., 2016). Furthermore, *Lacticaseibacillus* spp. are able to produce exopolysaccharides (EPS) impacting texture and viscosity, while also potentially exhibiting prebiotic or antioxidant properties that can improve the bioactivity of fermented cereal products (Cheirsilp et al., 2003; Polak-Berecka et al., 2015; Salazar et al., 2016). Several studies reported that lactate consumption by the yeast can probably enhance the production of kefiran or bacteriocins (nisin) under controlled pH in LAB–yeast co-culture (Minekus et al., 2014; Chanos and Mygind, 2016). Despite the fact that *S. cerevisiae* and LAB co-exist in cereal fermented products such as sourdough, improved understanding of their interactions and their effect on the bioaccessibility of phenolic acid compounds is still needed.

Static *in vitro* gastrointestinal digestion systems can replace animal and human models for rapidly screening food and bioingredients; additionally *in vitro* practices are faster and less expensive than *in vivo* approaches, while avoiding some ethical issues (Minekus et al., 2014). In food technology, the bioaccessibility and bioavailability of phenolic acid compounds can be estimated using *in vitro* simulated gastrointestinal digestion (Motilva et al., 2015; Zeng et al., 2016). However, little information has been published on these properties of bioactive compounds in ingredients obtained from fermented wheat bran subjected to *in vitro* gastrointestinal digestion. Therefore, this study focused on the effect of mono or co-culture as well as the presence of EPS on the bioaccessibility of phenolic acid compounds of fermented wheat bran. The first aim was to obtain bioingredients with bioactive properties through the fermentation of a wheat bran-whey permeate (WB/WP) mixture by 3 strains of *L. rhamnosus* in mono or co-culture with *S. cerevisiae.* The second aim was to investigate the influence of the type of culture on chemical composition of the bioingredients. The third aim was to evaluate the content of free and bound total phenolic compounds, antioxidant activity and the phenolic acid profile in the bioingredients. Finally, the bio-products were submitted to *in vitro* digestion in order to relate the properties to bioaccessibility and recovery of phenolic compounds.

MATERIALS AND METHODS

Bacteria and Culture Conditions

Lacticaseibacillus rhamnosus ATCC 9595 was obtained from the American Type Culture Collection (ATCC; Manassas, VA). *L. rhamnosus* RW-9595M (variant of ATCC 9595) and *L. rhamnosus* R0011 (also known as R or Rosell-11, from Lallemand Health Solutions) were obtained from our lactic acid bacteria culture collection (Université Laval, Quebec, Canada). These strains produced different quantities of the same EPS and their production was increased in co-culture with yeast in a previous study (van Calsteren et al., 2002; Bertsch et al., 2019). The stock culture was maintained at −80°C in 6% (v/v) rehydrated skim milk and 10% (v/v) glycerol. The commercial (Lallemand Instaferm Gold Instant dry yeast) baker's yeast

(Lallemand Instaferm) *S. cerevisiae* was grown in YEPAL medium (1% yeast extract, 2% peptone, and 1% lactic acid) at pH 5.0. This medium was used to adapt the yeast to lactic acid because the yeast can utilize lactic acid but cannot utilize lactose, which is the major carbon source in the WB/WP medium (Yamasaki-Yashiki et al., 2017).

Commercial Wheat Bran had a mean particle size of 750 μm and whey permeate WP was obtained from Agropur, Canada. Whey permeate powder was added to water to give a final concentration of 5% (w/w) and was autoclaved (121°C, 15 min) (Bergmaier et al., 2003). Analytical grade chemicals, solvents, and reagents were used unless specified otherwise.

Fermentation

The stock cultures of *L. rhamnosus* were incubated at 37°C for 8 h in 10 mL of MRS-L (MRS supplemented with 20 g/l lactose). Next, 2% (v/v) was added to 50 mL of WP supplemented with yeast extract, followed by incubation at 37°C for 12 h. A yeast colony from YEPAL agar was added to 20 mL of YEPAL broth, which was incubated at 30°C in a shaker at 180 rpm for 24 h.

A mixture of WB/WP (14:86% w/v) was inoculated with 3.5% cell suspension of *L. rhamnosus* for the monoculture or 1.75% of *L. rhamnosus* + 1.75% of yeast for the co-culture (1:1 ratio). Solid wheat bran fermentations were carried out in mono (lactic acid bacteria) or co-culture (lactic acid bacteria and baker's yeast) at 35°C without agitation (**Table 1**). A control (WB) sample containing a mixture of cereal and WP was prepared. All fermentations were sampled after 0, 3, 6, 9, 12, 15, and 24 h of incubation to monitor bacterial growth (by plate counts), pH, lactose consumption, and metabolite production (lactic acid, acetic acid). All fermentations were performed in triplicate.

Monitoring Bacterial Growth and pH

Fermented samples were diluted with sterile saline (1:9 w/v) for homogenization. Viable (cultivable) lacticaseibacillus and yeast counts were determined by spread-plating 10-fold serial dilutions [in 0.1% (w/v), sterilized peptone water] on MRS-L agar (selective for *Lacticaseibacillus* due to lack of lactose consumption by yeast) or in YEPAL agar (selective for the Yeast due to lack of consumption of lactic acid by *Lacticaseibacillus*). The plates were incubated aerobically during 48 h at 37°C for lactic acid bacteria strains and 30°C for yeast, followed by counting the number of colony-forming units (CFU) per g of WB in samples taken during mono- and co-culture. Each measurement was performed in triplicate. The pH value was measured by a VWR pH meter SB70P (VWR, Pennsylvania, United States).

TABLE 1 | Bioprocessing combinations of the wheat bran/whey permeate (WB/WP) mixture and strains* to obtain the fermented bioingredients and *in vitro* product of digestion.

Strain	Type of culture	Bioingredient
Lacticaseibacillus rhamnosus R0011	M	LR11M
Lacticaseibacillus rhamnosus R0011 + *S. cerevisiae*	C	LR11C
Lacticaseibacillus rhamnosus ATCC 9595	M	LR95M
Lacticaseibacillus rhamnosus ATCC 9595 + *S. cerevisiae*	C	LR95C
Lacticaseibacillus rhamnosus RW-9595M	M	LRWM
Lacticaseibacillus rhamnosus RW-9595M + *S. cerevisiae*	C	LRWC
Non-inoculated; non-fermented	NF	NFWB

M, monoculture; C, co-culture; NF, non-fermented.

Viscosity Analysis

Viscosity of fermented substrates was measured directly with a Rheometer AR-G2 (with a standard size vanned rotor, TA Instruments, Herts, United Kingdom). Before the measurement, the samples of WB/WP fermented (20 g) were mixed with sterile water (25 g). Sample viscosity was measured at 21°C in accelerating shear rate from 2 to 500 s^{-1}, followed by comparing samples at the 100 s^{-1} shear rate. The analysis was carried out in triplicate.

Scanning Electron Microscopy

The fermented bran samples were fixed with 2.5% glutaraldehyde buffered in sodium cacodylate 0.1 M, pH 7.3, and washed three times with buffer. Dehydration of the samples was carried out with ethanol from 30% (v/v) to 50% (v/v) to 70% (v/v) to 95% (v/v) and absolute, 3 min × 15 min then by hexamethyldisilazane (Fluka, Buchs, Switzerland). A scanning electronic microscope JEOL, JSM6360LV (Tokyo, Japan) was used to examine samples.

Analysis of Bioingredients and Digested Samples

At the end of the fermentation, the solid fermented medium was thermally treated (95°C for 15 min) and freeze-dried to obtain 6 different bioingredients and the control sample NFWB (**Table 1**). Water/salt-soluble extracts (WSE) were prepared according to the modified method described by Osborne (Weiss et al., 1993; Arte et al., 2015). An aliquot of the NFWB was diluted (1:10) with Tris-HCl 50 mM (pH 8.8), stirred for 1 h at room temperature, then centrifuged at 20,000 × *g* for 20 min. The water/salt-soluble fraction in the supernatants were stored at −20°C for further analyses.

In vitro Simulation of Digestion

The method described by Minekus et al. (2014) with some modifications was used for *in vitro* gastrointestinal digestion of bioingredients and NFWB. The three stages of digestion were mouth, gastric and small intestine. The composition of the salivary (SSF), gastric (SSG) and intestinal (SSI) juices were as described previously (Minekus et al., 2014). A saliva solution containing 1,500 U/mL α-amylase (Sigma, Germany) and diluted in 0.3 M $CaCl_2$ was used to simulated mastication. The simulated saliva 1.4 mL (75 U/mL in the final mixture) was added to 2.5 g of solid and mixed thoroughly to obtain a paste like-consistency with 10 mL of SSF electrolyte stock solution, 71.4 μL of $CaCl_2$ and 2.78 mL of water for 2 min at 37°C. In gastric conditions, 10.5 mL of SSG electrolyte stock solution, 7 μL of $CaCl_2$, 2.24 mL pepsin (2,000 U/mL in the final digestion mixture, Sigma) and 0.973 mL of water were added to the remaining fluid. Afterward, the pH was decreased until 3 using 6 M HCl and incubated for 2 h at 37°C and 80 rpm. For small intestine conditions, 15.4 mL of SSI electrolyte stock solution, 7 mL pancreatin from porcine

pancreas (100 U/mL final concentration, Sigma), 3.5 mL bile salt mixture (Sigma), 56 μL of $CaCl_2$ and 1.8 mL of water were added to the remainder of the mixture. The pH was increased to 7 with 4 M NaOH, continuing incubation for 2 h at 37°C and 80 rpm. The sample solution was then placed in 6–8 kDa molecular weight cut-off dialysis tubing and dialysed 24 h to remove low molecular mass digestion products. At the end, the digestion mixtures were lyophilized to obtain the digested samples LR11M to NFWB (**Table 1**).

Chemical Analysis

Samples were dried in an oven at 130°C for 5 h to determine moisture content [American Association of Cereal Chemists (AACC), 1975]. The Kjeldahl method was used to measure organic nitrogen concentration [American Association of Cereal Chemists (AACC), 1976]. Proteolysis was determined by measuring the concentration of proteins, peptides and free amino acids in the water/salt-soluble extracts (WSE) (Weiss et al., 1993; Arte et al., 2015). The concentration of soluble proteins and peptides were determined by the Bradford and the *o*-phthaldialdehyde (OPA) method, respectively (Bradford, 1976; Church et al., 1985). Quantitative analysis of free amino acids was performed using the EZ:faast kit obtained from Phenomenex (Torrance, CA, United States). After solid phase extraction, derivatization and liquid/liquid extraction of the derivatized amino acids, UHPLC-MS/MS was used to analyze the derivatized samples.

Sugars (lactose, glucose, and galactose), organic acids (lactic acid and acid acetic) and ethanol in all the samples were determined using HPLC following the same equipment and conditions reported previously (Bertsch et al., 2019). Before injection (15 μL), triplicate samples were diluted two-thirds with Milli-Q water, centrifuged at 20,000 × *g* for 15 min at 4°C, and filtered (pore size of 0.45 μm; Chromspec Syringe Filter; Chromatographic Specialties, Brockville, ON, Canada). Acetate, lactate (all from Sigma-Aldrich) and ethanol (JT Baker Chemical) were combined for use as an external standard for quantification. Assays from Megazyme International (Wicklow, Ireland) were used to determine the contents of xylose (K-XYLOSE), starch (K-TSTA-50A/K-TSTA-100A), β-glucan (K-EBHLG) and insoluble and soluble dietary fiber (K-RINTDF) from bioingredients or non-fermented wheat bran. The reducing sugar content was estimated with the dinitrosalicylic acid method (Miller, 1959).

Index of solubilisation of dietary fiber: IDF/SDF = Content of insoluble dietary fiber/content of soluble dietary fiber.

Determination of Water-Soluble Polysaccharides (WSP)

Ethanol precipitation was used for isolation and purification of water soluble polysaccharides (WSP) as described previously (Dubois et al., 1951; Miller, 1959; Tieking and Gänzle, 2005; Leroy and De Vuyst, 2016) with some modifications. Samples of bio-ingredients (0.5 g) were mixed with deionised water at 500 rpm × 1 h at room temperature. Then the solids from WB and cells were separated by centrifugation at 12,000 × *g* for 15 min at 4°C. The WSP were precipitated from the supernatant with 3 volumes 95% ethanol at 4°C for 24 h, and collected by centrifugation at 12,000 × *g* for 20 min. After dissolving the pellets in deionized water, the sample was freeze-dried. The lyophilized samples were treated with pancreatic amylase and amyloglucosidase 37°C for 4 h, then the pH was adjusted to 8.2 and heated to 95°C × 15 min (K-RINTDF Assay Kit). The next step was the protein hydrolysis with a protease at 60°C for 30 min (K-RINTDF Assay Kit). The pH was adjusted to 4.5, followed by two rinses of the precipitate with ethanol. After dialysis (3,500 Da MWCO, Fisher) for 3 days, with two changes of water per day, the WSP solution was freeze-dried. At the end, the total sugars were determined by the phenol/sulfuric acid method (Dubois et al., 1951) with glucose as a standard, and the results are expressed in g glucose per kg of sample. The NFWB was used as control.

Extraction and Separation of Free and Bound Fractions of Phenolic Compounds

Free and bound fractions of phenolic compounds were extracted as described previously (Singleton et al., 1999; Prückler et al., 2015) with the following changes: to obtain the free (non-bound) phenolic acid fraction, 50 mg DM was treated twice with 5 mL 80% methanol (Roth, HPLC grade). The extract was centrifuged, the final volume was measured, filtered (pore size of 0.45 μm) and used to determine free phenolic acid. To obtain the fraction of bound phenolic compounds, the residues of the above extraction were hydrolyzed with 1.5 mL of 2 M NaOH at 25°C for 4 h with shaking. The solution was then brought to pH 2 with 6 M HCl, extracted with ethyl acetate and evaporated to dryness under continuous nitrogen gas flush. Finally, after dissolving in 10 ml methanol, centrifugation at 10,000 × *g* for 10 min, the supernatant was stored at −20°C.

Determination of Total Phenolic Content (TPC)

Total phenolic content was determined in free and bound fractions using the procedure described previously (Singleton et al., 1999) with slight modifications. Briefly, the extracts (20 μL) were added to 100 μL Folin-Ciocalteu (Sigma-Aldrich F9252) reagent for 8 min, then the reaction was neutralized with 80 μl 7.5% Na_2CO_3, followed by 60 min incubation, then measuring absorbance at 765 nm. A standard curve of gallic acid was prepared and total phenolic content expressed as milligrams of gallic acid equivalents per gram dry weight sample (mg GAL/g DW). The percentage of recovery (unabsorbed) of TPC in DS = (amount of TPC in DS after digestion/Amount of TPC before digestion)*100.

Total TPC = TPC of Free + TPC of bound fraction.

Oxygen Radical Scavenging Capacity (ORAC) Assay

The sample (extract from free or bound fractions of phenolic compounds) was diluted with 0.075 M phosphate buffer (pH 7.0) in black 96-well plates (Corning Scientific, Corning, NY, United States). The reaction mixture contained 20 μL of the sample or of Trolox standard and 200 μL of fluorescein (Sigma F6377). After incubation at 37°C for 20 min in a plate reader, 75 μL of (8.6 mg/mL) AAPH solution was quickly added to each well. A Fluostar Galaxy was used to measure fluorescence intensity at 485 nm for excitation and 520 nm for emission for 35 cycles every 210 s. The ORAC value was expressed as micromole Trolox equivalents per gram DM (μmol TE/100 g DM).

The percentage of antioxidant activity recovered in DS = (ORAC value in DS after digestion/ORAC value before digestion)*100.

Total ORAC value = ORAC value of Free + ORAC value of bound form in samples.

Profiling of Phenolic Acids

A Waters Acquity Ultra-Performance TM LC system (Waters), equipped with a quaternary pump system (Waters) was used for UPLC analysis, with an Acquity high-strength silica (HSS) T3 column (150 mm × 2.1 mm internal diameter, 1.8 mm particle size, Waters) containing 100% silica particles as the stationary phase. The separation of the phenolic compounds was carried out following the same conditions reported previously (Bertsch et al., 2019). A TQD mass spectrometer (Waters) equipped with a Z-spray electrospray interface was used for mass spectrometry in negative mode and multiple reaction monitoring (MRM) was used to acquire data with Mass Lynx 4.1 software.

% Bioaccessibility = (Amount of free phenolic acid before digestion - amount of free phenolic acid in DS after digestion/Amount of phenolic acid before digestion) × 100.

The percentage of total phenolic acids recovered (unabsorbed) in DS = (amount of total phenolic acid (TPC) in DS after digestion/Amount of total phenolic acid before digestion) × 100.

The percentage of bound phenolic acids recovered (unabsorbed) in DS = (amount of bound phenolic acid in DS after digestion/Amount of total phenolic acid before digestion) × 100.

Total phenolic acids = Sum of free phenolic acid + Sum of Bound phenolic acid of the samples.

Free phenolic acids = Sum of free phenolic acid of the samples (Singleton et al., 1999; Dall'Asta et al., 2016; Swieca et al., 2017).

Statistical Analyses

Results were expressed as the means of three triplicate analyses and three independent fermentations were conducted. One-way ANOVA was carried out with a Tukey adjustment to test for significance ($P > 0.05$) among the replicates using GraphPad Prism 6 (GraphPad software). Biochemical properties of the bioingredients were analyzed through discriminant analysis (DA), using the software XLSTAT-Premium version 2017 (Addinsoft). Correlations between variables were measured using the Pearson correlation test (r).

RESULTS

Growth and Metabolite Production During Fermentation of WB/WP

During fermentation, the strains of lactic acid bacteria reached cell densities ranging from 6.5 (at 0 h) to 9.8 log CFU/g (at 24 h) and from 6.3 to 7.3 log CFU/g for the yeast (**Figures 1A–C**). No differences in growth were observed between mono and co-culture for all strains. The pH decreased from 5.7 to 3.8 at the end of the culture (**Figures 1D–F**). The lactose from whey permeate was the major carbon source consumed by the LAB strains and consequently lactic acid was produced (**Figures 1G–I**). No significant differences were observed between strains or type of culture (mono or co-culture) in lactose consumption during fermentation ($P > 0.05$). The amount of lactic acid produced by strains ATCC 9595 and RW-9595M was higher (15–19%) than R0011 in both mono and co-culture ($P < 0.05$). In monoculture, the lactic acid in the medium was significantly higher (13–15%) than in co-culture for R0011 and ATCC 9595 ($P < 0.05$), respectively. In contrast, no differences were detected in lactic acid production by strain RW-9595M in mono or co-culture. Ethanol (2%) was identified after 6 h of fermentation in co-culture for all strains. Additionally, the results showed a decrease in soluble protein content of the medium in both mono and co-culture (**Figures 1J–L**).

Viscosity of the Fermented WB/WP Mixtures

The six fermented WB/WP mixtures revealed a shear thinning behavior (pseudoplastic) regardless of the strain used or the fermentation method (mono or co-culture) at 24 h (**Supplementary Figure S1A**). However, the WB/WP fermented by RW-9595M in mono or co-culture showed a more pronounced decrease in viscosity compared to non-fermented WB/WP (**Supplementary Figure S1**). The results show that the pseudoplastic behavior increased over time in mono as well as in co-culture samples for the mixture fermented by RW-9595M at 0, 4, 6, 12, and 24 h (**Supplementary Figures S1B,C**). Bacterial growth (log CFU/g) was negatively correlated with viscosity (Pa.s) (Pearson index $r = -0.89$, $P = 0.04$, and $r = -0.97$, $P = 0.006$ for mono and co-culture, respectively) (**Supplementary Figure S2**). When the shear rate was 100 s^{-1}, a decrease of 50% of the apparent viscosity was observed at 4 h for the monoculture or at 6 h for the co-culture (**Supplementary Figure S2A**). Interestingly, at this moment ropy strands were visible (**Supplementary Figure S3**) with a white pellicle during fermentation, which homogeneously covered the substrate in comparison to the medium fermented by R0011 or ATCC 9595. The three *L. rhamnosus* strains are known to produce different quantities of the same exopolysaccharide (EPS) associated with cell growth. At 24 h of fermentation (**Figure 2**), scanning electron microscopy showed that the fiber surface of fermented WB/WP was covered with a pellicle that was not present in non-fermented WB/WP (**Figures 2A,B**). At a higher magnification, the *L. rhamnosus* strains, yeast and exopolysaccharides are visible on the wheat bran surface (**Figures 2C–H**).

Chemical Composition of Bioingredients Before and After Digestion

Dried fermented cereal-based products were obtained from a WB/WP mixture. All the WB/WP preparations, fermented or not, contained insoluble dietary fiber at 34–39% of dry matter (**Table 2**). Soluble dietary fiber and starch content were similar between the fermented and non-fermented (NFWB) samples ($P > 0.05$). Nevertheless, the beta-glucan content of LR95C (co-cultured ATCC 9595) was significantly ($P < 0.05$) higher (45%) than LR95M (monocultured ATCC 9595). No

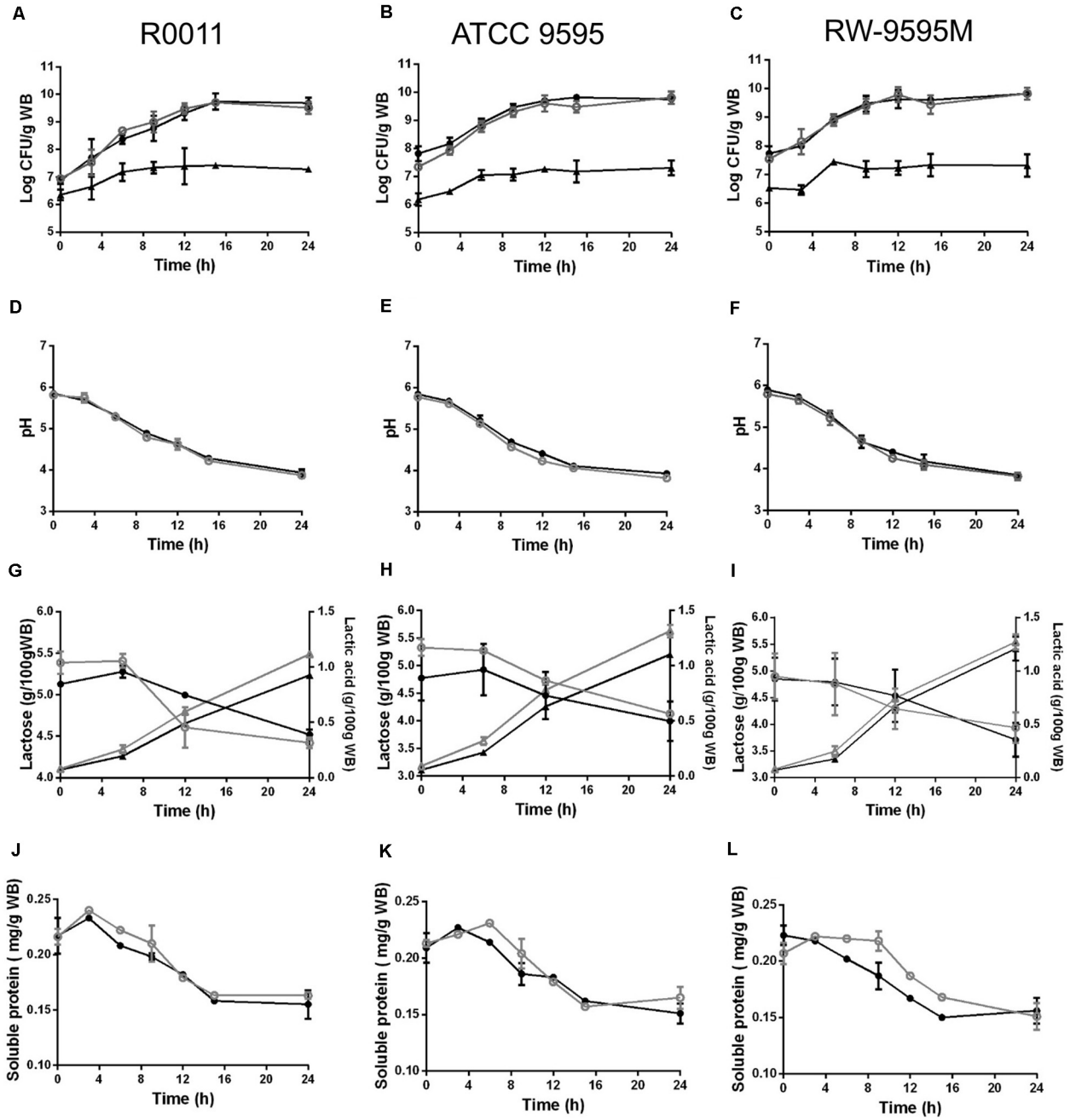

FIGURE 1 | Growth **(A–C)**, pH **(D–F)**, lactose consumption (○, ●); lactic acid production (Δ, ▲) **(G–I)**, and soluble protein **(J–L)** change during fermentation by *Lacticaseibacillus rhamnosus* R0011 in **(A,D,G,J)**; ATCC 9595 in **(B,E,H,K)** and RW-9595M in **(C,F,I L)** in mono (black) or co-culture (gray) with the yeast *S. cerevisiae*.

significant differences in beta-glucan content were found for bioingredients after mono or co-culture with R0011 (LR11M and LR11C) or monocultures of RW-9595M (LRWM) and ATCC 9595 (LR95M). In contrast, the co-cultured RW-9595M (LRWC) and ATCC 9595 (LR95C) bioingredients had similar beta-glucan content to NFWB. Moreover, the content of water-soluble polysaccharides (WSP) of the WB/WP mixtures increased significantly ($P < 0.05$) throughout the co-culture. The presence of yeast improved the content of WSP of WB/WP by 49%; 33.5 and 26.4% for the strains ATCC 9595, R0011 and RW-9595M, respectively (**Figure 3**). In co-culture, the WSP content was significantly higher ($P < 0.05$) than monoculture by 31% for R0011; 45.5% for ATCC 9595 and 9% for RW-9595M, respectively.

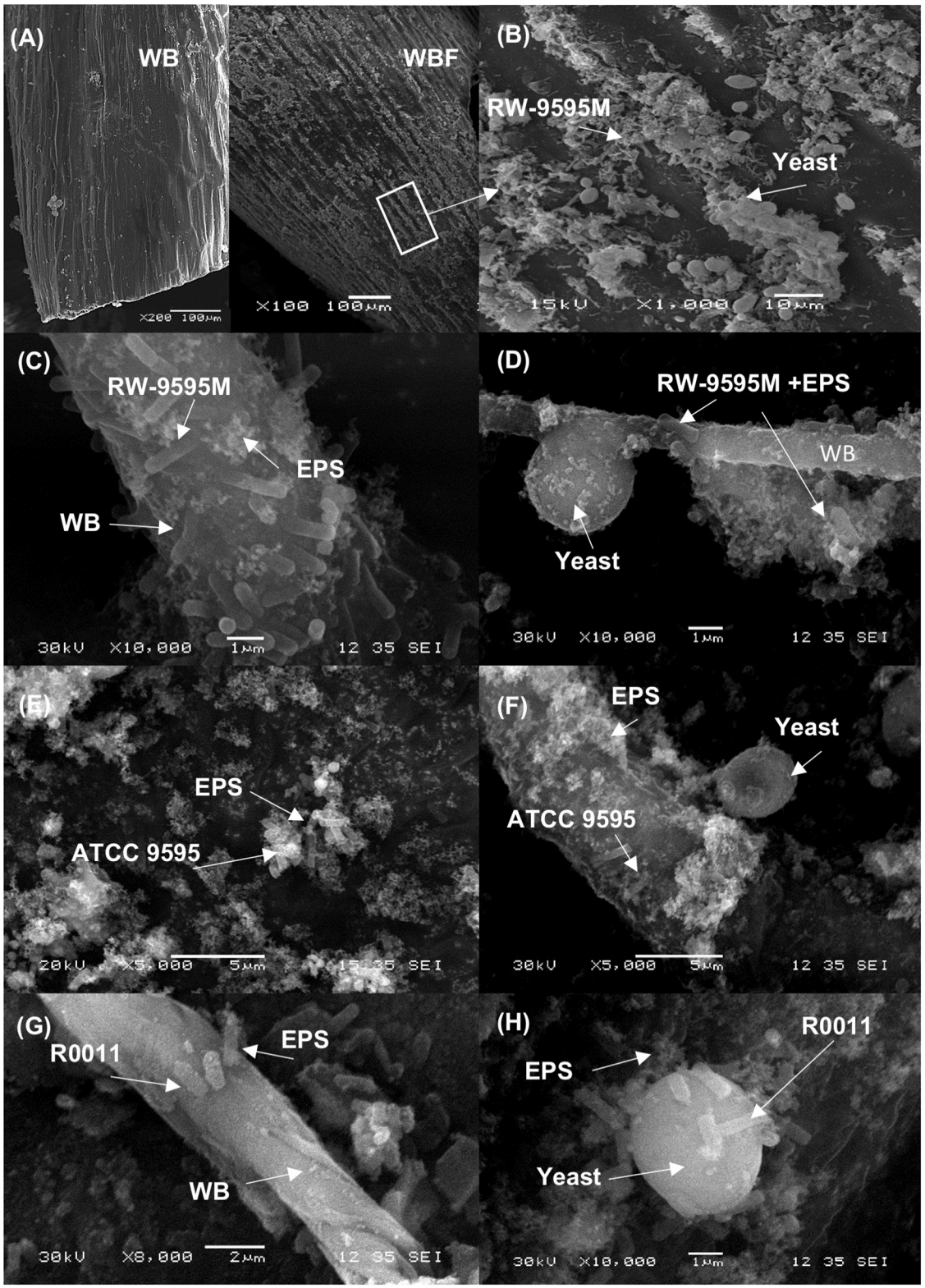

FIGURE 2 | Scanning electron micrograph of wheat bran (WB) fermented 24 h using the EPS producing *L. rhamnosus* RW-9595M and *S. cerevisiae*. In panel **(A)** the surface of non-fermented wheat bran (WB) and **(B)** the surfaces of fermented wheat bran (WBF) covered by material resembling microorganisms and EPS by appearance. In the panels a higher magnification of the bacterial cells of *L. rhamnosus* RW-9595M **(C,D)**, *L. rhamnosus* ATCC 9595 **(E,F)** or *L. rhamnosus* R0011 **(G,H)**, and EPS in mono and co-culture are observed on the fermented wheat bran surface.

TABLE 2 | Chemical composition (%DM) of bioingredients and control non-fermented wheat bran (NFWB).

Component	LR11M	LR11C	LR95M	LR95C	LRWM	LRWC	NFWB
Dry matter (%)	94.8 ± 0.4	94.7 ± 0.4	94.9 ± 0.2	95.0 ± 0.1	94.1 ± 0.1	95 ± 0.3	94.5 ± 0.1
Ash (%)	5.9 ± 0.1	5.5 ± 0.1	5.8 ± 0.3	5.4 ± 0.8	6.2 ± 0.3	5.9 ± 0.2	5.8 ± 0.1
Protein (%)	13.9 ± 0.1	14.3 ± 0.1	13.9 ± 0.3	14.1 ± 0.2	13.8 ± 0.4	14.5 ± 0.5	14.4 ± 0.3
IDF (%)	37.4 ± 2.9	38.0 ± 1.1	34.3 ± 0.8	36.7 ± 1.5	35.7 ± 1.2	39 ± 0.9	38.6 ± 0.6
SDF (%)	3.9 ± 0.3	3.7 ± 0.0	3.5 ± 0.1	2.8 ± 0.3	2.7 ± 0.2	3.2 ± 0.3	3.1 ± 0.6
Index SDF/IDF	0.104	0.097	0.102	0.076	0.075	0.08	0.08
Starch (%)	8.2 ± 0.2	8.7 ± 0.3	9.7 ± 0.3	8.6 ± 0.6	8.3 ± 0.1	8.5 ± 0.2	7.6 ± 1.9
BGluc (%)	2.9 ± 0.4^{a}	2.7 ± 0.0^{a}	2.3 ± 0.3^{a}	4.2 ± 0.0^{b}	3.2 ± 0.1^{ab}	3.9 ± 0.1^{ab}	3.6 ± 0.1^{ab}
Sol.protein (mg/g)	1.3 ± 0.1^{a}	1.4 ± 0.0^{a}	1.5 ± 0.0^{a}	1.6 ± 0.1^{a}	1.3 ± 0.05^{a}	1.4 ± 0.0^{a}	5.6 ± 0.3^{b}
Peptides (mg/g)	60.3 ± 3.7	40.9 ± 0.8	44.2 ± 2.6	63.1 ± 5.1	55.9 ± 17.1	53.3 ± 5.3	57.1 ± 4.4
Xylose (mg/g)	20.9 ± 1.7^{a}	17.2 ± 2.4^{a}	20.1 ± 0.6^{a}	26.2 ± 0.5^{a}	18.0 ± 0.5^{a}	23.1 ± 1.4^{a}	34.1 ± 1.1^{b}
Lactose (mg/g)	138.9 ± 11^{a}	155.1 ± 6.8^{a}	152.5 ± 7.6^{a}	153.4 ± 17.8^{a}	157.7 ± 22.3^{a}	156.4 ± 1.7^{a}	235 ± 0.0^{b}
Galactose (mg/g)	1.7 ± 0.1^{a}	nd*	1.6 ± 0^{a}	0.4 ± 0.0^{b}	1.5 ± 0.2^{a}	nd*^{b}	3.4 ± 0.6^{c}
Lactic acid (mg/g)	44.7 ± 2.8^{a}	40.0 ± 0.4^{a}	58.6 ± 3.7^{b}	52.4 ± 4.8^{b}	61.5 ± 7.8^{b}	53.7 ± 1.1^{b}	3.5 ± 0.6^{c}

The data are the means of three independent experiments ± standard deviations (n = 3). Data with different letters in the same column are significantly different (P < 0.05)
**nd, not detected; IDF, insoluble fiber; SDF, soluble dietary fiber; Sol.protein, soluble protein; BGluc, beta glucans.*

Galactose, lactose and xylose contents were higher in NFWB by 56–100, 33–41, and 24–50% in comparison to the fermented bio-products ($P < 0.05$), respectively (**Table 2**). Lactic acid was the major fermentation end-product and was higher (91–95%) in the bioingredients than in NFWB ($P < 0.01$). Total protein content did not significantly differ between the bioingredients and the non-fermented substrate ($P > 0.05$). Conversely, significant differences ($P < 0.05$) were observed in the fraction of soluble protein. Likewise, in culture medium, the amount of soluble protein was higher (72%) in the NFWB than in fermented WB/WP. The peptide content was similar between the non-fermented and fermented samples.

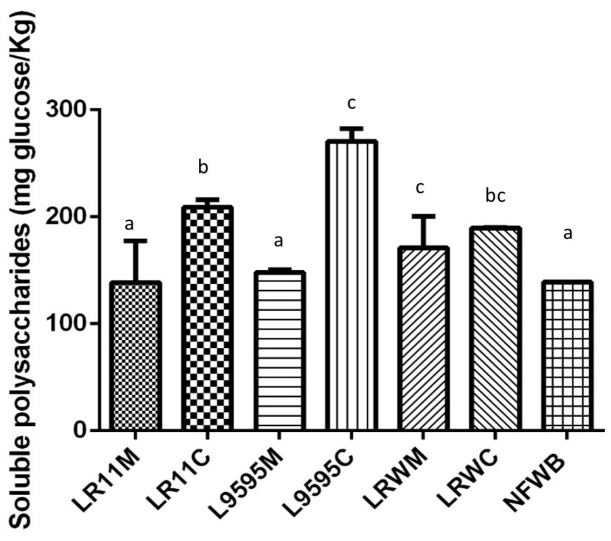

FIGURE 3 | Water soluble polysaccharide (WSP) content of bioingredients obtained in mono or co-culture by the strains of *L. rhamnosus* R0011, ATCC 9595, and RW-9595M. Data with different letters in the same column are significantly different ($P < 0.05$). The data are the means of three independent experiments ± standard deviations ($n = 3$).

In this study, the total free amino acid content was higher in the bioingredients (23.5–43%) compared to NFWB ($P < 0.05$) (**Table 2**). A heat map was constructed to visualize the result of hierarchical clustering of the profile data and to identify changes in free amino acid content among bio-products (**Supplementary Figure S4**). The dendrogram of the heat map shows groups of NFWB (non-fermented) and the bioingredients (fermented). Thus, in fermented bioproducts, 63% of the amino acids were significantly higher ($P < 0.05$) after bioprocessing (Arg, Gln, Ser, Gly, Thr, Ala, GABA, Pro, Asp, His, Glu, and Phe) in comparison to NFWB.

The concentration of GABA, a functional amino acid derivative, was slightly higher (between 26 and 47%) as a consequence of fermentation compared to non-fermented wheat bran (NFWB). Furthermore, the heat map shows that bioproducts LR11M (mono) and LR11C (co-culture) from *L. rhamnosus* R0011 were clustered together. Likewise, the analysis distinguished the amino acid profiles between the bioingredients from monoculture (LR95M and LRWM) or co-culture (LR95C and LRWC) of *L. rhamnosus* ATCC 9595 and RW-9595M. For strains ATCC 9595 and RW-9595M, the bioingredient obtained from co-culture showed an amino acid profile enriched in Lys, Val, Leu, Phe, Ile, and Glu.

Samples were hydrolyzed through simulated buccal, gastric and intestinal stages. The term digested sample (DS) refers to a portion (with a solubility ranging between 50 and 63%) which remained after the *in vitro* assay and would be degraded and converted in the colon by the intestinal microbiota. Dietary fiber was the major component of the digested samples, with values ranging from 54.3 to 58.5% (**Table 3**). The soluble dietary fiber was similar among the samples and ranged from 8.1 to 10.7%.

The protein content of the co-cultured bioingredients LR11C to LRWC was higher (9%) than digested NFWB and LR11M ($P < 0.01$). The soluble protein content in digested LR11M and

TABLE 3 | Chemical composition (%DM) of digested bioingredients and non-fermented mixture of wheat bran and whey permeate (NFWB).

Component	LR11M	LR11C	LR95M	LR95C	LRWM	LRWC	NFWB
Dry matter (%)	94.7 ± 0.3	95.3 ± 0.5	95.3 ± 0.6	95.4 ± 0.1	95.0 ± 0.1	95.0 ± 0.3	82.1 ± 2.6
Protein (%)	14.5 ± 0.3^{a}	15.6 ± 0.1^{b}	15.6 ± 0.0^{b}	14.9 ± 0.1^{b}	15.2 ± 0.1^{b}	15.1 ± 0.0^{b}	14.2 ± 0.0^{a}
IDF (%)	55.1 ± 0.3	54.3 ± 1.2	55.4 ± 0.8	58.5 ± 1.3	56.3 ± 0.1	57.7 ± 0.1	56.8 ± 0.5
SDF (%)	8.1 ± 1.1	10.4 ± 0.6	10.7 ± 0.5	9.3 ± 1.6	10.0 ± 1.1	9.4 ± 1.1	8.2 ± 0.1
Index ISF/IDF	0.145	0.19	0.19	0.154	0.175	0.161	0.145
Soluble protein (mg/g)	6.1 ± 0.4^{a}	7.3 ± 0.1^{a}	8.2 ± 0.05^{b}	7.4 ± 0.7^{a}	9.7 ± 0.07^{b}	8.7 ± 0.2^{b}	9.0 ± 0.1^{b}
Peptides (mg/g)	84.7 ± 3.2	95.2 ± 1.9	87.4 ± 1.3	89.6 ± 3.1	94.1 ± 2.3	83.9 ± 2.3	83.9 ± 4.4
Xylose (mg/g)	75.2 ± 14^{a}	46.0 ± 4.8^{a}	98.6 ± 1.7^{b}	83.6 ± 1.6^{b}	80.7 ± 0.0^{b}	101.7 ± 0.8^{b}	107 ± 0.2^{b}
Lactose (mg/g)	22.4 ± 0.2	23.0 ± 0.4	22.9 ± 0.6	21.2 ± 0.4	23.5 ± 0.3	25.4 ± 1.6	23.4 ± 0.0
Glucose (mg/g)	1.3 ± 0.0^{a}	1.2 ± 0.0^{ab}	1.5 ± 0.0^{c}	1.1 ± 0.1^{b}	1.4 ± 0.03^{c}	1.3 ± 0.1^{a}	1.5 ± 0.1^{a}
Lactic acid (mg/g)	6.4 ± 0.0^{a}	5.0 ± 0.0^{b}	7.6 ± 0.1^{c}	6.6 ± 0.2^{a}	7.9 ± 0.1^{c}	7.5 ± 0.5^{c}	0.4 ± 0.5^{d}

Data with different letters in the same column are significantly different ($P < 0.05$). IDF, insoluble fiber; SDF, soluble dietary fiber. The data are the means of three independent experiments ± standard deviations (n = 3).

LR11C was lower (33 and 19%, respectively) than the digested control NFWB, LR95M and LRWC ($P < 0.05$). In contrast, the peptide content in digested samples LR11C and LRWM was higher (12 and 11%, respectively) than in digested NFWB ($P < 0.05$). No differences were found in sugar content (reducing sugar, xylose, lactose, or glucose) between the digested samples from fermented or non-fermented products ($P > 0.05$), while the lactic acid in the digested bioingredients was higher (92–95%) than the non-fermented control.

Impact of Fermentation and *in vitro* Digestion on Bioactive Compounds and Antioxidant Activity

Total Phenolic and Antioxidant Activity

In general, the bound TPC and antioxidant activity of bioingredients and digested samples were higher than the free fraction (**Table 4**). The free fraction represented 3–32% of TPC and 29–45% of the antioxidant activity in bioingredients. Free TPC and antioxidant activity of the LRWM bio-product LRWM were similar to NFWB ($P > 0.05$) and higher than the other bioingredients. Nevertheless, free TPC content did not differ significantly between monoculture and co-culture for the bioingredients fermented using RW-9595M (LRWM-LRWC) or ATCC 9595 (LR95M-LR95C).

The amount of bound and total (sum of free and bound fractions) TPC as well as the antioxidant activity in all the bio-products (**Table 4**) were higher in fermented bioingredients than in NFWB ($P < 0.001$). The bioingredient fermented by RW-9595M in monoculture (LRWM) showed the maximum increase in TPC (bound and total), which was higher by 69.8 and 60% compared to NFWB. The bound and total TPC content was higher in monoculture in comparison to co-culture for RW-9595M (39 and 30% for bound and total phenolic content) and ATCC 9595 (23 and 19%) ($P < 0.01$). Likewise, the antioxidant activity of the bound fraction of LRWM was improved by 54% in comparison to NFWB. Furthermore, the antioxidant capacity of the bound and the total fractions of LRWM (monoculture) were higher (21 and 18%, respectively) than in the co-culture product LRWC ($P < 0.01$). Mono and co-cultured products fermented with R0011 (LR11M-LR11C) or ATCC 9595 (LR95M-LR95C) ($P > 0.05$) did not differ significantly. These results show a positive correlation between free and bound TPC and antioxidant activity (ORAC) of bioingredients (Pearson index $r = 0.86$ and $r = 0.92$, $P < 0.0001$, respectively).

After digestion, the free fraction of TPC represented 14–21% of TPC and 59–73% of the antioxidant activity (**Table 4**). The free TPC of LRWC (co-culture of RW-9595M) was similar to NFWB and it was the highest among the fermented samples. For strains R0011 and ATCC 9595, no differences in free TPC were observed between mono and co-culture. The antioxidant activity of the free fraction was similar in digested samples whatever their origin. On the other hand, the content of bound and total TPC in digested WB/WP after co-culture with R0011 and ATCC 9595 (LR11C and LR95C) and monoculture RW-9595M (LRWM) was similar to digested NFWB and higher than the other samples. The antioxidant activity of bound and total fractions revealed one group composed of digested samples from yeast co-culture with either ATCC 9595 (LR95C) or RW-9595M (LRWM-LRWC), which were similar to digested NFWB and higher than the second group containing the digested samples fermented with strain R0011 (LR11M-LR11C) and yeast co-culture of ATCC 9595 (LR95M) ($P < 0.01$).

Data collected from the free, bound and total TPC after and before the *in vitro* digestion were subjected to discriminant analysis (**Figure 4A**). Discriminant analysis was used to classify the data into groups according to discrete (categorical) variables. Two principal factors explained more than 92% of the variance of the independent variables. The F1 principal factor shows the effect of digestion. LRWM (monoculture of RW-9595M) is well separated from the other bioingredients and NFWB (left side of the figure). Interestingly, after digestion, the properties of the digested bioingredients and NFWB were more similar.

In spite of the similarity between fermented and non-fermented digested samples mentioned above, the recovery of unabsorbed TPC in digested NFWB was higher (23–61%) than that of the digested fermented bioingredients (**Figure 4B**). Monoculture resulted in a lower percentage of TPC and antioxidant activity than co-culture. LRWM-LRWC and LR95M

TABLE 4 | Total phenolic content (TPC) and antioxidant activity (ORAC) of bioingredients **(A)** and the digested samples **(B)**.

(A) Bioingredients before digestion.

Component	LR11M	LR11C	LR95M	LR95C	LRWM	LRWC	NFWB
Total phenolic content (mg/100 g DM)							
Free	7 ± 1.6^{a}	22 ± 3.7^{b}	27 ± 0.6^{b}	33 ± 3.3^{b}	52 ± 2.6^{cd}	48 ± 4.5^{c}	62 ± 5.1^{d}
Bound	231 ± 14.4^{a}	246 ± 38.2^{a}	308 ± 4.3^{b}	237 ± 7.5^{a}	437 ± 0.62^{c}	265 ± 0.37^{a}	132 ± 3.0^{d}
Total	238 ± 12.8^{a}	269 ± 34.4^{a}	336 ± 3.7^{b}	271 ± 4.2^{ab}	489 ± 1.9^{c}	313 ± 4.2^{b}	194 ± 2.1^{d}
ORAC (μmol Trolox/100 g DM)							
Free	$5,306 \pm 6^{a}$	$6,668 \pm 588^{b}$	$6,020 \pm 23^{ab}$	$6,811 \pm 118^{ab}$	$8,642 \pm 275^{c}$	$7,644 \pm 575^{a}b$	$7,990 \pm 134^{c}$
Bounded	$12,338 \pm 294^{a}$	$12,925 \pm 99^{a}$	$15,011 \pm 400^{a}$	$14,686 \pm 326^{a}$	$21,313 \pm 806^{b}$	$16,876 \pm 867^{a}$	$9,859 \pm 86^{c}$
Total	$17,644 \pm 288^{a}$	$19,593 \pm 687^{a}$	$21,031 \pm 377^{a}$	$21,497 \pm 444^{a}$	$29,954 \pm 1081^{b}$	$24,520 \pm 1442^{c}$	$17,849 \pm 49^{a}$

(B) Bioingredients after digestion

Component	LR11M	LR11C	LR95M	LR95C	LRWM	LRWC	NFWB
Total phenolic content (mg/100 g DM)							
Free	90 ± 1.6^{a}	94 ± 1.7^{a}	90 ± 0.1^{a}	98 ± 4.5^{a}	99 ± 1.1^{a}	108 ± 3.5^{ab}	116 ± 4.2^{b}
Bound	413 ± 27.3^{a}	589 ± 1.9^{b}	391 ± 0.4^{a}	559 ± 2.2^{bc}	527.6 ± 11^{bc}	429 ± 10.2^{a}	540 ± 5.1^{c}
Total	503 ± 26^{a}	683 ± 3.5^{b}	481 ± 0.5^{a}	656.1 ± 6.7^{b}	626.8 ± 12^{bc}	537 ± 6.7^{a}	656 ± 0.9^{b}
ORAC (μmol trolox/100 g DM)							
Free	$10,656 \pm 494^{a}$	$11,241 \pm 209^{ab}$	$10,469 \pm 1,636^{ab}$	$11,903 \pm 396^{c}$	$8,758 \pm 32^{b}$	$9,822 \pm 140^{b}$	$10,413 \pm 333^{a}$
Bound	$16,203 \pm 611^{a}$	$17,028 \pm 290^{a}$	$15,036 \pm 1,348^{a}$	$22,244 \pm 777^{b}$	$24,287 \pm 323^{b}$	$23,275 \pm 502^{b}$	$23,451 \pm 554^{b}$
Total	$26,859 \pm 1,105^{a}$	$28,269 \pm 81.3^{a}$	$25,505 \pm 984^{a}$	$34,148 \pm 381^{b}$	$3,3045 \pm 355^{b}$	$33,098 \pm 642^{b}$	$33,866 \pm 221^{b}$

Data with differents letters in the same column are significantly different ($P < 0.05$). The data are the means of three independent experiments ± standard deviations (n = 3).

had the lowest percentage of TPC recovered. Nevertheless, higher antioxidant activity (ORAC) kept the digested NFWB superior (34 and 40%) to those of LRWM and LR95M, respectively. This was in accordance with the lower correlation detected between TPC and antioxidant activity (Pearson $r = 0.564$ $P < 0.05$) in the digested samples.

Phenolic Acid Profile and Bioaccessibility

Gallic acid, protocatechuic acid, ferulic acid and caffeic acid content of bioingredients differed significantly from NFWB ($P < 0.01$) (**Table 5**). Total free phenolic acid content was higher for LR95M-LR95C (53–59%), LRWM-LRWC (45–46%), and LR11M-LR11C (29–39%) compared to non-fermented NFWB. There was no variation in 4-hydroxybenzoic acid and shikimic acid content between the bio-products and the control. The gallic acid content in LR11M, LR95C, LRWM, and LRWC was similar to NFWB and lower than that of LR95M. The protocatechuic acid content was lower by 14 and 47% in bioingredients compared to NFWB.

The free ferulic acid content was lower by 44.5% (LR11M-LR11C) to 88% (LR95M to LRWC) when compared with NFWB regardless of the type of culture employed (mono or co-culture) ($P < 0.01$). Free *p*-coumaric acid was present in NFWB but was absent in the fermented products. Interestingly, the content of free caffeic acid increased 97–98% in bioingredients compared to NFWB ($P < 0.001$).

After gastrointestinal digestion, the total free phenolic acid content was reduced by 73.6% in bioingredients and by 40% in NFWB, with no differences between mono and co-culture (**Table 5**). The content of shikimic acid was similar before and after digestion ($P > 0.05$). The digested NFWB sample showed the highest concentration of 4-hydroxybenzoic acid and ferulic acid in comparison to the digested samples from fermented bioingredients (higher by 51–95%). Similar to bioingredients, the free caffeic acid content of digested LR95M-LR95C was higher by 90% than in digested NFWB, followed by LRWM-LRWC (85%) and LR11M-LR11C (70–80%) ($P < 0.01$).

Based on free phenolic acid content, discriminant analysis separated bioingredients from NFWB (**Figure 5A**). Two principal factors explained more than 86% of the variance. As observed previously, the bioingredients fermented by R0011 (LR11M-LR11C) were similar in mono and co-culture and different from the bioingredients fermented by strains ATCC 9595 (LR95M-LR95C) and RW-9595M (LRWM-LRWC). As was expected, digestion results in more uniformity among bioingredients and non-fermented NFWB (**Figure 5A**).

The bioaccessibility of the free total phenolic acids was improved by 42-48% in fermented bioingredients compared to NFWB ($P < 0.05$) (**Figure 5B**). Bioaccessibility of free gallic and shikimic acids (in general >70%) was similar to NFWB while the bioaccessibility of caffeic and 4-hydroxybenzoic acids in bioingredients showed values superior to 60–75% (**Figure 5C**), which was significantly higher than NFWB ($P < 0.01$). The bioaccessibility of free protocatechuic acid was higher in LR11C through to LRWM when compared to NFWB. The bioingredients from R0011 and ATCC 9595 showed higher values (58% and more than 65%) of bioaccessible ferulic acid, respectively (**Figure 5C**). In contrast, both bioingredients

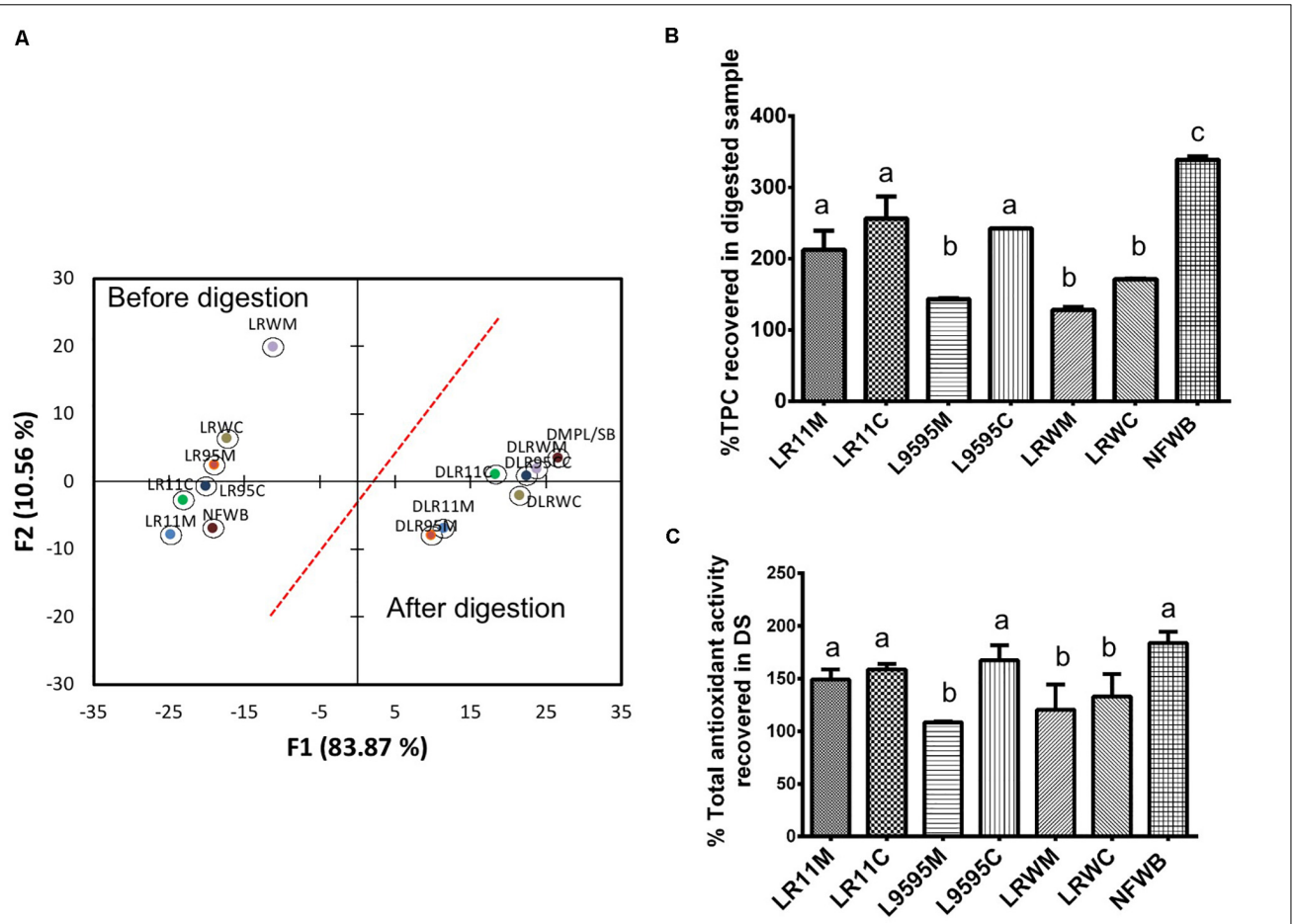

FIGURE 4 | (A) Biplot showing the results of the discriminant analysis of total (free and bound) phenolic content (TPC) and antioxidant activity (ORAC total) of bioingredients before and after *in vitro* digestion. The **(B)** Comparison of the percentage of TPC and **(C)** antioxidant activity recovered (unabsorbed) in the bioingredients and non-fermented sample (NFWB). Data with different letters in the same column are significantly different ($P < 0.05$). The data are the means of three independent experiments ± standard deviations ($n = 3$).

from RW-9595M (LRWM and LRWC) showed lower ferulic acid bioaccessibility (values inferior to 35%) compared to NFWB and the other bioingredients. The discriminant analysis showed that NFWB and LRWM are different from the other bioingredients (**Figure 5D**). Thus, the proportion of bioaccessible phenolic acids was strain and culture dependent. The monoculture resulted in higher bioaccessibility of ferulic acid for ATCC 9595 and RW-9595M. The bioingredients contained a higher quantity of bound 4-dihydroxybenzoic, *p*-coumaric, ferulic acid and its isomer, isoferulic acid, than free forms (**Figure 6A**). The bioingredient from RW-9595M showed higher values of bound phenolic acid compared to the other bioingredients and NFWB.

After gastrointestinal digestion, the bound phenolic acid content increased compared to before digestion (**Table 5**). Discriminant analysis of bound phenolic acid content showed that digested bioingredients LRWC and LR11M could be differentiated from NFWB, except for LRWC (**Figure 6A**). The two principal factors explained more than 90% of the variance of variables.

The recovery of individual bound phenolic acids was superior from LLR11M (32%) compared to NFWB and the other bioingredients (**Figure 6C**). In contrast, compared to NFWB, the LR95M bioingredient LR95M (19% inferior) and LRWC (27% inferior) showed the lowest recovery index values (**Figure 6C**). For *L. rhamnosus* strains R0011 and RW-9595M, the recovery of individual bound phenolic acids was significantly higher in mono (LR11M and LRWM) than in co-culture (LR11C and LRWC) ($P < 0.05$) while no differences were found for ATCC 9595 (LR95M-LR95C) (**Figures 6B,D**). The LRWC bioingredient showed the lowest recovery index values for bound caffeic, isoferulic and protocatechuic acids.

DISCUSSION

Growth and Viscosity During Fermentation of WB/WP

In both mono and co-culture, *L. rhamnosus* strains R0011, ATCC 9595, and RW-9595M showed similar profiles

TABLE 5 | Profile of free and bound phenolic acids of **(A)** bioingredients and **(B)** digested samples.

Bio-ingredients	LR11M	LR11C	LR95M	LR95C	LRWM	LRWC	NFWB
(A) Bioingredients before digestion							
Free acid phenolic (μg/100g DM)							
Gallic acid	76 ± 10^{a}	59 ± 26^{a}	167 ± 13^{b}	147 ± 4.8^{b}	126 ± 19^{c}	81 ± 11^{a}	106 ± 0.3^{a}
4-Hyd acid*	288 ± 34^{a}	463 ± 57^{b}	283 ± 53^{b}	336 ± 47^{b}	245 ± 92^{a}	336 ± 7.0^{b}	201 ± 3.0^{a}
Caffeic acid	4,662 ± 285^{a}	4,265 ± 224^{a}	8,053 ± 35^{b}	8,359 ± 931^{b}	6,292 ± 487^{c}	6,579 ± 738^{c}	142 ± 11^{d}
Ferulic acid	1,414 ± 108^{a}	852 ± 53^{b}	262 ± 37^{c}	380 ± 53^{d}	423 ± 15^{d}	296 ± 28^{d}	2,547 ± 10^{e}
Protocatechuic acid	1,210 ± 294^{a}	876 ± 91^{a}	1,201 ± 17^{a}	2,064 ± 199^{c}	1,428 ± 117^{a}	1,363 ± 74^{a}	1,660 ± 468^{a}
Shikimic acid	20 ± 3.9^{a}	28 ± 2.5^{b}	21 ± 0.6^{b}	26 ± 4.3^{b}	14 ± 0.3^{a}	19 ± 3.6^{a}	19 ± 3^{a}
p-Coumaric	nd	nd	nd	nd	nd	359 ± 46	nd
Total	7,671 ± 310	6,545 ± 361	9,988 ± 78	11,311 ± 864	8530 ± 553	8,676 ± 828	4,677 ± 1215
Bound acid phenolic (mg/100 g DM)							
4-Hyd acid*	5 ± 0.02^{a}	6 ± 0.22^{a}	7 ± 0.18^{b}	8 ± 0.40^{c}	6 ± 0.05^{b}	8 ± 0.53^{c}	7 ± 0.30^{b}
p-Coumaric acid	10 ± 1.25^{a}	16 ± 0.28^{b}	19 ± 2.3^{b}	20 ± 0.30^{b}	15 ± 0.21^{b}	24 ± 0.50^{c}	19 ± 0.18^{b}
Caffeic acid	0.2 ± 0.03^{a}	0.4 ± 0.02^{a}	nd	nd	nd	0.74 ± 0.04^{b}	nd
Ferulic acid	116 ± 7.8^{a}	174 ± 6.9^{b}	203 ± 2.1^{b}	166 ± 5.45^{b}	148 ± 7.5^{b}	221 ± 9.1^{c}	162 ± 5.5^{b}
IsoFerulic acid	39 ± 1.5^{a}	68 ± 3.2^{b}	55 ± 5.9^{b}	53 ± 0.2^{b}	50 ± 5.3^{b}	102 ± 4.7^{c}	60 ± 2.3^{b}
Protocatechuic acid	nd	113 ± 16^{a}	nd	nd	nd	218 ± 70^{b}	nd
Total	170.2 ± 10.6	264.2 ± 9.9	285.5 ± 13.1	246.6 ± 6.4	219.5 ± 13.1	356.4 ± 13.9	248.4 ± 8.3
(B) Bioingredients after digestion							
Free acid phenolic (μg/100g DM)							
Gallic Acid	31 ± 0.1^{a}	15 ± 0.1^{b}	15.1 ± 0.9^{b}	23.9 ± 0.9^{a}	22.1 ± 0.9^{a}	9.3 ± 0.2^{c}	17 ± 0.3^{b}
4-Hyd acid*	91 ± 8^{a}	145 ± 0.1^{a}	33 ± 0.1^{b}	78 ± 1.1^{b}	69 ± 4.1^{b}	47 ± 1^{b}	223 ± 38^{c}
Caffeic acid	687 ± 151^{a}	1,025 ± 140^{a}	2,113 ± 343^{b}	2,014 ± 156^{b}	1,299 ± 166^{ab}	1,370 ± 317^{ab}	202 ± 0.1^{a}
Ferulic acid	589 ± 127^{a}	383 ± 65^{a}	65 ± 27^{b}	138 ± 15^{c}	285 ± 67^{c}	274 ± 27^{c}	1,210 ± 268^{d}
Protocatechuic acid	550 ± 64^{a}	205 ± 9^{b}	193 ± 126^{b}	399 ± 139^{b}	308 ± 92^{b}	1,049 ± 8^{c}	1,043 ± 4^{c}
Shikimic acid	4.4 ± 0.3^{a}	3 ± 0.2^{a}	4.4 ± 0.8^{a}	4 ± 0.2^{a}	5 ± 0.1^{a}	6 ± 2.2^{a}	4 ± 0.2^{a}
Total	1,953 ± 96	1,778 ± 201	2,524 ± 363	2,705 ± 98	2,059 ± 134	2,757 ± 335	2,704 ± 302
Bound phenolic acids (mg/100 g DM)							
4-Hyd acid*	8 ± 0.4^{a}	8 ± 0.2^{a}	7 ± 0.6^{a}	8 ± 0.1^{a}	8 ± 0.4^{a}	10 ± 0.4^{b}	7 ± 0.5^{a}
p-Coumaric acid	32 ± 0.5^{a}	29 ± 2.8^{a}	26 ± 2.3^{a}	28 ± 0.5^{a}	28 ± 2.2^{a}	34 ± 2.5^{a}	28 ± 0.2^{a}
Caffeic acid	nd	0.6 ± 0.03^{b}	0.9 ± 0.07^{b}	1.7 ± 0.02^{c}	1.4 ± 0.2^{c}	nd	19 ± 0.1^{c}
Ferulic acid	262 ± 6.9^{a}	283 ± 10.3^{a}	259 ± 9.8^{a}	266 ± 0.41^{a}	276 ± 12.78^{a}	268 ± 12.8^{a}	257 ± 15.5^{a}
Isoferulic acid	96 ± 1.1^{a}	91 ± 3.5^{a}	78 ± 2.2^{b}	100 ± 0.8^{a}	102 ± 4.7^{ba}	102 ± 4.7^{a}	105 ± 5.4^{a}
Protocatechuic acid	nd	0.5 ± 0.06^{a}	0.3 ± 0.07^{a}	0.6 ± 0.12^{b}	0.3 ± 0.1^{a}	nd	0.4 ± 0.01^{a}
Total	398 ± 11.5	413 ± 13.9	371 ± 15	404 ± 2.4	417 ± 28.9	413 ± 27.8	399 ± 29.2

*The data are the means of three independent experiments ± standard deviations (n = 3). *4 Hyd acid, 4 hydroxybenzoic acid.*

during fermentation of WB/WP medium. *L. rhamnosus* R0011 produced the lowest quantity of lactic acid in 48 h of fermentation compared to the two other strains. The presence of ethanol in co-culture was related to the metabolism of the yeast, as *S. cerevisiae* is able to convert lactic acid to pyruvate to produce ethanol and decrease the levels of lactic acid in the medium (Cheirsilp and Radchabut, 2011). The interaction of yeast with LAB during co-culture in the presence of lactose can be considered as mutualism (Ponomarova et al., 2017).

The rheological behavior in terms of viscosity of WB/WP fermented by R0011 or ATCC 9595 was not different from that of non-fermented WB. While the shear intensity increases, the apparent viscosity decreases until the viscosity reaches a plateau of limit viscosity, this pseudoplastic behavior is characteristic of WB (Dikeman et al., 2006). In contrast, as the fermentation time increases, WB/WP fermented by RW-9595M showed a lower viscosity than non-fermented WB and the other fermented samples. This behavior suggests different chemical interactions between the components of fermented WB/WP mixture (protein/polysaccharides) and EPS produced by RW-9595M (visible white pellicle, ropy strand formation) during fermentation. In this sense, the ratio of low-molecular-mass EPS may affect the viscosity of an EPS solution (Pham et al., 2000). The EPS fractions produced by *L. rhamnosus* E/N on a medium with galactose, lactose, or sucrose show heterogeneous molecular weight, while those produced on a medium with maltose and glucose show only high-molecular-weight EPS (Polak-Berecka et al., 2015). The same authors reported that the reduction of viscosity was correlated with the thickness of the EPS chain. The rheology of the EPS from *L. rhamnosus* RW-9595M, due to its acidic nature, may also be affected

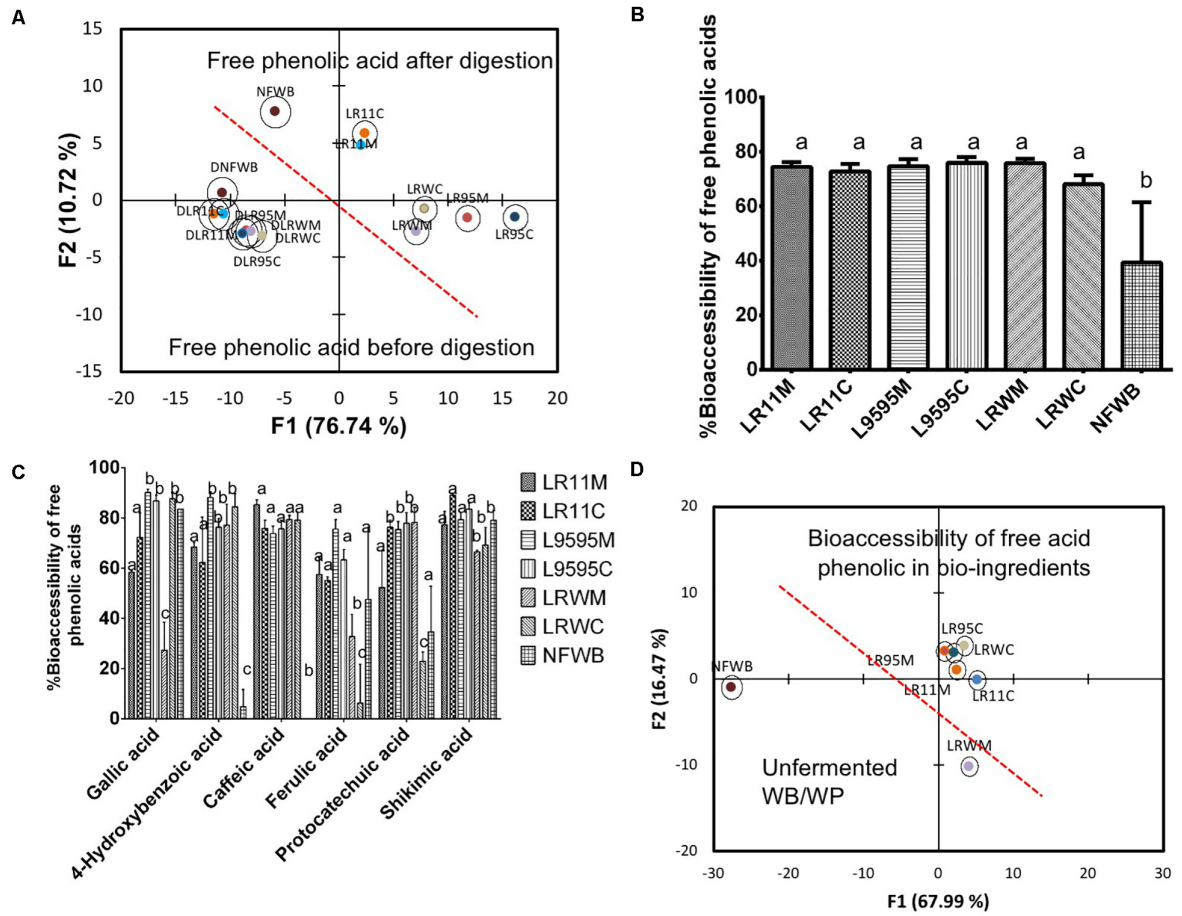

FIGURE 5 | Biplot showing the results of the discriminant analysis (DA) of **(A)** free phenolic acid content of bioingredients before and after *in vitro* digestion, **(B)** % bioaccessibility of free total phenolic acids (absorbed), **(C)** % bioaccessibility of individual free phenolic acids, and **(D)** bi-plot showing the classification of the bioingredients according their free phenolic acid bioaccessibility. Data with different letters in the same column are significantly different ($P < 0.05$). The data are the means of three independent experiments ± standard deviations ($n = 3$).

by electrostatic interactions between charged residues such as occurs with high-methoxyl pectin (Polak-Berecka et al., 2015; Bertsch et al., 2019).

In vitro Digestion of Bioingredients

In this work, the macro-components such as dietary fiber, ash and total protein of fermented products did not differ from the non-fermented NFWB. In contrast, the bioingredients showed a lower content of the sugars lactose, galactose and xylose than NFWB, indicating the utilization of sugars from whey permeate or wheat bran (xylose) as a carbon source for growth of the strains. Furthermore, the content of water-soluble polysaccharides increased, principally in LR95C, LR11C, and LRWC in comparison to NFWB. The presence of the yeast possibly influenced the content of water-soluble polysaccharides of bio-ingredients after co-culture. The content of WSP includes EPS and non-hydrolyzed soluble polysaccharides retained by dialysis from wheat bran such as arabinoxylan, beta-glucans and yeast cell wall polysaccharides. In previous studies, co-culture with the yeast resulted in increased EPS production compared to monoculture by these three strains (49% for ATCC 9595; 42% RW-9595M, and 39% R0011) in WP medium (Bertsch et al., 2019). The more complex nature of the WB/WP matrix compared to WP alone could influence the production of EPS by RW-9595M. The reduction in viscosity observed during fermentation could be related to EPS heterogeneity of molecular mass distribution and the fraction of low molecular weight that cannot be retained by the dialysis membrane used for WSP quantification in this work. This may explain the slight differences of WSP content in BI from RW-9595M in mono and co-culture for a strain reported to produce high amounts of EPS.

Also as a result of fermentation, the content of soluble protein was lower, and the free amino acid profile was enriched in the bioingredients. The fermentation of WB/WP led to an increase in amino acids such Pro (49–77%) and Glu (46 to 68%), which could also partially originate from prolamin degradation. Arte et al. (2015) reported that primary proteolysis occurs when oligopeptides are released during cereal fermentation, mainly by the activity of cereal endoproteases. In fermented wheat bran or sourdough, microbial peptidase activity from lactic acid

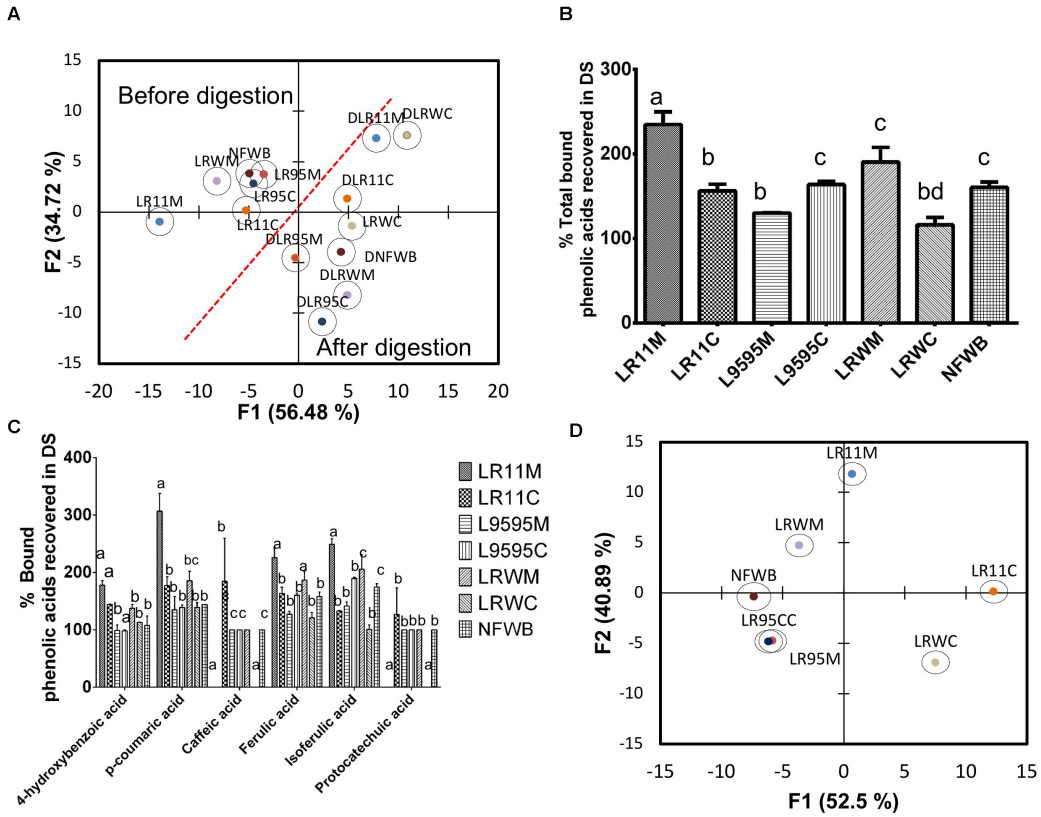

FIGURE 6 | (A) Biplot showing the results of the discriminant analysis (DA) of bound phenolic acid content before and after *in vitro* digestion, **(B)** % of total phenolic acids recovered in digested samples of bioingredients, **(C)** % bound individual phenolic acids recovered (unabsorbed) in digested samples of bioingredient. **(D)** Biplot showing the classification of bioingredients according the % of phenolic acids recovered in digested samples by discriminant analysis. Data with different letters in the same column are significantly different ($P < 0.05$). The data are the means of three independent experiments ± standard deviations ($n = 3$).

bacteria such as *L. rhamnosus* could be responsible for secondary proteolysis to release free amino acids and small-sized peptides (Coda et al., 2012). Accumulation of amino acids in dough during fermentation with lactobacilli depends on the strain (Gänzle et al., 2008). In this work, the co-culture revealed an enriched amino acid profile compared to monoculture. In this sense, the relative expression of the gene coding for dipeptidyl aminopeptidase (*R0011_04490*) was overexpressed in co-culture with yeast for these strains in a medium with WP (Bertsch et al., 2019). Further experiments would be necessary to determine how peptides and amino acids impact the bioactivity of bioingredients for use as antioxidants or their potential ACE-inhibitory activity due to peptide accumulation.

Impact of Fermentation and *in vitro* Digestion on Bioactive Compounds and Antioxidant Activity

Fermentation had an effect on free and bound TPC and antioxidant activity of bioingredients. In general, the bound TPC and antioxidant activity of bioingredients were higher than the free fraction and the non-fermented samples. This agrees with previous reports revealing that fermentation improved the free and/or bound phenolic content of lentils, soy bean, black cow gram and mottled cowpea, wheat, rye and whole barley (Gan et al., 2016; Shumoy et al., 2017). The structural breakdown of the complex cereal cell wall induced by the endogenous enzymes of the cereals releases bioactive compounds. These enzymes are activated by the changes of pH during the fermentation process (Mateo Anson et al., 2011). Hence, fermentation could improve extraction efficiency of both free and bound phenolic compounds, leading to a higher TPC after processing (Gan et al., 2016). These TPC can act as reducing agents and singlet oxygen quenchers (Hur et al., 2014), thus increasing antioxidant activity.

In monoculture, the TPC (bound and total) and the antioxidant activity were higher than in co-culture for ATCC 9595 and especially for RW-9595M. Dordevic et al. (2010) also reported higher antioxidant activity in fermented buckwheat, wheat germ, barley and rye with *L. rhamnosus*, compared with samples fermented with *S. cerevisiae*. Hur et al. (2014) reported that lactic acid bacteria have antioxidant activity themselves, with mechanisms to reduce the impact of reactive oxygen species on cells. In addition, these three strains are EPS producers and these polysaccharides are synthesized in the WB/WP medium, as shown by scanning electron microscopy. In this sense, Polak-Berecka et al. (2015) reported antioxidant activity of the EPS

produced by *L. rhamnosus* E/N, which produces EPS with the same structure as those produced by the strains used in this work.

Common groups of phenolic acids in cereals are hydroxybenzoic acid and hydroxycinnamic acid derivatives. Protocatechuate is one of the microbial degradation products of various aromatic compounds, including phytic acid, hydroxybenzoic acid, or hydroxycinnamic acid compounds such as ferulic acid. In a previous study, yeast co-culture with *L. rhamnosus* R0011, ATCC 9595 and principally RW-9595M showed an important increase of relative gene expression of carboxymuconolactone decarboxylase (*pcaC*) involved in the conversion of protocatechuate to 3-oxoadypate in co-culture with *S. cerevisiae* (Bertsch et al., 2019). In the β-ketoadipate pathway, 3-oxoadipate is then converted to succinyl-CoA and acetyl-CoA, which are processed by the tricarboxylic acid cycle (TCA) to release stored energy through the oxidation of acetyl-CoA into adenosine triphosphate (ATP) and carbon dioxide.

The increase in the amount of caffeic acid after fermentation of the bioingredients varied among the three strains (ATCC 9595 > RW-9595M > R0011) in both types of culture (mono or co-culture). The increase in free caffeic acid and the resulting decrease of ferulic acid or *p*-coumaric acid was also obtained for these strains of *L. rhamnosus* in a culture medium with WP and corn steep liquor (Bertsch et al., 2019). Possible mechanisms for microbial bioconversion could be (a) caffeic acid produced by hydroxylation of *p*-coumaric acid at the meta position similar to *Streptomyces caeruleus* (Sachan et al., 2006); (b) caffeic acid produced by the *o*-demethylation of ferulic acid. This pathway was shown in *Enterobacter cloacae* and *Clostridium methoxybenzovorans* and in human colonic fermentation of rye bran fortified bread (Micard et al., 2002; Filannino et al., 2014). Filannino et al. (2014) had confirmed the ability of some lactic acid bacteria such as *Lactobacillus* spp. to convert protocatechuic acid to catechol; *p*-coumaric to phloteric acid or *p*-vinylphenol. (c) chlorogenic acid may be transformed into either vynilcatechol, dihydrocaffeic or dihydroshikimic acid. Caffeic acid and shikimic acid appeared in the culture medium as intermediary products of the metabolism of phenolic acids (Sánchez-Maldonado et al., 2011). The enrichment with caffeic acid can have numerous beneficial properties: this phenolic acid has a stronger inhibition of *Staphylococcus aureus* (Stojković et al., 2013); colonic pathology and inflammation could be improved in mice with DSS colitis, and a proportional increase in *Akkermansia* may be associated (Zhang et al., 2016). Finally, caffeic acid may restrain the progression of type 2 diabetes through attenuating the output of hepatic glucose and enhancing uptake of adipocyte glucose, insulin secretion, and antioxidant capacity (Jung et al., 2006).

The total individual bound phenolic acid content increased after fermentation. Similarly, a previous study (Gan et al., 2016) reported that fermentation increased the bound phenolic acid contents of ferulic acid and *p*-coumaric acid in mottled cowpea. The individual content in bound phenolic acids was enhanced more from strain RW-9595M in co-culture compared with monoculture. In this study, bio-processing coupled with *in vitro* digestion resulted in higher TPC and antioxidant activity (ORAC), as found after *in vitro* digestion of bread made with buckwheat flour (Szawara-Nowak et al., 2016). The authors hypothesized that the TPC and antioxidant activity increase may be associated with pH and enzymatic interactions that occur during *in vitro* digestion resulting in the gradual release of total polyphenols during digestion. In contrast, the free individual phenolic acid content in digested samples was mainly solubilized during the simulated gastrointestinal process resulting in a decrease of their concentration in the non-soluble residue. The individual bound phenolic acid content was concentrated in the non-soluble residue, which might result in the appearance of higher TPC and antioxidant activity (ORAC) in the digested samples.

In order to evaluate the bioavailability of phenolic compounds for potential benefits, we determined the portion that was released from the food matrix, converted during digestion and accessible for absorption in the small intestine as well as the portion that undergoes degradation by the gut microbiota (unabsorbed) during gastrointestinal digestion. The quantity of recovered (unabsorbed) TPC and antioxidant activity remaining in the samples was highest in non-fermented NFWB. For all three strains, TPC recovery was higher from ingredients produced by co-culture than from those produced by monoculture, although the bioingredients obtained with *L. rhamnosus* RW-9595M showed the lowest percentage value of TPC recovered. Bioingredients from monoculture showed the highest release of TPC and antioxidant activity through *in vitro* digestion.

At the same time, the process enhanced the bioaccessibility of free phenolic acid compounds such as caffeic and 4-hydroxybenzoic acids. This is in accordance with Dall'Asta et al. (2016) who reported that in aleurone-enriched bread and whole-grain bread, sinapic and caffeic acid were better absorbed than ferulic acid or *p*-coumaric acids. One of the most abundant phenolic compounds in WB is ferulic acid, accounting for 90% of TPC in wheat grain (Mateo Anson et al., 2009). In WB, ferulic acid and its isomers represent aleurone and pericarp cell wall components, mainly esterified with arabinoxylans (Cömert and Gökmen, 2017). Fermentation of WB/WP provides added value for the production of new fermented cereal-based foods with enhanced bioaccessibility of free phenolic acids which is a prerequisite for their bioavailability.

Bioingredients derived from RW-9595M showed lower bioaccessibility of free ferulic acid compared with NFWB and the other bioingredients. On the other hand, the recovery of individual bound phenolic acids was higher from monoculture bioingredients compared to co-culture for strains R0011 and RW-9595M while no difference was found between mono and co-culture for strain ATCC 9595. The type of culture (mono or co-culture) of the three strains influenced the bioaccessibility of free phenolic acid and the recovery of TPC, antioxidant activity or bound phenolic acid of the bioingredients. Gullon et al. (2015) reported interaction with other diet compounds during digestion, such as iron, polysaccharides, other minerals or proteins as well as modification of chemical structure. Solubility changes are known to impact phenolic bioaccessibility and bioavailability. The chemical interactions between EPS or WSP from *L. rhamnosus* and phenolic acid compounds in WB/WP have not been elucidated to date. The EPS produced

by these strains are acidic and could find applications where high-methoxyl pectin is used (van Calsteren et al., 2002). Phan et al. (2015) noted interactions of water-soluble phenolic compounds (phenolic acids, phenolic acid esters, flavan-3-ols, and anthocyanidins) with cellulose. Also, phenolic acids such as caffeic acid and ferulic acid interact with pectin. Bread fortified with high-methoxyl pectin and polyphenols from fruits showed a modification of protein structure exhibiting hydrophilic characteristics during processing via the formation of H bonds with water, polyphenols and polysaccharides (Sivam et al., 2013). These results are the first step to evaluating the effects of fermentation by EPS producer strains on the bioactivity of combined cereal/whey permeate bioingredients.

CONCLUSION

The presence of free and bound phenolic compounds in bio-ingredients is an advantage in products which could act to control oxidative radical species (balance of soluble and insoluble antioxidant compounds) along the entire digestive tract (Cömert and Gökmen, 2017). The bound phenolic acid of fermented WB could reach the colon, where they would be converted by the gut microbiota into their metabolites such as 3-phenylpropionic acid (Mateo Anson et al., 2009). At the same time, phenolic compounds remaining after digestion may exert antioxidant action and antibacterial activity to limit pathogenic bacteria in the colon (Gong et al., 2018). In this sense, future experiments should involve the determination of colonic bioaccessibility of the residual bound phenolic compounds of these bioingredients and evaluate the potential prebiotic activity of foods containing EPS. Furthermore, the evaluation of functionality of BI should be done in order to reveal the impact of fermentation on the characteristic of EPS (molecular weight), rheology, water absorption of the mixture WB/WP to determine applications in sourdough. The research in this area appears to be a challenge, but promising, as results will have direct impact on the development of fermented dairy-cereal-containing functional foods to add value to wheat milling by-products.

DATA AVAILABILITY STATEMENT

The raw data supporting the conclusions of this article will be made available by the authors, without undue reservation, to any qualified researcher.

AUTHOR CONTRIBUTIONS

DR, AB, and GL: conceptualization and formal analysis. AB: methodology and writing – original draft preparation. GL and DR: resources, writing – review and editing, and funding acquisition. GL: data curation, supervision, and project administration. All authors contributed to the article and approved the submitted version.

FUNDING

We gratefully acknowledge funding provided by Novalait and the Fonds de Recherche du Quebec – Nature and Technologie (FRQNT). AB is the recipient of a scholarship from RECYC-QUEBEC.

SUPPLEMENTARY MATERIAL

The Supplementary Material for this article can be found online at: https://www.frontiersin.org/articles/10.3389/fbioe.2020.00956/full#supplementary-material

REFERENCES

American Association of Cereal Chemists (AACC) (1975). "CEREALS, and GRAINS association AACC international," in *Approved Methods of Analysis*, 11th Edn, *Method 44-15.02. Moisture—Air-oven Methods* (St. Paul, MN: AACC International).

American Association of Cereal Chemists (AACC) (1976). "CEREALS, and GRAINS association AACC international," in *Approved Methods of Analysis*, 11th Edn, *Method 46-11.02. Crude Protein—Kjeldahl Method* (St. Paul, MN: AACC International).

Anson, N. M., Havenaar, R., Vaes, W., Coulier, L., Venema, K., Selinheimo, E., et al. (2011). Effect of bioprocessing of wheat bran in wholemeal wheat breads on the colonic SCFA production in vitro and postprandial plasma concentrations in men. *Food Chem.* 128, 404–409. doi: 10.1016/j.foodchem.2011.03.043

Anson, N. M., Hemery, Y. M., Bast, A., and Haenen, G. R. M. M. (2012). Optimizing the bioactive potential of wheat bran by processing. *Food Funct.* 3, 362–375. doi: 10.1039/c2fo10241b

Arte, E., Rizzello, C. G., Verni, M., Nordlund, E., Katina, K., and Coda, R. (2015). Impact of enzymatic and microbial bioprocessing on protein modification and nutritional properties of wheat bran. *J. Agric. Food Chem.* 63, 8685–8693. doi: 10.1021/acs.jafc.5b03495

Bergmaier, D., Champagne, C. P., and Lacroix, C. (2003). Exopolysaccharide production during batch cultures with free and immobilized *Lactobacillus rhamnosus* RW-9595M. *J. Appl. Microbiol.* 95, 1049–1057. doi: 10.1046/j.1365-2672.2003.02084.x

Bertsch, A., Roy, D., and LaPointe, G. (2019). Enhanced Exopolysaccharide production by *Lactobacillus rhamnosus* in co-culture with *Saccharomyces cerevisiae*. *Appl. Sci.* 9:4026. doi: 10.3390/app9194026

Bradford, M. M. (1976). A rapid and sensitive method for the quantitation of microgram quantities of protein utilizing the principle of protein-dye binding. *Anal. Biochem.* 72, 248–254. doi: 10.1016/0003-2697(76)90527-3

Chanos, P., and Mygind, T. (2016). Co-culture-inducible bacteriocin production in lactic acid bacteria. *Appl. Microbiol. Biotechnol.* 100, 4297–4308. doi: 10.1007/s00253-016-7486-8

Cheirsilp, B., and Radchabut, S. (2011). Use of whey lactose from dairy industry for economical kefiran production by *Lactobacillus kefiranofaciens* in mixed cultures with yeasts. *New Biotechnol.* 28, 574–580. doi: 10.1016/j.nbt.2011.01.009

Cheirsilp, B., Shimizu, H., and Shioya, S. (2003). Enhanced kefiran production by mixed culture of *Lactobacillus kefiranofaciens* and *Saccharomyces cerevisiae*. *J. Biotechnol.* 100, 43–53.

Church, F. C., Porter, D. H., Catignani, G. L., and Swaisgood, H. E. (1985). An o-phthalaldehyde spectrophotometric assay for proteinases. *Anal. Biochem.* 146, 343–348. doi: 10.1016/0003-2697(85)90549-4

Coda, R., Rizzello, C. G., Curiel, J. A., Poutanen, K., and Katina, K. (2014). Effect of bioprocessing and particle size on the nutritional properties of wheat bran fractions. *Innov. Food Sci. Emerg. Technol.* 25, 19–27. doi: 10.1016/j.ifset.2013.11.012

Coda, R., Rizzello, C. G., Pinto, D., and Gobbetti, M. (2012). Selected lactic acid bacteria synthesize antioxidant peptides during sourdough fermentation of cereal flours. *Appl. Environ. Microbiol.* 78, 1087–1096. doi: 10.1128/AEM.06837-11

Cömert, E. D., and Gökmen, V. (2017). Antioxidants bound to an insoluble food matrix: their analysis, regeneration behavior, and physiological importance: insoluble bound antioxidants. *Compr. Rev. Food Sci. Food Saf.* 16, 382–399. doi: 10.1111/1541-4337.12263

Dall'Asta, M., Bresciani, L., Calani, L., Cossu, M., Martini, D., Melegari, C., et al. (2016). In vitro bioaccessibility of phenolic acids from a commercial aleurone-enriched bread compared to a whole grain bread. *Nutrients* 8:42. doi: 10.3390/nu8010042

Dikeman, C. L., Murphy, M. R., and Fahey, G. C. (2006). Dietary fibers affect viscosity of solutions and simulated human gastric and small intestinal digesta. *J. Nutr.* 136, 913–919. doi: 10.1093/jn/136.4.913

Dordevic, T. M., Śiler-Marinkovi, S. S., and Dimitrijevi-Brankovi, S. I. (2010). Effect of fermentation on antioxidant properties of some cereals and pseudo cereals. *Food Chem.* 119, 957–963. doi: 10.1016/j.foodchem.2009.07.049

Dubois, M., Gilles, K., Hamilton, J. K., Rebers, P. A., and Smith, F. (1951). A Colorimetric method for the determination of sugars. *Nature* 168:167. doi: 10.1038/168167a0

Filannino, P., Gobbetti, M., De Angelis, M., and Di Cagno, R. (2014). Hydroxycinnamic acids used as external acceptors of electrons: an energetic advantage for strictly heterofermentative lactic acid bacteria. *Appl. Environ. Microbiol.* 80, 7574–7582. doi: 10.1128/AEM.02413-14

Gan, R.-Y., Shah, N. P., Wang, M.-F., Lui, W.-Y., and Corke, H. (2016). Fermentation alters antioxidant capacity and polyphenol distribution in selected edible legumes. *Int. J. Food Sci. Technol.* 51, 875–884. doi: 10.1111/ijfs.13062

Gänzle, M. G., Loponen, J., and Gobbetti, M. (2008). Proteolysis in sourdough fermentations: mechanisms and potential for improved bread quality. *Trends Food Sci. Technol.* 19, 513–521. doi: 10.1016/j.tifs.2008.04.002

Gong, L., Cao, W., Chi, H., Wang, J., Zhang, H., Liu, J., et al. (2018). Whole cereal grains and potential health effects: involvement of the gut microbiota. *Food Res. Int.* 103, 84–102. doi: 10.1016/j.foodres.2017.10

Gullon, B., Pintado, M. E., Barber, X., Fernández-López, J., Pérez-Álvarez, J. A., and Viuda-Martos, M. (2015). Bioaccessibility, changes in the antioxidant potential and colonic fermentation of date pits and apple bagasse flours obtained from co-products during simulated in vitro gastrointestinal digestion. *Food Res. Int.* 78, 169–176. doi: 10.1016/j.foodres.2015.10.021

Hur, S. J., Lee, S. Y., Kim, Y.-C., Choi, I., and Kim, G.-B. (2014). Effect of fermentation on the antioxidant activity in plant-based foods. *Food Chem.* 160, 346–356. doi: 10.1016/j.foodchem.2014.03.112

Jung, U. J., Lee, M.-K., Park, Y. B., Jeon, S.-M., and Choi, M.-S. (2006). Antihyperglycemic and antioxidant properties of caffeic acid in db/db mice. *J. Pharmacol. Exp. Ther.* 318, 476–483. doi: 10.1124/jpet.106.105163

Kajala, I., Makela, J., Coda, R., Shukla, S., Shi, Q., Maina, N. H., et al. (2016). Rye bran as fermentation matrix boosts in situ dextran production by *Weissella* confusa compared to wheat bran. *Appl. Microbiol. Biotechnol.* 100, 3499–3510. doi: 10.1007/s00253-015-7189-6

Katina, K., Juvonen, R., Laitila, A., Flander, L., Nordlund, E., Kariluoto, S., et al. (2012). Fermented wheat bran as a functional ingredient in baking. *Cereal Chem. J.* 89, 126–134. doi: 10.1094/CCHEM-08-11-0106

Laddomada, B., Caretto, S., and Mita, G. (2015). Wheat bran phenolic acids: bioavailability and stability in whole wheat-based foods. *Molecules* 20, 15666–15685. doi: 10.3390/molecules200915666

Leroy, F., and De Vuyst, L. (2016). Advances in production and simplified methods for recovery and quantification of exopolysaccharides for applications in food and health. *J. Dairy Sci.* 99, 3229–3238. doi: 10.3168/jds.2015-9936

Macedo, M. G., Lacroix, C., Gardner, N. J., and Champagne, C. P. (2002). Effect of medium supplementation on exopolysaccharide production by *Lactobacillus rhamnosus* RW-9595M in whey permeate. *Int. Dairy J.* 12, 419–426. doi: 10.1016/S0958-6946(01)00173-X

Mateo Anson, N., Aura, A.-M., Selinheimo, E., Mattila, I., Poutanen, K., van den Berg, R., et al. (2011). Bioprocessing of wheat bran in whole wheat bread increases the bioavailability of phenolic acids in men and exerts antiinflammatory effects ex vivo. *J. Nutr.* 141, 137–143. doi: 10.3945/jn.110.127720

Mateo Anson, N., van den Berg, R., Havenaar, R., Bast, A., and Haenen, G. R. M. M. (2009). Bioavailability of ferulic acid is determined by its bioaccessibility. *J. Cereal Sci.* 49, 296–300. doi: 10.1016/j.jcs.2008.12.001

Micard, V., Landazuri, T., Surget, A., Moukha, S., Labat, M., and Rouau, X. (2002). Demethylation of ferulic acid and feruloyl-arabinoxylan by microbial cell extracts. *LWT Food Sci. Technol.* 35, 272–276. doi: 10.1006/fstl.2001.0856

Miller, G. L. (1959). Use of dinitrosalicylic acid reagent for determination of reducing sugar. *Anal. Chem.* 31, 426–428. doi: 10.1021/ac60147a030

Minekus, M., Alminger, M., Alvito, P., Ballance, S., Bohn, T., Bourlieu, C., et al. (2014). A standardised static in vitro digestion method suitable for food – an international consensus. *Food Funct.* 5, 1113–1124. doi: 10.1039/c3fo60702j

Motilva, M.-J., Serra, A., and Rubió, L. (2015). Nutrikinetic studies of food bioactive compounds: from in vitro to in vivo approaches. *Int. J. Food Sci. Nutr.* 66, S41–S52. doi: 10.3109/09637486.2015.1025721

Onipe, O. O., Jideani, A. I. O., and Beswa, D. (2015). Composition and functionality of wheat bran and its application in some cereal food products. *Int. J. Food Sci. Technol.* 50, 2509–2518. doi: 10.1111/ijfs.12935

Pham, P. L., Dupont, I., Roy, D., Lapointe, G., and Cerning, J. (2000). Production of exopolysaccharide by *Lactobacillus rhamnosus* R and analysis of its enzymatic degradation during prolonged fermentation. *Appl. Environ. Microbiol.* 66, 2302–2310. doi: 10.1128/AEM.66.6.2302-2310.2000

Phan, A. D. T., Netzel, G., Wang, D., Flanagan, B. M., D'Arcy, B. R., and Gidley, M. J. (2015). Binding of dietary polyphenols to cellulose: structural and nutritional aspects. *Food Chem.* 171, 388–396. doi: 10.1016/j.foodchem.2014.08.118

Polak-Berecka, M., Choma, A., Waśko, A., Górska, S., Gamian, A., and Cybulska, J. (2015). Physicochemical characterization of exopolysaccharides produced by *Lactobacillus rhamnosus* on various carbon sources. *Carbohydr. Polym.* 117, 501–509. doi: 10.1016/j.carbpol.2014.10.006

Ponomarova, O., Gabrielli, N., Sévin, D. C., Mülleder, M., Zirngibl, K., Bulyha, K., et al. (2017). Yeast creates a niche for symbiotic lactic acid bacteria through nitrogen overflow. *Cell Syst.* 5, 345.e6–357.e6. doi: 10.1016/j.cels.2017.09.002

Poutanen, K., Flander, L., and Katina, K. (2009). Sourdough and cereal fermentation in a nutritional perspective. *Food Microbiol.* 26, 693–699. doi: 10.1016/j.fm.2009.07.011

Prückler, M., Lorenz, C., Endo, A., Kraler, M., Dürrschmid, K., and Hendriks, K. (2015). Comparison of homo- and heterofermentative lactic acid bacteria for implementation of fermented wheat bran in bread. *Food Microbiol.* 49, 211–219. doi: 10.1016/j.fm.2015.02.014

Russo, P., de Chiara, M. L. V., Capozzi, V., Arena, M. P., Amodio, M. L., Rascon, A., et al. (2016). *Lactobacillus plantarum* strains for multifunctional oat-based foods. *LWT Food Sci. Technol.* 68, 288–294. doi: 10.1016/j.lwt.2015.12.040

Sachan, A., Ghosh, S., Sen, S. K., and Mitra, A. (2006). Co-production of caffeic acid and p-hydroxybenzoic acid from p-coumaric acid by Streptomyces caeruleus MTCC 6638. *Appl. Microbiol. Biotechnol.* 71, 720–727. doi: 10.1007/s00253-005-0197-1

Salazar, N., Gueimonde, M., de los Reyes-Gavilán, C. G., and Ruas-Madiedo, P. (2016). Exopolysaccharides produced by lactic acid bacteria and bifidobacteria as fermentable substrates by the intestinal microbiota. *Crit. Rev. Food Sci.* Nutr56, 1440–1453. doi: 10.1080/10408398.2013.770728

Sánchez-Maldonado, A. F., Schieber, A., and Gänzle, M. G. (2011). Structure-function relationships of the antibacterial activity of phenolic acids and their metabolism by lactic acid bacteria: antibacterial phenolic acids. *J. Appl. Microbiol.* 111, 1176–1184. doi: 10.1111/j.1365-2672.2011.05141.x

Shumoy, H., Gabaza, M., Vandevelde, J., and Raes, K. (2017). Soluble and bound phenolic contents and antioxidant capacity of tef injera as affected by traditional fermentation. *J. Food Compos Anal.* 58, 52–59. doi: 10.1016/j.jfca.2017.01.004

Singleton, V. L., Orthofer, R., and Lamuela-Ravents, R. M. (1999). "[14] Analysis of total phenols and other oxidation substrates and antioxidants by means of Folin-ciocalteu reagent," in *Methods in Enzymology*, eds J. Abelson, M. Simon, G. Verdine, and A. Pyle, (Amsterdam: Elsevier), 152–178. doi: 10.1016/S0076-6879(99)99017-1

Sivam, A. S., Sun-Waterhouse, D., Perera, C. O., and Waterhouse, G. I. N. (2013). Application of FT-IR and raman spectroscopy for the study of biopolymers in breads fortified with fibre and polyphenols. *Food Res. Int.* 50, 574–585. doi: 10.1016/j.foodres.2011.03.039

Slukovà, M., Hinkovà, A., Henke, S., Smrz, F., Lukacikovà, M., Pour, V., et al. (2016). Cheese whey treated by membrane separation as a valuable ingredient for barley sourdough preparation. *J. Food Eng.* 172, 38–47. doi: 10.1016/j.jfoodeng.2015.03.023

Stevenson, L., Phillips, F., O'sullivan, K., and Walton, J. (2012). Wheat bran: its composition and benefits to health, a European perspective. *Int. J. Food Sci. Nutr.* 63, 1001–1013. doi: 10.3109/09637486.2012.687366

Stojković, D., Petroviæ, J., Sokoviæ, M., Glamoèlija, J., Kukiæ-Markoviæ, J., and Petroviæ, S. (2013). In situ antioxidant and antimicrobial activities of naturally occurring caffeic acid, p -coumaric acid and rutin, using food systems: In situ antioxidant and antimicrobial activities of naturally occurring caffeic acid. *J. Sci. Food Agric.* 93, 3205–3208. doi: 10.1002/jsfa.6156

Swieca, M., Gawlik-Dziki, U., Dziki, D., and Baraniak, B. (2017). Wheat bread enriched with green coffee? In vitro bioaccessibility and bioavailability of phenolics and antioxidant activity. *Food Chem.* 221, 1451–1457. doi: 10.1016/j.foodchem.2016.11.006

Szawara-Nowak, D., Baczek, N., and Zielinski, H. (2016). Antioxidant capacity and bioaccessibility of buckwheat-enhanced wheat bread phenolics. *J. Food Sci. Technol.* 53, 621–630. doi: 10.1007/s13197-015-2074-y

Tieking, M., and Gänzle, M. G. (2005). Exopolysaccharides from cereal-associated Lactobacilli. *Trends Food Sci. Technol.* 16, 79–84. doi: 10.1016/j.tifs.2004.02.015

Valdés, L., Cuervo, A., Salazar, N., Ruas-Madiedo, P., Gueimonde, M., and González, S. (2015). The relationship between phenolic compounds from diet and microbiota: impact on human health. *Food Funct.* 6, 2424–2439. doi: 10.1039/C5FO00322A

van Calsteren, M.-R., Pau-Roblot, C., BéGin, A., and Roy, D. (2002). Structure determination of the exopolysaccharide produced by *Lactobacillus rhamnosus* strains RW-9595M and R. *Biochem. J.* 363, 7–17. doi: 10.1042/bj3630007

Verni, M., Rizzello, C. G., and Coda, R. (2019). Fermentation biotechnology applied to cereal industry by-products: nutritional and functional insights. *Front. Nutr.* 6:42. doi: 10.3389/fnut.2019.00042

Weiss, W., Vogelmeier, C., and Görg, A. (1993). Electrophoretic characterization of wheat grain allergens from different cultivars involved in bakers' asthma. *Electrophoresis* 14, 805–816. doi: 10.1002/elps.1150140 1126

Xu, Y., Coda, R., Shi, Q., Tuomainen, P., Katina, K., and Tenkanen, M. (2017). Exopolysaccharides production during the fermentation of soybean and fava bean flours by *Leuconostoc mesenteroides* DSM 20343. *J. Agric. Food Chem.* 65, 2805–2815. doi: 10.1021/acs.jafc.6b05495

Yamasaki-Yashiki, S., Sawada, H., Kino-Oka, M., and Katakura, Y. (2017). Analysis of gene expression profiles of *Lactobacillus paracasei* induced by direct contact with *Saccharomyces cerevisiae* through recognition of yeast mannan. *Biosci. Microbiota Food Health* 36, 17–25. doi: 10.12938/bmfh.BMFH-2016-015

Zeng, Z., Liu, C., Luo, S., Chen, J., and Gong, E. (2016). The Profile and bioaccessibility of phenolic compounds in cereals influenced by improved extrusion cooking treatment. *PLoS One* 11:e0161086. doi: 10.1371/journal.pone.0161086

Zhang, Z., Wu, X., Cao, S., Wang, L., Wang, D., Yang, H., et al. (2016). Caffeic acid ameliorates colitis in association with increased Akkermansia</i> population in the gut microbiota of mice. *Oncotarget* 31 7, 31790–31799. doi: 10.18632/oncotarget.9306

Zhao, H.-M., Guo, X.-N., and Zhu, K.-X. (2017). Impact of solid state fermentation on nutritional, physical and flavor properties of wheat bran. *Food Chem.* 217, 28–36. doi: 10.1016/j.foodchem.2016.08.062

Conflict of Interest: The authors declare that the research was conducted in the absence of any commercial or financial relationships that could be construed as a potential conflict of interest.

frontiers in Bioengineering and Biotechnology

ORIGINAL RESEARCH
published: 19 August 2020
doi: 10.3389/fbioe.2020.01024

Characterization of Highly Mucus-Adherent Non-GMO Derivatives of *Lacticaseibacillus rhamnosus* GG

Pia Rasinkangas[1†‡], Hanne L. P. Tytgat[2‡], Jarmo Ritari[1†], Justus Reunanen[1†], Seppo Salminen[3], Airi Palva[1], François P. Douillard[1†] and Willem M. de Vos[1,2,4*]

[1] Department of Veterinary Biosciences, Faculty of Veterinary Medicine, University of Helsinki, Helsinki, Finland, [2] Laboratory of Microbiology, Wageningen University, Wageningen, Netherlands, [3] Functional Foods Forum, Faculty of Medicine, University of Turku, Turku, Finland, [4] Human Microbiome Research Program, Faculty of Medicine, University of Helsinki, Helsinki, Finland

Lacticaseibacillus rhamnosus GG is one of the best studied lactic acid bacteria in the context of probiotic effects. *L. rhamnosus* GG has been shown to prevent diarrhea in children and adults and has been implicated to have mitigating or preventive effects in several disorders connected to microbiota dysbiosis. The probiotic effects are largely attributed to its adhesive heterotrimeric sortase-dependent pili, encoded by the *spaCBA-srtC1* gene cluster. Indeed, the strain-specific SpaCBA pili have been shown to contribute to adherence, biofilm formation and host signaling. In this work we set out to generate non-GMO derivatives of *L. rhamnosus* GG that adhere stronger to mucus compared to the wild-type strain using chemical mutagenesis. We selected 13 derivatives that showed an increased mucus-adherent phenotype. Deep shotgun resequencing of the strains enabled division of the strains into three classes, two of which revealed SNPs (single nucleotide polymorphisms) in the *spaA* and *spaC* genes encoding the shaft and tip adhesive pilins, respectively. Strikingly, the other class derivatives demonstrated less clear genotype – phenotype relationships, illustrating that pili biogenesis and structure is also affected by other processes. Further characterization of the different classes of derivatives was performed by PacBio SMRT sequencing and RNAseq analysis, which resulted in the identification of molecular candidates driving pilin biosynthesis and functionality. In conclusion, we report on the generation and characterization of three classes of strongly adherent *L. rhamnosus* GG derivatives that show an increase in adhesion to mucus. These are of special interest as they provide a window on processes and genes driving piliation and its control in *L. rhamnosus* GG and offer a variety of non-GMO derivatives of this key probiotic strain that are applicable in food products.

Keywords: pili, mucus, *Lacticaseibacillus rhamnosus* GG, adhesion, probiotics, non-GMO

OPEN ACCESS

Edited by:
Jian-Ming Liu,
Technical University of Denmark, Denmark

Reviewed by:
Jun Chen,
Samplix ApS, Denmark
Rabia Ladjouzi,
Université de Lille, France
Paloma López,
Margarita Salas Center for Biological Research (CSIC), Spain
Egon Bech Hansen,
Technical University of Denmark, Denmark

***Correspondence:**
Willem M. de Vos
willem.devos@wur.nl

†Present address:
Pia Rasinkangas,
DuPont Nutrition & Biosciences, Kantvik, Finland
Jarmo Ritari,
Finnish Red Cross Blood Service, Helsinki, Finland
Justus Reunanen,
Biocenter Oulu, Faculty of Medicine, University of Oulu, Oulu, Finland
François P. Douillard,
Department of Food Hygiene and Environmental Health, Faculty of Veterinary Medicine, University of Helsinki, Helsinki, Finland

‡*These authors have contributed equally to this work*

Specialty section:
This article was submitted to Synthetic Biology, a section of the journal Frontiers in Bioengineering and Biotechnology

Received: *27 May 2020*
Accepted: *05 August 2020*
Published: *19 August 2020*

INTRODUCTION

The last decade of microbiome analysis has rendered a plethora of information on the bacteria inhabiting a healthy or diseased microbiota-gut ecosystem. Dysbiosis of the gut microbiota has been correlated to a large variety of non-communicable diseases, like diabetes, obesity and even autism (Qin et al., 2010). Building further on this knowledge, it is key to support these correlations with hard-core microbiology insights: understanding how bacteria can mediate and influence human physiology. These insights also pave the way for novel application opportunities, for instance by understanding how microbiota composition and crosstalk can be modulated. One possibility is the use of beneficial microbes or probiotics, defined as live microorganisms, that, when administered in adequate amounts, confer a health benefit to the host (FAO/WHO, 2001).

Many of the most widely studied probiotics are lactic acid bacteria, with *Lacticaseibacillus rhamnosus* GG being a prime example (de Vos, 2011). This strain was previously known as *Lactobacillus rhamnosus* GG (Zheng et al., 2020). Its probiotic potential ranges from the prevention of antibiotic-associated diarrhea in children and adults (Arvola et al., 1999; Szajewska and Kolodziej, 2015), over atopic diseases (Kalliomaki et al., 2001; Nermes et al., 2011), to respiratory tract infections in children (Hatakka et al., 2001; Kumpu et al., 2012; Luoto et al., 2014). As also demanded by EFSA (European Food Safety Authority), health claims should be corroborated by defined studies of probiotic effectors (Binnendijk and Rijkers, 2013).

One of the key features of *L. rhamnosus* GG are its highly adherent, long (1 or more microns) SpaCBA-pili (Kankainen et al., 2009) that play a key role in adherence, host signaling, biofilm formation and competitive exclusion of pathogens like *Enterococcus faecium* (Lebeer et al., 2012; Ardita et al., 2014; Tytgat et al., 2016a,b; Chandrasekharan et al., 2019). These sortase-dependent pili are heterotrimers of a major, shaft-forming pilin SpaA, a SpaB polymerization termination signaling pilin and a pilus-decorating SpaC pilin (Reunanen et al., 2012; Douillard et al., 2014). It has been shown that these species-specific pili, encoded in a *spaCBA-srtC1* cluster, are the main drivers of the high colonization phenotype of *L. rhamnosus* GG and are for instance absent in the closely related Lc705 strain (Kankainen et al., 2009; von Ossowski et al., 2010; Lebeer et al., 2012; Ardita et al., 2014). Especially the SpaC pilin was found to be crucial, as it is the major contributor to mucus binding of *L. rhamnosus* GG, probably via its C-terminal collagen-binding and N-terminal von Willebrand factor domains (Tripathi et al., 2013; Kant et al., 2016). The three pilin subunits are assembled into the mature SpaCBA pili by a pilin-specific transpeptidase, SrtC1, which is encoded in the same gene cluster as the three pilins, whilst a housekeeping sortase, SrtA, assures attachment to the cell wall (Hendrickx et al., 2011; Reunanen et al., 2012). The mechanisms and motifs by which these sortases act, have been studied in-depth in *L. rhamnosus* GG (Douillard et al., 2014, 2016). This has enhanced the general knowledge on pilus assembly and function of these key cell wall appendages of a multitude of Gram-positive species, including pathogens (Mandlik et al., 2008).

To further expand our insights in the structure and function of the SpaCBA pili, we use random chemical mutagenesis to generate non-GMO derivatives (The European Union, 2001) of *L. rhamnosus* GG. This approach has a three-fold goal: (1) the generation, screening and characterization of strains with an aberrant pilosotype, (2) the generation of strains safe to use in human trials with potential enlarged beneficial properties, and (3) advancing our understanding of the processes and genes driving piliation and its control. We already successfully used this non-GMO approach to produce and describe non-piliated variants of *L. rhamnosus* GG (Rasinkangas et al., 2014).

In this work we focus on the generation of derivatives of *L. rhamnosus* GG showing an increased capacity to adhere to mucus, using a similar approach: random chemical mutagenesis followed by genome resequencing. In what follows we describe the generation, selection and isolation of 13 highly mucus-adherent *L. rhamnosus* GG derivatives, followed by their phenotypic, biochemical, genomic and transcriptomic characterization.

MATERIALS AND METHODS

Bacterial Strains and Growth Conditions

Lacticaseibacillus rhamnosus GG (ATCC53103) was obtained from Valio Ltd., Helsinki, Finland. As a pilus-less control, the previously characterized *L. rhamnosus* GG PB12 strain was included (Rasinkangas et al., 2014). Strains were grown in De Man-Rogosa-Sharpe (MRS) medium and 1.5% agar (Difco) at 37°C.

EMS Mutagenesis

Ethyl methanesulphonate (EMS, Sigma Aldrich) was used as an alkylating mutagen (Sega, 1984; Parekh et al., 2000), as described in our previous work on the production of non-piliated derivatives of *L. rhamnosus* GG (Rasinkangas et al., 2014). In particular, stationary-phase *L. rhamnosus* GG cells were treated with 2% (v/v) EMS and incubated at 37°C for 2 h. After incubation, samples were washed several times with phosphate-buffered saline (PBS, pH 7.3, Oxoid) and resuspended in MRS broth. Bacterial survival was estimated by plating a dilution series of the samples at 16%. At various stages in the mutation selection process, cultures were stored at −80°C, after supplementation with 20% glycerol.

Enrichment of Highly Piliated Strains and High-Throughput Dot Blot Screening of Derivatives

A screening was set up for derivatives of *L. rhamnosus* GG that could present a stronger interaction with mucus. Given that the SpaC pilin is the main mucus-interacting component of the SpaCBA-pili, and by extension of *L. rhamnosus* GG, an anti-SpaC antibody based screen was set up (Kankainen et al., 2009; von Ossowski et al., 2010; Lebeer et al., 2012; Nishiyama et al., 2016). A dense EMS-treated bacterial suspension of $OD_{600\ nm}$ 4 was incubated in wells coated with anti-SpaC IgG, purified from

anti-SpaC rabbit antiserum (Kankainen et al., 2009). After 3–4 h incubation, wells were washed ten times with PBS, followed by scraping to release potentially highly adherent *L. rhamnosus* GG derivatives. These scraped cells were incubated overnight in MRS medium. This enrichment scheme was repeated a total of three times. Following the last round of enrichment, a dilution series was prepared and plated. Colonies were picked, grown and screened using a dot blot assay as described earlier (Rasinkangas et al., 2014). The strains exhibiting the strongest interaction with anti-SpaC IgG in the dot blot screening were selected for further characterization.

Illumina-Based Genome Screening of Derivatives

Genomic DNA was extracted using the Wizard Genomic DNA purification kit (Promega). Genomes were sequenced in paired-end mode using the MiSeq Illumina platform. MUMmer 3.0 software (Kurtz et al., 2004) was used to align sequence assemblies to the *L. rhamnosus* GG genome (Kankainen et al., 2009). MIRA software was then used to align sequences and annotate mutations (Chevreux et al., 1999). Illumina paired end Fastq reads were mapped against *L. rhamnosus* GG (FM179322.1) annotated GenBank file using MIRA v4.0.2 with the following parameters: "job = mapping,genome,accurate," "parameters = COMMON_SETTINGS -NW:cac = no," "technology = solexa" and "autopairing." Commands "miraconvert -t asnp" and "miraconvert -t hsnp" were used to generate single nucleotide polymorphisms (SNP) analysis results. Mutations residing in the *spaCBA-srtC1* gene cluster were further verified with Sanger sequencing.

PacBio Next-Generation Sequencing of Class Representatives

Genomic DNA extraction was performed as described above. Further processing, sequencing and variant detection (SNP) in representative strains (PS17, PS24, PS31, and PS41) of each class was performed by BaseClear (Leiden, Netherlands) according to their procedures (paired-end sequencing Illumina HiSeq2500). In the case of PS24 and PS31, representatives of Class II and III, de novo hybrid genome assemblies were performed by BaseClear and compared to the genome of wild-type *L. rhamnosus* GG to detect any large aberrations in the genome structure of these derivatives (PacBio Sequel Instrument, gapped regions were closed with Illumina reads).

Qualitative and Quantitative Analysis of Surface-Located Pilins Using Immunofluorescence

Conforming to our earlier studies, we performed immunofluorescence labeling, quantification and microscopy of pilins on the cell surface of the selected derivatives (Rasinkangas et al., 2014). SpaA and SpaC antisera were used as primary labeling agent, followed by detection via secondary labeling with Alexa Fluor 488-labeled goat anti-rabbit antibody (Invitrogen). DAPI (1:1000 dilution, Dilactate form, Thermo Fisher Scientific) was used to stain and thus quantify all cells present in a sample, thus enabling normalization of the fluorescence intensity results for SpaA and SpaC. Fluorescence intensities of each stain were measured separately using a Victor3 1460 multilabel counter (Perkin Elmer). Normalization was performed by dividing the obtained fluorescence intensity values by the corresponding DAPI intensity for each strain. Both quantitative and qualitative data from a representative experiment is shown.

Immuno-Electron Microscopy of SpaA and SpaC Pilins

Experimental details are in accordance with (Douillard et al., 2014; Rasinkangas et al., 2014). In short, stationary grown cells were washed with PBS and incubated for 1 h on top of Formvar-carbon-coated grids. Grids were subsequently washed several times with 0.02 M Glycine in PBS and blocked using 1% BSA in PBS for 15 min. After blocking, grids were incubated with antiserum diluted 1:100 in blocking solution for 1 h. A protein A-gold suspension either containing 5 or 10 nm gold particles was diluted 1:55 and incubated with the grids for 20 min after several washes with 0.1% BSA in PBS. SpaA and SpaC pilins were detected by coupling SpaA antiserum to 10 nm and SpaC to 5 nM protein A-gold particles. Grids were fixed with 1% (v/v) gluteraldehyde (Sigma-Aldrich) and washed with water, followed by staining them using a 1.8% methylcellulose-0.4% uranyl acetate mixture on ice. Samples were visualized using a JEM-1400 transmission electron microscope (JEOL).

Western Blot Analysis of SpaC and SpaA Pilins

Cell wall proteins were extracted from cultures of which the $OD_{600\ nm}$ was adjusted to 8 prior to extraction, as described in Rasinkangas et al. (2014). Protein extracts were diluted 1:300 and 1:200 respectively for detection using SpaA and SpaC antisera on Western blot. To visualize the total quantity of proteins in the blots, a Western blot of 1:200 diluted samples (similar to SpaC blot) was developed using a whole cell antibody (WCA, 1:25000 dilution) against *L. rhamnosus* GG (Tytgat et al., 2016b).

Mucus Adherence Measurements

Strains were grown overnight in the presence of ^{3}H-labeled thymidine (Perkin Elmer). Cultures were then incubated in a Maxisorp 96-well plate coated with either porcine type II mucus (Sigma-Aldrich) or human mucus, followed by extensive washing with PBS (Oxoid) and lysis of the remaining adherent cells. Sample radioactivity was measured using a Wallac 1480 Wizard 3 automatic gamma counter (Perkin Elmer). Full experimental details are described in Vesterlund et al. (2005). Each assay was performed in three biological repeats, with each a minimum of three technical replicates per strain.

Transcriptomic Analysis of *L. rhamnosus* GG Derivatives

Wild-type *L. rhamnosus* GG, PS24 and PB12 as negative control were grown in MRS till $OD_{600\ nm}$ 2 (early exponential) and $OD_{600\ nm}$ 7 (late exponential, early stationary phase). Cell pellets were resuspended in TRIzol (Life technologies) and RNA

extraction was performed with the RNeasy kit (Qiagen) according to manufacturers' instructions (triplicate for wild-type). Quality and quantity of RNA was monitored using Qubit (Thermo Fisher) and Experion (Bio-Rad). rRNA was depleted using the RiboZero kit (Epicentre, Ilumina), followed by cDNA library preparation according to the guidelines of the ScriptSeq v2 RNA-Seq Library Preparation Kit (Epicentre, Illumina).

HighPrep PCR magnetic beads (Magbio) enabled cDNA purification prior to barcoding with ScriptSeq Index PCR Primers (Epicentre, Illumina). The RNA-Seq library was again further purified using HighPrep PCR magnetic beads (Magbio) and quantity and quality was assessed using Nanodrop (Thermo Fisher Scientific). Barcoded cDNA libraries were pooled and sent to Baseclear (Leiden, Netherlands) for sequencing on one single lane using the Illumina HiSeq2500 platform. All bioinformatic work was performed on a local Galaxy webserver (Giardine et al., 2005; Blankenberg et al., 2010; Goecks et al., 2010). rRNA reads were removed with SortMeRNA version 2.0 (Kopylova et al., 2012) and all included databases. Trueseq adapters were trimmed with Cutadapt v1.8.1 (Martin, 2011) using default settings. Quality trimming was performed with Sickle version 1.33 (Joshi and Fass, 2011) with a minimum sequence length of 50 bp and a minimum quality threshold of 30. Reads were mapped to the genome with Bowtie2 version 2.2.4 (Langmead and Salzberg, 2012) using default settings and mapping rate was inspected with Samtools version 0.1.19 (Li et al., 2009). Gene coverage was calculated with R version 3.1.2 (R Core Team, 2014) and the R package HTSeq-count version 0.6.1 (Anders et al., 2015). GFF files were obtained by converting Genbank files via Readseq version 2.1.19 (Gilbert, 2003). Differential expression was calculated with the R package DESeq2 version 2.1.8.0 (Love et al., 2014).

Sequence Accession Numbers

The genome sequences and RNASeq data of the described derivatives can be found in the NCBI Sequence Read Archive (SRA) database under BioProject accession code PRJNA309744. Specific codes of the highly mucus-adherent strains are:

PS11 – SAMN04440341;
PS12 – SAMN04440342;
PS13 – SAMN04440343;
PS14 – SAMN04440344;
PS15 – SAMN04440345;
PS16 – SAMN04440346;
PS17 – SAMN04440347;
PS21 – SAMN04440348;
PS22 – SAMN04440349;
PS23 – SAMN04440350;
PS24 – SAMN04440351;
PS31 – SAMN04440352;
PS41 – SAMN04440353.

Data Analysis

All analyses were performed using GraphPad Prism 8. Significant differences between two groups were calculated using unpaired *t*-tests and the significance level was set at $p < 0.05$.

RESULTS

Selection of Highly Mucus-Adherent *L. rhamnosus* GG Derivatives

The aim of the present study was to decipher whether it would be possible to produce highly mucus-adherent derivatives of *L. rhamnosus* GG using random mutagenesis induced by the chemical mutagen ethyl methanesulfonate. Benefits of these derivatives include that they are considered to be non-GMO (The European Union, 2001) and that they can offer unique insights in the genes driving *L. rhamnosus* GG piliation.

By coating a plate with anti-SpaC IgG we aimed to enrich derivatives that presented a higher fraction of SpaC pilins, the major adhesive pilin of the *L. rhamnosus* GG SpaCBA pili, on their cell surface. A total of 384 strains that matched this phenotype was screened, to ultimately obtain 13 strains, which, according to dot blot analysis, produced higher quantities of SpaC compared to the parental wild-type *L. rhamnosus* GG strain (results not shown). This results in a discovery rate of 3.4%, which is in line with our earlier work on the production of pilus-less derivatives (Rasinkangas et al., 2014). In what follows we characterize these 13 "PS" strains in-depth by focusing on their genotypes and phenotypes.

Genomic Resequencing of the Selected Derivatives

The genotype of the 13 selected strains was analyzed by shotgun genomic resequencing using Illumina technology to identify SNPs (Singe Nucleotide Polymorphisms) (**Table 1** for a summary, **Supplementary File S1** for the detailed results of all selected strains). Based on the mutation profile that emerged, the 13 strains were divided into three classes (**Table 1**): Class I consists of 7 strains denoted as PS11–PS17, Class II of 5 strains termed PS21-PS24 and PS31, and Class III of the single strain, PS41,

TABLE 1 | Mutations detected by Illumina resequencing in the selected highly adherent derivatives of *L. rhamnosus* GG.

		Phenotype driving mutation			Other mutations
Strain	**Class**	**Gene**	**Mutation**	**AA change**	**SNP#**
PS11	I	*spaC*	C → T	Pro552Ser	46
PS12			C → T	Pro552Ser	58
PS13			C → T	Pro552Ser	59
PS14			C → T	Pro552Ser	47
PS15			C → T	Pro552Ser	62
PS16			C → T	Pro552Ser	54
PS17			C → T	Pro552Ser	51
PS21	II	Unknown	–	–	41
PS22			–	–	65
PS23			–	–	73
PS24			–	–	44
PS31			–	–	80
PS41	III	*spaA*	C → T	Thr35Met	35

SNP#: Quantity of other single nucleotide mutations in the strain.

respectively. A total of 7 mutations, localized both in coding sequences (3) and intergenic regions (4) were found to be shared amongst all derivatives (**Supplementary Table S1**).

Class I strains PS11–PS17 were clustered based on the emergence of the same mutation in the gene encoding SpaC (**Table 1**). The mutation resulted in an amino acid change (Pro → Ser) of residue 552 of the SpaC protein, which is located at the C-terminal end of the collagen-binding domain of SpaC (Tripathi et al., 2013; Kant et al., 2016). Apart from this SNP in the *spaCBA-srtC1cluster*, there are 38 SNPs shared by all Class I mutants (see **Supplementary Table S1**).

Genomic analysis of derivatives belonging to Class II (PS21–PS24, PS31) did not result in a clear genotype (**Table 1**). Based on the shotgun sequencing, no mutations in genes that were in a direct way related to piliation could be detected.

The strain constituting Class IV, PS41, presented a mutation in the gene encoding SpaA. The mutation resulted in a Thr → Met substitution in residue 35, which is close to the predicted secretion signal peptide cleavage site (residues 1–33) of this pilin (**Table 1**).

Quantification of Pilins Using Immuno-Fluorescence Labeling

To be able to evaluate whether the strains produce higher quantities of pili compared to the parental strain *L. rhamnosus* GG, both SpaA and SpaC pilins of all derivatives were both qualitatively and quantitatively assessed in immuno-fluorescence labeling assays (**Figure 1A**). Quantitative measurements were obtained by normalizing fluorescence to DAPI staining of nucleic acids, and ultimately to values of the wild-type strain.

Pilin quantities were highly similar for all derivatives of Class I, and slightly higher for the SpaA pilin (1.0–1.4 for SpaA and 1.0–1.1 for SpaC) compared to wild-type (SpaA and SpaC normalized to 1.0). For the two other classes, a slight increase in pilin abundance, especially of SpaC pilin quantities, could be recorded (**Figure 1C**). Indeed, the strains of Class II all had an increased abundance of SpaC (1.3–1.9), compared to SpaA. Interestingly, in Class III the increase in abundance of SpaA and SpaC pilins seems to be balanced, both showing a considerable (almost 50%) increase in abundance compared to the parental strain (resp. 1.4 and 1.5).

These results indicate that the mutation in the *spaC* gene in the Class I mutants seems to slightly affect the abundance of SpaC in the pili, without affecting overall pili quantity. Classes II and III, in contrast, do show an increase of both SpaA and SpaC pilins, which might point toward a higher degree of piliation of these strains.

Analysis of the Architecture and Size of the Pili in the Different Derivative Classes Using Immuno-Electron Microscopy and Western Blot Analysis

Since immuno-fluorescence does not provide information about the architecture and size of the pili, we used immuno-electron microcopy (EM) to visualize the pili in the different classes of the 13 highly mucus adherent strains (**Figure 1B**). In general, the pili produced by the strains seemed to be similar in size to the parental strain *L. rhamnosus* GG, and no apparent large differences in pili morphology could be observed.

To investigate potential differences in the pilus ladder (Kankainen et al., 2009), cell wall-associated pilins from all strains were analyzed by Western blot and probed with anti-SpaC and -SpaA antibody (**Figure 1D**). These analyses revealed that the pilus ladder was highly similar for all strains and did not reveal apparent aberrations in the pilin ladders of PS strains compared to each other or the parental strain, *L. rhamnosus* GG.

Mucus Adhesion of the Selected Derivatives

As the SpaCBA pili of *L. rhamnosus* GG play a key role in its strong adhesive phenotype (Kankainen et al., 2009), we tested how the altered piliation of the different derivative classes affected mucus adhesion. Binding to porcine mucus, as a proxy for human mucus, was evaluated for all strains.

Wild-type *L. rhamnosus* GG presented an adhesion percentage of 40.4% (standard error of mean, SEM 6.7%) (**Figure 1E**). The earlier-characterized pilus-less derivative PB12 was used as a negative control and exhibited a statistically significant lower adhesion to mucus compared to wild-type and all derivatives (1.3%, SEM 0.2%, $p < 0.05$) (Rasinkangas et al., 2014). All derivative strains showed an increase in mucus adhesion with percentages ranging between 44.7 and 55.6% of cells irreversibly bound to mucus (**Figure 1E**). Strikingly, no clear differences or trends could be discerned between the different derivatives or classes.

Since porcine mucus was used for this analysis, two derivatives Class II (resp. PS24 and PS31) were retested on human mucus in order to evaluate if results were comparable between the two mucus sources (**Figure 1F**). Indeed, both strains showed a higher adherence to human mucus (44.1 and 48.4% resp.) compared to wild-type *L. rhamnosus* GG (39.7%) and certainly compared to the negative control strain, the pilus-less PB12 derivative (1.5%, $p < 0.05$) (**Figure 1F**).

Genomic Characterization of Derivatives by Single-Molecule Sequencing

For both Class I and Class III derivatives, shotgun (Illumina) sequencing could identify a mutation respectively in the adhesive pilin SpaC or in the major pilin SpaA. However, for the Class II derivatives the driving mutation affecting a higher SpaC antibody interaction remained elusive. Therefore, we performed single-molecule (PacBio) analysis of a representative of each class to confirm the genotype uncovered by the shotgun sequencing (**Supplementary File S2**). All classes had several SNPs in a pseudogene in common, *LGG_RS15025*.

The single-molecule analysis confirmed the genotype of the Class I representative PS17, namely a SNP in the adhesive pilin subunit SpaC, and for Class III strain PS41, a SNP in the major pilin SpaA (**Supplementary File S2**). Of particular interest was the analysis of two representative strains of Class II, PS24 and PS31 respectively. Whole genome alignment of both PS strains did not reveal gaps, large indels, inversions or other

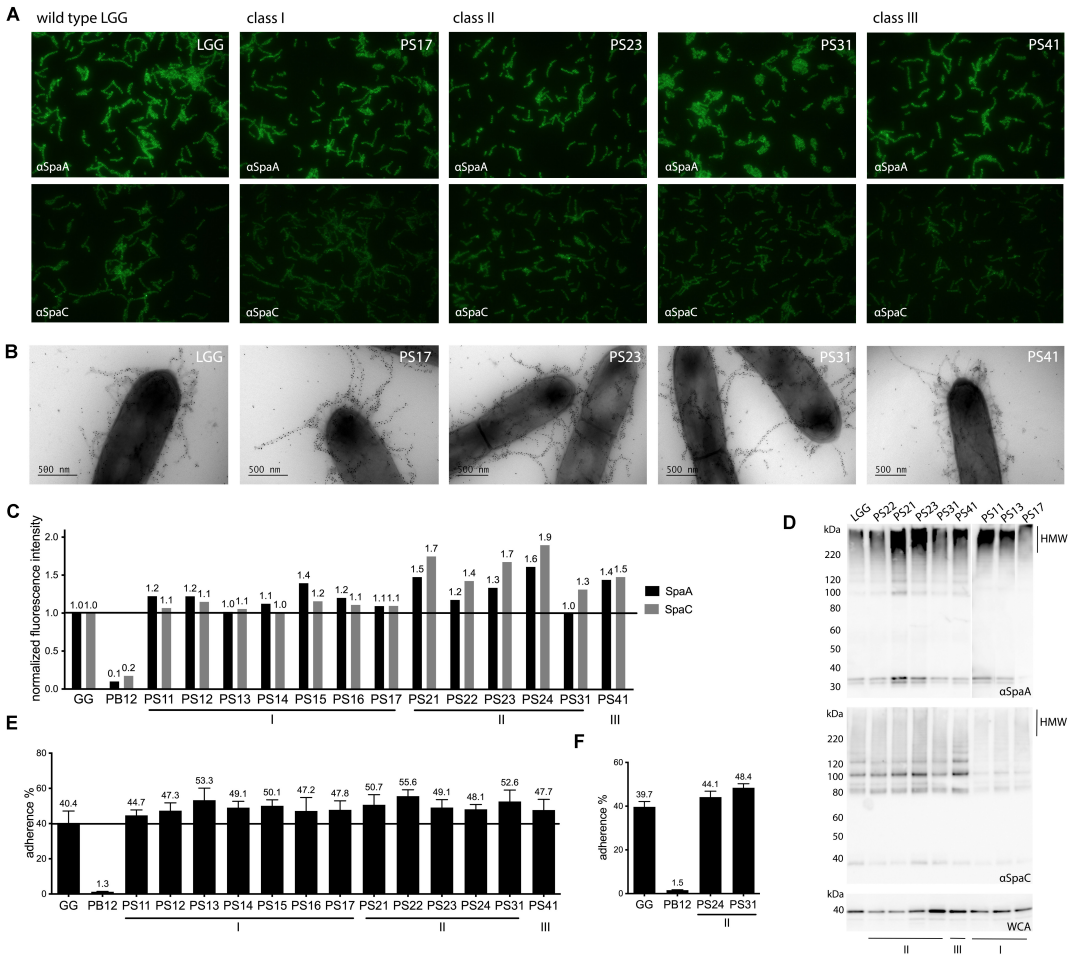

FIGURE 1 | Phenotypic assessment of piliation and mucus adhesion of highly mucus-adherent derivatives of *L. rhamnosus* GG. **(A)** Immunofluorescent labeling of SpaA and SpaC on cell surface of derivatives. Strains were labeled with either SpaA or SpaC antisera and detected with Alexa 488-labeled secondary antibody. Representative images are included for each strain. **(B)** Immunoelectron micrographs of strains double labeled with SpaC and SpaA antibodies. Both SpaC (5 nm gold particles) and SpaA (10 nm gold particles) are imaged on the pili of the different derivative strains (a representative figure is shown for each strain). **(C)** Quantitative immunofluorescent labeling results of SpaA and SpaC. Fluorescent signals of strains labeled with either SpaA and SpaC (detected by Alexa 488-labeled antibodies) were normalized to DAPI fluorescence. These values were further normalized to the fluorescence of the parental *L. rhamnosus* GG strain (indicated with a line to facilitate interpretation). A representative experiment is depicted. **(D)** Western blot analysis of cell wall associated proteome of each derivative. The pilus ladder (HMW for High Molecular Weight fraction) of the derivatives was visualized by probing cell wall extracts of each strain with SpaA and SpaC antibodies. Total amount of proteins is shown as a reference with a whole cell antibody (WCA) blot. **(E)** Mucus adhesion of the derivatives. The average result of 3 biological measurements (with each 3–6 technical repeats) is depicted for each derivative with wild-type *L. rhamnosus* GG as a positive control and the non-piliated derivative PB12 as a negative control. Standard error of mean (SEM) is shown. **(F)** Adhesion to human mucus. Adhesion of two derivatives, together with the positive and negative controls, to mucus isolated out of a human specimen, to validate porcine results. The average of three biological repeats is depicted with standard error of mean (SEM).

apparent anomalies compared to wild-type *L. rhamnosus* GG (**Supplementary File S3**).

The single-molecule analysis of PS24 resulted in an updated list of 43 genes affected by single nucleotide variations (**Supplementary File S2**). None of the SNPs was located in the *spaCBA-srtC1* gene cluster, confirming the shotgun results (**Supplementary File S1**). Also in accordance with the shotgun sequencing results, a SNP was detected in the SpaD pilus protein (Asp → Asn). SpaD is the major pilin of a second pili cluster (SpaFED) present in *L. rhamnosus* GG, which is thought to only play a minor role in interaction with the environment compared to the SpaCBA pili cluster, as only the latter seem to be expressed by the bacterium (von Ossowski et al., 2010; Reunanen et al., 2012). Of note, another LPXTG-motif harboring adhesin encoded by *LGG_RS13990* (*LGG_02923*) also harbors a SNP.

Further striking observations include the high amount of mutations in genes potentially affecting pilin production, like the gluconate operon repressor family regulator *farR* (*LGG_RS13185, LGG_02757*), transporters, surface and membrane proteins. Especially the large amount metal and cation transporters affected by SNPs stand out: *LGG_RS11535* (*LGG_02411,*

mntH), *LGG_RS11610* (*LGG_02426, psaA*), *LGG_RS12705* (*LGG_02658*), and *LGG_RS11565* (*LGG_02417*).

In the Class II derivative PS31, a total of 79 genes were affected by SNPs. It is hard to discern any large trends in the results, but one of the potential effector mutations could be in the gene of a transcriptional regulator belonging to the MarR family (*LGG_RS10240*, *LGG_02127*).

Transcriptome Analysis of the Class II Derivative PS24

To further investigate the different leads resulting from the SNP analysis of the Class II derivative PS24, the transcriptome of the strain was investigated at early ($OD_{600\,nm}$ 2) and late exponential phase ($OD_{600\,nm}$ 7) and compared to wild-type *L. rhamnosus* GG and the pili-less PB12 derivative (Rasinkangas et al., 2014).

RNA was isolated from wild-type *L. rhamnosus* GG, PB12 and PS24 and analyzed by RNASeq using deep Illumina sequencing. All resulting count tables and differential expression analysis comparing expression between *L. rhamnosus* GG and the PS24 derivative are compiled in **Supplementary File S4**.

In line with our observations described above and the goal of the experiment, the genes of the *spaCBA-srtC1* cluster are among the genes that are strongly upregulated in the PS24 derivative compared to the parental strain in early exponential phase (**Figure 2A**). Transcription levels of the genes of the other pili cluster, *spaFED-srtC2*, in contrast were extremely low in all strains and conditions tested (**Supplementary File S4**), confirming earlier observations stating that the SpaFED-pili do not play a role in the strong adhesion capacity of *L. rhamnosus* GG strains. Further comparison of normalized counts for the *spaCBA-srtC1* cluster for wild-type, the pilus-less PB12 and the PS24 strain resulted in a strong increase in expression of the *SpaCBA-srtC1* gene cluster in the PS24 strain (**Figure 2B**). This trend is both apparent at the early ($OD_{600\ nm}$ 2) (**Figure 2B**) and late exponential growth phase ($OD_{600\ nm}$ 7) time points (see **Supplementary File S4**).

Analysis of the 20 most upregulated genes in PS24, compared to wild-type, further corroborate the hypothesis that cation homeostasis might play a regulatory role affecting piliation and mucus adhesion in *L. rhamnosus* GG. Approximately 40% of the top hits belong to a cluster of genes related to cation transport (**Figures 2A,C**, green). Two genes in particular stand out, as they are harboring a SNP in the PS24 strain and both encode for a

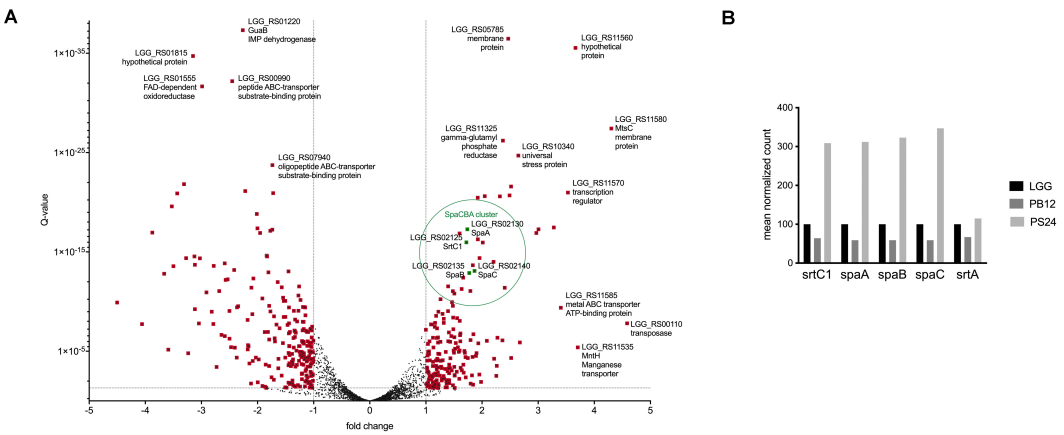

C upregulated genes in PS24

Locus tag	Old locus tag	Gene name	Gene product	Log2 fold	Q value
LGG_RS05775	LGG_01204		hypothetical protein	7.315250391	1.35E-169
LGG_RS00115	LGG_00023		membrane protein	6.096473706	1.09E-103
LGG_RS11530	LGG_02407		hypothetical protein	6.024038216	2.42E-38
LGG_RS00110	LGG_00022	is2	transposase	4.583730931	1.55E-08
LGG_RS11580	LGG_02420	mtsC	metal ABC transporter permease	4.304009645	3.74E-28
LGG_RS11545	LGG_02413		hypothetical protein	4.277183284	7.63E-108
LGG_RS11575	LGG_02419	mtsA	manganese ABC transporter substrate-binding protein	3.791242659	1.15E-43
LGG_RS11535	LGG_02411	mntH	manganese transporter	3.705819469	4.06E-06
LGG_RS11565	LGG_02417		cation transporter	3.699046823	1.50E-53
LGG_RS11560	LGG_02416		hypothetical protein	3.666097906	2.87E-36
LGG_RS11570	LGG_02418	czrA	ArsR family transcriptional regulator	3.529811204	1.06E-21
LGG_RS11585	LGG_02421	mtsB	manganese transporter	3.404515288	4.13E-10
LGG_RS02910	LGG_00616	proY	alanine glycine permease	3.304553869	1.97E-73
LGG_RS00440	LGG_00088		hypothetical protein	3.278598971	3.45E-18
LGG_RS05780	LGG_01205		hypothetical protein	3.130887971	3.10E-43
LGG_RS01420	LGG_00293		hydrolase	3.006256866	5.25E-18
LGG_RS00445	LGG_00089		membrane protein	2.967079731	1.24E-17
LGG_RS00125	LGG_00025		ABC transporter	2.674104626	1.31E-06
LGG_RS10340	LGG_02151	usp	universal stress protein A	2.647267385	1.99E-25
LGG_RS02375	LGG_00497		hypothetical protein	2.519258157	4.82E-05

D upregulated genes in wild type GG

Locus tag	Old locus tag	Gene name	Gene product	Log2 fold	Q value
LGG_RS08715	LGG_01810	purQ	phosphoribosylformylglycinamidine synthase	-8.486030209	3.79E-153
LGG_RS08720	LGG_01811	purS	phosphoribosylformylglycinamidine synthase	-8.428785719	5.47E-116
LGG_RS08725	LGG_01812	purC	phosphoribosylaminoimidazole-succinocarboxamide synthase	-8.39426168	4.66E-121
LGG_RS08730	LGG_01813	purK	phosphoribosylaminoimidazole carboxylase	-8.35037715	6.87E-109
LGG_RS08710	LGG_01809	purL	phosphoribosylformylglycinamidine synthase	-8.350022463	7.42E-174
LGG_RS08705	LGG_01808	purF	amidophosphoribosyltransferase	-8.251551375	1.53E-171
LGG_RS08700	LGG_01807	purM	phosphoribosylaminoimidazole synthetase	-8.144073489	3.69E-168
LGG_RS08690	LGG_01805	purH	purine biosynthesis protein purH	-8.118399886	1.14E-241
LGG_RS08695	LGG_01806	purN	phosphoribosylglycinamide formyltransferase	-8.116348352	1.95E-187
LGG_RS08685	LGG_01803	purD	phosphoribosylamine--glycine ligase	-8.055760314	3.62E-232
LGG_RS08735	LGG_01814	purE	N5-carboxyaminoimidazole ribonucleotide mutase	-7.913348641	5.23E-100
LGG_RS00360	LGG_00072		membrane protein	-5.826715138	1.43E-32
LGG_RS02840	LGG_00600	oxlT	MFS transporter	-5.281770215	4.21E-54
LGG_RS00365	LGG_00073		membrane protein	-4.501292055	1.24E-10
LGG_RS00355	LGG_00071		amidohydrolase	-4.057811454	1.84E-08
LGG_RS00350	LGG_00070		hypothetical protein	-3.874030315	1.13E-17
LGG_RS02020	LGG_00419		LacI family transcriptional regulator	-3.664221176	1.59E-13
LGG_RS00835	LGG_00168	pbuO	guanine permease	-3.58909389	6.90E-06
LGG_RS13470	LGG_02817	argG	argininosuccinate synthase	-3.526812291	2.61E-20
LGG_RS12870	LGG_02692		AraC family transcriptional regulator	-3.497747383	2.74E-14

FIGURE 2 | Transcriptomic analysis of PS24 compared to wild-type *L. rhamnosus* GG at $OD_{600\ nm}$ 2. **(A)** Volcano plot of differential expression compared for *L. rhamnosus* GG and PS24. Log2 fold change versus *q*-value is depicted. Data points marked in red have a log2 fold larger than 1 and a *q*-value smaller than 0.05. Positive fold change implies higher expression in the PS24 strain. **(B)** Mean normalized pili transcript count. Normalized expression of the *spaCBA-srtC1*gene cluster in the pilus-less PB12 derivative and PS24 derivative relative to wild-type *L. rhamnosus* GG. The housekeeping sortase A was included for comparison. **(C)** Top 20 upregulated genes in PS24 derivative. The top 20 genes with the highest log2fold value compared to wild-type *L. rhamnosus* GG at $OD_{600\ nm}$ 2. **(D)** Top 20 downregulated genes in PS24 derivative. The top 20 genes with the highest log2fold value in wild-type *L. rhamnosus* GG at $OD_{600\ nm}$ 2, compared to the PS24 derivative.

cation transporter, namely *LGG_RS11535* (*LGG_02411, mntH*) and *LGG_RS11565* (*LGG_02417*) (**Supplementary File S3**).

Analysis of the counterpart, the 20 most downregulated genes in PS24 compared to the parental strain (**Figure 2D**), showed a strong downregulation of the C1 metabolism in PS24, more in particular genes involved in purine metabolism (purple in **Figure 2D**). Two genes that are also strongly downregulated in PS24, include two transcriptional regulators (orange in **Figure 2D**).

DISCUSSION

In this study, we sought to find highly mucus adherent derivatives of *L. rhamnosus* GG with the means of random chemical mutagenesis. Such derivatives not only can render invaluable insights in processes steering pili biogenesis and functionality, but also can safely be used in a human trial setting as these derivatives are considered as non-GMO (The European Union, 2001).

Increased binding to anti-SpaC IgG was chosen as a readout to select strains, as SpaC is the pilin mainly responsible for the strong adhesive properties attributed to the SpaCBA pili of *L. rhamnosus* GG (Kankainen et al., 2009; von Ossowski et al., 2010; Lebeer et al., 2012; Reunanen et al., 2012; Tripathi et al., 2013). Combined mutagenesis and selection led to the isolation of 13 highly mucus-adherent strains. Illumina genomic re-sequencing revealed mutations underlying the observed phenotype and allowed classification of the derivatives into 3 classes. The strains were also subjected to further phenotypic analyses to assess how piliation was affected in the different classes.

All selected strains showed an increased capability to adhere to mucus compared to wild-type *L. rhamnosus* GG (**Figure 1D**). This confirms the validity of our screening set-up, where interaction with anti-SpaC IgG is used as a predictor of mucus adhesion capacity. These findings also corroborate the key role of SpaC in the strong mucus adhesion phenotype of *L. rhamnosus* GG. Our results also further validate the use of porcine mucus as a proxy for human mucus as the heightened mucus adhesion phenotype could be replicated for two selected strains (**Figure 1F**).

With mucus adherence of wild-type *L. rhamnosus* GG being around 40% both for porcine and human mucus, a 15% increase in adhesion (PS22, approximately 55%) was the strongest increase in mucus adhesion that could be registered for the derivatives. This is a further attestation of the known superb adhesion capacity of wild-type *L. rhamnosus* GG (Kankainen et al., 2009; von Ossowski et al., 2010; Reunanen et al., 2012; Tytgat et al., 2016a) and suggesting that this is highly optimized through evolution as only relatively modest increases in mucus adhesion could be achieved.

Class I mutants were found to harbor a mutation in the C-terminal of the *spaC* gene, close to its collagen-binding domain. These strains, however, did not appear to produce more pili in general or represent more SpaC on their cell surface (**Figure 1**). The higher adhesion efficacy of Class I strains is likely due to a direct impact of the mutation on the adherence properties of the SpaC tip pilin itself, potentially by altering its collagen-binding domain. Further studies are needed to understand the exact mechanisms driving SpaC adherence and the role of its different domains. Interestingly, all derivatives of Class I also share SNPs in other genes and intergenic regions. Further research is necessary to assess the importance, if any, of these SNPs, by for instance reverse engineering.

The strain designated as a Class III strain, PS41, harbors a mutation in the gene encoding SpaA, the shaft pilin, which is located close to its secretion signal. This mutation may affect the secretion efficiency of backbone pilin SpaA and hence result in higher pilus production. Another potential explanation is the production of longer pili. In *Corynebacterium diphtheriae,* pilus length is shown to be regulated by the ratio of major pilin SpaA to basal pilin SpaB, and a higher quantity of SpaA tends to lead to formation of longer pili (Swierczynski and Ton-That, 2006). Our selection of the PS41 strain based on strong interaction with anti-SpaC IgG might thus be due either to a higher presentation of SpaC along the pilus, or on more pili, or more accessible SpaC units on longer pilins. PS41 was found to produce a higher amount of both SpaA and SpaC pilins compared to the parental strain (**Figure 1C**). This, however, did not result in a significant increase in the length of the pili or changes in the pilin protein ladder (**Figures 1B,D**). Our results do point toward a higher degree of piliation in general on the surface of PS41, which is likely coming from a higher secretion of SpaA (**Figures 1A,B**). This is corroborated by the balanced increase in relative abundance of SpaA and SpaC subunits in PS41 compared to wild-type and the other derivatives.

In contrast to Class I and III, where a SNP was found that could be directly linked to genes driving SpaCBA biogenesis, the genotype of the Class II strains remains more elusive, nevertheless this class harbors the strains that demonstrate the most dramatic increase in the amount of SpaCBA pili (**Figure 1**). Considering the phenotype, i.e., high mucus adherence and high production of pilins, it is likely that mutations lead to more efficient gene transcription or increased secretion of the pilins by an unknown mechanism. However, at this point no mutations that are known to influence pilin biogenesis or functionality could be identified in genomic analyses of strains this class. As the secretion machinery of *L. rhamnosus* GG is still largely unknown, it is difficult to evaluate which of the genes would impact the quantity of the pilins that are secreted and competent for pili production. Single-molecule re-sequencing of two representatives of this class (PS24 and PS31) showed that no large indels, inversions or other genomic events could explain the observed phenotype (**Supplementary File S3**).

Dedicated PacBio SNP analysis of Class II mutant PS24 revealed mutations in the *spaFED-srtC2* pili cluster (von Ossowski et al., 2010) and the adhesin encoding *LGG_RS13990* gene. Further research is necessary to investigate if defects in these two minor adhesive units of *L. rhamnosus* GG have an impact on the overall adhesion capacity of the *L. rhamnosus* GG via changes in their own adhesive function or by affecting the SpaCBA pili.

Another mutated gene that might affect pilin production in the Class II derivative PS24, could be the *farR* transcriptional regulator belonging to the gluconate operon repressor

(GntR) family (*LGG_RS13185, LGG_02757*). A member of this family, YtrA, has been shown to regulate expression of type III protein secretion system and control several biological processes, such as adhesion and extracellular enzyme production, in a plant pathogen *Xanthomonas citri* (Zhou et al., 2017). Further of note, are the SNPs in several metal and cation transporters: *LGG_RS11535* (*LGG_02411, mntH*), *LGG_RS11610* (*LGG_02426, psaA*), *LGG_RS12705* (*LGG_02658*) and *LGG_RS11565* (*LGG_02417*). ABC transporters are a group of enzymes coupling substrate transport to hydrolysis of ATP. In *Streptococcus pneumoniae*, mutations in PsaA, characterized as a component of a Mn^{2+}-transporter, have been shown to cause deficiencies in virulence and adherence of the bacterium (Johnston et al., 2004). Several studies have addressed the connections between the function of certain metal ABC transporters and secretion of fimbrial proteins (Fenno et al., 1995; Claverys, 2001). These data suggested the coupling of pilin secretion and metal ion transport. Additionally, metal ions may act as co-factors for many proteins: manganese has been shown to be important for the function of fibronectin binding protein (Fbp68) of *Clostridium difficile* (Lin et al., 2011). These findings in other strains, coupled to our observations might indicate that cation metabolism plays a role in steering pilin secretion. The potential impact of cation metabolism was confirmed in transcriptomic evaluation of the PS24 derivative, with a whole cluster of genes linked to metal ion transport and regulation being among the top differentially expressed genes compared to wild-type *L. rhamnosus* GG (**Figures 2A,C**). Here again the overexpression of the *mntH* managanese transporter stands out, the overproduction of which has recently been linked to increased antifungal activity (Siedler et al., 2020).

This transcriptomic analysis also confirmed the increase in transcription of the *spCBA-srtC1* gene cluster in the PS24 strain (**Figures 2A,B**), which is in accordance with our observations of a higher degree of piliation in Class II strains (**Figure 1**).The higher piliation phenotype, especially the increase of SpaC at the strains surface, is likely caused by more efficient gene transcription of the pilins. Indeed, especially the transcription counts of the *spaC* gene are strongly increased in an absolute sense compared to the other genes of the *spaCBA-srtC1* operon in PS24, both at $OD_{600\ nm}$ 2 and $OD_{600\ nm}$ 7 (**Supplementary File S4**). A potential explanation is that one of the other genes that have been affected by the EMS mutagenesis normally acts as a repressor of the *spaCBA* promoter that is mapped in the IS30 element upstream of the *spaC* gene (Douillard et al., 2013). Our results indicate that genes related to metal cation homeostasis potentially play a role in regulating *L. rhamnosus* GG adhesion properties, with mutations in key regulators and transporters potentially affecting pilin secretion causing the observed phenotype. Furthermore, this effect seems to be situated at the transcription level. Further research is needed to address the details of the transcriptional regulation of the *spaCBA* gene cluster identified here.

Similar efforts, i.e., using single-molecule genomic analysis to identify SNPs in genes potentially affecting SpaCBA pili, were performed for another Class II derivative, PS31 (**Supplementary File S2**). This, however, did not lead to clear hypotheses on genes that might drive its highly piliated phenotype, illustrating that much remains to be uncovered on the regulation of SpaCBA biogenesis and functionality in *L. rhamnosus* GG. One lead might be the SNP in the transcriptional regulator belonging to the MarR family (*LGG_RS10240, LGG_02127*). A regulator in *Enterococcus faecalis* belonging to the same family, SlyA, has been shown to be involved in virulence and persistence in the host, and similar effects have been noted for other MarR regulators in other pathogens (Michaux et al., 2011). Additionally, Obg, a CgtA GTPase, plays a role in the bet-hedging behavior of *Escherichia coli* and *Pseudomonas aeruginosa*, increasing their persistence and resistance toward stresses (Verstraeten et al., 2015). It remains to be confirmed if and how these genes play a role in SpaCBA pilin regulation and function in *L. rhamnosus* GG.

Taken together, we report on the generation and characterization of highly adherent derivatives of the model probiotic *L. rhamnosus* GG. Given its strong mucus adhesion properties attributed to its unique SpaCBA pili, we investigated if an increase in anti-SpaC IgG interaction translated in an increase in mucus adhesion. According to our phenotypic analyses, we conclude that the observed highly adherent phenotypes of the derivatives was caused either by mutations resulting in a higher adherence ability (Class I) or production of higher quantity of pilins (Classes II–III). We uncovered novel insights in mechanisms regulating the biogenesis and functionality of the SpaCBA pili and propose a coupling between ion homeostasis and piliation in *L. rhamnosus* GG. It will be interesting to investigate and validate these leads further using site-directed mutagenesis approaches in future studies. Our study also delivers a unique set of strains to study the effect of increased quantity of pili on host interactions in human trials, as the strains are not considered as GMOs.

Together with the non-piliated derivatives of *L. rhamnosus* GG (Rasinkangas et al., 2014) we characterized earlier, the here described highly adherent derivatives make up a complete toolset of strains that can aid in further functional dissection of *L. rhamnosus* GG – host interactions, and particularly the role of the SpaCBA pili therein. These insights will ultimately stimulate the development of next-generation probiotics and identification of probiotic effectors.

DATA AVAILABILITY STATEMENT

The datasets presented in this study can be found in online repositories and **Supplementary Material**. The names of the repository/repositories and accession number(s) can be found in the article.

AUTHOR CONTRIBUTIONS

PR, FD, AP, and WV contributed to conception and design of the study. PR and HT carried out the experimental procedures. JRe performed the immuno EM analysis. JRi was responsible for Illumina sequence processing of all strains. SS provided the human mucus and provided the general comments.

HT and PR wrote the manuscript and made the figures. All the authors contributed to manuscript revision, read, and approved the submitted version.

FUNDING

This project, including the efforts of PR, FD, JRe, and JRi, were funded by European Research Council (Grant 250172, Microbes Inside to WV) and Academy of Finland (Grants 252123 to FD, 299749 to JRe, and 137389 to WV). Work of HT and WV was partly funded by the SIAM Gravity Grant 024.002.002 and Spinoza Award of the Netherlands Organization for Scientific Research of WV.

ACKNOWLEDGMENTS

We are grateful to the personnel of Sequencing and Electron Microscopy Units of the Institute of Biotechnology, University of Helsinki. We gratefully acknowledge Dr. Ingemar von Ossowski of UHelsinki for providing the antibodies against SpaA and SpaC pilins. We thank Bart Nijsse and Bastian Hornung of the Laboratory of Systems and Synthetic Biology of Wageningen University for advice on RNA Seq analysis.

SUPPLEMENTARY MATERIAL

The Supplementary Material for this article can be found online at: https://www.frontiersin.org/articles/10.3389/fbioe.2020.01024/full#supplementary-material

FILE S1 | SNPs identified by shotgun Illumina sequencing in all highly adherent derivatives. Includes an SNP comparison sheet where similar SNPs in genes and intergenic regions between all selected derivatives are highlighted: green for the ones shared amongst all highly adherent derivatives and blue for the SNPs common amongst all Class I strains.

FILE S2 | SNPs identified by single-molecule genome PacBio resequencing in PS17, PS24, PS31, and PS41.

FILE S3 | Whole Genome Alignment results for PS24 and PS31 resulting from PacBio sequencing.

FILE S4 | RNASeq count tables of *L. rhamnosus* GG, PB12 and PS24 and differential expression of *L. rhamnosus* GG vs. PS24 at OD2 and OD7.

REFERENCES

Anders, S., Pyl, P. T., and Huber, W. (2015). HTSeq–a Python framework to work with high-throughput sequencing data. *Bioinformatics* 31, 166–169. doi: 10.1093/bioinformatics/btu638

Ardita, C. S., Mercante, J. W., Kwon, Y. M., Luo, L., Crawford, M. E., Powell, D. N., et al. (2014). Epithelial adhesion mediated by pilin SpaC is required for *Lactobacillus rhamnosus* GG-induced cellular responses. *Appl. Environ. Microbiol.* 80, 5068–5077. doi: 10.1128/AEM.01039-14

Arvola, T., Laiho, K., Torkkeli, S., Mykkanen, H., Salminen, S., Maunula, L., et al. (1999). Prophylactic Lactobacillus GG reduces antibiotic-associated diarrhea in children with respiratory infections: a randomized study. *Pediatrics* 104:e64. doi: 10.1542/peds.104.5.e64

Binnendijk, K. H., and Rijkers, G. T. (2013). What is a health benefit? An evaluation of EFSA opinions on health benefits with reference to probiotics. *Benef. Microbes.* 4, 223–230. doi: 10.3920/BM2013.0019

Blankenberg, D., Von Kuster, G., Coraor, N., Ananda, G., Lazarus, R., Mangan, M., et al. (2010). Galaxy: a web-based genome analysis tool for experimentalists. *Curr. Protoc. Mol. Biol. Chapter.* 19, 11–21. doi: 10.1002/0471142727.mb1910s89

Chandrasekharan, B., Saeedi, B. J., Alam, A., Houser, M., Srinivasan, S., Tansey, M., et al. (2019). Interactions between commensal bacteria and enteric neurons, via FPR1 induction of ROS, increase gastrointestinal motility in mice. *Gastroenterology* 157, 179.e172–192.e172. doi: 10.1053/j.gastro.2019.03.045

Chevreux, B., Wetter, T., and Suhai, S. (1999). Genome sequence assembly using trace signals and additional sequence information. *German Conference Bioinform.* 99, 45–56.

Claverys, J. P. (2001). A new family of high-affinity ABC manganese and zinc permeases. *Res. Microbiol.* 152, 231–243. doi: 10.1016/s0923-2508(01)01195-0

de Vos, W. M. (2011). Systems solutions by lactic acid bacteria: from paradigms to practice. *Microb. Cell Fact.* 10(Suppl. 1), S2. doi: 10.1186/1475-2859-10-S1-S2

Douillard, F. P., Rasinkangas, P., Bhattacharjee, A., Palva, A., and de Vos, W. M. (2016). The N-Terminal GYPSY motif is required for pilin-specific sortase SrtC1 functionality in *Lactobacillus rhamnosus* strain GG. *PLoS One* 11:e0153373. doi: 10.1371/journal.pone.0153373

Douillard, F. P., Rasinkangas, P., von Ossowski, I., Reunanen, J., Palva, A., and de Vos, W. M. (2014). Functional identification of conserved residues involved in *Lactobacillus rhamnosus* strain GG sortase specificity and pilus biogenesis. *J. Biol. Chem.* 289, 15764–15775. doi: 10.1074/jbc.M113.542332

Douillard, F. P., Ribbera, A., Jarvinen, H. M., Kant, R., Pietila, T. E., Randazzo, C., et al. (2013). Comparative genomic and functional analysis of Lactobacillus casei and *Lactobacillus rhamnosus* strains marketed as probiotics. *Appl. Environ. Microbiol.* 79, 1923–1933. doi: 10.1128/AEM.03467-12

The European Union (2001). *Directive 2001/18/EC of the European Parliament and of the Council of 12 March 2001 on the Deliberate Release into the Environment Of Genetically Modified Organisms and Repealing Council Directive 30/2203EEC*. Belgium: European Union.

FAO/WHO (2001). *Report on Joint FAO/WHO Expert Consultation of Health and Nutritional Properties of Probiotics in Food Including Powder Milk with Live Lactic Acid Bacteria*. Geneva: WHO.

Fenno, J. C., Shaikh, A., Spatafora, G., and Fives-Taylor, P. (1995). The fimA locus of Streptococcus parasanguis encodes an ATP-binding membrane transport system. *Mol. Microbiol.* 15, 849–863. doi: 10.1111/j.1365-2958.1995.tb02355.x

Giardine, B., Riemer, C., Hardison, R. C., Burhans, R., Elnitski, L., Shah, P., et al. (2005). Galaxy: a platform for interactive large-scale genome analysis. *Genome Res.* 15, 1451–1455. doi: 10.1101/gr.4086505

Gilbert, D. (2003). Sequence file format conversion with command-line readseq. *Curr. Protoc. Bioinformatics* A.1E.1–A.1E.4. doi: 10.1002/0471250953.bia01es00

Goecks, J., Nekrutenko, A., Taylor, J., and Galaxy, T. (2010). Galaxy: a comprehensive approach for supporting accessible, reproducible, and transparent computational research in the life sciences. *Genome Biol.* 11:R86. doi: 10.1186/gb-2010-11-8-r86

Hatakka, K., Savilahti, E., Ponka, A., Meurman, J. H., Poussa, T., Nase, L., et al. (2001). Effect of long term consumption of probiotic milk on infections in children attending day care centres: double blind, randomised trial. *BMJ* 322, 1327. doi: 10.1136/bmj.322.7298.1327

Hendrickx, A. P., Budzik, J. M., Oh, S. Y., and Schneewind, O. (2011). Architects at the bacterial surface - sortases and the assembly of pili with isopeptide bonds. *Nat. Rev. Microbiol.* 9, 166–176. doi: 10.1038/nrmicro2520

Johnston, J. W., Myers, L. E., Ochs, M. M., Benjamin, W. H. Jr., Briles, D. E., et al. (2004). Lipoprotein PsaA in virulence of Streptococcus pneumoniae: surface accessibility and role in protection from superoxide. *Infect. Immun.* 72, 5858–5867. doi: 10.1128/IAI.72.10.5858-5867.2004

Joshi, N. A., and Fass, J. N. (2011). *Sickle: A sliding-window, adaptive, quality-based trimming tool for FastQ files (version 1.33)*.

Kalliomaki, M., Salminen, S., Arvilommi, H., Kero, P., Koskinen, P., and Isolauri, E. (2001). Probiotics in primary prevention of atopic disease: a randomised

placebo-controlled trial. *Lancet* 357, 1076–1079. doi: 10.1016/S0140-6736(00)04259-8

Kankainen, M., Paulin, L., Tynkkynen, S., von Ossowski, I., Reunanen, J., Partanen, P., et al. (2009). Comparative genomic analysis of *Lactobacillus rhamnosus* GG reveals pili containing a human- mucus binding protein. *Proc. Natl. Acad. Sci. U.S.A.* 106, 17193–17198. doi: 10.1073/pnas.0908876106

Kant, A., von Ossowski, I., Palva, A., and Krishnan, V. (2016). Crystallization and X-ray crystallographic analysis of the adhesive SpaC pilin subunit in the SpaCBA Pilus of Gut-adapted *Lactobacillus rhamnosus* GG. *Protein Pept. Lett.* 23, 365–371. doi: 10.2174/0929866523666160106153055

Kopylova, E., Noe, L., and Touzet, H. (2012). SortMeRNA: fast and accurate filtering of ribosomal RNAs in metatranscriptomic data. *Bioinformatics* 28, 3211–3217. doi: 10.1093/bioinformatics/bts611

Kumpu, M., Kekkonen, R. A., Kautiainen, H., Jarvenpaa, S., Kristo, A., Huovinen, P., et al. (2012). Milk containing probiotic *Lactobacillus rhamnosus* GG and respiratory illness in children: a randomized, double-blind, placebo-controlled trial. *Eur. J. Clin. Nutr.* 66, 1020–1023. doi: 10.1038/ejcn.2012.62

Kurtz, S., Phillippy, A., Delcher, A. L., Smoot, M., Shumway, M., Antonescu, C., et al. (2004). Versatile and open software for comparing large genomes. *Genome Biol.* 5:R12. doi: 10.1186/gb-2004-5-2-r12

Langmead, B., and Salzberg, S. L. (2012). Fast gapped-read alignment with Bowtie 2. *Nat. Methods* 9, 357–359. doi: 10.1038/nmeth.1923

Lebeer, S., Claes, I., Tytgat, H. L., Verhoeven, T. L., Marien, E., von Ossowski, I., et al. (2012). Functional analysis of *Lactobacillus rhamnosus* GG pili in relation to adhesion and immunomodulatory interactions with intestinal epithelial cells. *Appl. Environ. Microbiol.* 78, 185–193. doi: 10.1128/AEM.06192-11

Li, H., Handsaker, B., Wysoker, A., Fennell, T., Ruan, J., Homer, N., et al. (2009). The Sequence Alignment/Map format and SAMtools. *Bioinformatics* 25, 2078–2079. doi: 10.1093/bioinformatics/btp352

Lin, Y. P., Kuo, C. J., Koleci, X., McDonough, S. P., and Chang, Y. F. (2011). Manganese binds to Clostridium difficile Fbp68 and is essential for fibronectin binding. *J. Biol. Chem.* 286, 3957–3969. doi: 10.1074/jbc.M110.184523

Love, M. I., Huber, W., and Anders, S. (2014). Moderated estimation of fold change and dispersion for RNA-seq data with DESeq2. *Genome Biol.* 15:550. doi: 10.1186/s13059-014-0550-8

Luoto, R., Ruuskanen, O., Waris, M., Kalliomaki, M., Salminen, S., and Isolauri, E. (2014). Prebiotic and probiotic supplementation prevents rhinovirus infections in preterm infants: a randomized, placebo-controlled trial. *J. Allergy Clin. Immunol.* 133, 405–413. doi: 10.1016/j.jaci.2013.08.020

Mandlik, A., Swierczynski, A., Das, A., and Ton-That, H. (2008). Pili in Gram-positive bacteria: assembly, involvement in colonization and biofilm development. *Trends Microbiol.* 16, 33–40. doi: 10.1016/j.tim.2007.10.010

Martin, M. (2011). Cutdadapt removes adapter sequences from high-throughput sequencing reads. *EMBnet. J.* 17, 10–12. doi: 10.14806/ej.17.1.200

Michaux, C., Sanguinetti, M., Reffuveille, F., Auffray, Y., Posteraro, B., Gilmore, M. S., et al. (2011). SlyA is a transcriptional regulator involved in the virulence of *Enterococcus faecalis*. *Infect. Immun.* 79, 2638–2645. doi: 10.1128/IAI.01132-10

Nermes, M., Kantele, J. M., Atosuo, T. J., Salminen, S., and Isolauri, E. (2011). Interaction of orally administered Lactobacillus rhamnosus GG with skin and gut microbiota and humoral immunity in infants with atopic dermatitis. *Clin. Exp. Allergy* 41, 370–377. doi: 10.1111/j.1365-2222.2010.03657.x

Nishiyama, K., Ueno, S., Sugiyama, M., Yamamoto, Y., and Mukai, T. (2016). Lactobacillus rhamnosus GG SpaC pilin subunit binds to the carbohydrate moieties of intestinal glycoconjugates. *Anim. Sci. J.* 87, 809–815. doi: 10.1111/asj.12491

Parekh, S., Vinci, V. A., and Strobel, R. J. (2000). Improvement of microbial strains and fermentation processes. *Appl. Microbiol. Biotechnol.* 54, 287–301. doi: 10.1007/s002530000403

Qin, J., Li, R., Raes, J., Arumugam, M., Burgdorf, K. S., Manichanh, C., et al. (2010). A human gut microbial gene catalogue established by metagenomic sequencing. *Nature* 464, 59–65. doi: 10.1038/nature08821

Rasinkangas, P., Reunanen, J., Douillard, F. P., Ritari, J., Uotinen, V., Palva, A., et al. (2014). Genomic characterization of non-mucus-adherent derivatives of Lactobacillus rhamnosus GG reveals genes affecting pilus biogenesis. *Appl. Environ. Microbiol.* 80, 7001–7009. doi: 10.1128/AEM.02006-14

R Core Team (2014). *The R Project for Statistical Computing. R Foundation for Statistical Computing*. Vienna: R Core Team.

Reunanen, J., von Ossowski, I., Hendrickx, A. P., Palva, A., and de Vos, W. M. (2012). Characterization of the SpaCBA pilus fibers in the probiotic *Lactobacillus rhamnosus* GG. *Appl, Environ. Microbiol.* 78, 2337–2344. doi: 10.1128/AEM.07047-11

Sega, G. A. (1984). A review of the genetic effects of ethyl methanesulfonate. *Mutat. Res.* 134, 113–142. doi: 10.1016/0165-1110(84)90007-1

Siedler, S., Rau, M. H., Bidstrup, S., Vento, J. M., Aunsbjerg, S. D., Bosma, E. F., et al. (2020). Competitive exclusion is a major bioprotective mechanism of lactobacilli against fungal spoilage in fermented milk products. *Appl. Environ. Microbiol.* 86:e02312-19. doi: 10.1128/AEM.02312-19

Swierczynski, A., and Ton-That, H. (2006). Type III pilus of corynebacteria: pilus length is determined by the level of its major pilin subunit. *J. Bacteriol.* 188, 6318–6325. doi: 10.1128/JB.00606-06

Szajewska, H., and Kolodziej, M. (2015). Systematic review with meta-analysis: *Lactobacillus rhamnosus* GG in the prevention of antibiotic-associated diarrhoea in children and adults. *Aliment. Pharmacol. Ther.* 42, 1149–1157. doi: 10.1111/apt.13404

Tripathi, P., Beaussart, A., Alsteens, D., Dupres, V., Claes, I., von Ossowski, I., et al. (2013). Adhesion and nanomechanics of pili from the probiotic *Lactobacillus rhamnosus* GG. *ACS Nano.* 7, 3685–3697. doi: 10.1021/nn400705u

Tytgat, H. L., Douillard, F. P., Reunanen, J., Rasinkangas, P., Hendrickx, A. P., Laine, P. K., et al. (2016a). *Lactobacillus rhamnosus* GG Outcompetes *Enterococcus faecium* via mucus-binding pili: evidence for a novel and heterospecific probiotic mechanism. *Appl. Environ. Microbiol.* 82, 5756–5762. doi: 10.1128/AEM.01243-16

Tytgat, H. L., van Teijlingen, N. H., Sullan, R. M., Douillard, F. P., Rasinkangas, P., Messing, M., et al. (2016b). Probiotic gut microbiota isolate interacts with dendritic cells via glycosylated heterotrimeric pili. *PLoS One* 11:e0151824. doi: 10.1371/journal.pone.0151824

Verstraeten, N., Knapen, W. J., Kint, C. I., Liebens, V., Van den Bergh, B., Dewachter, L., et al. (2015). Obg and membrane depolarization are part of a microbial bet-hedging strategy that leads to antibiotic tolerance. *Mol Cell* 59, 9–21. doi: 10.1016/j.molcel.2015.05.011

Vesterlund, S., Paltta, J., Karp, M., and Ouwehand, A. C. (2005). Measurement of bacterial adhesion-in vitro evaluation of different methods. *J. Microbiol. Methods* 60, 225–233. doi: 10.1016/j.mimet.2004.09.013

von Ossowski, I., Reunanen, J., Satokari, R., Vesterlund, S., Kankainen, M., Huhtinen, H., et al. (2010). Mucosal adhesion properties of the probiotic *Lactobacillus rhamnosus* GG SpaCBA and SpaFED pilin subunits. *Appl. Environ. Microbiol.* 76, 2049–2057. doi: 10.1128/AEM.01958-09

Zheng, J., Wittouck, S., Salvetti, E., Franz, C., Harris, H. M. B., Mattarelli, P., et al. (2020). A taxonomic note on the genus *Lactobacillus*: description of 23 novel genera, emended description of the genus *Lactobacillus* Beijerinck 1901, and union of *Lactobacillaceae* and *Leuconostocaceae*. *In. J. Syst. Evol. Microbiol.* 70, 2782–2858. doi: 10.1099/ijsem.0.004107

Zhou, X., Yan, Q., and Wang, N. (2017). Deciphering the regulon of a GntR family regulator via transcriptome and ChIP-exo analyses and its contribution to virulence in Xanthomonas citri. *Mol. Plant Pathol.* 18, 249–262. doi: 10.1111/mpp.12397

Conflict of Interest: The authors declare that the research was conducted in the absence of any commercial or financial relationships that could be construed as a potential conflict of interest.

Citation: Rasinkangas P, Tytgat HLP, Ritari J, Reunanen J, Salminen S, Palva A, Douillard FP and de Vos WM (2020) Characterization of Highly Mucus-Adherent Non-GMO Derivatives of Lacticaseibacillus rhamnosus GG. Front. Bioeng. Biotechnol. 8:1024. doi: 10.3389/fbioe.2020.01024

frontiers in Bioengineering and Biotechnology

REVIEW
published: 11 September 2020
doi: 10.3389/fbioe.2020.581778

Bacteriocins From LAB and Other Alternative Approaches for the Control of *Clostridium* and *Clostridiodes* Related Gastrointestinal Colitis

*Svetoslav D. Todorov[1], Hye-Ji Kang[1,2], Iskra V. Ivanova[3] and Wilhelm H. Holzapfel[1,2]**

[1] Advanced Green Energy and Environment Institute (AGEE), Handong Global University, Pohang, South Korea, [2] HEM Inc., Handong Global University, Pohang, South Korea, [3] Department of General and Applied Microbiology, Faculty of Biology, Sofia University "St. Kliment Ohridski", Sofia, Bulgaria

OPEN ACCESS

Edited by:
Csaba Fehér, Budapest University of Technology and Economics, Hungary

Reviewed by:
Javier Alberto Garza Cervantes, Monterrey Institute of Technology and Higher Education (ITESM), Mexico
Quang Duc Nguyen, Szent István University, Hungary

***Correspondence:**
Wilhelm H. Holzapfel
wilhelm@woodapple.net

Specialty section:
This article was submitted to Synthetic Biology, a section of the journal Frontiers in Bioengineering and Biotechnology

Received: *09 July 2020*
Accepted: *25 August 2020*
Published: *11 September 2020*

Citation:
Todorov SD, Kang H-J, Ivanova IV and Holzapfel WH (2020) Bacteriocins From LAB and Other Alternative Approaches for the Control of Clostridium and Clostridiodes Related Gastrointestinal Colitis. Front. Bioeng. Biotechnol. 8:581778. doi: 10.3389/fbioe.2020.581778

The gut microbiome is considered as a promising target for future non-conventional therapeutic treatment of inflammatory and infectious diseases. The search for appropriate safe and beneficial (lactic acid bacterial and other) putative probiotic strains and/or their antimicrobial metabolites represents a challenging approach for combating several problematic and emerging infections. The process of selecting suitable strains, especially of lactic acid bacteria (LAB) with superior properties, has been accelerated and intensified during the past two decades, also thanks to recent developments in lab techniques. Currently, special focus is on the potential of antimicrobial metabolites produced by some LAB strains and their application as active therapeutic agents. The vision is to develop a scientific basis for 'biotherapeutics' as alternative to conventional approaches in both human and veterinary medicine. Consequently, innovative and promising applications of LAB to the therapeutic practice are presently emerging. An overview of the existing literature indicates that some antimicrobial metabolites such as bacteriocins, widely produced by different bacterial species including LAB, are promising biotherapeutic agents for controlling infections caused by potential pathogens, such as *Clostridium* and *Clostridiodes*. Non-conventional, safe and well designed therapeutic treatments may contribute to the improvement of gut dysbiotic conditions. Thereby gut homeostasis can be restored and inflammatory conditions such as gastrointestinal colitis ameliorated. Combining the knowledge on the production, characterization and application of bacteriocins from probiotic LAB, together with their antibacterial properties, appears to be a promising and novel approach in biotherapy. In this overview, different scenarios for the control of *Clostridium* spp. by application of bacteriocins as therapeutic agents, also in synergistic combination with antibiotics, will be discussed.

Keywords: *Clostridium*, *Clostridiodes*, bacteriocins, probiotics, biotherapeutics, lactic acid bacteria, gut microbiota, dysbiosis

INTRODUCTION

Since early human history the beneficial influence of fermented foods on the human gut has been appreciated; numerous ancient societies and cultures have consumed fermented foods such as yogurt as a therapy for treatment of diarrhea and other adverse gut conditions (Holzapfel, 2006). The development of microbiology as a discipline during the second half of the 19th century soon revealed the beneficial association of lactic acid bacteria (LAB) as a major microbial group associated with fermented foods. This era has also provided a scientific foundation for bacteriotherapy which has probably been pioneered by Döderlein (1892) when he reported on a vaginal Gram-positive "bacillus" with antagonistic activity against staphylococci, also suggesting lactic acid as underlying basis of this antagonism. Called "Döderlein's bacillus," later studies have focused on these (catalase-negative) 'lacto-bacilli,' their beneficial association with the human host and their role in balancing vaginal ecology (Lash and Kaplan, 1926; Cruickshank, 1931). A beneficial association of LAB with the human host and the intestinal tract was underlined by Metchnikoff (1908) when he proposed the high intake of fermented milk products to be related to longevity.

Developments in biological sciences have been fundamental, at least during the recent history of 200 years, for the development and accumulation of knowledge in clinical practices. Gut microbiota are considered as a promising target for future therapeutic treatment of inflammatory and infectious diseases (Mukherjee et al., 2018). Current biotherapy approaches involve the careful selection of appropriate strains and/or specific antimicrobial metabolites in order to meet exigencies when targeting specific (intestinal) pathogens such as some *Clostridium* and *Clostridiodes* spp. In the past two decades the search for LAB with probiotic properties and strains for application as active therapeutic agents has intensified. Special attention is currently directed at non-conventional "anti-infective" therapies, some of which involve specific vaccines (Czaplewski et al., 2016), antimicrobial metabolites such as antimicrobial peptides (Mahlapuu et al., 2016) and bacteriocins (Cotter et al., 2013; Hanchi et al., 2017; Chikindas et al., 2018), and also includes bacteriophage therapy and the application of predatory bacteria (Allen, 2017; Vieco-Saiz et al., 2019). Moreover, thanks to their adjuvant properties, LAB have been suggested for potential replacement of classical, attenuated microbial carriers that may frequently induce pathogenicity in the host (Szatraj et al., 2017). These examples represent feasible alternatives to current approaches, and show potential of application both in human and veterinary medicine.

With innovative applications of LAB in the therapeutic practice currently emerging, the focus on "natural" or "biological" approaches (as opposed to the use of antibiotics and chemical drugs) for combating infectious diseases have moved toward a major research area. In particular the search for functional LAB strains with potential application in human and veterinary medicine, also in combination with the production of beneficial (anti-pathogenic) bacteriocins and probiotic characteristics, is actively being pursued. The challenge of finding specific antimicrobial properties of produced antimicrobial metabolites beyond organic acids (Tejero-Sariñena et al., 2012) by LAB, concomitantly with desirable (probiotic) characteristics in a single strain remains an ultimate goal (Lerner et al., 2019). Nevertheless, several innovative therapeutic applications of LAB have emerged, and, as research reports are increasingly showing, LAB can be considered as promising and additional/alternative therapeutic agents for the control of some infectious diseases. With the rapid technological development in various branches of the life sciences and the accumulation of new knowledge in microbiology, physiology and medicine, important changes to long-established practices are now being introduced. Aside from the novel potentially-beneficial properties of candidate probiotic LAB strains, their safety assessment requires special attention (Sanders et al., 2010; Brodmann et al., 2017), with particular focus on the presence of known virulence factors, the production of biogenic amines and antibiotic resistance determinants. Numerous well-known and recently characterized virulence determinants are now mapped in members of the genera *Enterococcus* and *Streptococcus*. However, recently some of these virulence related determinants have also been detected in lactobacilli with previous Generally Recognized As Safe (GRAS) status; this could possibly signify potential hurdles for developers and manufacturers of probiotics and strains for use as bio-therapeutic agents. A risk of horizontal transfer of virulence factors has been identified when (probiotic) LAB and pathogenic strains colonize the same ecological niche. Uncontrolled or wrong therapeutic use of antibiotics and even bacteriocinogenic LAB strains may increase this risk, thereby underlining the importance of reliable safety assessment of LAB strains at the intraspecies level, before their application (Leuschner et al., 2010; Brodmann et al., 2017; Holzapfel et al., 2018). It is acknowledged that GRAS status cannot be applied to entire species or genera. Intraspecies diversity underpins the fact that strain differences can be related to the presence of potential virulence factors, previously not investigated in a particular bacterial species, or neither have been transformed via horizontal gene transfer as a result of inter-bacterial interaction. Safety aspects of beneficial cultures (probiotics and bacteriocinogenic bacteria) are a critical point in the approval and distribution of new probiotic cultures for human and animal applications. This process includes not only strict evaluation of the expression of virulence factors by physiological and biochemical approaches, but deep bio-molecular investigations for presence of genes related to virulence factors, also including antibiotic resistance. Antibiotic resistance in beneficial LAB may be a delicate point. Comprehensive risk assessment on the spread of resistant genes to human health has apparently not been conducted yet. Investigations on the behavior, adaptation and dynamics of probiotics under conditions representing the human gut, also accounting for the presence of antibiotics, therefore appear imperative (Zheng et al., 2017). In particular, probiotic cultures should be free of transferable genetic determinants related to antibiotic resistance in order to prevent their transfer to recipient strains. Special attention should be given to genes located on transmittable genetic elements, such as plasmids, transposons, and chaperons. Antibiotic resistance genes located on the

bacterial chromosome are generally considered as a lower level of safety concern. However, every case needs to be evaluated on a strain specific basis also by considering the antibiotic specificity. On the other side, well defined antibiotic resistance of a probiotic culture might be considered as beneficial against the scope of its application in combination with a specific antibiotic. Thereby its synergetic interaction may be exploited by combining, e.g., an antibiotic and probiotic LAB strain under well controlled conditions.

Apart from the safety evaluation of viable bacterial strains, cytotoxicity of bacteriocins and other metabolites requires specific attention. Almost one century since the discovery of nisin its long history of safe food-associated use can be attributed to an extremely low cytotoxicity index similar to that of NaCl (Jozala et al., 2007), its sensitivity to digestive proteases, and the absence of any negative influence on the sensory properties of food (Pongtharangkul and Demirci, 2004). On other hand, some bacteriocins, including nisin, pediocin PA-1 and plantaricin A, appear to have elevated cytotoxicity against some kinds of cancer cells in comparison to normal cells. Altogether, application approval of a newly characterized bacteriocin should be supported by information on its cytotoxicity according to recommended accepted clinical standards.

In this overview we are looking into the potential of biological approaches for non-conventional therapeutic treatment of inflammatory and infectious diseases. A particular focus will deal with the combating of *Clostridium* infections and the prospect of widening the applications of beneficial LAB and their metabolites for this purpose. Reference will also be made to the inhibition of heterogeneous target organisms, including pathogens associated with colitis. Information basic to potential biological approaches is summarized, at least in part, in **Figure 1**.

With this paper we attempt to find answers on questions related to, e.g.:

- Realistic and practical applications of LAB and their metabolites as tools of therapeutic adjuncts, but also including major limitations;
- A clear borderline between reality and fiction in these approaches;
- Whether some of the more significant issues have been overlooked in recent reports on previously-unexplored applications of bacteriocins;
- Possible applications of bacteriocin producers as potential probiotic cultures with the concomitant effective control of pathogens related to colitis;
- The purification level of antimicrobial metabolites such as antimicrobial peptides and considerations whether combinations with conventional antibiotics might be one way of optimization toward application.

BACTERIOCINS

The beneficial practical application of antimicrobial peptides is not a novel concept. It may even be claimed that, for the centuries, bacteriocins and other antimicrobial metabolites have unknowingly been involved as natural preservatives when produced by LAB in traditional food fermentation processes. Nisin is the most well known, deepest researched, and commercially most widely used bacteriocin in food preservation, presently approved in at least 50 countries (Delves-Broughton et al., 1996). Its discovery in the 1930s was followed 30 years later by its first commercial introduction for food preservation in the United Kingdom. Since then the prospect of applying bacteriocins in food biopreservation has found general acceptance in food safety approaches (Abee et al., 1995; Silva et al., 2018).

Potential therapeutic application of bacteriocins and other antimicrobials produced by LAB in human and veterinary medicine represents a relatively new area of research investigations. It should be acknowledged that traditional medicine has recommended the application of some products resulting from (LAB associated) food fermentation processes as alternatives in the treatment of some diseases. Such practices are well known for the Maasai tribe of East Africa where the consumption of the traditional fermented milk product '*kule naoto*' is considered to have therapeutic value for curing of and/or protection against ailments such as diarrhea and constipation (Mathara et al., 2004). These beneficial effects are possibly related to antimicrobial metabolites, including bacteriocins, as components of such (traditional) fermented commodities. Since the first years of discovery of LAB bacteriocins, numerous have been the subject of intensive investigation (Favaro and Todorov, 2017; Chikindas et al., 2018). According to the current definition, bacteriocins are proteinaceous antimicrobials, produced by bacteria that primarily inhibit the growth of relatively closely-related bacteria; their mode of action is typically bactericidal. It is generally accepted that bacteriocins act by disrupting the cell membrane integrity while different receptors can be involved in this process (Cotter et al., 2013). However, additional mechanisms have also been proposed and may include cleavage of the bacterial DNA, interaction with some intracellular enzymes and/or interrupting bacterial protein synthesis as result of interaction between bacteriocins and ribosome (James et al., 1991; Heu et al., 2001; Todorov et al., 2019). The ability to produce bacteriocins (bacteriocinogenicity) is a common characteristic of many bacteria associated with complex natural ecosystems and may decisively influence the stability of their microbial population. Key focus areas of bacteriocin research have formerly been identified (Schillinger and Holzapfel, 1996), while bacteriocin classification of Gram-positive bacteria has continually developed over a period of more than 20 years (Klaenhammer, 1988; De Vuyst and Vandamme, 1994; Heng et al., 2007). Moreover, it appears that most bacteriocins of Gram-positive bacteria are small peptides, initially expressed as pro-peptides. Only a small number of bacteriocins are posttranslationally modified, as in the case of the lantibiotics (class I in the classification of Klaenhammer, 1988; Heng et al., 2007), while only a few others are relatively complex molecules that also incorporate non-protein moieties responsible for their antibacterial activity (class IV of the classification of Klaenhammer, 1988). Apart from bacteriocins, LAB may produce a variety of antimicrobial compounds, including organic

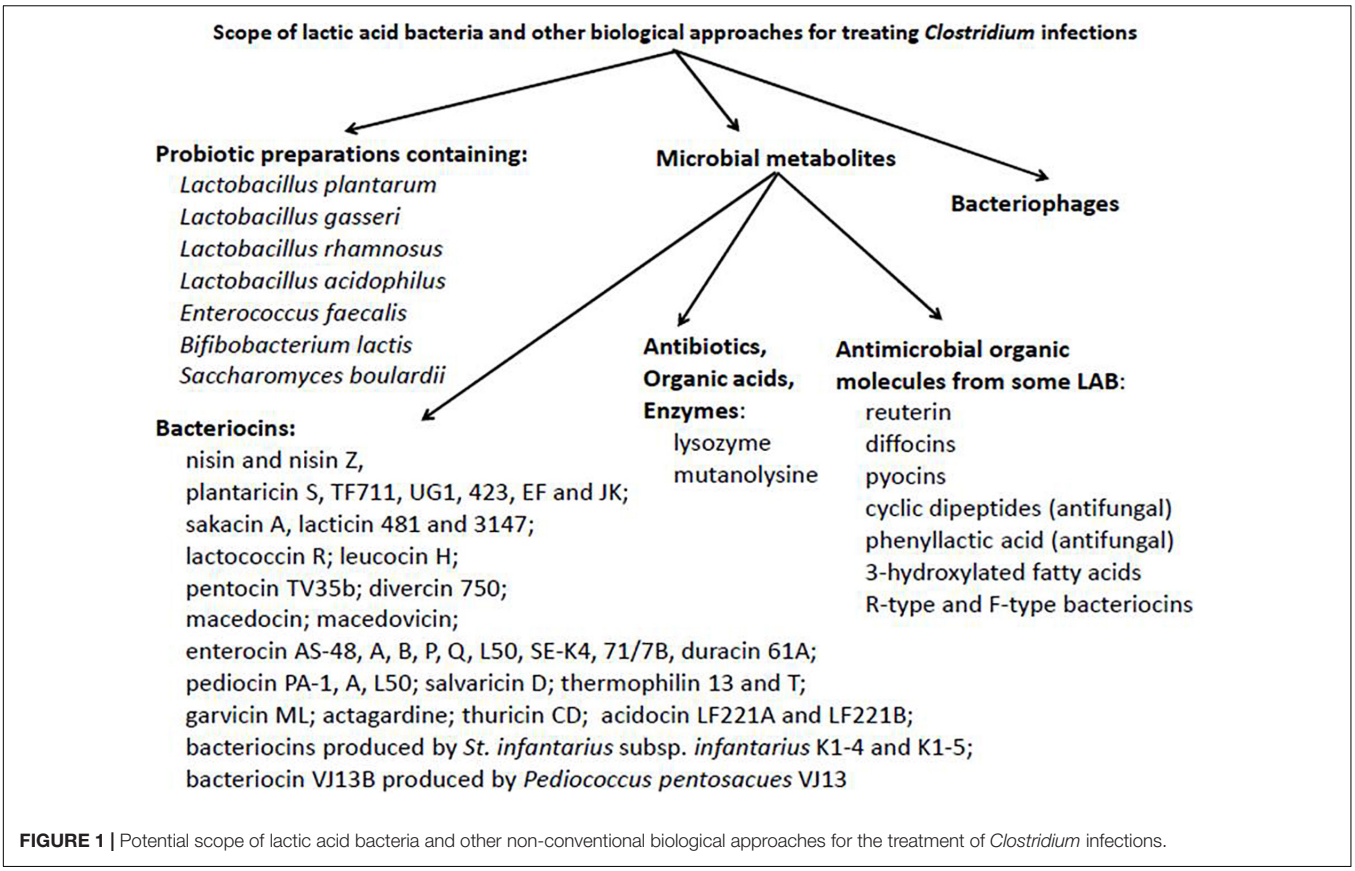

FIGURE 1 | Potential scope of lactic acid bacteria and other non-conventional biological approaches for the treatment of *Clostridium* infections.

acids, diacetyl, carbon dioxide, hydrogen peroxide, and organic antimicrobial compounds with low molecular mass (Favaro and Todorov, 2017). Particular low-molecular metabolites such as D-phenyllactic and 4-hydroxy-phenyllactic acids, 3-hydroxylated fatty acids and cyclic dipeptides show strong antifungal activity and are therefore of special interest for application in food biopreservation (Valerio et al., 2004; Svanström et al., 2013; Chen et al., 2016; Leyva Salas et al., 2018).

Commercial application of the best studied bacteriocin, nisin, is regulated by the European Food Safety Authority (EFSA) and is licensed as a food preservative (E234). Nisin was recognized as safe for application as a bio-preservative in food products by the Joint Food and Agriculture Organization/World Health Organization (FAO/WHO) Expert Committee on Food Additives in 1969 (Favaro et al., 2015). Subsequently, the FDA approved its use as an "anti-botulism" additive to canned food products in the United States to inhibit *Clostridium botulinum* (Jones et al., 2005). The FAO/WHO Codex Committee on milk and milk products has authorized nisin to be applied as a food additive for different processed cheeses, with an upper limit of 12.5 mg (applied as pure nisin) per kilogram of product (Reis et al., 2012). The exceptionally low cytotoxicity of nisin is comparable to that of NaCl, and it has been safely used in food and food products over a long time period (Jozala et al., 2007). Based on its proteinaceous nature, this may also be attributed to its proteolytic degradation while, at the same time, the sensory attributes of the food remain unchanged (Pongtharangkul and Demirci, 2004).

According to Wiedemann et al. (2001) the underlying mechanism basic to the antibacterial effect of nisin is related to lipid II (the main transporter of peptidoglycan subunits from the cytoplasm to the cell wall) that acts as a docking station (receptor) for nisin. In this way nisin induces the formation of short-lived pores in the cell membrane. The regulation of transport control is thereby disrupted thus leading to the loss of cytoplasmic components (Wiedemann et al., 2001). A similar mode of action has been described for mersacidin and also for the antibiotic vancomycin, both of which bind to a different part of the lipid II molecule (Cotter et al., 2005).

Clostridium AND *Clostridiodes* spp.

The enterotoxigenic *Clostridium* and *Clostridiodes* (*Cd.*) spp. can be directly related to food poisoning and non-food−borne human gastrointestinal diseases. Important is their ability to form highly resistant endospores, and, as anaerobes, they are of great concern to both the food canning industry and also to meat producing plants attempting to provide meat products free of *C. perfringens* contamination. *Clostridium* spp. can be transferred to humans and may cause gastrointestinal complications.

The genus *Clostridium* belongs to the family *Clostridiaceae* and, with presently an estimated of more than 203 metabolically diverse species, only a few species are recognized as being pathogenic to humans (NHS, 2016). Representatives are

Gram-positive, endospore-forming anaerobic bacteria that are ubiquitously found in virtually all anoxic habitats where organic compounds are present, including soils, aquatic sediments, and the intestinal tracts of animals and humans (Udaondo et al., 2017; Cebrian et al., 2019). By far the majority of the *Clostridium* spp. are considered to be commensal, but a few such as *C. perfringens, C. botulinum, C. tetani*, and *Clostridiodes (Cd.) difficile* are known to be opportunistic, toxin-producing pathogens in both animals and humans and may be associated with a high mortality rate (Cassir et al., 2016; Cebrian et al., 2019; Czepiel et al., 2019). One particular species of the pathogenic 'clostridia,' *Cd. difficile*, is receiving increased attention from the clinical community, due to its high resistance to antibiotics and the growing number of especially nosocomial infections with *Cd. difficile* as one of the most common causes (Cebrian et al., 2019; Czepiel et al., 2019). A recent proposal to restrict the genus *Clostridium* to the *C. butyricum* clade and related species resulted in ramifications for "unrelated" *Clostridium* spp. not forming part of this clade (Lawson and Rainey, 2015). With a similarity value of 94.7% between *C. difficile* and *C. mangenotii,* both species were shown to be phylogenetically only distantly related to other members of the genus *Clostridium sensu stricto*. Also by their location within the family *Peptostreptococcaceae* and by their comparatively converging physiological characteristics such as abundant production of H_2 gas in PYG broth, the reclassification of *C. difficile* and *C. mangenotii* into a new genus, *Clostridiodes*, was proposed by Lawson et al. (2016). For practical purposes the general term "clostridia" in this paper implicitly includes *Clostridiodes difficile*. Confusion still exists related to the simultaneous use of the genus names *Clostridium* and *Clostridioides*. The name *Clostridioides difficile* has been validated in "Validation List No. 171" (Oren and Garrity, 2016), and is acknowledged to meet requirements of the Rules of the International Code of Nomenclature of Prokaryotes (Oren and Rupnik, 2018). According to Oren and Rupnik (2018), the new genus name has not been overruled the use of the name *Clostridium* (yet), which, at present, can still be used equally to *Clostridioides*. We recognize the use of two different genus names (*Clostridium* and *Clostridioides*) in line with the nomenclatural recommendations of the International Committee on Systematics of Prokaryotes of the International Union of Microbiological Societies (IUMS), and accordingly use two different abbreviations (*C.* and *Cd.*) for these two genera.

Clostridiodes difficile infections (CDI) are considered as a significant health risk, particularly to an aging population. An estimated 250,000 hospitalizations and 14,000 deaths per year are caused by CDI in the United States alone (Kers et al., 2018), with an estimated annual cost of care amounting to $4.8 billion (Dieterle and Young, 2017). Moreover, recent studies indicate that 30 to 35% of North American CDI cases were due to BI/NAP1/027-type strains (Vaishnavi, 2015; Wilcox, 2016). Relapse following successful antibiotic treatment of CDI, especially when associated with RT027 strains, is not uncommon (Rogers and Whittier, 1928; Surawicz et al., 2013). A major pillar in present-day clinical practices are approaches toward the prevention of infectious diseases. However, current preventative options are limited to antibiotic stewardship and good hygienic practices (Chatterjee et al., 2005; Field et al., 2015). In order to reduce the application of antibiotics, new preventative approaches are urgently needed. An additional and early recognized problem accompanying the use of antibiotics is the elimination or reduction of beneficial microbiota, thereby resulting in dysbiosis and the disruption of gut homeostasis. The unintended loss of diversity and abundance in a stable gut microbiota has a dramatic detrimental impact on colonization resistance of the host to opportunistic pathogens, including *Cd. difficile*, in addition to other negative modulatory influences on gut metabolism (Smith and Hillman, 2008; Ross and Vederas, 2011; Piper et al., 2012; Goetz et al., 2014; Ongey et al., 2017). Discontinuing gut destabilizing antibiotics is considered a first and foremost step in the management of *Cd. difficile* infections (Wilcox and Dave, 2001).

BACTERIOCINS AND CONTROL OF *Clostridium* AND *Clostridiodes* spp.

The potential of Class II bacteriocins to modify gut microbiota and to improve host health have been recently reviewed by Umu et al. (2016). In their report the authors have discussed the crossroads between production of bacteriocins and the probiotic potential of LAB for preventing the growth of pathogens in the gut environment.

Antagonistic activity against *Clostridium* and *Clostridiodes* spp. has been reported for diverse bacteriocins representing different Classes, including nisin (Class I), pediocins (Class IIa), plantaricins (Class IIb), different (partly unnamed) enterocins (some belonging to Class IIc), and durancin (Class IV) (**Table 1**). A bacteriocin is not necessarily active against all tested strains of a species and under all given ecological conditions. A major drawback is the limited knowledge on bacteriocin production and activity in gastro-intestinal tract (GIT) environments *in situ* (e.g., simulation models) or *in vivo* in healthy animals (Umu et al., 2016). The potential of five bacteriocin-producing strains of LAB (producers of sakacin A; pediocin PA-1; enterocins P, Q and L50; plantaricins EF and JK; and garvicin ML), and their isogenic non-producing (bac^-) mutants were evaluated by Umu et al. (2016) for their probiotic effects by administering the strains to mice through drinking water; changes in the gut microbiota composition were evaluated via appropriate 16S rRNA gene sequencing analysis. Umu et al. (2016) concluded that the overall structure of the gut microbiota remained largely unaffected by the treatments, this also supporting the putative safety of the applied strains. More important observations were only pointing to some lower taxonomic levels. Some potentially problematic bacteria, including *Clostridium* spp., were inhibited when a producer of plantaricins was applied. This can be considered as positive indication that bacteriocin producing strains can be applied for the control of *Clostridium* spp. It appears indeed that they promote favorable changes in the host without major disturbance in the gut microbiota, important for the maintenance of the normal functional properties and gut homeostasis (Umu et al., 2016).

TABLE 1 | Bacteriocins and their producer strains showing activity against *Clostridium* (*C.*) and *Clostridiodes* (*Cd.*) species with special focus on those associated with infections.

Bacteriocins	Target species*	Experimental set-up	Bacteriocin characteristics	Bacteriocin classification	References
Bacteriocins produced by 6 strains of *E. faecalis*	*C. perfringens*	Vegetative cells	pH stability: 2.0–10.0 thermostability: 60 and 90°C for 30 min; 121°C for 15 min	NR**	Han et al., 2014
Bacteriocin produced by *Lb. plantarum*	*C. butyricum*, *C. difficile*, *C. perfringens*	Vegetative cells	NR	NR	Monteiro et al., 2019
Bacteriocins produced by 2 strains of *St. infantarius* subsp. *infantarius*	*C. perfringens*	Vegetative cells	pH stability: 2.0–12.0 thermostability: 100°C for 120 min; 121°C for 20 min	Class IIa (suggested)	dos Santos et al., 2020
Durancin 61A, produced by *E. durans;* pediocin PA-1 and nisin Z	*Cd. difficile*	Vegetative cells	Durancin 61A: NR pediocin PA-1: NR nisin Z: NR	Durancin 61A: Class IV (glycosylated polypeptide); pediocin PA-1: Class IIa; nisin Z: Class I	Hanchi et al., 2016, 2017
Enterocin AS-48, produced by *E. faecalis*	*Clostridium* spp. (broad spectrum)	Against vegetative cells and spores in food production	Thermostability: heat stable	Class IIc	Egan et al., 2016
Lacticin 481, produced by *L. lactis* subsp. *lactis*	*C. tyrobutyricum*	Cheese production	Thermostability: heat stable	Class I	O'Sullivan et al., 2003
Nisin, produced by *L. lactis*	*C. perfringens*	Endospore germination, vegetative cells	pH stability: 2.0–6.0; thermostability: heat stable	Class I	Udompijitkul et al., 2012
Nisin, produced by *L. lactis*	*Cd. difficile*	Vegetative cells and spores	pH stability: 5.0–9.0; thermostability: heat stable	Class I	Bartoloni et al., 2004; Egan et al., 2016
Nisin, produced by *L. lactis*	*C. tyrobutyricum*, *C. butyricum*, *C. beijerinckii*, *C. sporogenes*	Vegetative cells and spores	pH stability: 5.0–9.0; thermostability: heat stable	Class I	Avila et al., 2014
Nisin, produced by *L. lactis*	*Clostridium* spp.	Cheese production	pH stability: 5.0–9.0; thermostability: heat stable	Class I	Abee et al., 1995; Galvez et al., 2008; Silva et al., 2018
Nisin, lacticin 3147 and thuricin CD, produced by *L. lactis*, *L. lactis* subsp. *lactis* and *B. thuringiensis*	*Cd. difficile*	Vegetative cells	nisin: pH stability: 5.0–9.0; thermostability: heat stable lacticin 3147: pH stability: 5.0–9.0; thermostability: heat stable; thuricin CD: thermostability: heat stable	Nisin: Class I lacticin 3147: Class I	Rea et al., 2007
Plantaricins EF and JK, produced by *Lactobacillus plantarum*	*Clostridium* spp.	Vegetative cells, *in vivo* analysis, animal model	Thermostability: heat stable	Class IIb	Umu et al., 2016
R-type bacteriocin particles; diffocins from *Cd. difficile*	*Cd. difficile*	Vegetative cells	NR	NR	Gebhart et al., 2015; Schwemmlein et al., 2018

**Not all tested strains of a species are intrinsically sensitive to a bacteriocin; **NR, not reported in the cited reference paper.*

Udompijitkul et al. (2012) have evaluated the antimicrobial effect of nisin against two strains of *C. perfringens* (FP and NFB). They have not observed any inhibitory effect against endospore germination of both the food poisoning and non-food−borne strains in a laboratory medium. However, more important was that nisin effectively arrested the outgrowth of germinated spores of *C. perfringens* in a rich medium. Interestingly, Udompijitkul et al. (2012) pointed out that germinated spores of non-food−borne isolates possessed higher resistance to nisin than those of food poisoning strains, pointing to a possible application of nisin in the selective control of *C. perfringens*. Furthermore, nisin exhibited an inhibitory effect against vegetative growth of both FP and NFB isolates in a laboratory medium, with vegetative cells of NFB isolates showing a higher resistance than the FP

isolates. Udompijitkul et al. (2012) also reported an inhibitory effect of nisin against both endospore outgrowth and vegetative cells of *C. perfringens* FP and NFB isolates under laboratory conditions, and emphasized the potential of nisin for the control of *C. perfringens*.

Bartoloni et al. (2004) evaluated the effect of nisin activity against clinical isolates of *Cd. difficile* in comparison to the effect of vancomycin and metronidazole based on minimal inhibitory concentrations (MIC), minimum bactericidal concentrations (MBC) and time-kill studies. In this study nisin was found to be more active than the other agents, with a MIC_{90} of 0.256 mg/L and a strong bactericidal activity. Therefore nisin was suggested as a promising agent for the management of *Cd. difficile* associated diarrhea.

The inhibitory influence of several antimicrobial compounds (reuterin, nisin, lysozyme, and sodium nitrite) on both vegetative cells and endospores of *C. tyrobutyricum*, *C. butyricum*, *C. beijerinckii*, and *C. sporogenes* was investigated by Avila et al. (2014) using the experimental protocols of Bartoloni et al. (2004). the effect was compared in two different media, milk and modified RCM (mRCM), after a period of 7 days. Based on the minimal inhibitory concentration (MIC), most *Clostridium* strains showed higher resistance in milk than in mRCM while their endospores were more resistant than the vegetative cells. Vegetative cells and also spores of the investigated clostridia were inhibited in each medium by both reuterin, at MIC values ranging from 0.51–32.5 mM, and nisin at MIC values between 0.05–12.5 μg/mL. Reuterin and nisin, with a broad inhibitory activity spectrum against *Clostridium* spp. spores and vegetative cells, were therefore suggested as the best options to control *Clostridium* growth (Avila et al., 2014).

Several other bacteriocins and antimicrobial proteins from LAB show promise for application in the control of *Clostridium* spp. However, compliance with the safety requirements of the final product should be warranted. Based on the absence of cytotoxicity nisin is considered as safe (Jozala et al., 2007). Moreover, a low cytotoxicity was also reported for several other bacteriocins (Wachsman et al., 2003; Martinez et al., 2013; Carneiro et al., 2014; Quintana et al., 2014; Todorov et al., 2014; Cavicchioli et al., 2018). However, some report have referred to observations on potential cytotoxicity of some bacteriocins, and posed questions on their potential as health hazards (Carneiro et al., 2014; Kaur and Kaur, 2015). However, cytotoxicity of bacteriocins against specific cell lines can be of potential advantage. As Kaur and Kaur (2015) have pointed out, high (selective) bacteriocin cytotoxicity against cancer cells but without similar action against healthy cells, can be explored as an advantage in the control and treatment of some types of cancers.

The safety of bacteriocin producers may constitute an additional concern. Generally the LAB are recognized as safe, and most species have GRAS status. As a large group of Gram-positive, non-sporeforming, catalase-negative, fermentative and generally aerotolerant bacteria, the LAB include diverse organisms, adapted to specific and partly extreme environments, and with some (most *Streptococcus* spp.) considered as typical pathogenic. On the other hand, clinical cases of *Lactobacillus* associated bacteremia and sepsis have been reported, yet, only in rare cases and in particular for patients with underlying conditions (Castro-González et al., 2019). Therefore, any declaration on safety requires critical assessment and careful specification, also taking into account both general phenotypic heterogeneity and subspecies diversity. Some *Enterococcus* species are considered as opportunists and are frequently associated with nosocomial infections (Holzapfel et al., 2018); strains from clinical origin are known to carry virulence factors (Favaro et al., 2014; Perin et al., 2014; Ribeiro et al., 2014). With almost all species of the genus *Streptococcus* considered as pathogenic, *Streptococcus thermophilus* represents a rare exception with GRAS status, and with relatively strict specialization in the dairy environment (Leuschner et al., 2010; dos Santos et al., 2020). Some recent papers have reported on the safety of *Streptococcus diacetylactis* subps. *macedonicus* and suggested its safe application as starter and probiotic culture (De Vuyst and Tsakalidou, 2008; Pieterse et al., 2010; Laiño et al., 2019).

Streptococcus infantarius subsp. *infantarius* is reported to be the predominant species in several dairy products in West Africa and Brazil (Schlegel et al., 2000; Hoshino et al., 2005; Abdelgadir et al., 2008; Herrera et al., 2009; dos Santos et al., 2020). Interestingly, bacteriocin production have been reported for two strains of *St. infantarius* subsp. *infantarius*, isolated from the dairy environment, showing a strong activity not only against *Listeria monocytogenes*, but against *C. perfringens* (dos Santos et al., 2020). Such activity suggests the potential of the producer strains (*St. infantarius* subsp. *infantarius* K1-4 and K5-1) as candidates for application as starter cultures, and even as putative probiotics. dos Santos et al. (2020) explored different characteristics and thee physiological behavior of *St. infantarius* subsp. *infantarius* strains K1-4 and K5-1 and, while suggesting their potential as beneficial strains, also mentioned the detection of several virulence factors. Declaring these strains as safe for human and animal applications therefore appears premature. This report (dos Santos et al., 2020) serves as a good example for the importance of safety evaluation of each particular strain before recommending it for use as beneficial culture. On the other hand, biotechnological production of a bacteriocin of even an unsafe strain may be feasible in view of the appropriate application of the purified bacteriocin as antimicrobial agent.

Han et al. (2014) reported on bacteriocin-producing *Enterococcus faecalis* strains with activity against *C. perfringens*, isolated from domestic animals an with a potential for application as probiotics. From a total of 1370 evaluated bacterial isolates, 6 were selected on basis of their activity against the pathogenic indicator strains *C. perfringens* KCTC 3269 and *C. perfringens* KCTC 5100. All selected 6 isolates were identified as *E. faecalis* by 16S rRNA sequencing. Apart from their anti-*Clostridium* activity, selected strains showed potential as probiotics based on their behavior under *in vitro* gut model conditions. Some of the evaluated *E. faecalis* strains also showed strong inhibitory activity against different strains of *Listeria monocytogenes*. The produced bacteriocins were partially characterized, and Han et al. (2014) suggested the use of these bacteriocin producing strains and/or their bacteriocins in feed manufacturing in the livestock industry as alternatives to antibiotics.

The *in vitro* antimicrobial activity and potential probiotic application of *Bifidobacterium* and *Lactobacillus* against *Clostridium* species were investigated by Monteiro et al. (2019). Based on its inhibitory activity the authors suggested the application of *Lb. plantarum* ATCC 8014 as promising candidate against *Clostridium* spp. In addition, this strain may be considered as probiotic based on its functional properties. Referring to its potential for controlling infections by *Clostridium* species, Monteiro et al. (2019) suggested safety evaluation of *Lb. plantarum* ATCC 8014 in *in vivo* animal models in order to clarify open questions before its application as beneficial organism.

Accumulating knowledge on the importance of human gut microbiota diversity suggests that reduction in microbial diversity may result in vulnerability to many diseases (Vujkovic-Cvijin et al., 2013; Gevers et al., 2014; Xuan et al., 2014; Gebhart et al., 2015). A definitive link between human gut microbial diversity, gut homeostasis and health appears to be firmly established. Even when acknowledging the extraordinary importance of conventional antibiotics, the other side is pointing to negative consequences resulting from the inadverse antibiotic application for (sometimes extended) treatment of bacterial diseases, also resulting in off-target effects (Gebhart et al., 2015). There is a clear need for more selective and highly effective, so-called "smart," antibacterial agents by which rapid and accurate molecular diagnostic information can be exploited at the point of intervention toward precisely targeted protection against a pathogen. Such new generation antimicrobials pose a low risk of drug resistance transfer to off-target organisms or disrupting gut homeostasis by the elimination of protective/beneficial microbiota. Precision antibacterials can be deployed both as safe prophylactics and therapeutics. Safe antibacterials such as bacteriocins, combinations of bacteriocins and selected drugs, and bioengineered antimicrobial or chemically modified peptides may be considered as the next frontier in the combat of humans and animals against pathogens (Gebhart et al., 2015).

Antibiotic resistance is widely known and well described for, e.g., methicillin-resistant *Staphylococcus aureus* (MRSA) and *Cd. difficile*. There is wide consensus on an urgent need for alternatives to antibiotics and for finding novel antimicrobial compounds to combat these pathogens (Allen, 2017). In the last decade a strong increase in outbreaks of *Cd. difficile*-associated disease (CDAD) were registered. These presented significant challenges to health care facilities worldwide (Dieterle and Young, 2017). *Cd. difficile* was recognized as a causative agent of nosocomial diarrhea since the early 1970s (George et al., 1978; Rea et al., 2010). Moreover, it is generally acknowledged that CDAD is increasing, not only quantitatively, but also in severity in many parts of the world (Redelings et al., 2007). The scientific community accepts the fact that the main predisposing factor for CDAD is antibiotic therapy, which often eradicates the commensal and beneficial gut microbiota of the host and enables the opportunistic establishment of a *Cd. difficile* infection. Several antibiotics, hitherto considered as effective therapeutic agents, have been implicated in CDAD, and include clindamycin, ampicillin, and amoxicillin as well as the cephalosporins and fluoroquinolones (Aronsson et al., 1985; Wiström et al., 2001; Bartlett, 2006). However, their negative effects on the commensal gut microbiota are recognized, while the increase in antibiotic resistance constitutes an additional problem. Moreover, the increasing prevalence of hypervirulent strains of *Cd. difficile* (Bartlett, 2006; Kuijper et al., 2007) adds urgency to the search for alternative treatment of CDAD. Thus far, small-molecule antibiotics have generally proven unsuccessful in mitigating the development of resistance in bacterial pathogens, indicating a need to examine alternative classes of antimicrobial compounds. Linked to this, there has been considerable interest in bacteriocins as antimicrobial bacterial peptides with either narrow- or broad-spectrum antimicrobial activities. It has already been established that bacteriocins such as nisin and lacticin 3147 can effectively kill *Cd. difficile* at concentrations that compare favorably with therapeutic levels of vancomycin and metronidazole, the most commonly used antibiotics in the treatment of CDAD (Rea et al., 2007). Moreover, thuricin CD, a two-component antimicrobial showed activity against *Cd. difficile* in the nanomolar range. This antimicrobial peptide (thuricin CD) is produced by *Bacillus thuringiensis* DPC 6431, a strain originally isolated from a human fecal sample, and consisting of two distinct peptides, Trn-α and Trn-β, that act synergistically to kill a wide range of clinical *Cd. difficile* isolates, including ribotypes commonly associated with CDAD (Rea et al., 2010). Very important is the fact that thuricin CD has little impact on most other genera, including many gut commensal microorganisms. The amino acid sequences of thuricin SD molecules were determined using infusion tandem mass spectrometry and revealing that each peptide is posttranslationally modified at its respective 21st, 25th, and 28th residues. The thuricin CD gene cluster contains genes responsible for encoding two S′-adenosylmethionine proteins that are typically involved in uncommon posttranslational modifications. The two components of the thuricin CD antimicrobial peptide system are connected by sulfur to α-carbon linkages. It shows prospects for therapeutic implementation targeted against CDAD, with the additional benefit of not disturbing normal gut microbial homeostasis (Rea et al., 2010).

Some strains of *Cd. difficile* produce phage tail-like particles upon induction of the SOS response. These particles have bactericidal activity against several *Cd. difficile* strains and can therefore be classified as bacteriocins, similar to the R-type pyocins of *Pseudomonas aeruginosa*. Each of these R-type bacteriocin particles, purified from different strains, shows a different *C. difficile*-killing spectrum, with no single bacteriocin killing all *C. difficile* isolates tested. The genetic locus has been identified for these "diffocins" and was found to be common within the species (Schwemmlein et al., 2018). Moreover, the entire diffocin genetic locus of more than 20 kb was cloned and expressed in *Bacillus subtilis*, resulting in the production of bactericidal particles. One of the interesting features of these particles is a very large structural protein of 200 kDa. It determines the lethal spectrum of the particles and is likely the receptor-binding protein. Diffocins may provide an alternative bactericidal agent to prevent or treat infections and to decolonize individuals that are asymptomatic carriers (Schwemmlein et al., 2018).

Some specific bacteriocin-like metabolites such as high-molecular-weight or phage tail-like bacteriocins appear to be common throughout the Eubacteria domain (Gebhart et al., 2012). From this family of antimicrobials, the best-studied examples are possibly the R-type pyocins produced by some strains of *P. aeruginosa* (Michel-Briand and Baysse, 2002); these have in fact been well reported earlier for other Gram-negative (Coetzee et al., 1968; Strauch et al., 2001) and also Gram-positive bacteria (Kautter et al., 1966; Ellison and Kautter, 1970; Thompson and Pattee, 1981; Zink et al., 1995; Gebhart et al., 2012). These phage tail-like bacteriocins are produced as intracellular metabolites in response to SOS induction and are liberated only after cell lysis. Gebhart et al. (2012) subdivided phage tail-like bacteriocins in R and F-types, of which the R-type resembles the structures of the tail apparatus of the Myoviridae phages (contractile, non-flexible tails), while the F-type is described for *P. aeruginosa* with genetic resemblance to the Siphoviridae phages (non-contractile, flexible tails) (Nakayama et al., 2000). In their mode of action, R-type bacteriocins kill target cells by attachment through interaction between a receptor binding protein (tail fiber protein) and a bacterial surface receptor. This leads to insertion of the core through the envelope of the target bacterium and rapid depolarization of the cell membrane potential and immediate cell death (Uratani and Hoshino, 1984). The activity spectrum of R-type bacteriocins generally includes very closely related species, normally other strains from the same species, although rare coincidental killing of other species by R-type pyocins has been noted; moreover, autoimmune phenomena have been reported (Gebhart et al., 2012). R-type phage tail-like bacteriocins ("diffocins") can be mapped in the genomes of different strains of *Cd. difficile*. Some strains of this species can produce diffocin particles as a result of SOS response induction; these strains may show bactericidal effects against other *Cd. difficile* strains (Gebhart et al., 2012).

Biotechnical application of "diffocin" was proposed by Gebhart et al. (2015) in designing a specific genetically modified contractile R-type bacteriocin from *Cd. difficile* strain CD4 with the purpose to kill BI/NAP1/027-type strains. Gebhart et al. (2015) proposed that the natural receptor binding protein (RBP) responsible for diffocin targeting can be replaced by a RBP identified protein from the prophage of a BI/NAP1/027-type target strain. The resulting modified diffocins, called avidocin-CD type Av-CD291.1 and Av-CD291.2, respectively, were reported to be more stable and to kill the 16 BI/NAP1/027-type strains (applied as target strains) investigated. In addition, Gebhart et al. (2015) evaluated the efficacy of Av-CD291.2 in an animal model, providing the constructed diffocin via the drinking water. Sufficient survival levels during the passage through the mouse GIT were reported, yet, not notably modulating the mouse gut microbiota or even disrupting natural colonization resistance to *Cd. difficile* or a vancomycin-resistant *E. faecium* (VREF) strain. Moreover, antibiotic-induced colonization of the mice inoculated with BI/NAP1/027-type *Cd. difficile* spores was prevented (Gebhart et al., 2015), thereby reducing presence of the most severe CDIs. In conclusion, this modified diffocin can be considered as a prototype of an "Avidocin-CD platform," for producing targetable agents with high precision and efficacy against *Cd. difficile*. This represents a basis for the prevention and combating of CDIs without a negative impact on commensal (protective) indigenous microbiota (Gebhart et al., 2015).

BACTERIOCINS, CHEESE PRESERVATION AND CONTROL/PREVENTION OF *Clostridium*

Control of clostridia is a challenging issue, not only in human and veterinary medicine, but also a serious problem in the dairy industry. Bacterial contamination of dairy products with *L. monocytogenes*, some *Staphylococcus* spp., and/or sporeformers such as *Bacillus* and *Clostridium* spp. is considered as a potential health hazard. Nisin has been confirmed as effective antimicrobial agent for the control of numerous Gram-positive bacteria, including spoilage LAB and pathogens (such as *L. monocytogenes*, *S. aureus*, some *Bacillus* spp., and *Clostridium* spp.) (Silva et al., 2018). Nisin application to prevent late blowing in cheese caused by gas-producing *Clostridium* spp. was widely explored and applied by the dairy industry (Galvez et al., 2008). Nisin also finds application in cheeses and pasteurized cheese spreads as alternative to nitrate for preventing the outgrowth of *Clostridium* spores (Abee et al., 1995; Silva et al., 2018).

Another lantibiotic, lacticin 481, was also suggested as an alternative for the control of *Clostridium tyrobutyricum* (O'Sullivan et al., 2003) and *L. monocytogenes* (Ribeiro et al., 2016). The advantage of lactacin 481 is its specific spectrum of activity, also by generally being not active against other LAB, thus rendering it a good candidate for use in fermented food products (Silva et al., 2018). Moreover, a mild bacteriostatic activity has been shown for non-purified lacticin 481 in milk stored at refrigeration temperatures (Arqués et al., 2011). Also, semi-purified lacticin 481 can be applied with high success to fresh cheeses stored at refrigeration temperatures in reducing *L. monocytogenes* viable numbers by 3 log cycles within 3–7 days (Ribeiro et al., 2016).

Enterocin AS-48, a cyclic bacteriocin, produced by *E. faecalis* is active against a number of *Bacillus* and *Clostridium* strains (Egan et al., 2016). The activity of several enterocins against foodborne pathogens, including *Listeria* spp. and *Clostridium* spp., has been well established Yet, their application in food systems needs more precise evaluation. This especially includes their optimization, e.g., by addition of possible synergistic components for improved prevention of the re-growth of pathogens throughout storage (Khan et al., 2010; Zacharof and Lovitt, 2012; Barbosa et al., 2015a,b). A possible hypothesis maybe related to insufficient activity of these bacteriocins against *Clostridium* endospores.

Apart from nisin producing strains, other bacteriocin-producing LAB have also been proposed as alternatives for the prevention of *Clostridium* associated late blowing of cheeses, commonly related to the ubiquitous presence of *Clostridium* spores in the dairy environment (Gómez-Torres et al., 2015). It could be that one single alternative for reducing germination of *Clostridium* spores might not be effective to prevent late blowing in cheeses (Garde et al., 2011). Approaches involving combined factors therefore deserve further investigation, and may include

bacteriocins and/or bacteriocinogenic LAB as alternative starters or adjustment cultures for cheese-making.

BACTERIOCIN SYNERGISM STUDIES AND DELIVERY SYSTEMS

There appears to be promising scope for the application of different non-antibiotic antimicrobial agents such as bacteriocins for controlling pathogenic microbes in therapeutic practices. This approach needs to be viewed as part of a potentially complex treatment procedure that may also incorporate synergies with conventional antimicrobial agents. Some studies have already pointed to benefits of synergistic interactions between bacteriocins and antibiotics with the clear objective of reducing the usage of antibiotics and other conventional drugs, and also of increasing their efficacy (Minahk et al., 2004; Todorov and Dicks, 2009; Salvucci et al., 2010; Todorov et al., 2010; Todorov, 2010). To our best of knowledge, only limited studies have dealt with the evaluation of combined applications and for exploring synergistic mode(s) of action of bacteriocins and antibiotics against *Clostridium* spp. (Mathur et al., 2013; Hanchi et al., 2017). However, activity against *Listeria* spp. has been well documented and the anti-*Listeria* efficacy of enterocin CRL35 was shown when combining with the cell wall membrane-acting antibiotics (monensin, bacitracin, and gramicidin) and muralytic enzymes (mutanolysin and lysozyme) (Salvucci et al., 2010). A number of benefits from this combined application, positive interactions and possible synergistic effects were reported. According to Salvucci et al. (2010) the combination of not only the naturally produced bacteriocin, enterocin CRL35, but also of its synthetic equivalent with some antibiotics can provide substantial inhibitory effects against *L. innocua* and *L. monocytogenes* growth in culture; even more importantly, this combination can significantly reduce the amount of antibiotic required for effective treatment of infections caused by *Listeria* spp. Enterocin CRL35 appears to be a promising agent with applications not only for maintenance of food quality and safety, but also for medical applications in combination with conventional therapeutic agents. The former examples suggest a therapeutic potential of antibiotic and bacteriocin combinations by which the risk of the possible misuse of antibiotics in human and veterinary medicine can be reduced. This may also be a precaution against the development of antibiotic-resistant strains.

Actagardine, the lipid II-binding lantibiotic, was applied in combination with the antibiotics metronidazole, vancomycin and ramoplanin in an assay against several *Cd. difficile* isolates (Mathur et al., 2013). In combination with ramoplanin actagardine behaved in a partial synergistic/additive fashion against 61.5% of the target *Cd. difficile* strains assessed in this study (Mathur et al., 2013). Actagardine-metronidazole and actagardine-vancomycin combinations also showed partial synergistic/additive effects against 54 and 38% of *Cd. difficile* strains, respectively (Mathur et al., 2013).

Combinations of durancin 61A with reuterin or with pediocin showed strong synergistic effects against *Cd. difficile*. With this approach the MIC of *Cd. difficile* could be reduced from 16 mg/L to respectively 0.12 (in presence of reuterin) and 0.06 mg/L (with pediocin) (Hanchi et al., 2017). Durancin 61A, a glycosylated broad-spectrum bacteriocin produced by *E. durans* 61A, was active against clinical drug-resistant *C. difficile*, in addition to *E. faecium* vancomycin- resistant enterococcus (VRE) and MRSA. Synergistic inhibition of *Cd. difficile* was also detected when durancin 61A was combined with reuterin and pediocin (Hanchi et al., 2017). Durancin 61A was shown to be bactericidal and to act on the bacterial membrane via the pore formation mechanism that includes pore and vesicle formation followed by cell disruption and loss of membrane integrity and cytoplasm content (Hanchi et al., 2016). Combinations of durancin 61A with antibiotics and other bacteriocins showed highly synergistic inhibitory patterns against multi-resistant pathogens related to clinical cases, including *S. aureus, Cd. difficile* and *Streptococcus* spp. (Hanchi et al., 2017).

Although bacteriocins have clearly been reported in recent years to show promise as therapeutic antimicrobial agents, the development of appropriate delivery systems remains a considerable challenge for successful therapeutic applications. In an overview on existing bacteriocin delivery systems, Arthur et al. (2014) referred to their potential for application both in food bio-preservation and in human and veterinary medicine. Several promising delivery systems for bacteriocins have been suggested such as silver- or carbohydrate-based nanoparticles, nanofiber scaffolds, nanospheres, impregnated implants, catheter coating, hydrogel, oral tablets, gums, livestock feed, aquaculture dry spray, and also the incorporation in food packaging, and of either the bacteriocin or its producer strain in food products (Favaro et al., 2015).

PHAGES IN COMBAT AGAINST *Clostridium* spp.

Naturally occurring bacteriophages (phages) appears to be an interesting alternative option for therapeutic treatment of infected livestock, even before conventional antibiotics have been used in farming practice for this purpose (Gravitz, 2012; Ghosh and Kim, 2019). In general, bacteriophages can act bactericidal by anchoring onto the bacterial cell surface, followed by injection of phage genetic material into the bacterial cytoplasm. This results in the take-over of the host cell machinery and the synthesis of phage components, followed by the assembly of new phages within the infected bacterial cell. In most cases, this leads to bacterial lysis and the release of phage progeny that can commence a second infection cycle. Phages are known to be highly selective in target (host) selection and therefore will attack only specific bacterial species or even strains, according to their mode of selectivity. This is a well-know principle and highly promising for exploitation of the lytic cycle of bacteriophages.

Further development that may lead to practical application of phage therapy for selectively targeting pathogenic bacteria over commensal bacteria is justified (Clark and March, 2006). However, despite the successful use of phage therapy in Eastern European countries and especially in the former Soviet Republics,

the Western world previously failed to follow up on the development of phage therapy (Pelfrene et al., 2016). Currently, phage therapy is the subject of increased research, and is driven by emerging needs for alternatives to traditional antibiotics (Kutter et al., 2010; Abedon et al., 2011). Bacteriophages present promising alternatives for the treatment of various bacterial infections, including *Cd. difficile*.

Even when phage therapy offers several advantages, some concerns exist about its practical application. Bacterial resistance to homologous phages has been reported (Labrie et al., 2010), and assessing the susceptibility of bacteria to a particular phage is therefore crucial. Unfortunately, rapid diagnostic platforms are not yet available, thereby frequently requiring a cocktail of multiple bacteriophages for the treatment of selected pathogen/s. Another problem may be the release of endotoxins from the bacteria after bacteriophage lysis; this could potentially lead to sepsis. Moreover, the pharmacokinetics of bacteriophages is a concern as they are known to easily diffuse into several organs of the body (Abedon et al., 2011). A possibly more serious concern is the immunogenicity of bacteriophages (Abedon et al., 2011). These aspects may limit to the uses of bacteriophages beyond a single application, as they would be efficiently cleared by the body the next time they are administered. Still, advances in genetic engineering during the recent decades have ensured that bacteriophages can be used in innovative ways to combat bacterial infections (Braff et al., 2016). On the other hand, inadequate methodology for phage preparation may constitute a major hurdle toward their development for successful therapy. The presence of endotoxins and pyrogenic substances poses a high degree of toxicity potential, and their removal would therefore be essential for safe application (Ghosh and Kim, 2019).

PROBIOTICS IN COMBAT AGAINST *Clostridiodes difficile*

Different probiotics have been suggested over a long period as potential and effective agents for prevention and control of diarrhea. The potential of probiotics such as *Saccharomyces boulardii* in biotherapeutic approaches for restoration of gut microbiota and combating *Cd. difficile* associated infections has already been recommended earlier (Buts et al., 1993; Rolfe, 2000; Wilcox and Dave, 2001; Aslam et al., 2005).

The clinical characteristics of diarrhea can be very different, but this condition is generally associated with a disbalance (dysbiosis) in the GIT microbiota; it frequently results from (inadverse) antibiotic treatment. *Cd. difficile* is typically involved in nosocomial antibiotic-associated diarrhea and is also considered to be the major agent in the etiology of pseudomembranous colitis (Hopkins and Macfarlane, 2003). Active drug therapy of diarrhea normally involves antibiotic treatment, also based on the expected presence of pathogenic bacteria involved in the production of toxins, thereby resulting in the disruption of gut homeostasis. Such therapies can, in some cases, even provoke life-threatening conditions for a patient and is also related to the possible destruction of both beneficial and commensal GIT microbiota by antibiotics. The use of probiotics in such cases can be considered as superior and potentially more effective alternative to antibiotics, also because the specificity of probiotics in targeting some specific pathogens constitutes a well-documented advantage. In addition, probiotics can be applied as a prevention therapy by not altering the beneficial microbiota and rather supporting the stabilization the gut microbiome.

Recommendations of the European Society of Clinical Microbiology and Infectious Diseases (ESCMID) for treatment of *Cd. difficile* infections include therapy with antibiotics, toxin-binding resins and polymers, immunotherapy, probiotics and fecal or bacterial intestinal transplantation (Debast et al., 2014). Generally, antibiotic treatment is a first choice in clinical practice and includes the application of metronidazole, vancomycin and fidaxomicin (Debast et al., 2014). However, antibiotic resistance and collateral effects of overdosing antibiotic applications are reasons for searching alternative therapies including the application of probiotics, live therapeutics and even bacteriocins such as thuricin CD. These were suggested as effective alternatives to reduce incidences and recurring infections (Rea et al., 2013).

Bacteriocins represent viable alternatives to antimicrobials due to their specificity, related to either a narrow or broad spectrum of antimicrobial activity. In addition, the potential of bacteriocins is also underlined by their low toxicity, the possibility of their *in situ* production by probiotic organisms, and their modulatory potential for bioengineering (Mathur et al., 2014). However, as potential alternative bacteriocin therapy for specifically combating *Cd. difficile* infections, their comparative effectivity relative to currently used antibiotics needs to proven while the risk of damage to the GIT microbiota should be excluded. Nisin and lacticin 3147 are bacteriocins showing efficacy in killing *Cd. difficile in vitro* at concentrations comparable to those used in the application of vancomycin and metronidazole (Mathur et al., 2014). Thuricin CD, a two-component peptide shows potential in the treatment of *Cd. difficile* infections (Rea et al., 2010; Mathur et al., 2014). Mathur et al. (2014) reported on GE2270 and its semi-synthetic derivative LFF571 as two additional bacteriocins with antimicrobial activity against *Cd. difficile*. Trzasko et al. (2012) conducted a pre-clinical study on survival benefits of peptide LFF571 compared to vancomycin at a lower dose, resulting in fewer recurrences in the hamster *Cd. difficile* infection model. In addition, the safety, tolerability and pharmacokinetics of single and multiple ascending oral doses of LFF571 were investigated. Trzasko et al. (2012) further reported that among 56 subjects, protein LFF571 was well tolerated and no serious side-effects were noted. A low concentration of protein LFF571 remained in the serum compared to a high concentration in the fascia. These results suggest the scope for the future development of protein LFF571 as potential agent for treatment for CDI (Trzasko et al., 2012).

Strategies based on the (beneficial) modulation of gut microbiota including the application of life microorganisms, are strongly pointing to the potential of alternative (biological) approaches for the control of CDI. The use of probiotics and prebiotics (non-digestible oligosaccharides) constitutes two of several alternatives for successfully preventing CDI and antibiotic-associated diarrhea in children (Hopkins and

Macfarlane, 2003). Especially in the case of infants and young children, only carefully selected probiotic strains should find specified clinical application (Zheng et al., 2017), also by considering the strain related functionality (McFarland, 2005) and safety (Brodmann et al., 2017) of a probiotic. Moreover, current developments in both precision medicine and precision nutrition are taking into account the diversity patterns of the human gut microbiome (Jobin, 2018; Mills et al., 2019). Individual differences in the commensal microbiota and genes of the human gut indeed constitute a strong basis for the rapid development of personalized disease management toward so-called "microbiomics" (Shukla et al., 2015). Detecting changes in the relative abundance of particular gut microbiota may serve as a strong diagnostic tool for analyzing health conditions including a variety of gut related diseases (Kitsios et al., 2016; Almonacid et al., 2017). On this basis the association of *Cd. difficile* with diarrhea could be clearly identified. In fact, individualized host–microbiome phenotypes are reflected by the maintenance of host–microbe associations across populations, thereby constituting an essential key for precision medicine (Petrosino, 2018). In a wider sense, tungstate treatment for modulating ("precision editing") the gut microbial population has been suggested for ameliorating dysbiotic conditions such as colitis (Zhu et al., 2018).

Using a co-culture method, Quigley et al. (2019) proposed the use of different *Lactobacillus* strains for the control of *Cd. difficile* activity. Following preliminary screening for inhibitory ability, the efficacy of *Lb. gasseri* APC 678 and *Lb. rhamnosus* DPC 6111 to combat *Cd. difficile* was shown in a murine model of CDI (Quigley et al., 2019). The beneficial effects of *Lb. gasseri* APC 678 was confirmed by the significant reduction of viable *Cd. difficile* VPI 10463 numbers in the feces of mice. Moreover, additional analysis based on the sequencing of the cecal microbiota showed that application of *Lb. gassei* APC 678 in a mouse model resulted in a significant increase in bacterial diversity (Quigley et al., 2019). At the same time, application of *Lb. gassei* APC 678 did not significantly affect the relative abundance of Firmicutes or Bacteroidetes, relative to the control.

The hypothesis related to strain specific benefits of probiotics was discussed and defended in different cases (Quigley et al., 2019). Consequently Quigley et al. (2019) strongly defended the idea of strain specificity, evaluating the range of *Lactobacillus* species for their efficacy to inhibit *Cd. difficile* with the aim to select an appropriate potential strain/s to target CDI in humans. Based on these results Quigley et al. (2019) highlighted the potential of *Lb. gasseri* APC 678 as a live therapeutic agent for targeting CDI.

In a micro-calometric study, Fredua-Agyeman et al. (2017) evaluated the *in vitro* inhibition of *Cd. difficile* by commercial probiotic strains and mixtures (*Lb. acidophilus* LA-51, *B. lactis* BB-121, Probio 71, and Symprove^{TM}). Li et al. (2019) reported on the successful attenuation of *Cd. difficile* colonization by a probiotic consortium of five *Lactobacillus* and two *Bifidobacterium* strains in a mouse model, and proposed the modulation of gut microbiota and bile acids as the underlying mechanism for this effect.

Saccharomyces boulardii is a probiotic yeast that can upregulate the expression of anti-toxin A secretory IgA and that secretes a protease that degrades toxin A and B produced by *Cd. difficile* and, in this way, effectively contributes to the control of CDI (Hickson, 2011). McFarland (2005) reported on a double-blind placebo-controlled trial, performed with high doses of vancomycin in combination with *S. boulardii*, and detected a significant reduction in recurrence of CDI compared to patients receiving only a high dose vancomycin and placebo patients.

FINAL REMARKS

In a report of 31 July 2020[1], the World Health Organization (WHO) describes the current antibiotic resistance situation as "one of the biggest treats to global health, food security and development." Multiple factors are underlying to the emerging rise of antibiotic resistance, with over- or mal-prescription, and extended (and wrong) use as some of the major complicating contributors, both in human medicine and animal husbandry. Looking for therapeutic alternatives to classical antibiotics constitutes an enormous but rewarding challenge. Thanks to a better understanding of the underlying antibiotic resistance mechanisms, and the access to information on the whole genome of resistant pathogens, a rapidly widening spectrum of potential antimicrobial agents has become a focus of current research. With this paper we intended to highlight the antimicrobial peptides, including bacteriocins, as a highly promising group of biotherapeutics, as alternatives to conventional antibiotics, for the treatment and prevention, especially of *Clostridium* infections. Several bacteriocins have already displayed efficacy in the laboratory and pre-clinical experiments. Some bacteriocins, and in particular nisin, have found successful commercial application in the food industry. We expect that *in vivo* (and in part also clinical) studies will be imperative before bacteriocins can be more regularly integrated in approaches for the control of bacterial and viral infections in human and veterinary medicine.

AUTHOR CONTRIBUTIONS

WH and ST planned and developed the manuscript. H-JK and II contributed to further expanding the text. ST contributed to the semifinal version, while WH added further amendments and did the final editing. All authors contributed to the article and approved the submitted version.

FUNDING

Support to ST and WH from the Bio&Medical Technology Program of the Korean National Research Foundation (NRF) of the Korean Ministry of Science and Technology (Nos. 2016M3A9A5923160 and 2018M3A9F3021964), and also from HEM Inc., Handong Global University, Techno-Incubator Center 103, Pohang-si, Gyeongbuk, South Korea, is gratefully acknowledged.

[1]https://www.who.int/news-room/fact-sheets/detail/antibiotic-resistance

REFERENCES

Abdelgadir, W., Nielsen, D. S., Hamad, S., and Jakobsen, M. (2008). A traditional Sudanese fermented camel's milk product, gariss, as a habitat of *Streptococcus infantarius* subsp. *infantarius*. *Int. J. Food Microbiol.* 127, 215–219. doi: 10.1016/j.ijfoodmicro.2008.07.008

Abedon, S. T., Kuhl, S. J., Blasdel, B. G., and Kutter, E. M. (2011). Phage treatment of human infections. *Bacteriophage* 1, 66–85. doi: 10.4161/bact.1.2.15845

Abee, T., Kröckel, L., and Hill, C. (1995). Bacteriocins: mode of action and potentials in food preservation and control of food poisoning. *Int. J. Food Microbiol* 28, 169–185.

Allen, H. K. (2017). *Alternatives to Antibiotics: Why and How. NAM Perspectives. Discussion Paper*. Washington, DC: National Academy of Medicine. doi: 10.31478/201707g

Almonacid, D. E., Kraal, L., Ossandon, F. J., Budovskaya, Y. V., Cardenas, J. P., Bik, E. M., et al. (2017). 16S rRNA gene sequencing and healthy reference ranges for 28 clinically relevant microbial taxa from the human gut microbiome. *PLoS One* 12:e0176555. doi: 10.1371/journal.pone.0176555

Aronsson, B., Möllby, R., and Nord, C. E. (1985). Antimicrobial agents and *Clostridium difficile* in acute enteric disease: epidemiological data from Sweden, 1980–1982. *J. Infect. Dis.* 151, 476–481. doi: 10.1093/infdis/151.3.476

Arqués, J. L., Rodriguez, E., Nunez, M., and Medina, M. (2011). Combined effect of reuterin and lactic acid bactéria bacteriocins on the inactivation of food-borne pathogens in milk. *Food Control* 22, 457–461. doi: 10.1016/j.foodcont.2010.09.027

Arthur, T. D., Cavera, V. L., and Chikindas, M. L. (2014). On bacteriocin delivery system and potential applications. *Future Microbiol.* 9, 235–248. doi: 10.2217/fmb.13.148

Aslam, S., Hamill, R. J., and Musher, D. M. (2005). Treatment of *Clostridium difficile*-associated disease: old therapies and new strategies. *Lancet* 9, 549–557. doi: 10.1016/S1473-3099(05)70215-2

Avila, M., Gomez-Torres, N., Hernandez, M., and Garde, S. (2014). Inhibitory activity of reuterin, nisin, lysozyme and nitrate against vegetative cells and spores of dairy-related *Clostridium* species. *Int. J. Food Microbiol.* 172, 70–75. doi: 10.1016/j.ijfoodmicro.2013.12.002

Barbosa, M. S., Todorov, S. D., Ivanova, I., Chobert, J.-M., Haertlé, T., and De Melo Franco, B. D. G. (2015a). Improving safety of salami by application of bacteriocins produced by an autochthonous *Lactobacillus curvatus* isolate. *Food Microbiol.* 46, 254–262. doi: 10.1016/j.fm.2014.08.004

Barbosa, M. S., Todorov, S. D., Jurkiewicz, C. H., and Franco, B. D. G. M. (2015b). Bacteriocin production by *Lactobacillus curvatus* MBSa2 entrapped in calcium alginate during ripening of salami for control of *Listeria monocytogenes*. *Food Control* 47, 147–153. doi: 10.1016/j.foodcont.2014.07.005

Bartlett, J. G. (2006). Narrative review: the new epidemic of *Clostridium difficile* associated enteric disease. *Ann. Intern. Med.* 145, 758–764. doi: 10.7326/0003-4819-145-10-200611210-00008

Bartoloni, A., Mantella, A., Goldstein, B. P., Dei, R., Benedetti, M., Sbaragli, S., et al. (2004). *In vitro* activity of nisin against clinical isolates of *Clostridium difficile*. *J. Chemother.* 16, 119–121. doi: 10.1179/joc.2004.16.2.119

Braff, D., Shis, D., and Collins, J. J. (2016). Synthetic biology platform technologies for antimicrobial applications. *Adv. Drug. Deliv. Rev.* 105, 35–43. doi: 10.1016/j.addr.2016.04.006

Brodmann, T., Endo, A., Gueimonde, M., Vinderola, G., Kneifel, W., de Vos, W. M., et al. (2017). Safety of novel microbes for human consumption: practical examples of assessment in the European union. *Front. Microbiol.* 8:1725. doi: 10.3389/fmicb.2017.01725

Buts, J. P., Corthier, G., and Delmeé, M. (1993). *Saccharomyces boulardii* for *Clostridium difficile*-associated enteropathies in infants. *J. Pediatr. Gastroenterol. Nutr.* 16, 419–425. doi: 10.1097/00005176-199305000-00013

Carneiro, B. M., Braga, A. C. S., Batista, M. N., Rahal, P., Favaro, L., Penna, A. L. B., et al. (2014). *Lactobacillus plantarum* ST202Ch and *Lactobacillus plantarum* ST216Ch – what are the limitations for application? *J. Nutr. Health Food Eng.* 1, 61–63.

Cassir, N., Benamar, S., and La Scola, B. (2016). *Clostridium butyricum*: from beneficial to a new emerging pathogen. *Clin. Microbiol. Infect.* 22, 37–45. doi: 10.1016/j.cmi.2015.10.014

Castro-González, J. M., Castro, P., Sandoval, H., and Castro-Sandoval, D. (2019). Probiotic Lactobacilli Precautions. *Front. Microbiol.* 10:375. doi: 10.3389/fmicb.2019.00375

Cavicchioli, V. Q., de Carvalho, O. V., de Paiva, J. C., Todorov, S. D., Júnior, A. S., and Nero, L. A. (2018). Inhibitionof Herpes simplex virus 1 and Poliovirus (PV 1 -1) by bacteriocins from *Lactococcus lactis* subsp. *lactis* and Enterococcus durans strains isolated from goat milk. *Int. J. Antimicrob. Agents* 51, 33–37. doi: 10.1016/j.ijantimicag.2017.04.0200924-8579

Cebrian, R., Macia-Valero, A., Jato, A. P., and Kuipers, O. P. (2019). Design and expression of specific hybrid lantibiotics active against pathogenic *Clostridium* spp. *Front. Microbiol.* 24:2154. doi: 10.3389/fmicb.2019.02154

Chatterjee, C., Paul, M., Xie, L., and van der Donk, W. A. (2005). Biosynthesis and mode of action of lantibiotics. *Chem. Rev.* 105, 633–684. doi: 10.1021/cr030105v

Chen, Y. Y., Liang, N. Y., Curtis, J. M., and Gänzle, M. (2016). Characterization of Linoleate 10-Hydratase of *Lactobacillus plantarum* and Novel Antifungal Metabolites. *Front. Microbiol.* 7:1561. doi: 10.3380/fmicb.2016.01561

Chikindas, M. L., Weeks, R., Drider, D., Chistyakov, V. A., and Dicks, L. M. T. (2018). Functions and emerging applications of bacteriocins. *Curr. Opin. Biotechnol.* 49, 23–28. doi: 10.1016/j.copbio.2017.07.011

Clark, J. R., and March, J. B. (2006). Bacteriophages and biotechnology: vaccines, gene therapy and antibacterials. *Trends Biotechnol.* 24, 212–218. doi: 10.1016/j.tibtech.2006.03.003

Coetzee, H. L., De Klerk, H. C., Coetzee, J. N., and Smit, J. A. (1968). Bacteriophage tail-like particles associated with intra-species killing of *Proteus vulgaris*. *J. Gen. Virol.* 2, 29–36. doi: 10.1099/0022-1317-2-1-29

Cotter, P. D., Hill, C., and Ross, R. P. (2005). Bacteriocins: developing innate immunity for foods. *Nat. Rev. Microbiol.* 3, 777–788. doi: 10.1038/nrmicro1273

Cotter, P. D., Ross, R. P., and Hill, C. (2013). Bacteriocins – A viable alternative to antibiotics. *Nat. Rev. Microbiol.* 11, 95–105. doi: 10.1038/nrmicro2937

Cruickshank, R. (1931). Döderlein's vaginal bacillus: a contribution to the study of the lacto-bacilli. *J. Hyg.* 31, 375–381.

Czaplewski, L., Bax, R., Clokie, M., Dawson, M., Fairhead, H., Fischetti, V. A., et al. (2016). Alternatives to antibiotics-a pipeline portfolio review. *Lancet Infect. Dis.* 16, 239–251. doi: 10.1016/S1473-3099(15)00466-1

Czepiel, J., Drozdz, M., Pituch, H., Kuijper, E. J., Perucki, W., Aleksandrova, M., et al. (2019). *Clostridium difficile* infection: review. *Eur. J. Microbiol. Infect. Dis.* 38, 1211–1221. doi: 10.1007/s10096-019-03539-6

De Vuyst, L., and Tsakalidou, E. (2008). *Streptococcus macedonicus*, a multi-functional and promising species for dairy fermentations. *Int. Dairy J.* 18, 476–485. doi: 10.1016/j.idairyj.2007.10.006

De Vuyst, L., and Vandamme, E. (1994). *Bacteriocins of Lactic Acid Bacteria*. Berlin: Springer, 539.

Debast, S. B., Bauer, M. P., and Kuijper, E. J. (2014). European society of clinical microbiology and infectious diseases: update of the treatment guidance document for *Clostridium difficile* infection. *Clin. Microbiol. Infect.* 20(Suppl. 2), 1–26. doi: 10.1111/1469-0691.12418

Delves-Broughton, J., Blackburn, P., Evans, R. J., and Hugenholtz, J. (1996). Applications of the bacteriocin, nisin. *Antonie Van Leeuwenhoek* 69, 193–202. doi: 10.1007/BF00399424

Dieterle, M. G., and Young, V. B. (2017). Reducing Recurrence of *C. difficile* Infection. *Cell* 169, 375. doi: 10.1016/j.cell.2017.03.039

Döderlein, A. (1892). Das Scheidensekret und seine Bedeutungfür das Puerperalfieber ('The vaginal transsudate and its significance forchildbed fever'). *Centralblatt Bacteriol.* 11, 699–700.

dos Santos, K. M. O., de Matos, C. R., Salles, H. O., Franco, B. D. G. M., Arellano, K., Holzapfel, W. H., et al. (2020). Exploring beneficial/virulence properties of two dairy related strains of *Streptococcus infantarius* subsp. *infantarius*. *Probiot. Antimicrob. Prot.* (in press). doi: 10.1007/s12602-020-09637-8

Egan, K., Field, D., Rea, M. C., Ross, R. P., Hill, C., and Cotter, P. D. (2016). Bacteriocins: novel solutions to age old spore-related problems? *Front. Microbiol.* 7:461. doi: 10.3389/fmicb.2016.00461

Ellison, J. S., and Kautter, J. A. (1970). Purification and some properties of two botocins. *J. Bacteriol.* 104, 19–26.

Favaro, L., Basaglia, M., Casella, S., Hue, I., Dousset, X., Franco, B. D. G. M., et al. (2014). Bacteriocinogenic potential and safety evaluation of non starter *Enterococcus faecium* strains isolated from home made white brine cheese. *Food Microbiol.* 38, 228–239. doi: 10.1016/j.fm.2013.09.008

Favaro, L., Penna, A. L. B., and Todorov, S. D. (2015). Bacteriocinogenic LAB from cheeses - application in biopreservation? *Trends Food Sci. Technol.* 41, 37–48. doi: 10.1016/j.tifs.2014.09.001

Favaro, L., and Todorov, S. D. (2017). Bacteriocinogenic LAB strains for fermented meat preservation: perspectives, challenges and limitations. *Probiotics Antimicrob. Prot.* 9, 444–458. doi: 10.1007/s12602-017-9330-6

Field, D., Cotter, P. D., Hill, C., and Ross, R. P. (2015). Bioengineering lantibiotics for therapeutic success. *Front. Microbiol.* 6:1363. doi: 10.3389/fmicb.2015.01363

Fredua-Agyeman, M., Stapleton, P., Basit, A. W., Beezer, A. E., and Gaisford, S. (2017). *In vitro* inhibition of *Clostridium difficile* by commercial probiotics: a microcalorimetric study. *Int. J. Pharm.* 517, 96–103. doi: 10.1016/j.ijpharm.2016.12.005

Galvez, A., Lopez, R. L., Abriouel, H., Valdivia, E., and Omar, N. B. (2008). Application of bacteriocins in the control of foodborne pathogens and spoilage bacteria. *Crit. Rev. Biotechnol.* 28, 125–152. doi: 10.1080/07388550802107202

Garde, S., Avila, M., Arias, R., Gaya, P., and Nunez, M. (2011). Outgrowth inhibition of *Clostridium beijerinckii* spores by a bacteriocin-producing lactic culture in ovine milk cheese. *Int. J. Food Microbiol.* 150, 59–65. doi: 10.1016/j.ijfoodmicro.2011.07.018

Gebhart, D., Lok, S., Clare, S., Tomas, M., Stares, M., Scholl, D., et al. (2015). A modified R-type bacteriocin specifically targeting *Clostridium difficile* prevents colonization of mice without affecting gut microbiota diversity. *mBio* 6:e02368-14. doi: 10.1128/mBio.02368-14

Gebhart, D., Williams, S. R., Bishop-Lilly, K. A., Govoni, G. R., Willner, K. M., Butani, A., et al. (2012). Novel high-molecular-weight, R-type bacteriocins of *Clostridium difficile*. *J. Bacteriol.* 194, 6240–6247. doi: 10.1128/JB.01272-12

George, R. H., Symonds, J. M., Dimock, F., Brown, J. D., Arabi, Y., Shinagawa, N., et al. (1978). Identification of *Clostridium difficile* as a cause of pseudomembranous colitis. *Br. Med. J.* 1:695. doi: 10.1136/bmj.1.6114.695

Gevers, D., Kugathasan, S., Denson, L. A., Vázquez-Baeza, Y., Van Treuren, W., Ren, B., et al. (2014). The treatment-naive microbiome in new-onset Crohn's disease. *Cell Host Microbe* 15, 382–392. doi: 10.1016/j.chom.2014.02.005

Ghosh, K., and Kim, K. P. (2019). Complete nucleotide sequence analysis of a novel *Bacillus subtilis*-infecting phage, BSP38, possibly belonging to a new genus in the subfamily Spounavirinae. *Arch. Virol.* 164, 875–878. doi: 10.1007/s00705-018-4110-5

Goetz, F., Perconti, S., Popella, P., Werner, R., and Schlag, M. (2014). Epidermin and gallidermin: Staphylococcal lantibiotics. *Int. J. Med. Microbiol.* 304, 63–71. doi: 10.1016/j.ijmm.2013.08.012

Gómez-Torres, N., Garde, S., Peiroten, A., and Avila, M. (2015). Impact of *Clostridium* spp. on cheese characteristics: microbiology, color, formation of volatile compounds and off-flavors. *Food Control* 56, 186–194. doi: 10.1016/j.foodcont.2015.03.025

Gravitz, L. (2012). Turning a new phage. *Nat. Med.* 18, 1318–1320. doi: 10.1038/nm0912-1318

Han, S.-K., Shin, M.-S., Park, H.-E., Kim, S.-Y., and Lee, W.-K. (2014). Screening of bacteriocin-producing *Enterococcus faecalis* strains for antagonistic activities against *Clostridium perfringens*. *Korean J. Food Sci. Anim. Resour.* 34, 614–621. doi: 10.5851/kosfa.2014.34.5.614

Hanchi, H., Hammami, R., Gingras, H., Kourda, R., Bergeron, M. G., Hamida, J. B., et al. (2017). Inhibition of MRSA and of *Clostridium difficile* by durancin 61A: synergy with bacteriocins and antibiotics. *Future Microbiol.* 12, 205–212. doi: 10.2217/fmb-2016-0113

Hanchi, H., Hammami, R., Kourda, R., Bem Hamida, J., and Fliss, I. (2016). Simultaneous production of formylated and non-formylated enterocins L50A and L50B, and 61A, a new glycosylated durancin, by *Enterococcus durans* 61A, a strain isolated from artisanal fermented milk in Tunisia. *J. Agric. Food Chem.* 64, 3584–3590. doi: 10.1021/acs.jafc.6b00700

Heng, N. C. K., Wescombre, P. A., Burton, J. P., Jack, R. W., and Tagg, J. R. (2007). *The Diversity of Bacteriocins in Gram-Positive Bacteria Bacteriocins: Ecology and Evolution*, eds M. A. Riley and M. A. Chavan (Berlin: Springer-Verlag).

Herrera, P., MinKwon, Y., and Ricke, S. C. (2009). Ecology and pathogenicity of gastrointestinal *Streptococcus bovis*. *Anaerobe* 15, 44–54. doi: 10.1016/j.anaerobe.2008.11.003

Heu, S., Oh, J., Kang, Y., Ryu, S., Cho, S. K., Cho, Y., et al. (2001). Gly gene cloninig and expression and purification of Glycinecin A, a bacteriocin produced by *Xantomonas campestris* pv. *glycines* 8ra. *Appl. Environ. Microbiol.* 67, 4105–4110. doi: 10.1128/AEM.67.9.4105-4110.2001

Hickson, M. (2011). Probiotics in the prevention of antibiotic-associated diarrhoea and *Clostridium difficile* infection. *Therap. Adv. Gastroenterol.* 4, 185–197. doi: 10.1177/1756283X11399115

Holzapfel, W., Arini, A., Aeschbacher, M., Coppolecchia, R., and Pot, B. (2018). *Enterococcus faecium* SF68 as a model for efficacy and safety evaluation of pharmaceutical probiotics. *Benef. Microbes* 9, 375–388. doi: 10.3920/BM2017.0148

Holzapfel, W. H. (2006). "Introduction to prebiotics and probiotics," in *Probiotics in Food Safety and Human Health*, eds I. Goktepe, V. K. Juneja, and M. Ahmedna (Boca Raton, FL: CRC Press), 1–33.

Hopkins, M. J., and Macfarlane, G. T. (2003). Nondigestible oligosaccharides enhance bacterial colonization resistance against *Clostridium difficile in vitro*. *Appl. Environ. Microbiol.* 69, 1920–1927.

Hoshino, T., Fujiwara, T., and Kilian, M. (2005). Use of phylogenetic and phenotypicanalyses to identify non hemolytic streptococci isolated from bacteremic patients. *J. Clin. Microbiol.* 43, 6073–6085. doi: 10.1128/JCM.43.12.6073-6085.2005

James, R., Lazdunski, C., and Pattis, F. (1991). *Bacteriocins, Microcins and Lantibiotics*. New York, NY: Springer-Verlag, 519.

Jobin, C. (2018). Precision medicine using microbiota. *Science* 359, 32–34. doi: 10.1126/science.aar2946

Jones, E., Salin, V., and Williams, G. W. (2005). *Nisin and the Market for Commercial Bacteriocins. TAMRC Consumer and ProductResearch Report No. CP-01–05*. Lubbock, TX: Texas Agribusiness Mark Research Center.

Jozala, A. F., De Andrade, M. S., De Arauz, L. J., Pessoa, A. Jr., and Penna, T. C. V. (2007). Nisin production utilizing skimmed milk aiming to reduce process cost. *Appl. Biochem. Biotechnol.* 137-140, 515–528. doi: 10.1007/s12010-007-9076-9

Kaur, S., and Kaur, S. (2015). Bacteriocins as potential anticancer agents. *Front. Pharmacol.* 6:272. doi: 10.3389/fphar.2015.00272

Kautter, D. A., Harmon, S. M., Lynt, R. K. Jr., and Lilly, T. (1966). Antagonistic effect on *Clostridium botulinum* type E by organisms resembling it. *Appl. Microbiol.* 14, 616–622.

Kers, J. A., Sharp, R. E., Defusco, A. W., Park, J. H., Xu, J., Pulse, M. E., et al. (2018). Mutacin 1140 lantibiotic variants are efficacious against *Clostridium difficile* infection. *Front. Microbiol.* 9:415. doi: 10.3389/fmicb.2018.00415

Khan, H., Flint, S. H., and Yu, P.-L. (2010). Enterocins in food preservation. *Int. J. Food Microbiol.* 141, 1–10. doi: 10.1016/j.ijfoodmicro.2010.03.005

Kitsios, G. D., Morowitz, M. J., Dickson, R. P., Huffnagle, G. B., McVerry, B. J., and Morris, A. (2016). Dysbiosis in the intensive care unit: microbiome science coming to the bedside. *J. Crit. Care* 38, 84–91. doi: 10.1016/j.jcrc.2016.09.029

Klaenhammer, T. (1988). Bacteriocins of lactic acid bacteria. *Biochimie* 70, 337–349. doi: 10.1016/0300-9084(88)90206-4

Kuijper, E. J., Dissel, J. T., and Wilcox, M. H. (2007). *Clostridium difficile*: changing epidemiology and new treatment options. *Curr. Opin. Infect. Dis.* 20, 376–383. doi: 10.1097/QCO.0b013e32818be71d

Kutter, E., de Vos, D., Gvasalia, G., Alavidze, Z., Godokhia, L., Kuhl, S., et al. (2010). Phage therapy in clinical practice: treatment of human infections. *Curr. Pharm. Biotechnol.* 11, 69–86. doi: 10.2174/138920110790725401

Labrie, S. J., Samson, J. E., and Moineau, S. (2010). Bacteriophage resistance mechanisms. *Nat. Rev. Microbiol.* 8, 317–327. doi: 10.1038/nrmicro2315

Laiño, J. E., LeBlanc, J. G., and Savoy de Giori, G. (2019). Production of naturalfolates by lactic acid bacteria starter cultures isolated from artisanal Argentinian yogurt. *Can. J. Microbiol.* 58, 581–585. doi: 10.1139/w2012-0

Lash, A. F., and Kaplan, B. (1926). A study of Döderlein's vaginal bacillus. *J. Infect. Dis.* 38, 333–340.

Lawson, P. A., Citron, D. M., Tyrrell, K. L., and Finegold, S. M. (2016). Reclassification of *Clostridium difficile* as *Clostridioides difficile* (Hall and O'Toole 1935) Prévot 1938. *Anaerobe* 40, 95–99. doi: 10.1016/j.anaerobe.2016.06.008

Lawson, P. A., and Rainey, F. A. (2015). Proposal to restrict the genus *Clostridium* Prazmowski to *Clostridium butyricum* and related species. *Int. J. Syst. Evol. Microbiol.* 66, 1009–1016. doi: 10.1099/ijsem.0.000824

Lerner, A., Shoenfield, Y., and Matthias, T. (2019). Probiotics: If it does not help it does not do any harm. Really? *Microorganisms* 7:104. doi: 10.3390/microorganisms7040104

Leuschner, R. G. K., Robinson, T. P., Hugas, M., Cocconcelli, P. S., Richard-Forget, F., Klein, G., et al. (2010). Qualified presumption of safety (QPS): a generic risk assessment approach for biological agents notified to the European Food Safety Authority (EFSA). *Trends Food Sci. Technol.* 21, 425–435. doi: 10.1016/j.tifs.2010.07.003

Leyva Salas, M., Thierry, A., Lemaître, M., Garric, G., Harel-Oger, M., Chatel, M., et al. (2018). Antifungal activity of lactic acid bacteria combinations in dairy

mimicking models and their potential as bioprotective cultures in pilot scale applications. *Front. Microbiol.* 9:1787. doi: 10.3389/fmicb.2018.01787

Li, X., Chu, Q., Huang, Y., Xiao, Y., Song, L., Zhu, S., et al. (2019). Consortium of probiotics attenuates colonization of *Clostridioides difficile*. *Front. Microbiol.* 10:2871. doi: 10.3389/fmicb.2019.02871

Mahlapuu, M., Håkansson, J., Ringstad, L., and Bjorn, C. (2016). Antimicrobial peptides: an emerging category of therapeutic agents. *Front. Cell. Infect. Microbiol.* 6:194. doi: 10.3389/fcimb.2016.00194

Martinez, R. R. C., Wachsman, M., Torres, N. I., LeBlanc, J. G., Todorov, S. D., and Franco, B. D. G. M. (2013). Biochemical, antimicrobial and molecular characterization of a noncytotoxic bacteriocin produced by *Lactobacillus plantarum* ST71KS. *Food Microbiol.* 34, 376–381. doi: 10.1016/j.fm.2013.01.011

Mathara, M. J., Schillinger, U., Kutima, P. M., Mbugua, K. S., and Holzapfel, W. H. (2004). Isolation, identification and characterisation of the dominant microorganisms of *kulenaoto*: the Maasai traditional fermented milk in Kenya. *Int. J. Food Microbiol.* 94, 269–278. doi: 10.1016/j.ijfoodmicro.2004.01.008

Mathur, H., O'Connor, P. M., Hill, C., Cotter, P. D., and Ross, R. P. (2013). Analysis of anti-*Clostridium difficile* activity of thuricin CD, vancomycin, metronidazole, ramoplanin, and actagardine, both singly and in paired combinations. *Antimicrob. Agents Chemother.* 57, 2882–2886. doi: 10.1128/AAC.00261-13

Mathur, H., Rea, M. C., Cotter, P. D., Ross, R. P., and Hill, C. (2014). The potential for emerging therapeutic options for *Clostridium difficile* infection. *Gut Microbes* 5, 696–710. doi: 10.4161/19490976.2014.983768

McFarland, L. V. (2005). Alternative treatments for *Clostridium difficile* disease: what really works? *J. Med. Microbiol.* 54, 101–111. doi: 10.1099/jmm.0.45753-0

Metchnikoff, E. (1908). *Prolongation of Life*. New York, NY: Putmans Sons.

Michel-Briand, Y., and Baysse, C. (2002). The pyocins of *Pseudomonas aeruginosa*. *Biochimie* 84, 499–510. doi: 10.1016/s0300-9084(02)01422-0

Mills, S., Stanton, C., Lane, J. A., Smith, G. J., and Ross, R. P. (2019). Precision nutrition and the microbiome, Part I: current state of the science. *Nutrients* 11:923. doi: 10.3390/nu11040923

Minahk, C. J., Dupuy, F., and Morero, R. D. (2004). Enhancement of antibiotic activity by sub-lethal concentrations of enterocin CRL35. *J. Antimicrob. Chemother.* 53, 240–246. doi: 10.1093/jac/dkh079

Monteiro, C. R. A. V., do Carmo, M. S., Melo, B. O., Alves, M. S., dos Santos, C. I., Monteiro, S. G., et al. (2019). *In vitro* antimicrobial activity and probiotic potential of *Bifidobacterium* and *Lactobacillus* against species of *Clostridium*. *Nutrients* 11:448. doi: 10.3390/nu11020448

Mukherjee, S., Joardar, N., Senguota, S., and Sinha Babu, S. (2018). Gut microbes as future therapeutics in treating inflammatory and infectious diseases: lessons from recent findings. *J. Nutr. Biochem.* 61, 111–128. doi: 10.1016/j.jnutbio.2018.07.010

Nakayama, K., Takashima, K., Ishihara, H., Shinomiya, T., Kegeyama, M., Kanaya, S., et al. (2000). The R-type pyocin of *Pseudomonas aeruginosa* is related to P2 phage, and the F-type is related to lambda phage. *Mol. Microbiol.* 38, 213–231. doi: 10.1046/j.1365-2958.2000.02135.x

NHS (2016). UK Standards for Microbiology Investigations. Identification of Clostridium species. Issued by the Standard Unit, Microbiology Sevices, PHE. Available online at: https://assets.publishing.service.gov.uk/government/uploads/system/uploads/attachment_data/file/504183/ID_8i4.1.pdf (accessed July 1, 2020).

Ongey, E. L., Yassi, H., Pflugmacher, S., and Neubauer, P. (2017). Pharmacological and pharmacokinetic properties of lanthipeptides undergoing clinical studies. *Biotechnol. Lett.* 39, 473–482. doi: 10.1007/s10529-016-2279-9

Oren, A., and Garrity, G. M. (2016). Notification that new names of prokaryotes, new combinations, and new taxonomic opinions have appeared in volume 69, part 5 of the IJSEM. *Int. J. Syst. Evol. Microbiol.* 69, 2177–2178. doi: 10.1099/ijsem.0.003470

Oren, A., and Rupnik, M. (2018). *Clostridium difficile* and *Clostridioides difficile*: two validly published and correct names. *Anaerobe* 52, 125–126. doi: 10.1016/j.anaerobe.2018.07.005

O'Sullivan, L., Ryan, M. P., Ross, R. P., and Hill, C. (2003). Generation of food-grade lactcoccal starters which produce the lantibioticslactacin 3143 and lactacin 481. *Appl. Environ. Microbiol.* 69, 3681–3685.

Pelfrene, E., Willebrand, E., Sanches, A. C., Sebris, Z., and Cavaleri, M. (2016). Bacteriophage therapy: a regulatory perspective. *J. Antimicrob Chemother.* 71, 2071–2074. doi: 10.1093/jac/dkw083

Perin, L. M., Miranda, R. O., Todorov, S. D., Franco, B. D. G. M., and Nero, L. A. (2014). Virulence, antibiotic resistance and biogenic amines of bacteriocinogenic lactococci and enterococci isolated from goatmilk. *Int. J. Food Microbiol.* 185, 121–126. doi: 10.1016/j.ijfoodmicro.2014.06.001

Petrosino, J. (2018). The microbiome in precision medicine: the way forward. *Genome Med.* 10:12. doi: 10.1186/s13073-018-0525-6

Pieterse, R., Todorov, S. D., and Dicks, L. M. T. (2010). Mode of action and *in vitro* susceptibility of mastitis pathogens to macedocin ST91KM and preparation of a teat seal containing the bacteriocin. *Braz. J. Microbiol.* 41, 133–145. doi: 10.1590/S1517-838220100001000020

Piper, C., Casey, P. G., Hill, C., Cotter, P. D., and Ross, R. P. (2012). The lantibiotic lacticin 3147 prevents systemic spread of *Staphylococcus aureus* in a murine infection model. *Int. J. Microbiol.* 2012:806230. doi: 10.1155/2012/806230

Pongtharangkul, T., and Demirci, A. (2004). Evaluation of agar diffusion bioassay for nisin quantification. *Appl. Microbiol. Biotechnol.* 65, 268–272. doi: 10.1007/s00253-004-1579-5

Quigley, L., Coakley, M., Alemayehu, D., Rea, M. C., Casey, P. G., O'Sullivan, O., et al. (2019). *Lactobacillus gasseri* APC 678 reduces shedding of the pathogen *Clostridium difficile* in a murine model. *Front. Microbiol.* 10:273. doi: 10.3389/fmicb.2019.00273

Quintana, J., Bayona, L. M., Castellanos, L., Puyana, M., Camargo, P., Aristizabal, F., et al. (2014). Almiramide D, cytotoxic peptide from the marine cyanobacterium *Oscillatoria nigroviridis*. *Bioorg. Med. Chem.* 22, 6789–6795. doi: 10.1016/j.bmc.2014.10.039

Rea, M. C., Alemayehu, D., Ross, P. R., and Hill, C. (2013). Gut solutions to a gut problems: bacteriocins, probiotics and bacteriophage for control of *Clostridium difficile* infection. *J. Med. Microbiol.* 62, 1369–1378. doi: 10.1099/jmm.0.058933-0

Rea, M. C., Clayton, E., O'Connor, P. M., Shanahan, F., Kiely, B., Ross, R. P., et al. (2007). Antimicrobial activity of lacticin 3,147 against clinical *Clostridium difficile* strains. *J. Med. Microbiol.* 56, 940–946. doi: 10.1099/jmm.0.47085-0

Rea, M. C., Sit, C. S., Clayton, E., O'Connor, P. M., Whittal, R. M., Zheng, J., et al. (2010). Thuricin CD, a posttranslationally modified bacteriocin with a narrow spectrum of activity against *Clostridium difficile*. *Proc. Natl. Acad. Sci. U.S.A.* 107, 9352–9357. doi: 10.1073/pnas.0913554107

Redelings, M. D., Sorvillo, F., and Mascola, L. (2007). Increase in *Clostridium difficile*-related mortality rates, United States, 1999-2004. *Emerg. Infect. Dis.* 13, 1417–1419. doi: 10.3201/eid1309.061116

Reis, J. A., Paula, A. T., Casarotti, S. N., and Penna, A. L. B. (2012). Lactic acid bacteria antimicrobial compounds: characteristics and applications. *Food Eng. Rev.* 4, 124–140. doi: 10.1007/s12393-012-9051-2

Ribeiro, S. C., Costa, M. C., Todorov, S. D., Franco, B. D. G. M., Dapkevicius, M. L. E., and Silva, C. C. G. (2014). Characterization of bacteriocin-producing bacteria isolated from Pico Cheese an artisanal cow's milk cheese. *J. Appl. Microbiol.* 116, 573–585. doi: 10.1111/jam.12388

Ribeiro, S. C., O'Connor, P. M., Ross, R. P., Stanton, C., and Silva, C. C. G. (2016). An anti-listrerial *Lactococcus lactis* strain isolated from Azorean Pico cheese produces lactacin 481. *Int. Dairy J.* 63, 18–28. doi: 10.1016/j.idairyj.2016.07.017

Rogers, L. A., and Whittier, E. O. (1928). Limiting factors in the lactic fermentation. *J. Bacteriol.* 16, 211–229.

Rolfe, R. D. (2000). The role of probiotic cultures in the control of gastrointestinal health. *J. Nutr.* 130, S396–S402.

Ross, A. C., and Vederas, J. C. (2011). Fundamental functionality: recent developments in understanding the structure activity relationships of lantibiotic peptides. *J. Antibiot.* 64, 27–34. doi: 10.1038/ja.2010.136

Salvucci, E., Hebert, E. M., Sesma, F., and Saavedra, L. (2010). Combined effect of synteticenterocin CRL35 with cell wall, membrane-acting antibiotics and muranolytic enzymes against *Listeria* cells. *Lett. Appl. Microbiol.* 51, 191–195. doi: 10.1111/j.1472-765x.2010.02879.x

Sanders, M. E., Akkermans, L. M. A., Haller, D., Hammerman, C., Heimbach, J., Hörmannsperger, G., et al. (2010). Safety assessment of probiotics for human use. *Gut Microbes* 1, 164–185.

Schillinger, U., and Holzapfel, W. H. (1996). Guidelines for manuscripts on bacteriocins of lactic acid bacteria. *Int. J. Food Microbiol.* 33, iii–v. doi: 10.1016/0168-1605(96)82773-5

Schlegel, L., Grimont, F., Collins, M. D., Régnault, B., Grimont, P. A. D., and Bouvet, A. (2000). *Streptococcus infantarius* sp. nov., *Streptococcus infantarius* subsp. *infantarius* subsp. nov. and *Streptococcus infantarius* subsp. *coli* subsp. nov., isolated from humans and food. *Int. J. System. Evol. Microbiol.* 50, 1425–1434. doi: 10.1099/00207713-50-4-1425

Schwemmlein, N., Pippel, J., Gazdag, E. M., and Blankenfeldt, W. (2018). Crystal structures of R-type bacteriocin sheath and tube proteins CD1363 and CD1364 from *Clostridium difficile* in the pre-assembled State. *Front. Microbiol.* 9:1750. doi: 10.3389/fmicb.2018.01750

Shukla, S. K., Murali, N. S., and Brillian, M. H. (2015). Personalizted medicine going precise: from genomics to microbiomics. *Trends Mol. Med.* 21, 461–461. doi: 10.1016/j.molmed.2015.06.002

Silva, C. C. G., Silva, S. P. M., and Ribeiro, S. C. (2018). Application of bacteriocins and protective cultures in dairy food preservation. *Front. Microbiol.* 9:594. doi: 10.3389/fmicb.2018.00594

Smith, L., and Hillman, J. D. (2008). Therapeutic potential of type A (I) lantibiotics, a group of cationic peptide antibiotics. *Curr. Opin. Microbiol.* 11, 401–408. doi: 10.1016/j.mib.2008.09.008

Strauch, E., Kaspar, H., Schaudinn, C., Dersch, P., Madala, K., Gewinner, C., et al. (2001). Characterization of enterocoliticin, a phage tail-like bacteriocin, and its effect on pathogenic *Yersinia enterocolitica* strains. *Appl. Environ. Microbiol.* 67, 5634–5642. doi: 10.1128/AEM.67.12.5634-5642.2001

Surawicz, C. M., Brandt, L. J., Binion, D. G., Ananthakrishnan, A. N., Curry, S. R., Gilligan, P. H., et al. (2013). Guidelines for diagnosis, treatment, and prevention of *Clostridium difficile* infections. *Am. J. Gastroenterol.* 108, 478–498. doi: 10.1038/ajg.2013.4

Svanström, Å., Boveri, S., Boström, E., and Melin, P. (2013). The lactic acid bacteria metabolite phenyllactic acid inhibits both radial growth and sporulation of filamentous fungi. *BMC Res. Notes* 6:464. doi: 10.1186/1756-0500-6-464

Szatraj, K., Szczepankowska, A. K., and Chmielewska-Jeznac, M. (2017). Lactic acid bacteria — promising vaccine vectors: possibilities, limitations, doubts. *J. Appl. Microbiol.* 123, 325–339. doi: 10.1111/jam.13446

Tejero-Sariñena, S., Barlow, J., Costabile, A., Gibson, G. R., and Rowland, I. (2012). *In vitro* evaluation of the antimicrobial activity of a range of probiotics against pathogens: evidence for the effects of organic acids. *Anaerobe* 18, 530–538. doi: 10.1016/j.anaerobe.2012.08.004

Thompson, N. E., and Pattee, P. A. (1981). Genetic transformation in *Staphylococcus aureus*: demonstration of a competence-conferring factor of bacteriophage origin in bacteriophage 80a lysates. *J. Bacteriol.* 148, 294–300.

Todorov, S. D. (2010). Diversity of bacteriocinogenic lactic acid bacteria isolated from boza, a cereal-based fermented beverage from Bulgaria. *Food Control* 21, 1011–1021. doi: 10.1016/j.foodcont.2009.12.020

Todorov, S. D., and Dicks, L. M. T. (2009). Bacteriocin production by *Pediococcus pentosaceus* isolated from marula (Scerocaryabirrea). *Int. J. Food Microbiol.* 132, 117–126. doi: 10.1016/j.ijfoodmicro.2009.04.010

Todorov, S. D., Franco, B. D. G. M., and Tagg, J. R. (2019). Bacteriocins of Gram positive bacteria having activity spectra extending beyond closely-related species. *Benef. Microbes* 10, 315–328. doi: 10.3920/BM2018.0126

Todorov, S. D., Wachsman, M., Tomé, E., Dousset, X., Destro, M. T., Dicks, L. M. T., et al. (2010). Characterisation of an antiviral pediocin-like bacteriocin produced by *Enterococcus faecium*. *Food Microbiol.* 27, 869–879. doi: 10.1016/j.fm.2010.05.001

Todorov, S. D., Wachsman, M., Ignatova-Ivanova, T. S., and Ivanova, I. (2014). *Lactobacillus plantarum* ST16Pa – are we ready to use it as bio-preservative culture? *Bulg. J. Agric. Sci.* 20(Suppl. 1), 55–58.

Trzasko, A., Leeds, J. A., Praestgaard, J., LaMarche, M. J., and McKenney, D. (2012). Efficacy of LFF571 in a hamster model of *Clostridium difficile* infection. *Antimicrob. Agents Chemother.* 56, 4459–4462. doi: 10.1128/AAC.06355-11

Udaondo, Z., Duque, E., and Ramos, J. L. (2017). The pangenome of the genus *Clostridium*. *Environ. Microbiol.* 19, 2588–2603. doi: 10.1111/1462-2920.13732

Udompijitkul, P., Paredes-Sabja, D., and Sarker, M. R. (2012). Inhibitory effects of nisin against *Clostridium perfringens* food poisoning and nonfood-borne isolates. *J. Food Sci.* 77, M51–M56. doi: 10.1111/j.1750-3841.2011.02475.x

Umu, ÖC., Bäuerl, C., Oostindjer, M., Pope, P. B., Hernandez, P. E., Perez-Martinez, G., et al. (2016). The potential of class II Bacteriocins to modify gut microbiota to improve host health. *PLoS One* 11:e0164036. doi: 10.1371/journal.pone.0164036

Uratani, Y., and Hoshino, T. (1984). Pyocin R1 inhibits active transport in *Pseudomonas aeruginosa* and depolarizes membrane potential. *J. Bacteriol.* 157, 632–636. doi: 10.1128/JB.157.2.632-636.1984

Vaishnavi, C. (2015). Fidaxomicin, the new drug for *Clostridium difficile* infection. *Indian J. Med. Res.* 141, 398–407. doi: 10.4103/0971-5916.159251

Valerio, F., Lavermicocca, P., Pascale, M., and Visconti, A. (2004). Production of phenyllactic acid by lactic acid bacteria: an approach to the selection of strains contributing to food quality and preservation. *FEMS Microbiol. Lett.* 233, 289–295. doi: 10.1111/j.1574-6968.2004.tb09494.x

Vieco-Saiz, N., Belguesmia, Y., Raspoet, R., Auclair, E., Gancel, F., Kempf, I., et al. (2019). Benefits and inputs from lactic acid bacteria and their bacteriocins as alternatives to antibiotic growth promoters during food-animal production. *Front. Microbiol.* 10:57. doi: 10.3389/fmicb.2019.00057

Vujkovic-Cvijin, I., Dunham, R. M., Iwai, S., Maher, M. C., Albright, R. G., Broadhurst, M. J., et al. (2013). Dysbiosis of the gut microbiota is associated with HIV disease progression and tryptophan catabolism. *Sci. Transl. Med.* 5:193ra191. doi: 10.1126/scitranslmed.3006438

Wachsman, M. B., Castilla, V., de Ruiz Holgado, A. P., de Torres, P. A., Sesma, F., and Coto, C. E. (2003). Enterocin CRL35 inhibits late stages of HSV-1 and HSV-2 replication *in vitro*. *Antiviral Res.* 58, 17–24. doi: 10.1016/s0166-3542(02)00099-2

Wiedemann, I., Breukink, E., van Kraaij, C., Kuipers, O. P., Bierbaum, G., and de Kruijff, B. (2001). Specific binding of nisin to the peptidoglycan precursor lipid II combines pore formation and inhibition of cell wall biosynthesis for potent antibiotic activity. *J. Biol. Chem.* 276, 1772–1779. doi: 10.1074/jbc.M006770200

Wilcox, M. (2016). Interview with professor Mark Wilcox. *Future Microbiol.* 11, 991–994. doi: 10.2217/fmb-2016-0123

Wilcox, M. H., and Dave, J. (2001). Treatment options in *Clostridium difficile* infections. *Rev. Med. Microbiol.* 12, 21–28. doi: 10.1097/00013542-200101000-00003

Wiström, J., Norrby, S. R., Myhre, E. B., Eriksson, S., Granstrom, G., Lagergren, L., et al. (2001). Frequency of antibiotic-associated diarrhoea in 2462 antibiotic-treated hospitalized patients: a prospective study. *J. Antimicrob. Chemother.* 47, 43–50. doi: 10.1093/jac/47.1.43

Xuan, C., Shamonki, J. M., Chung, A., Di Nome, M. L., Chung, M., Sieling, P. A., et al. (2014). Microbial dysbiosis is associated with human breast cancer. *PLoS One* 9:e83744. doi: 10.1371/journal.pone.0083744

Zacharof, M. P., and Lovitt, R. W. (2012). Bacteriocins produced by lactic acid bacteria a review article. *APCBEE Procedia* 2, 50–56. doi: 10.1016/j.apcbee.2012.06.010

Zheng, M., Zhang, R., Tian, X., Zhou, X., Pan, X., and Wong, A. (2017). Assessing the risk of probiotic dietary supplements in the context of antibiotic resistance. *Front. Microbiol.* 8:908. doi: 10.3389/fmicb.2017.00908

Zhu, W., Winter, M., Byndloss, M., Spiga, L., Duerkop, B. A., Hughes, E. R., et al. (2018). Precision editing of the gut microbiota ameliorates colitis. *Nature* 553, 208–211. doi: 10.1038/nature25172

Zink, R., Loessner, M. J., and Scherer, S. (1995). Characterization of cryptic prophages (monocins) in *Listeria* and sequence analysis of a holin/endolysin gene. *Microbiology* 141, 2577–2584. doi: 10.1099/13500872-141-10-2577

Conflict of Interest: H-JK and WH are employed by company HEM Inc.

The remaining authors declare that the research was conducted in the absence of any commercial or financial relationships that could be construed as a potential conflict of interest.

frontiers in Bioengineering and Biotechnology

ORIGINAL RESEARCH
published: 08 October 2020
doi: 10.3389/fbioe.2020.580090

A Novel Method for Long-Term Analysis of Lactic Acid and Ammonium Production in Non-growing *Lactococcus lactis* Reveals Pre-culture and Strain Dependence

Avis Dwi Wahyu Nugroho[1,2,3], *Michiel Kleerebezem*[1,3] *and Herwig Bachmann*[1,2,4]*

[1] TiFN, Wageningen, Netherlands, [2] Health Department, NIZO Food Research, Ede, Netherlands, [3] Laboratory of Host-Microbe Interactomics, Wageningen University and Research Centers, Wageningen, Netherlands, [4] Systems Biology Lab, Vrije Universiteit Amsterdam, Amsterdam, Netherlands

OPEN ACCESS

Edited by:
Peter Ruhdal Jensen,
Technical University of Denmark, Denmark

Reviewed by:
Dave Siak-Wei Ow,
Bioprocessing Technology Institute (A*STAR), Singapore
Feng Li,
Tianjin University, China

***Correspondence:**
Herwig Bachmann
herwig.bachmann@nizo.com

Specialty section:
This article was submitted to Synthetic Biology, a section of the journal Frontiers in Bioengineering and Biotechnology

Received: 04 July 2020
Accepted: 15 September 2020
Published: 08 October 2020

Citation:
Nugroho ADW, Kleerebezem M and Bachmann H (2020) A Novel Method for Long-Term Analysis of Lactic Acid and Ammonium Production in Non-growing Lactococcus lactis Reveals Pre-culture and Strain Dependence. Front. Bioeng. Biotechnol. 8:580090. doi: 10.3389/fbioe.2020.580090

In various (industrial) conditions, cells are in a non-growing but metabolically active state in which *de novo* protein synthesis capacity is limited. The production of a metabolite by such non-growing cells is dependent on the cellular condition and enzyme activities, such as the amount, stability, and degradation of the enzyme(s). For industrial fermentations in which the metabolites of interest are mainly formed after cells enter the stationary phase, the investigation of prolonged metabolite production is of great importance. However, current batch model systems do not allow prolonged measurements due to metabolite accumulation driving product-inhibition. Here we developed a protocol that allows high-throughput metabolic measurements to be followed in real-time over extended periods (weeks). As a validation model, sugar utilization and arginine consumption by a low density of translationally blocked *Lactococcus lactis* was designed in a defined medium. In this system *L. lactis* MG1363 was compared with its derivative HB60, a strain described to achieve higher metabolic yield through a shift toward heterofermentative metabolism. The results showed that in a non-growing state HB60 is able to utilize more arginine than MG1363, and for both strains the decay of the measured activities were dependent on pre-culture conditions. During the first 5 days of monitoring a ∼25-fold decrease in acidification rate was found for strain HB60 as compared to a ∼20-fold decrease for strain MG1363. Such measurements are relevant for the understanding of microbial metabolism and for optimizing applications in which cells are frequently exposed to long-term suboptimal conditions, such as microbial cell factories, fermentation ripening, and storage survival.

Keywords: high throughput screening, long-term biocatalysis, conversion decay, prolonged acidification, arginine utilization, lactic acid bacteria

INTRODUCTION

The widespread use of bacteria in many biotechnological applications is not only attributed to their growth ability but also to their metabolic persistence under non-growing/dormant condition. The arrest of cell division coincides with limited de-novo protein synthesis, whereas metabolic activity and survival can be maintained over a long period of time (Ercan et al., 2015; Erkus et al., 2016). This non-growing state can be induced by adverse circumstances, e.g., starvation, lethal stress or inhibitory compounds (Oliver et al., 1995; Keren et al., 2004; Magajna and Schraft, 2015), as commonly found in industrial processes, such as bioreactor metabolite production (Förberg et al., 1983), wastewater treatment (Witzig et al., 2002), and food processes (Millet and Lonvaud-Funel, 2000). In some applications, for example microbial cell factories, such physiological state might be desired since metabolic fluxes are diverted away from cell growth, resulting in the increase of metabolic yield (Sonderegger et al., 2005). In food fermentation applications, the long-term metabolic activity is an important function of starter cultures that contributes to product quality, stability and safety (Marcobal et al., 2006; Liu et al., 2018). Therefore, the study of persisting metabolic activity in non-growing cells is of relevance for food fermentation processes, and the ability to steer the activity of such cells can strongly contribute to process control.

Lactic acid bacteria (LAB) and *Lactococcus lactis* in particular are important industrial microorganisms and the ability to steer their metabolic activities in non-growing cultures is of great interest. As an example, the majority of flavor volatiles is produced by the starter culture during cheese ripening, where the most relevant ones are derived from nitrogen catabolism, such as 3-methylbutanal, 2-methylbutanal, and 2-methylpropanal (Smid and Kleerebezem, 2014). The combination of cheese production-related environments, such as the dynamic processing conditions, low temperatures, high salt concentrations, and carbon starvation results in non-growing but metabolically active starter culture cells. Despite the loss of culturability during cheese ripening, it has been shown that a high level of cellular intactness was retained and only a small fraction of the starter population appeared to exhibit membrane injury (Erkus et al., 2016). Furthermore, studies on the metabolite production of *Lactococcus lactis* have shown that the cheese-related volatile profile can be mimicked best with near-zero growth conditions achieved by retentostat cultivation (van Mastrigt et al., 2018b) or by incubation in nutrient-free buffer (van de Bunt et al., 2014). Conversely, the prolonged metabolic activity of non-growing starter cultures can also pose challenges in ensuring product quality during storage. Post-production acidification is an important example of such phenomenon, in which slow but persistent lactic acid production in stored yogurts eventually leads to shorter shelf life due to perceivable changes in flavor and acidity leading to lower consumer appreciation and acceptance (Shah et al., 1995; Settachaimongkon et al., 2016).

Since the renewal of proteins is limited, the role of repair, maintenance and active degradation becomes particularly important. During prolonged incubation of non-growing cells, enzyme decay is inevitable but can be minimized by intracellular mechanisms that ensure protein quality control, such as the Clp-related protease machinery (Frees et al., 2001; Kock et al., 2004). Upon carbon starvation, lactococci were shown to lose the ability to be cultured but at the same time they could maintain intact membranes and showed metabolic activity for up to 3.5 years (Ganesan et al., 2007). The overall cell fitness and performance can be greatly affected by the cellular proteome composition that is dependent on the conditions applied during the growing phase (Dijkstra et al., 2014; Settachaimongkon et al., 2015). Consequently, the initial enzyme amount and the rate of enzyme-activity decay will influence the overall production of metabolites over prolonged periods of incubation. In addition, environmental conditions, such as pH, and temperature, as well as the level of oxidative conditions, and inhibitor exposure also affect protein and cellular stability. Collectively, these environmental parameters determine the actual rate and stability of metabolite formation, but they are often determined as separate entities and/or in a simplified *in vitro* system.

In this study, we developed a method that allows us to measure catalytic activity of a complete pathway based on continuous pH monitoring through a fluorescent readout in a 384-well plate format. pH-monitoring is employed as a model since it applies to primary metabolism but also amino acid catabolism, that both involve a substantial metabolic flux. The system is designed to prevent product inhibition, which is achieved by employing cultures at low cell densities combined with the translation-inhibiting antibiotic erythromycin. Blockage of de-novo protein synthesis enabled us to compare the impact on acidification and arginine consumption rate of distinct strains and cellular proteome compositions, that were generated through different (pre)-culture conditions. The method allowed continuous pH measurements in real-time over periods of several weeks, without the emergence of detectable product inhibition as commonly found in batch systems.

MATERIALS AND METHODS

Strain and Cultivation Conditions

Lactococcus lactis subsp. *cremoris* NCDO712 (Gasson, 1983), HB60 (Bachmann et al., 2013), and MG1363 (Wegmann et al., 2007) were grown on chemically defined medium for prolonged cultivation (CDMPC) as described previously (Price et al., 2019). Medium was supplemented with either lactose 30 mM, galactose 55 mM, or glucose 55 mM depending on experimental design. All pre-cultures were standardized and started with a single use aliquot of glycerol stock which was 1,000-fold diluted in medium and cultured overnight (as described in Price et al., 2019). Overnight cultures were sub-cultured (40-fold dilution) in fresh medium and harvested during the early exponential phase (OD 0.1–0.2). *Lactococcus lactis* was routinely cultured at 30°C without aeration. The growth rate of *L. lactis* NCDO712 in CDM+0.5% glucose is approximately 0.7/h, which is a bit slower compared to 0.8/h reached in the rich medium M17 supplemented with 0.5% glucose.

Prolonged Measurements of Culture pH

Exponentially growing cells were centrifuged at 5,000 g for 10 min and washed twice with an equal volume of PBS, followed by resuspending the cells at a standard density between 1E+07 and 2.5E+07 cells/mL in fresh CDMPC (Mn-omitted) supplemented with erythromycin (5 μg/mL) and 10μM 5(6)-carboxyfluorescein (Sigma-Aldrich 21877). Individual sugar was supplemented as the sole carbon source in the media depending on experimental design at concentration of 30 mM (lactose) or 55 mM (glucose or galactose). In experiments measuring arginine utilization, the CDMPC pH was set to 5.5 (rather than 6.5 in standard CDMPC) and instead of one of the sugars, L-arginine was supplemented at a final concentration of 30 mM. All measurements were performed with at least four replicates in black clear bottom 384-well plate (Greiner Bio-One 781076). Fluorescence (λex/em: 485/535 nm) was measured at constant gain, at 30 min intervals during a period of up to 3 weeks at 30°C in a microplate reader (Tecan Safire 2). The gain was determined to ensure standard pH solutions (4.0–7.0) were in the detectable range.

Viable Count and Membrane Integrity Determination

Measurements of culturable bacteria were performed through plating on CDMPC supplemented with 1% glucose and 0.5% UltraPure agarose (Invitrogen 16500500). Serial dilutions were prepared in PBS and 100 μL of the diluted cultures were plated on agar plates. Plates were incubated at 30°C for 24–48 h and colonies were enumerated.

Membrane integrity of cells during prolonged incubation was analyzed using Live/Dead BacLightTM Bacterial viability and counting kit (Invitrogen L34856) and a BD LSR Fortessa Flow Cytometry instrument (BD Biosciences), according to manufacturer instructions with some modifications. A staining mixture was prepared with 1.5 μL of PI, 1.5 μL of SYTO 9 stock-solutions, 5 μL microsphere standard (1E+08 beads/mL), 892 μL of running buffer (FACS Flow), and 100 μL of sample resulting in a total of 1 mL assay reaction. Fluorescence signals were measured with FITC and PE-Texas Red detectors. Gating was set on the basis of fresh overnight culture (live) and cells incubated in 60% ethanol (dead).

Fermentation End Product Analysis

The concentrations of organic acids in media (lactic acid, formic acid, acetic acid, and ethanol) were determined by high performance anion exchange chromatography (HPAEC) with UV and refractive index (RI) detection as previously described (Hugenholtz and Starrenburg, 1992). Culture supernatant samples were collected and filtered using 0.20 μm polyethersulfone (PES) membranes and stored at -20°C before analysis.

Calculation of Lactic Acid or Ammonia Production Rate

Raw data files from the microplate reader were analyzed and plotted with R (v 3.6.1). Fluorescent signals were converted to pH values based on a standard curve obtained with fluorophore-containing medium set at a range of pH values. To correct for buffering capacity, the proton equivalent of the pH values were calculated. Subsequently, the acid production was determined based on the logarithmic equation which relates the accumulation of acid and the change in proton equivalent. This relation was obtained from a titration curve which was prepared by step-wise addition of lactic acid (2 M) to CDMPC in the presence of 2.5E+07 cells/mL for the extended operational range of the measurement (pH 6.5–4.0). In case of arginine consumption, the ammonia production was analogously determined using a titration curve of ammonia from pH 5.5–7.0. The production rate (M/h) was calculated periodically in equal intervals of lactate or ammonium production e.g., every 0.001 M.

RESULTS

Optimization of Cell Density and Medium Composition Allows Acidification Measurements for Weeks Without Product Inhibition in Non-growing Cells

The glycolytic flux of *Lactococcus lactis* has been reported to run at maximal rate during balanced growth in batch culture (Koebmann et al., 2002b). The high flux through glycolysis and lactic acid production leads to a fast decline in pH and high accumulation of lactate, which eventually stops acidification. In non-growing cells of *L. lactis*, the glycolytic flux was found to be 37% of exponentially growing cells (Koebmann et al., 2002a), which is still relatively high. To enable a prolonged measurement of the product formation rate, a number of challenges, such as product inhibition, continuous monitoring, sufficient throughput, and the maintenance of non-growing state need to be overcome. To achieve this, we established a microplate-based assay in which the pH of non-growing cells can be continuously followed in a microplate reader through the use of commercially available fluorescent pH indicator (5/6-carboxyfluorescein). The assay consists of a defined medium in which cells are fully translationally blocked with erythromycin (5 μg/mL) and provided with excess supply of a catabolizable substrate. Under circumstances with e.g., sugar (1% w/v) as a substrate and high cell densities (e.g., 1E+08 cells/mL), this setup leads to full acidification of the solution within 24–48 h, when further acidification is blocked by product inhibition. In contrast, in the absence of translation inhibition, the exponential growth of cells and the concomitant increase of glycolytic flux will typically lead to complete acidification within less than 8–12 h. Therefore, to enable long term acidification online monitoring, we ensured the cell density is kept constant by complete inhibition of protein translation.

Cell concentration in the range of 1–2.5E+07 /mL in 20 mM phosphate buffer resulted in slow but detectable acidification activity that remains in a high-buffering range. This allowed us to follow measurements for 3 weeks. The results consistently showed that acidification ranged in pH from 6.5 to 5.75 and produced less than 20 mM lactate over the complete period.

Considering the pKa of lactate at 3.8, the majority of lactate (∼99%) will be in a deprotonated state, which will not readily diffuse across the cell membrane. During the long period of measurement, the fluorescent signal was stable and showed negligible change in signal intensity (**Figure 1A**). The detection accuracy and frequent reading interval (30 min) allows real-time and precise monitoring. We opted to use a defined medium as it allows well-defined alterations of individual constituents, however, it is possible to use undefined medium, such as M17, but medium-composition manipulations will be less defined and higher fluorescence background might reduce measurement resolution. Furthermore, the use of assay medium that closely resembles growing medium of the bacteria aims to optimize conditions for all cellular processes. In combination with the use of a microplate (384-wells), the setup allows high-throughput comparisons of prolonged acidification profiles.

Conversion of the Fluorescent Signal to Acid Production Rate

The fluorescent signal in our assay was not directly reflecting organic acid production because of the buffer capacity being higher at the initial (near neutral) pH compared to the buffering capacity toward the end of the fermentation (>pH 5). To get a better representation of lactic acid production, we established an analysis pipeline where the fluorescent signal (**Figure 1A**) is first converted to pH (**Figure 1B**) based on a calibration curve of medium prepared at different pH values (pH was set by hydrochloric acid addition). Subsequently, the pH value is converted to the proton equivalent, which is then used to obtain the equivalent of acid produced (**Figure 1C**). The latter conversion was based on the titration of pure lactic acid to the assay medium in the presence of cells to accommodate the contribution of cells to buffering capacity. Once the acid formation over time was calculated, the rate of formation and its decline could be derived as a function of time. However, large differences in rate could result in unfair comparison due to the difference in total reaction number per enzyme. Therefore, the production rate was calculated within periods of equal production of acid e.g., 1 mM starting from the period above the noise threshold determined from a negative control (**Figure 1C**). In multiple experiments, the signal considered as noise was consistently found to be the first 7.5–10 mM of lactate produced. This can be seen in the negative control that showed signal noise at 5–10 mM of lactate produced (**Figure 1C**). This sensitivity to noise is possibly due to the high buffering capacity in this pH region, which leads to small signal variation resulting in relatively large noise in lactate production (with a relatively constant signal of approximately 40,000 RFU in the control sample (**Figure 1A**) noise of 1,000–1,500 RFU is responsible for the observed 5–10 mM variation in lactate). The measurements from this initial region were therefore not considered in the data analysis. The decline in lactic acid production rate over time was plotted against lactate accumulation (**Figure 1D**) and typically resulted in a straight-line when transformed to its log-values (**Figure 1E**) or its inverse (**Figure 1F**), following the first order or second order of rate kinetic, respectively. From this plot, the kinetic of rate decline could be determined from the slope and the maximum/initial production rate was predicted from Y-intercept. Based on these kinetic parameters, the behavior in longer period of time could be estimated, e.g., lactate yield in 2 months. As an exemplary case, *L. lactis* NCDO712 (2.5E+07 cells/mL) pre-cultured in lactose was transferred into the assay medium containing the same sugar and followed for 2 weeks. A 15-fold reduction of the lactic acid production rate from 3.98E-04 to 2.51E-05 M/h was observed (**Figure 1D**).

Translational Blocking Leads to Non-culturable Cells and Has No Influence on Organic Acid Profiles

The addition of erythromycin results in the physical blocking of the nascent-peptide exit tunnel in the ribosome which halts translation (Tenson et al., 2003). We tested different erythromycin concentrations and found that 5 μg/mL was sufficient to prevent an increase in culture density over 2 weeks, indicating that cell growth was blocked due to continuous translational blocking. Such treatment may cause cell dormancy or induce cell death which is influenced by not only the kinetics of drug-ribosome interactions, but also species or strains, growth conditions, cell density, and the antibiotic concentration (Svetlov et al., 2017). When prolonged translation inhibition is applied, cell death is inevitable and can be responsible to the decline in product formation to some extent. Antibiotic exposure to *Lactococcus lactis* has also been reported to induce heterogenous population response regarding dormancy states and the corresponding death rates and metabolic activity (van Tatenhove-Pel et al., 2019). To characterize the effects of erythromycin in our experiments, a combination of CFU counting and live-dead staining measurements was employed to determine how cellular viability and integrity relate to the observed decline in acidification. For *L. lactis* NCDO712 pre-cultured and transitioned to lactose, the amount of colony forming units was decreasing from 7.25 to 5.65 log10 CFU/mL in 11 days (**Figure 2A**), which is equivalent to roughly a 40-fold overall decline. On the other hand, the number of intact cells according to live-dead stained flow cytometry counts was more or less constant at approximately 7 log cells/mL. Moreover, the fraction of cells classified as intact (live+injured-cells) remained constantly above 75% (**Figure 2B**), displaying a slow progression toward cell populations with compromised membrane-integrity ("injured cells" in the analysis). In the 2-week incubation period, approximately 40% of the cells initially qualified as "live" cells progressed to the "injured" population, representing only a 2.5-fold reduction of the "live" population, which is much less than the observed 40-fold reduction in CFU enumerations. This observation is in agreement with the detection of so-called "viable but non-culturable" (VBNC) *L. lactis* cells during 2 weeks of retentostat cultivation (van Mastrigt et al., 2018a) and cheese ripening (Erkus et al., 2016). Overall, the 40-fold decrease in CFU does not match the 15-fold decrease in acidification rate and the results of the live-dead staining. This suggests that VBNC cells appear in the population, but the current methodology does not allow to

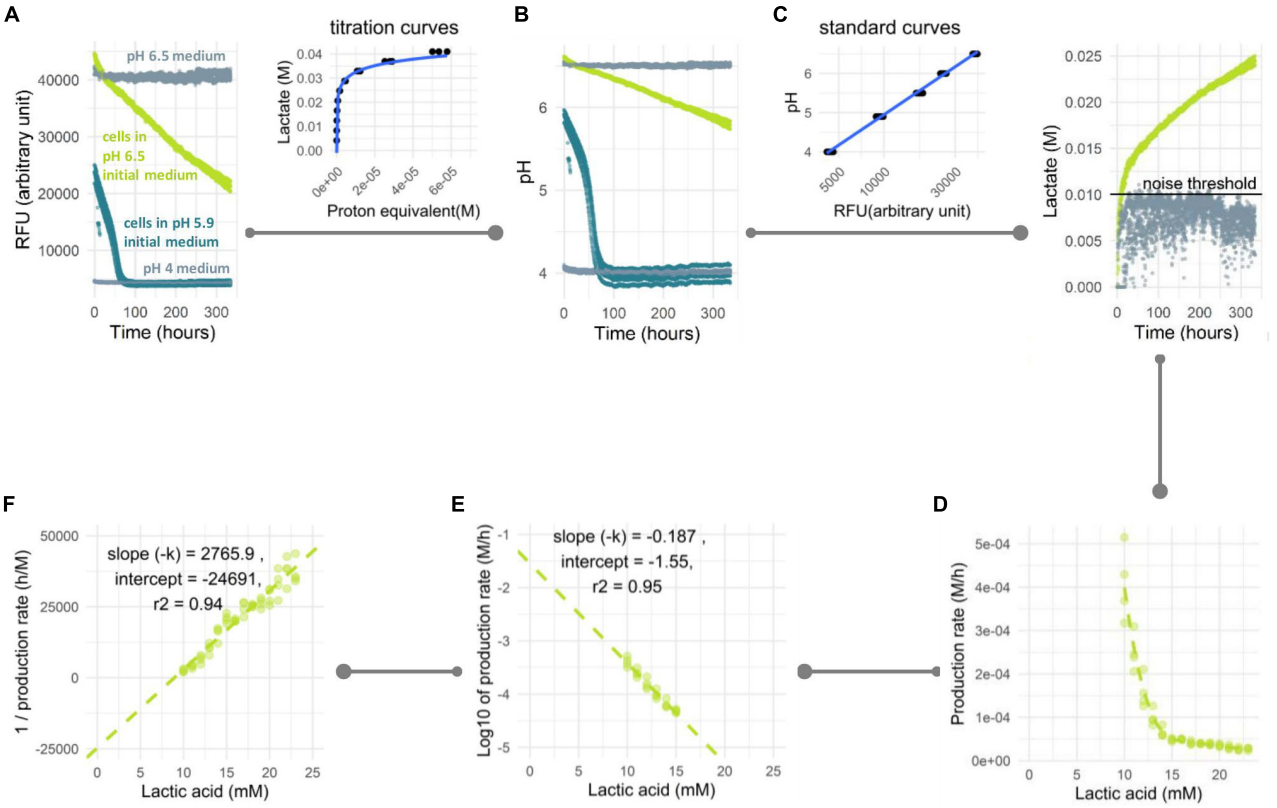

FIGURE 1 | Analysis pipeline of prolonged acidification in non-growing cells. *L. lactis* NCDO712 cells were pre-cultured in lactose 1%, harvested at mid-exponential growth and transferred to the assay medium with lactose 1%. **(A)** Fluorescent signal was measured for assay medium without cells at pH 4 and 6.5 (light gray), cells (2.5E+07/mL) in assay medium at an initial pH of 6.5 (light green) and an initial pH of 5.9 (dark green). **(B)** Based on a standard curve, the RFU were converted to pH. In samples with a low starting pH (dark green) acidification stopped due to product inhibition at pH 4 while for a high starting pH acidification was still ongoing after more than 300 h. **(C)** Based on a titration curve, the pH profile was converted to the amount of lactic acid produced. The noise threshold was determined from the non-biological fluctuation of signal based on a negative control at pH 6.5. **(D)** The lactate production rate is plotted as a function of the total amount of lactic acid produced. Decline in production could be calculated following first order **(E)** or second order **(F)** reaction kinetics. The experiment was carried out three times with four replicates with reproducible results. Four replicate curves are shown in this plot.

discern the contribution of different cell populations to the acidification profiles.

Besides cell viability, we also determined the concentration of organic acids during the prolonged acidification measurements to confirm the fluorescence-based result. While it is known that the strain used produces predominantly lactic acid (>90%) during growth on lactose, low levels of acetic acid production might lead to slight misestimation of the lactic acid production level. The switch to heterofermentative metabolism (acetic and lactic acid formation) is known to occur in conditions with reduced glycolytic flux (Thomas et al., 1979, 1980) or increased exposure to molecular oxygen and intracellular redox balance (Garrigues et al., 1997; Lopez de Felipe et al., 1998; Melchiorsen et al., 2000), which could both be apparent during the prolonged assay developed here. Therefore, we investigated whether the induced non-growing state led to changes in fermentation pathways. Under the experimental conditions used, the cells remained a homofermentative (>90% of carbon flux toward lactic acid) metabolite profile during the 2-week incubation (**Figure 2D**). The final concentrations of lactic acid determined reached almost 20 mM, whereas concentrations of formic and acetic acid did not exceed 1 mM (**Figure 2D**). Moreover, the lactic acid concentrations determined matched accurately (R-squared value of 0.94) with the concentrations estimated based on fluorescence measurements using the lactic acid titration curve (**Figure 2C**).

Sugar and Arginine Utilization Are Strain and Pre-culture Dependent

The presented standardized protocol allows for the testing of numerous modulations of environmental parameters as well as the comparison of different strains. To demonstrate this, the developed protocol was used to test the influence of pre-culture conditions on the long-term acidification activity using different pre-culture and assay substrates. In addition, the wild-type strain *L. lactis* MG1363 (plasmid-free derived of NCDO712) and its experimentally evolved derivative HB60 (Bachmann et al., 2013) were employed to further characterize the phenotype difference of these strains. Expression for carbon

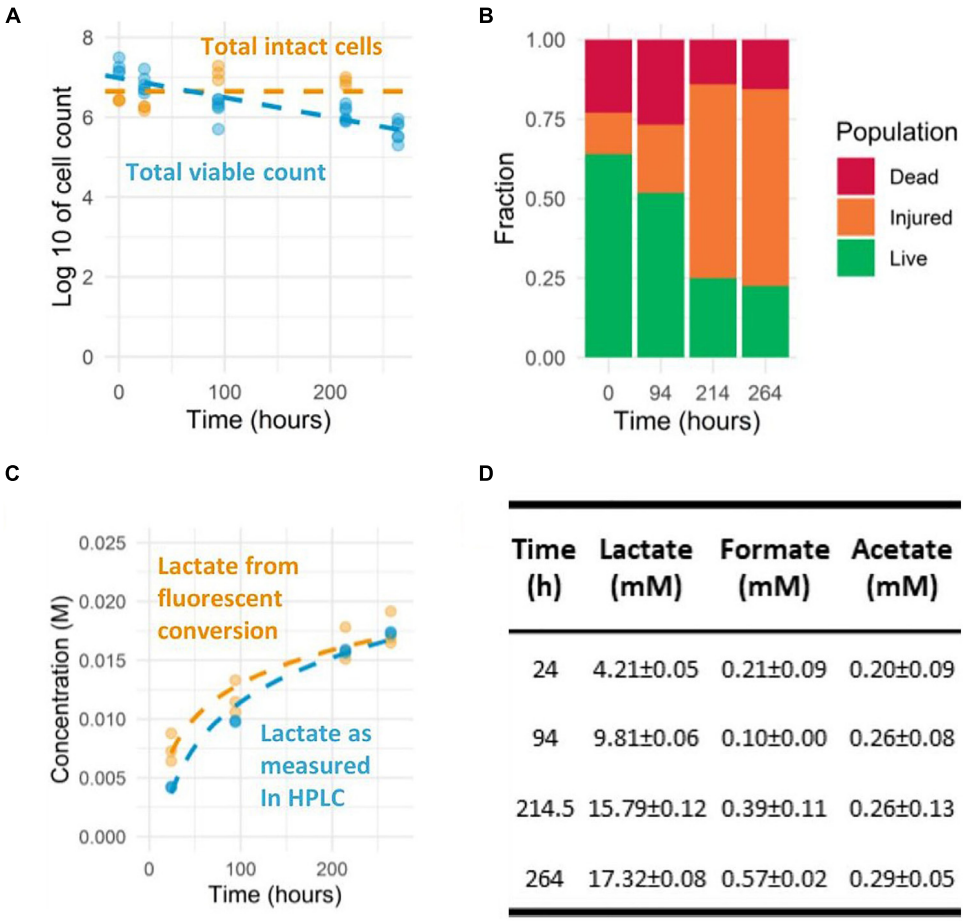

D

Time (h)	Lactate (mM)	Formate (mM)	Acetate (mM)
24	4.21±0.05	0.21±0.09	0.20±0.09
94	9.81±0.06	0.10±0.00	0.26±0.08
214.5	15.79±0.12	0.39±0.11	0.26±0.13
264	17.32±0.08	0.57±0.02	0.29±0.05

FIGURE 2 | Prolonged observation of *L. lactis* NCDO712 pre-cultured in CDMpc-lactose 1%, harvested at mid-exponential growth and transferred to the assay medium with lactose 1%. **(A)** Colony forming units and intact cell count as measured by flow-cytometry. **(B)** The different cell fractions of the life-dead staining as measured by flow-cytometry. **(C)** Lactate accumulation derived from fluorescent measurements and HPLC determination show good agreement (R-squared value of 0.94) (dashed lines indicate semi-logarithmic fit). **(D)** The organic acid production profiles as determined by HPLC were dominated by lactic acid throughout the experiment.

source utilization pathways is governed by carbon catabolite repression to ensure hierarchical utilization of preferred carbon source. As a consequence of catabolite repression, it was not unexpected to find that mid-exponential *L. lactis* MG1363 and HB60 pre-cultured in glucose showed no detectable utilization of galactose when it was provided to translationally blocked cells in the assay medium (data not shown). Growth on glucose is known to effectively repress the expression of the enzymes of the Leloir pathway that is required to import and utilize galactose as a carbon and energy source. In contrast, galactose pre-cultured *L. lactis* could effectively utilize either glucose or galactose during the translationally blocked assay conditions (**Figure 3A** middle and left). However, the glucose utilization rate (as measured by lactic acid formation rate) rapidly declined and halted within 75 h (**Figure 3B** middle). Interestingly, we observed higher acidification rates in MG1363 than HB60, which is in agreement with previous findings where due to a point-mutation (F65L) in *ptnD*, HB60 displays reduced glucose import activity and consequently a lower glycolytic flux compared to its parental strain (Bachmann et al., 2013). Higher acidification rates were also observed for galactose pre-cultured MG1363 in the prolonged assay in comparison to galactose pre-cultured HB60, irrespective of the carbon source provided during the assay (glucose or galactose). Notably, the acidification rates seem to decline faster in HB60 as compared to MG1363 (**Figure 3B**) under all assay conditions. Within 5 days of measurement, up to 25-fold decrease in acidification rates was found for strain HB60 as opposed to roughly 20-fold for strain MG1363. Since *L. lactis* MG1363 grown on galactose and HB60 displays a mixed-acid fermentation profile, it may be that the calculated acid production is somewhat misestimated, but the kinetics of production decline remains reliable due to normalization to the produced amount of acid. Moreover, the pH values during the prolonged acidification assay are between 5.75 and 6.5, where both acetic (pKa = 4.75) and formic (pKa = 3.75) acid are predominantly present in their deprotonated form (>90 and >99%, respectively). The calculated proton equivalent is barely affected by undissociated H^+ ions from formic acid, but rather slightly affected by undissociated H^+

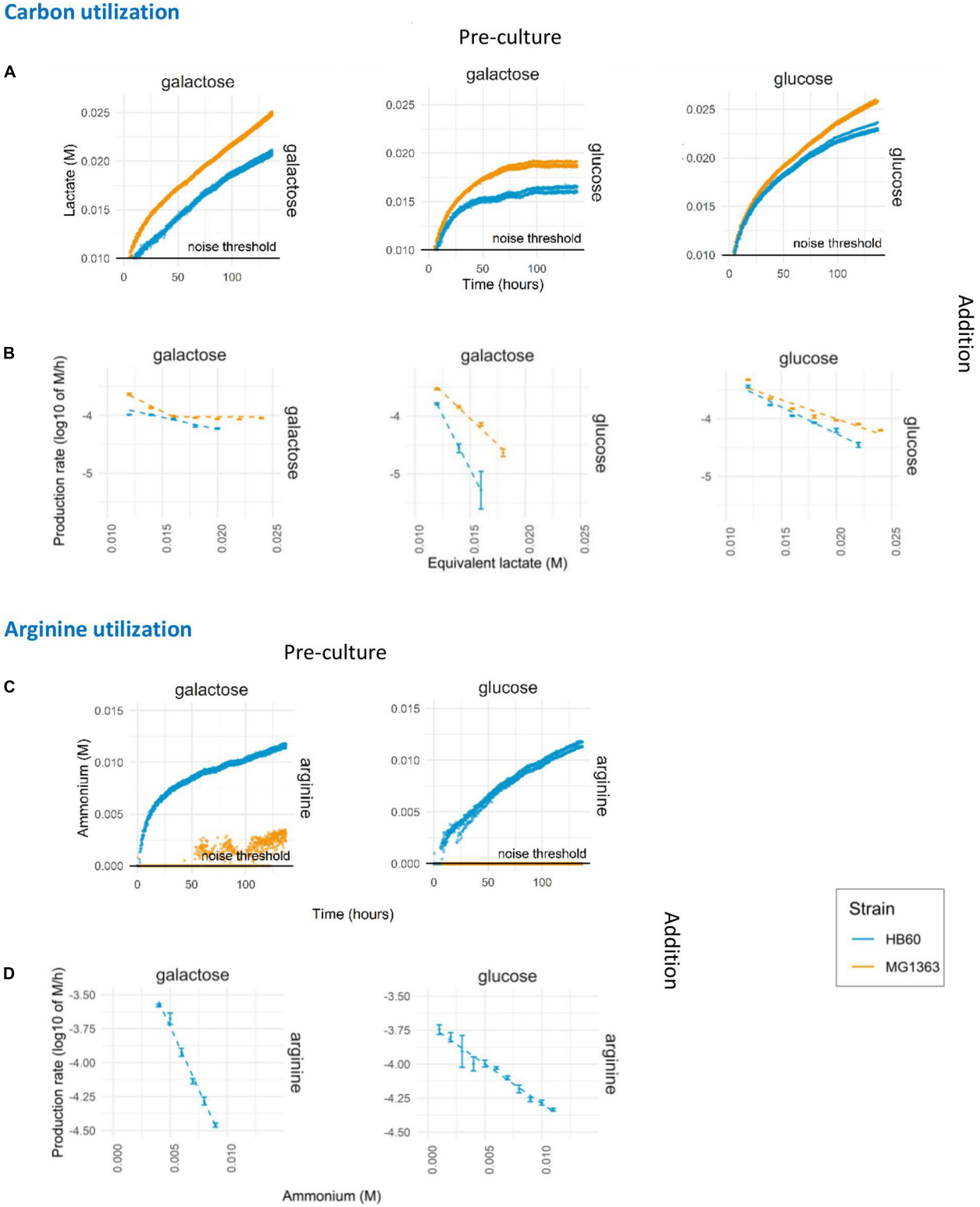

FIGURE 3 | Prolonged assay of carbon and arginine utilization. *L. lactis* MG1363 (orange) and HB60 (blue) were harvested at mid-exponential growth following pre-culture (top label) in 1% w/v of glucose or galactose and subsequently transferred to translationally blocked assay mediums with different carbon source (right side label) at 2.0E+07/mL cell density. **(A)** Lactate production. **(B)** The decline in lactate production rates. **(C)** Ammonium production. **(D)** The decline in ammonium production rates. Dashed lines indicate the linear fits of the data. Noise threshold was determined from the non-biological fluctuation of signal based on a negative control at pH 6.5 (lactate production) and pH 5.5 (ammonium production). Error bars indicate standard deviation of the experiment (n = 4).

ions from acetic acid. In our setup, a higher flux toward acetate would potentially result in more protons released due to the stoichiometry of the end products and the high buffer pH which ensures that lactate and acetate are deprotonated. This means our system might underestimate the differences in acidification rate between MG1363 and HB60 and the discussed effect might actually be larger than what is shown.

Next to lowering the pH by carbon fermentation and organic acid production, the presented method also allows for similar measurements of pathways that lead to metabolite production that increase the environmental pH. To exemplify this possibility, we characterized the arginine utilization pathway activity over extended periods of time in *L. lactis* strains MG1363 and HB60 that were incubated in assay media that lack a carbon source, and with an initial pH set to 5.5. This enables the detection of a pH increase due to the formation of one of the arginine pathway products, ammonium (**Figure 3C**). Besides ammonium, arginine catabolism by the arginine deiminase (ADI) pathway also generates ornithine, CO_2 and ATP (Poolman et al., 1987), which contribute to the enhanced acid stress tolerance observed in cells that actively express this pathway (Budin-Verneuil et al., 2004). The detected pH-increase curves established that there is significant ammonium production in *L. lactis* HB60, but that this activity could not readily be detected in MG1363 (**Figure 3C**). Especially glucose pre-cultured cells of MG1363 appeared to lack ammonium production entirely, whereas the very modest pH increase observed in galactose pre-cultured MG1363 cells suggests that these cells did convert arginine to ammonium, albeit at a marginal and barely detectable level. Strikingly, when analyzing the ammonium production rates decline over time in *L. lactis* HB60 (**Figure 3D**), we observed a faster decline in galactose pre-cultured cells compared to glucose pre-cultured cells. Overall, this demonstrates the suitability and sensitivity of the method to capture the metabolic pathway activity levels over prolonged periods of time, and it enables the study of strain and pre-culture dependent differences.

DISCUSSION

Here we describe a high-throughput approach and analysis pipeline for prolonged measurements of metabolic activity using translationally blocked *L. lactis* cells. As model pathways, we employed carbohydrate and amino acid utilization of which the products can be readily detected by measurement of the pH of the medium. The novelty in the presented approach lies in the fact that real-time monitoring of lactic acid formation or ammonium accumulation due to arginine deamination can be performed for up to several weeks by a relatively straightforward and simple microplate-based assay. Prolonged product-formation measurements can be readily tracked in low-density, translation-blocked cells, which is critical to prevent cell growth and adaptation and product inhibition. To some extent, these translationally blocked cells may also mimic aspects of cellular physiology and pathway persistence in the non-growing state that many cells experience during environmental and industrial conditions. This possible parallel opens several avenues to test industrially and environmentally interesting phenotypic properties in changing environments. In the case that strains of interest carry erythromycin resistance cassettes, there are multiple antibiotic alternatives that could likely be employed for the same purpose, such as chloramphenicol, and azithromycin (Svetlov et al., 2017; Yerlikaya, 2019). Alternatively, a non-growing state can be achieved by nitrogen starvation or omission of essential nutrients, although in such a system the complete inhibition of translation cannot be guaranteed as internal turnover of the limiting molecules might occur.

The presented method was used to compare the metabolic capacity of two closely related strains. *L. lactis* MG1363 and HB60 which is a derivative of MG1363 that contains a point-mutation (F65L) in its *ptnD* gene. HB60 is reported to have a higher ATP yield when growing on glucose at the expense of its growth rate (Bachmann et al., 2013). However, the expression of other ATP-generating pathways, such as arginine deiminase pathway was not investigated in this strain, to date. While the mutated phosphotransferase system (PTS^{Man}) serves mainly as a high-affinity glucose transport system in *L. lactis*, it has also been suggested to be involved in galactose transport in *L. lactis* MG1363 (Neves et al., 2010). Investigating carbon and arginine utilization, we demonstrated that acidification rates of MG1363 were higher than those of HB60 not only for glucose utilization, but also for galactose utilization. Interestingly, we also observed significantly higher ammonium production through arginine deimination in translationally blocked cells of strain HB60 than MG1363. While the amount of arginine in the initial study with this strain was relatively low, the catabolization of arginine in HB60 could potentially contribute to the observed increased biomass yield. It has been reported that arginine utilization during active growth could increase biomass yield up to 25% in another *L. lactis* strain (Palmfeldt et al., 2004). The expression of the arginine deiminase pathway has been linked to carbon catabolite repression (Gaudu et al., 2003; Zomer et al., 2007). The lower growth rate of HB60 might possibly play a role in relieving repression of this pathway either directly through interaction of CcpA with the *cre* elements in the *arc* operon or indirectly through, e.g., FBP levels which are expected to be lower in the slow growing HB60 (Bachmann et al., 2013). In chemostat cultures, it was observed that arginine consumption increases up to a dilution rate of 0.5 h^{-1} above which it rapidly drops again (Goel et al., 2015). Based on this data it seems plausible that a reduction of the maximum growth rate can result in a higher arginine utilization, indicating that exploration of this activity in strains that are known to display reduced growth rates e.g., *ldh* or *ccpA* mutants (Platteeuw et al., 1995; Luesink et al., 1998; Bongers et al., 2003) would be of interest.

Next to the ability of the assay to measure pathway activities, we also observed differences in production rate decline in relation to pre-culture conditions or strains. A prominent example was the glucose-utilization assay of galactose- pre-cultured cells which showed rapid acidification decline and complete halt within 100 h of measurement. The underlying mechanism that caused acidification to stop after the transition to the preferred carbon source glucose remains to be deciphered, but it has been suggested that large overshoots in intracellular metabolites

can be toxic due to osmotic and hydration effects (Korem Kohanim et al., 2018). Such activity decline could potentially be associated with changes in the physiological state of the population over time, including rate of cellular viability and membrane integrity loss. Detailed analysis of such underlying effects, may reveal heterogeneity in the bacterial population, including the potential presence of persister subpopulations in cultures produced under different pre-culture conditions that may explain the (bi-phasic) decline in metabolic activities during the subsequent assay conditions. The current approach is a valuable addition toward answering fundamental questions on catalytic stability and cellular fitness, particularly in non-growing environmental conditions.

The presented method provides additional insight on the complete pathway activity of intact cells. While omics analysis produces substantial information on composition and level of transcripts and proteins in response to variation in a specific growth condition, they have a reduced throughput and are not necessarily able to distinguish between active and non-active proteins/pathways. The combination of omics technologies with extensive physiological measurement contributes to our understanding of cellular performance during long-term incubations under non-growing conditions. In addition, determination of the specific activity level of relevant enzymes or pathways in cells harvested from the assay conditions could be used to determine enzyme decay. The simplicity of the method developed is very attractive, while it does not compromise on the level of assay condition definition. Consequently, omission, addition and dose titration of single components (e.g., metals, vitamins, amino acids, etc.) can be performed in a high throughput manner to decipher the effect of environmental conditions on the flux through certain pathways. Moreover, the influence of biochemical parameters on pathway activities, such as allosteric regulation, co-factor availability, pH, and temperature, can also be explored and related to its longevity. Although the present assay was on pathways that modulate the environmental pH (i.e., carbon flux and lactic acid production, and arginine utilization, and ammonium formation) that is monitored by a pH-dependent fluorescent reporter, one can envision the expansion to other metabolic pathways provided that product formation can be measured by fluorescence or other means of detection (e.g., luminescence and absorbance) that are compatible with high-throughput methodologies. Ultimately, this approach will allow to investigate the effect of environmental and genetic modulation on phenotypic properties and the optimization during prolonged catalysis in biotechnological applications, which is largely unexplored despite of its commercial interest.

DATA AVAILABILITY STATEMENT

All datasets generated for this study are included in the article/supplementary material.

AUTHOR CONTRIBUTIONS

ADWN executed the experimental work. All authors designed the study, participated in data interpretation, and wrote the manuscript, have read and approved the final manuscript.

FUNDING

This study was funded by the TiFN (TIFN, Program 16MF01, Wageningen, Netherlands).

ACKNOWLEDGMENTS

We would like to thank Stephanie Agnes Bachtiar for technical assistance in viability and membrane integrity measurement and Roelie Holleman for the HPLC measurement of organic acids.

REFERENCES

Bachmann, H., Fischlechner, M., Rabbers, I., Barfa, N., Dos Santos, F. B., Molenaar, D., et al. (2013). Availability of public goods shapes the evolution of competing metabolic strategies. *Proc. Natl. Acad. Sci. U.S.A.* 110, 14302–14307. doi: 10.1073/pnas.1308523110

Bongers, R. S., Hoefnagel, M. H. N., Starrenburg, M. J. C., Siemerink, M. A. J., Arends, J. G. A., Hugenholtz, J., et al. (2003). IS*981*-mediated adaptive evolution recovers lactate production by *ldhB* transcription activation in a lactate dehydrogenase-deficient strain of *Lactococcus lactis*. *J. Bacteriol.* 185, 4499–4507. doi: 10.1128/JB.185.15.4499-4507.2003

Budin-Verneuil, A., Maguin, E., Auffray, Y., Dusko Ehrlich, S., and Pichereau, V. (2004). An essential role for arginine catabolism in the acid tolerance of *Lactococcus lactis* MG1363. *Lait* 84, 61–68. doi: 10.1051/lait:2003033

Dijkstra, A. R., Alkema, W., Starrenburg, M. J. C., Hugenholtz, J., van Hijum, S. A. F. T., and Bron, P. A. (2014). Fermentation-induced variation in heat and oxidative stress phenotypes of *Lactococcus lactis* MG1363 reveals transcriptome signatures for robustness. *Microb. Cell Fact.* 13:148. doi: 10.1186/s12934-014-0148-6

Ercan, O., Wels, M., Smid, E. J., and Kleerebezem, M. (2015). Molecular and metabolic adaptations of *Lactococcus lactis* at near-zero growth rates. *Appl. Environ. Microbiol.* 81, 320–331. doi: 10.1128/AEM.02484-14

Erkus, O., De Jager, V. C. L., Geene, R. T. C. M., Van Alen-Boerrigter, I., Hazelwood, L., Van Hijum, S. A. F. T., et al. (2016). Use of propidium monoazide for selective profiling of viable microbial cells during Gouda cheese ripening. *Int. J. Food Microbiol.* 228, 1–9. doi: 10.1016/j.ijfoodmicro.2016.03.027

Förberg, C., Enfors, S. O., and Häggström, L. (1983). Control of immobilized, non-growing cells for continuous production of metabolites. *Eur. J. Appl. Microbiol. Biotechnol.* 17, 143–147. doi: 10.1007/BF00505878

Frees, D., Varmanen, P., and Ingmer, H. (2001). Inactivation of a gene that is highly conserved in Gram-positive bacteria stimulates degradation of non-native proteins and concomitantly increases stress tolerance in *Lactococcus lactis*. *Mol. Microbiol.* 41, 93–103. doi: 10.1046/j.1365-2958.2001.02503.x

Ganesan, B., Stuart, M. R., and Weimer, B. C. (2007). Carbohydrate starvation causes a metabolically active but nonculturable state in *Lactococcus lactis*. *Appl. Environ. Microbiol.* 73, 2498–2512. doi: 10.1128/AEM.01832-06

Garrigues, C., Loubiere, P., Lindley, N. D., and Cocaign-Bousquet, M. (1997). Control of the shift from homolactic acid to mixed-acid fermentation in

Lactococcus lactis: predominant role of the NADH/NAD+ ratio. *J. Bacteriol.* 179, 5282–5287. doi: 10.1128/jb.179.17.5282-5287.1997

Gasson, M. J. (1983). Plasmid complements of *Streptococcus lactis* NCDO 712 and other lactic streptococci after protoplast-induced curing. *J. Bacteriol.* 154, 1–9. doi: 10.1128/jb.154.1.1-9.1983

Gaudu, P., Lamberet, G., Poncet, S., and Gruss, A. (2003). CcpA regulation of aerobic and respiration growth in *Lactococcus lactis*. *Mol. Microbiol.* 50, 183–192. doi: 10.1046/j.1365-2958.2003.03700.x

Goel, A., Eckhardt, T. H., Puri, P., de Jong, A., Branco dos Santos, F., Giera, M., et al. (2015). Protein costs do not explain evolution of metabolic strategies and regulation of ribosomal content: does protein investment explain an anaerobic bacterial Crabtree effect? *Mol. Microbiol.* 97, 77–92. doi: 10.1111/mmi.13012

Hugenholtz, J., and Starrenburg, M. J. C. (1992). Diacetyl production by different strains of *Lactococcus lactis* subsp. *lactis* var. *diacetylactis* and *Leuconostoc* spp. *Appl. Microbiol. Biotechnol.* 38, 17–22. doi: 10.1007/BF00169412

Keren, I., Kaldalu, N., Spoering, A., Wang, Y., and Lewis, K. (2004). Persister cells and tolerance to antimicrobials. *FEMS Microbiol. Lett.* 230, 13–18. doi: 10.1016/S0378-1097(03)00856-5

Kock, H., Gerth, U., and Hecker, M. (2004). The ClpP peptidase is the major determinant of bulk protein turnover in *Bacillus subtilis*. *J. Bacteriol.* 186, 5856–5864. doi: 10.1128/JB.186.17.5856-5864.2004

Koebmann, B. J., Andersen, H. W., Solem, C., and Jensen, P. R. (2002a). "Experimental determination of control of glycolysis in *Lactococcus lactis*," in *Lactic Acid Bacteria: Genetics, Metabolism and Applications*, eds R. J. Siezen, J. Kok, T. Abee, and G. Schasfsma (Cham: Springer), 237–248. doi: 10.1007/978-94-017-2029-8_14

Koebmann, B. J., Westerhoff, H. V., Snoep, J. L., Solem, C., Pedersen, M. B., Nilsson, D., et al. (2002b). The extent to which ATP demand controls the glycolytic flux depends strongly on the organism and conditions for growth. *Mol. Biol. Rep.* 29, 41–45. doi: 10.1023/A:1020398117281

Korem Kohanim, Y., Levi, D., Jona, G., Towbin, B. D., Bren, A., and Alon, U. (2018). A Bacterial Growth Law out of Steady State. *Cell Rep.* 23, 2891–2900. doi: 10.1016/j.celrep.2018.05.007

Liu, J., Deng, Y., Li, L., Li, B., Li, Y., Zhou, S., et al. (2018). Discovery and control of culturable and viable but non-culturable cells of a distinctive *Lactobacillus harbinensis* strain from spoiled beer. *Sci. Rep.* 8:11446. doi: 10.1038/s41598-018-28949-y

Lopez de Felipe, F., Kleerebezem, M., de Vos, W. M., and Hugenholtz, J. (1998). Cofactor engineering: a novel approach to metabolic engineering in *Lactococcus lactis* by controlled expression of NADH oxidase. *J. Bacteriol.* 180, 3804–3808.

Luesink, E. J., van Herpen, R. E. M. A., Grossiord, B. P., Kuipers, O. P., and de Vos, W. M. (1998). Transcriptional activation of the glycolytic *las* operon and catabolite repression of the *gal* operon in *Lactococcus lactis* are mediated by the catabolite control protein CcpA. *Mol. Microbiol.* 30, 789–798. doi: 10.1046/j.1365-2958.1998.01111.x

Magajna, B. A., and Schraft, H. (2015). *Campylobacter jejuni* biofilm cells become viable but non-culturable (VBNC) in low nutrient conditions at 4 °C more quickly than their planktonic counterparts. *Food Control* 50, 45–50. doi: 10.1016/j.foodcont.2014.08.022

Marcobal, Á, Martín-Álvarez, P. J., Polo, M. C., Muñoz, R., and Moreno-Arribas, M. V. (2006). Formation of biogenic amines throughout the industrial manufacture of red wine. *J. Food Protoc.* 69, 397–404. doi: 10.4315/0362-028X-69.2.397

Melchiorsen, C. R., Jokumsen, K. V., Villadsen, J., Johnsen, M. G., Israelsen, H., and Arnau, J. (2000). Synthesis and posttranslational regulation of pyruvate formate-lyase in *Lactococcus lactis*. *J. Bacteriol.* 182, 4783–4788. doi: 10.1128/JB.182.17.4783-4788.2000

Millet, V., and Lonvaud-Funel, A. (2000). The viable but non-culturable state of wine micro-organisms during storage. *Lett. Appl. Microbiol.* 30, 136–141. doi: 10.1046/j.1472-765x.2000.00684.x

Neves, A. R., Pool, W. A., Solopova, A., Kok, J., Santos, H., and Kuipers, O. P. (2010). Towards enhanced galactose utilization by *Lactococcus lactis*. *Appl. Environ. Microbiol.* 76, 7048–7060. doi: 10.1128/AEM.01195-10

Oliver, J. D., Hite, F., McDougald, D., Andon, N. L., and Simpson, L. M. (1995). Entry into, and resuscitation from, the viable but nonculturable state by *Vibrio vulnificus* in an estuarine environment. *Appl. Environ. Microbiol.* 61, 2624–2630.

Palmfeldt, J., Paese, M., Hahn-Hägerdal, B., and Van Niel, E. W. J. (2004). The pool of ADP and ATP regulates anaerobic product formation in resting cells of *Lactococcus lactis* downloaded from. *Appl. Environ. Microbiol.* 70, 5477–5484. doi: 10.1128/AEM.70.9.5477-5484.2004

Platteeuw, C., Hugenholtz, J., Starrenburg, M., Van Alen-Boerrigter, I., and De Vos, W. M. (1995). Metabolic engineering of *Lactococcus lactis*: influence of the overproduction of α-acetolactate synthase in strains deficient in lactate dehydrogenase as a function of culture conditions. *Appl. Environ. Microbiol.* 61, 3967–3971. doi: 10.1128/aem.61.11.3967-3971.1995

Poolman, B., Driessen, A. J. M., and Konings, W. N. (1987). Regulation of Arginine-Ornithine Exchange and the Arginine Deiminase Pathway in *Streptococcus lactis*. *J. Bacteriol.* 169, 5597–5604.

Price, C. E., Branco Dos Santos, F., Hesseling, A., Uusitalo, J. J., Bachmann, H., Benavente, V., et al. (2019). Adaption to glucose limitation is modulated by the pleotropic regulator CcpA, independent of selection pressure strength. *BMC Evol. Biol.* 19:15. doi: 10.1186/s12862-018-1331-x

Settachaimongkon, S., van Valenberg, H. J. F., Gazi, I., Nout, M. J. R., van Hooijdonk, T. C. M., Zwietering, M. H., et al. (2016). Influence of *Lactobacillus plantarum* WCFS1 on post-acidification, metabolite formation and survival of starter bacteria in set-yoghurt. *Food Microbiol.* 59, 14–22. doi: 10.1016/j.fm.2016.04.008

Settachaimongkon, S., van Valenberg, H. J. F., Winata, V., Wang, X., Nout, M. J. R., van Hooijdonk, T. C. M., et al. (2015). Effect of sublethal preculturing on the survival of probiotics and metabolite formation in set-yoghurt. *Food Microbiol.* 49, 104–115. doi: 10.1016/j.fm.2015.01.011

Shah, N. P., Lankaputhra, W. E. V., Britz, M. L., and Kyle, W. S. A. (1995). Survival of *Lactobacillus acidophilus* and *Bifidobacterium bifidum* in commercial yoghurt during refrigerated storage. *Int. Dairy J.* 5, 515–521. doi: 10.1016/0958-6946(95)00028-2

Smid, E. J., and Kleerebezem, M. (2014). Production of aroma compounds in lactic fermentations. *Annu. Rev. Food Sci. Technol.* 5, 313–326. doi: 10.1146/annurev-food-030713-092339

Sonderegger, M., Schümperli, M., and Sauer, U. (2005). Selection of quiescent *Escherichia coli* with high metabolic activity. *Metab. Eng.* 7, 4–9. doi: 10.1016/J.YMBEN.2004.05.005

Svetlov, M. S., Vázquez-Laslop, N., and Mankin, A. S. (2017). Kinetics of drug-ribosome interactions defines the cidality of macrolide antibiotics. *Proc. Natl. Acad. Sci. U.S.A.* 114, 13673–13678. doi: 10.1073/pnas.1717168115

Tenson, T., Lovmar, M., and Ehrenberg, M. (2003). The mechanism of action of macrolides, lincosamides and streptogramin B reveals the nascent peptide exit path in the ribosome. *J. Mol. Biol.* 330, 1005–1014. doi: 10.1016/S0022-2836(03)00662-4

Thomas, T. D., Ellwood, D. C., and Longyear, V. M. C. (1979). Change from homo- to heterolactic fermentation by *Streptococcus lactis* resulting from glucose limitation in anaerobic chemostat cultures. *J. Bacteriol.* 138, 109–117. doi: 10.1128/jb.138.1.109-117.1979

Thomas, T. D., Turner, K. W., and Crow, V. L. (1980). Galactose fermentation by *Streptococcus lactis* and *Streptococcus cremoris*: pathways, products, and regulation. *J. Bacteriol.* 144, 672–682.

van de Bunt, B., Bron, P. A., Sijtsma, L., de Vos, W. M., and Hugenholtz, J. (2014). Use of non-growing *Lactococcus lactis* cell suspensions for production of volatile metabolites with direct relevance for flavour formation during dairy fermentations. *Microb. Cell Fact.* 13:176. doi: 10.1186/s12934-014-0176-2

van Mastrigt, O., Abee, T., Lillevang, S. K., and Smid, E. J. (2018a). Quantitative physiology and aroma formation of a dairy *Lactococcus lactis* at near-zero growth rates. *Food Microbiol.* 73, 216–226. doi: 10.1016/J.FM.2018.01.027

van Mastrigt, O., Gallegos Tejeda, D., Kristensen, M. N., Abee, T., and Smid, E. J. (2018b). Aroma formation during cheese ripening is best resembled by

Lactococcus lactis retentostat cultures. *Microb. Cell Fact.* 17, 1–8. doi: 10.1186/s12934-018-0950-7

van Tatenhove-Pel, R. J., Zwering, E., Solopova, A., Kuipers, O. P., and Bachmann, H. (2019). Ampicillin-treated *Lactococcus lactis* MG1363 populations contain persisters as well as viable but non-culturable cells. *Sci. Rep.* 9, 1–10. doi: 10.1038/s41598-019-46344-z

Wegmann, U., O'Connell-Motherway, M., Zomer, A., Buist, G., Shearman, C., Canchaya, C., et al. (2007). Complete genome sequence of the prototype lactic acid bacterium *Lactococcus lactis* subsp. *cremoris* MG1363. *J. Bacteriol.* 189, 3256–3270. doi: 10.1128/JB.01768-06

Witzig, R., Manz, W., Rosenberger, S., Krüger, U., Kraume, M., and Szewzyk, U. (2002). Microbiological aspects of a bioreactor with submerged membranes for aerobic treatment of municipal wastewater. *Water Res.* 36, 394–402. doi: 10.1016/S0043-1354(01)00221-4

Yerlikaya, O. (2019). Probiotic potential and biochemical and technological properties of *Lactococcus lactis* ssp. *lactis* strains isolated from raw milk and kefir grains. *J. Dairy Sci.* 102, 124–134. doi: 10.3168/jds.2018-14983

Zomer, A. L., Buist, G., Larsen, R., Kok, J., and Kuipers, O. P. (2007). Time-resolved determination of the CcpA regulon of *Lactococcus lactis* subsp. *cremoris* MG1363. *J. Bacteriol.* 189, 1366–1381. doi: 10.1128/JB.01013-06

Conflict of Interest: The project was organized by and executed under the auspices of TiFN, a public—private partnership on pre-competitive research in food and nutrition. Funding for this research was obtained from Friesland Campina (Wageningen, Netherlands), CSK Food Enrichment (Wageningen, Netherlands) and the Top-sector Agri and Food.

The public partners were responsible for the study design, data collection and analysis, decision to publish, and preparation of the manuscript. The private partners have contributed to the project through regular discussion.

HB was employed by NIZO Food Research.

The remaining authors declare that the research was conducted in the absence of any commercial or financial relationships that could be construed as a potential conflict of interest.

frontiers in Bioengineering and Biotechnology

HYPOTHESIS AND THEORY
published: 22 December 2020
doi: 10.3389/fbioe.2020.613986

Modeled Structure of the Cell Envelope Proteinase of *Lactococcus lactis*

Egon Bech Hansen[1]* *and Paolo Marcatili*[2]

[1] National Food Institute, Technical University of Denmark, Kongens Lyngby, Demark, [2] Department of Health Technology, Technical University of Denmark, Kongens Lyngby, Demark

The cell envelope proteinase (CEP) of *Lactococcus lactis* is a large extracellular protease covalently linked to the peptidoglycan of the cell wall. Strains of *L. lactis* are typically auxotrophic for several amino acids and in order to grow to high cell densities in milk they need an extracellular protease. The structure of the entire CEP enzyme is difficult to determine experimentally due to the large size and due to the attachment to the cell surface. We here describe the use of a combination of structure prediction tools to create a structural model for the entire CEP enzyme of *Lactococcus lactis*. The model has implications for how the bacterium interacts with casein micelles during growth in milk, and it has implications regarding the energetics of the proteolytic system. Our model for the CEP indicates that the catalytic triad is activated through a structural change caused by interaction with the substrate. The CEP of *L. lactis* might become a useful model for the mode of action for enzymes belonging to the large class of S8 proteinases with a PA (protease associated) domain and a downstream fibronectin like domain.

Keywords: lactic acid bacteria (LAB), cell envelope associated peptidases, protein structure prediction, proteolytic system, casein micelle, subtilisin, S8 proteinase, substrate specificity

OPEN ACCESS

Edited by:
Csaba Fehér,
Budapest University of Technology and Economics, Hungary

Reviewed by:
Eddy J. Smid,
Wageningen University & Research, Netherlands
Gisele LaPointe,
University of Guelph, Canada

***Correspondence:**
Egon Bech Hansen
egbh@food.dtu.dk

Specialty section:
This article was submitted to Synthetic Biology, a section of the journal Frontiers in Bioengineering and Biotechnology

Received: *04 October 2020*
Accepted: *02 December 2020*
Published: *22 December 2020*

Citation:
Hansen EB and Marcatili P (2020) Modeled Structure of the Cell Envelope Proteinase of Lactococcus lactis. Front. Bioeng. Biotechnol. 8:613986. doi: 10.3389/fbioe.2020.613986

INTRODUCTION

Lactic acid bacteria (LAB) are commonly found in ecological niches rich in nutrients. The adaption to nutrient rich environments has resulted in extensive genome reduction and fastidious growth requirements including the demand for multiple amino acids (Jensen and Hammer, 1993; Makarova et al., 2006; Gänzle, 2015). In nutrient rich environments LAB compete against other microorganisms by fast growth and rapid accumulation of lactic acid from carbohydrate fermentation. The demand for essential amino acids will typically lead to a depletion of low molecular weight peptides and free amino acids. Growth beyond this point requires protein hydrolysis (Juillard et al., 1995b; Vermeulen et al., 2005). Proteolytic phenotypes are widespread among LAB (Kliche et al., 2017) whereas also the strategy of relying on symbiosis with proteolytic strains seems to be competitive (Sodini et al., 2000; Bachmann et al., 2012). The proteolytic system of LAB consist of an extracellular proteinase, various transporters allowing peptides and amino acids to be imported into the cell, and a range of intracellular peptidases completing the hydrolysis of peptides into amino acids (reviewed by Savijoki et al., 2006). The extracellular proteinase is typically a large serine proteinase attached to the cell envelope with a proteinase

domain homologous to the *Bacillus* protease subtilisin (Siezen, 1999; Siezen and Leunissen, 2010; Broadbent and Steele, 2013).

The proteinases of LAB used in the dairy industry have been studied for two main reasons: speed of acidification and flavor formation. Particularly the *Lactococcus lactis* cell envelope proteinases (CEP) have been extensively studied. The *L. lactis* CEP is a large multi domain enzyme covalently attached to the peptidoglycan layer at the outside of the cell wall (Siezen, 1999). The CEPs from different strains of *L. lactis* differ very little in sequence with identities larger than 98%. However, the enzymes differ regarding flavor development and substrate specificity (Visser et al., 1986; Exterkate, 1990; Exterkate et al., 1993; Broadbent et al., 1998; Exterkate and Alting, 1999; Børsting et al., 2015).

It was recently demonstrated that proteolysis is the bottleneck for acidification of camel milk with commercially available dairy starter cultures (Berhe et al., 2018). LAB strains able to acidify camel milk have been isolated (Abdelgadir et al., 2008; Drici, 2008; Drici et al., 2010; Gabed et al., 2015; Fugl et al., 2017) and several of these have been genome sequenced (Drici, 2008; Gabed et al., 2015; Bragason et al., 2020).

Comparison of CEP from strains of *Lactococcus lactis* with different properties toward caseins from camel and cow milk is likely to reveal fundamental properties of this important enzyme. Knowledge of the structure of the protein is useful for the fundamental understanding of an enzyme. In this paper we describe the development of a structural model of the PrtP enzyme starting from the amino acid sequence of PrtP from *Lactococcus lactis* MS22337, a strain isolated from spontaneously acidified camel milk.

The architecture of the *L. lactis* CEP shares features with a large number of serine proteases. The subtilisins annotated in the Pfam database[1] are characterized by the shared domain S8 (PF00082). Domain S8 is found in 43564 sequences and a large class of those contain an insertion of a protease associated domain, PA(PF02225) within the S8 domain. Among those, there is often a fibronectin-like domain just downstream for the S8 domain. In prokaryotic proteases the fibronectin-like domain has been termed Fn3_5(PF06280). Fn3_5 is found in 1515 sequences and always together with S8. In plant proteases, the fibronectin-like domain is termed Fn3_6(PF17766) and this domain is found in 5862 sequences. The possible interaction between PA, S8, and Fn in the CEP of *L. lactis* might reveal a common principle used by this large class of proteases. The objective of this study is to use current state of the art structure prediction algorithms to establish a structural model of the CEP of *L. lactis* and to examine if the predicted model have implications for the function of the enzyme.

MATERIALS AND METHODS

CEP Sequences

The *prtP* genes of *Lactococcus lactis* strains Wg2 and SK11 were the first CEP genes to be cloned and sequenced (Kok et al., 1988; Vos et al., 1989a). The amino acid sequences of these two enzymes are available in Uniprot under the accession numbers P16271 and P15292 respectively. We did however during this work realize that the sequence at Uniprot accession P15292 deviates from the sequence given in the original papers and several subsequent papers on SK11 PrtP. We therefore used the PrtP sequence translated from the DNA sequence for the complete proteinase plasmid pSK11P with accession DQ149245 (Siezen et al., 2005). The two sequences for the same protein differ in 23 positions. We also compared the 2005 PrtP sequence to the original SK11 PrtP sequence from 1989 (Vos et al., 1989a) and found deviation at 3 positions, I109T, S592F, and D899E, of which the first is located in the pro-peptide. In this paper we also use the sequences of the CEP enzymes from two *Lactococcus lactis* subsp. *lactis* strains MS22333 and MS22337 isolated from spontaneously acidified camel milk in Ethiopia (Fugl et al., 2017), these two sequences have been deposited at the NCBI GenBank under the accession numbers WWDI00000000 and WWDK00000000 respectively. An alignment of the four PrtP amino acid sequences is given in **Supplementary Figure S1**. The two strains isolated from camel milk differ from each other in 39 positions and with Wg2 in 50 and 54 positions respectively. They show the largest difference to the SK11 PrtP where differences are found for 68 and 73 positions within the first 1800 amino acids. In the last domain, W, composed of a variable number of a 60 aa repeat unit we see differences of up to seven amino acids between repeat units from different strains and up to two differences in amino acid sequence between units from the same strain.

Protein Structure Modeling

Protein structures were modeled using the four different methods given in **Table 1**. Restrictions on sequence length apply for I-TASSER and RaptorX forcing the modeling of large proteins to be conducted in segments. Swiss-Model has a feature allowing a template to be provided for the modeling. This feature was used to impose the repeated use of the same template on a longer segment of the protein sequence. The PyMOL software (version 2.3.3)[2] was used for visualization and editing of protein structure PDB files. Comparison of protein structures and calculation of TM-scores and RMSD values was done using the TM-score and TM-align programs at University of Michigan[3] (Zhang and Skolnick, 2004). Individual domains were assembled into larger models using the DEMO program (Zhou et al., 2019).

[1] pfam.org

[2] https://pymol.org

[3] http://zhanglab.ccmb.med.umich.edu/TM-score

TABLE 1 | Algorithms used for structure prediction.

Algorithm	Server address	Reference
Phyre2	http://www.sbg.bio.ic.ac.uk/~{}phyre2	Kelley et al., 2015
Swiss-Model	https://swissmodel.expasy.org/	Waterhouse et al., 2018
I-TASSER	https://zhanglab.ccmb.med.umich.edu/I-TASSER/	Yang et al., 2015
RaptorX	http://raptorx.uchicago.edu/	Wang et al., 2017; Xu, 2019

RESULTS – MODELING THE STRUCTURE OF CEP

One Step Modeling of CEP

The *L. lactis* PrtP enzyme starts from the N-terminal end with a signal peptide assuring the translocation of the protein across the membrane via the seg pathway (Cranford-Smith and Huber, 2018). Following the signal peptide comes a long propeptide which is autocatalytically cleaved by the PrtP enzyme to make an aspartic acid at position 188 to become the N-terminus of the mature enzyme (Kok et al., 1988; de Vos et al., 1989; Haandrikman et al., 1989; Vos et al., 1989a). We find a two amino acid deletion in the pro-peptide of PrtP enzymes in all *L. lactis* isolates from Ethiopian camel milk. In our sequence the N-terminal D residue thus has the residue number 186 rather than 188.

Two of the three modeling servers accept long amino acid sequences and as a first approach we attempted to model the entire PrtP molecule. The sequence of the mature PrtP protease from strain MS22337 was submitted to the servers of Phyre2 and Swiss Model. The sequence submitted was starting with the sequence DAK predicted to be the first amino acids in the mature PrtP protein after autocatalytic cleavage of the pro-peptide. The C-terminus of the sequence was the PKT predicted to be covalently linked to the peptidoglycan of the cell wall. The entire length of the protein sequence is 1725 amino acids.

Protein structures identified as best templates by the modeling servers are listed in **Table 2**.

Although Swiss model accepts the entire sequence as input, the output is a model for only the first half of the sequence containing 912 amino acids ending at position 1100. Phyre2 also accepts the entire sequence as input and proposes the model shown in **Supplementary Figure S2**. In the Phyre2 model the first 1308 amino acids have been assigned a structure quite similar to the Swiss model, where the remaining 415 amino acids, for which no template has been identified, are modeled as random coils.

Phyre2 and Swiss model both use two streptococcal serine proteinases as templates for the structure models of the first half of the molecule. Both programs detect homology to a protein from *Marinomonas primoryensis* with the structure given by 4p99. The homology to this protein is found in the region from 996 to 1396 in the PrtP sequence. Phyre2 also detects a homology to 2yn5 in the region 1212–1496.

From the analysis of the templates identified by these tools and of the resulting models, we can see that the C-terminal region of the protein has not been modeled with sufficient accuracy, and additional remote homology templates and modeling constraints are needed to improve the modeling confidence.

TABLE 2 | Protein structures identified as best templates for modeling the structure of the sequence of MS22337 PrtP.

Phyre2	Swiss Model	iTASSER	Protein	Reference
Protease domain				
5xyr/5xxz	5xyr/5xya		*Streptococcus pyogenes* ScpC virulence protease	Jobichen et al., 2018
1xf1	1xf1	1xf1	*Streptococcus agalactiae* C5a peptidase	Brown et al., 2005
	3eif	3eif	*Streptococcus pyogenes* C5a peptidase	Kagawa et al., 2009
		1r6v	Fervidolysin, *Fervidobacterium pennivorans*	Kim et al., 2004
		3vta	Cucumisin, *Cucumis melo*	Murayama et al., 2012
A + B domain				
4p99	4p99	4p99	MpAFP, *Marinomonas primoryensis*	Vance et al., 2014
2yn5			SiiE, *Salmonella enterica*	Griessl et al., 2013
		4rm6	HxuA, *Haemophilus influenzae*	Zambolin et al., 2016
		5ftx	SbsC, *Geobacillus stearothermophilus*	https://www.rcsb.org/structure/5ftx
		4om9	Pet passenger domain, *Escherichia coli*	Domingo Meza-Aguilar et al., 2014

The actual structures can be downloaded from the Protein Data Bank at https://www.ebi.ac.uk/pdbe/.

Identification of Domains of CEP by Evolutionary Information

In recent years, evolutionary constraints (Marks et al., 2012) have revolutionized the field of protein modeling, by introducing the ability to identify long- and short-term interactions between residues solely on the base of residue conservation and co-variation as observed in multiple sequence alignments. RaptorX exploits such methods to predict contacts and use additional information for the identification of remote homologs. In order to use modeling servers with restriction on the length we need to split the PrtP sequence into sections. The split can be done according to assumed domains or just random in overlapping segments. The RaptorX server allows contact maps to be generated for segments up to a length of 800 amino acids. A number of overlapping maps were generated and the contacts predicted were independent on how the protein sequence was segmented. By superimposing the maps for overlapping segments it is possible to generate a "full length diagonal" contact map for the amino acids separated by less than about 200 amino acids as shown in **Figure 1**.

The contact map allows us to identify regions of the protein with distinct structural features. The first 520 amino acid residue region is predicted to have numerous short range and long-range contacts. This region has previously been recognized as the protease domain with homology to subtilisin (Siezen, 1999). After the protease domain comes a long region where antiparallel β-sheets seems to be a characteristic feature. Antiparallel β-sheets are characteristic for fibronectin like domains. Fibronectin domains are quite common among the subtilisins and for the bacterial subtilisins the domain has been termed Fn3.5 (see footnote 1). In the structure of the *Streptococcus pyogenes* C5a protease three fibronectin like domains were identified downstream for the protease domain (Kagawa et al., 2009; Kagawa and Cooney, 2013). In the region between aa 500 and 1400, **Figure 1** shows a pattern which seems to be repeated

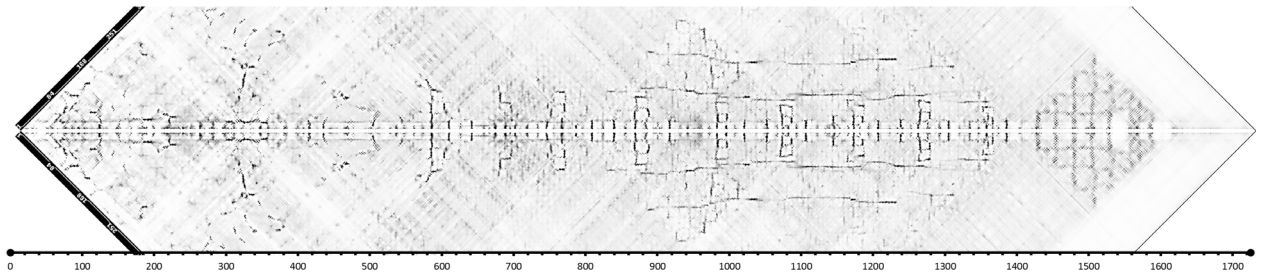

FIGURE 1 | Contact map for *L. lactis* MS22337 PrtP generated by RaptorX by superimposing 799 aa long segments of the PrtP sequence starting from the first aa of the mature protein (D186). As the map covers only the region around the diagonal, the composite map has been tilted by 45°. The four segments are 1–799, 301–1099, 501–1299, and 926–1725 (in this figure, positions are relative to D186).

nine times with intervals of about 100 aa. Each of these 9 patterns might represent individual fibronectin like domains. The three first units seem to be different from the last six and particularly the second unit seems to be involved in short-range and long-range contacts. The last six units appear to have long-range interactions between parallel β-sheets in addition to short-range antiparallel interactions. The long-range interactions are between parallel β-sheets separated by about 100 or 200 aa. These interactions could suggest that the structure is able to adopt alternative configurations with parallel β-sheets organized into β-barrels.

After the region with the fibronectin like domains, the contact map of **Figure 1** shows a region from 1400 to 1620 (1570–1800 relative to start of the reading frame) with patterns indicative of α helixes. The pattern is consistent with a bundle of α helixes shoving parallel and antiparallel interactions. This region coincides with the domain termed H for helix by Siezen (1999). The region following the H domain has no predicted interactions. This domain was termed W by Siezen, based on a hypothetical role as a cell wall spanning domain (Siezen, 1999).

The Proteinase Domain

Phyre2 and Swiss model gave structure predictions of the MS22337 PrtP enzyme. In addition we also used iTASSER to obtain models for the proteinase domain. The minimal domain was modeled by presenting a 511 aa long sequence starting from D 186 in the MS22337 PrtP sequence. The output from iTASSER contains several possible structures and two models, iTAS_1 and iTAS_2, are used for further analysis. In addition to the minimal protease domain we also used iTASSER to model an extended version of the proteinase domain by presenting a sequence starting with the amino acid following the predicted cleavage site of the signal peptidase. The 1077 aa long sequence presented to iTASSER was starting at K32. This sequence covers the proteinase domain preceded by the pro-peptide and followed by the A domain. Two models, iTAS_3 and iTAS_4 are retained for further analysis.

The four iTASSER models and the two models predicted by Phyre2 and Swiss model are compared in **Table 3**. When comparing only the structure of the "proteinase core" (residue 186-698) TM values are in the range from 0.55 to 0.95 indicating that that the predicted structures are in general consistent and belong to the same fold. The structure iTAS_4 is the structure differing the most from any of the other structures. iTAS_1, iTAS_2, and iTAS_3 are rather similar to each other and the Phyre2 and the Swiss models are also rather similar to each

TABLE 3 | Comparison of protein structure models of *Lactococcus lactis* MS22337 PrtP.

		Model:					
"Core" Model:		**iTAS_1**	**iTAS_2**	**iTAS_3**	**iTAS_4**	**Phyre2**	**Swiss**
iTAS_1_I	Shared residues		513	513	513	513	511
	RMSD Å		3.666	4.393	14.084	7.568	7.251
	TM-score		0.916	0.439	0.303	0.250	0.440
iTAS_2_K	Shared residues	513		513	513	513	511
	RMSD Å	3.666		2.864	13.298	6.966	6.262
	TM-score	0.916		0.459	0.323	0.256	0.464
iTAS_3_M	Shared residues	513	513		1077	923	913
	RMSD Å	4.393	2.864		40.628	8.599	7.455
	TM-score	0.892	0.950		0.370	0.431	0.792
iTAS_4_O	Shared residues	513	513	513		923	913
	RMSD Å	14.084	13.298	13.374		21.854	22.044
	TM-score	0.559	0.608	0.606		0.244	0.395
Phyre2_P	Shared residues	513	513	513	513		913
	RMSD Å	7.568	6.966	6.191	14.516		6.859
	TM-score	0.739	0.773	0.791	0.573		0.812
Swiss_S	Shared residues	511	511	511	511	511	
	RMSD Å	7.251	6.262	6.332	14.325	5.879	
	TM-score	0.731	0.782	0.777	0.574	0.847	

Models were compared using the TM-score program at the server of Zhanglab at University of Michigan (http://zhanglab.ccmb.med.umich.edu/TM-score). The values for each pairwise comparison are: the number of common residues; root-mean-square deviation (RMSD) of α-carbons; TM-score. The TM-score is a measure of structure similarity ranging from 0 to 1 (Zhang and Skolnick, 2004). The values above the diagonal (upper right) give the value for comparison of the "full length" models and the values below the diagonal (lower left) gives the value for comparing only the "proteinase core structure" (residue nr 186–698).

other. iTAS_2 seems to be the structure differing the least from any of the other structures within the "core proteinase region." The five other structures were each aligned to the iTAS_2 structure and all structures were then superimposed using these five alignments. The modeled structures have been deposited at modelarchive.org[4, 5, 6, 7, 8, 9]. **Figure 2** show the aligned structures for the "core protease region."

The Catalytic Site

An interesting aspect of the structure is the position of the amino acid residues of the catalytic site. The subtilisins (Pfam and Merops S8) are serine proteases with a catalytic triad consisting of three amino acids, aspartic acid, histidine, and serine. In the sequence of PrtP of MS22337 these amino acids are at the positions D215, H279, and S618. The relative positioning of these three amino acids in the six structures is given in **Figure 3**. It is remarkable that the aspartic acid and the serine residues, separated by 402 residues in the sequence, in all six models coincide at positions separated by seven Å. In four models; iTAS_2, iTAS_3, iTAS_4, and Swiss; the active site histidine is located at coinciding positions close to the two other amino acids of the catalytic triad. However, in the iTAS_1 and Phyre2 models, the histidine is located far from the active site. In these two models the histidine is displaced by 10–13 Å from the position presumably defining the position of the histidine in an active triad. It is tempting to speculate that the differences between the six models might reflect dynamics in the molecule and not only inaccuracy in the structure prediction. If this is the case, the different positions of the histidine of the catalytic triad might illustrate the possible mode of action of this enzyme. The enzyme could in the "ground state" be inactive due to a large distance

[4]https://modelarchive.org/doi/10.5452/ma-qijqu
[5]https://modelarchive.org/doi/10.5452/ma-jnx5p
[6]https://modelarchive.org/doi/10.5452/ma-04l8v
[7]https://modelarchive.org/doi/10.5452/ma-59xz0
[8]https://modelarchive.org/doi/10.5452/ma-9zlh3
[9]https://modelarchive.org/doi/10.5452/ma-298jo

FIGURE 2 | Predicted structures of the MS22337 PrtP proteinase for the domain spanning residue nr 186–698. The superimposed structures are shown for iTAS_1 in green, iTAS_3 in cyan, iTAS_4 in yellow, Phyre2 in salmon, and Swiss in gray. The protein backbones are shown as cartoons with the catalytic triad shown as stick models with D in red, H in magenta, and S in blue.

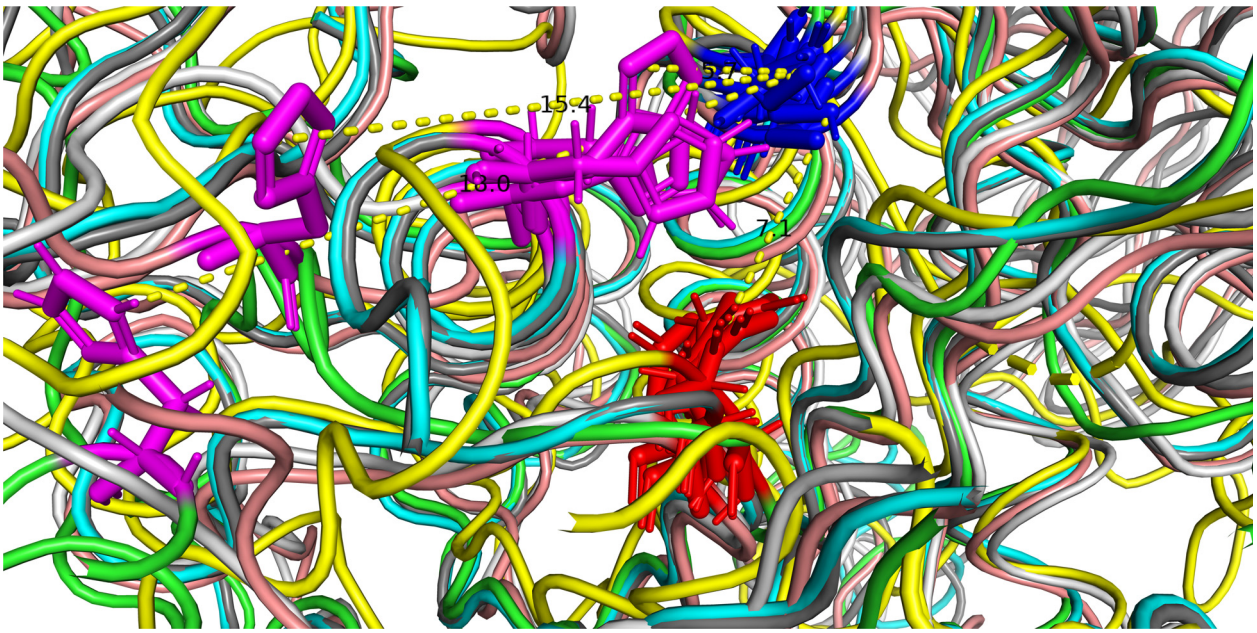

FIGURE 3 | The catalytic triad of MS22337 PrtP in the six structural models predicted based on the amino acid sequence. Aspartic acid, D215, is shown in red; Histidine, H279, is shown in magenta; and Serine, S618, is shown in blue. The protein backbone of the α carbons are shown as tubes with different color: iTAS_1 in green, iTAS_2 in light blue, iTAS_3 in dark gray, iTAS_4 in yellow, Phyre2 in amber, and Swiss in light gray. All six structures have the aspartic acid (215) at the same position and they have the serine (618) at coinciding positions in a distance of 7 Å from the aspartic acid. The histidine (279) of four models (iTAS_2, iTAS_3, iTAS_4, and Swiss) are located a the same position in a distance of 6 Å from the two other amino acids of the triad, whereas the histidines of iTAS_1 and Phyre2 are located far from the active site with distances of 18 and 15 Å respectively to the S618.

between the histidine and the D and S residues. Recognition of a suitable substrate might lead to a change in structure moving the histidine to the active position in the active site. **Figure 4** show the alternative structures for the region carrying the histidine 279.

Interaction With Substrate

By including the pro-peptide in the iTASSER modeling the two structures iTAS_3 and iTAS_4 were obtained as the two top ranking structures. The iTAS_3 model carries the pro-peptide as a long appendage whereas the pro-peptide in iTAS_4 is molded into the structure of the proteinase domain. The path of the pro-domain is passing the D and S of the catalytic triad in a distance of 4–8 Å from the amino acids of the catalytic triad. The path of the pro-peptide in this model seems to follow the catalytic cleft and thus defines the orientation of substrate bound to the protease. The pro-peptide is the very first substrate for the newly synthesized enzyme molecule and must therefore fit into the active site of the protease. In the iTAS_4 model the amino acid of the pro-peptide closest to the catalytic triad is residue number 161 whereas the activation is supposed to be a cleavage between residue 185 and 186. **Figure 5A** shows the position of the pro-peptide on the surface of the PrtP model iTAS_4. On the iTAS_4 model the pro-peptide (the substrate) follows a free trajectory along the length of more than 50 amino acids. On the iTAS_3 model (**Figure 5B**) the trajectory of the substrate is blocked at either side in a distance of 7–10 amino acids on either side of the position of the catalytic triad. Several of the other models also show structures blocking the substrate from fitting into the active site. The regions of the PrtP enzyme blocking at the access of the substrate are loops at either side of the catalytic triad one loop centered around residue 320 and the other around residue 429. These interactions are visualized in **Figures 5B,C**.

The possible interaction between substrate and the PrtP enzyme at domains further downstream has previously been suggested (Vos et al., 1991; Exterkate et al., 1993; Siezen et al., 1993; Børsting et al., 2015). From the iTAS_4 and iTAS_5 models, this region could likely be the site of interactions with residues in the region 930–950 as illustrated in **Figure 5D**.

Fibronectin Like Domains, Domain A + B

Four of the six models described in section "The proteinase domain" extends beyond the catalytic domain and covers also the A domain as defined by Siezen (1999) and the Phyre2 structure extends well into the B domain before turning into an unstructured leash. However, the regularity of the patterns in the contact maps obtained with RaptorX (cfr. **Figure 1**) prompted us to conduct a specific analysis of this region. As listed in **Table 2**; Phyre2, Swiss Model, and iTASSER all identify homology to a calcium-stabilized adhesin from the Antarctic bacterium *Marinomonas primoryensis* of which the structure has been determined and listed under the accession 4p99 in the PDB database. The reported structure is for a unit cell containing a tetramer of four antiparallel chains of identical structure. Each of the four chains contain four fibronectin like domains surrounded by calcium ions (Vance et al., 2014). When using this structure

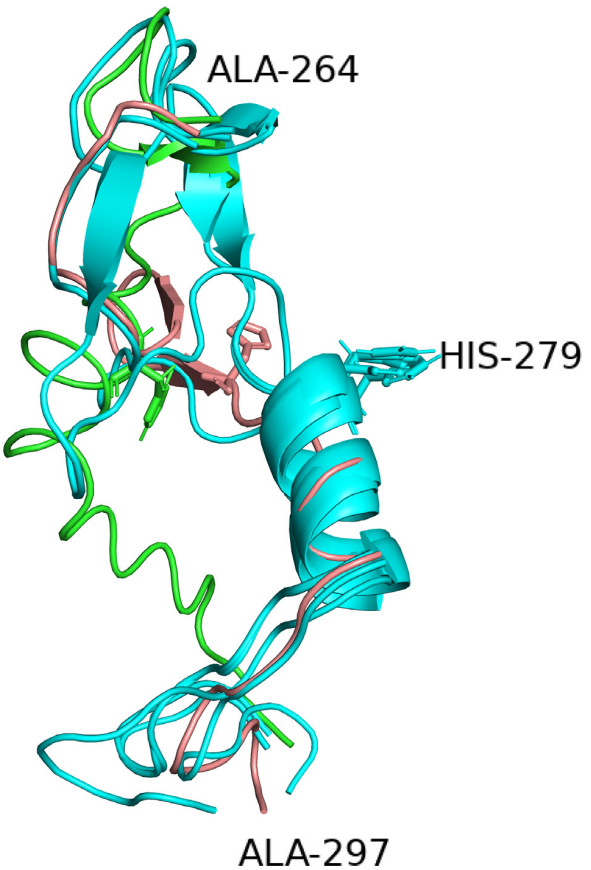

FIGURE 4 | The alternative structures for the segment containing the histidine (279) of the catalytic triad. Four of the six structures have identical structures and are all shown in cyan whereas the two deviating structures iTAS_1 and Phyre2 are shown in green and salmon respectively. His 279s are shown as stick models in all structures.

as template for molding the structure of MS22337 PrtP, Swiss Model proposes two models which are basically identical. One model corresponds to using the 4p99 structure on the last four (6–9) "aeroplane like patterns" in the contact map (cf. **Figure 1**). In the other model the same mold is just shifted one pattern upstream to cover "aeroplane" 5–8. In order to test if more of the patterns could be squeezed into the same mold we used a monomer chain from 4p99 as template on overlapping segments of the PrtP sequence. The resulting structure of 6 fibronectin like domains is shown in **Figure 6**.

The region was also modeled by submitting the sequence from 699 to 1574 to the iTASSER server. The highest-ranking model was a structure resembling a tube build of parallel β-sheets with three faces organized as an α-helical solenoid with three β-strands per turn (**Figure 7**). The templates selected by i-TASSER to build this model are mainly 4rm6 and 4om9, a hemopexin binding protein from *Haemophilus influenza* and a plasmid encoded auto-transporter enterotoxin from *Escherichia coli* respectively. This tube-like structure is suggestive for a function of the A and B domains as a drain, funneling the peptides produced by the enzyme down toward the C-terminus.

The two alternative structures of **Figures 6**, **7** seem to be very different and mutually exclusive. However, both models seem to have biological relevant implications like maintaining a distance to the cell surface and a stability depending on the presence of calcium ions. The two models might represent different states and the function of this region might be a rod able to metamorphose into a tube transporting peptides.

The Helical Domain, H

The domain between residue 1570 and 1800 was termed the H-domain by Siezen due to the predicted helical secondary structure (Siezen, 1999). The contact map produced by RaptorX (**Figure 1**) also give an immediate impression of this region being helical in the entire length with the helixes being folded several times to give parallel and antiparallel interactions between helixes. The highest-ranking model proposed by Raptor X is shown in **Figure 8**.

Domain W

The W domain is the last domain before the anchor domain. The W domain shows the largest variability of the *L. lactis* PrtP domains. The W domain varies both in sequence and in length. The length of the W domain ranges from 63 to 183 amino acids as the domain is composed of a unit of 60 amino acids repeated from 1 to 3 times with strains having 1, 1.5, 2, or 3 repeats of the basic element. Variability in sequence is seen at 11 positions within the basic unit. However, differences within repeats in the same strain is typically limited to two positions.

The function of the W domain was hypothesized to be a cell wall spanning domain allowing the proteinase to raise above the S-layer of the cell wall (Siezen, 1999). However, it has later been shown that the W-domain is involved in cell adhesion, either between *Lactococcus* cells or between lactococci and epithelia cells (Gajic, 2003). It has recently been shown that *L. lactis* expressing PrtP adheres to mucin and fibronectin (Radziwill-Bienkowska et al., 2017). It is therefore reasonable to assume that the W domain is an adhesin, and that the function of this domain during growth in milk might be to bind the casein micelle probably through binding to kappa casein located at the surface of the casein micelle.

The contact map (**Figure 1**) did not reveal any interactions with or within the W region, and neither of the servers listed in **Table 1** gave good hits for homologous structures and they did not produce structure models with high predictive values. iTasser detected some homology to an adhesin, BoaA, from *Burkholderia pseudomallei* with structure 3s6l (Balder et al., 2010). This structure can be used as template for molding a possible structure for the MS22337 PrtP W-domain. This structure is shown in **Supplementary Figure S3**. However, the selection of this template is mainly based on:

- the template being an adhesin
- the structure can easily be varied in length by multiples of the turn

The structure in **Supplementary Figure S3** has a pitch of 14 amino acids per turn in the solenoid. A pitch of 15 might have

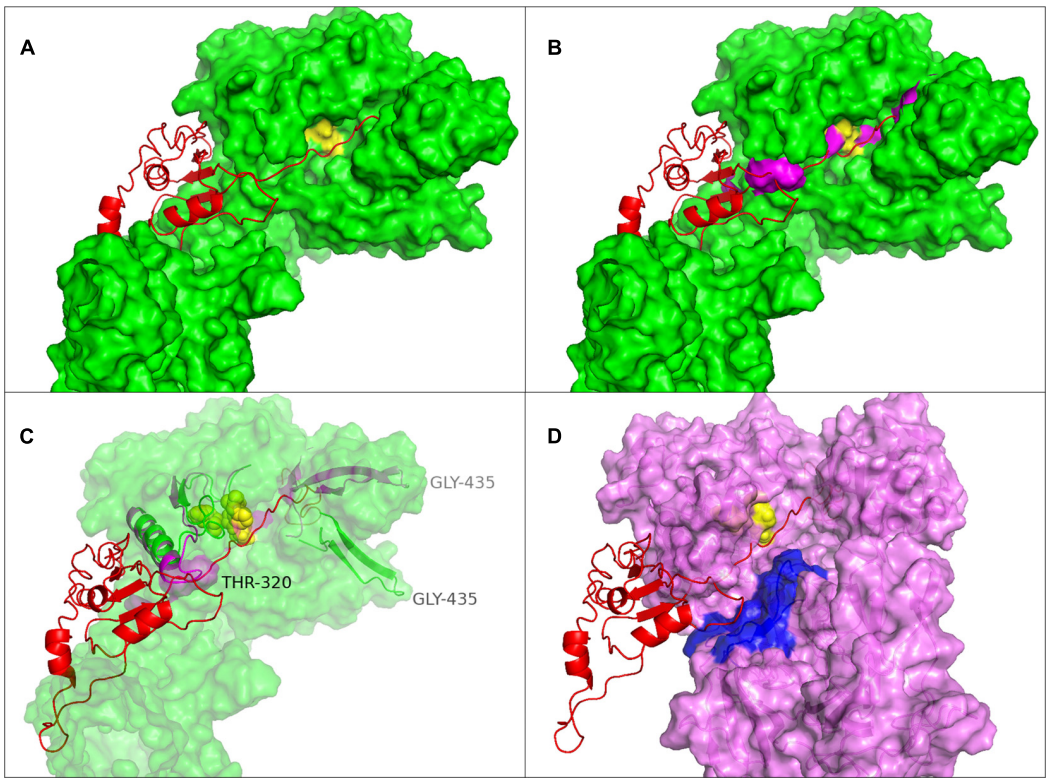

FIGURE 5 | Substrate position in the catalytic cleft of PrtP. **(A)** The iTAS4 model. The pro-peptide (shown as cartoon in red) is positioned in the catalytic cleft on iTAS_4 (shown as green surface. The catalytic triad is shown in yellow. **(B)** The obstructions in path of substrate posed by the iTAS_3 model is shown as magenta surfaces in the same model as **(A)**. **(C)** The underlying change in structure allowing the substrate access to the catalytic cleft. Residue 320 is obstructing to one side and residue 429 is obstructing at the other site. The segments from 300–340 and 422–445 of iTAS_3 and iTAS_4 are shown as cartoons in magenta and green respectively inside the same surface as **(B)** (now transparent). **(D)** Possible substrate interaction in the area of fibronectin like structures. The surface of the iTAS_3 structure is shown in magenta. The position of substrate is shown in red and the catalytic triad is shown in yellow. The same obstacles for the substrate as seen in **(C)** is also obvious in this figure. The area in blue is a region within the fibronectin like domains spanning residue 930–950. This area might interact with larger substrates like entire caseins or long peptides.

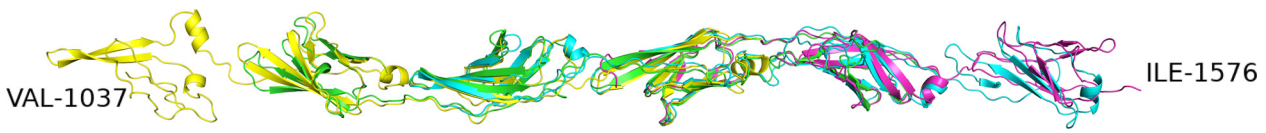

FIGURE 6 | Possible fibronectin like structure of the B domain established as a superposition of four overlapping structures build by Swiss model using a monomer of 4p99 as template. Only the six last units of the nine (based on **Figure 1**) fibronectin like structures could be fitted to the 4p99 template and only the five last gave a complete fit to this structure. The four overlapping structures are colored in yellow, green, cyan, and magenta.

been more appealing as this would give a better match with repeat units of length 60. In the lack of a better structure for W, we will use the structure of **Supplementary Figure S3** for the assembly of the complete structure of PrtP.

DISCUSSION

The purpose prompting us toward assembling a model for the structure of the cell wall proteinase of *Lactococcus lactis* was to understand the behavior of this bacterium during growth in milk. Differences in the PrtP enzyme seems to have a profound influence on the speed of acidification and to influence the ability of the bacterium to grow in different types of milk. We propose for the first time a structural model for the entire cell envelope proteinase of *Lactococcus lactis*. The model is constructed from the PrtP amino acid sequence of strain MS22337 deduced from an Illumina whole genome DNA sequence of this strain. We have used a combination of four different structure prediction servers to generate several models for overlapping segments of this large enzyme. The output from the different modeling algorithms gave structures showing differences that might represent alternative states of the enzyme. These differences have inspired us to propose

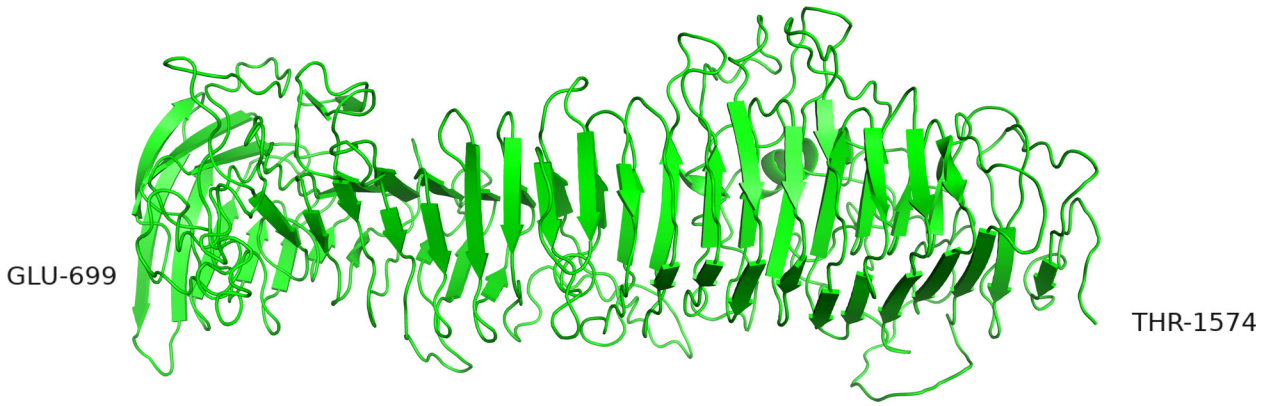

FIGURE 7 | Alternative structure of the AB domain modeled by iTASSER. In this structure the β-sheets are organized in parallel orientations.

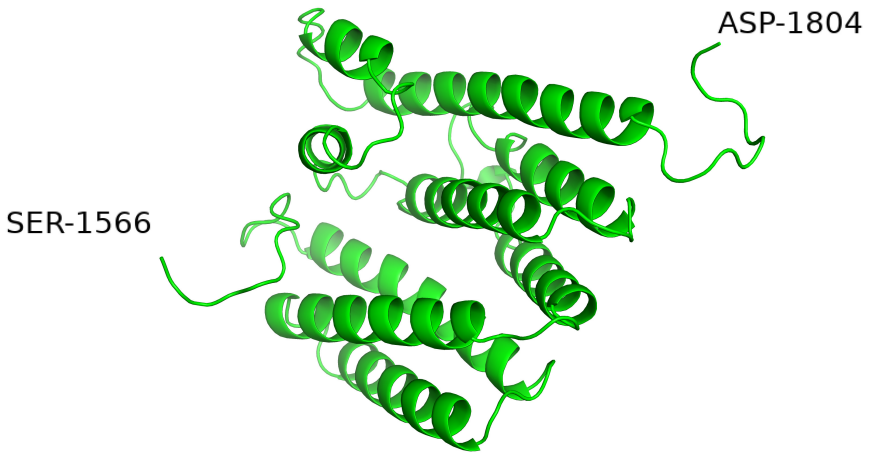

FIGURE 8 | The H domain of *Lactococcus lactis* PrtP modeled by RaptorX.

a model for how the enzyme interacts with substrate during growth in milk.

Implications for the Proteolytic System of LAB

The model of PrtP emerging by combining the various domain structures seems to be a large protease with the proteinase domain sitting on top of a high structure being either a rod of fibronectin like units or a tube-like solenoid structure (**Figure 9**). The height of the enzyme will obviously depend on the shape of the stalk, with the tube structure being shorter than the fibronectin like structure, if only one fibronectin domain at the time adopts a barrel-like structure, the difference in height would be minimal. The total height of PrtP will be in the range of 200–400 Å, equal to 20–40 nM.

It is interesting to compare the dimension of the enzyme to the dimensions of the other components of milk, particularly the casein micelle, which must be the actual substrate during the early growth-phase in milk. Caseins are organized into micelles of quite variable size. A median size of 150 nM has been reported for cow milk whereas camel milk has considerable larger casein micelles (Horne, 2008; Broyard and Gaucheron, 2015). Different models for the internal structure of the casein micelle has been proposed. In spite of the differences, all models include nanoclusters of calcium phosphate kept in suspension by caseins. The surface of the micelle is covered by kappa casein having a hydrophilic glycosylated c-terminal half (Holt, 2016). In **Figure 9** the PrtP and casein micelles models are superimposed in the same relative scale. The size of the bacterium will be approximately 10 times the size of a casein micelle.

It is evident that a configuration with the proteinase more or less permanently submerged into a casein micelle would give the cell several advantages. Substrate is readily available; the peptide import will be more efficient; the cell might reserve the peptides for own use rather than supporting neighboring non-proteolytic cells; the energetics of protein hydrolysis plus peptide uptake would seem to be advantageous compared to a dissociated protease.

The main peptide import system used by *Lactococcus lactis* is the oligo peptide transporter Opp able to transport peptides up to the length of 18 amino acids (Doeven et al., 2005). The

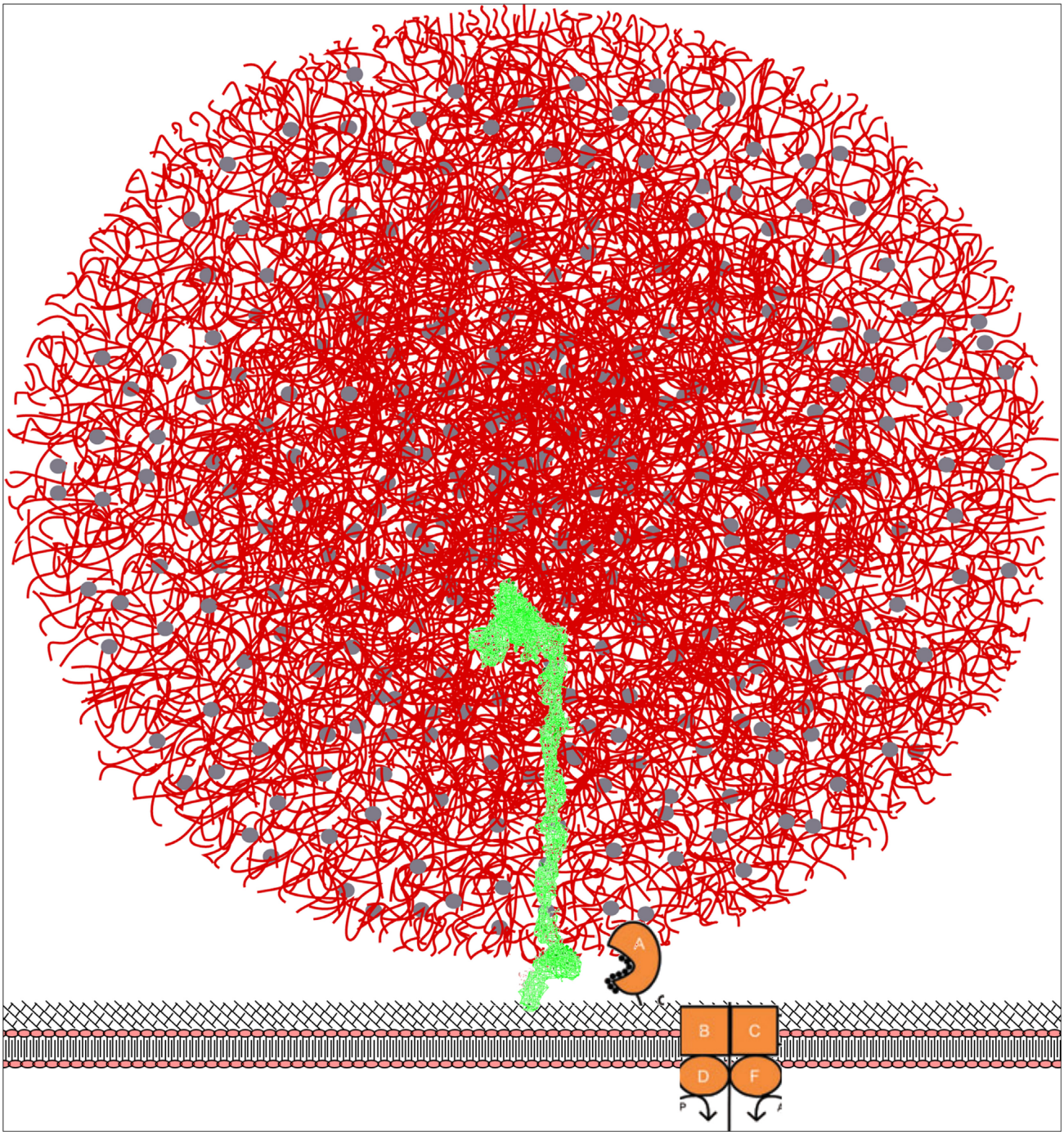

FIGURE 9 | Model for the surface bound PrtP enzyme (shown in green) hydrolyzing caseins within the casein micelle. PrtP is covalently attached to the surface of the bacterium through a C-terminal threonine joined to peptidoglycan. The height of the enzyme is approximately 40 nm with the N-terminal proteinase domain at the top of molecule. The casein micelle (shown in red) has a diameter of 100 nm and is presented as the "Holt model" (Holt, 2016). We propose that the bacterium attach to the surface of the micelle and thereby position the proteinase domain in an environment of rich in casein substrates. The oligopeptide transporter proteins OppA, OppB, OppC, OppD, and OppF are shown as cartoons inspired by Doeven et al. (2005).

uptake of a molecule by an ABC transporter will typically cost two moles of ATP per mole of substance imported (Locher, 2016; Scheepers et al., 2016). Hydrolyzing peptides inside the cell might allow the bacterium to capture the energy released by the hydrolysis, and for the longer peptides, this might result in a net gain of energy as the energy released can exceed the energy required to re-phosphorylate two moles of ATP (Martin, 1998; Bergman et al., 2010). Surplus amino acids can be used as fuel

for antiporters, to import other nutrients or to export protons allowing production of ATP via the ATPase system. For LAB this route of ATP generation might be particularly favored under acidic condition as protein hydrolysis below pH 6 would "consume" protons and reduce acidity.

The proteolytic system might accordingly play a role in energy production and not only in satisfying the need for nitrogen. If the cell also captures the energy stored in the phosphoserines of the caseins, this contribution might actually be quite substantial.

The optimal proteinase for growth in milk would thus seem to be a protease able to grab entire micelles and showing a relatively broad specificity allowing hydrolysis of caseins at any part of the molecule. The resulting peptides should preferably be shorter than 18 amino acids to allow uptake. However, the peptides should be as long as possible to minimize the energy required to import the peptides. Ideally, the enzyme should be able to hold on to the peptides until they can be handed over to the peptide binding protein OppA which subsequently pass it on to the OppBC complex. In light of this, it is tempting to propose that the hydrolyzed peptides are trickling down the shaft of domain A + B either along the outside or within a "peristaltic tube." Upon reaching the H domain, the peptides are stocked within the bundle of helices until OppA comes along to collect peptides. In this model, the logical role of the W domain would be to bind to the surface of the casein micelle, possibly via the glycosylated kappa casein.

This model for the functioning of PrtP during growth in milk could also explain the reduced acidification rate in camel milk. Larger casein micelles would allow fewer micelles to attach to the surface of the bacterium. As micelles of camel milk are four times bigger than in bovine milk, the maximal number of micelles accommodated on the surface would be reduced by approximately 16-fold.

Matching the Model Toward Published Research

All dairy associated PrtP enzymes utilize caseins and leave whey proteins untouched. Some PrtP enzymes (P_I type) prefer β-casein and all types cleave β- casein at multiple sites with no obvious specificity (Visser et al., 1986; Exterkate et al., 1993; Børsting et al., 2015). Researchers at NIZO and University of Groningen have over the last three decades contributed considerably to the understanding of the specificity of the cell wall proteinases of *Lactococcus*. They have characterized the diversity in specificity of natural enzymes and they have used protein engineering to explore the molecular basis of the specificity. Mainly four types of assays have been used: (1) growth rate in reconstituted milk of strains expressing the proteinase in question, (2) hydrolysis of intact α_{S1} casein and β- casein, (3) hydrolysis of chromogenic peptide substrates containing a *p*-nitroaniline at the C-terminal end, and (4) hydrolysis pattern of a 23 amino acid long peptide from the N-terminus of α_{S1} casein. A body of knowledge and a large number of enzymes with altered properties have been the result of this research. However, it seems that it has been somewhat elusive to get a firm grasp on the specificity of lactocepin. Maybe we need to make a slight shift in our approach to understand the specificity of this type of proteases. Understanding protease specificity based on the Schechter and Berger model for the active site of papain (Schechter and Berger, 1967) has been very successful for a long range of proteases where the amino acids around the cleavage site determine the specificity. This model has also been guiding the research on the CEP enzymes. The underlying assumption has been that if we understand all the cleavage sites we will understand the enzyme.

Several results point toward this being a misconception:

- The CEP enzymes are rather unspecific and able to cleave at almost any position in β- casein (Visser et al., 1988, 1991, 1994; Juillard et al., 1995a; Børsting et al., 2015)
- The CEP enzymes are very selective regarding short peptide substrates. Most chromogenic substrates are not cleaved at all; and the few substrates which are cleaved, require particular salt concentrations; and the specific activity is orders of magnitude lower than for subtilisin (Exterkate, 1990)
- The CEP enzymes cleave only at very few positions within the peptide α_{S1}(1–23) (Exterkate, 1990)
- The CEP enzymes are selective regarding which caseins to hydrolyze and they leave whey proteins unhydrolyzed (Visser et al., 1986).

This seemingly contradictory behavior of an enzyme being unspecific and yet very selective can be reconciled if the enzyme is non-selective regarding the site cleaved but selective regarding the length or the nature of the substrate. An enzyme with these properties would also fit the needs of the bacterium for growth in milk.

We find that the model emerging from our investigations seems to support such a mechanism:

- The active site is similar to subtilisin which is a rather unspecific enzyme. However, in PrtP the enzyme is in the off position due to a slight displacement of the histidine of the catalytic triad
- The catalytic cleft has at either site an obstruction which might function as push-buttons needing to be activated by substrate to activate and switch on the histidine. This feature might assure that short peptides are not being "over degraded." Long peptides might be cleaved at several positions whereas short peptides are not cleaved at all.
- Entire proteins might require auxiliary binding domains to allow for a bulky protein to squeeze into the catalytic cleft. This function might be served by the area on the surface of the fibronectin domains in the A-domain (**Figure 5D**)

This model fits well also with the published protein engineering investigations.

Vos et al. (1991) conducted swapping of domains between the SK11 and the Wg2 proteinases and demonstrated that a two amino acid difference in the A domain are having a profound effect on the preference for α_{S1}-casein or β- casein (Vos et al., 1991). The coordinates of the two amino acids are 747 and 748 in the mature form of the enzyme. This corresponds to 932 and 933 in the numbering on the MS22337 sequence, a position within

the "blue area" on **Figure 5D**. The two amino acids in SK11 are arginine and lysine whereas Wg2 has leucine and threonine. The much stronger positive charge of the SK11 proteinase in this region might determine how the enzyme interacts with the negatively charged caseins and it is tempting to speculate that the clusters of phosphoserines might influence how the two enzymes make the first attack on the caseins. Vos et al. (1991) also demonstrated that differences within the N-terminal 173 amino acids also contributed to the preference for α or β- casein. Bruinenberg et al. (1994b) showed that an entire loop of the SK11 proteinase is dispensable by removal of 151 residues between position 238 and 388 (423–573 in this papers coordinates). The mutant proteinase supported growth in milk although with a reduced growth rate and the mutant retained the ability to hydrolyze α_{S1}-casein (Bruinenberg et al., 1994b). **Figure 10A** shows the position of this dispensable loop on our enzyme model and **Figure 10B** shows the appearance of the enzyme without this loop. The residues just before and just after the loop are in our model quite close, with a distance of 10 Å and the structure of the remaining molecule might therefore be only minimally disturbed. The loop is not close to the site in the A domain demonstrated to be essential for the affinity for α_{S1} casein, and this might explain why the deletion mutant retains the P_{III} type specificity. The change might give easier access to the active site, and it would be interesting to analyze if the average length of products has changed.

In a different study Bruinenberg et al. (1994a) determined another shorter loop to be essential. Residues 205–219 (391–405 in our coordinates) could not be deleted without loss of enzyme activity whereas a triple mutant with substitutions of amino acids in both ends caused almost no change in activity (Bruinenberg et al., 1994a). In our model, the ends of this loop are separated by 24 Å and complete removal of the loop would most likely cause structural changes.

In a third engineering study, the same group investigated the effect of changes at specific positions of the SK11 proteinase. These positions were AKT(137–139), N166, S433, and K748 corresponding to position 322–324, 351, 618, and 933 in the MS22337 PrtP sequence. Except for the serine, which is the serine of the catalytic triad, all the positions could be mutated without losing the proteolytic activity of the enzyme. Change of the serine of the catalytic triad to an alanine led to complete inactivation of the enzyme. The AKT triplet could even be deleted or have insertions of 6 or 12 amino acids and still support growth with only minimal reduction in growth rate (Siezen et al., 1993). The AKT is located in one of the regions shown in **Figure 5** to change position at contact with substrate. In our proposed model this contact with substrate could be the trigger switching the histidine to the on-position in the active site. It is interesting that the residues between 322 and 324 can be deleted and mutated without loss of activity. This might support the conclusion that this region of the molecule is adopting variable conformations. It certainly must lead to the conclusion that these residues do not play an essential role in recognizing a specific cleavage site. If the region serves a role as sensor of the length of substrate to avoid digesting small peptides even further, one would expect the phenotypes of the mutants to lead to altered length requirements for the substrate and give a different mix of positions of the actual cleavage sites. This phenotype was exactly what was observed by Siezen et al. (1993) Wild-type SK11 PrtP cleave α_{S1}(1–23) at three sites between 16 and 23 with the site closest to the N-terminus being between 16 and 17. Mutant GLA is able to cleave closer to the N-terminus at bond 13–14, mutant GDT goes as close to the N-terminus as the Wg2 PrtP and cleaves at bond 8–9, whereas mutant GPP is changed in the other direction to give a longer product by only cleaving at one site between 21 and 22 (Siezen et al., 1993).

An interesting aspect of PrtP of *Lactococcus lactis* is the need for a maturation protein PrtM for activity (Vos et al., 1989b). PrtM is a prolyl *cis/trans* isomerase needed as a chaperone for PrtP to attain activity (Siezen, 1999). It is not known which of

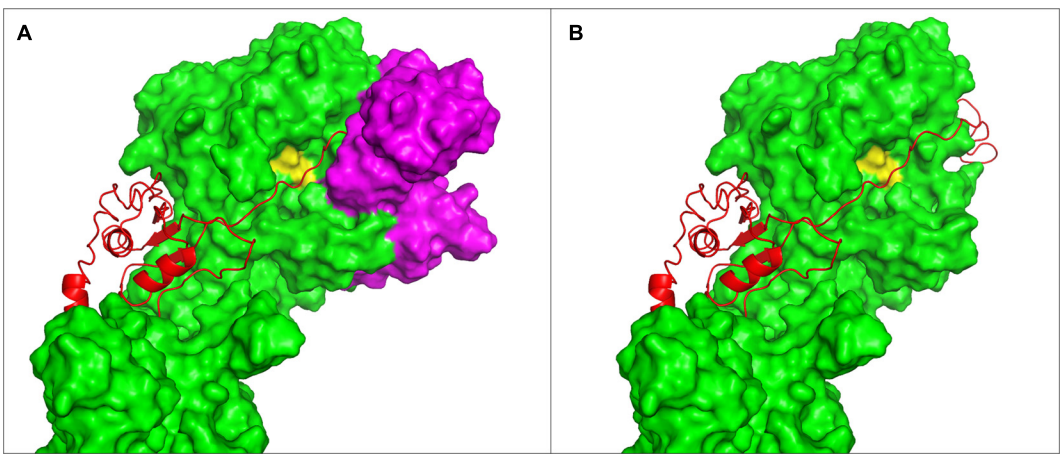

FIGURE 10 | Position of the dispensable loop of Bruinenberg et al. (1994b). The structure of PrtP iTAS_4 model is shown as surface in green. Substrate positioned in the catalytic cleft is shown as red cartoon. The catalytic triad is shown as yellow on the surface of the enzyme. **(A)** The loop from 423 to 573 is shown in magenta, on **(B)** the entire loop has been removed. Residues 422 and 574 are quite close in the model (10 Å distance).

the 69 prolines in PrtP are depending on PrtM to attain the active conformation. That the prolines of domain W should be the target, as suggested by Siezen (1999)is not likely, as truncated versions lacking W also depend on PrtM (Vos et al., 1989b). The proteolytic domain must depend on some of the critical prolines as autocatalytic processing of PrtP does not occur in absence of prtM (Vos et al., 1989b).

The templates used for modeling the structure of *Lactococcus lactis* MS22337 PrtP by iTASSER, Phyre2, and Swiss model come from the streptococcal C5a proteases ScpA and ScpB from *Streptococcus pyogenes* and *Streptococcus agalactiae* respectively (Brown et al., 2005; Kagawa et al., 2009). The structure determined by Brown et al. (2005) was obtained with a recombinant mutant protein expressed in *Escherichia coli* with the asp and ser of the catalytic triad replaced by alanines and without the pro-peptide. This structure has the histidine of the catalytic triad separated by 20 Å from the active position (Brown et al., 2005). The structure determined by Kagawa et al. (2009) was determined on a recombinant protein produced in *E. coli* containing the pro-peptide and only omitting the signal peptide. No substitutions were made and the protein had enzymatic activity (Kagawa et al., 2009). It is an open question if the different position of the histidine residue has biological relevance or if it is due to an artifact caused by the absence of the pro-peptide. The pro-peptide of subtilisin is a catalyst for correct folding of the active enzyme (Zhu et al., 1989). It is plausible that the pro-peptide serves a similar role for these much larger proteases and that this explains the extraordinary length of the pro-peptides. The C5 proteinase is a very specific proteinase with only one known substrate complement factor C5a, a 74 amino acid peptide (Kagawa and Cooney, 2013). Kagawa et al. (2009) modeled the interaction between the C5a protease and the C5a peptide and concluded that the specificity arises from complementarity between the surface of the Fn2 domain and the core structure of the peptide (Kagawa et al., 2009). Eighteen amino acids of C5a peptide between 1 and 64 could form hydrogen-, ionic-, and hydrophobic interactions with 24 amino acids on the proteinase in the region between residue 751–887 (Kagawa et al., 2009). This region would correspond to the region between residues 857–993 in MS22337 PrtP, and thus include "the blue region" of **Figure 5D** which also include the residues shown to determine the SK11 PrtP preference for α_{S1} casein.

The role of domains B, H, and W in determining the specificity of CEP has been investigated by Bruinenberg et al. (2000), and they concluded that these domains are dispensable for protease activity and that they have no role in determining the specificity of the CEP enzyme. These results are important, but leaves the question of the actual function unanswered. It seems unlikely that such large domains would be maintained through evolution if they were entirely dispensable. The B domain contains the protease sensitive site exposed in absence of Ca ions and leading to autocatalytic release of the CEP from the cell wall (Bruinenberg et al., 1994a). We here propose that the function of the B domain is to position the proteinase deeply into the casein micelle. A low calcium concentration will indicate that the proteinase does not reside in a casein micelle, and under such conditions, the release of the protease might be advantageous. We suggest that the H domain might be a domain stocking the peptide products until received by OppA.

The function of domain W has been the subject of very little experimental investigation. Most researchers seem to accept the plausible suggestion of this domain being a spacer allowing the CEP enzyme to raise above the various surface layers of Gram positive bacteria (Chapot-Chartier et al., 2010; Chapot-Chartier and Kulakauskas, 2014; Mercier-Bonin and Chapot-Chartier, 2017). However, a study designed to determine the required number of W-units needed to lift an antigen above the surface layers gave the surprising result that the W-domain is an adhesin able to bind to itself and to epithelial surfaces (Gajic, 2003). In a different study the adhesive properties of PrtP were found to result in adhesion to polystyrene, mucin, and fibronectin (Radziwill-Bienkowska et al., 2017). The actual structure for the W-domain proposed by us could be far from the true structure as we picked this structure among other weak candidates based on the function as adhesin and because the structure seems to fit well with a domain which can be expanded by repeating the same unit or even fractions of the unit. The exact structure of W is not critical for our model but the function as an adhesin binding to kappa casein would be essential.

CONCLUSION

From the sequence of the *Lactococcus lactis* MS22337 cell envelope proteinase, PrtP, we have modeled a structure for the complete enzyme of 1942 amino acids. Based on the model we could assign probable functions for the domains of this multi domain enzyme. These predictions are useful for guiding further experimental investigations of cell wall proteinases of lactic acid bacteria, including pathogens. The model has a general implication for serine proteases carrying a PA domain and fibronectin like domains downstream for the protease domain. This combination of domains seems to allow evolution of almost any type of specificity as substrate recognition at a fibronectin like domain activates an unspecific protease residing at a separate domain.

DATA AVAILABILITY STATEMENT

The datasets presented in this study can be found in online repositories. The names of the repository/repositories and accession number(s) can be found in the article.

AUTHOR CONTRIBUTIONS

EH conceived the research strategy, conducted the modeling analyses, and drafted the manuscript. PM contributed with expertise on protein modeling particularly the use of evolutionary algorithms and participated in writing the manuscript. Both authors contributed to the article and approved the submitted version.

FUNDING

We are grateful for the financial support from Innovation Fund Denmark to the project PROVIDE, grant number: 7045-00021B.

ACKNOWLEDGMENTS

We want to thank Carl Holt for sharing his casein micelle artwork and for permission to include the micelle representation in our illustrations. We also want to thank Dr. Girbe Buist for alerting us to the research of Dr. Gajic.

SUPPLEMENTARY MATERIAL

The Supplementary Material for this article can be found online at: https://www.frontiersin.org/articles/10.3389/fbioe.2020.613986/full#supplementary-material

REFERENCES

Abdelgadir, W., Nielsen, D. S., Hamad, S., and Jakobsen, M. (2008). A traditional Sudanese fermented camel's milk product, gariss, as a habitat of *Streptococcus infantarius* subsp. infantarius. *Int. J. Food Microbiol.* 127, 215–219. doi: 10.1016/j.ijfoodmicro.2008.07.008

Bachmann, H., Starrenburg, M. J. C., Molenaar, D., Kleerebezem, M., and van Hylckama Vlieg, J. E. T. (2012). Microbial domestication signatures of *Lactococcus lactis* can be reproduced by experimental evolution. *Genome Res.* 22, 115–124. doi: 10.1101/gr.121285.111

Balder, R., Lipski, S., Lazarus, J. J., Grose, W., Wooten, R. M., Hogan, R. J., et al. (2010). Identification of *Burkholderia mallei* and *Burkholderia pseudomallei* adhesins for human respiratory epithelial cells. *BMC Microbiol.* 10:250. doi: 10.1186/1471-2180-10-250

Bergman, C., Kashiwaya, Y., and Veech, R. L. (2010). The effect of pH and free Mg2+ on ATP linked enzymes and the calculation of Gibbs free energy of ATP hydrolysis. *J. Phys. Chem. B* 114, 16137–16146. doi: 10.1021/jp105723r

Berhe, T., Ipsen, R., Seifu, E., Kurtu, M. Y., Eshetu, M., and Hansen, E. B. (2018). Comparison of the acidification activities of commercial starter cultures in camel and bovine milk. *LWT* 89, 123–127. doi: 10.1016/j.lwt.2017.10.041

Børsting, M. W., Qvist, K. B., Brockmann, E., Vindeløv, J., Pedersen, T. L., Vogensen, F. K., et al. (2015). Classification of *Lactococcus lactis* cell envelope proteinase based on gene sequencing, peptides formed after hydrolysis of milk, and computer modeling. *J. Dairy Sci.* 98, 68–77. doi: 10.3168/jds.2014-8517

Bragason, E., Svendsen, C. A., Guya, M. E., Berhe, T., and Hansen, E. B. (2020). Draft Genome Sequences of *Lactococcus lactis* strains MS22314, MS22333, MS22336, and MS22337, Isolated from Fermented Camel Milk in Ethiopia. *Microbiol. Resour. Announc.* 9:e00862-20. doi: 10.1128/MRA.00862-20

Broadbent, J. R., and Steele, J. L. (2013). Lactocepin: the cell envelope-associated Endopeptidase of lactococci. *Handb. Proteolytic Enzym.* 3, 3188–3195. doi: 10.1016/B978-0-12-382219-2.00703-1

Broadbent, J. R., Strickland, M., Weimer, B. C., Johnson, M. E., and Steele, J. L. (1998). Peptide accumulation and bitterness in cheddar cheese made using single-strain *Lactococcus lactis* starters with distinct proteinase specificities. *J. Dairy Sci.* 81, 327–337. doi: 10.3168/jds.S0022-0302(98)75581-X

Brown, C. K., Gu, Z.-Y., Matsuka, Y. V., Purushothaman, S. S., Winter, L. A., Cleary, P. P., et al. (2005). Structure of the streptococcal cell wall C5a peptidase. *Proc. Natl. Acad. Sci. U.S.A.* 102, 18391–18396. doi: 10.1073/pnas.0504954102

Broyard, C., and Gaucheron, F. (2015). Modifications of structures and functions of caseins: a scientific and technological challenge. *Dairy Sci. Technol.* 95, 831–862. doi: 10.1007/s13594-015-0220-y

Bruinenberg, P. G., de Vos, W. M., and Siezen, R. J. (1994a). Prevention of C-terminal autoprocessing of *Lactococcus lactis* SK11 cell-envelope proteinase by engineering of an essential surface loop. *Biochem. J.* 302, 957–963. doi: 10.1042/bj3020957

Bruinenberg, P. G., Doesburg, P., Alting, A. C., Exterkate, F. A., Vos, W. M. D., and Siezen, R. J. (1994b). Evidence for a large dispensable segment in the subtilisin-like catalytic domain of the *Lactococcus lactis* cell-envelope proteinas. *Protein Eng. Des. Sel.* 7, 991–996. doi: 10.1093/protein/7.8.991

Bruinenberg, P. G., De Vos, W. M., and Siezen, R. J. (2000). Deletion of various carboxy-terminal domains of *Lactococcus lactis* SK11 proteinase: effects on activity, specificity, and stability of the truncated enzyme. *Appl. Environ. Microbiol.* 66, 2859–2865. doi: 10.1128/AEM.66.7.2859-2865.2000

Chapot-Chartier, M. P., and Kulakauskas, S. (2014). Cell wall structure and function in lactic acid bacteria. *Microb. Cell Fact.* 13:S9. doi: 10.1186/1475-2859-13-S1-S9

Chapot-Chartier, M. P., Vinogradov, E., Sadovskaya, I., Andre, G., Mistou, M. Y., Trieu-Cuot, P., et al. (2010). Cell surface of *Lactococcus lactis* is covered by a protective polysaccharide pellicle. *J. Biol. Chem.* 285, 10464–10471. doi: 10.1074/jbc.M109.082958

Cranford-Smith, T., and Huber, D. (2018). The way is the goal: how SecA transports proteins across the cytoplasmic membrane in bacteria. *FEMS Microbiol. Lett.* 365, 1–16. doi: 10.1093/femsle/fny093

de Vos, W. M., Vos, P., de Haard, H., and Boerrigter, I. (1989). Cloning and expression of the *Lactococcus lactis* subsp. cremoris SK11 gene encoding an extracellular serine proteinase. *Gene* 85, 169–176. doi: 10.1016/0378-1119(89)90477-0

Doeven, M. K., Kok, J., and Poolman, B. (2005). Specificity and selectivity determinants of peptide transport in *Lactococcus lactis* and other microorganisms. *Mol. Microbiol.* 57, 640–649. doi: 10.1111/j.1365-2958.2005.04698.x

Domingo Meza-Aguilar, J., Fromme, P., Torres-Larios, A., Mendoza-Hernández, G., Hernandez-Chiñas, U., Arreguin-Espinosa De Los Monteros, R. A., et al. (2014). X-ray crystal structure of the passenger domain of plasmid encoded toxin(Pet), an autotransporter enterotoxin from enteroaggregative *Escherichia coli* (EAEC). *Biochem. Biophys. Res. Commun.* 445, 439–444. doi: 10.1016/j.bbrc.2014.02.016

Drici, H., Gilbert, C., Kihal, M., and Atlan, D. (2010). Atypical citrate-fermenting *Lactococcus lactis* strains isolated from dromedary's milk. *J. Appl. Microbiol.* 108, 647–657. doi: 10.1111/j.1365-2672.2009.04459.x

Drici, H. (2008). Analyse Physiologique, Génétique et Moléculaire de Lactocoques Protéolytiques Issus du lait cru de Chamelle d ' Algérie. Thesis, Université Claude Bernard, Lyon, France.

Exterkate, F. A. (1990). Differences in short peptide-substrate cleavage by two cell-envelope-located serine proteinases of *Lactococcus lactis* subsp. cremoris are related to secondary binding specificity. *Appl. Microbiol. Biotechnol.* 33, 401–406. doi: 10.1007/BF00176654

Exterkate, F. A., and Alting, A. C. (1999). Role of calcium in activity and stability of the *Lactococcus lactis* cell envelope proteinase. *Appl. Environ. Microbiol.* 65, 1390–1396. doi: 10.1128/AEM.65.4.1390-1396.1999

Exterkate, F. A., Alting, A. C., and Bruinenberg, P. G. (1993). Diversity of cell envelope proteinase specificity among strains of *Lactococcus lactis* and its relationship to charge characteristics of the substrate-binding region. *Appl. Environ. Microbiol.* 59, 3640–3647. doi: 10.1128/aem.59.11.3640-3647.1993

Fugl, A., Berhe, T., Kiran, A., Hussain, S., Laursen, M. F., Bahl, M. I., et al. (2017). Characterisation of lactic acid bacteria in spontaneously fermented camel milk and selection of strains for fermentation of camel milk. *Int. Dairy J.* 73, 19–24. doi: 10.1016/j.idairyj.2017.04.007

Gabed, N., Yang, M., Bey, M., Hamed, B., Drici, H., Gross, R., et al. (2015). Draft genome sequence of the moderately heat-tolerant *Lactococcus lactis* subsp . lactis bv . diacetylactis Strain GL2 from Algerian. *Genome Announc* 3, 13–14. doi: 10.1128/genomeA.01334-15

Gajic, O. (2003). *Relationships Between MDR Proteins, Bacteriocin Production and Proteolysis in Lactococcus lactis*. PhD Thesis, University of. Groningen, Netherlands.

Gänzle, M. G. (2015). Lactic metabolism revisited: metabolism of lactic acid bacteria in food fermentations and food spoilage. *Curr. Opin. Food Sci.* 2, 106–117. doi: 10.1016/j.cofs.2015.03.001

Griessl, M. H., Schmid, B., Kassler, K., Braunsmann, C., Ritter, R., Barlag, B., et al. (2013). Structural insight into the giant Ca2+-binding adhesin siie: implications for the adhesion of *Salmonella enterica* to polarized epithelial cells. *Structure* 21, 741–752. doi: 10.1016/j.str.2013.02.020

Haandrikman, A. J., Kok, J., Laan, H., Soemitro, S., Ledeboer, A. M., Konings, W. N., et al. (1989). Identification of a gene required for maturation of an extracellular lactococcal serine proteinase. *Environ. Microbiol.* 171, 2789–2794. doi: 10.1128/jb.171.5.2789-2794.1989

Holt, C. (2016). Casein and casein micelle structures, functions and diversity in 20 species. *Int. Dairy J.* 60, 2–13. doi: 10.1016/j.idairyj.2016.01.004

Horne, D. S. (2008). *Casein Micelle Structure and Stability*, 2nd Edn. Amsterdam: Elsevier Inc, doi: 10.1016/B978-0-12-374039-7.00005-2

Jensen, P. R., and Hammer, K. (1993). Minimal requirements for exponential growth of *Lactococcus lactis*. *Appl. Environ. Microbiol.* 59, 4363–4366. doi: 10.1093/emboj/16.12.3533

Jobichen, C., Tan, Y. C., Prabhakar, M. T., Nayak, D., Biswas, D., Pannu, N. S., et al. (2018). Structure of ScpC, a virulence protease from *Streptococcus pyogenes*, reveals the functional domains and maturation mechanism. *Biochem. J.* 475, 2847–2860. doi: 10.1042/BCJ20180145

Juillard, V., Laan, H., Kunji, E. R. S., Jeronimus-Stratingh, C. M., Bruins, A. P., and Konings, W. N. (1995a). The extracellular P(I)-type proteinase of *Lactococcus lactis* hydrolyzes β-casein into more than one hundred different oligopeptides. *J. Bacteriol.* 177, 3472–3478. doi: 10.1128/jb.177.12.3472-3478.1995

Juillard, V., le Bars, D., Kunji, E. R. S., Konings, W. N., Gripon, J.-C., and Richard, J. (1995b). Oligopeptides are the main source of nitrogen for *Lactococcus lactis* during growth in milk. *Appl. Environ. Microbiol.* 61, 3024–3030. doi: 10.1128/aem.61.8.3024-3030.1995

Kagawa, T. F., and Cooney, J. C. (2013). "C5a Peptidase," in *Handbook of Proteolytic Enzymes*, eds N. D. Rawlings, and G. Salvesen (Amsterdam: Elsevier), 3202–3208. doi: 10.1016/B978-0-12-382219-2.00705-5

Kagawa, T. F., O'Connell, M. R., Mouat, P., Paoli, M., O'Toole, P. W., and Cooney, J. C. (2009). Model for Substrate Interactions in C5a Peptidase from *Streptococcus pyogenes*: a 1.9 Å Crystal Structure of the Active Form of ScpA. *J. Mol. Biol.* 386, 754–772. doi: 10.1016/j.jmb.2008.12.074

Kelley, L. A., Mezulis, S., Yates, C. M., Wass, M. N., and Sternberg, M. J. E. (2015). The Phyre2 web portal for protein modeling, prediction and analysis. *Nat. Protoc.* 10, 845–858. doi: 10.1038/nprot.2015.053

Kim, J.-S., Kluskens, L. D., de Vos, W. M., Huber, R., and van der Oost, J. (2004). Crystal structure of fervidolysin from fervidobacterium pennivorans, a keratinolytic enzyme related to subtilisin. *J. Mol. Biol.* 335, 787–797. doi: 10.1016/j.jmb.2003.11.006

Kliche, T., Li, B., Bockelmann, W., Habermann, D., Klempt, M., de Vrese, M., et al. (2017). Screening for proteolytically active lactic acid bacteria and bioactivity of peptide hydrolysates obtained with selected strains. *Appl. Microbiol. Biotechnol.* 101, 7621–7633. doi: 10.1007/s00253-017-8369-3

Kok, J., Leenhouts, K. J., Haandrikman, A. J., Ledeboer, A. M., and Venema, G. (1988). Nucleotide sequence of the cell wall proteinase gene of *Streptococcus cremoris* Wg2. *Appl. Environ. Microbiol.* 54, 231–238. doi: 10.1128/AEM.54.1.231-238.1988

Locher, K. P. (2016). Mechanistic diversity in ATP-binding cassette (ABC) transporters. *Nat. Struct. Mol. Biol.* 23, 487–493. doi: 10.1038/nsmb.3216

Makarova, K., Slesarev, A., Wolf, Y., Sorokin, A., Mirkin, B., Koonin, E., et al. (2006). Comparative genomics of the lactic acid bacteria. *Proc. Natl. Acad. Sci. U.S.A* 103, 15611–15616. doi: 10.1073/pnas.0607117103

Marks, D. S., Hopf, T. A., and Sander, C. (2012). Protein structure prediction from sequence variation. *Nat. Biotechnol.* 30, 1072–1080. doi: 10.1038/nbt.2419

Martin, R. B. (1998). Free energies and equilibria of peptide bond hydrolysis and formation. *Biopolymers* 45, 351–353. doi: 10.1002/(SICI)1097-0282(19980415)45:5<351::AID-BIP3<3.0.CO;2-K

Mercier-Bonin, M., and Chapot-Chartier, M.-P. (2017). Surface proteins of *Lactococcus lactis*: bacterial resources for muco-adhesion in the gastrointestinal tract. *Front. Microbiol.* 8:2247. doi: 10.3389/fmicb.2017.02247

Murayama, K., Kato-Murayama, M., Hosaka, T., Sotokawauchi, A., Yokoyama, S., Arima, K., et al. (2012). Crystal structure of cucumisin, a subtilisin-like endoprotease from *Cucumis melo* L. *J. Mol. Biol.* 423, 386–396. doi: 10.1016/j.jmb.2012.07.013

Radziwill-Bienkowska, J. M., Robert, V., Drabot, K., Chain, F., Cherbuy, C., Langella, P., et al. (2017). Contribution of plasmid-encoded peptidase S8 (PrtP) to adhesion and transit in the gut of *Lactococcus lactis* IBB477 strain. *Appl. Microbiol. Biotechnol.* 101, 5709–5721. doi: 10.1007/s00253-017-8334-1

Savijoki, K., Ingmer, H., and Varmanen, P. (2006). Proteolytic systems of lactic acid bacteria. *Appl. Microbiol. Biotechnol.* 71, 394–406. doi: 10.1007/s00253-006-0427-1

Schechter, I., and Berger, A. (1967). On the size of the active site in proteases. I. Papain. *Biochem. Biophys. Res. Commun.* 27, 157–162. doi: 10.1016/s0006-291x(67)80055-x

Scheepers, G. H., Lycklama, A., Nijeholt, J. A., and Poolman, B. (2016). An updated structural classification of substrate-binding proteins. *FEBS Lett.* 590, 4393–4401. doi: 10.1002/1873-3468.12445

Siezen, R. J. (1999). Multi-domain, cell-envelope proteinases of lactic acid bacteria. *Antonie van Leeuwenhoek* 76, 139–155. doi: 10.1023/A:1002036906922

Siezen, R. J., Bruinenberg, P. G., Vos, P., van Alen-Boerrigter, I., Nijhuis, M., and Alting, A. C. (1993). Engineering of the substrate-binding region of the sublilisin-like, cell-envelop proteinase of *Lactococcus lactis*. *Protein Eng. Des. Sel.* 6, 927–937. doi: 10.1093/protein/6.8.927

Siezen, R. J., and Leunissen, J. A. M. (2010). Subtilases: the superfamily of subtilisin-like serine proteases. *Protein Sci.* 6, 501–523. doi: 10.1002/pro.5560060301

Siezen, R. J., Renckens, B., Van Swam, I., Peters, S., Van Kranenburg, R., Kleerebezem, M., et al. (2005). Complete sequences of four plasmids of *Lactococcus lactis* subsp. *cremoris SK*11 reveal extensive adaptation to the dairy environment. *Appl. Environ. Microbiol.* 71, 8371–8382. doi: 10.1128/AEM.71.12.8371-8382.2005

Sodini, I., Latrille, E., and Corrieu, G. (2000). Identification of interacting mixed cultures of lactic acid bacteria by their exclusion from a model predicting the acidifying activity of non-interacting mixed cultures. *Appl. Microbiol. Biotechnol.* 54, 715–718. doi: 10.1007/s002530000460

Vance, T. D. R., Olijve, L. L. C., Campbell, R. L., Voets, I. K., Davies, P. L., and Guo, S. (2014). Ca2+-stabilized adhesin helps an Antarctic bacterium reach out and bind ice. *Biosci. Rep.* 34, 357–368. doi: 10.1042/BSR20140083

Vermeulen, N., Pavlovic, M., Ehrmann, M. A., Ganzle, M. G., and Vogel, R. F. (2005). Functional Characterization of the proteolytic system of *Lactobacillus sanfranciscensis* DSM 20451T during Growth in Sourdough. *Appl. Environ. Microbiol.* 71, 6260–6266. doi: 10.1128/AEM.71.10.6260-6266.2005

Visser, S., Exterkate, F. A., Slangen, C. J., and de Veer, G. J. C. M. (1986). Comparative study of action of cell wall proteinases from various strains of *Streptococcus cremoris* on Bovine α s1-, β-, and κ-Casein. *Appl. Environ. Microbiol.* 52, 1162–1166. doi: 10.1128/AEM.52.5.1162-1166.1986

Visser, S., Robben, A. J. P. M., and Slangen, C. J. (1991). Specificity of a cell-envelope-located proteinase (Pro-type) from *Lactococcus lactis* subsp, cremoris AM1 in its action on bovine//-casein. *Appl. Microbiol. Biotechnol.* 35, 477–483.

Visser, S., Slangen, C. J., Exterkate, F. A., and de Veer, G. J. C. M. (1988). Action of a cell wall proteinase (PI) from *Streptococcus cremoris* HP on bovine β-casein. *Appl. Microbiol. Biotechnol.* 29, 61–66. doi: 10.1007/BF00258352

Visser, S., Slangen, C. J., Robben, A. J. P. M., van Dongen, W. D., Heerma, W., and Haverkamp, J. (1994). Action of a cell-envelope proteinase (CEPIII-type) from *Lactococcus lactis* subsp. *cremoris AM*1 on bovine κ-casein. *Appl. Microbiol. Biotechnol.* 41, 644–651. doi: 10.1007/BF00167279

Vos, P., Boerrigter, I. J., Buist, G., Haandrikman, A. J., Nijhuis, M., de Reuver, M. B., et al. (1991). Engineering of the *Lactococcus lactis* serine proteinase by construction of hybrid enzymes. *Protein Eng. Des. Sel.* 4, 479–484. doi: 10.1093/protein/4.4.479

Vos, P., Simons, G., Siezen, R. J., and de Vos, W. M. (1989a). Primary structure and organization of the gene for a procaryotic, cell envelope-located serine proteinase. *J. Biol. Chem.* 264, 13579–13585.

Vos, P., van Asseldonk, M., van Jeveren, F., Siezen, R., Simons, G., and de Vos, W. M. (1989b). A maturation protein is essential for production of active forms of *Lactococcus lactis* SK11 serine proteinase located in or secreted from the cell envelope. *J. Bacteriol.* 171, 2795–2802. doi: 10.1128/JB.171.5.2795-2802.1989

Wang, S., Sun, S., Li, Z., Zhang, R., and Xu, J. (2017). Accurate de novo prediction of protein contact map by ultra-deep learning model. *PLoS Comput. Biol.* 13:e1005324. doi: 10.1371/journal.pcbi.1005324

Waterhouse, A., Bertoni, M., Bienert, S., Studer, G., Tauriello, G., Gumienny, R., et al. (2018). SWISS-MODEL: homology modelling of protein structures

and complexes. *Nucleic Acids Res.* 46, W296–W303. doi: 10.1093/nar/gky427

Xu, J. (2019). Distance-based protein folding powered by deep learning. *Proc. Natl. Acad. Sci. U.S.A.* 116, 16856–16865. doi: 10.1073/pnas.1821309116

Yang, J., Yan, R., Roy, A., Xu, D., Poisson, J., and Zhang, Y. (2015). The I-TASSER Suite: protein structure and function prediction. *Nat. Methods* 12, 7–8. doi: 10.1038/nmeth.3213

Zambolin, S., Clantin, B., Chami, M., Hoos, S., Haouz, A., Villeret, V., et al. (2016). Structural basis for haem piracy from host haemopexin by *Haemophilus influenzae*. *Nat. Commun.* 7:11590. doi: 10.1038/ncomms11590

Zhang, Y., and Skolnick, J. (2004). Scoring function for automated assessment of protein structure template quality. *Proteins Struct. Funct. Bioinforma* 57, 702–710. doi: 10.1002/prot.20264

Zhou, X., Hu, J., Zhang, C., Zhang, G., and Zhang, Y. (2019). Assembling multidomain protein structures through analogous global structural alignments. *Proc. Natl. Acad. Sci. U.S.A.* 116, 15930–15938. doi: 10.1073/pnas.1905068116

Zhu, X., Ohta, Y., Jordan, F., and Inouye, M. (1989). Pro-sequence of subtilisin can guide the refolding of denatured subtilisin in an intermolecular process. *Nature* 339, 483–484. doi: 10.1038/339483a0

Conflict of Interest: The authors declare that the research was conducted in the absence of any commercial or financial relationships that could be construed as a potential conflict of interest.

frontiers in Bioengineering and Biotechnology

ORIGINAL RESEARCH
published: 06 January 2021
doi: 10.3389/fbioe.2020.611701

Efficient Production of Pyruvate Using Metabolically Engineered *Lactococcus lactis*

Fan Suo[1], *Jianming Liu*[1], *Jun Chen*[1], *Xuanji Li*[2], *Christian Solem*[1]* *and Peter R. Jensen*[1]*

[1] Division of Production and Microbiology, National Food Institute, Technical University of Denmark, Lyngby, Denmark,
[2] Section of Microbiology, Department of Biology, University of Copenhagen, Copenhagen, Denmark

Microbial production of commodity chemicals has gained increasing attention and most of the focus has been on reducing the production cost. Selecting a suitable microorganism, which can grow rapidly on cheap feedstocks, is of key importance when developing an economically feasible bioprocess. We chose *Lactococcus lactis*, a well-characterized lactic acid bacterium, as our microbial host to produce pyruvate, which is a commodity chemical with various important applications. Here we report the engineering of *Lactococcus lactis* into becoming an efficient microbial platform for producing pyruvate. The strain obtained, FS1076 (MG1363 Δ^3*ldh Δpta ΔadhE Δals*), was able to produce pyruvate as the sole product. Since all the competitive pathways had been knocked out, we achieved growth-coupled production of pyruvate with high yield. More than 80 percent of the carbon flux was directed toward pyruvate, and a final titer of 54.6 g/L was obtained using a fed-batch fermentation setup. By introducing lactose catabolism into FS1076, we obtained the strain FS1080, which was able to generate pyruvate from lactose. We then demonstrated the potential of FS1080 for valorizing lactose contained in dairy side-streams, by achieving a high titer (40.1 g/L) and high yield (78.6%) of pyruvate using residual whey permeate (RWP) as substrate. The results obtained, show that the *L. lactis* platform is well-suited for transforming lactose in dairy waste into food-grade pyruvate, and the yields obtained are the highest reported in the literature. These results demonstrate that it is possible to achieve sustainable bioconversion of waste products from the dairy industry (RWP) to valuable products.

Keywords: high-yield pyruvate production, *Lactococcus lactis*, metabolic engineering, dairy side-stream, fermentation

OPEN ACCESS

Edited by:
Pasquale Stano, University of Salento, Italy

Reviewed by:
Kaemwich Jantama, Suranaree University of Technology, Thailand
Aron Nemeth, Budapest University of Technology and Economics, Hungary

***Correspondence:**
Christian Solem
chso@food.dtu.dk
Peter R. Jensen
perj@food.dtu.dk

Specialty section:
This article was submitted to Synthetic Biology, a section of the journal Frontiers in Bioengineering and Biotechnology

Received: *29 September 2020*
Accepted: *27 November 2020*
Published: *06 January 2021*

Citation:
Suo F, Liu J, Chen J, Li X, Solem C and Jensen PR (2021) Efficient Production of Pyruvate Using Metabolically Engineered Lactococcus lactis. Front. Bioeng. Biotechnol. 8:611701. doi: 10.3389/fbioe.2020.611701

INTRODUCTION

Pyruvic acid (pyruvate), the simplest of the α-keto acids, serves a key role in living organisms. Pyruvate has many important applications, e.g., as a food supplement and as a precursor for chemicals and pharmaceuticals, and the demand for this compound has greatly increased over the past few decades (Park et al., 1998; Rosche et al., 2001; Zelić et al., 2003; Reiße et al., 2016). Pyruvate can be made by classical chemical synthesis or by microbial fermentation, where the latter approach is preferred, especially for sensitive applications such as use in food (Li et al., 2001; Stottmeister et al., 2005; Maleki and Eiteman, 2017). Chemically synthesized pyruvate is expensive, and Li et al.

estimated the total cost of production from tartaric acid by dehydration and decarboxylation to be US 8,000–9,000/ton (Li et al., 2001). The fermentative approach for producing pyruvate was developed much later, probably due to the difficulties associated with getting microorganisms to secrete a central metabolite (Li et al., 2001). In the late 1980s, Toray Industries in Japan submitted several patent applications for fermentative production of pyruvate using the multi-vitamin auxotrophic yeast *Candida glabrata* (previously named *Torulopsus glabrata*) (Miyata et al., 1989a,b,c, 1990), and *C. glabrata* continues to be one of the best pyruvate producers available. The *C. glabrata* strains used are auxotrophic for thiamine (vitamin B1), nicotinic acid, biotin and pyridoxine (vitamin B6), and when grown with limiting amount of these vitamins start to secrete large amounts of pyruvate due to low activities of pyruvate dehydrogenase, pyruvate decarboxylase (PDC), pyruvate carboxylase (PC), and transaminase (Li et al., 2016). *C. glabrata* is a good pyruvate producer as it possesses a high tolerance to low pH, which lowers product recovery costs, and since it can grow on relatively simple and cheap media (Li et al., 2016), albeit with a low growth rate. Using a pH-controlled fermentation setup and an osmotolerant *C. glabrata* mutant, Liu et al. achieved a high titer of 94.3 g/L, however, the fermentation lasted 82 h and the yield was fairly low (0.635 g pyruvate/g glucose), resulting in a low productivity of 1.15 g L^{-1} h^{-1}, despite using a large inoculum of 10% (Liu et al., 2007). Miyata and Yonehara achieved a somewhat lower titer of 67.8 g/L after an almost 70 h fermentation using a medium containing soy bean hydrolysate, and the yield was less than 50% (Miyata and Yonehara, 1996). There is thus great opportunity for improving the fermentation process, perhaps by using other organisms. There have been several efforts aiming to achieve pyruvate production in prokaryotes. *E. coli* is commonly used as a production host for various compounds, mainly due to its well-characterized metabolism and the plethora of genetic tools available for its manipulation. Yokota et al., using a lipoic acid auxotroph of *E. coli*, managed to produce 25.5 g/L with a 51% yield in 32–40 h, in a pH-controlled fermentation using a mineral medium, however, a 4% inoculum grown in rich medium was needed (Yokota et al., 1994). *E. coli*, despite of its ease of manipulation, is not always a suitable production host, especially for organic acids for which its tolerance is low.

Lactic acid bacteria (LAB) are immensely important within food manufacturing, e.g., the cheese bacterium *Lactococcus lactis* is annually inoculated into more than 100 million tons of milk (Teuber, 1995). Recently, LAB have been widely engineered into producing various valuable biochemicals (Ghaffar et al., 2014; Liu et al., 2016a,b,c,d). Because these bacteria rely on a purely fermentative metabolism, they usually have a high glycolytic capacity. They are also able to metabolize a broad range of carbohydrates, and are becoming increasingly easy to manipulate genetically (Kleerebezem et al., 2000; Liu et al., 2017). They naturally thrive in carbohydrate-rich environments, and usually produce lactic acid as the main fermentation product. In this study, we explored the potential of *Lactococcus lactis*, the model organism of LAB, as a pyruvate producer. We rerouted its metabolism from lactate to pyruvate, characterized its performance in various media and optimized the fermentation. We successfully managed to produce pyruvate from glucose, and also from lactose contained in dairy waste. We found that *L. lactis* has a high potential for pyruvate production, and the fermentation process developed should have industrial relevance.

MATERIALS AND METHODS

Strains and Plasmids

The bacterial strains and plasmids used in this study have been listed in **Table 1**. *L. lactis* subsp. *cremoris* MG1363 (Gasson, 1983) or derivatives were used as described in this article. The plasmid pCS1966als, a derivative of plasmid pCS1966 (Solem et al., 2008), was used to delete *als* in *L. lactis*. The plasmid pCS4564 with a thermosensitive replicon carrying *E. coli ldh* (Liu et al., 2016a), was used to increase transformation efficiency of *L. lactis* strains deficient in lactate dehydrogenase. The plasmid pLP712, which carries the lactose utilization gene cluster, was obtained from the dairy isolate NCDO712 (Wegmann et al., 2012). pLC17 (Dorau et al., 2019) contains the *als* gene from *Lactococcus lactis* MG1363, and was used to re-introduce the *als* gene into FS1072.

Growth Experiments

L. lactis was grown at 30°C, either in rich M17 broth (Oxoid TM) and defined SAL medium (Jensen and Hammer, 1993) supplemented with glucose (Terzaghi and Sandine, 1975) and various concentrations of hemin. The compositions of both media can be found in **Supplementary Table 5**. When needed, antibiotics were added to the cultures in the following concentrations: 200 mg/mL erythromycin for *E. coli* and 5 mg/mL erythromycin for *L. lactis*; 8 mg/mL tetracycline for *E. coli* and 5 mg/mL tetracycline for *L. lactis*.

Analytical Methodology

To monitor cell growth, the optical density at 600 nm (OD600) was measured. Glucose, lactate, and pyruvate were quantified using an Ultimate 3000 high-pressure liquid chromatography system (Dionex, Sunnyvale, USA) equipped with a Shodex RI-101 detector (Showa Denko K.K., Tokyo, Japan) and a diode array detector (DAD-3000, Dionex, Sunnyvale, USA), where glucose and lactate were detected using the former and pyruvate using the latter detector. The column used was an Aminex HPX-87H. The oven temperature was set to 60°C, and the flow rate of the mobile phase, which consisted of 5 mM H_2SO_4, was set to 0.5 mL/min.

DNA Techniques

All manipulations were carried out according to Sambrook and Russell (2001). *E. coli* cells were transformed using electroporation. *L. lactis* cells grown in GM17 medium containing 1% glycine were made electrocompetent and transformed by electroporation according to Holo and Nes (1989). Gene deletions were achieved using the method developed by Solem et al. (2008). The plasmid pCS1966als was employed to delete *als* gene in *L. lactis*. When deleting *als* gene, ∼800 bp regions upstream and downstream of the

TABLE 1 | Strains and plasmids.

Designation	Genotype or description	References
***L. lactis* strains**		
CS4363	MG1363 Δ^3*ldh Δpta ΔadhE*	Solem et al., 2013
FS1068	MG1363 Δ^3*ldh Δpta ΔadhE* pCS4564	This work
FS1069	MG1363 Δ^3*ldh Δpta ΔadhE Δals* pCS4564	This work
FS1072	MG1363 Δ^3*ldh Δpta ΔadhE Δals*	This work
FS1073	MG1363 Δ^3*ldh Δpta ΔadhE Δals* pLC17	This work
FS1076	Adaptive mutants derived from FS1072	This work
FS1080	FS1076 with pLP712	This work
Plasmids		
pCS4564	pG$^+$host8::SP-*ldhA* (*E. coli*)	Liu et al., 2016a
pCS1966	The selection/counter selection vector	Solem et al., 2008
pCS1966als	Plasmid used for deleting *als*	This work
pLP712	Plasmid from *L. lactis* NCDO712 encoding lactose utilization gene custer	Wegmann et al., 2012
pLC17	pLC0 inserted with the *als* gene from *Lactococcus lactis* MG1363	Dorau et al., 2019

deleted *als* gene were amplified by PCR and inserted into the plasmid pCS1966. The resulting plasmid pCS1966als was then transformed to *L. lactis*, where integration resulted in erythromycin resistance. Subsequently, counterselection was carried out in the presence of 5-fluoroorotic (5FO), where excision and loss of the plasmid resulted in 5FO resistance (Solem et al., 2008). The upstream region was amplified by using the primers 5′- CTAGTCTAGATTATATAAAATCGCTCTTCTTTATG-3′ and 5′- AAAACTGCAGTTTTTATTTTACCTCTATTTGTTC−3′. The primers used to amplify the downstream region were 5′- AAAACTGCAGTAAAAAACAAGCAAATTGTGAAAT−3′ and 5′- CGGGGTACCTATTTCTTGATCTAGCTGATTAAA -3′.

Strain Construction

Plasmid pCS1966als for deleting *als* was constructed as described above. To assist further manipulations, plasmid pCS4564 with a thermosensitive replicon carrying *E. coli ldh* (Liu et al., 2016a), was transformed into CS4363 inducing FS1068. The *als* gene deletion strain was named FS1069 (MG1363 Δ^3*ldh Δpta ΔadhE Δals* pCS4564). The plasmid pCS4564 was lost by incubation at 36°C in the presence of 5 μg/mL hemin and the resultant strain was FS1072 (MG1363 Δ^3*ldh Δpta ΔadhE Δals*). We further obtained the mutant strain FS1076 through adaptive evolution of FS1072. Moreover, plasmid pLP712 was introduced into strain FS1076 to generate FS1080, which enables the use of residual whey permeate (RWP) as feedstock.

Adaptive Evolution

The strain FS1072 was re-streaked, and a single colony was used as a starting point for the adaptive evolution experiment. The adaption was carried out in a 15 mL centrifuge tube filled with 5 mL SAL medium, supplemented with 1% glucose. Every 24 h, 500 μL of the culture was transferred into a new tube containing fresh medium. Every 7 days, samples were taken from the growing culture, and streaked on an SAL plate, and the largest colony was inoculated into a new tube, whereafter the evolution experiment continued. The entire experiment lasted 21 days.

Pre-culture

For the pre-culture, the strains were grown in 250 mL Erlenmeyer flasks with 25 mL M17 medium supplemented with different concentrations of hemin (0–1 μg/mL) and 1% (w/v) glucose. The bacterial cultures were grown at 200 rpm, 30°C. Alternatively, for strain FS1080, pre-culturing was carried out in diluted residual whey permeate (RWP) containing 1% lactose, and supplemented with yeast extract (0.5–2% w/v). The cultures were grown aerobically with 200 rpm shaking in 250 mL Erlenmeyer flasks at 30°C.

Pyruvate Fermentation

All the fermentation experiments were performed in a 500 mL maximum working volume bioreactor (Sartorius Biostat Q) equipped with standard control units for stirring speed, temperature, pH, aeration, etc. The pH was adjusted to 7.0. All the fermentation experiments were performed at 30°C with a constant aeration rate of 0.2 vvm and a constant stirring speed of 150 rpm. The pH and dissolved oxygen were monitored during the fermentation, and samples were withdrawn regularly to determine glucose, cell density (OD600) and pyruvate concentration.

RNA Analysis

All the RNAseq data analysis in the study were done after data trimming. These included mapping, gene reads counts, normalization, statistical analysis, and gene annotation, and this was done using R (R Development Core Team, 2011). After trimming the reads and checking the quality, we mapped the clean reads to the reference Genome (GenBank accession number: NC_009004) using the function "align" in the Bioconductor package "Rsubread" (Liao et al., 2019). The R function "featureCounts" in the package "Rsubread" was used to summarize the reads and give the number of reads mapped per gene. Before proceeding with the differential expression analysis, we filtered out genes that were expressed to a very low level, meaning less than 1 count-per-million (CPM). Calculating the CPM values were done using the R function "cpm" in the package "edgeR" (Robinson et al., 2009). The R function "voom" in the package "limma" (Ritchie et al., 2015) was used to normalize the read counts as log2CPM and apply a linear model to the normalized data for computing moderated t-statistics of differential expression. The R function "eBayes" in the package "limma" (Ritchie et al., 2015) computed moderated t-statistics of differential expression (DE). The R "topTable" function in the package "limma" (Ritchie et al., 2015) summarized the DE genes

in a table format. The annotation of gene IDs was done manually using the reference genome GFF (General Feature Format) file in R, which consists of the gene annotations. The RNA-Seq data have been deposited at the Sequence Read Archive (SRA) under the accession number PRJNA 669338. https://www.ncbi.nlm.nih.gov/bioproject/PRJNA669338/.

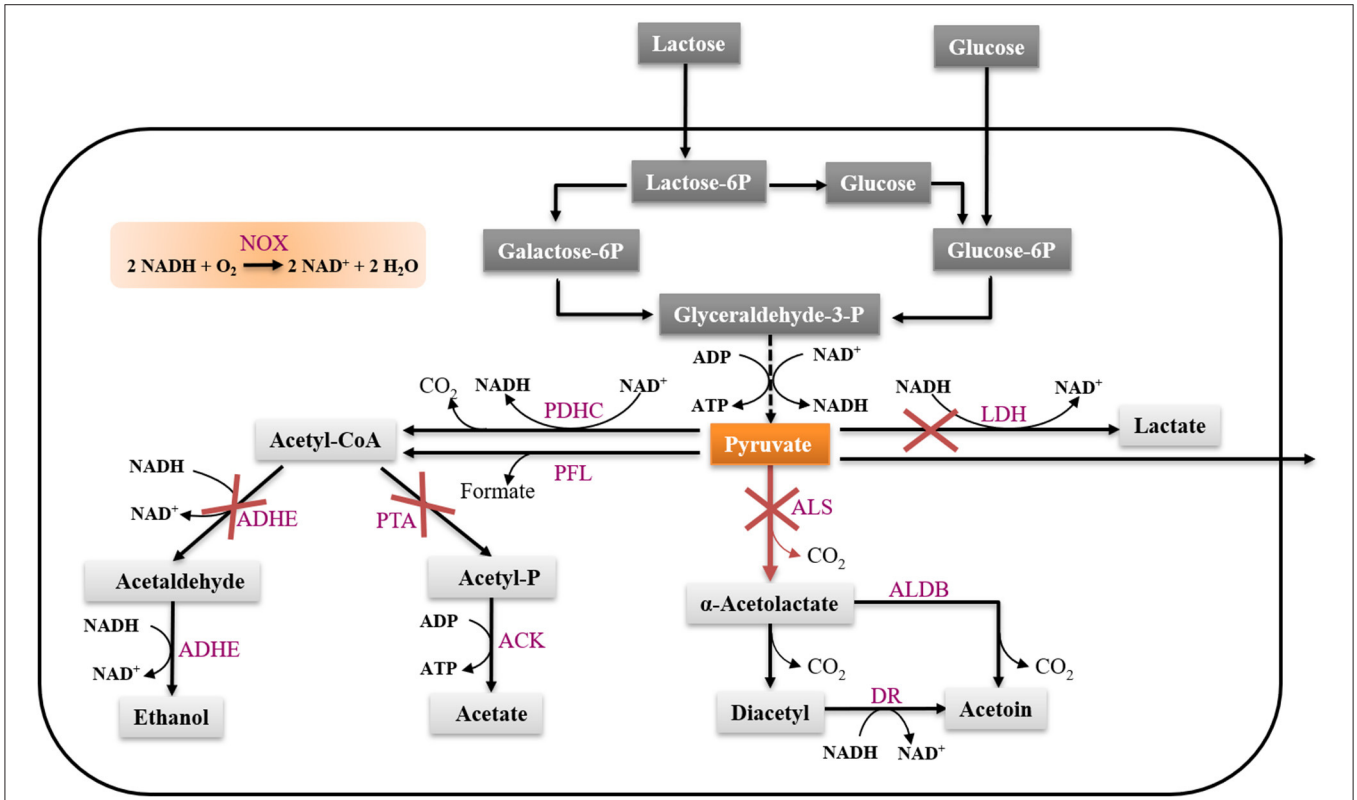

FIGURE 1 | Metabolism of lactose and glucose in *L. lactis*. LDH, lactate dehydrogenase; ALS, α-acetolactate synthase; ALD, α-acetolactate decarboxylase; PDHc, pyruvate dehydrogenase complex; PFL, pyruvate formate lyase; PTA, phosphotransacetylase; ADHE, alcohol dehydrogenase; ACK, acetate kinase; Nox, NADH oxidase; DR, diacetyl reductase.

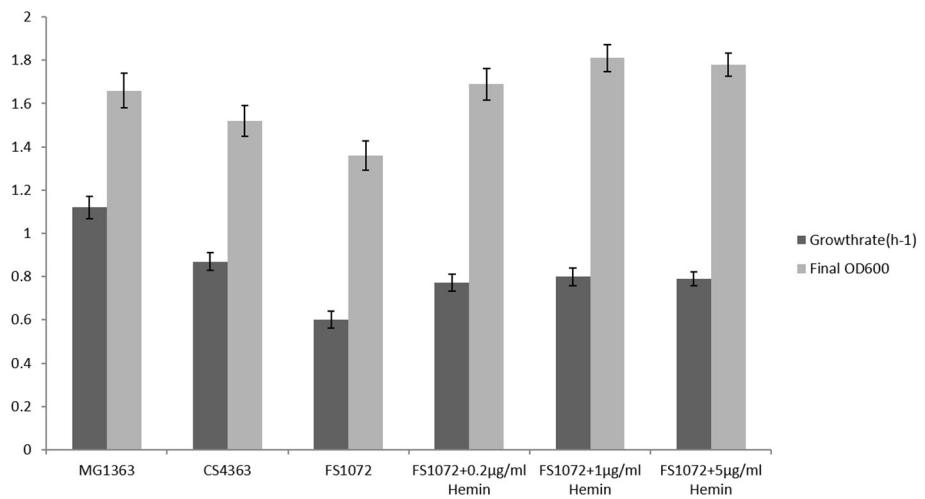

FIGURE 2 | Growth characterization of the recombinant pyruvate-producing strain in rich medium. Strains were grown in M17 with 0.2% glucose. Measurements are the average value ± standard error from independent duplicate cultivations.

RESULTS

Construction, Characterization, and Adaptive Evolution of the Pyruvate-Producing *Lactococcus lactis* Strain

Pyruvate is a central metabolite that some microorganisms produce in small amounts, usually due to leakage across the cell membrane (Maleki and Eiteman, 2017). Efficient microbial production of pyruvate usually requires a limitation in the catabolism (Maleki and Eiteman, 2017). In *L. lactis*, in order to achieve efficient pyruvate accumulation, it is necessary to inactivate the pyruvate consuming pathways. In this study, we used the previously constructed strain CS4363 as a starting point, where genes encoding three lactate dehydrogenase (LDH) homologs (*ldh*, *ldhB*, *ldhX*), phosphotransacetylase (PTA) and alcohol dehydrogenase (ADHE) had been deleted (Solem et al., 2013; Liu et al., 2016a). After deleting these pathways, a strain mainly producing acetoin under aerobic conditions was obtained. To achieve pyruvate production, we further needed to inactivate the *als* gene, encoding α-acetolactate synthase (**Figure 1**). We attempted to delete the *als* gene using the genetic tool pCS1966, as described in the section Materials and Methods, which was challenging. However, after screening more than 800 colonies, we obtained the pyruvate-producing strain FS1072 (MG1363 Δ^3*ldh Δpta ΔadhE Δals*) (**Table 1**).

We tested the growth performance of the pyruvate-producing strain in rich medium M17 and minimal medium SAL. FS1072 relies on oxygen in order to grow, as oxygen is needed by the cytoplasmic NADH oxidase (NoxE) for regenerating NAD^+, and we therefore examined the growth capacity of the engineered strain under aerobic conditions. As shown in **Figure 2**, both the specific growth rate and the final biomass yield of the recombinant strain FS1072 were lower than for the wild-type strain MG1363 and the strain CS4363, its immediate precursor. This indicated that the absence of a functional α-acetolactate synthase could have an adverse effect on growth. Normally, the H_2O-forming NADH oxidase, NoxE, is responsible for the majority of NADH oxidase activity under aerobic conditions (Jensen et al., 2001). However, *L. lactis* also is capable of respiring, when hemin is added, which is a more efficient way to regenerate NAD^+, improve biomass formation and help alleviate oxidative stress (Blank et al., 2001; Duwat et al., 2001; Koebmann et al., 2008). Indeed, the presence of hemin resulted in a significant increase of the growth capacity of the recombinant strain. As shown in **Figure 2**, the introduction of 0.2 μg/mL hemin significantly increased the growth rate of the recombinant strain FS1072. Higher hemin concentrations did not further improve growth rate or biomass formation. We also found that a high concentration of glucose inhibited the growth of strain FS1072, with 5% glucose having a slightly negative effect and 10% glucose significantly repressed the growth of the strain. This phenomenon was probably due to osmotic effects, why limiting the glucose content to 5% appeared to be a good choice.

In minimal medium SAL, as shown in **Figure 3**, the strain FS1072 could hardly grow, and the final cell density (OD_{600}) was only 0.11. When we knocked-out the *als* gene, we had to use the defined medium SAL, as is deficient in pyrimidine compounds that interfere with the 5FO counterselection, and the poor growth of the *als* mutant on SAL medium probably explains why it was so difficult to obtain the mutant in the first place. To ascertain that deletion of the als gene caused the poor growth on SAL,

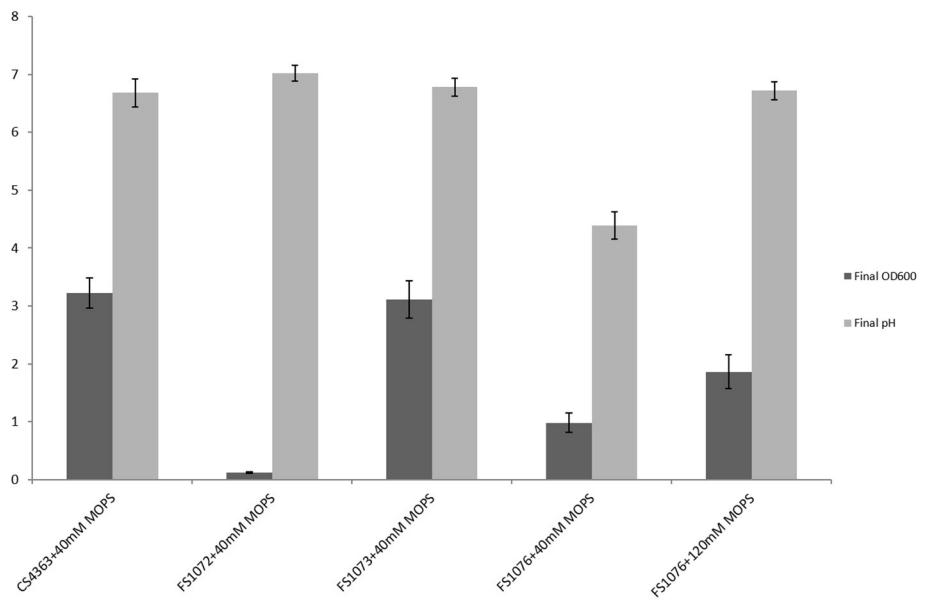

FIGURE 3 | Growth characterization of the recombinant pyruvate-producing strain in minimal medium. Strains were grown in SAL with 1% glucose. Measurements are the average value ± standard error from independent duplicate cultivations.

we complemented FS1072 with a plasmid expressing *als*, pLC17, and obtained the strain FS1073 (MG1363 Δ^3*ldh* *Δpta* *ΔadhE* *Δals* pLC17). As shown in **Figure 3**, the strain FS1073 had a drastically recovered growth capacity. Apparently, the absence of a functional α-acetolactate synthase had a significant effect on the cell growth in SAL medium. In an attempt to overcome the slow growth, we carried out a 21 days adaptive evolution experiment, and obtained the mutant strain FS1076 which grew better. Strain FS1076 was able to reach a cell density of 0.98 (OD_{600}) in SAL containing 1% glucose and 40 mM MOPS buffer, and as high as 1.86 when 120 mM MOPS buffer was added, to compensate for the pH drop caused by pyruvate (**Figure 3**). In M17 medium, the growth capacity of strains FS1072 and FS1076 were quite similar.

Transcriptomics Analysis With the Recombinant Pyruvate-Producing Strains

To find the reason for the improved growth of the mutant achieved after the adaptive evolution experiment, we compared the transcriptomes of FS1072 and FS1076 grown on the M17 and SAL medium, and for this purpose we relied on RNA-sequencing. A number of genes relevant to Arginine metabolism and pyrimidine metabolism were found to be differentially regulated under the various conditions (All the significantly expressed genes on the various conditions can be found in **Supplementary Tables 1–4**). The expression of 15 genes involved in these two pathways were downregulated in FS1072 in M17 medium as compared to in SAL medium (**Figure 4A**), which indicates that there are insufficient amounts of arginine in SAL medium. SAL medium does not contain pyrimidines. This conclusion was supported by the poor growth of FS1072 observed in SAL medium (**Figure 3**). However, the adapted strain FS1076, did not display any big differences between the two media (**Figure 4B**), which is reflected in the similar growth of FS1076 in these two media. In addition, we also compared the expression levels of genes between FS1072 and FS1076 in SAL medium (**Figure 4C**). The expression of almost all the genes involved in these two pathways in FS1076 down regulated compared to in

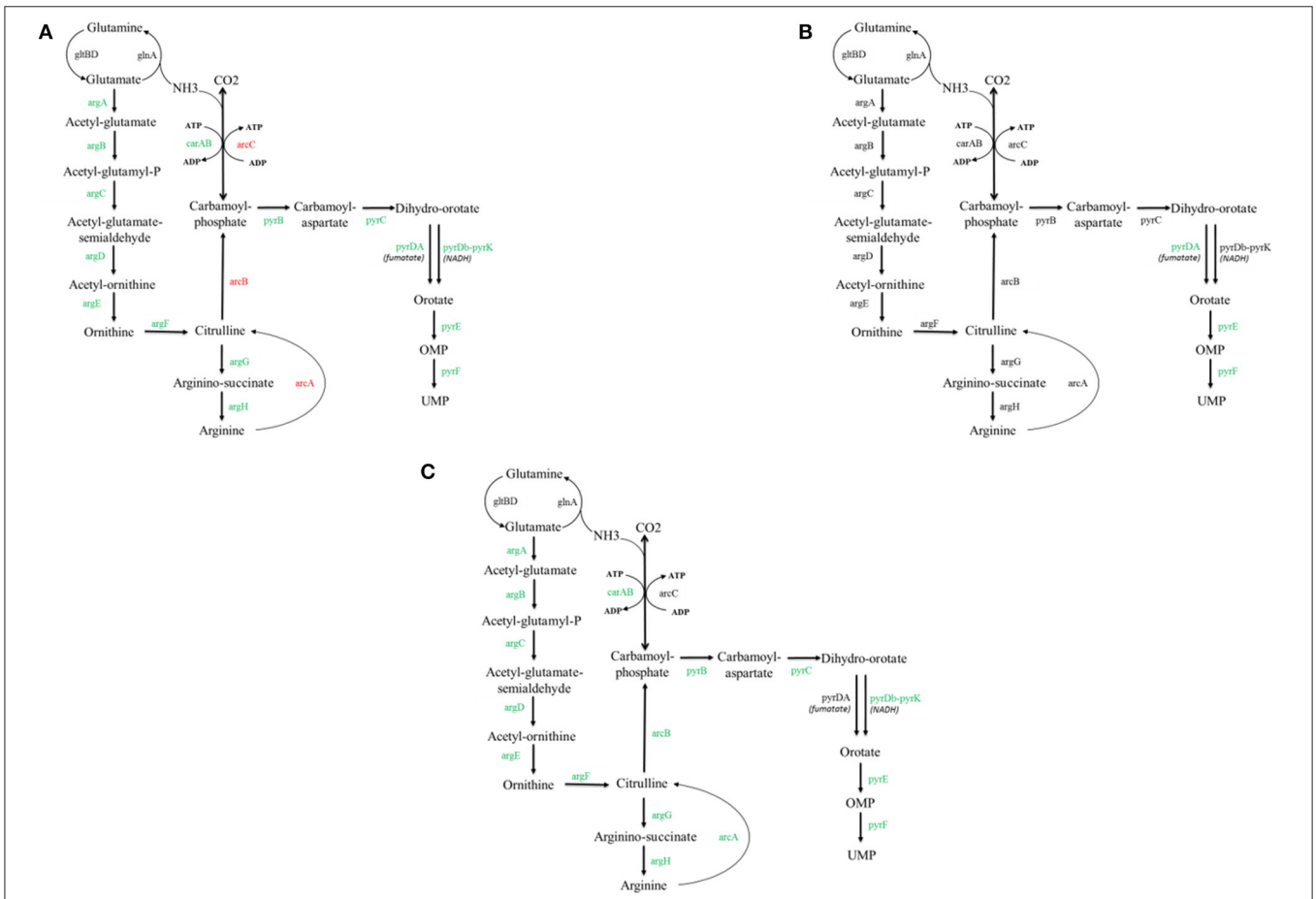

FIGURE 4 | Transcriptomics analysis with the recombinant pyruvate-producing strain. Comparison of transcriptional level of selected genes for the FS1072 and FS1076 strains. All the genes involved in arginine metabolism and pyrimidine metabolism cycle are included. Red color represents up-regulated and Green color represents down-regulated in the metabolic network. **(A)** FS1072 in M17/SAL (SAL as control), **(B)** FS1076 in M17/SAL (SAL as control), **(C)** FS1076/FS1072 in SAL (FS1072 as control).

FS1072, suggesting arginine and pyrimidine starvation in FS1072 in SAL medium. This observation correlated with the ability of FS1076 to grow better than FS1072 in SAL medium.

To experimentally verify the arginine and pyrimidine starvation indicated by the transcriptomic analysis, we supplemented the SAL medium with arginine and nucleosides, and recorded the effect of this on FS1072 and FS1076, respectively (**Figure 5**). As expected, by adding the two compounds, it was possible to increased the final cell density (OD_{600}) of the two strains, in particular for FS1072, and furthermore, the specific growth rate of FS1072 approached that of FS1076. These results clearly demonstrated that FS1072 was starved for arginine and pyrimidines in SAL medium, however, the underlying reason remained unclear. After inspecting the metabolic pathways for arginine and pyrimidine, we speculated that the poor growth of FS1072 might be due to insufficient CO_2. CO_2 is necessary for cell growth, and when *als* is knocked out in the CS4363, this would block a source of CO_2 production (**Figure 1**). To test this hypothesis, we added 20 mM $NaHCO_3$ into the SAL medium, and as seen in **Figure 5**, this had a beneficial effect on the growth of FS1072 and FS1076, similar to the effect of arginine and nucleosides (**Figure 5**). We thus conclude that knocking out *als*

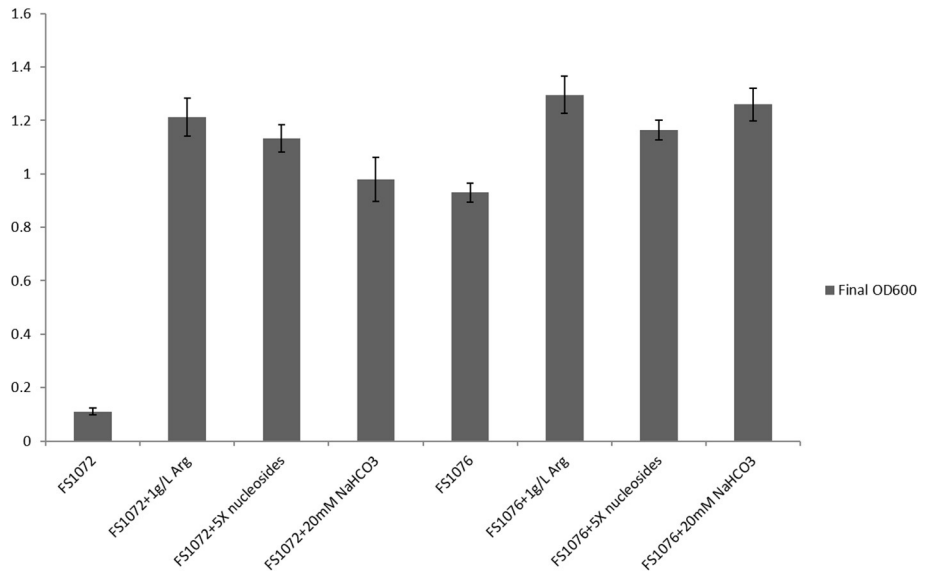

FIGURE 5 | Growth characterization of the recombinant pyruvate-producing strain in minimal medium with different compounds. Strains were grown in SAL with 1% glucose. Measurements are the average value ± standard error from independent duplicate cultivations.

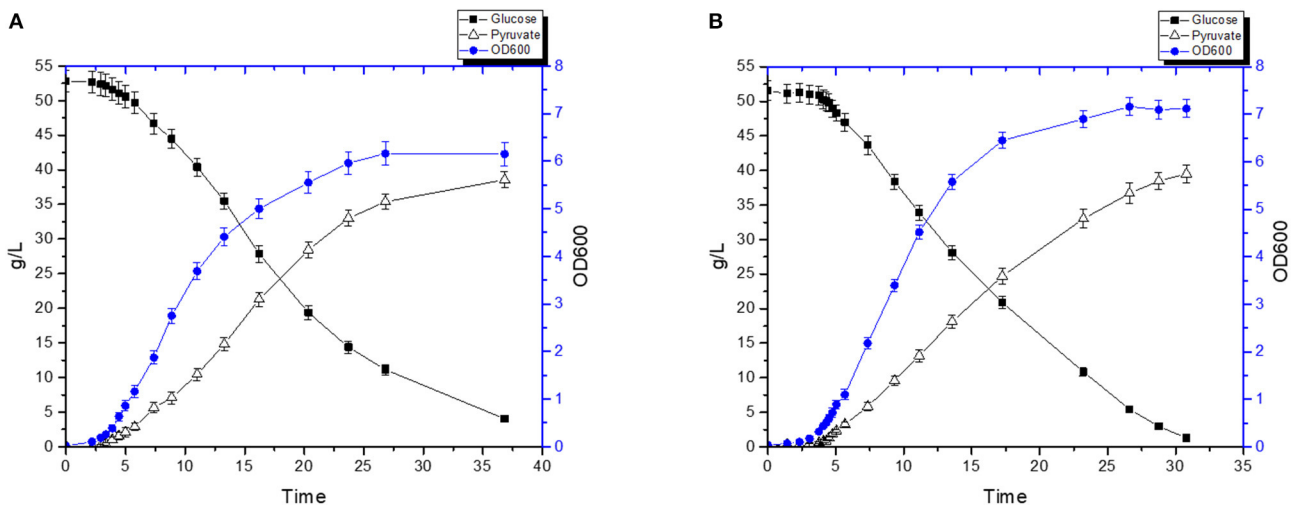

FIGURE 6 | Pyruvate production by the recombinant strain FS1076. The recombinant strain FS1076 was grown in M17 with 5% glucose. **(A)** 0 μg/mL hemin, **(B)** 1 μg/mL hemin. Measurements are the average value ± standard error from independent duplicate cultivations.

leads to deprivation of CO_2, and that this is the reason for why it was so difficult to isolate *als* mutants on SAL medium.

Pyruvate Production From Glucose in a Bioreactor With pH Control

We tested the efficiency of our new pyruvate platform under controlled settings using a bioreactor (**Figure 6**). Without hemin, FS1076 produced 38.6 g/L pyruvate in 36.8 h (**Figure 6A**) from an initial glucose concentration of 52.8 g/L and around 4 g/L glucose remained in the broth. The pyruvate productivity was 1.05 g/L·h and the yield was 80.8% of the theoretical maximum. In contrast, FS1076 with hemin had higher pyruvate productivity. As **Figure 6B** shows, FS1076 with 1 μg/mL hemin resulted in 39.51 g/L pyruvate in 30.8 h, corresponding to a productivity of 1.28 g/L·h and a yield of 80.4%. Thus, hemin was clearly beneficial for reducing the fermentation time and thereby increasing productivity. These results demonstrate that the yield of pyruvate for FS1076 was high and despite a very low inoculum (OD_{600} only 0.038), we achieved a good pyruvate productivity. Pyruvate production in different strains, especially *E. coli*, has been extensively investigated (Zhu et al., 2008; Maleki and Eiteman, 2017; Yang and Xing, 2017). Zhu et al. reported the highest pyruvate concentration achieved using *E. coli* in defined medium, 90 g/L pyruvate with an overall productivity of 2.1 g/L·h and yield of 0.68 g/g (Zhu et al., 2008). Compared to the *E. coli* strain, the titer we achieved in this study is not the highest, but our yield is higher. Looking into the setup used by Zhu et al. reveals that they relied on fed-batch fermentation with a high initial cell density of 3 (OD600), where our initial cell density was only 0.038 (OD600). In addition the high titer Zhu et al. obtained required feeding of a mixture of acetate & glucose, which is far more complicated than the simple setup used here.

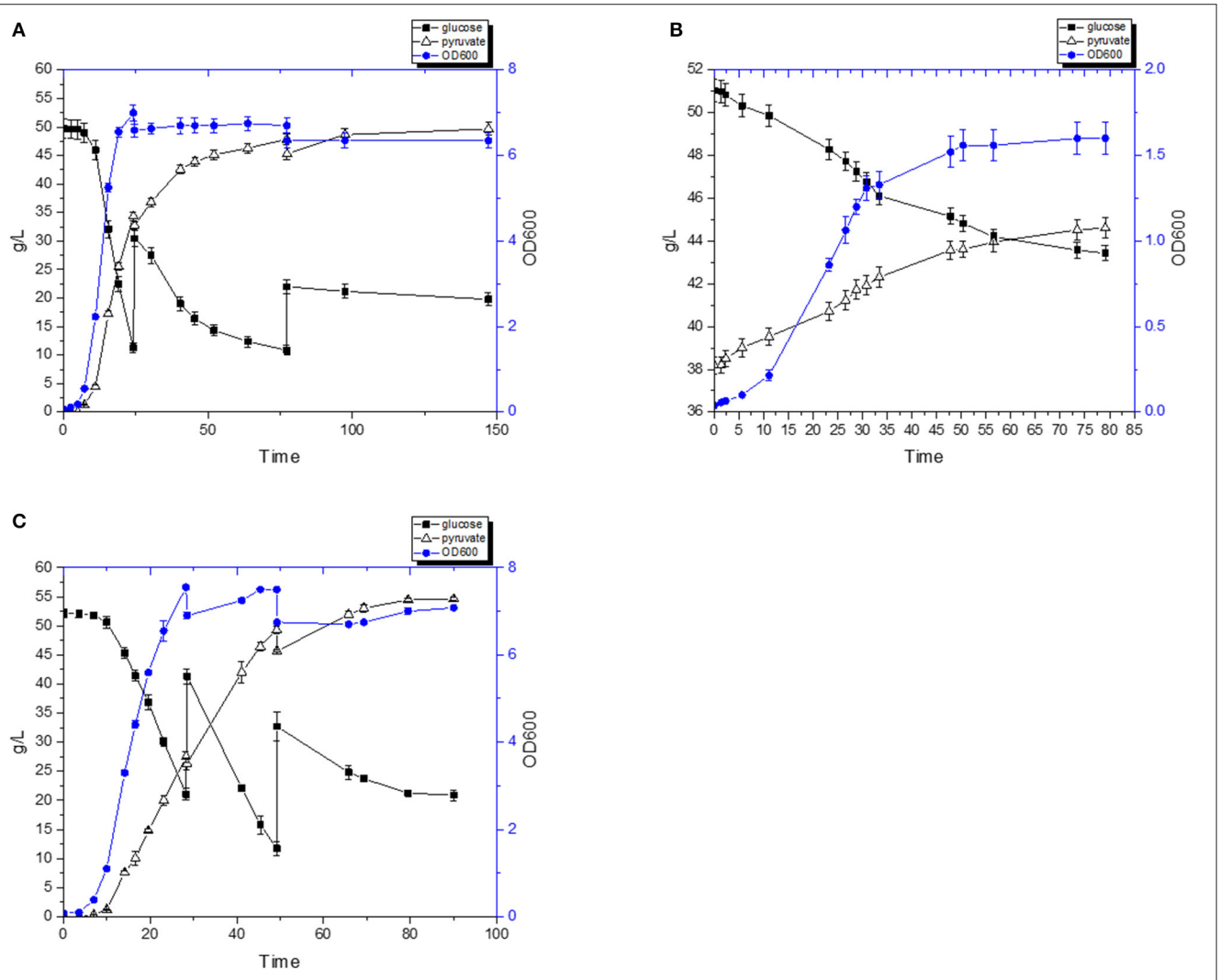

FIGURE 7 | Pyruvate production by the recombinant strain FS1076. The recombinant strain FS1076 was grown in M17 medium. **(A)** Fed-batch culture with 1 μg/mL hemin. **(B)** Fermentation with an initial 38 g/L of pyruvate. **(C)** Fed-batch culture with 1 μg/mL hemin with 10 mM betaine. Measurements are the average value ± standard error from independent duplicate cultivations.

In order to establish cost-efficient biotechnological production of pyruvate, it is not only necessary to have a fermentation process that delivers a high yield, high titer, and a high productivity. It is an obvious advantage if the fermentation process is simple, as it is in our case.

In an attempt to further increase the pyruvate titer, a fed-batch fermentation strategy was devised (**Figure 7A**). After 50 h of fermentation, pyruvate production had almost ceased, and after 150 h the titer was 49.7 g/L. We speculated that the main limiting factor for achieving higher pyruvate titer probably was a high osmotic pressure or product inhibition. We tested this by carrying out a fermentation experiment where 38 g/L of pyruvate was present from the beginning. As shown in **Figure 7B**, both the specific growth rate and final biomass of the strain FS1076 were significantly repressed by the pyruvate present in the medium. The specific growth rate and final biomass only reached 0.13 h^{-1} and 1.6, respectively. Moreover, the final concentration of pyruvate, including the initial pyruvate, was only 46 g/L. Therefore, we speculate that the tolerance of pyruvate or high osmotic stress maybe the limiting factor preventing further accumulation of pyruvate. An explanation for the observed termination of cell growth and pyruvate formation is the high osmotic stress caused by high concentration of pyruvate as well as the Na^+ accumulated due to NaOH added to maintain the pH. To overcome this problem, many microorganisms can accumulate organic osmolytes, such as betaine, which naturally protect them from high osmotic stress (Yancey, 2005). By adding betaine to the fermentation medium, various fermentation processes have been optimized, e.g., production of pyruvate (Zhu et al., 2008), ethanol (Underwood et al., 2004), and lactate (Zhou et al., 2006). Thus, we tested whether the compatible solute betaine could have a beneficial effect in a fed-batch fermentation setup. After optimization, as shown in **Figure 7C**, with the help of 10 mM betaine, the growth of the pyruvate strain was improved and after 90 h the pyruvate titer reached 54.6 g/L which is 10% higher than without betaine. This is encouraging but the reasons for the benefits of betaine in this case are still unclear. We believe that adaptive evolution is a good approach for obtaining mutants with improved tolerance to osmotic stress, and that pyruvate production can be further improved by using these mutants.

Pyruvate Production From Lactose Contained in Dairy Waste

Recent trends toward the production of green chemicals calls for processes that are efficient, cost-effective and sustainable, and an important element is to find cheap and renewable feedstocks. Residual whey permeate (RWP), which is a lactose rich side stream generated by the dairy industry, is a good candidate as a cheap carbon source for producing food-grade pyruvate. Strain FS1076 is a derivative of the plasmid-free laboratory strain MG1363, which lacks the ability to metabolize lactose, and to restore this ability, we therefore introduced the lactococcal plasmid pLP712 into strain FS1076 to generate FS1080.

A fermentation was carried out using a combination of diluted RWP and 2% (w/v) yeast extract. FS1080 produced pyruvate as main product during the fermentation. **Figure 8** shows that, without hemin, FS1080 produced 38.21 g/L pyruvate in 52.7 h and with a yield of 78.9% (**Figure 8A**). Adding 1 μg/mL hemin resulted in 40.1 g/L pyruvate in 44.7 h with a yield of 78.6% (**Figure 8B**). Thus, the pyruvate productivity using RWP with 2% yeast extract added was slightly lower compared to what was achieved in M17 medium containing glucose.

To further reduce the cost of the medium, we also carried out the fermentation using 0.5% (w/v) yeast extract. Without hemin, the pyruvate titer reached 27.9 g/L in 48.6 h with a yield of 79.9% (**Figure 9A**), whereas FS1080 with 1 μg/mL hemin resulted in a pyruvate titer of 29.9 g/L in 48.6 h with a yield of 79.1% (**Figure 9B**). Compared with the fermentation where 2% YE was used, the pyruvate yield obtained using 0.5% YE was very similar, but since FS1080, when grown with 0.5%YE, did not consume all the sugar in the medium, the final titer of pyruvate

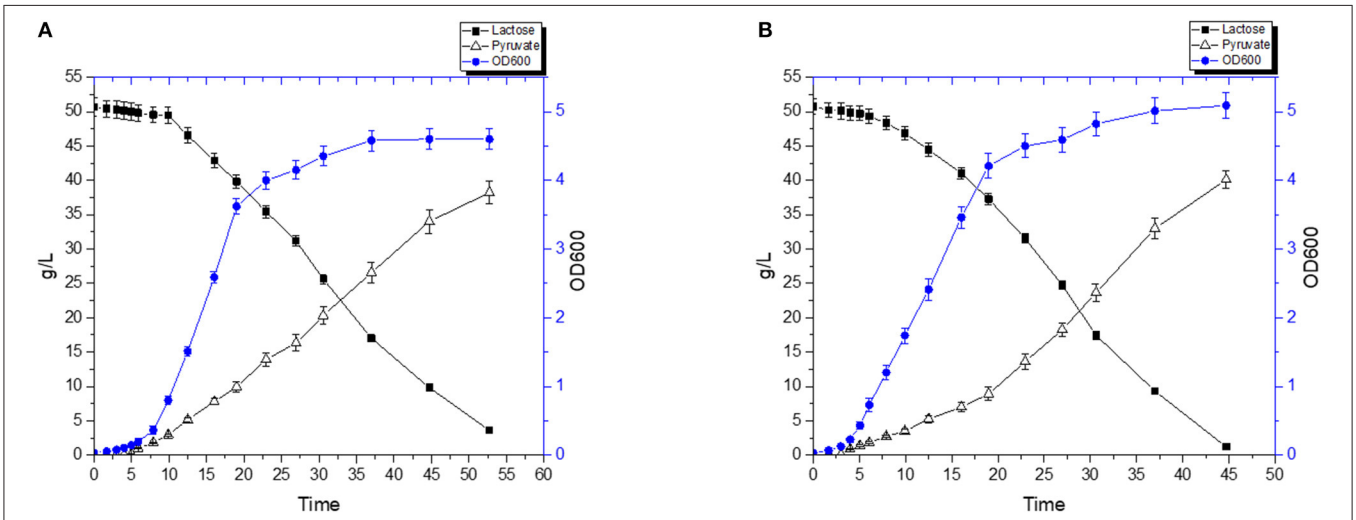

FIGURE 8 | Pyruvate production with RWP and 2% Yeast extract. The recombinant strain FS1080 was grown in the diluted whey with 2% yeast extract. **(A)** 0 μg/mL hemin, **(B)** 1 μg/mL hemin. Measurements are the average value ± standard error from independent duplicate cultivations.

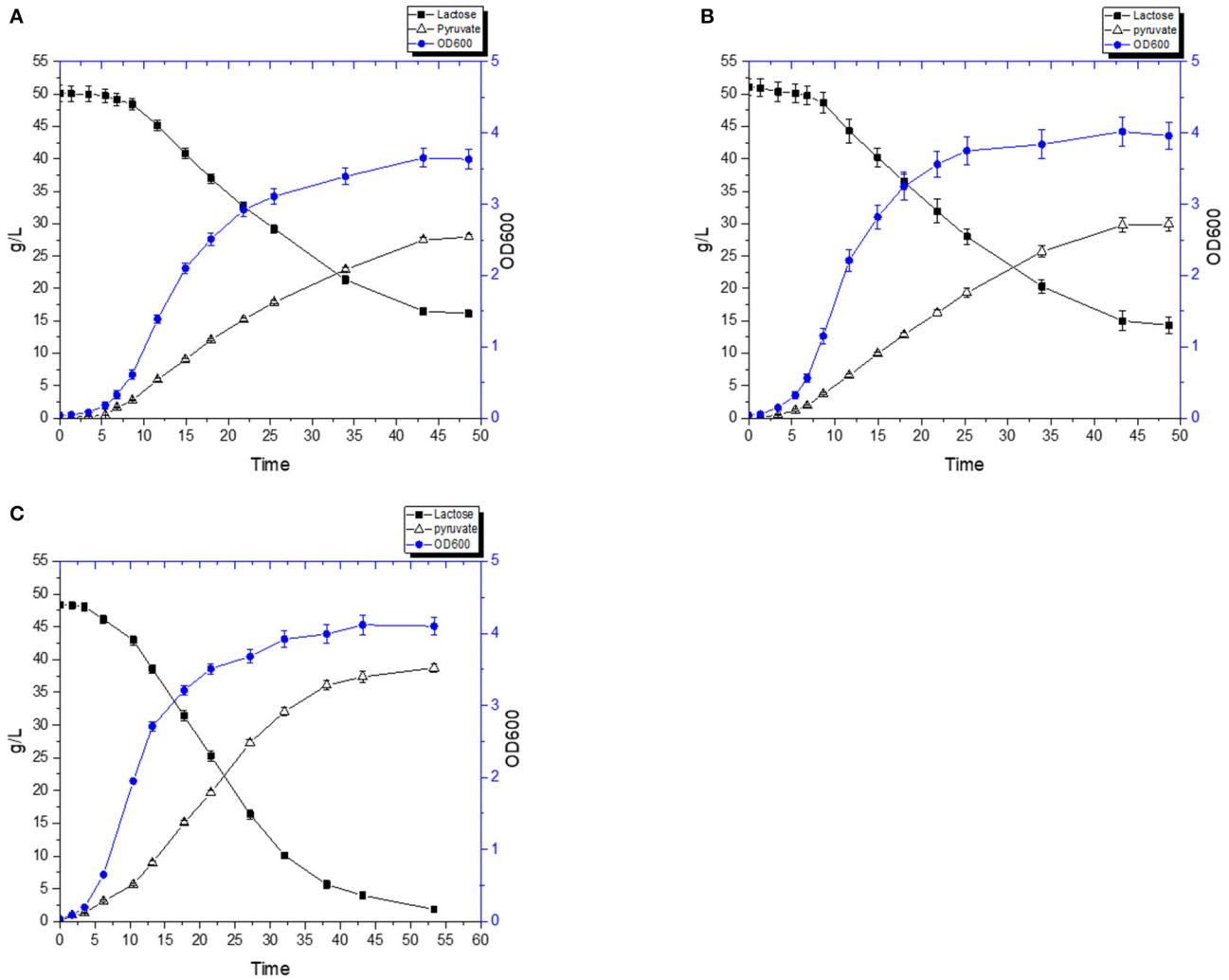

FIGURE 9 | Pyruvate production with 0.5% Yeast extract. The recombinant strain FS1080 was grown in the diluted whey with 0.5% yeast extract. **(A)** 0 μg/mL hemin, **(B)** 1 μg/mL hemin, **(C)** 1 μg/mL hemin with 2 μg/L $CoCl_2.6H_2O$ with 2 μg/L $MnSO_4.H_2O$. Measurements are the average value ± standard error from independent duplicate cultivations.

was much lower. To solve this problem, we tried to add various components to the fermentation medium, including different metal ions. Shorb reported growth stimulation of *L. lactis* by adding crystalline vitamin B12 (Shorb, 1948). Cobalt is at the center of the vitamin B12 complex, and is an essential factor for growth of a number of lactic acid bacteria (Hoff-Jorgensen, 1949). Manganese has also been found to be essential for many lactic acid bacteria, and manganese plays an important role in many enzymes, including oxidoreductases, transferases, hydrolases, lyases, ligases, and isomerases (Archibald, 1986). Eventually we found that adding a low concentration of the two metal ions Co^{2+} and Mn^{2+} improved the growth and sugar consumption. Thus, by including 1 μg/mL hemin, 2 μg/L $CoCl_2 \bullet 6H_2O$ and 2 μg/L $MnSO_4 \bullet H_2O$, the lactose in medium could almost completely be consumed, and the pyruvate titer was enhanced to 38.7 g/L in 53.4 h with a yield of 80.9% (theoretical maximum) (**Figure 9C**), similar to the outcomes under glucose. The high cost of yeast extract (4000 $/ton, Angel Yeast China), could be a limiting factor for the process described here, e.g., when using 0.5% YE the cost of the fermentation medium alone would amount to $0.5 per kg pyruvate produced (assuming that RWP is zero cost). It is likely that by re-using the cells, the fermentation medium associated costs could be further reduced, which we will explore in the future.

CONCLUSION

In this study, *L. lactis* was engineered as a new cell factory yielding pyruvate and a fermentation based on a cheap renewable feedstock was developed. The engineered *L. lactis* can convert different sugars into pyruvate efficiently. The results demonstrate that *L. lactis* has a good potential as a cell factory for producing pyruvate. It is possible to achieve sustainable and cost-efficient bioconversion of waste products from the dairy industry (RWP)

to pyruvate, and the process developed shows great potential for commercial realization.

DATA AVAILABILITY STATEMENT

The datasets presented in this study can be found in online repositories. The names of the repository/repositories and accession number(s) can be found at: https://www.ncbi.nlm.nih.gov/bioproject/PRJNA669338/.

AUTHOR CONTRIBUTIONS

PJ, CS, JL, JC, and FS designed the experiments and revised the manuscript. FS performed this experiment and wrote this manuscript. XL worked on RNAseq analysis. All authors read and approved the final manuscript.

FUNDING

This work was supported by the China Scholarships Council (No. 201406220127) and through a DTU Food stipend.

SUPPLEMENTARY MATERIAL

The Supplementary Material for this article can be found online at: https://www.frontiersin.org/articles/10.3389/fbioe.2020.611701/full#supplementary-material

REFERENCES

Archibald, F. (1986). Manganese: its acquisition by and function in the lactic acid bacteria. *Crit. Rev. Microbiol.* 13, 63–109. doi: 10.3109/10408418609108735

Blank, L. M., Koebmann, B. J., Michelsen, O., Lars, K., Jensen, P. R., Michelsen, O. L. E., et al. (2001). DNP and nisin for HighOD medium. *J. Bacteriol.* 183, 6707–6709. doi: 10.1128/JB.183.22.6707

Dorau, R., Chen, L., Liu, J., Jensen, P. R., and Solem, C. (2019). Efficient production of α-acetolactate by whole cell catalytic transformation of fermentation-derived pyruvate. *Microb. Cell Fact.* 18, 1–11. doi: 10.1186/s12934-019-1271-1

Duwat, P., Sourice, S., Cesselin, B., Vido, K., Gaudu, P., Loir, Y., et al. (2001). Respiration capacity of the fermenting bacterium *Lactococcus lactis* and its positive effects on growth and survival respiration capacity of the fermenting bacterium *Lactococcus lactis* and its positive effects on growth and survival †. *J. Bacteriol.* 183, 4509–4516. doi: 10.1128/JB.183.15.4509

Gasson, M. J. (1983). Genetic transfer systems in lactic acid bacteria. *Antonie Van Leeuwenhoek* 49, 275–282. doi: 10.1007/BF00399500

Ghaffar, T., Irshad, M., Anwar, Z., Aqil, T., Zulifqar, Z., Tariq, A., et al. (2014). Recent trends in lactic acid biotechnology: a brief review on production to purification. *J. Radiat. Res. Appl. Sci.* 7, 222–229. doi: 10.1016/j.jrras.2014.03.002

Hoff-Jorgensen, E. (1949). Difference in growth-promoting effect of desoxyribosides and vitamin BU on three strains of lactic acid bacteria. *J. Biol. Chem.* 178, 525–526.

Holo, H., and Nes, I. F. (1989). High-frequency transformation, by electroporation, of *Lactococcus lactis* subsp. cremoris grown with glycine in osmotically stabilized media. *Appl. Environ. Microbiol.* 55, 3119–3123.

Jensen, N. B. S., Melchiorsen, C. R., Jokumsen, K. V., and Villadsen, J. (2001). Metabolic behavior of *Lactococcus lactis* MG1363 in microaerobic continuous cultivation at a low dilution rate. *Appl. Environ. Microbiol.* 67, 2677–2682. doi: 10.1128/AEM.67.6.2677-2682.2001

Jensen, P. R., and Hammer, K. (1993). Minimal requirements for exponential-growth of *Lactococcus lactis*. *Appl. Environ. Microbiol.* 59, 4363–4366.

Kleerebezem, M., Hols, P., and Hugenholtz, J. (2000). Lactic acid bacteria as a cell factory: rerouting of carbon metabolism in *Lactococcus lactis* by metabolic engineering. *Enzyme Microb. Technol.* 26, 840–848. doi: 10.1016/S0141-0229(00)00180-0

Koebmann, B., Blank, L. M., Solem, C., Petranovic, D., Nielsen, L. K., and Jensen, P. R. (2008). Increased biomass yield of *Lactococcus lactis* during energetically limited growth and respiratory conditions. *Biotechnol. Appl. Biochem.* 50:25. doi: 10.1042/BA20070132

Li, S., Chen, X., Liu, L., and Chen, J. (2016). Pyruvate production in *Candida glabrata*: manipulation and optimization of physiological function. *Crit. Rev. Biotechnol.* 36, 1–10. doi: 10.3109/07388551.2013.811636

Li, Y., Chen, J., and Lun, S. Y. (2001). Biotechnological production of pyruvic acid. *Appl. Microbiol. Biotechnol.* 57, 451–459. doi: 10.1007/s002530100804

Liao, Y., Smyth, G. K., and Shi, W. (2019). The R package Rsubread is easier, faster, cheaper and better for alignment and quantification of RNA sequencing reads. *Nucleic Acids Res.* 47:e47. doi: 10.1093/nar/gkz114

Liu, J., Chan, S. H. J., Brock-Nannestad, T., Chen, J., Lee, S. Y., Solem, C., et al. (2016a). Combining metabolic engineering and biocompatible chemistry for high-yield production of homo-diacetyl and homo-(S,S)-2,3-butanediol. *Metab. Eng.* 36, 57–67. doi: 10.1016/j.ymben.2016.02.008

Liu, J., Dantoft, S. H., Würtz, A., Jensen, P. R., and Solem, C. (2016b). A novel cell factory for efficient production of ethanol from dairy waste. *Biotechnol. Biofuels* 9, 1–11. doi: 10.1186/s13068-016-0448-7

Liu, J., Kandasamy, V., Würtz, A., Jensen, P. R., and Solem, C. (2016c). Stimulation of acetoin production in metabolically engineered *Lactococcus lactis* by increasing ATP demand. *Appl. Microbiol. Biotechnol.* 100, 9509–9517. doi: 10.1007/s00253-016-7687-1

Liu, J., Solem, C., and Jensen, P. R. (2016d). Integrating biocompatible chemistry and manipulating cofactor partitioning in metabolically engineered *Lactococcus lactis* for fermentative production of (3S)-acetoin. *Biotechnol. Bioeng.* 113, 2744–2748. doi: 10.1002/bit.26038

Liu, J., Wang, Z., Kandasamy, V., Lee, S. Y., Solem, C., and Jensen, P. R. (2017). Harnessing the respiration machinery for high-yield production of chemicals in metabolically engineered *Lactococcus lactis*. *Metab. Eng.* 44, 22–29. doi: 10.1016/j.ymben.2017.09.001

Liu, L., Xu, Q., Li, Y., Shi, Z., Zhu, Y., Du, G., et al. (2007). Enhancement of pyruvate production by osmotic-tolerant mutant of *Torulopsis glabrata*. *Biotechnol. Bioeng.* 97, 825–832. doi: 10.1002/bit.21290

Maleki, N., and Eiteman, M. (2017). Recent progress in the microbial production of pyruvic acid. *Fermentation* 3:8. doi: 10.3390/fermentation3010008

Miyata, R., Tsutsui, H., and Yonehara, T. (1989a). Manufacture of pyruvic acid with Torulopsis species. *JP Patent*. No. 0155185.

Miyata, R., Tsutsui, H., and Yonehara, T. (1989b). Manufacture of pyruvic acid with aminooxyacetic acid-resistant Torulopsis species. *JP Patent*. No. 0155186.

Miyata, R., and Yonehara, T. (1996). Improvement of fermentative production of pyruvate from glucose by *Torulopsis glabrata* IFO 0005. *J. Ferment. Bioeng.* 82, 475–479. doi: 10.1016/S0922-338X(97)86986-3

Miyata, R., Yonehara, T., Yotsumoto, K., and Tsutsui, H. (1989c). Preparing pyruvic acid by fermentation with Torulopsis species. *JP Patent*. No. 8901523.

Miyata, R., Yonehara, T., Yotsumoto, K., and Tsutsui, H. (1990). Method for producing pyruvic acid by fermentation. *U.S. Patent*. No. 4,971,907. Washington, DC: U.S. Patent and Trademark Office.

Park, H. S., Lee, J. Y., and Kim, H. S. (1998). Production of L-DOPA(3,4-dihydroxyphenyl-L-alanine) from benzene by using a hybrid pathway. *Biotechnol. Bioeng.* 58, 339–343.

R Development Core Team (2011). *R: A Language and Environment for Statistical Computing. Vienna: R Foundation for Statistical Computing*. Available online at: http://www.R-project.org

Reiße, S., Haack, M., Garbe, D., Sommer, B., Steffler, F., Carsten, J., et al. (2016). *In vitro* bioconversion of pyruvate to n-butanol with minimized cofactor utilization. *Front. Bioeng. Biotechnol.* 4:74. doi: 10.3389/fbioe.2016.00074

Ritchie, M. E., Phipson, B., Wu, D., Hu, Y., Law, C. W., Shi, W., et al. (2015). Limma powers differential expression analyses for RNA-sequencing and microarray studies. *Nucleic Acids Res.* 43:e47. doi: 10.1093/nar/gkv007

Robinson, M. D., McCarthy, D. J., and Smyth, G. K. (2009). edgeR: a Bioconductor package for differential expression analysis of digital gene expression data. *Bioinformatics* 26, 139–140. doi: 10.1093/bioinformatics/btp616

Rosche, B., Sandford, V., Breuer, M., Hauer, B., and Rogers, P. (2001). Biotransformation of benzaldehyde into (R)-phenylacetylcarbinol by filamentous fungi or their extracts. *Appl. Microbiol. Biotechnol.* 57, 309–315. doi: 10.1007/s002530100781

Sambrook, J. W., and Russell, D. (2001). *Molecular Cloning: A Laboratory Manual*. Cold Spring Harb. NY: Cold Spring Harb. Lab. Press, 999.

Shorb, M. S. (1948). Activity of vitamin B12 for the growth of *Lactobacillus lactis*. *Sci.* 107, 397–398.

Solem, C., Defoor, E., Jensen, P. R., and Martinussen, J. (2008). Plasmid pCS1966, a new selection/counterselection tool for lactic acid bacterium strain construction based on the oroP gene, encoding an orotate transporter from Lactococcus lactis. *Appl. Environ. Microbiol.* 74, 4772–4775. doi: 10.1128/AEM.00134-08

Solem, C., Dehli, T., and Jensen, P. R. (2013). Rewiring *Lactococcus lactis* for ethanol production. *Appl. Environ. Microbiol.* 79, 2512–2518. doi: 10.1128/AEM.03623-12

Stottmeister, U., Aurich, A., Wilde, H., Andersch, J., Schmidt, S., and Sicker, D. (2005). White biotechnology for green chemistry: fermentative 2-oxocarboxylic acids as novel building blocks for subsequent chemical syntheses. *J. Ind. Microbiol. Biotechnol.* 32, 651–664. doi: 10.1007/s10295-005-0254-x

Terzaghi, B. E., and Sandine, W. E. (1975). Improved medium for lactic streptococci and their bacteriophages. *Appl. Microbiol.* 29, 807–813.

Teuber, M. (1995). *"The Genus Lactococcus." The Genera of Lactic Acid Bacteria*. Boston, MA: Springer.

Underwood, S. A., Buszko, M. L., Shanmugam, K. T., and Ingram, L. O. (2004). Lack of protective osmolytes limits final cell density and volumetric productivity of ethanologenic *Escherichia coli* KO11 during xylose fermentation. *Appl. Environ. Microbiol.* 70, 2734–2740. doi: 10.1128/AEM.70.5.2734-2740.2004

Wegmann, U., Overweg, K., Jeanson, S., Gasson, M., and Shearman, C. (2012). Molecular characterization and structural instability of the industrially important composite metabolic plasmid pLP712. *Microbiology* 158, 2936–2945. doi: 10.1099/mic.0.062554-0

Yancey, P. H. (2005). Organic osmolytes as compatible, metabolic and counteracting cytoprotectants in high osmolarity and other stresses. *J. Exp. Biol.* 208, 2819–2830. doi: 10.1242/jeb.01730

Yang, M., and Xing, J. (2017). Improvement of pyruvate production based on regulation of intracellular redox state in engineered *Escherichia coli*. *Biotechnol. Bioprocess. Eng.* 22, 376–381. doi: 10.1007/s12257-017-0061-z

Yokota, A., Shimizu, H., Terasawa, Y., Takaoka, N., and Tomita, F. (1994). Pyruvic acid production by a lipoic acid auxotroph of *Escherichia coli* W1485. *Appl. Microbiol. Biotechnol.* 41, 638–646. doi: 10.1007/BF00167278

Zelić, B., Gerharz, T., Bott, M., Vasić-Rački, Đ., Wandrey, C., and Takors, R. (2003). Fed-batch process for pyruvate production by recombinant *Escherichia coli* YYC202 strain. *Eng. Life Sci.* 3, 299–305. doi: 10.1002/elsc.200301756

Zhou, S., Grabar, T. B., Shanmugam, K. T., and Ingram, L. O. (2006). Betaine tripled the volumetric productivity of D(-)-lactate by *Escherichia coli* strain SZ132 in mineral salts medium. *Biotechnol. Lett.* 28, 671–676. doi: 10.1007/s10529-006-0033-4

Zhu, Y., Eiteman, M. A., Altman, R., and Altman, E. (2008). High glycolytic flux improves pyruvate production by a metabolically engineered *Escherichia coli* strain. *Appl. Environ. Microbiol.* 74, 6649–6655. doi: 10.1128/AEM.01610-08

Conflict of Interest: The authors declare that the research was conducted in the absence of any commercial or financial relationships that could be construed as a potential conflict of interest.

frontiers in Bioengineering and Biotechnology

ORIGINAL RESEARCH
published: 13 January 2021
doi: 10.3389/fbioe.2020.623700

Use of Cell Envelope Targeting Antibiotics and Antimicrobial Agents as a Powerful Tool to Select for Lactic Acid Bacteria Strains With Improved Texturizing Ability in Milk Fermentations

Kim I. Sørensen[1], Inge Kjærbølling[1†], Ana Rute Neves[1†], Ronnie Machielsen[1] and Eric Johansen[2†]*

[1] Discovery, Research and Development, Chr. Hansen A/S, Hørsholm, Denmark, [2] Emerging Technology, Chr. Hansen A/S, Hørsholm, Denmark

Many antibiotics and antimicrobial agents have the bacterial cell envelope as their primary target, interfering with functions such as synthesis of peptidoglycan, membrane stability and permeability, and attachment of surface components. The cell envelope is the outermost barrier of the bacterial cell, conferring protection against environmental stresses, and maintaining structural integrity and stability of the growing cell, while still allowing for required metabolism. In this work, inhibitory concentrations of several different cell envelope targeting antibiotics and antimicrobial agents were used to select for derivatives of lactic acid bacteria (LAB) with improved properties for dairy applications. Interestingly, we observed that for several LAB species a fraction of the isolates had improved milk texturizing capabilities. To further improve our understanding of the mechanisms underlying the improved rheology and to validate the efficacy of this method for strain improvement, genetic and physiological characterization of several improved derivatives was performed. The results showed that the identified genetic changes are diverse and affect also other cellular functions than the targeted cell surface. In short, this study describes a new versatile and powerful toolbox based on targeting of the cell envelope to select for LAB derivatives with improved phenotypic traits for dairy applications.

Keywords: antimicrobial agents, resistance, toolbox, improved texture, lactic acid bacteria, yogurt

OPEN ACCESS

Edited by:
Jian-Ming Liu,
Technical University of Denmark, Denmark

Reviewed by:
Jun Chen,
Samplix ApS, Denmark
Fernanda Mozzi,
CONICET Centro de Referencia para Lactobacilos (CERELA), Argentina

****Correspondence:***
Kim I. Sørensen
dkksr@chr-hansen.com

†Present address:
Inge Kjærbølling,
Department of Microbiomics and Microbe, Discovery, Novozymes, Bagsvaerd, Denmark
Ana Rute Neves,
Discover, Arla Foods Ingredients, Viby, Denmark
Eric Johansen,
Retired, Hørsholm, Denmark

Specialty section:
This article was submitted to Synthetic Biology, a section of the journal Frontiers in Bioengineering and Biotechnology

Received: *30 October 2020*
Accepted: *07 December 2020*
Published: *13 January 2021*

Citation:
Sørensen KI, Kjærbølling I, Neves AR, Machielsen R and Johansen E (2021) Use of Cell Envelope Targeting Antibiotics and Antimicrobial Agents as a Powerful Tool to Select for Lactic Acid Bacteria Strains With Improved Texturizing Ability in Milk Fermentations. Front. Bioeng. Biotechnol. 8:623700. doi: 10.3389/fbioe.2020.623700

INTRODUCTION

Lactic acid bacteria (LAB) have been used for millennia for the fermentation of food and feed. In the dairy industry, they are used for the production of cheese and fermented milk products such as yogurt and buttermilk. The LAB not only contribute with taste and texture to dairy products, they also help to preserve them by lowering the pH, producing inhibitory compounds and through competitive exclusion of spoilage organisms (Siedler et al., 2020). Today, most food fermentations are initiated by the addition of commercial starter cultures and there is a constant need for new cultures with improved properties (Derkx et al., 2014; Johansen, 2018). One major

trend in yogurt products is high texture and yogurt producers strive to make yogurt with the desired texture without the addition of thickening agents. Thus, a starter culture with the ability to improve texture of fermented milks would be a desirable solution and help manufacturers reduce cost while maintaining a simple product label. While modern biotechnology has developed multiple tools for strain improvement, public concerns about the use of gene technology in the food chain have resulted in a need to develop alternate methods of strain improvement (Johansen, 2017). These include the use of natural selection and evolution (Johansen, 2018) as well as the use of dominant selection, for example, based on resistance to inhibitory substances (Derkx et al., 2014; Cardoso et al., 2018).

Antimicrobial agents have been developed primarily for the control of pathogenic organisms. They have a specific mode-of-action, targeting a specific component of bacterial metabolism. However, since these components are common to a wide range of microbes, most antimicrobials also inhibit non-pathogens. One feature of the bacterial cell that is commonly targeted directly by antimicrobials is the cell surface and especially the assembly of the peptidoglycan layer. Ampicillin (AMP) acts on peptidoglycan crosslinking, inhibiting the transpeptidase responsible for the crosslinking, while vancomycin binds the D-ala-D-ala terminal of the growing peptidoglycan chain, inhibiting both the polymerization and cross-linking steps (Barna and Williams, 1984) (**Figure 1**). Other antimicrobials interfere with the synthesis of peptidoglycan precursors in the cytosol. For example, D-cycloserine (DCS) targets two enzymes, alanine racemase and D-ala:D-ala ligase, involved in the production of D-ala-D-ala which forms the terminal end of the UDP-MurNAc pentapeptide while fosfomycin targets UDP-*N*-acetylglucosamine enolpyruvyl transferase, the first committed step in peptidoglycan biosynthesis (Lambert and Neuhaus, 1972; Prosser and de Carvalho, 2013). Triclosan provokes oxidative stress in bacteria and damages the cell membrane (Lu et al., 2018). We have previously characterized several LAB variants spontaneously resistant to DCS and AMP (Kibenich et al., 2012; Johansen et al., 2013). Some of these derivatives showed reduced whey syneresis as well as increased texture formation when grown in milk compared to the parent strain. The other growth properties were found to be unaffected relative to that of the parent strain. Subsequently, we wanted to explore the potential of using other cell envelope targeting antimicrobials for the selection of strains with improved texture in milk. We therefore applied a dominant selection strategy based on resistance to several different antimicrobials to generate a strain development toolbox for improved rheological properties. Here we describe the characterization of the obtained resistant derivatives with improved texture for dairy application.

MATERIALS AND METHODS

Bacteria and Growth Conditions

All bacterial strains are listed in **Table 1**. Wild-type strains are from the Chr. Hansen culture collection (Johansen et al., 2015) and were originally isolated from dairy cultures or dairy products.

Lactobacillus delbrueckii subsp. *bulgaricus* strains were cultured using MRS medium (de Man et al., 1960) (Oxoid) at 37°C. Liquid cultures were propagated without shaking; plate cultures (1% w/v agar; Oxoid) were incubated in anaerobic jars (Anaerocult A, Millipore). *Streptococcus thermophilus* strains were grown in M17 medium (Terzaghi and Sandine, 1975) (Difco Laboratories) with 2% (w/v) lactose, under the same environmental conditions. Milk fermentations for screening purposes were carried out in B-milk, which consists of skim milk powder at a level of dry matter of 9.5% (w/v) reconstituted in distilled water and pasteurized at 99°C for 30 min, followed by cooling to 30°C (Sørensen et al., 2016). Full fat milk with 2% added whey protein was used for rheologic characterization of selected strains. Full fat (whole) cow's milk contains 3.5% fat and was obtained from Arla Food Ingredients.

Selection of Antimicrobial Resistant Isolates

To identify a suitable concentration of an antimicrobial agent for selection of resistant isolates, a single colony of the parental strain was inoculated into the preferred broth containing various concentrations of the antimicrobial and incubated 20 h. The suitable concentration was typically identified as the concentration that reduced the OD_{600} measured growth, after 20 h growth at 37°C. The suitable concentration was identified as the concentration that reduced the OD_{600} measured after 20 h to approximately 20% of that obtained during growth in the same medium without added antibiotic. A standardized approach was used for the isolation of variants. A single colony of the parent strain was inoculated into the appropriate broth containing the antimicrobial agent at the predetermined suitable concentration and incubated to saturation. Saturated cultures were plated on appropriate agar without the antimicrobial agent. Isolated colonies were picked and screened in microtiter plates (Johansen et al., 2015) for the ability to grow in the presence of the antimicrobial agent at the selective concentration. Typically, 25% of the resistant isolates were identified as fast growing derivatives. After purification, the isolates were screened for their basic texturizing properties when grown in B-milk (Kibenich et al., 2012; Johansen et al., 2013). The selective concentrations of the antimicrobial agents were: DCS, 50 or 100 μg/ml; AMP, 0.3 or 0.5 μg/ml; fosfomycin, 70 μg/ml; vancomycin, 0.05 μg/ml; and triclosan, 4 μg/ml. All antimicrobials were from Sigma–Aldrich.

Texturizing Properties of Antibiotic Resistant Derivatives in Milk

The screening of the selected resistant derivatives was performed using two different approaches. DCS and AMP resistant derivatives, showing improved rheological properties, were identified as having reduced whey syneresis and perceived improved texture when grown in milk compared to the parent strain (Kibenich et al., 2012). While to identify the fosfomycin, vancomycin, and triclosan resistant derivatives with improved texturizing properties, the selected isolates were grown to saturation in broth and inoculated 1% vol/vol into 96-well deep-well plates containing 1.8 ml/well B-milk including

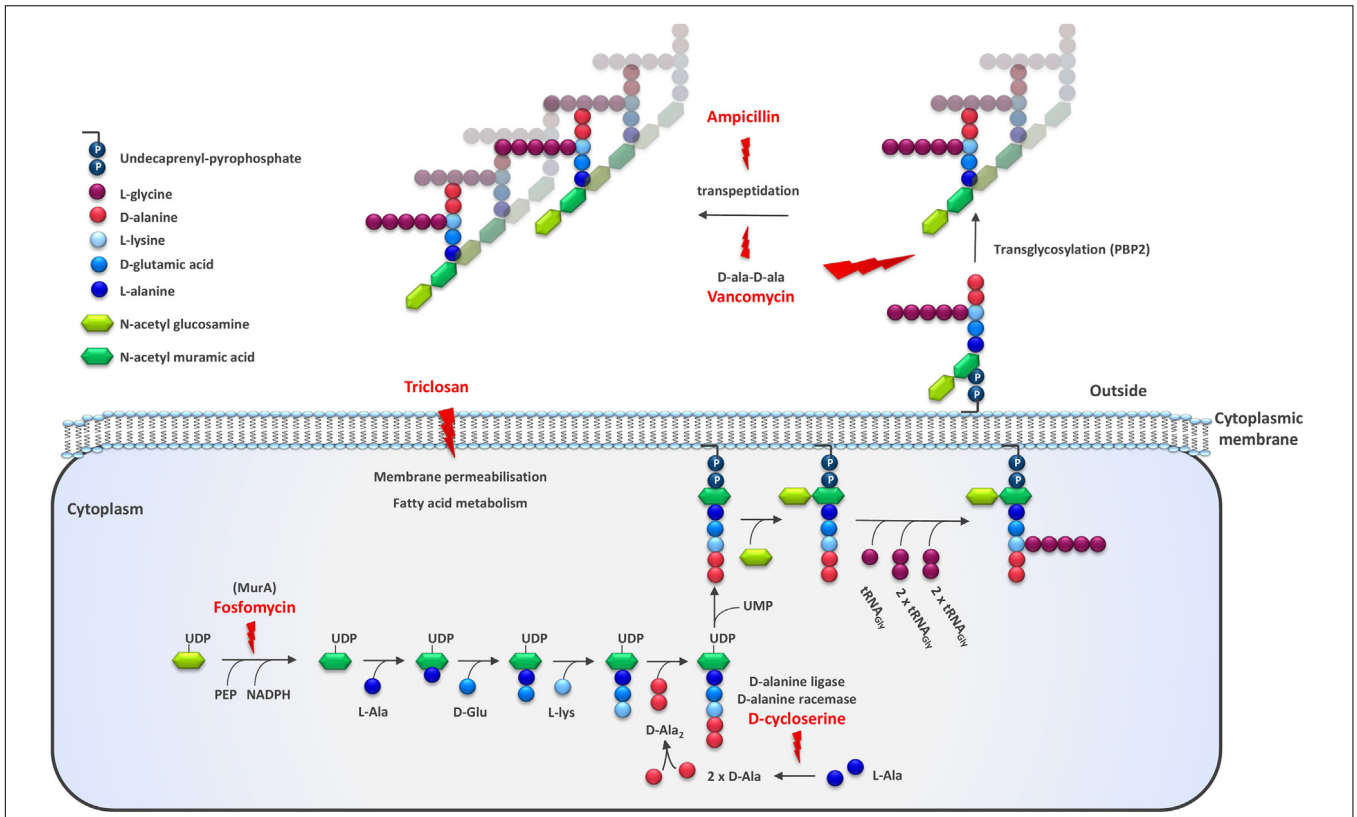

FIGURE 1 | Schematic representation of the enzymatic steps involved in Gram positive cell wall synthesis. The targets of cell envelope targeting antibiotics and antimicrobial agents used for strain improvement are indicated with a lightning symbol. The illustration is adapted from McCallum et al. (2011) and depicts the cell wall of *Staphylococcus aureus*. Among the different LAB species, the nature of interpeptide cross-bridge, the fifth residue stem peptide, the glycan chain length, and other features may vary.

the pH indicators bromocresol purple and bromocresol green (Poulsen et al., 2019). After fermentation at 37°C, the texturizing properties of the derivatives were assessed using the TADM-based method described in Poulsen et al. (2019). Finally, the most interesting candidates from all selections were grown to saturation in the appropriate broth and inoculated 1% vol/vol into 200 ml full fat milk and then fermented overnight at 40°C. The milk used for rheology measurement was added 2% whey protein to standardize the protein content of the milk. Acidification was followed using a CINAC system (Corrieu et al., 1992) or an ICINAC system (AMS alliance). Fermentation was stopped at pH 4.55 and the contents of the bottle were carefully stirred and placed at 6°C overnight before rheology measurements. Rheologic properties were measured in a StressTech rheometer (RheoLogica Instruments AB, Sweden) equipped with a C25 coaxial measuring system (Folkenberg et al., 2011). The viscometry test was made with shear rates varying from 0.27 to 300 s^{-1} in 21 steps. Shear rates were increased and then decreased and the upward and downward curves of shear stress and apparent viscosity were recorded. Delay and integration times were 5 and 10 s, respectively. Shear stress at 300 s^{-1} was chosen as a standard for comparisons. G*, reflecting gel firmness, was measured by oscillation at frequency of 1 Hz. We found that among the fast growing isolates, 1–5% were found to have improved texturizing properties. The rheological data of the strains studied here are presented in **Table 1**. For most strains, the values represent an average of duplicate experiments but due to milk variations over the experimental period, the values for each group of strains are set relative to that of the respective parent strain.

Genome Sequencing and SNP/INDEL Analysis

Genomic DNA for *de novo* short-read whole genome sequencing (WGS) was extracted from 1 ml of overnight culture (at OD_{600} = 1) of wild-type and mutant strains with DNeasy Blood and Tissue kit on QiaCube system (Qiagen) following the manufacturer's protocol. Sequencing was done at BGI using Illumina Hiseq 2000 machines or in-house at Chr. Hansen using an Illumina MiSeq machine. The genome sequences were assembled, annotated, and finished using CLC genomic workbench software (CLCBio). Reference-quality hybrid genome assemblies were created for selected strains using the Oxford Nanopore Technologies (ONT) long reads and the corresponding Illumina short reads. Poor quality reads (≤30 bases, ≤quality 20) were trimmed using AdapterRemoval v.2.2.4 based on the PHREDscale. The hybrid genome assembler Unicycler v.0.4.7

TABLE 1 | Strain list and texture properties.

Streptococcus thermophilus		**Relative shear stress***	**Relative gel firmness***
CHCC13994	Wild-type	100	100
CHCC13235	Cycloserine resistant derivative of CHCC13994	93	121
CHCC13236	Cycloserine resistant derivative of CHCC13994	114	119
CHCC15914	Wild-type	100	100
STFOS92	Fosfomycin resistant derivative of CHCC15914	111	113
STVAN16	Vancomycin resistant derivative of CHCC15914	100	120
CHCC27806	Wild-type	100	100
STTRI97	Triclosan resistant derivative of CHCC27806	99	103
STVAN19	Vancomycin resistant derivative of CHCC27806	100	123
STVAN20	Vancomycin resistant derivative of CHCC27806	108	115
STVAN24	Vancomycin resistant derivative of CHCC27806	100	103
Lactobacillus delbrueckii* subsp. *bulgaricus			
CHCC13995	Wild-type	100	100
CHCC12944	Cycloserine resistant derivative of CHCC13995	109	150
CHCC12945	Cycloserine resistant derivative of CHCC13995	110	158
CHCC15461	Ampicillin resistant derivative of CHCC13995	101	134
CHCC15466	Ampicillin resistant derivative of CHCC13995	100	114
CHCC759	Wild-type	100	100
CHCC15470	Ampicillin resistant derivative of CHCC759	109	105

**For each group of strains, the values are relative to the respective parent strain. The absolute values for the wild-type strains are in Pascal units (shear stress, gel firmness): CHCC13994 (70, 137), CHCC15914 (83, 225), CHCC27806 (77, 229), CHCC13995 (99, 59), and CHCC759 (45, 199).*

was used for the *de novo* assembly of the trimmed short reads and the raw ONT reads. In order to reduce sequence misassembly, the non-default parameter: "conservative" was selected for the hybrid assembly. The annotated genome sequences of all variant strains were aligned and compared with the respective mother strains using Mauve 2.3.1 software. After alignment, a single-nucleotide polymorphism (SNP) analysis was performed using Mauve 2.3.1 software. Breseq v. 0.35.0 was used as a secondary method to assess SNPs, small deletions, and insertions by mapping reads from variant sequences to the reference genome of the mother strain (Deatherage and Barrick, 2014). Subsequently, gdtool was used to compare and collect the identified SNPs. The similarities with identified genes from other organisms available in GenBank[1] were assessed by using the Basic Local AlignmentSearchTool (BLAST) (Altschul et al., 1990), provided by the National Center for Biotechnology Information[2].

[1]http://www.ncbi.nlm.nih.gov/GenBank/

[2]http://blast.ncbi.nlm.nih.gov/Blast.cgi

Intracellular Magnesium and Manganese Concentrations

To prepare the cellular extracts, fresh overnight cultures in MRS were inoculated at 1% (vol/vol) into 100 ml MRS and incubated anaerobically overnight at 37°C. Cultures were then split into two cultures of 50 ml and cells were collected by centrifugation at 5000 r/min for 10 min (A and B samples for each strain). After first centrifugation, the cells were washed once at 4°C with MRS and then twice with 5 ml 1x phosphate buffered saline (PBS) buffer (pH 7.4). The PBS buffer had been treated overnight with 10 mg/ml Chelex (Bio-Rad Inc.). All tubes were then centrifuged for 10 min at 5000 r/min, and washed with 5 ml PBS buffer, centrifuged for 10 min at 5000. After washing and resuspension in 1 ml PBS buffer, the contents were transferred to 2 ml Eppendorf tube. The Eppendorf tubes were centrifuged for 15 min at 15,000 x *g* and the supernatants were discarded. The cell pellets were dried in a rotary evaporator at room temperature, weighed and resuspended in 200 µl (vol/vol) concentrated (65%) nitric acid containing 0.1% Triton-X 100. The tubes were incubated at 95°C with shaking for 10 min followed by vigorous vortexing for 20 s. Finally, the tubes were centrifuged at 15,000 x *g* for 5 min and the supernatants transferred to new tubes. The supernatants for each strain (samples A and B) were sent to Hans van der Velde, Micro-analyse, Rijksuniversiteit Groningen, Netherlands where they were analyzed for total content of magnesium and manganese using inductively coupled plasma mass spectroscopy (ICP-MS) using a Perkin Elmer Optima 7000 DV (Wilschefski and Baxter, 2019). Both extractions showed the same tendency but only sample B was sufficiently extracted and these data are presented in **Figure 2**.

EDTA Chelating Experiments

The CHCC13995 wild-type strain and derivatives, CHCC12945, CHCC12944, CHCC15461, and CHCC15466 were grown anaerobically at 40°C for approximately 20 h and inoculated 1% vol/vol into 200 ml B-milk. The cultures were incubated overnight at 40°C and the development of pH was followed continuously over approximately 20 h using an ICINAC system (AMS alliance). When used, EDTA (Sigma–Aldrich) was added to a final concentration of 100 µg/ml, $MgSO_4$ (Sigma–Aldrich) was added to a final concentration of 50 µg/ml, and $MnSO_4$ was added to the final concentrations of 10, 25, 50, or 100 µ g/ml.

RESULTS AND DISCUSSION

Application of Antimicrobial Agents for Industrial Strain Improvement

We used a number of antimicrobials, including the antibiotics DCS, AMP, vancomycin, and fosfomycin, as well as the biocide triclosan to select resistant variants which were subsequently screened for desirable traits for industrial application. For each compound, we developed a selection protocol optimized for the particular strain and antimicrobial (for details, see section "Materials and Methods") and obtained a suitable number of variants for screening purposes. In the dairy industry, strains

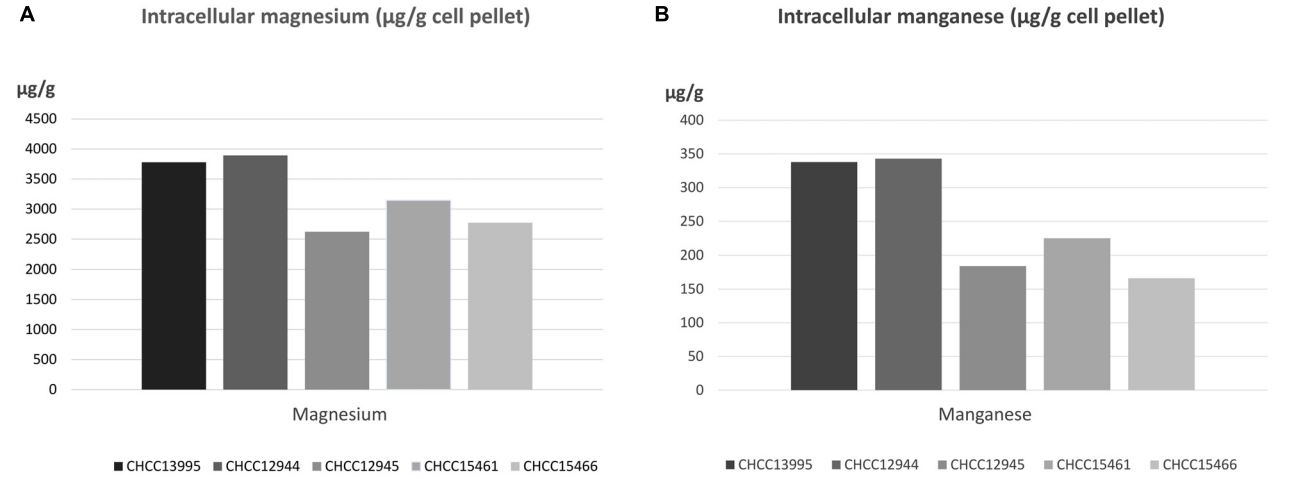

FIGURE 2 | Intracellular levels of **(A)** magnesium (µg/ml) and **(B)** manganese (µg/ml) measured in wild-type strain CHCC13995 and texturizing derivatives CHCC12944, CHCC12945, CHCC15461, and CHCC15466 measured by inductively coupled plasma–mass spectrometry (ICP-MS) analysis.

with optimal rheological traits are in high demand. With this in mind, we screened all isolates obtained upon selection with antimicrobial compounds for their texturing potential in milk. The best milk texturizing strains had up to 14% improved shear stress or up to 58% higher gel firmness (**Table 1**). Especially gel firmness was higher in many of the selected derivatives. These strains were selected for further characterization, including WGS to identify mutations that may confer resistance to the compound of choice as well as mutations presumably involved in the improved texturizing phenotype. Data from wild-type and variant strains were compared and analyzed for non-synonymous SNPs and gaps. The outcome of this analysis is presented in **Table 2**.

Genetic Changes in Derivatives Obtained After Antimicrobial Selection

Analysis of Genetic Changes in *Streptococcus thermophilus* Strains Resistant to D-Cycloserine

Two *S. thermophilus* strains with improved texture formation were isolated among DCS resistant derivatives (Kibenich et al., 2012; Johansen et al., 2013). Genome sequence analysis of these derivatives, strains CHCC13235 and CHCC13236, revealed three non-synonymous SNPs resulting in amino acid replacement in the encoded proteins, possibly altering the enzyme activity and therefore potentially involved in the observed DCS resistance. CHCC13235 has an SNP in a gene annotated as EAM type sugar transporter (glcU) (302C to 302T, resulting in amino acid change V101A). GlcU encodes a novel non-PTS glucose permease (Castro et al., 2009), which previously has been shown to play a role in fitness cost in nisin-resistant variants of *Streptococcus faecalis* (Kumar et al., 2019). In addition, CHCC13235 carries an SNP in the promoter region upstream of a LacI type regulator potentially regulating the neighboring gene maltodextrin phosphorylase, whose role in milk fermentations is unknown but was previously found to be upregulated in *S. thermophilus* under acidic growth conditions (Wu et al., 2019). CHCC13236 has an SNP in a gene encoding an MFS transporter (nucleotide change A337 to G337, resulting in amino acid change I113V). Thus, both strains have non-synonymous substitutions in a protein with a transporter function which have previously been suggested to be involved in resistance to DCS via an antibiotic efflux mechanism (Versluis et al., 2016). No direct linkage to the observed improved texturizing properties could be identified.

Analysis of Genetic Changes in *L. delbrueckii* subsp. *bulgaricus* Strains Resistant to D-Cycloserine and Ampicillin

The most texturizing derivative of CHCC13995 is the DCS resistant CHCC12945. This strain has T to A substitutions at positions 897 and 898, and a 1 bp deletion at nucleotide position 899 of a gene encoding a Mg^{2+} transporting P-type ATPase, while CHCC15461, an AMP resistant derivative, was found to have a 4 bp deletion in the same gene starting at nucleotide position 181. In both cases, the change results in premature termination of the protein. In addition, CHCC12945 harbors an SNP in a gene encoding a PTS sugar (cellobiose) transporter subunit IIC (nucleotide change 536C to 536G, resulting in the predicted amino acid sequence alteration A179G). Chen et al. (2017) also found a sugar transporter encoding gene among the novel genes conferring DCS resistance. Potentially, the sugar transporter can mediate transport of DCS facilitating contact with the target enzymes (Versluis et al., 2016; Chen et al., 2017). Strain CHCC15466, an AMP resistant derivative, has an SNP in the same ATPase (nucleotide change 2273C to 2273A, resulting in P758Q). In addition, the two AMP resistant isolates, CHCC15461 and CHCC15466, both have the identical SNP in a gene annotated as encoding a glycerol uptake facilitator protein GlpF (nucleotide change 115A to 115C, resulting in I39L) while in CHCC15466, another SNP was identified in a polyamine (spermidine/putrescine) ABC transporter encoding

TABLE 2 | Gene modifications identified in resistant and texturizing derivatives.

Resistance	Species[1]	Texturizing derivative	Background	Gene modification	Gene accession[2]
Cycloserine	St	CHCC13235	CHCC13994	EAM type sugar transporter glcU (302T to 302C, V101A)	MW084972, MW084973
				LacI type regulator (−202A to −202C)	MW292712, MW292713
Cycloserine	St	CHCC13236	CHCC13994	MFS transporter (337A to 337G, I113V)	MW292666, MW292667
Cycloserine	Lb	CHCC12945	CHCC13995	Mg^{2+} transporting P-type ATPase (898T to 898A, 899T to 899A, Δ916C) Truncated	MW292668, MW292669
				PTS sugar transporter subunit IIC—cellebiose: (536C to 536G, A179G)	MW292672, MW262673
Ampicillin	Lb	CHCC15461	CHCC13995	Mg^{2+} transporting P-type ATPase (Δ181 - 184) Truncated	MW262668, MW292670
				Aquaporin/glycerol uptake facilitator. (115A to 115C, I39L)	MW292674, MW292675
Ampicillin	Lb	CHCC15466	CHCC13995	Mg^{2+} transporting P-type ATPase (2273C to 2273A, P758Q)	MW292668, MW292671
				Spermidine/putrescine ABC transporter, ATP-binding protein (254A to 254C, Y85S)	MW292677, MW292678
				Aquasporin/glycerol uptake facilitator protein (115A to 115C, I39L)	MW292674, MW292676
Ampicillin	Lb	CHCC15470	CHCC759	Beta-subunit DNA polymerase (1504G to 1504T, G502C)	MW292679, MW292680
				Tyrosine-protein phosphatase (73G to 73C, G25R)	MW292681, MW292682
Fosfomycin	ST	STFOS92	CHCC15914	UDP-*N*-acetylglucos-amine_1-carboxyvinyl-transferase – murA. (122G to 112A, E38stop). Truncated	MW292682, MW292684
				Pyruvate kinase (653G to 653A, A218T)	MW292685, MW292686
				Calcium-translocating P-type ATPase, PMCA-type (1990G to 1990A, G664R)	MW292687, MW292688
Vancomycin	ST	STVAN16	CHCC15914	PBP1A family penicillin-binding protein (966A to 966C, E322D)	MW292689, MW292690
				LysM peptidoglycan-binding domain-containing protein (541T to 541C, S181P)	MW292691, MW292692
				Anthranilate phosphoribosyltransferase. (979A to 979C, R327S)	MW292693, MW292694
				Hypothetical protein (1630A to 1630T, S544C)	MW292695, MW292696
				Glycine-tRNA ligase subunit alpha (438C to 438A, F146L)	MW292697, MW292698
Vancomycin	St	STVAN19	CHCC27806	Large subunit carbamoyl-phosphate synthase (452C to 452T, T151M)	MW292699, MW292700
Vancomycin	St	STVAN20	CHCC27806	Dihydroxyacetone kinase (140C to 140T, T47I)	MW292701, MW292702
				Cell wall CHAP hydrolase (−67C to −67T)	MW292703, MW292704
				Response regulator transcription factor (lytR family). T insertion at −109	MW292705, MW292706
Vancomycin	St	STVAN24	CHCC27806	Glycosyltransferase polysaccharide biosynthesis gene—rgp. (282G to 282A, M94I)	MW292707, MW292708
				Ribosome silencing factor. (166C to 166T, R56C)	MW292709, MW292710
Triclosan	St	STTRI97	CHCC27806	Glutathione-disulfide reductase (104G to 104A, G35E)	MW292711, MW292712

[1]St (S. thermophilus); Lb (L. bulgaricus). [2]Accession numbers: Background strain, derivative. Nucleotide positions: +1 defines A in AUG start codon.

gene (254Ato 254C, Y85S). In *Staphylococcus aureus*, the GlpF level correlates with formation of the L-form of the bacteria which is more tolerant to antibiotics such as AMP and secretes more exopolysaccharide (EPS) (Han et al., 2014). If a similar mode of action exists in *L. delbrueckii* subsp. *bulgaricus*, the amino acid change predicted should result in a more active GlpF protein. Interestingly, exposure of *Streptococcus pneumoniae* to penicillin resulted in down-regulation of the polyamine transporter (Rogers et al., 2007) while spermidine was found to stimulate biofilm formation in *Bacillus subtilis* (Hobley et al., 2017).

In another *L. delbrueckii* subsp. *bulgaricus* strain background, CHCC759, a more texturizing and AMP resistant derivative was also selected, CHCC15470. This derivative had no SNP in the cation transporting P-type ATPase but instead we identified an SNP in a gene encoding a tyrosine-protein phosphatase (73G to 73C, resulting in aa change G25R) and in the beta-subunit of DNA polymerase (1504G to 1504T, resulting in aa change G502C) (**Table 2**). While the relationship between changes in the DNA polymerase and improved texture or antibiotic resistance is not apparent, tyrosine-protein phosphatases have been shown to be involved in the regulation of extracellular polysaccharide synthesis and assembly (Vincent et al., 2000). Strains with higher extracellular polysaccharide production have been found to exhibit a significantly higher resistance to antibiotics (Arciola et al., 2005) and extracellular polysaccharide is known to be involved in texture formation in dairy products.

Interestingly, three derivatives of *L. delbrueckii* subsp. *bulgaricus* strain CHCC13995 with improved texturizing properties were found to have genetic changes, at different positions, in the same gene; a gene annotated as a Mg^{2+} transporting P-type ATPase (*mgtA*). Two of these derivatives, CHCC15461 and CHCC15466, were selected as resistant to AMP and one strain, CHCC12945, as DCS resistant. A more thorough characterization of these derivatives was therefore carried out as described in a subsequent section.

Analysis of Genetic Changes in Strains Resistant to Vancomycin

Vancomycin was used to select a number of derivatives with improved rheological properties in two different background strains of *S. thermophilus,* CHCC15914 and CHCC27806. **Table 2** presents the changes detected in four vancomycin resistant derivatives of *S. thermophilus* showing improved rheological properties. Three of the derivatives, STVAN19, STVAN20, and STVAN24 are derived from CHCC27806. STVAN19 contains a single SNP present in the *carB* gene encoding the large subunit of carbamoyl phosphate synthetase (452C to 452T, resulting in aa change T151M), which is located in ATP-grasp fold 1 of this subunit. It is not known if this change results in a more or less active enzyme. Interestingly, vancomycin binds to D-alanyl-D-alanine and the active site of CarAB is very similar to that previously described for D-alanine:D-alanine ligase (Stapleton et al., 1996). In addition, *carB* was found to be the most highly induced gene in a vancomycin sensitive *S. aureus* strain when grown in the presence of vancomycin (Awad et al., 2013) and has previously been found to be involved in multiple cellular functions including biofilm formation and EPS formation (Zhuo et al., 2015). In STVAN20, we identified four SNPs with two occurring in promoter regions of different genes. These are: a cell wall CHAP hydrolase (C to T change at position −67 from ATG start codon) and a transcription factor annotated as a response regulator (a T insertion in a long row of T's at −109 from ATG start codon). In both cases, such promoter changes may alter the level of expression for the downstream genes. The CHAP hydrolases play a role in cell wall biosynthesis which could affect vancomycin resistance and trigger EPS production (Monteiro et al., 2017). Response regulators have been shown to regulate vancomycin resistance in *E. faecium* (Haldimann et al., 1997). The third SNP was found in the coding region of the *dak* gene encoding the cytoplasmic enzyme dihydroxyacetone kinase (140C to 140T, T47I). This change might result in an altered activity of the enzyme. A potential *dak* gene has been identified as a target for vancomycin in *S. aureus* (Haag et al., 2015) and DHA-induced genes have been found to be involved in a biofilm growth state in *E. coli* (Peiro et al., 2019). The last vancomycin resistant derivative in the CHCC27806 background, STVAN24, was found to contain two SNPs. One SNP was identified in a glycosyltransferase polysaccharide biosynthesis gene *cspB* (282G to 282A, M94I) and the second occurred in a gene predicted to encode a ribosome silencing factor (166C to 166T, R56C). Both are amino acid changes that are likely to change the activity of their respective encoded proteins. Only the change in *cspB* is expected to be directly involved in polysaccharide biosynthesis and texture formation (Schmid et al., 2016).

Finally, strain STVAN16 derived from the CHCC15914 strain background, was found to possess 5 different SNPs, all within the coding region of the encoded protein. SNP1 is in the gene encoding PBP1A family penicillin-binding protein (966A to 966C, E322D), SNP2 in the gene encoding LysM (543T to 543C, S191P), SNP3 is in a gene encoding Anthranilate phosphoribosyltransferase (979A to 979C, R327S), SNP4 occurred in a hypothetical protein (1630A to 1630T, S544C) while the last SNP in the alpha subunit of Glycine-tRNA ligase (438C to 438A, F146L).

Only the first two of these five genes have previously been associated with vancomycin resistance and texturizing properties; the PBP1A family penicillin-binding protein and LysM peptidoglycan-binding domain-containing protein. Both proteins are involved in cell wall biosynthesis and are induced in the vancomycin resistant *Enterococcus faecium* strain AUS0004 (Cacaci et al., 2018). Furthermore, disruption of the gene encoding penicillin-binding protein 2b was resulted in reduction of EPS production in *S. thermophilus* Sfi6 (Stingele and Mollet, 1996). No direct correlation to vancomycin resistance or texture could be made for the three other SNPs in STVAN16.

Analysis of Genetic Changes in a Strain Resistant to Fosfomycin

From CHCC15914, one fosfomycin resistant derivative with improved texturizing properties was isolated. The strain, STFOS92, contains three SNPs (**Table 2**). SNP1 results in a truncated UDP-*N*-acetylglucosamine-1-carboxyvinyltransferase protein due to a nucleotide change resulting in premature translation termination after amino acid 38E, SNP2 is in the gene

encoding pyruvate kinase (653G to 653A, A218T) while SNP3 occurs in a gene annotated as a calcium-translocating P-type ATPase, PMCA-type (1990G to 1990A, G664R). From these three observed changes, only the change in *murA* is expected to be associated with the observed phenotype as MurA catalyzes the first step in the biosynthesis of the bacterial cell wall and is a target of fosfomycin (**Figure 1**). Furthermore, it is likely that the potential accumulation of the EPS precursor UDP-N-acetyl-alpha-D-glucosamine leads to increased formation of EPS (Zeidan et al., 2017). This derivative was found to aggregate significantly.

Analysis of Genetic Changes in a Strain Resistant to Triclosan

One triclosan resistant derivative with improved texturizing properties was isolated. The strain, STTRI97, a derivative of CHCC27806, contains an SNP in the gene encoding glutathione-disulfide reductase (nucleotide change G104A resulting in amino acid change G35E) (**Table 2**). Triclosan provokes oxidative stress and damages the bacterial membrane (Lu et al., 2018). A change in glutathione disulfide reductase activity may help the bacteria to overcome this oxidative damage (Patel et al., 1998).

Intracellular Magnesium and Manganese Concentrations of Variants With Changes in the P-Type ATPase

The observation that three of the DCS or AMP resistant isolates, CHCC12945, CHCC15461, and CHCC15466, carried mutations in the same gene, annotated as encoding a Mg^{2+} transporting P-type ATPase, suggested an inactivation of function which could lead to a lower intracellular magnesium concentration. Furthermore, we speculated that a lower intracellular concentration of magnesium could play a role in texture formation and/or resistance to the two antimicrobial agents. Cell pellets from the individual cultures were therefore subjected to ICP-MS analysis of the total intracellular magnesium and manganese content. We included another DCS resistant mutant, CHCC12944, that shows improved texture but has no genetic changes in the ATPase. Surprisingly, the data obtained from the analysis showed that the ATPase variants all have reduced intracellular levels of both magnesium and manganese when compared to the parental strain (CHCC13995) and the non-ATPase derivative CHCC12944. The reduction in intracellular levels of magnesium ranged from 17% in CHCC15461 and up to 31% in CHCC12945 and the reduction in manganese levels was from 33% (CHCC15461) and up to 51% (CHCC15466) when compared to the levels found for the CHCC13995 mother strain. The intracellular level of magnesium is approximately 10-fold higher than for manganese.

EDTA Inhibits and Mn^{2+} Restores Milk Acidifications of the P-Type ATPase Variants

EDTA is a chelating agent with high affinity for calcium, magnesium, and other divalent metal cations. The effect of addition of EDTA to milk acidifications was assessed for the three ATPase variants, the DCS resistant mutant CHCC12944, and the CHCC13995 mother strain. The effect of adding various concentrations of Mg^{2+} and Mn^{2+} to milk containing 100 μg/ml EDTA was also determined. The pH achieved after 20 h incubation is shown in **Figure 3**. In the absence of EDTA, a pH of 4.0 was attained after 20 h for all strains (**Figure 3A**). Addition of 100 μg/ml EDTA inhibited the ATPase variants more than CHCC12944 and CHCC13995 (**Figure 3B**). Addition of 50–200 μg/ml $MgSO_4$ (only 50 μg/ml is shown) did not restore the EDTA inhibited acidification but had a minor effect on acidification of CHCC15466 at 50 μg/ml (**Figure 3D**). On the other hand, addition of 10 μg/ml $MnSO_4$ partly restored the acidification of the mother strain and for derivatives CHCC15461 and CHCC15466 but to a lesser extent for the derivative CHCC12945 (not shown). Addition of 50 μg/ml $MnSO_4$ completely restored acidification of both mother strain and the derivatives (**Figure 3C**). Addition of 50 μg/ml $MgSO_4$ to cultures supplemented with $MnSO_4$ had no additional effect (not shown).

P-Type ATPase—A Role for Antibiotic Resistance and Texture?

P-type ATPases transport a variety of different compounds, including ions and phospholipids, across a membrane using ATP hydrolysis for energy (Axelsen and Palmgren, 1998; Chan et al., 2010). The MgtA and MgtB ATPase type, described here, are normally associated with active influx of Mg^{2+}, which is the most abundant divalent intracellular cation and a cofactor with ATP in many enzymatic reactions (Smith and Maguire, 1998). Manganese transporting P-type ATPases are not well known but at least one was described for mycobacteria (Padilla-Benavides et al., 2013). Instead, two other manganese uptake systems have been reported for LAB: the NRAMP-type transporter MntH and the ABC transporter SitABC (Kehres and Maguire, 2003). MntH is the major transporter under acidic conditions while SitABC is active at neutral pH (Porcheron et al., 2013; Siedler et al., 2020). Mn^{2+}, an important trace element, also plays a role in bacterial physiology and protection against oxidative stress (Kehres and Maguire, 2003).

The genetic changes detected in the variants described here are expected to either inactivate the ATPase completely due to premature translation termination (CHCC12945 and CHCC15461) or reduce the activity (CHCC15466). All derivatives were found to have lower intracellular levels of both magnesium and manganese when grown in standard medium. Another DCS resistant and texturizing derivative with no genetic change in the ATPase encoding gene, CHCC12944, had levels of magnesium and manganese similar to the mother strain CHCC13995. The addition of EDTA to milk inhibited acidification of the ATPase variants to a greater extent than the other derivatives and the mother strain. The EDTA mediated inhibition was restored by addition of Mn^{2+} while addition of Mg^{2+} had only minor effect. We interpret these results to indicate that the change in the ATPase leads to an intracellular Mn^{2+} deficiency in the presence of EDTA while the intracellular reduction in Mg^{2+} is less critical. Together, these results suggest that the P-type ATPase is a not a specific Mg^{2+} transporter but rather a transporter of both Mg^{2+} and Mn^{2+} and potentially other cations. Interestingly, the most texturizing derivative, CHCC12945, is more inhibited

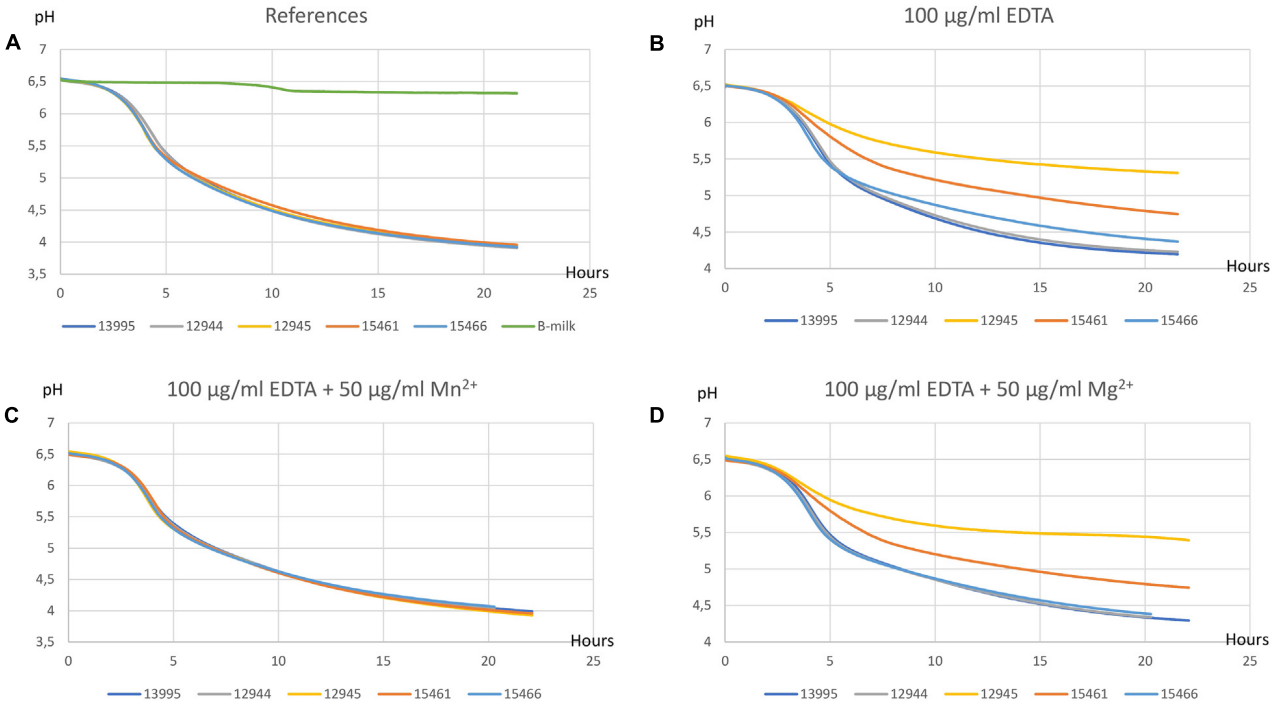

FIGURE 3 | Milk acidification curves. All experiments were performed for wild-type strain CHCC13995 and texturizing derivatives CHCC12944, CHCC12945, CHCC15461, and CHCC15466 at 40°C in B-milk **(A)**, with 100 µg/ml EDTA **(B)**, with 100 µg/ml EDTA + 50 µg/ml Mn^{2+} **(C)**, and with 100 µg/ml EDTA + 50 µg/ml Mg^{2+} added **(D)**.

by EDTA than the other derivative with a truncated ATPase, CHCC15461. This could indicate that the potential PTS sugar transporter, found to be altered in CHCC12945, also plays a role in texture formation. Whether the reduced intracellular levels of magnesium and manganese are directly or indirectly related to the observed antibiotic resistance and observed texture improvement is unclear but the only genetic change common to these three derivatives is in the gene encoding the P-type ATPase. The results from Lew et al. (2013) indicated that the ratio between manganese and magnesium ions in *Lactocaseibacillus rhamnosus* affected biosynthesis of lipoteichoic acid and these authors discussed whether the ratio between the metals indirectly affected the level of peptidoglycan by modifying the activity of the enzymes MurA to MurF. Similarly, the target for DCS, D-ala:D-alanine ligase, can itself be affected. Finally, it can be speculated that the P-type ATPase plays a more direct role in the uptake of DCS and AMP but this seems unlikely due to the different nature of the two antibiotics.

CONCLUSION

We have presented a new powerful toolbox to select for strains with improved texture formation in milk. By using inhibitory concentrations of different cell envelope targeting antibiotics and antimicrobial agents to select variants, we were able to identify a number of isolates that showed improved rheological properties in milk. Surprisingly, the characterization of these derivatives showed that the identified genetic changes occurred, in only a few cases, in target genes typically associated with resistance to the antimicrobial compounds. The versatility of this method and the diversity of mutations detected were unexpected. Therefore, we also expect this tool to be useful to select for other improved traits in bacteria used for dairy and other fermentation applications. Together these results show that mechanisms leading to resistance to antibiotics and antimicrobials are complex and we speculate this to be dependent on the growth medium used during the application of these dominant selection strategies. Similar observations have also been made by others (Baisa et al., 2013.) who described that individual resistance mechanisms are typically well defined in minimal and defined medium but more complex in rich media and can involve several different genetic loci. This highlights the necessity of understanding the mode of action for each specific antibiotic and antimicrobial agent in a particular medium, especially when new antibiotic targets are to be identified for the prevention and treatment of disease. In our case, the selections were done in complex media like M17 and MRS medium and the genetic characterization of the selected resistant derivatives led to the discovery of mutations in a variety of different genes. The characterized resistant strains generally comprise mutations in genes associated with transport functions, formation of the outer surface of the cell or stress responses. Some of the genes have not previously been associated with resistance to the compounds used. However, our results will only partly reflect the resistance

mechanism to be found in the complex media used in these studies because the isolates investigated were a subset of the total number of resistant derivatives, specifically selected for their improved texturizing ability. This also complicates the understanding of how the genetic changes link to the observed resistance and texturizing phenotype because the two phenotypes are not separated. This is especially the case when multiple genetic changes occur in an isolate. In a number of cases, there was a predictable link to the improved texturizing phenotype that was observed. For example, in the AMP^R derivative CHCC15470 and the VAN^R derivative STVAN24, SNPs were identified in genes encoding a tyrosine-protein phosphatase and a glycosyltransferase polysaccharide biosynthetic enzyme CspB, respectively. Both genes are predicted to directly play a role in polysaccharide biosynthesis.

A number of independent isolates of *L. delbrueckii* subsp. *bulgaricus*, obtained with either DCS or AMP selection, had mutations in a gene annotated as a putative Mg^{2+}-transporting P-type ATPase. The finding that P-type ATPase derivatives were found with both types of antimicrobials indicates a secondary target mechanism. Despite an extra effort to understand the mode of action for the observed phenotypes, we can only speculate that reduced intracellular levels of manganese or eventually magnesium can alter the activity of enzymes crucial for cell envelope formation and indirectly lead to production of more capsular polysaccharide (CPS) or EPS. When nutrients are limited, formation of EPS and biofilm is induced and bacteria become highly tolerant to antibiotics (Mulcahy and Lewenza, 2011; Nguyen et al., 2011). Moreover, strains with higher extracellular polysaccharide production have been shown to have a significantly higher resistance to antibiotics (Arciola et al., 2005). Since most of the observed changes occur in genes encoding transport functions, cell wall formation, or stress responses, this potential link between stress, starvation, texture, and antibiotic resistance might be a hypothesis to explain the link between texture and antibiotic resistance in several of the derivatives found here.

Antibiotic resistance is considered to be one of the most important public health issues of our time, primarily due to the development of transmissible antibiotic resistance genes which can transfer between bacterial hosts. However, the use of cell envelope targeting antibiotics and antimicrobial agents to select the derivatives described here does not pose a threat to public health because the resistance is host specific and not based on transmissible antibiotic resistance genes.

The selective methods described in this study can therefore be used directly as an effective toolbox for strain improvement for the food industry.

DATA AVAILABILITY STATEMENT

The datasets presented in this study can be found in online repositories. The names of the repository/repositories and accession number(s) can be found in the article/supplementary material.

AUTHOR CONTRIBUTIONS

KS was involved in design of and performing the experiments, writing of the manuscript, and drawing of the figures. EJ was involved in design of the experiments and writing of the manuscript. IK was involved in writing of the manuscript and genome sequence analysis. All authors contributed to revising the manuscript.

ACKNOWLEDGMENTS

The authors thank Annette Kibenich, Minna Wernegreen, and Mette Junge for excellent technical assistance, Anna Koza and Martin Holm Rau for their great help in genomic sequencing and analyses, and Michael Broberg Palmgren for many helpful discussions.

REFERENCES

Altschul, S. F., Gish, W., Miller, W., Myers, E. W., and Lipman, D. J. (1990). Basic local alignment search tool. *J. Mol. Biol.* 215, 403–410. doi: 10.1016/S0022-2836(05)80360-2

Arciola, C. R., Campoccia, D., Gamberini, S., Donati, M. E., Pirini, V., Visai, L., et al. (2005). Antibiotic resistance in exopolysaccharide-forming *Staphylococcus epidermidis* clinical isolates from orthopaedic implant infections. *Biomaterial* 26, 6530–6535. doi: 10.1016/j.biomaterials.2005.04.031

Awad, S., Alharbi, A. E., and Alshami, I. (2013). Exposure of vancomycin-sensitive *Staphylococcus aureus* to subinhibitory levels of vancomycin leads to upregulated capsular gene expression. *Br. J. Biomed. Sci.* 70, 58–61. doi: 10.1080/09674845.2013.11669936

Axelsen, K. B., and Palmgren, M. G. (1998). Evolution of substrate specificities in the P-type ATPase superfamily. *J. Mol. Evol.* 46, 84–101. doi: 10.1007/pl00006286

Baisa, G., Stabo, N. J., and Welch, R. A. (2013). Characterization of *Escherichia coli* D-cycloserine transport and resistant mutants. *J. Bacteriol.* 195, 1389–1399. doi: 10.1128/JB.01598-12

Barna, J. C., and Williams, D. H. (1984). The structure and mode of action of glycopeptide antibiotics of the vancomycin group. *Annu. Rev. Microbiol.* 38, 339–357. doi: 10.1146/annurev.mi.38.100184.002011

Cacaci, M., Giraud, C., Leger, L., Torelli, R., Martini, C., Posteraro, B., et al. (2018). Expression profiling in a mammalian host reveals the strong induction of genes encoding LysM domain-containing proteins in *Enterococcus faecium*. *Sci. Rep.* 8:12412. doi: 10.1038/s41598-018-30882-z

Cardoso, J. G. R., Zeidan, A. A., Jensen, K., Sonnenschein, N., Neves, A. R., and Herrgård, M. J. (2018). MARSI: metabolite analogues for rational strain improvement. *Bioinformatics* 34, 2319–2321. doi: 10.1093/bioinformatics/bty108

Castro, R., Neves, A. R., Fonseca, L. L., Pool, W. A., Kok, J., Kuipers, O. P., et al. (2009). Characterization of the individual glucose uptake systems of *Lactococcus lactis*: mannose-PTS, cellobiose-PTS and the novel GlcU permease. *Mol. Microbiol.* 71, 795–806. doi: 10.1111/j.1365-2958.2008.06564.x

Chan, H., Babayan, V., Blyumin, E., Gandhi, C., Hak, K., Harake, D., et al. (2010). The P-type ATPase superfamily. *J. Mol. Microbiol. Biotechnol.* 19, 5–104. doi: 10.1159/000319588

Chen, J., Zhang, S., Cui, P., Shi, W., Zhang, W., and Zhang, Y. (2017). Identification of novel mutations associated with cycloserine resistance in *Mycobacterium tuberculosis*. *J. Antimicrob. Chemother.* 72, 3272–3276. doi: 10.1093/jac/dkx316

Corrieu, G., Picque, D., Perret, B., and Quemener, P. (1992). CINAC, an automated system for control of lactic starters. *Process Magazine* 1068, 24–27.

de Man, J., Rogosa, M., and Sharpe, M. (1960). A medium for the cultivation of lactobacilli. *J. Appl. Bacteriol.* 23, 130–135. doi: 10.1111/j.1365-2672.1960.tb00188.x

Deatherage, D. E., and Barrick, J. E. (2014). Identification of mutations in laboratory-evolved microbes from next-generation sequencing data using breseq. *Methods Mol. Biol.* 1151, 165–188. doi: 10.1007/978-1-4939-0554-6_12

Derkx, P. M. F., Janzen, T., Sørensen, K. I., Christensen, J. E., Stuer-Lauridsen, B., and Johansen, E. (2014). The art of strain improvement of industrial lactic acid bacteria without the use of recombinant DNA technology. *Microb. Cell Fact.* 13(Suppl. 1):S5. doi: 10.1186/1475-2859-13-S1-S5

Folkenberg, D. M., Øregaard, G., Bennedsen, M., and Poulsen, L. (2011). *Method for Producing a Fermented Milk Product*. International Patent Application WO/2011/000883. Geneva: WIPO.

Haag, N., Velk, K., McCune, T., and Wu, C. (2015). Bioinformatics and molecular biological characterization of a hypothetical protein SAV1226 as a potential drug target for methicillin/vancomycin *Staphylococcus aureus* infections. *World Acad. Sci. Eng. Technol.* 9, 587–591.

Haldimann, A., Fisher, S. L., Daniels, L. L., Walsh, C. T., and Wanner, B. L. (1997). Transcriptional regulation of the Enterococcus faecium BM4147 vancomycin resistance gene cluster by the VanS-VanR two-component regulatory system in *Escherichia coli* K-12. *J. Bacteriol.* 179, 5903–5913. doi: 10.1128/jb.179.18.5903-5913.1997

Han, J., He, L., Shi, W., Xu, X., Wang, S., Zhang, S., et al. (2014). Glycerol uptake is important for L-form formation and persistence in *Staphylococcus aureus*. *PLoS One* 9:e108325. doi: 10.1371/journal.pone.0108325

Hobley, L., Li, B., Wood, J. L., Kim, S. H., Naidoo, J., Ferreira, A. S., et al. (2017). Spermidine promotes Bacillus subtilis biofilm formation by activating expression of the matrix regulator slrR. *J. Biol. Chem.* 292, 12041–12053. doi: 10.1074/jbc.M117.789644

Johansen, E. (2017). Future access and improvement of industrial lactic acid bacteria cultures. *Microb. Cell Fact.* 16:230. doi: 10.1186/s12934-017-0851-1

Johansen, E. (2018). Use of natural selection and evolution to develop new starter cultures for fermented foods. *Ann. Rev. Food Sci. Technol.* 9, 411–425. doi: 10.1146/annurev-food-030117-012450

Johansen, E., Øregaard, G., Sørensen, K., and Derkx, P. (2015). "Modern approaches for isolation, selection and improvement of bacterial strains for fermentation applications," in *Advances in Fermented Foods and Beverages: Improving Quality, Technologies and Health Benefits*, ed. W. Holzapfel (Cambridge: Woodhead Publishing Ltd).

Johansen, E., Sørensen, K. I., and Kibenich, A. (2013). *Ampicillin Resistant Texturizing Lactic Acid Bacteria Strains*. Patent Application WO/2013/160270. Geneva: WIPO.

Kehres, D. G., and Maguire, M. E. (2003). Emerging themes in manganese transport, biochemistry and pathogenesis in bacteria. *FEMS Microbiol. Rev.* 27, 263–290. doi: 10.1016/S0168-6445(03)00052-4

Kibenich, A., Sørensen, K. I., and Johansen, E. (2012). *Texturizing Lactic Acid Bacteria Strains*. International Patent Application WO/2012/052557. Geneva: WIPO.

Kumar, S., Narayan, K. S., Shandilya, S., Sood, S. K., and Kapila, S. (2019). Role of non-PTS dependent glucose permease (GlcU) in maintaining the fitness cost during acquisition of nisin resistance by *Enterococcus faecalis*. *FEMS Microbiol. Lett.* 366:fnz230. doi: 10.1093/femsle/fnz230

Lambert, M. P., and Neuhaus, F. C. (1972). Mechanism of D-cycloserine action: alanine racemase from *Escherichia coli* W. *J. Bacteriol.* 110, 978–987. doi: 10.1128/JB.110.3.978-987.1972

Lew, L. C., Liong, M. T., and Gan, C. Y. (2013). Growth optimization of *Lactobacillus rhamnosus* FTDC 8313 and the production of putative dermal bioactives in the presence of manganese and magnesium ions. *J. Appl. Microbiol.* 114, 526–535. doi: 10.1111/jam.12044

Lu, J., Wang, Y., Li, J., Mao, L., Nguyen, S. H., Duarte, T., et al. (2018). Triclosan at environmentally relevant concentrations promotes horizontal transfer of multidrug resistance genes within and across bacterial genera. *Environ. Int.* 121, 1217–1226. doi: 10.1016/j.envint.2018.10.040

McCallum, N., Meier, P. S., Heusser, R., and Berger-Bächi, B. (2011). Mutational analyses of open reading frames within the vraSR operon and their roles in the cell wall stress response of *Staphylococcus aureus*. *Antimicrob. Agents Chemother.* 55, 1391–1402. doi: 10.1128/AAC.01213-10

Monteiro, A., Wallace, R. N. N., Mendes, A. R. S., Pinto, B. L., Nascimento da Silva, L. C., and Ferreira, G. F. (2017). "Effects of alterations in *Staphylococcus aureus* cell membrane and cell wall in antimicrobial resistance," in *The Rise of Virulence and Antibiotic Resistance in Staphylococcus aureus*, eds S. Enany and L. Crotty Alexander (London: IntechOpen).

Mulcahy, H., and Lewenza, S. (2011). Magnesium limitation is an environmental trigger of the *Pseudomonas aeruginosa* biofilm lifestyle. *PLoS One* 6:e23307. doi: 10.1371/journal.pone.0023307

Nguyen, D., Joshi-Datar, A., Lepine, F., Bauerle, E., Olakanmi, O., Beer, K., et al. (2011). Active starvation responses mediate antibiotic tolerance in biofilms and nutrient-limited bacteria. *Science* 334, 982–986. doi: 10.1126/science.1211037

Padilla-Benavides, T., Long, J. E., Raimunda, D., Sassetti, C. M., and Argüello, J. M. (2013). A novel P(1B)-type Mn2+-transporting ATPase is required for secreted protein metallation in mycobacteria. *J. Biol. Chem.* 288, 11334–11347. doi: 10.1074/jbc.M112.448175

Patel, M. P., Marcinkeviciene, J., and Blanchard, J. S. (1998). Enterococcus faecalis glutathione reductase: purification, characterization and expression under normal and hyperbaric O2 conditions. *FEMS Microbiol. Lett.* 166, 155–163. doi: 10.1111/j.1574-6968.1998.tb13197.x

Peiro, C., Millard, P., de Simone, A., Cahoreau, E., Peyriga, L., Enjalbert, B., et al. (2019). Chemical and metabolic controls on dihydroxyacetone metabolism lead to suboptimal growth of *Escherichia coli*. *Appl. Environ. Microbiol.* 85:e00768-19. doi: 10.1128/AEM.00768-19

Porcheron, G., Garenaux, A., Proulx, J., Sabri, M., and Dozois, C. M. (2013). Iron, copper, zinc, and manganese transport and regulation in pathogenic Enterobacteria: correlations between strains, site of infection and the relative importance of the different metal transport systems for virulence. *Front. Cell. Infect. Microbiol.* 3:90. doi: 10.3389/fcimb.2013.00090

Poulsen, V., Derkx, P., and Øregaard, G. (2019). High-throughput screening for texturing *Lactococcus* strains. *FEMS Microbiol. Lett.* 366:fnz001. doi: 10.1093/femsle/fnz001

Prosser, G. A., and de Carvalho, L. P. (2013). Kinetic mechanism and inhibition of *Mycobacterium tuberculosis* D-alanine:D-alanine ligase by the antibiotic D-cycloserine. *FEBS J.* 280, 1150–1166. doi: 10.1111/febs.12108

Rogers, P., Liu, T., Barker, K., Hilliard, G., English, B., Thornton, J., et al. (2007). Gene expression profiling of the response of *Streptococcus pneumoniae* to penicillin. *J. Antimicrob. Chemother.* 59, 616–626. doi: 10.1093/jac/dkl560

Schmid, J., Heider, D., Wendel, N. J., Sperl, N., and Sieber, V. (2016). Bacterial glycosyltransferases: challenges and opportunities of a highly diverse enzyme class toward tailoring natural products. *Front. Microbiol.* 18:182. doi: 10.3389/fmicb.2016.00182

Siedler, S., Rau, M. H., Bidstrup, S., Vento, J. M., Aunsbjerg, S. D., Bosma, E. F., et al. (2020). Competitive exclusion is a major bioprotective mechanism of lactobacilli against fungal spoilage in fermented milk products. *Appl. Environ. Microbiol.* 86:e02312-19. doi: 10.1128/AEM.02312-19

Smith, R. L., and Maguire, M. E. (1998). Microbial magnesium transport: unusual transporters searching for identity. *Mol. Microbiol.* 28, 217–226. doi: 10.1046/j.1365-2958.1998.00810.x

Sørensen, K., Curic-Bawden, M., Junge, M. P., Janzen, T., and Johansen, E. (2016). Enhancing the sweetness of yoghurt through metabolic remodeling of carbohydrate metabolism in *Streptococcus thermophilus* and *Lactobacillus delbrueckii* subsp. bulgaricus. *Appl. Environ. Microbiol.* 82, 3683–3692. doi: 10.1128/AEM.00462-16

Stapleton, M. A., Javid-Majd, F., Harmon, M. F., Hanks, B. A., Grahmann, J. L., Mullins, L. S., et al. (1996). Role of conserved residues within the carboxy phosphate domain of carbamoyl phosphate. *Biochemistry* 35, 14352–14361. doi: 10.1021/bi961183y

Stingele, F., and Mollet, B. (1996). Disruption of the gene encoding penicillin-binding protein 2b (pbp2b) causes altered cell morphology and cease in exopolysaccharide production in *Streptococcus thermophilus* Sfi6. *Mol. Microbiol.* 22, 357–366. doi: 10.1046/j.1365-2958.1996.00121.x

Terzaghi, B., and Sandine, W. (1975). Improved medium for lactic streptococci and their bacteriophages. *Appl. Microbiol.* 29, 807–813. doi: 10.1128/aem.29.6.807-813.1975

Versluis, D., Rodriguez de Evgrafov, M., Sommer, M. O. A., Sipkema, D., Smidt, H., and van Passel, M. W. J. (2016). Sponge microbiota are a reservoir of functional antibiotic resistance genes. *Front. Microbiol.* 7:1848. doi: 10.3389/fmicb.2016.01848

Vincent, C., Duclos, B., Grangeasse, C., Vaganay, E., Riberty, M., Cozzone, A. J., et al. (2000). Relationship between exopolysaccharide production and protein-tyrosine phosphorylation in gram-negative bacteria. *J. Mol. Biol.* 304, 311–321. doi: 10.1006/jmbi.2000.4217

Wilschefski, S. C., and Baxter, M. R. (2019). Inductively coupled plasma mass spectrometry: introduction to analytical aspects. The clinical biochemist. *Reviews* 40, 115–133. doi: 10.33176/AACB-19-00024

Wu, Q., Chu, H., Padmanabhan, A., and Shah, N. P. (2019). Functional genomic analyses of exopolysaccharide-producing *Streptococcus thermophilus* ASCC 1275 in response to milk fermentation conditions. *Front. Microbiol.* 10:1975. doi: 10.3389/fmicb.2019.01975

Zeidan, A. A., Poulsen, V. C., Janzen, T., Buldo, P., Derkx, P. M. F., Øregaard, G., et al. (2017). Polysaccharide production by lactic acid bacteria: from genes to industrial applications. *FEMS Microbiol. Rev.* 41, 168–200. doi: 10.1093/femsre/fux017

Zhuo, T., Rou, W., Song, X., Kamau, G. G., and Zou, H. (2015). Molecular study on the carAB operon reveals that carB gene is required for swimming and biofilm formation in *Xanthomonas citri* subsp. citri. *BMC Microbiol.* 15:225.

Conflict of Interest: All authors were employed by Chr Hansen A/S during the writing of this manuscript. Chr. Hansen A/S is a major commercial supplier of starter cultures to the fermentation industry. Additionally, some authors are shareholders in the company and/or inventors on patents and patent applications related to the described technology.

frontiers in Bioengineering and Biotechnology

ORIGINAL RESEARCH
published: 27 January 2021
doi: 10.3389/fbioe.2020.614498

A SH3_5 Cell Anchoring Domain for Non-recombinant Surface Display on Lactic Acid Bacteria

*Pei Kun Richie Tay, Pei Yu Lim and Dave Siak-Wei Ow**

*Microbial Cells Group, Bioprocessing Technology Institute, Agency for Science, Technology and Research (A*STAR), Singapore, Singapore*

Lactic acid bacteria (LAB) are a group of gut commensals increasingly recognized for their potential to deliver bioactive molecules *in vivo*. The delivery of therapeutic proteins, in particular, can be achieved by anchoring them to the bacterial surface, and various anchoring domains have been described for this application. Here, we investigated a new cell anchoring domain (CAD4a) isolated from a Lactobacillus protein, containing repeats of a SH3_5 motif that binds non-covalently to peptidoglycan in the LAB cell wall. Using a fluorescent reporter, we showed that C-terminal CAD4a bound *Lactobacillus fermentum* selectively out of a panel of LAB strains, and cell anchoring was uniform across the cell surface. Conditions affecting CAD4a anchoring were studied, including temperature, pH, salt concentration, and bacterial growth phase. Quantitative analysis showed that CAD4a allowed display of 10^5 molecules of monomeric protein per cell. We demonstrated the surface display of a functional protein with superoxide dismutase (SOD), an antioxidant enzyme potentially useful for treating gut inflammation. SOD displayed on cells could be protected from gastric digestion using a polymer matrix. Taken together, our results show the feasibility of using CAD4a as a novel cell anchor for protein surface display on LAB.

Keywords: lactic acid bacteria, cell anchoring domain, bacteria surface display, bacteria protein delivery, superoxide dismutase, probiotics

OPEN ACCESS

Edited by:
Mingfeng Cao,
University of Illinois at Urbana-Champaign, United States

Reviewed by:
Aleš Berlec,
Institut JoŽef Stefan (IJS), Slovenia
Muralikannan Maruthamuthu,
Purdue University, United States

****Correspondence:***
Dave Siak-Wei Ow
dave_ow@bti.a-star.edu.sg

Specialty section:
This article was submitted to Synthetic Biology, a section of the journal Frontiers in Bioengineering and Biotechnology

Received: *06 October 2020*
Accepted: *30 December 2020*
Published: *27 January 2021*

Citation:
Tay PKR, Lim PY and Ow DS-W (2021) A SH3_5 Cell Anchoring Domain for Non-recombinant Surface Display on Lactic Acid Bacteria. Front. Bioeng. Biotechnol. 8:614498. doi: 10.3389/fbioe.2020.614498

INTRODUCTION

Microbial cell-surface display has a wide range of biotechnological and industrial applications. It can be used to screen protein and peptide libraries in directed evolution, epitope mapping and drug discovery (Rockberg et al., 2008; Hudson et al., 2012; Fleetwood et al., 2013; Robert and Gouet, 2014). Microbes displaying proteins are also useful as remedial biosorbents (Tang et al., 2014; Hui et al., 2018; Maruthamuthu et al., 2018), biosensors (Han et al., 2018; Park, 2020), whole-cell biocatalysts (Pontes et al., 2012), and as vaccines and delivery vectors for therapeutics (Cano-Garrido et al., 2015; Plavec and Berlec, 2019). Lactic acid bacteria (LAB) are a heterogeneous group of Gram-positive bacteria, commonly of the genera *Lactococcus*, *Lactobacillus*, *Streptococcus*, *Pediococcus*, and *Leuconostoc*. They have a long history as components of fermented foods and are thus considered GRAS ("generally regarded as safe" per U.S. Food and Drug Administration). They are used industrially in feed and food fermentation, and in the production of various fine chemicals (Mora-Villalobos et al., 2020). Many lactobacilli also colonize mucosa in humans and animals, forming part of the intestinal and vaginal microbiomes, and probiotic strains of *Lactobacillus* have been identified that confer health benefits to the host (Gill and Prasad, 2008; Walter, 2008). These characteristics make LAB valuable candidates for protein display in numerous industrial and biomedical applications.

LAB displaying enzymes can be used as biocatalysts for industrial processes. Nguyen et al. displayed β-mannanase on the surface of *Lactobacillus plantarum* for the production of manno-oligosaccharides, a class of prebiotic oligosaccharides (Nguyen et al., 2019). Similarly, Pham et al. displayed dimeric β-galactosidases on *L. plantarum* for lactose conversion and production of galacto-oligosaccharides (Pham et al., 2019). In both cases, the bacterial catalysts could be used for multiple rounds of bioconversion. Other groups displayed cohesins on *L. plantarum* and *Lactococcus lactis* to assemble multi-enzyme cellulosomal complexes for the degradation of complex polymers (Wieczorek and Martin, 2012; Stern et al., 2018). Surface display could also be used to introduce substrate-binding domains on LAB to enable cell immobilization on solid supports for continuous bioprocessing, as has been demonstrated for *L. lactis* displaying a chitin-binding domain (Simşek, 2014).

LAB have also been investigated for therapeutic use, for instance, to treat metabolic and gastrointestinal diseases. Companies like Aurealis Pharma and Precigen ActoBio are developing "live biotherapeutics" using engineered strains of *Lactococcus lactis* that secrete therapeutic proteins and peptides in the oral and gastrointestinal tract. Anchoring these therapeutic entities to the bacteria surface could provide protection against proteolysis during gastrointestinal transit (Mao et al., 2016). Proteins that have been successfully displayed on *L. lactis* include β-galactosidase to manage lactose intolerance; an insulin analog (SCI-59) to manage diabetes; and the thrombolytic agent subtilisin QK-2 (Mao et al., 2016, 2017; Yin et al., 2018). Various protein domains that block pro-inflammatory cytokines and chemokines have been also displayed on LAB to treat inflammatory bowel disease (IBD) (Kosler et al., 2017; Škrlec et al., 2017; Plavec et al., 2019). Škrlec et al. displayed a pentadecapeptide BPC-157 to reduce the production of reactive oxygen species (ROS) to moderate gut inflammation (Skrlec et al., 2018). Protein display on LAB can also be used to develop bacterial vaccine vectors. Here the innate immunogenicity of certain probiotic strains may obviate the need for adjuvants. Lactic acid bacteria engineered to display antigens from influenza A, pneumococcus, *Mycobacterium tuberculosis*, and SARS-CoV have shown efficacy as mucosal vaccines against their respective viral and bacterial pathogens in animal models (Lee et al., 2006; Hernani Mde et al., 2011; Chowdhury et al., 2014; Mustafa et al., 2018). LAB can also be developed into efficient vectors for DNA delivery through the surface display of targeting proteins that directly interact with host epithelial or immune cells (Pontes et al., 2012; Liu et al., 2019).

To enable surface display, a protein or peptide is fused to an anchoring domain that binds to the LAB cell wall. Such anchoring domains may be covalently linked to a cell wall component, or they may bind non-covalently. Examples of covalent anchors include lipoproteins like BmpA and PrsA (Fredriksen et al., 2012; Zadravec et al., 2014); transmembrane proteins like PgsA (Narita et al., 2006; Lei et al., 2011); and more commonly, LPXTG domains derived from the streptococcal M6 protein or the *L. plantarum* Lp_2578 protein, which are anchored to peptidoglycans by cell wall sortases (Dieye et al., 2001; Fredriksen et al., 2010). Bacteria are usually genetically modified for covalent display, but the use of GM bacteria raises safety concerns and may encounter lower consumer acceptance and more severe regulatory scrutiny, especially when used in food or pharmaceutical preparations. Non-covalent anchoring strategies avoid the use of recombinant bacteria as hosts for protein display. Proteins containing non-covalent anchoring domains can be produced in an expression strain, then anchored *in trans* to a wild-type (non-GM) host LAB strain. Another advantage of this approach is that protein production is not limited by the biosynthetic capabilities of the host bacterium, and can undergo further post-translational modifications prior to surface anchoring.

The success of a non-covalent cell surface display system depends on choosing an appropriate anchoring motif for the target protein and host cell. Each anchoring domain has a different capacity for protein display, and can be highly selective of its target LAB. While several non-covalent binding domains have been identified, only a few have been applied for protein surface display. These include: lactobacillal S-layer homology domains (Åvall-Jääskeläinen et al., 2002; Hu et al., 2011); WxL (Brinster et al., 2007), SH3 (Plavec et al., 2019); CW_1 (Plavec et al., 2019) and LysM (Raha et al., 2005; Hu et al., 2010; Ravnikar et al., 2010; Xu et al., 2011). Although many of these domains have known binding partners, the mechanism of binding is still ambiguous for some (Desvaux et al., 2018). The LysM domain from the lactococcal protein AcmA is a commonly used non-covalent anchor for LAB surface display (Steen et al., 2005; Bosma et al., 2006; Ravnikar et al., 2010). New anchoring motifs are constantly being sought to target a wide range of LAB, and to allow surface display of different proteins on the same cell. The bacterial SH3 type 5 motif (SH3_5; Pfam PF08460) is known to bind cell wall peptidoglycans in Gram-positive bacteria (Becker et al., 2009; Mitkowski et al., 2019). It contains 60–65 amino acids and is mainly found among Firmicutes, especially of the *Streptococcus* and *Lactobacillus* genera (Desvaux et al., 2018). A recent report described the use of a lactococcal phage SH3_5 motif for surface display in *L. lactis* (Plavec et al., 2019). Nonetheless, SH3_5 has not been widely investigated for bacterial protein display. The goal of the present study was to test a newly-identified anchoring domain (CAD4a) containing SH3_5 repeats for heterologous protein display on LAB. The CAD4a domain was isolated from an *L. plantarum* protein. We appended this domain to two proteins—a fluorescent reporter and a dimeric enzyme—and examined functional display on LAB, as well as conditions for optimal anchoring, and resistance of the anchored proteins to gastric digestion.

MATERIALS AND METHODS

Bacterial Strains, Culture Conditions, and Plasmid Assembly

The bacteria strains and plasmids used in this study are listed in **Table 1**. Cloning was performed in *E. coli* Turbo and proteins were expressed in *E. coli* BL21(DE3) as detailed in the next section. *E. coli* was selected on LB agar supplemented with

TABLE 1 | Bacterial strains and plasmids used in this study.

	Feature	Source
Strains		
E. coli Turbo	Cloning host, TG1 derivative *glnV44 thi-1* Δ*(lac-proAB) galE15 galK16 R(zgb-210*::Tn*10)*Tet^S *endA1 fhuA2* Δ*(mcrB-hsdSM)5*, ($r_K^- m_K^-$) F′[*traD36 proAB*$^+$ *lacI*^{q} *lacZ*Δ*M15*]	NEB
E. coli BL21(DE3)	Expression host, *E. coli* str. B F^- *ompT gal dcm lon hsdS*$_B$($r_B^- m_B^-$) λ(DE3 [*lacI lacUV5-T7p07 ind1 sam7 nin5*]) [*malB*$^+$]$_{K-12}$(λ^S)	Thermo Fisher
Lactococcus lactis NZ9000	Binding host, MG1363 derivative *pepN*::*nisRK*	MoBiTec
Lactobacillus casei 393	Binding host, wild type	ATCC
Lactobacillus fermentum 14931	Binding host, wild type	ATCC
Lactobacillus plantarum 8014	Binding host, wild type	ATCC
Lactobacillus rhamnosus GG	Binding host, wild type	Lesaffre
Plasmids		
pET22b	P_{T7}, Amp^R, *lacI* gene, N-terminal pelB seq	Novagen
pET22b-Sirius	His-tagged Sirius	This study
pET22b-Sirius-CAD4a12	12-residue spacer between Sirius and CAD4a	This study
pET22b-Sirius-CAD4a24	24-residue spacer between Sirius and CAD4a	This study
pET22b-Sirius-CAD4a36	36-residue spacer between Sirius and CAD4a	This study
pET22b-SOD	His-tagged SOD	This study
pET22b-SOD-CAD4a12	12-residue spacer between SOD and CAD4a	This study
pET22b-SOD-CAD4a24	24-residue spacer between SOD and CAD4a	This study
pET22b-SOD-CAD4a36	36-residue spacer between SOD and CAD4a	This study

100 μg/ml carbenicillin. Lactic acid bacteria were grown in static, unaerated MRS broth (Sigma-Aldrich) at 37°C.

Supplementary Table 1 lists the primers and synthetic gene fragments used in this study. Primers and gene fragments were synthesized by Integrated DNA Technologies (USA). Gibson assembly was used to construct all plasmids. The pET22b plasmid was linearized with primers F1 and R1, and assembled with fragment G10 to give pET22b-Sirius. pET22b-Sirius was linearized with primers F1 and either R7 or R6, to give pET22b-Si-CAD4a12 and -Si-CAD4a24, respectively, after assembly with gene fragment G5. CAD4a was subcloned from pET22b-Si-CAD4a24 using primers F15 and R5, then assembled with pET-Sirius linearized with F1 and R26, to give pET22b-Si-CAD4a36.

For the SOD constructs, G29 was amplified with primers F18 and R37, and pET22b-Sirius linearized with primers F1 and R4. Both fragments were then assembled to give pET22b-SOD. pET22b-SOD was linearized with primers F1 and either R24 or R25, to give pET22b-SOD-CAD4a12 and -SOD-CAD4a24, respectively, after assembly with gene fragment G5. CAD4a was subcloned from pET22b-Si-CAD4a24 with primers F15 and R5, then assembled with pET-SOD linearized with F1 and R27, to give pET22b-SOD-CAD4a36.

Protein Expression

Overnight *E. coli* BL21(DE3) cultures were diluted 1:100 in Terrific Broth and grown to optical density OD_{600} ∼0.8. At that point, the temperature was reduced to 20°C and sorbitol was added to a concentration of 0.4 M. Sorbitol was added only for expression of CAD4a protein conjugates, to reduce protein aggregation. Expression was induced with 0.2 mM IPTG and allowed to proceed for 6 h at 20°C. Cells were then pelleted at 4,000 g for 10 min, resuspended in Tris buffer (50 mM Tris, 0.3 M NaCl, pH 8), and subjected to one freeze-thaw cycle before lysis on ice with a probe sonicator (Microson XL2000, 10 s ON, 10 s OFF, 8 cycles). The lysate was pelleted at 12,000 g for 30 min at 4°C, and separated on Ni-NTA resin (Qiagen, USA) in a PD-10 column. His-tagged protein was eluted with 200 mM imidazole, then concentrated and buffer-exchanged into 1×PBS (pH 7.4) and stored at 4°C until use.

SDS-PAGE and Western Blot

Protein concentrations were determined using Bradford reagent (Biorad). Protein samples were analyzed on NuPAGE 4–12% Bis-Tris gels (Life Technologies), following manufacturer's protocols. Gels were stained with InstantBlue (Expedeon) or transferred onto nitrocellulose membranes using the semi-dry method at 20 V for 20 min (Trans-Blot, Bio-Rad). The membrane was washed with TBST (1×TBS, 0.1% Tween 20), blocked with 5% w/v non-fat dry milk in TBST for 1 h at room temperature, then exposed to a 1:10,000 dilution of HRP-conjugated anti-His antibody (Merck) for 1 h at room temperature before detection with Clarity Western ECL Blotting Substrate (Bio-Rad) using the manufacturer's protocol. Gel images were acquired on a ChemiDoc MP imaging system (Bio-Rad), and blots were imaged on an ImageQuant LAS 500 imager (GE Healthcare).

Anchoring of Sirius-CAD4a to Lactic Acid Bacteria

Lactobacillus casei, *L. fermentum*, *L. plantarum*, *L. rhamnosus*, and *Lactococcus lactis* were grown to mid-log (OD_{600} 0.8–1.2) or stationary phase (overnight culture), washed once with 10% glycerol, then resuspended in a 50:50 mix of MRS and 20% glycerol, aliquoted, and frozen at −80°C to obtain stocks for subsequent cell binding studies. Except where stated otherwise, the following protocol was used for binding studies. Frozen log-phase cells were thawed and washed twice with binding buffer (1×PBS, pH 5), diluted to OD_{600} = 1.5, and resuspended in 75 μl of binding buffer containing 2 μM of Sirius-CAD4a12. The mixture was incubated for 1.5 h at 37°C with periodic mixing, then pelleted and washed twice with the same binding buffer before transfer to a black 96-well-polystyrene plate for fluorescence measurement. Cell-associated fluorescence was measured on a spectrophotometer (Tecan, USA) with

excitation at 355 nm and emission at 424 nm. The background fluorescence of the cells was subtracted to obtain a reading in relative fluorescence units (RFU). All studies were performed in triplicate. Cell imaging was performed on a Nikon Eclipse Ni-U microscope using a DAPI filter and 60× oil immersion lens.

Influence of Cell Growth Phase, Salt Concentration, pH, and Binding Temperature on CAD4a Anchoring

The effect of cell growth phase on CAD4a binding capacity was investigated with frozen *L. fermentum* at mid-log and stationary phase. The influence of salt concentration on CAD4a binding to *L. fermentum* was tested using phosphate buffer (pH 5) supplemented with NaCl to final concentrations of 0.05, 0.1, 0.15, 0.2, 0.3, 0.4 M NaCl. The influence of pH was evaluated using PBS at pH 4.5, 5, 5.5, 6, 6.5, 7, 8, and 9. The effect of binding temperature was tested at 25, 30, and 37°C, with half-hourly timepoints up to 3 h. Protein concentration used was 2 μM in these studies; protein binding and fluorescence measurement were carried out as described above.

Effect of Cell Pre-Treatment on CAD4a Anchoring

Frozen *L. fermentum* aliquots were treated with either 5 M LiCl or 10% v/v trichloroacetic acid (TCA) at 37°C with shaking for 1 h. Cells were washed twice with pH 7 PBS and once with pH 5 PBS before binding experiments.

Binding Capacity of CAD4a on *L. fermentum*

Fresh overnight cultures of *L. fermentum* were washed twice with binding buffer (pH 5 PBS), diluted to $OD_{600} = 1.5$, and incubated with 70 μl of various concentrations of Sirius-CAD4a12 (0, 0.5, 1, 2, 3, 4, 5 μM). This was used to set up a standard curve to correlate RFU to protein concentration in the presence of cells. Subsequently, cell mixtures were pelleted and cell fluorescence determined as described above. All data points represent the average of at least three experiments. Non-linear regression analysis was used to fit the binding data to the Langmuir adsorption model to determine B_{max}, the protein concentration at saturation. Assuming that the distribution of the anchored protein was uniform across the entire cell population, we calculated the average binding capacity per cell using B_{max} and the standard curve.

Influence of Spacer Length on Activity of Surface-Displayed Superoxide Dismutase

Superoxide dismutase (SOD) from *Potentilla atrosanguinea* (Kumar et al., 2012) was engineered with C-terminal CAD4a and three different spacer lengths (12-, 24-, and 36-residues) between the enzyme and anchoring domain. A flexible $(GGSG)_x$ spacer was used, where $x = 3$ for the 12-residue spacer, $x = 6$ for the 24-residue spacer, and $x = 9$ for the 36-residue spacer. Proteins were expressed in *E. coli*, and protein binding was performed with frozen log-phase *L. fermentum* as described above. After washing, cells were resuspended in binding buffer for the SOD activity assay.

Superoxide Dismutase Activity Assay

SOD activity assay was done using a commercial SOD kit (Sigma-Aldrich 19160) according to the manufacturer's protocol. The average gradient over the first 10 min (linear range) from triplicates was used to calculate the activity for each sample.

Cell Encapsulation

Cell encapsulation was adapted from a previously-described protocol (Nualkaekul et al., 2012). Low-viscosity alginate (Sigma-Aldrich) was prepared as a 6% w/v stock in distilled water. Low molecular weight chitosan (Sigma-Aldrich) was dissolved in 0.1 M acetic acid to a concentration of 0.5% w/v, and the final pH adjusted to 5. Fresh overnight cultures of *L. fermentum* were washed twice with binding buffer (pH 5 PBS), diluted to $OD_{600} = 1.5$, and incubated with 2 μM SOD-CAD4a12 or SOD-CAD4a36. After washing, 2 ml of cells was resuspended in 1.2 ml of 4% low-viscosity alginate (6% stock diluted with binding buffer) and mixed vigorously. The mixture was extruded dropwise into a 0.15 M $CaCl_2$ bath (pH 5) using a 21G needle, and the beads were left to stir at room temperature for 1 h, then rinsed once with binding buffer. The beads were subsequently added to 0.5% chitosan and left to stir for 10 min, then washed twice with binding buffer and kept at 4°C till use. Empty beads and beads containing 1 μM SOD (without cells) were prepared as controls.

In vitro Digestion

Simulated gastric fluid (SGF) was modified from Minekus et al. (2014) and prepared as a 1× concentrate. This consisted of: 6.9 mM KCl, 0.9 mM KH_2PO_4, 25 mM $NaHCO_3$, 47.2 mM NaCl, 0.1 mM $MgCl_2(H_2O)_6$, and 0.5 mM $(NH_4)_2CO_3$. Pepsin (Sigma-Aldrich P6887) and all necessary chemicals were purchased from Sigma-Aldrich. Sodium citrate was dissolved in PBS (pH 5) at a concentration of 0.15 M. Ten alginate-chitosan beads were used for each condition tested. Beads were suspended in 125 μl distilled water and equivolume SGF, with addition of $CaCl_2$ (final concentration 0.075 mM) and pepsin (final concentration 0.5 mg/ml). The mixture was incubated with shaking at 37°C for 2 hr, then rinsed twice with PBS (pH 7). Beads were incubated with pH 5 PBS as a control. The beads were dispersed in 250 μl citrate buffer held at 40°C, then centrifuged at 10,000 g for 10 min. The cell pellet was resuspended in 250 μl 1 × PBS (pH 5) for the SOD assay. Residual activity represents enzyme activity of SGF-treated beads relative to the control (beads in PBS).

Statistical Analyses

Statistical analyses were performed using GraphPad Prism v8.0.1 for Windows. Two-tailed Student's *t*-tests were performed to determine the significance of differences in the binding studies. For curve fitting to the Langmuir model, non-linear regression analysis was performed assuming single-site saturation binding. B_{max} from the analysis was taken as the saturation RFU.

RESULTS

Isolation of a Putative Cell Anchoring Domain (CAD4a) From *L. plantarum*

A search of the Pfam database revealed 83 homologs of the bacterial SH3 type 5 motif (SH3_5, Pfam PF08460) across the *Lactobacillus* and *Lactococcus* genera and their phages. This study focused on a previously uncharacterized SH3_5 anchoring domain in Lys2 (GenBank CCC80137), a muramidase from *L. plantarum* WCFS1. The full-length muramidase is an 860-amino acid protein with an expected molecular weight of 84 kDa, with five SH3_5 repeats (R1–5) at its C-terminus spanning residues 471 and 860 (**Figure 1**). Each repeat in Lys2 contains 61 residues, and the similarity between the five repeats vary from 50% to over 90%. The SH3_5 anchoring domain of Lys2 has 54% identity to that of Acm2 (GenBank CCC79778), another *L. plantarum* autolysin with similar molecular organization (Rolain et al., 2012). Comparing the first SH3_5 repeat of Lys2 to SH3_5 motifs in the proteins of *Streptococcus* (GenBank EQC72385, four SH3_5 repeats), *Staphylococcus* (GenBank AAB53783, single SH3_5), *L. lactis* phage 1358 (NCBI YP_009140409, single SH3_5), *Lactobacillus* phage ATCC 8014-B2 (NCBI YP_009783998, single SH3_5), and *Staphylococcus* phage K (GenBank AHB79986) showed identities of 40, 22, 27, 31, and 21%, respectively, thus the lactobacillal domain is homologous to but quite distinct from other SH3_5 domains in the group of Firmicutes (**Supplementary Figure 1**).

To assess the surface display potential of this five-repeat SH3_5 domain, we used the Sirius blue fluorescent protein as a reporter (Tomosugi et al., 2009). Sirius was chosen for its photostability at low pH (pKa < 3). The five-repeat domain was cloned downstream of Sirius in the pET22b plasmid, but the fusion protein was insoluble and difficult to purify (data not shown). A truncated domain containing only R1–R3 (henceforth called CAD4a) gave more tractable expression, and the Sirius conjugate (Si-CAD4a) was easily detected by SDS-PAGE and Western blot against the N-terminal His-tag (**Figure 2B**). There was some protein degradation during expression, but the bulk of the soluble fraction was the full-length protein.

CAD4a Anchoring to LAB

Heterologous binding of Si-CAD4a12 (with a 12-residue spacer between Sirius and CAD4a) to LAB was tested using *L. lactis, L. casei*, *L. fermentum*, *L. plantarum*, and *L. rhamnosus* (**Table 1**). Bacteria in log-phase growth were incubated with 2 μM protein without shaking for 2 h at 37°C. As shown in **Figure 3A**, there was >2-fold increase in cell-associated fluorescence on *L. fermentum* after exposure to Si-CAD4a12, compared to Sirius without the anchoring domain. Fluorescence microscopy showed that the protein was displayed uniformly across the cell surface (**Figure 3D**). Negligible binding was seen with *L. lactis*, *L. casei*, *L. plantarum*, and *L. rhamnosus*, suggesting that the interaction between CAD4a and *L. fermentum* was selective. There was also more binding to log-phase compared to stationary-phase *L. fermentum* (**Figure 3B**). This could be due to actively dividing cells having more exposed cell wall structure and fewer surface proteins inhibiting access to the cell wall. Except where otherwise stated, all subsequent binding experiments were carried out with log-phase bacteria.

Cell Wall Target of CAD4a

The SH3_5 domain is known to bind cross-linked peptidoglycan (PGN) (Desvaux et al., 2018). To confirm that CAD4a binds PGN, *L. fermentum* was pre-treated with either 5 M LiCl or 10% v/v TCA before exposure to Si-CAD4a12. TCA hydrolyzes teichoic acids (TAs), one of the major cell wall components, whereas 5 M LiCl removes non-covalently bound surface proteins. As shown in **Figure 3C**, treatment with LiCl led to a

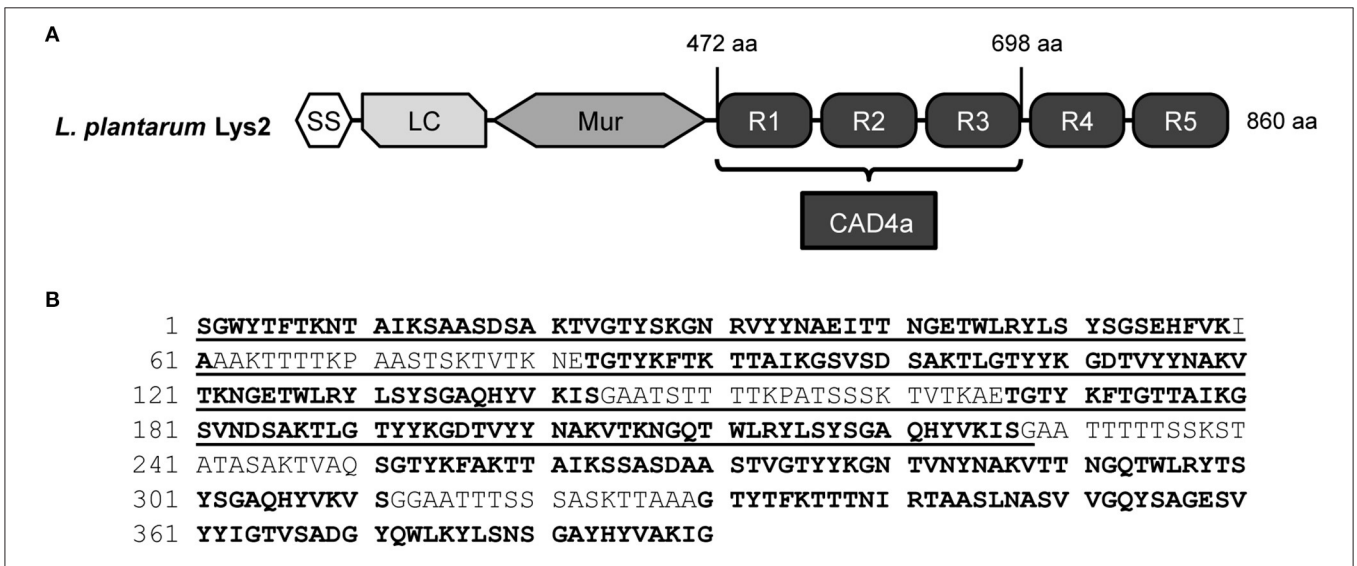

FIGURE 1 | (A) Molecular organization of *L. plantarum* Lys2 with the C-terminal anchoring region. SS, signal sequence; LC, low complexity region; Mur, muramidase; R1–R5, SH3_5 repeats. **(B)** Amino acid sequence of the Lys2 anchoring region. Individual SH3_5 repeats are in bold, and the CAD4a domain has been underlined.

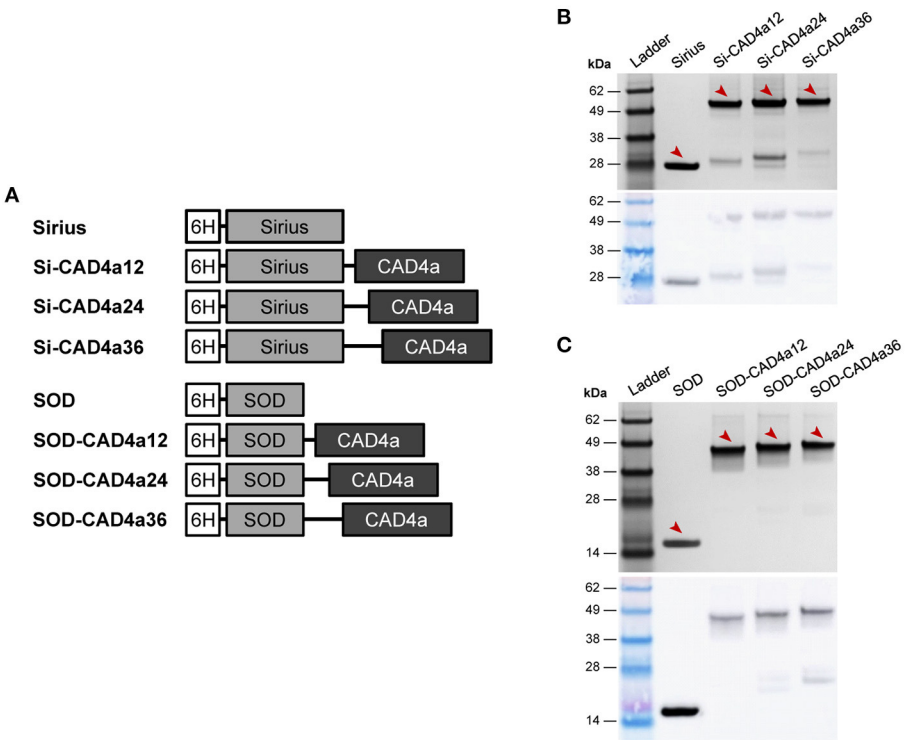

FIGURE 2 | (A) Fusion protein constructs for surface display. 6H, His-tag; CAD4a, SH3_5 anchoring domain containing repeats R1–R3 (25 kDa); Si, Sirius blue fluorescent protein (28 kDa); SOD, superoxide dismutase from *Potentilla atrosanguinea* (17 kDa). Coomassie blue-stained SDS-PAGE gel (top) and western blot (bottom) of **(B)** Sirius and Si-CAD4a conjugates, and **(C)** SOD and SOD-CAD4a conjugates, all purified from *E. coli* cultures. Blots were labeled with anti-His antibody conjugated to HRP. Arrows indicate expected band position of the full-length proteins.

2-fold increase in cell anchoring, likely because the removal of surface proteins exposed more binding sites within the cell wall. TCA treatment did not significantly impact CAD4a binding, thus the anchoring domain was not targeting cell wall TAs. Taken together, these results suggest that CAD4a is binding to PGN, the other major component of the Gram-positive cell wall. Further, since TCA treatment significantly reduced cell viability (results not shown) but not CAD4a anchoring, changes to cell viability are not likely to impact CAD4a-mediated protein display, so long as the PGN matrix remains intact.

Factors Influencing Binding of CAD4a to *L. fermentum*

We investigated several binding conditions to see if we could improve surface display on *L. fermentum*. Ambient temperature had an effect on the rate of binding, with noticeably slower binding at 25°C compared to 37°C (**Figure 4A**). At 30 and 37°C, maximum binding was achieved within 1.5 h. Ionic strength had a negligible effect on binding at low and physiological salt concentrations ($\leq$ 150 mM NaCl), but high salt concentrations ($>$ 200 mM NaCl) adversely affected anchoring, possibly by disrupting the non-covalent interactions between CAD4a and PGN (**Figure 4B**). We found that pH 5 was optimal for CAD4a anchoring; there was no binding above pH 6, whereas below pH 5, non-specific binding of Sirius became significant and the contribution of CAD4a was less clear (**Figure 4C**).

To determine the binding capacity of CAD4a on stationary-phase *L. fermentum*, different concentrations of Si-CAD4a were mixed with overnight cultures diluted to $OD_{600} = 1.5$ ($\sim 10^9$ cells/ml). As shown in **Figure 5A**, cell-associated fluorescence increased in a dose-dependent manner before reaching a plateau, with B_{max} determined to be ~378 RFU after fitting to a Langmuir adsorption isotherm ($r^2 = 0.766$). This corresponded to a saturation concentration of 1.05 μM protein (**Figure 5B**), or an average of 5×10^5 molecules per cell.

Heterologous Display of Superoxide Dismutase via CAD4a

To demonstrate the surface display of a functional protein using CAD4a, we cloned and expressed a superoxide dismutase (SOD) from *P. atrosanguinea* with CAD4a at its C-terminus. SOD is an enzyme that scavenges reactive oxygen radicals and has potential application in treating intestinal inflammation, based on positive outcomes in mouse models (Seguí et al., 2004). We constructed three SOD-CAD4a variants with 12-, 24-, and 36-residue glycine-serine (GS) spacers (**Figure 2A**) to examine if spacer length affects protein activity after anchoring. Active SOD is a homodimeric complex, and a short linker could

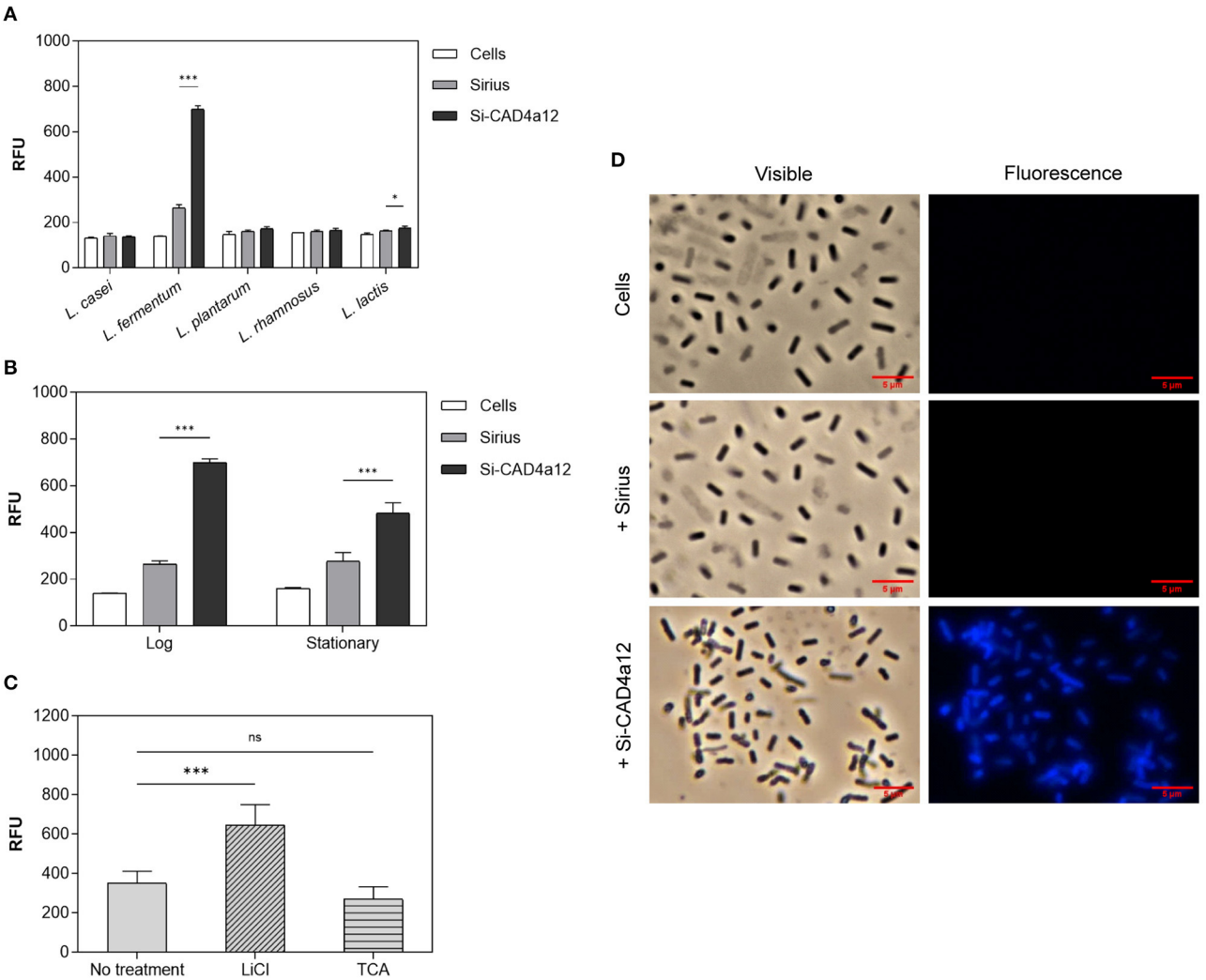

FIGURE 3 | CAD4a12 anchors selectively to *L. fermentum*. Cell-associated fluorescence after Si-CAD4a12 was exposed to **(A)** *L. casei*, *L. fermentum*, *L. plantarum*, *L. rhamnosus*, and *L. lactis* in log-phase growth; and **(B)** *L. fermentum* in log- and stationary-phase growth. **(C)** Effect of pre-treatment of *L. fermentum* with 5 M LiCl or 10% v/v TCA on CAD-4a12 anchoring. **(D)** Fluorescence micrographs of log-phase *L. fermentum* (top), and cells exposed to Sirius (middle) and Si-CAD4a12 (bottom). Phase contrast image on left and fluorescence image on right (DAPI filter). $n = 3$. *ns*, $p > 0.05$; $^{*}p \leq 0.05$; $^{***}p \leq 0.001$ vs. control.

have impacted its dimerization and thus enzyme activity. Full-length protein was obtained for all three variants following expression and purification from *E. coli* cultures (**Figure 2C**). A comparison of enzyme activity showed that SOD-CAD4a12 had slightly reduced activity compared to SOD and the other spacer variants, although the difference was not statistically significant (**Supplementary Figure 2A**). We did not observe the same effect of spacer length on the monomeric Sirius, as fluorescence output of Sirius conjugates with different spacer lengths did not differ significantly (**Supplementary Figure 2B**).

The SOD variants were used for subsequent binding experiments. As shown in **Figure 6**, there was more non-specific binding for SOD compared to Sirius, but the addition of the anchoring domain increased cell-associated enzyme activity by ∼40%. All three spacer variants gave very similar activity after cell anchoring (**Figure 6**), thus spacer length had minimal effect on the functionality of the anchored domain. The native spacer in the *L. plantarum* muramidase is 33 amino acids long. Our results suggest that shorter spacers could be used, although the ideal length is protein-dependent, and should be optimized based on size and multimericity of the target protein.

Gastric Resistance of Encapsulated SOD-Coated Bacteria

We found that anchored Si-CAD4a was sufficiently surface-exposed to be digested when cells underwent simulated gastric digestion (**Supplementary Figure 3**). There was thus a need to protect surface-displayed protein from detachment and/or degradation under changing and potentially adverse ambient conditions. Nualkaekul et al. showed that a matrix of alginate

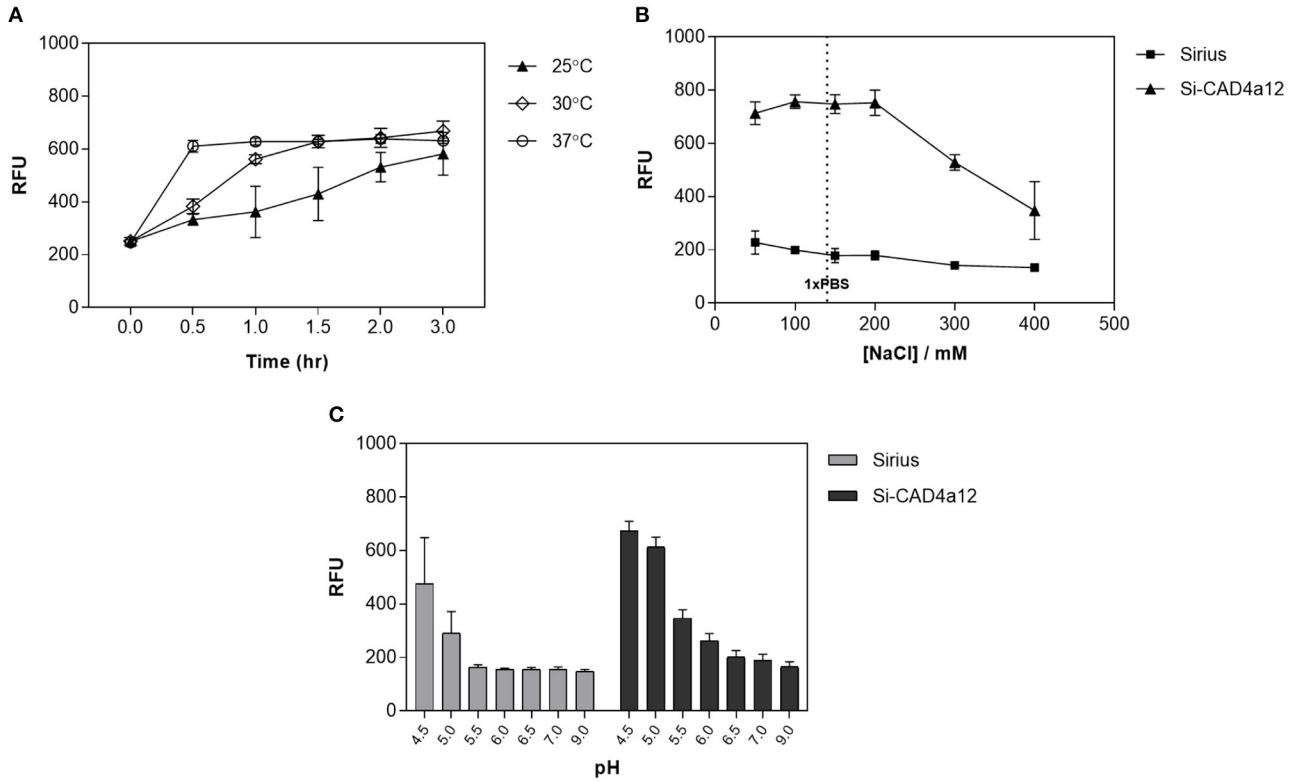

FIGURE 4 | Anchoring of Si-CAD4a12 under different conditions. **(A)** Time-course of anchoring at different temperatures. Anchoring at **(B)** different NaCl concentrations, and **(C)** different pH. $n = 3$.

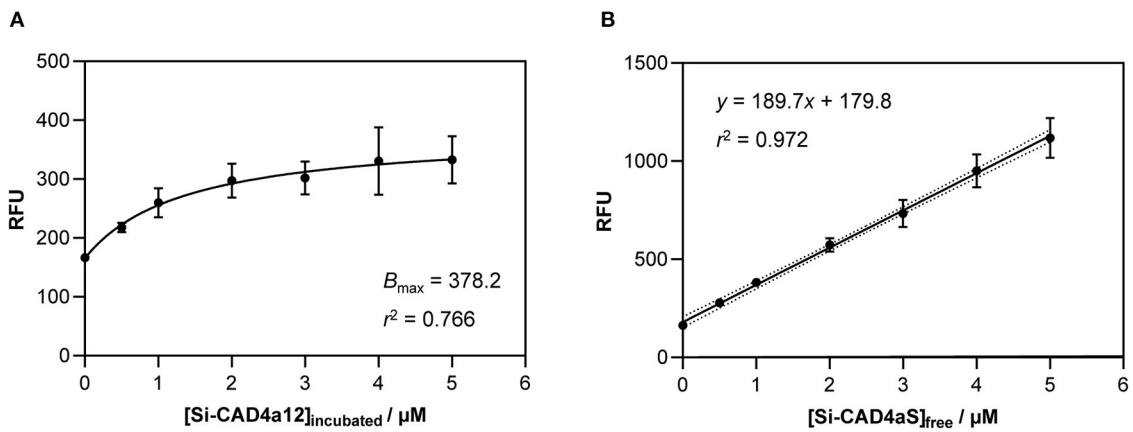

FIGURE 5 | Binding curve for anchoring of Si-CAD4a12 to overnight cultures of *L. fermentum*. Data points represent the average and standard deviation of at least three independent experiments. Points were fitted to a Langmuir adsorption isotherm to determine fluorescence at saturation **(A)**, and concentration at saturation was calculated from a standard curve **(B)**.

coated in chitosan helped to buffer pH changes and maintained the viability of *L. plantarum* in acidic media (Nualkaekul et al., 2012). To maintain optimal conditions for CAD4a anchoring during encapsulation, SOD-coated cells mixed with alginate were gelled in a Ca^{2+} bath at pH 5, and the alginate beads were then coated with a chitosan solution, also at pH 5. Gastric resistance was evaluated using simulated gastric fluid (SGF) at pH 3 containing the gastric protease pepsin (Minekus et al., 2014). Following gastric digestion, beads were treated with a citrate solution at pH 5 to chelate the Ca^{2+} ions and disperse the matrix. Subsequent activity assays on the pelleted cells showed that over 90% of cell-associated enzyme activity was retained (**Figure 7A**),

thus the polymer matrix offered substantial protection for the surface-displayed enzyme. In comparison, there was less residual enzyme activity (72%) in beads that contained unanchored SOD (**Figure 7A**), suggesting that cell anchoring also confers some protection to the protein, perhaps by limiting protein diffusion within the matrix. A Western blot of the cell pellet showed that the anchoring domain was intact, thus the enzyme likely remained anchored to the cell surface (**Figure 7B**).

DISCUSSION

The first SH3_5 anchoring motif was identified in staphylococcal endolysins and helped to localize the latter to its cell wall targets (Baba and Schneewind, 1996; Gründling and Schneewind, 2006). These domains, along with similar ones from phages, contained a single SH3_5 motif. In contrast, SH3_5-based anchoring domains from *Streptococcus* and *Lactobacillus* can have multiple SH3_5 repeats, up to six in tandem for some species. Such domains from *Lactobacillus* have not been investigated for protein surface display, where the multiplicity of SH3_5 may provide stronger cell wall binding. This work examined the anchoring domain of the *L. plantarum* Lys2 autolysin, which contains five terminal SH3_5 repeats. From the Lys2 cell wall targeting region, a truncated three-repeat domain, which we named CAD4a, was successfully expressed as part of fusion proteins. We tested five strains of LAB for anchoring of CAD4a, and found selective binding to *L. fermentum*. It was surprising that CAD4a bound poorly to the *L. plantarum* strain that we tested (ATCC 8014), since it was derived from another *L. plantarum* strain (WCFS1). However, the surface of *L. plantarum* is known to be covered in capsular polysaccharides, which were shown to inhibit Acm2 binding in a previous study (Beaussart et al., 2013), and could have had a similar shielding effect toward CAD4a anchoring. Although the surface composition of *L. fermentum* is not well-characterized, it is likely that a lack of significant polysaccharide coverage made this bacterium a more ideal host for CAD4a binding. Alternatively, all five of the SH3_5 repeats might be essential for proper binding to the *L. plantarum* cell wall, similar to the LysM domain in lactococcal AcmA, which requires all three of its LysM repeats for optimal PGN binding (Steen et al., 2005).

We have shown that CAD4a binds to cell wall peptidoglycan (PGN), though its ligand is uncertain. Existing molecular models for PGN-SH3_5 interactions were based on staphylococcal domains, where it was shown that SH3_5 recognized pentapeptide cross-bridges in PGN (Mitkowski et al., 2019; Gonzalez-Delgado et al., 2020). However, such cross-bridges are absent in lactobacilli (Kleerebezem et al., 2010), and the section in staphylococcal SH3_5 that binds the cross-bridges

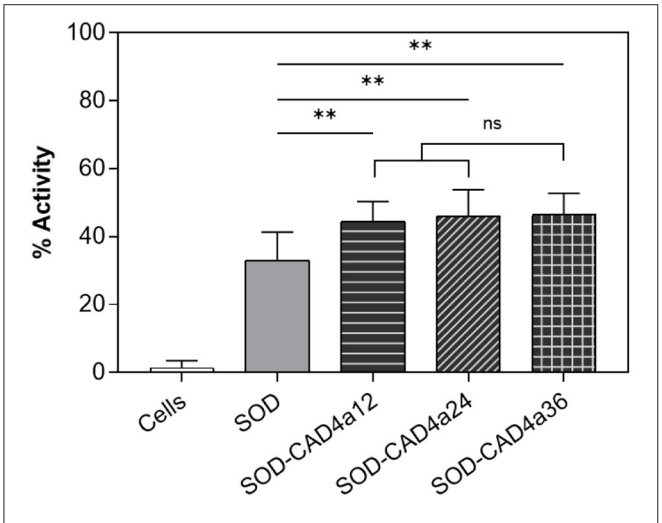

FIGURE 6 | Cell-associated enzyme activity after exposure of SOD and SOD-CAD4a variants to log-phase *L. fermentum*. $n = 3$. *ns*, $p > 0.05$; $^{**}p \leq 0.01$ vs. control.

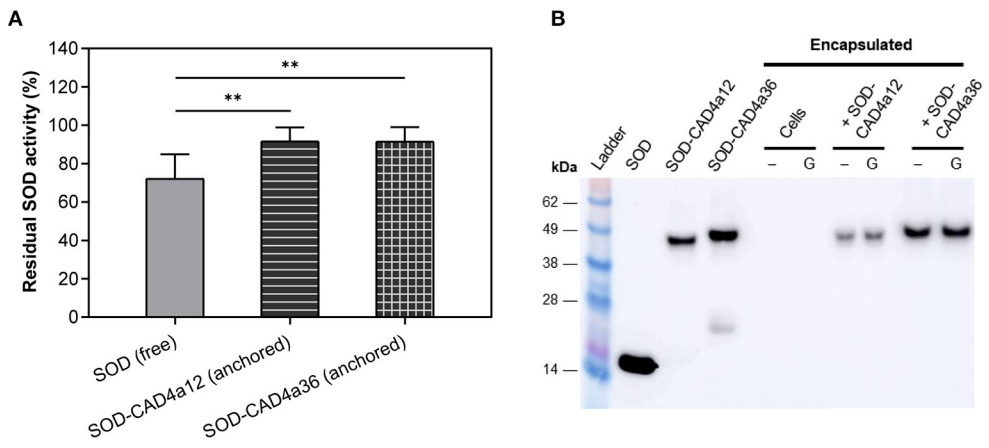

FIGURE 7 | Outcome of *in vitro* gastric digestion of free SOD and SOD-coated *L. fermentum*, both in chitosan-alginate beads. Beads were digested with pH 3 SGF containing pepsin, then dispersed and the cells pelleted down for the SOD activity assay. **(A)** Residual enzyme activity, calculated as cell-associated activity after digestion relative to undigested control beads left in pH 5 PBS. **(B)** Western blot of resuspended cell pellets that were untreated (–) or underwent gastric digestion (G). Proteins were labeled with anti-His antibody. The first three lanes after the protein ladder are pure proteins for reference. $^{**}p \leq 0.01$ vs. control.

is notably absent from CAD4a. Instead, CAD4a may anchor similar to LysM, another PGN-binding motif commonly used for surface display. LysM recognizes a generic GlcNAc-X-GlcNAc motif in PGN glycans, but its binding affinity is modulated by neighboring peptide stems, thus providing some measure of selectivity (Mesnage et al., 2014). It was recently shown that the SH3_5 domain of *L. plantarum* Acm2 autolysin also has an affinity for PGN glycan chains containing GlcNAc, although the authors did not examine the influence of PGN peptide stems (Beaussart et al., 2013). It is thus possible that the SH3_5 and LysM binding motifs recognize similar PGN ligands, and cannot be used concurrently for protein display.

Stationary-phase bacteria bound less protein than log-growth bacteria, but are more robust to handling and gastrointestinal transit, and are thus of greater practical importance, especially for *in vivo* delivery applications that require viable cells (Brashears and Gilliland, 1995; Lorca and De Valdez, 1999; Corcoran et al., 2004; Broeckx et al., 2020). Stationary-phase *L. fermentum* bound 10^5 molecules of monomeric protein per cell. This compares well with previously reported binding capacities for LysM and S-layer-derived anchoring domains, which ranged from 10^3 to 10^6 molecules/cell (Bosma et al., 2006; Hu et al., 2010, 2011; Ravnikar et al., 2010). The binding capacity is likely to vary with the size and multimericity of the protein. Improvement in binding was reported for other anchoring domains after pre-treating bacteria with various solvents and detergents (Hu et al., 2010, 2011; Xu et al., 2011); we have also shown that 5 M LiCl treatment improves binding of CAD4a (**Figure 3C**). However, such treatments disrupt the proteosurfaceome of bacteria, and could have knock-on effects on cell viability and host-microbe interactions *in vivo*, and so should be used judiciously.

The optimal pH for CAD4a anchoring (pH 5) means that coated bacteria must be kept under slightly acidic conditions to maintain surface display. This precludes the display of acid-sensitive proteins—an important limitation of the CAD4a anchoring domain—although many lactobacilli can still thrive under these conditions, and *L. fermentum* is known to tolerate pH values down to 4.5 (Calderon Santoyo et al., 2003; LeBlanc et al., 2004). Encapsulation in a polymer matrix can further protect the anchored protein from the harsh conditions of gastrointestinal transit. We have shown that one such matrix, a composite of the natural polymers alginate and chitosan which can be assembled under acidic conditions, can protect surface-anchored protein from gastric digestion; other enteric coatings are reviewed elsewhere (Ramos et al., 2018; Gomand et al., 2019).

We have shown that CAD4a could be used to display SOD on the surface of *L. fermentum*, with minimal effect on enzyme functionality. Various strains of *L. fermentum* are known to have probiotic effects (Geier et al., 2007; Peran et al., 2007; Mikelsaar and Zilmer, 2009; Garcia-Castillo et al., 2019); whether these could enhance the therapeutic outcome of displayed functionalities could form the basis of future studies. It was shown previously that recombinant lactobacilli engineered to secrete SOD can ameliorate intestinal inflammation in mouse models of inflammatory bowel disease (Carroll et al., 2007; Watterlot et al., 2010; Hou et al., 2014). The SOD produced complemented inherent antioxidative and immunomodulatory properties of the probiotic *Lactobacillus* strains. However, such genetically modified bacteria might face stringent regulatory scrutiny and poor public acceptance. Heterologous display of therapeutic domains like SOD using CAD4a on wild-type LAB could get around these constraints, since no recombinant DNA is introduced to lactobacilli, and these bacteria could potentially be sourced from healthy microbiomes. We are currently looking into protein surface display using CAD4a for treatment of intestinal disease and for mucosal vaccination.

To conclude, we have characterized the use of CAD4a, a novel SH3_5-based anchoring domain, for surface display of heterologous proteins on LAB. C-terminal conjugation of the domain enabled the anchoring and display of two different proteins on *L. fermentum*, with optimal anchoring at pH 5, and up to 10^5 monomeric protein displayed per cell. Besides the delivery of therapeutic proteins to the gut, we foresee that surface display mediated by CAD4a could be also be used in the development of mucosal vaccines and for industrial biocatalysis.

DATA AVAILABILITY STATEMENT

The original contributions presented in the study are included in the article/**Supplementary Material**, further inquiries can be directed to the corresponding author/s.

AUTHOR CONTRIBUTIONS

PT and DO conceptualized the study and interpreted the results. PT designed and performed the experiments. PL helped with cloning and performed experiments involving SOD. PT drafted the manuscript and DO edited it. All authors reviewed the final manuscript.

FUNDING

This research was supported by the Agency for Science, Technology and Research (A*STAR), Singapore, under its Industry Alignment Fund (Pre-Positioning) Food Structure Engineering for Nutrition and Health (FSENH) programme (H18/01/a0/C11).

ACKNOWLEDGMENTS

The authors thank Lesaffre APAC for contributing a sample of *Lactobacillus rhamnosus* GG.

SUPPLEMENTARY MATERIAL

The Supplementary Material for this article can be found online at: https://www.frontiersin.org/articles/10.3389/fbioe.2020.614498/full#supplementary-material

REFERENCES

Åvall-Jääskeläinen, S., Kylä-Nikkilä, K., Kahala, M., Miikkulainen-Lahti, T., and Palva, A. (2002). Surface display of foreign epitopes on the *Lactobacillus brevis* S-Layer. *Appl. Environ. Microbiol.* 68:5943. doi: 10.1128/AEM.68.12.5943-5951.2002

Baba, T., and Schneewind, O. (1996). Target cell specificity of a bacteriocin molecule: a C-terminal signal directs lysostaphin to the cell wall of *Staphylococcus aureus*. *EMBO J.* 15, 4789–4797. doi: 10.1002/j.1460-2075.1996.tb00859.x

Beaussart, A., Rolain, T., Duchene, M. C., El-Kirat-Chatel, S., Andre, G., Hols, P., et al. (2013). Binding mechanism of the peptidoglycan hydrolase Acm2: low affinity, broad specificity. *Biophys. J.* 105, 620–629. doi: 10.1016/j.bpj.2013.06.035

Becker, S. C., Foster-Frey, J., Stodola, A. J., Anacker, D., and Donovan, D. M. (2009). Differentially conserved staphylococcal SH3b_5 cell wall binding domains confer increased staphylolytic and streptolytic activity to a streptococcal prophage endolysin domain. *Gene* 443, 32–41. doi: 10.1016/j.gene.2009.04.023

Bosma, T., Kanninga, R., Neef, J., Audouy, S. A., Van Roosmalen, M. L., Steen, A., et al. (2006). Novel surface display system for proteins on non-genetically modified gram-positive bacteria. *Appl. Environ. Microbiol.* 72, 880–889. doi: 10.1128/AEM.72.1.880-889.2006

Brashears, M. M., and Gilliland, S. E. (1995). Survival during frozen and subsequent refrigerated storage of *Lactobacillus acidophilus* cells as influenced by the growth phase. *J. Dairy Sci.* 78, 2326–2335. doi: 10.3168/jds.S0022-0302(95)76859-X

Brinster, S., Furlan, S., and Serror, P. (2007). C-terminal WxL domain mediates cell wall binding in *Enterococcus faecalis* and other gram-positive bacteria. *J. Bacteriol.* 189, 1244–1253. doi: 10.1128/JB.00773-06

Broeckx, G., Kiekens, S., Jokicevic, K., Byl, E., Henkens, T., Vandenheuvel, D., et al. (2020). Effects of initial cell concentration, growth phase, and process parameters on the viability of Lactobacillus rhamnosus GG after spray drying. *Drying Technol.* 38, 1474–1492. doi: 10.1080/07373937.2019.1648290

Calderon Santoyo, M., Loiseau, G., Rodriguez Sanoja, R., and Guyot, J.-P. (2003). Study of starch fermentation at low pH by *Lactobacillus fermentum* ogi E1 reveals uncoupling between growth and a-amylase production at pH 4.0. *Int. J. Food Microbiol.* 80, 77–87. doi: 10.1016/S0168-1605(02)00140-X

Cano-Garrido, O., Seras-Franzoso, J., and Garcia-Fruitós, E. (2015). Lactic acid bacteria: reviewing the potential of a promising delivery live vector for biomedical purposes. *Microb. Cell Fact.* 14, 137–137. doi: 10.1186/s12934-015-0313-6

Carroll, I. M., Andrus, J. M., Bruno-Barcena, J. M., Klaenhammer, T. R., Hassan, H. M., and Threadgill, D. S. (2007). Anti-inflammatory properties of *Lactobacillus gasseri* expressing manganese superoxide dismutase using the interleukin 10-deficient mouse model of colitis. *Am. J. Physiol. Gastrointest. Liver Physiol.* 293, G729–738. doi: 10.1152/ajpgi.00132.2007

Chowdhury, M. Y., Li, R., Kim, J. H., Park, M. E., Kim, T. H., Pathinayake, P., et al. (2014). Mucosal vaccination with recombinant *Lactobacillus casei*-displayed CTA1-conjugated consensus matrix protein-2 (sM2) induces broad protection against divergent influenza subtypes in BALB/c mice. *PLoS ONE* 9:e94051. doi: 10.1371/journal.pone.0094051

Corcoran, B. M., Ross, R. P., Fitzgerald, G. F., and Stanton, C. (2004). Comparative survival of probiotic lactobacilli spray-dried in the presence of prebiotic substances. *J. Appl. Microbiol.* 96, 1024–1039. doi: 10.1111/j.1365-2672.2004.02219.x

Desvaux, M., Candela, T., and Serror, P. (2018). Surfaceome and proteosurfaceome in parietal monoderm bacteria: focus on protein cell-surface display. *Front. Microbiol.* 9:100. doi: 10.3389/fmicb.2018.00100

Dieye, Y., Usai, S., Clier, F., Gruss, A., and Piard, J. C. (2001). Design of a protein-targeting system for lactic acid bacteria. *J. Bacteriol.* 183:4157. doi: 10.1128/JB.183.14.4157-4166.2001

Fleetwood, F., Devoogdt, N., Pellis, M., Wernery, U., Muyldermans, S., Ståhl, S., et al. (2013). Surface display of a single-domain antibody library on Gram-positive bacteria. *Cell. Mol. Life Sci.* 70, 1081–1093. doi: 10.1007/s00018-012-1179-y

Fredriksen, L., Kleiveland, C. R., Olsen Hult, L. T., Lea, T., Nygaard, C. S., Eijsink, V. G. H., et al. (2012). Surface display of N-terminally anchored invasin by *Lactobacillus plantarum* activates NF-κB in monocytes. *Appl. Environ. Microbiol.* 78, 5864–5871. doi: 10.1128/AEM.01227-12

Fredriksen, L., Mathiesen, G., Sioud, M., and Eijsink, V. G. H. (2010). Cell wall anchoring of the 37-kilodalton oncofetal antigen by *Lactobacillus plantarum* for mucosal cancer vaccine delivery. *Appl. Environ. Microbiol.* 76:7359. doi: 10.1128/AEM.01031-10

Garcia-Castillo, V., Komatsu, R., Clua, P., Indo, Y., Takagi, M., Salva, S., et al. (2019). Evaluation of the immunomodulatory activities of the probiotic strain *Lactobacillus fermentum* UCO-979C. *Front. Immunol.* 10:1376. doi: 10.3389/fimmu.2019.01376

Geier, M. S., Butler, R. N., Giffard, P. M., and Howarth, G. S. (2007). *Lactobacillus fermentum* BR11, a potential new probiotic, alleviates symptoms of colitis induced by dextran sulfate sodium (DSS) in rats. *Int. J. Food Microbiol.* 114, 267–274. doi: 10.1016/j.ijfoodmicro.2006.09.018

Gill, H., and Prasad, J. (2008). "Probiotics, immunomodulation, and health benefits," in *Bioactive Components of Milk,* ed. Z. Bösze (New York, NY: Springer), 423–454. doi: 10.1007/978-0-387-74087-4_17

Gomand, F., Borges, F., Burgain, J., Guerin, J., Revol-Junelles, A. M., and Gaiani, C. (2019). Food matrix design for effective lactic acid bacteria delivery. *Ann. Rev. Food Sci. Technol.* 10, 285–310. doi: 10.1146/annurev-food-032818-121140

Gonzalez-Delgado, L. S., Walters-Morgan, H., Salamaga, B., Robertson, A. J., Hounslow, A. M., Jagielska, E., et al. (2020). Two-site recognition of *Staphylococcus aureus* peptidoglycan by lysostaphin SH3b. *Nat. Chem. Biol.* 16, 24–30. doi: 10.1038/s41589-019-0393-4

Gründling, A., and Schneewind, O. (2006). Cross-linked peptidoglycan mediates lysostaphin binding to the cell wall envelope of *Staphylococcus aureus*. *J. Bacteriol.* 188, 2463–2472. doi: 10.1128/JB.188.7.2463-2472.2006

Han, L., Zhao, Y., Cui, S., and Liang, B. (2018). Redesigning of microbial cell surface and its application to whole-cell biocatalysis and biosensors. *Appl. Biochem. Biotechnol.* 185, 396–418. doi: 10.1007/s12010-017-2662-6

Hernani Mde, L., Ferreira, P. C., Ferreira, D. M., Miyaji, E. N., Ho, P. L., and Oliveira, M. L. (2011). Nasal immunization of mice with *Lactobacillus casei* expressing the pneumococcal surface protein C primes the immune system and decreases pneumococcal nasopharyngeal colonization in mice. *FEMS Immunol. Med. Microbiol.* 62, 263–272. doi: 10.1111/j.1574-695X.2011.00809.x

Hou, C. L., Zhang, J., Liu, X. T., Liu, H., Zeng, X. F., and Qiao, S. Y. (2014). Superoxide dismutase recombinant *Lactobacillus fermentum* ameliorates intestinal oxidative stress through inhibiting NF-κB activation in a trinitrobenzene sulphonic acid-induced colitis mouse model. *J. Appl. Microbiol.* 116, 1621–1631. doi: 10.1111/jam.12461

Hu, S., Kong, J., Kong, W., Guo, T., and Ji, M. (2010). Characterization of a novel LysM domain from *Lactobacillus fermentum* bacteriophage endolysin and its use as an anchor to display heterologous proteins on the surfaces of lactic acid bacteria. *Appl. Environ. Microbiol.* 76, 2410–2418. doi: 10.1128/AEM.01752-09

Hu, S., Kong, J., Sun, Z., Han, L., Kong, W., and Yang, P. (2011). Heterologous protein display on the cell surface of lactic acid bacteria mediated by the s-layer protein. *Microb. Cell Fact.* 10:86. doi: 10.1186/1475-2859-10-86

Hudson, E. P., Uhlen, M., and Rockberg, J. (2012). Multiplex epitope mapping using bacterial surface display reveals both linear and conformational epitopes. *Sci. Rep.* 2:706. doi: 10.1038/srep00706

Hui, C., Guo, Y., Zhang, W., Gao, C., Yang, X., Chen, Y., et al. (2018). Surface display of PbrR on *Escherichia coli* and evaluation of the bioavailability of lead associated with engineered cells in mice. *Sci. Rep.* 8:5685. doi: 10.1038/s41598-018-24134-3

Kleerebezem, M., Hols, P., Bernard, E., Rolain, T., Zhou, M., Siezen, R. J., et al. (2010). The extracellular biology of the lactobacilli. *FEMS Microbiol. Rev.* 34, 199–230. doi: 10.1111/j.1574-6976.2009.00208.x

Kosler, S., Strukelj, B., and Berlec, A. (2017). Lactic acid bacteria with concomitant IL-17, IL-23 and TNFα-binding ability for the treatment of Inflammatory Bowel Disease. *Curr. Pharm. Biotechnol.* 18, 318–326. doi: 10.2174/1389201018666170210152218

Kumar, A., Dutt, S., Bagler, G., Ahuja, P. S., and Kumar, S. (2012). Engineering a thermo-stable superoxide dismutase functional at sub-zero to >50°C, which also tolerates autoclaving. *Sci. Rep.* 2:387. doi: 10.1038/srep00387

LeBlanc, J. G., Garro, M. S., and Savoy De Giori, G. (2004). Effect of pH on *Lactobacillus fermentum* growth, raffinose removal, alpha-galactosidase activity and fermentation products. *Appl. Microbiol. Biotechnol.* 65, 119–123. doi: 10.1007/s00253-003-1532-z

Lee, J. S., Poo, H., Han, D. P., Hong, S. P., Kim, K., Cho, M. W., et al. (2006). Mucosal immunization with surface-displayed severe acute respiratory syndrome coronavirus spike protein on *Lactobacillus casei* induces neutralizing antibodies in mice. *J. Virol.* 80, 4079–4087. doi: 10.1128/JVI.80.8.4079-4087.2006

Lei, H., Sheng, Z., Ding, Q., Chen, J., Wei, X., Lam, D. M.-K., et al. (2011). Evaluation of oral immunization with recombinant avian influenza virus HA1 displayed on the *Lactococcus lactis* surface and combined with the mucosal adjuvant cholera toxin subunit B. *Clin. Vacc. Immunol.* 18, 1046–1051. doi: 10.1128/CVI.00050-11

Liu, J., Yang, G. L., Gao, X., Zhang, Z., Liu, Y., Yang, X., et al. (2019). Immunomodulatory properties of Lact*obacillus plantarum* NC8 expressing an anti-CD11c single-chain Fv fragment. *J. Microbiol. Biotechnol.* 29, 160–170. doi: 10.4014/jmb.1809.09017

Lorca, G. L., and De Valdez, G. F. (1999). The effect of suboptimal growth temperature and growth phase on resistance of *Lactobacillus acidophilus* to environmental stress. *Cryobiology* 39, 144–149. doi: 10.1006/cryo.1999.2193

Mao, R., Wu, D., Hu, S., Zhou, K., Wang, M., and Wang, Y. (2017). Secretory expression and surface display of a new and biologically active single-chain insulin (SCI-59) analog by lactic acid bacteria. *Appl. Microbiol. Biotechnol.* 101, 3259–3271. doi: 10.1007/s00253-017-8125-8

Mao, R., Zhou, K., Han, Z., and Wang, Y. (2016). Subtilisin QK-2: secretory expression in *Lactococcus lactis* and surface display onto gram-positive enhancer matrix (GEM) particles. *Microb. Cell Fact.* 15:80. doi: 10.1186/s12934-016-0478-7

Maruthamuthu, M. K., Selvamani, V., Nadarajan, S. P., Yun, H., Oh, Y.-K., Eom, G. T., et al. (2018). Manganese and cobalt recovery by surface display of metal binding peptide on various loops of OmpC in *Escherichia coli*. *J. Indust. Microbiol. Biotechnol.* 45, 31–41. doi: 10.1007/s10295-017-1989-x

Mesnage, S., Dellarole, M., Baxter, N. J., Rouget, J.-B., Dimitrov, J. D., Wang, N., et al. (2014). Molecular basis for bacterial peptidoglycan recognition by LysM domains. *Nat. Comm.* 5:4269. doi: 10.1038/ncomms5269

Mikelsaar, M., and Zilmer, M. (2009). *Lactobacillus fermentum* ME-3 - an antimicrobial and antioxidative probiotic. *Microb. Ecol. Health Dis.* 21, 1–27. doi: 10.1080/08910600902815561

Minekus, M., Alminger, M., Alvito, P., Ballance, S., Bohn, T., Bourlieu, C., et al. (2014). A standardised static *in vitro* digestion method suitable for food – an international consensus. *Food Funct.* 5, 1113–1124. doi: 10.1039/C3FO60702J

Mitkowski, P., Jagielska, E., Nowak, E., Bujnicki, J. M., Stefaniak, F., Niedzialek, D., et al. (2019). Structural bases of peptidoglycan recognition by lysostaphin SH3b domain. *Sci. Rep.* 9:5965. doi: 10.1038/s41598-019-42435-z

Mora-Villalobos, J. A., Montero-Zamora, J., Barboza, N., Rojas-Garbanzo, C., Usaga, J., Redondo-Solano, M., et al. (2020). Multi-product lactic acid bacteria fermentations: a review. *Fermentation* 6:23. doi: 10.3390/fermentation6010023

Mustafa, A. D., Kalyanasundram, J., Sabidi, S., Song, A., a,.-L., Abdullah, M., et al. (2018). Proof of concept in utilizing in-trans surface display system of *Lactobacillus plantarum* as mucosal tuberculosis vaccine via oral administration in mice. *BMC Biotechnol.* 18:63. doi: 10.1186/s12896-018-0461-y

Narita, J., Okano, K., Kitao, T., Ishida, S., Sewaki, T., Sung, M. H., et al. (2006). Display of alpha-amylase on the surface of *Lactobacillus casei* cells by use of the PgsA anchor protein, and production of lactic acid from starch. *Appl. Environ. Microbiol.* 72, 269–275. doi: 10.1128/AEM.72.1.269-275.2006

Nguyen, H.-M., Pham, M.-L., Stelzer, E. M., Plattner, E., Grabherr, R., Mathiesen, G., et al. (2019). Constitutive expression and cell-surface display of a bacterial β-mannanase in *Lactobacillus plantarum*. *Microb. Cell Fact.* 18:76. doi: 10.1186/s12934-019-1124-y

Nualkaekul, S., Lenton, D., Cook, M. T., Khutoryanskiy, V. V., and Charalampopoulos, D. (2012). Chitosan coated alginate beads for the survival of microencapsulated *Lactobacillus plantarum* in pomegranate juice. *Carbohydr. Polym.* 90, 1281–1287. doi: 10.1016/j.carbpol.2012.06.073

Park, M. (2020). Surface display technology for biosensor applications: a review. *Sensors* 20:2775. doi: 10.3390/s20102775

Peran, L., Sierra, S., Comalada, M., Lara-Villoslada, F., Bailón, E., Nieto, A., et al. (2007). A comparative study of the preventative effects exerted by two probiotics, *Lactobacillus reuteri* and *Lactobacillus fermen*tum, in the trinitrobenzenesulfonic acid model of rat colitis. *Brit. J. Nutrition* 97, 96–103. doi: 10.1017/S0007114507257770

Pham, M.-L., Tran, A.-M., Kittibunchakul, S., Nguyen, T.-T., Mathiesen, G., and Nguyen, T.-H. (2019). Immobilization of β-galactosidases on the *Lactobacillus* cell surface using the peptidoglycan-binding motif LysM. *Catalysts* 9, 443–443. doi: 10.3390/catal9050443

Plavec, T. V., and Berlec, A. (2019). Engineering of lactic acid bacteria for delivery of therapeutic proteins and peptides. *Appl. Microbiol. Biotechnol.* 103, 2053–2066. doi: 10.1007/s00253-019-09628-y

Plavec, T. V., Štrukelj, B., and Berlec, A. (2019). Screening for new surface anchoring domains for *Lactococcus lactis*. *Front. Microbiol.* 10:1879. doi: 10.3389/fmicb.2019.01879

Pontes, D., Innocentin, S., Del Carmen, S., Almeida, J. F., Leblanc, J.-G., De Moreno De Leblanc, A., et al. (2012). Production of fibronectin binding protein A at the surface of *Lactococcus lactis* increases plasmid transfer *in vitro* and *in vivo*. *PLoS ONE* 7:e44892. doi: 10.1371/journal.pone.0044892

Raha, A. R., Varma, N. R. S., Yusoff, K., Ross, E., and Foo, H. L. (2005). Cell surface display system for *Lactococcus lactis*: a novel development for oral vaccine. *Appl. Microbiol. Biotechnol.* 68, 75–81. doi: 10.1007/s00253-004-1851-8

Ramos, P. E., Cerqueira, M. A., Teixeira, J. A., and Vicente, A. A. (2018). Physiological protection of probiotic microcapsules by coatings. *Crit. Rev. Food Sci. Nutrit.* 58, 1864–1877. doi: 10.1080/10408398.2017.1289148

Ravnikar, M., Strukelj, B., Obermajer, N., Lunder, M., and Berlec, A. (2010). Engineered lactic acid bacterium *Lactococcus lactis* capable of binding antibodies and tumor necrosis factor alpha. *Appl. Environ. Microbiol.* 76, 6928–6932. doi: 10.1128/AEM.00190-10

Robert, X., and Gouet, P. (2014). Deciphering key features in protein structures with the new ENDscript server. *Nuc. Acids Res.* 42, W320–W324. doi: 10.1093/nar/gku316

Rockberg, J., Löfblom, J., Hjelm, B., Uhlén, M., and Ståhl, S. (2008). Epitope mapping of antibodies using bacterial surface display. *Nat. Methods* 5, 1039–1045. doi: 10.1038/nmeth.1272

Rolain, T., Bernard, E., Courtin, P., Bron, P. A., Kleerebezem, M., Chapot-Chartier, M.-P., et al. (2012). Identification of key peptidoglycan hydrolases for morphogenesis, autolysis, and peptidoglycan composition of *Lactobacillus plantarum* WCFS1. *Microb. Cell Fact.* 11:137. doi: 10.1186/1475-2859-11-137

Seguí, J., Gironella, M., Sans, M., Granell, S., Gil, F., Gimeno, M., et al. (2004). Superoxide dismutase ameliorates TNBS-induced colitis by reducing oxidative stress, adhesion molecule expression, and leukocyte recruitment into the inflamed intestine. *J. Leukocyte Biol.* 76, 537–544. doi: 10.1189/jlb.0304196

Simşek, Ö. (2014). Nisin production in a chitin-including continuous fermentation system with *Lactococcus lactis* displaying a cell wall chitin-binding domain. *J. Indust. Microbiol. Biotechnol.* 41, 535–543. doi: 10.1007/s10295-013-1388-x

Škrlec, K., Pucer, J. A., Rogelj, B., Štrukelj, B., and Berlec, A. (2017). Evasin-displaying lactic acid bacteria bind different chemokines and neutralize CXCL8 production in Caco-2 cells. *Microb. Biotechnol.* 10, 1732–1743. doi: 10.1111/1751-7915.12781

Skrlec, K., Rucman, R., Jarc, E., Sikiric, P., Svajger, U., Petan, T., et al. (2018). Engineering recombinant *Lactococcus lactis* as a delivery vehicle for BPC-157 peptide with antioxidant activities. *Appl. Microbiol. Biotechnol.* 102, 10103–10117. doi: 10.1007/s00253-018-9333-6

Steen, A., Buist, G., Horsburgh, G. J., Venema, G., Kuipers, O. P., Foster, S. J., et al. (2005). AcmA of *Lactococcus lactis* is an N-acetylglucosaminidase with an optimal number of LysM domains for proper functioning. *FEBS J.* 272, 2854–2868. doi: 10.1111/j.1742-4658.2005.04706.x

Stern, J., Moraïs, S., Ben-David, Y., Salama, R., Shamshoum, M., Lamed, R., et al. (2018). Assembly of synthetic functional cellulosomal structures onto the cell surface of *Lactobacillus plantarum*, a potent member of the gut microbiome. *Appl. Environ. Microbiol.* 84:e00282-18. doi: 10.1128/AEM.00282-18

Tang, X., Liang, B., Yi, T., Manco, G., Ilariapalchetti, and Liu, A. (2014). Cell surface display of organophosphorus hydrolase for sensitive spectrophotometric detection of p-nitrophenol substituted organophosphates. *Enzyme Microb. Technol.* 55, 107–112. doi: 10.1016/j.enzmictec.2013.10.006

Tomosugi, W., Matsuda, T., Tani, T., Nemoto, T., Kotera, I., Saito, K., et al. (2009). An ultramarine fluorescent protein with increased photostability and pH insensitivity. *Nat. Methods* 6, 351–353. doi: 10.1038/nmeth.1317

Walter, J. (2008). Ecological role of lactobacilli in the gastrointestinal tract: implications for fundamental and biomedical research. *Appl. Environ. Microbiol.* 74:4985. doi: 10.1128/AEM.00753-08

Watterlot, L., Rochat, T., Sokol, H., Cherbuy, C., Bouloufa, I., Lefevre, F., et al. (2010). Intragastric administration of a superoxide dismutase-producing recombinant *Lactobacillus casei* BL23 strain attenuates DSS colitis in mice. *Int. J. Food Microbiol.* 144, 35–41. doi: 10.1016/j.ijfoodmicro.2010.03.037

Wieczorek, A. S., and Martin, V. J. (2012). Effects of synthetic cohesin-containing scaffold protein architecture on binding dockerin-enzyme fusions on the surface of *Lactococcus lactis*. *Microb. Cell Fact.* 11:160. doi: 10.1186/1475-2859-11-160

Xu, W., Huang, M., Zhang, Y., Yi, X., Dong, W., Gao, X., et al. (2011). Novel surface display system for heterogonous proteins on *Lactobacillus plantarum*. *Lett. Appl. Microbiol.* 53, 641–648. doi: 10.1111/j.1472-765X.2011.03160.x

Yin, S., Zhu, H., Shen, M., Li, G., Lu, S., Zhao, Y., et al. (2018). Surface display of heterologous β-galactosidase in food-grade recombinant *Lactococcus lactis*. *Curr. Microbiol.* 75, 1362–1371. doi: 10.1007/s00284-018-1531-z

Zadravec, P., Mavrič, A., Bogovič Matijasic, B., Štrukelj, B., and Berlec, A. (2014). Engineering BmpA as a carrier for surface display of IgG-binding domain on *Lactococcus lactis*. *Protein Eng. Des. Sel.* 27, 21–27. doi: 10.1093/protein/gzt059

Conflict of Interest: The authors declare that the research was conducted in the absence of any commercial or financial relationships that could be construed as a potential conflict of interest.

frontiers in Bioengineering and Biotechnology

ORIGINAL RESEARCH
published: 05 February 2021
doi: 10.3389/fbioe.2021.612105

Combinational Antibacterial Activity of Nisin and 3-Phenyllactic Acid and Their Co-production by Engineered *Lactococcus lactis*

Jiaheng Liu[1,2,3†], Rongrong Huang[1†], Qianqian Song[1,2†], Hui Xiong[1,2], Juan Ma[1], Rui Xia[1] and Jianjun Qiao[1,2,3]*

[1] Department of Pharmaceutical Engineering, School of Chemical Engineering and Technology, Tianjin University, Tianjin, China, [2] Key Laboratory of Systems Bioengineering, Ministry of Education, Tianjin, China, [3] Collaborative Innovation Center of Chemical Science and Engineering, SynBio Research Platform, Tianjin, China

OPEN ACCESS

Edited by:
Jian-Ming Liu,
Technical University of Denmark, Denmark

Reviewed by:
Zheng-Jun Li,
Beijing University of Chemical Technology, China
Javier Alberto Garza Cervantes,
Monterrey Institute of Technology and Higher Education (ITESM), Mexico

***Correspondence:**
Jianjun Qiao
jianjunq@tju.edu.cn

[†] These authors have contributed equally to this work

Specialty section:
This article was submitted to Synthetic Biology, a section of the journal Frontiers in Bioengineering and Biotechnology

Received: 30 September 2020
Accepted: 20 January 2021
Published: 05 February 2021

Citation:
Liu J, Huang R, Song Q, Xiong H, Ma J, Xia R and Qiao J (2021) Combinational Antibacterial Activity of Nisin and 3-Phenyllactic Acid and Their Co-production by Engineered Lactococcus lactis. Front. Bioeng. Biotechnol. 9:612105. doi: 10.3389/fbioe.2021.612105

Nisin produced by certain *Lactococcus lactis* strains is commercially used in meat and dairy industries because of its effective antibacterial activity and food safety characteristics. It has been proved that the antibacterial activity could be enhanced when combined with other antimicrobial agents. In this study, we demonstrated that nisin and 3-phenyllactic acid (PLA) in combination displayed excellent combinational antibacterial activity against foodborne pathogens including *S. xylosus* and *M. luteus*. The potential application in food preservation was further verified *via* microbial analysis during the storage of meat and milk, and determination of strawberry rot rate. Scanning electron microscopy observation indicated a distinct mode of PLA with nisin, which may target at the dividing cell, contributing to their combinational antibacterial effect of nisin and PLA. Considering the positive results, a nisin-PLA co-producing strain was constructed based on the food-grade strain *L. lactis* F44, a nisin Z producer. By the knockout of two L-lactate dehydrogenase (LDH) and overexpression of D-LDH^{Y25A}, the yield of PLA was significantly increased 1.77-fold in comparison with the wild type. Anti-bacterial assays demonstrated that the fermentation product of the recombinant strain performed highly effective antibacterial activity. These results provided a promising prospect for the nisin-PLA co-expressing *L. lactis* in food preservation on account of its considerable antibacterial activity and cost-effective performance.

Keywords: *Lactococcus lactis*, nisin, 3-phenyllactic acid, antimicrobial activity, food preservative, metabolic engineering

INTRODUCTION

Food safety is generally recognized as an essential public safety issue worldwide. Microbial contamination of food products is of great importance effecting food safety, which can bring about great economic losses and prevalent foodborne diseases (Chatterjee and Abraham, 2017). Although various synthetic preservatives, such as sodium benzoate, potassium sorbate, and butylated hydroxyanisole, have been investigated and applied to inhibit microbial growth during food storage, the increasingly serious threat of synthetic preservatives to human health has prompted

investigations into exploring natural preservatives (KBauera et al., 2001; Przybylski et al., 2016; de Oliveira Pateis et al., 2018).

Nisin, produced by certain strains of *Lactococcus lactis*, is a natural antimicrobial peptide exhibiting broad-spectrum antimicrobial activity against a majority of Gram-positive foodborne bacteria and some Gram-negative pathogens when combined with EDTA or physical treatments (Gharsallaoui et al., 2015). It exerts its antimicrobial activity by both pore formation on the surface of cells and inhibition of cell wall biosynthesis (Chatterjee et al., 2005). More importantly, nisin is easily degradable by proteolytic enzymes in mammalian and presents no risk to human health. Thus, the application of nisin in preservation of many food products, such as cheese and meat, has a long and impressive history (Cotter et al., 2005; Barbosa et al., 2017). However, it has less significance for fruit or bread preservation due to its weak antifungal activity.

Another major problem is that pure product of nisin (>99%) is commercially unavailable due to its time-consuming separation and purification (Juturu and Wu, 2018). The commercial nisin preparation called Nisaplin contains only 2.5% (w/w) nisin, and the rest are mainly NaCl and proteins. In some cases, the nisin fermentation broth is immediately applied in food preservation to reduce the cost, while the bounding effect between nisin and proteins could decrease its preservative effectiveness (Cleveland et al., 2002).

The above issues prompted us to turn to the strategy of combined application of nisin and other antimicrobial agents. PLA, an organic acid, has been reported to be an antimicrobial compound with broad-spectrum activity against bacteria including *Listeria monocytogenes* (Dieuleveux et al., 1998), *Staphylococcus aureus*, and *Escherichia coli* (Ohhira et al., 2010), and fungi including yeasts (Schwenninger et al., 2008) and a wide range of molds, such as *Aspergillus ochraceus*, *Penicillium roqueforti*, and *Penicillium citrinu* (Lavermicocca et al., 2003b). Its antimicrobial mechanism of action is still under investigation, and some researchers supposed that the interaction between PLA and cell surface could contribute to the damage of cellular structures (Ning et al., 2017; Sorrentino et al., 2018). It has been reported that PLA could be produced by a wide range of lactic acid bacteria species, such as *Lactobacillus* and *Enterococcus* (Lavermicocca et al., 2000; Valerio et al., 2004).

Therefore, the objectives of this research were to: (1) examine whether there is a combinational antibacterial activity of nisin and PLA against foodborne pathogens, (2) evaluate the efficacy of combined application of nisin-PLA in food preservation, and (3) construct an *L. lactis* strain co-producing nisin and PLA, the fermentation product of which could exhibit both antibacterial and antifungal activities and serve as a potential preservative candidate in food industry more widely.

MATERIALS AND METHODS

Strains, Plasmids, and Growth Conditions

All bacteria strains and plasmids used in this study are listed in **Supplementary Table S1**. *Lactococcus lactis* F44 (Genome accession number: PRJNA 419050), a nisin Z producer, was derived from *L. lactis* YF11 *via* genome shuffling in our previous study (Zhang et al., 2014b). *L. lactis* F44 and the engineered strains were incubated at 30°C with no agitation in seed medium or fermentation medium. The seed medium contained the following (wt/vol): yeast extract (1.5%), peptone (1.5%), KH_2PO_4 (2.0%), sucrose (2.0%), NaCl (0.15%), and $MgSO_4{\cdot}7H_2O$ (0.015%), pH 7.2. For the fermentation medium, additional corn steep liquor (0.3%) and cysteine (0.26%) were needed. Three g/L phenylpyruvic acid (PPA) was supplemented in the fermentation medium for PLA production.

Escherichia coli TG1 was applied for the construction of expression vector. *Staphylococcus xylosus* and *Micrococcus luteus* ATC10240 were used as indicators and cultured in Nutrient Broth (NB). 5 μg/mL erythromycin (Em) and 5 μg/mL chloramphenicol (Cm) were employed for *L. lactis*, while for *E. coli*, 200 μg/mL Em and 50 μg/mL Cm were applied, if necessary.

Anti-bacterial Activity

Agar diffusion assay was performed to detect the anti-bacterial activities of PLA and nisin, or the culture supernatants. Briefly, 25 mL of NB agar and 200 μL indicator strain (5×10^8 CFU/mL) were mixed and poured onto a plate with Oxford cups (6 mm). The wells of the dried agar plates were added with 100 μl of samples and the plates were incubated overnight at 37°C. The standards PLA and nisin were applied to verify the combinational effect of PLA and nisin in antibacterial. The concentrations of the standards were set as follows: 10 mg/mL PLA (Liu et al., 2018), 100 IU/mL nisin (Wu et al., 2020) and a mixture of PLA-nisin (10 mg/mL PLA and 100 IU/mL nisin), and 0.02 M HCl was taken as blank. Besides, the boiled supernatant (100°C, 5 min) from fermentation sample were used to evaluate the antibacterial activities of F44/P, F44/DLDH and F44ΔLDHΔLDHB/DLDH. For the inhibitory effect against *M. luteus*, a dilution of 1:8 was used, and the culture supernatant without dilution for *S. xylosus*.

Microbiology Analysis in Pork Samples

The microbial analysis was performed to assess the application of PLA and nisin in pork preservation with a modified method (Liu et al., 2020b). Fresh ground pork was purchased in local market (Tianjin, China). It was divided into 4 groups and mixed with sterilized water in a ratio of 1 g/1 mL. Three experimental groups were supplemented with nisin and PLA in a final concentration of 0.1% (wt/vol), and 0.1% nisin-0.1%PLA mixture in combination, respectively. Sterilized water served as the blank. Subsequently, the samples were stored in sterile containers at 4°C. 5 g sample was taken at days 1, 2, and 3 and mixed with 30 mL saline to calculate the number of microorganism. One milliliter supernatant was serially diluted with saline and 100 μL of dilution was spread on the NB agar plate. The plate was incubated at 30°C for 24 h. The results were expressed as $\log_{10}$ CFU per gram of pork ($\log_{10}$ CFU/g). All the samples were carried out in triplicate.

Microbiology Analysis in Pasteurized Milk

S. xylosus belongs to Staphylococcus, one of the microbiota in many dairy products and meat products, and has strong drug resistance (Martuscelli et al., 2000). *S. xylosus* (10^3 CFU/mL) was added to 1 L of pasteurized milk and divided into 4 groups which were mixed with 0.1% nisin solution, 0.1% PLA solution, and 0.1% nisin-0.1% PLA solution, respectively. The mixtures were stored in sterile containers at 4°C. 1 mL of pasteurized milk sample was carried out at 0, 3, 6, and 9 h to count the number of *S. xylosus via* spreading an appropriate dilution on the NB agar plate. The result was showed as $\log_{10}$CFU per milliliter pasteurized milk ($\log_{10}$ CFU/mL). All the samples were tested in triplicate.

Determination of Rotting Rate in Strawberry

Strawberries with uniform size and no visible damage were selected in a local farm. The rotting rate was determined with a modified method (Liu et al., 2020b). Then 100 strawberries were randomly divided into 4 groups, dipping in sterilized water as blank and the solution of nisin, PLA, and nisin-PLA mixture for 30 s, respectively, and the concentration of each preservative was 0.1% (wt/vol). The strawberries were stored at room temperature after air drying in Clean Bench. The number of rotten strawberries with mildew, injury, or black spot surface, was counted at days 0, 1, 2, 3, 4, 5, and 6. The rotting rate was calculated as the following:

$$Rotting\ rate = \frac{the\ number\ of\ rotten\ strawberries}{the\ \ initial\ number\ of\ strawberries} \times 100\%.$$

Scanning Electron Microscopy (SEM)

S. xylosus, grown to logarithmic phase, was collected and washed twice with PBS buffer. The cells were treated with nisin (50 IU/mL), PLA (5 mg/mL) or their combination and 0.9% NaCl solution (control) for 1 h at 37°C. After incubation, the cells were collected, washed with PBS and fixed in 2.5% glutaraldehyde overnight at 4°C. Following washes of three times with the same buffer, the samples were dehydrated with ethanol of gradient concentrations (50, 70, 80, 90, 100%). The samples were lyophilized and prepared for SEM (Hitachi High-Technologies, Tokyo, Japan) analysis.

Construction of Plasmids and PLA Producing Strains

Primers used in this study were listed in **Supplementary Table S2**. *d-ldh*^{Y52A} from *Lactobacillus pentosus* (Ishikura et al., 2005), encoding lactate dehydrogenase mutant D-LDH^{Y25A}, was synthesized in GENEWIZ Inc. (Suzhou, China). Seamless cloning technology was applied to construct the *d-ldh*^{Y52A} expression vector. The expression fragment *d-ldh*^{Y52A} was amplified using Phanta Max Super-Fidelity DNA polymerase (Vazyme Biotech Co., Ltd., Nanjing, China) and purified with Universal DNA Purification kit (TIANGEN, Biotech, Beijing, China). Then, the fragment was cloned into *Hin*dIII-*Bam*HI digested pLEB124 to produce pLEB124-DLDH *via* Minerva Super Fusion Cloning Kit (US EVERBRIGHT® INC.). The recombinant plasmid was transformed into *E. coli* TG1 and then electroporated into *L. lactis* F44 and F44ΔLDHΔLDHB, respectively, obtaining the overexpressing strains F44/DLDH and F44ΔLDHΔLDHB/DLDH.

For knockout of lactate dehydrogenase genes *ldh* and *ldhB* in *L. lactis* F44, an *oroP*-based selection/counterselection vector pCS1966 was employed (Solem et al., 2008). The upstream and downstream (∼1,000 bp) of *ldh* or *ldhB* were inserted into the plasmid pCS1966 to constructed the recombinant plasmid pCS1966-LDH or pCS1966-LDHB. The plasmid pCS1966-LDH was then introduced into F44 and the successful integration was selected by Em resistance. Subsequently, the transformant was plated on SA glucose plates supplemented with 5-fluoroorotate (5-FOA, 20 μg/mL) to screen the resistant strain where the secondary homologous recombination was occurred. Eventually, the *ldh*-deleted strain F44ΔLDH was gained. In the same method, the double knockout strain F44ΔLDHΔLDHB was obtained.

Determination of PLA and PPA Contents in Fermentation Broth

The 12 h-culture supernatants of F44/P, F44/DLDH and F44ΔLDHΔLDHB/DLDH were collected for content analysis of PLA and PPA by high performance liquid chromatography (HPLC), equipped with a HC-C18 column (3.5 μm, 4.6 × 250 mm, Agilent) and a 2489 UV/Vis Detector. A gradient separation was programmed with the mobile phase of 0.05% trifluoroacetic acid (TFA)-0.05% TFA methanol and at a flow rate of 1 mL/min. The detection wavelength was 210 nm. The PLA and PPA standards were purchased from Meryer (Shanghai, China).

Statistical Analysis

Experimental data in this study were expressed as means ± standard deviations (SD). SPSS 18.0 software (SPSS, Chicago, IL, United States) was used for the statistical analyses. One-way analysis of variance (ANOVA) was applied to determine the differences for diameter of inhibition zone, microbial count, rotting rate, and PLA concentration between experimental and control groups. A $p < 0.05$ was considered statistically significant.

RESULTS

Combinational Antibacterial Activity of Nisin and PLA

To verify whether the combination of nisin and PLA possessed a positive effect in antimicrobial activity, pathogens of *M. luteus* and *S. xylosus* were used as indictors. The suppressive effects of PLA (10 mg/mL), nisin (100 IU/mL), nisin-PLA (mixture of 10 mg/mL PLA and 100 IU/mL nisin) were compared, with 0.02 M HCl served as negative control, and the result was shown in **Figure 1**. Both PLA and nisin showed antibacterial activities against *M. luteus* and *S. xylosus*. The control group, by contrast, exhibited no inhibition zone. Larger diameters of

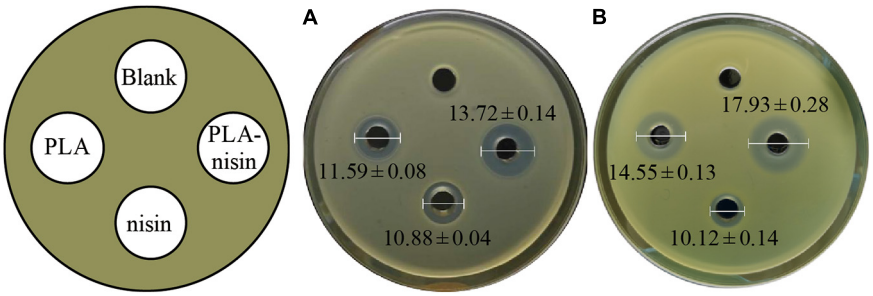

FIGURE 1 | The antibacterial activities of PLA and nisin against *S. xylosus* **(A)** and *M. luteus* **(B)**. The wells (6 mm) of the plates were added with 100 μL 0.02 M HCl as blank, 10 mg/mL PLA, 100 IU/mL nisin and a mixture of PLA-nisin with the same concentrations. The differences in inhibition diameters (unit: mm) represents bacteriostasis activities of PLA and nisin. The differences among the four groups were compared by One-way ANOVA. The diameter of inhibition zone of PLA-nisin was significantly different ($P < 0.01$) compared with PLA, nisin and control.

inhibition zones of nisin-PLA (13.72 ± 0.14 mm for *S. xylosus* and 17.93 ± 0.28 mm for *M. luteus*) were observed, than those of PLA and nisin alone, suggesting a superior antibacterial activity of the combined nisin-PLA. Interestingly, PLA appeared to work better in inhibiting the growth of *M. luteus*, while for nisin, slight difference was observed between the two indicators. Similarily, the combined nisin-PLA also performed a stronger bacteriostatic efficacy against *M. luteus*. All these results demonstrated that the antibacterial efficacy of nisin was substantially enhanced when combined with PLA.

Preservation Effect of Nisin and PLA on Fresh Pork

To evaluate the application of a combination of nisin and PLA in food preservation, chilled pork was taken as an example. Considering microorganisms are the major cause of food spoilage, microbial colony counting was used to assess the spoilage degree of chilled pork. As shown in **Figure 2A**, the growth of microbials in which groups were mixed with 0.1% nisin and 0.1% PLA alone or in combination, was effectively suppressed, compared with that of the sample treated with sterilized water. The viable count of microbials was reduced by more than 2 $\log_{10}$ CFU/mL in the group treated with the combination of nisin and PLA at day 3. However, the microbial count in the combination one (6.25 ± 0.27 $\log_{10}$ CFU/mL) was slightly better ($p < 0.05$) than that of the nisin-treated one (6.61 ± 0.35 $\log_{10}$ CFU/mL) at day 3, indicating a dominated role of nisin in pork preservation, instead of PLA.

Preservation Effect of Nisin and PLA on Pasteurized Milk

To further investigate whether nisin and PLA in combination had the advantages of inhibiting the growth of bacteria in food preservation, the antibacterial activity in pasteurized milk was evaluated. As fresh milk is usually kept in the refrigerator after opening, the experiment was carried out at 4°C. One box of Pasteurized milk after incubation of *S. xylosus* was divided into four parts and mixed with sterilized water, 0.1% nisin and 0.1% PLA alone or in combination, respectively. **Figure 2B** showed that the addition of PLA alone or nisin and PLA in combination significantly slowed down the growth of *S. xylosus*, and the inhibition effect was especially remarkable when the storage time was less than 9 h. However, the inhibition effect of nisin was weak and no obvious difference in viable microbial counts was observed between the nisin-addition sample and the control sample. The viable microbial count of the sample treated with nisin-PLA was decreased almost 3.5 $\log_{10}$ CFU/mL before 9 h and the number of microbials was lowest, which decreased 27.5% ($p < 0.01$), 25.2% ($p < 0.01$), 23.5% ($p < 0.01$), and 12.1% ($p < 0.05$) compared with those of the PLA-treated group, respectively, at 3, 6, 9, and 12 h. Interestingly, unlike the preservation effect in fresh pork which nisin played the chief role, PLA performed better antibacterial activity in this assay. These results further illustrated that a combination of nisin and PLA exhibited an enhanced effect in Pasteurized milk preservation against *S. xylosus*.

Preservation Effect of Nisin and PLA on Strawberry

The increasing demand for fruit products, as well as maintaining their natural characteristics (Olaimat and Holley, 2012), makes nisin as a candidate in the preservation of fruits and vegetables in recent years (Komitopoulou et al., 2001; Barbosa et al., 2017). We speculated whether nisin in the presence of PLA, could have a better performance on fruit preservation. Strawberry, easy to be damaged and rotten, was chosen for the test. The fresh strawberries were dipped in sterilized water, 0.1% nisin and 0.1% PLA alone or in combination for 30 s, respectively, kept dry and stored at room temperature. The rotting rates were summarized in **Figure 2C**. The rotting rates of three experimental groups were lower than those of the control in 6 days, especially the groups treated with 0.1% PLA alone and nisin-PLA in combination, which was corresponding with the results presented in the Pasteurized milk preservation assay. The rotting rate in the PLA-treating group performed better within 3 days, while the combined nisin-PLA treatment was more effective ($p < 0.05$) in days 5 and 6 which the rotting rates dropped considerably (35% decrease in day 5 and 30% decrease in the day 6) than those of the control. Significantly, the combination of nisin and

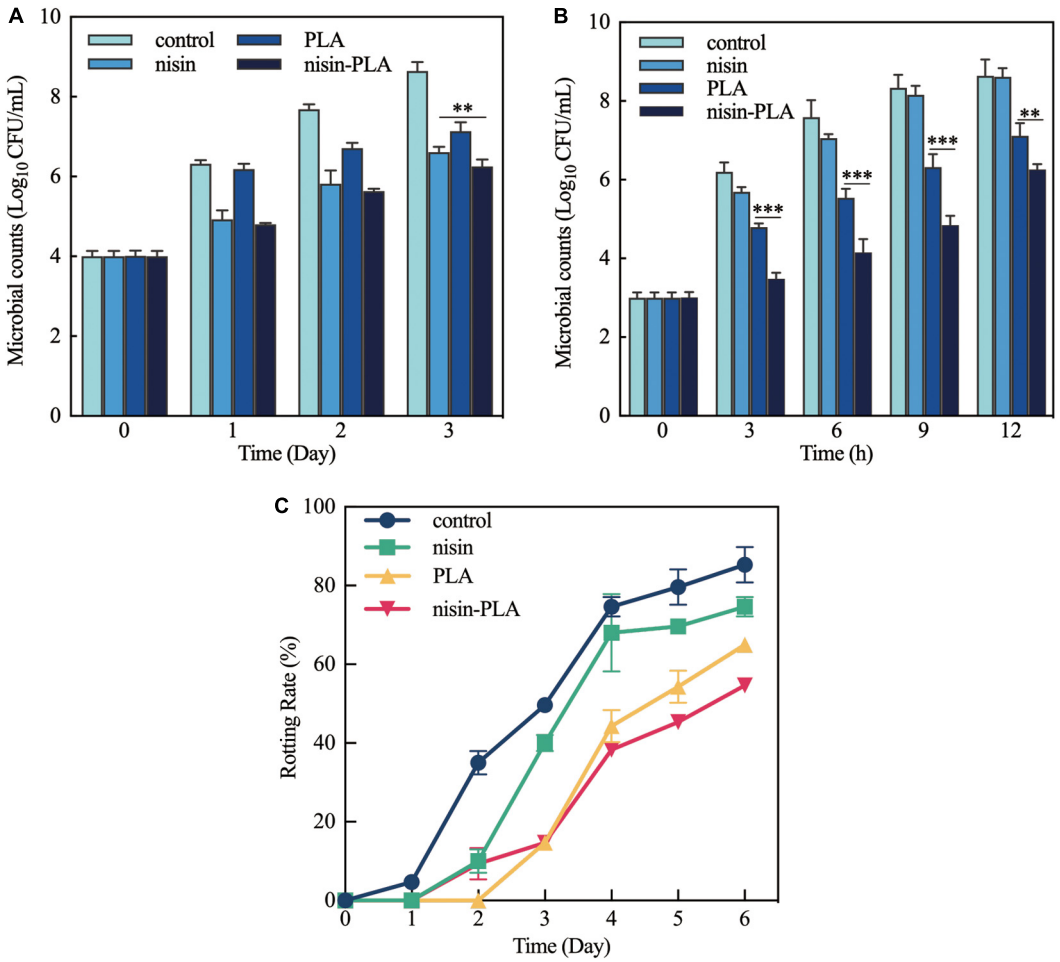

FIGURE 2 | Effects of food preservation of nisin and PLA alone, or in combination. **(A)** Microbial changes in chilled pork stored at refrigerator (4°C), **(B)** microbial changes of pasteurized milk at a starting inoculum concentration of 10^3 CFU/mL, and **(C)** the rot rate of strawberry during storage at room temperature. The samples were treated with sterilized water (control), nisin (0.1%), PLA (0.1%), and nisin (0.1%)-PLA (0.1%), respectively. The data were carried out in triplicate and the standard deviation (SD) of data was shown as error bar. The differences between the four groups were determined by One-way ANOVA, and the significantly differences (**$P < 0.05$; ***$P < 0.01$) between the groups were presented in the figure.

PLA demonstrated better potential in the fruits preservation in comparision with nisin.

Effect of Nisin and PLA on Bacterial Morphology

The morphological changes of *S. xylosus* were directly observed through SEM, to clarify the antibacterial effects of nisin and PLA alone or in combination (**Figure 3**). Evident changes in cell morphology were observed which suggesting a severe cell damage. The *S. xylosus* sample without nisin or PLA treatment maintained a regular spherical shape and displayed a relative flat and smooth surface (**Figure 3A**). Cells treated with nisin exhibited irregular shape and cell shrinkage (**Figure 3B**). Similar observations were earlier reported by Tong et al. (2010) for *Streptococcus sanguinis* and *Lactobacillus acidophilus* treated with nisin. Surprisingly, some hemispherical-shaped cells with wrinkled outer surface were observed in the PLA-treating sample which just as the dividing cell was split in half, indicating a distinct antibacterial mechanism with nisin (**Figure 3C**). For nisin and PLA in combination (**Figure 3D**), a more significant damage was evidenced from collapsed and split cell or even cell debris. These alterations of surface properties in *S. xylosus* revealed that the inhibition of bacterial growth could be due to the disruption in membrane permeability and blocked division of cells, which further confirmed that the combination of nisin and PLA displayed strong antibacterial activity.

Construction of Nisin and PLA Co-producing *L. lactis* Strain

As the combination of nisin and PLA has shown strong antimicrobial activity and exhibited good performance in food preservation, we considered to construct a nisin-PLA co-producing strain, based on the nisin-producing strain *L. lactis* F44. Although F44 had the ability to produce

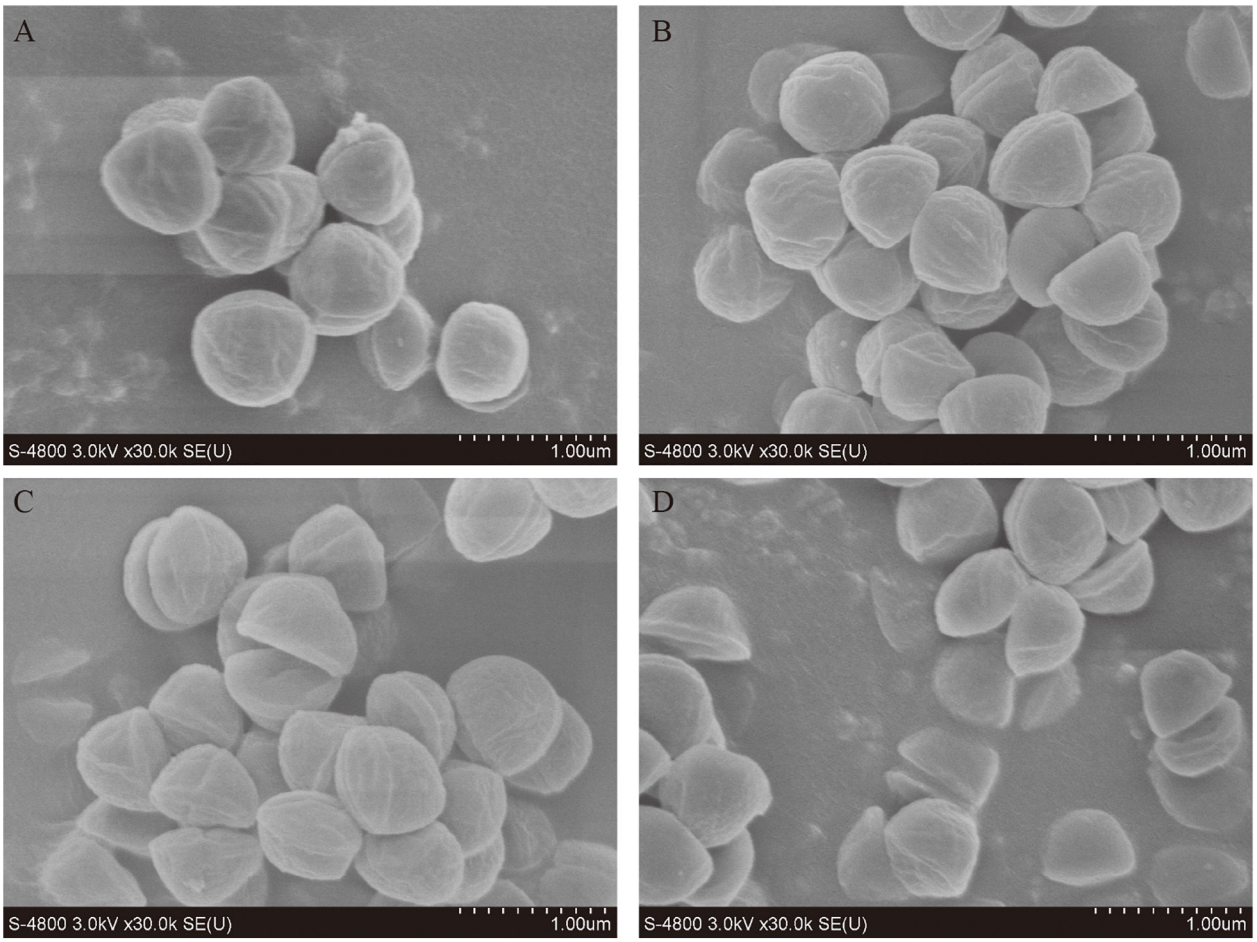

FIGURE 3 | Scanning electron microscopy (SEM) observation of *S. xylosus* treated with nisin and PLA alone and in combination. **(A)** Control cells treated with 0.9% NaCl, **(B)** cells treated with nisin (50 IU/mL), **(C)** cells treated with PLA (5 mg/mL), and **(D)** cells treated with the combination of nisin (50 IU/mL) and PLA (5 mg/mL).

PLA, the yield was only 54 mg/L in our previous work. Then 3 g/L PPA was added into the medium for PLA production. Additionally, a D-LDH mutant (D-LDH^{Y52A}) (Ishikura et al., 2005), which exhibited higher catalytic activity and PPA preference, was also introduced into F44. As shown in **Figure 4**, the PLA yield of F44/P was 0.943g/L, which was dramatically improved compared with that of no PPA added. After the introduction of D-LDH^{Y52A}, the PLA yield of F44/DLDH reached 1.344 g/L which further increased by 42.5% ($p < 0.01$), indicating a key role of D-LDH^{Y52A}. The exogenous PPA was almost used up in the 12 h-fermentation supernatant.

It was considered that LDH in F44 is the L-type, which led to a mixture of L-PLA and D-PLA in the production of F44/DLDH. It motivated us to knock out the two main lactate dehydrogenases LDH and LDHB in F44. The LDH-deficient strain F44ΔLDHΔLDHB was constructed *via* a selection/counter-selection tool based on 5-FOA sensitivity (Solem et al., 2008). And then, a recombinant strain F44ΔLDHΔLDHB/DLDH (**Supplementary Figure S1**) was obtained by overexpression of D-LDH^{Y52A}. An enhanced yield of PLA (1.670 g/L) was detected which had increases of 24.3% ($p < 0.01$) and 77.1% ($p < 0.01$) than F44/DLDH and the control F44/P, respectively. Notably, the recombinant strain F44ΔLDHΔLDHB/DLDH had a considerable production of PLA, and we further explored its antibacterial activity.

Determination of the Bacteriostatic Efficacy of Fermentation Supernatants

The antibacterial activities of fermentation supernatants of nisin and PLA co-producing strains were shown in **Figure 5**. The inhibitory activities of the constructed strains against *S. xylosus* and *M. luteus* were as follows: F44ΔLDHΔLDHB/DLDH > F44/DLDH > F44/P. After the introduction of D-LDH^{Y52A}, the diameters of inhibition zones of F44/DLDH were increased 14.3% ($p < 0.01$) and 7.7% ($p < 0.01$) against *S. xylosus* and *M. Luteus*, respectively, when compared to F44/P. The inhibitory effects were further raised [31.8% ($p < 0.01$) and 29.8% ($p < 0.01$) increases against *S. xylosus* and *M. luteus,* respectively] for F44ΔLDHΔLDHB/DLDH. The antibacterial effect was in accordance with the findings of

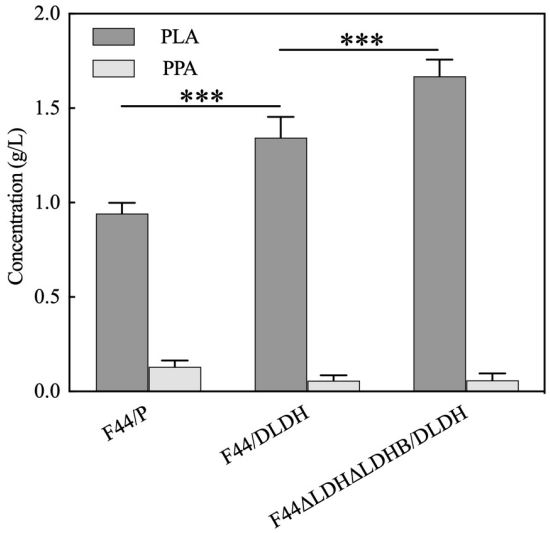

FIGURE 4 | PLA and PPA concentrations of 12 h-culture supernatants of *L. lactis* F44/P and PLA-producing strain F44/DLDH, F44ΔLDHΔLDHB/DLDH. The error bar presented SD indicating the repeatability of the data in three-testing. The data were analyzed by One-way ANOVA. The yield of PLA in strain F44ΔLDHΔLDHB/DLDH was significantly different (***$P < 0.01$) from that in F44/P and F44/DLDH, respectively.

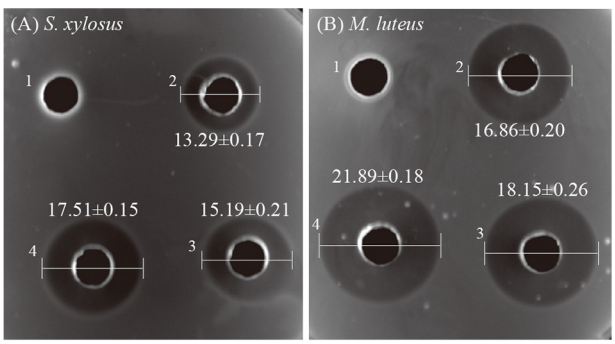

FIGURE 5 | Results of agar-diffusion experiment with the fermentation broths of nisin and PLA co-producing *L. lactis* strains. *S. xylosus* **(A)** and *M. luteus* **(B)** were served as the indicators. The wells (6 mm) of the plates were added with 80 μL of (1) normal saline; (2) *L. lactis* F44/P; (3) *L. lactis* F44/DLDH; and (4) *L. lactis* F44ΔLDHΔLDHB/DLDH. Three repeated measurements were conducted. The differences between the four groups were compared by One-way ANOVA. The diameter of inhibition zone of strain F44ΔLDHΔLDHB/DLDH was significantly different ($P < 0.01$) from that in F44/P, F44/DLDH and control, respectively.

PLA contents of the recombinant strains, revealing a valuable fermentation product of the constructed strains.

DISCUSSION

Nisin, produced by certain *Lactococcus lactis* ssp. *lactis*, is the only bacteriocin allowed to be used as food additive which is generally recognized as safe (GRAS) by FDA. And it has strong inhibitory effect on many Gram-positive bacteria, i.e., food spoilage bacteria and pathogens (Turner et al., 2004; Nguyen and Mittal, 2007; Costas Malvido et al., 2016), contributing to the wide application in food industry as preservative. While nisin exhibited little effect on Gram-negative bacteria or molds. Recently, growing evidence suggested PLA possessed a broad antimicrobial spectrum of activity against both Gram-positive and Gram-negative bacteria (Liu et al., 2020a; Zhou et al., 2020), as well as fungi (Lavermicocca et al., 2003a), especially the D-PLA (Xu et al., 2016), which showed potentials as natural food antiseptic agent (Mu et al., 2012). Moreover, PLA could be cost-effectively produced *via* lactic acid bacteria fermentation.

This research demonstrated the combination of nisin and PLA could provide better antibacterial effect against *M. luteus* and *S. xylosus* (**Figure 1**). Studies suggested that nisin show additive or synergistic effects when used in combination with other antimicrobial agents, such as lysozyme (Chung and Hancock, 2000), lactates (Nykanen et al., 2000), and essential oils (Razavi Rohani et al., 2011), which is consistent with our result. *S. xylosus*, is not only common in fermented meat and milk, but is also one of the main pathogen in clinical infection with strong drug resistance (Martuscelli et al., 2000). This finding may imply their potential applications in food preservation and clinical treatment of bacterial infection. Several studies displayed the mechanism of antibacterial activity of nisin (Tong et al., 2010; Barbosa et al., 2013). Nisin can interact with the cytoplasmic membrane to form transient pores, which allow the efflux of intracellular substances with low molecular weights, such as adenosine triphosphate, amino acids and ions. While the anti-bacterial mechanism of PLA has not been well characterized, although it was suggested that PLA could interrupt the membrane permeability and damage genomic DNA as an intercalator, when investigated in *Listeria monocytogenes* and *E. coli* (Ning et al., 2017). Interestingly, our results first demonstrated a different mode, PLA affected the division of *S. xylosus* which caused the dividing cell to split from the septum (**Figure 3C**), implying divisome as a target. we hypothesized that it was the shape might result in the difference, rod-shaped bacteria and the spherical cocci ones displayed distinct elongation and septation models (Pérez-Núñez et al., 2011), which remained to be investigated. Moreover, in the presented study, it is revealed that nisin and PLA target cell membrane and septum, respectively, indicating a possible synergistic antibacterial efficacy. Generally, the use of nisin and PLA in combination exhibit better antibacterial effects, indicating a positive action. It is a novel combination worth to investigate the potent of practical application as preservative.

Our previous study showed that nisin in cooperation with γ-aminobutytic acid could prolonged the storage of meat and strawberry (Liu et al., 2020b). Combined use of nisin and leucocin C could work effectively against *Listeria monocytogenes* in pasteurized milk (Fu et al., 2018). In this study, the further research on practical application of a combination of nisin and PLA was carried out. For the pork preservation assay, there was no significant difference in the microbial acounts between nisin alone and nisin-PLA in combination until the day 3(**Figure 2A**),

which might be due to the insufficient preservation time (Liu et al., 2020b). We conjectured the combination of nisin and PLA might be more suitable to the long-term preservation of meat, which remained to be discussed further. What was different from the above is that nisin in combination with PLA performed greater anti-microbial activity in the storage of pasteurized milk inoculated with *S. xylosus* and strawberry, compared with nisin and PLA alone (**Figures 2B,C**). It was the result that PLA presented better inhibitory activity against *S. xylosus* than nisin contributing for pasteurized milk storage. Additionally, PLA can also inhibit the growth of mold to some extent (Lavermicocca et al., 2003a), which was the key factor resulting in the rot of strawberry. Although some literatures on the PLA production and function have been reported (Nykanen et al., 2000; Zhang and Li, 2018), few presented the combined use of nisin and PLA. Our results promised a combinational effect of nisin and PLA on the antimicrobial activity during food preservation. The combination of nisin and PLA exhibited a potential candidate as food preservative, as well as an expanded scope of application.

As the limitation of the low cost-efficient, no pure nisin was commercially available. Nisaplin, the first commercial preparation, contains only 2.5% (w/w) nisin which is usually the fermentation product. In more cases, the fermentation broth of nisin is immediately applied for its "food-grade quality" producer (Barbosa et al., 2017), which to a certain extent lowers the cost. The food-grade strain *L. lactis* F44, because of its nisin production capacity, was used to construct the nisin-PLA co-expression strain, and a new antimicrobial agent PLA was induced into this fermented broth. The results of PLA content determination and antibacterial assay verified that the recombinant strains can successfully produce PLA (**Figure 4**) and the fermented broth with higher PLA content presented superior inhibitory effects against *S. xylosus* and *M. luteus* (**Figure 5**). It demonstrated that the F44ΔLDHΔLDHB/DLDH was more suitable for commercial application in industrial fermentation.

The biosynthetic pathway of PLA is initiated from phenylalanine which was converted to PPA by transaminase and then was further reduced into PLA by LDH in LAB (Lavermicocca et al., 2003a). Our results showed that the addition of PPA in the culture significantly increased the yield of PLA (0.054 g/L for no addition and 0.943 g/L for 3 g/L PPA) in F44/P, implying a serious shortage of biosynthesis of PPA in F44, which is in accordance with the previous literature of Zhang et al. (Zhang et al., 2014a). In addition, LDH is also a key for the improvement of PLA production and various activity gives rise to the disparity in PLA production (Li et al., 2008). Interestingly, D-PLA has a better performance against microbials than L-PLA (Xu et al., 2016). These findings revealed that the introduction of D-LDH^{Y52A} in F44 significantly improved the conversion rate of PPA to PLA (an increase of 42.5%). However, only L-LDH exists in F44, which leads to a mixture of L-PLA and D-PLA in the fermentation broth of F44/DLDH. Then, we deleted the two main LDH (LDH and LDHB) in F44 and induced D-LDH^{Y52A}, where L-PLA could be reduced to a considerable extent, and a further 24.3% increase of PLA yield was obtained for F44ΔLDHΔLDHB/DLDH. Notably this study was a first preliminary attempt to endow a nisin-producing *L. lactis* strain with capacity of PLA synthesis using PPA as substrate. Since the synthesis of nisin is not involved in central carbon metabolism in *L. lactis*, further studies on realizing *de novo* synthesis of PLA from glucose was recommended to make co-production of nisin and PLA more cost effective.

CONCLUSION

This study found that the cooperation of nisin and PLA performed a significant antibacterial activity and exhibited high potential as food preservative. Moreover, it is the first study to construct the nisin and PLA co-expressing engineered *L. lactis* and the fermentation product was demonstrated to be effective against bacteria. In contrast with nisin, PLA showed a different mode of action, contributing to the combinational antibacterial activity of nisin and PLA. The present study describes the potent application of the engineered *L. lactis* co-produing nisin and PLA, and gives insight to the development of natural food preservatives.

DATA AVAILABILITY STATEMENT

The original contributions presented in the study are included in the article/**Supplementary Material**, further inquiries can be directed to the corresponding author/s.

AUTHOR CONTRIBUTIONS

JQ and JL designed the experiment and guided the writing. QS and RH performed the major experiments and wrote the manuscript. HX, JM, and RX provided the additional experimental assistance and helped to revise the manuscript. All authors contributed to the article and approved the submitted version.

FUNDING

This research was financially supported by the National Natural Science Foundation of China (31770076, 32070073, and 31900029), the National Key Research and Development Project of China (2017YFD0201400), the Funds for Creative Research Groups of China (21621004), and the Opening Project of Key Laboratory of Storage of Agricultural Products (KF2018003).

SUPPLEMENTARY MATERIAL

The Supplementary Material for this article can be found online at: https://www.frontiersin.org/articles/10.3389/fbioe.2021.612105/full#supplementary-material

REFERENCES

Barbosa, A. A., Silva, de Araujo, H. G., Matos, P. N., Carnelossi, M. A., Almeida, et al. (2013). Effects of nisin-incorporated films on the microbiological and physicochemical quality of minimally processed mangoes. *Int. J. Food Microbiol.* 164, 135–140. doi: 10.1016/j.ijfoodmicro.2013.04.004

Barbosa, A. A. T., Mantovani, H. C., and Jain, S. (2017). Bacteriocins from lactic acid bacteria and their potential in the preservation of fruit products. *Crit. Rev. Biotechnol.* 37, 852–864. doi: 10.1080/07388551.2016.1262323

Chatterjee, A., and Abraham, J. (2017). Microbial contamination, prevention, and early detection in food industry. *Microb. Contaminat. Food Degrad.* 2017, 0–2. doi: 10.1016/B978-0-12-811515-2.00002-0

Chatterjee, C., Pau, M., Xie, L., and Donk, W. A. V. D. (2005). Biosynthesis and mode of action of lantibiotics. *Chem. Rev.* 105, 633–683. doi: 10.1021/cr030105v

Chung, W., and Hancock, E. W. R. (2000). Action of lysozyme and nisin mixtures against lactic acid bacteria. *Int. J. Food Microbiol.* 60, 25–32.

Cleveland, J., Chikindas, M., and Montville, T. J. (2002). Multimethod assessment of commercial nisin preparations. *J. Ind. Microbiol. Biotechnol.* 29, 228–232. doi: 10.1038/sj.jim.7000315

Costas Malvido, M., Alonso Gonzalez, E., and Perez Guerra, N. (2016). Nisin production in realkalized fed-batch cultures in whey with feeding with lactose- or glucose-containing substrates. *Appl. Microbiol. Biotechnol.* 100, 7899–7908. doi: 10.1007/s00253-016-7558-9

Cotter, P. D., Hill, C., and Ross, R. P. (2005). Bacteriocins: developing innate immunity for food. *Nat. Rev. Microb.* 3, 777–778. doi: 10.1038/nrmicro1273

de Oliveira Pateis, V., Bracht, L., Dos Santos, Castro, L., Bueno Franco, Salla, G., et al. (2018). The food additive BHA modifies energy metabolism in the perfused rat liver. *Toxicol. Lett.* 299, 191–200. doi: 10.1016/j.toxlet.2018.10.005

Dieuleveux, V., Pyl, D. V. D., Chataud, J., and Gueguen, M. (1998). Purification and Characterization of Anti-Listeria Compounds Produced by Geotrichum candidum. *Appl. Environ. Microbiol.* 64, 800–803. doi: 10.1128/AEM.64.2.800-803.1998

Fu, Y., Mu, D., Qiao, W., Zhu, D., Wang, X., Liu, F., et al. (2018). Co-expression of Nisin Z and Leucocin C as a Basis for Effective Protection Against *Listeria monocytogenes* in Pasteurized Milk. *Front. Microbiol.* 9:547. doi: 10.3389/fmicb.2018.00547

Gharsallaoui, A., Oulahal, N., Joly, C., and Degraeve, P. (2015). Nisin as a Food Preservative: Part 1: Physicochemical Properties, Antimicrobial Activity, and Main Uses. *Crit. Rev. Food Sci. Nutrit.* 56, 1262–1274. doi: 10.1080/10408398.2013.763765

Ishikura, Y., Tsuzuki, S., Takahashi, O., Tokuda, C., Nakanishi, R., Shinoda, T., et al. (2005). Recognition site for the side chain of 2-ketoacid substrate in d-lactate dehydrogenase. *J. Biochem.* 138, 741–749. doi: 10.1093/jb/mvi170

Juturu, V., and Wu, J. C. (2018). Microbial production of bacteriocins: Latest research development and applications. *Biotechnol. Adv.* 36, 2187–2200. doi: 10.1016/j.biotechadv.2018.10.007

KBauera, A., Dwyer-Nield, L. D., Hankin, J. A., CMurphy, R., and MMalkinson, A. (2001). The lung tumor promoter, butylated hydroxytoluene (BHT), causes chronic inflammation in promotion-sensitive BALB:cByJ mice but not in promotion-resistant CXB4 mice. *Toxicology* 169, 1–15.

Komitopoulou, E., Boziaris, I. S., Davies, E. A., Delves−Broughton, J., and Adams, M. R. (2001). *Alicyclobacillus acidoterrestris* in fruit juices and its control by nisin. *Int. J. Food Technol.* 2001:34.

Lavermicocca, P., Valerio, F., Evidente, A., Lazzaroni, S., Corsetti, A., and Gobbetti, M. (2000). Purification and characterization of novel antifungal compounds from the sourdough Lactobacillus plantarum strain 21B. *Appl. Environ. Microbiol.* 66, 4084–4090. doi: 10.1128/aem.66.9.4084-4090.2000

Lavermicocca, P., Valerio, F., and Visconti, A. (2003a). Antifungal activity of phenyllactic acid against molds isolated from bakery products. *Appl. Environ. Microbiol.* 69, 634–640. doi: 10.1128/aem.69.1.634-640.2003

Lavermicocca, P., Valerio, F., and Visconti, A. (2003b). Antimicrobial effectiveness of Phenyllactic acid against foodborne pathogenic bacteria and Penicillium and Aspergillus molds. *Appl. Environ. Microb.* 69, 634–640.

Li, X., Jiang, B., Pan, B., Mu, W., and Zhang, T. (2008). Purification and Partial Characterization of *Lactobacillus* Species SK007 Lactate Dehydrogenase (LDH) Catalyzing Phenylpyruvic Acid (PPA) Conversion into Phenyllactic Acid (PLA). *J. Agricul. Food Chem.* 56:2392.

Liu, F., Sun, Z., Wang, F., Liu, Y., Zhu, Y., Du, L., et al. (2020a). Inhibition of biofilm formation and exopolysaccharide synthesis of *Enterococcus faecalis* by phenyllactic acid. *Food Microbiol.* 86:103344. doi: 10.1016/j.fm.2019.103344

Liu, F., Wang, F., Du, L., Zhao, T., Doyle, M. P., Wang, D., et al. (2018). Antibacterial and antibiofilm activity of phenyllactic acid against *Enterobacter cloacae*. *Food Control.* 84, 442–448. doi: 10.1016/j.foodcont.2017.09.004

Liu, J., Meng, F., Du, Y., Nelson, E., Zhao, G., Zhu, H., et al. (2020b). Co-production of Nisin and γ-Aminobutyric Acid by Engineered *Lactococcus lactis* for Potential Application in Food Preservation. *Front. Microb.* 11:00049. doi: 10.3389/fmicb.2020.00049

Martuscelli, M., Crudele, M. A., Gardini, F., and Suzzi, G. (2000). Biogenic amine formation and oxidation by *Staphylococcus xylosus* strains from artisanal fermented sausages. *Lett. Appl. Microb.* 31, 228–232.

Mu, W., Yu, S., Zhu, L., Zhang, T., and Jiang, B. (2012). Recent research on 3-phenyllactic acid, a broad-spectrum antimicrobial compound. *Appl. Microbiol. Biotechnol.* 95, 1155–1163. doi: 10.1007/s00253-012-4269-8

Nguyen, P., and Mittal, G. S. (2007). Inactivation of naturally occurring microorganisms in tomato juice using pulsed electric field (PEF) with and without antimicrobials. *Chem. Eng. Proc. Process Inten.* 46, 360–365. doi: 10.1016/j.cep.2006.07.010

Ning, Y., Yan, A., Yang, K., Wang, Z., Li, X., and Jia, Y. (2017). Antibacterial activity of phenyllactic acid against *Listeria monocytogenes* and *Escherichia coli* by dual mechanisms. *Food Chem.* 228, 533–540. doi: 10.1016/j.foodchem.2017.01.112

Nykanen, A., Weckman, K., and Lapvetelainen, A. (2000). Synergistic inhibition of *Listeria monocytogenes* on cold-smoked rainbow trout by nisin and sodium lactate. *Int. J. Food Microb.* 61, 63–72.

Ohhira, I., Kuwaki, S., Morita, H., Suzuki, T., Tomita, S., Hisamatsu, S., et al. (2010). Identification of 3-Phenyllactic Acid As a Possible Antibacterial Substance Produced by *Enterococcus faecalis* TH 10. *Biocontrol Sci.* 9, 77–81. doi: 10.4265/bio.9.77

Olaimat, A. N., and Holley, R. A. (2012). Factors influencing the microbial safety of fresh produce: a review. *Food Microbiol.* 32, 1–19. doi: 10.1016/j.fm.2012.04.016

Pérez-Núñez, D., Briandet, R., David, B., Gautier, C., Renault, P., Hallet, B., et al. (2011). A new morphogenesis pathway in bacteria: unbalanced activity of cell wall synthesis machineries leads to coccus-to-rod transition and filamentation in ovococci. *Mole. Microb.* 79, 759–771. doi: 10.1111/j.1365-2958.2010.07483.x

Przybylski, R., Firdaous, L., Chataigne, G., Dhulster, P., and Nedjar, N. (2016). Production of an antimicrobial peptide derived from slaughterhouse by-product and its potential application on meat as preservative. *Food Chem.* 211, 306–313. doi: 10.1016/j.foodchem.2016.05.074

Razavi Rohani, S. M., Moradi, M., Mehdizadeh, T., Saei-Dehkordi, S. S., and Griffiths, M. W. (2011). The effect of nisin and garlic (*Allium sativum L.*) essential oil separately and in combination on the growth of *Listeria monocytogenes*. *LWT - Food Sci. Technol.* 44, 2260–2265. doi: 10.1016/j.lwt.2011.07.020

Schwenninger, S. M., Lacroix, C., Truttmann, S., Jans, C., Spörndli, C., Bigler, L., et al. (2008). Characterization of low-molecular-weight antiyeast metabolites produced by a food-protective Lactobacillus-Propionibacterium coculture. *J. Food Prot.* 71, 2481–2487. doi: 10.4315/0362-028x-71.12.2481

Solem, C., Defoor, E., Jensen, P. R., and Martinussen, J. (2008). Plasmid pCS1966, a new selection/counterselection tool for lactic acid bacterium strain construction based on the oroP gene, encoding an orotate transporter from *Lactococcus lactis*. *Appl. Environ. Microbiol.* 74, 4772–4775. doi: 10.1128/AEM.00134-08

Sorrentino, E., Tremonte, P., Succi, M., Iorizzo, M., Pannella, G., Lombardi, S. J., et al. (2018). Detection of Antilisterial Activity of 3-Phenyllactic Acid Using *Listeria innocua* as a Model. *Front. Microbiol.* 9:1373. doi: 10.3389/fmicb.2018.01373

Tong, Z., Dong, L., Zhou, L., Tao, R., and Ni, L. (2010). Nisin inhibits dental caries-associated microorganism in vitro. *Peptides* 31, 2003–2008. doi: 10.1016/j.peptides.2010.07.016

Turner, S. R., Love, R. M., and Lyons, K. M. (2004). An in-vitro investigation of the antibacterial effect of nisin in root canals and canal wall radicular dentine. *Int. Endodontic J.* 37, 664–671.

Valerio, F., Lavermicocca, P., Pascale, M., and Visconti, A. (2004). Production of phenyllactic acid by lactic acid bacteria: an approach to the selection of strains contributing to food quality and preservation. *FEMS Microbiol. Lett.* 233, 289–295. doi: 10.1016/j.femsle.2004.02.020

Wu, H., Xue, E., Zhi, N., Song, Q., Kairen, T., Caiyin, Q., et al. (2020). D-Methionine and D-Phenylalanine Improve *Lactococcus lactis* F44 Acid Resistance and Nisin Yield by Governing Cell Wall Remodeling. *Appl. Environ. Microb.* 86, e2981–e2919. doi: 10 .1128/AEM.02981-19

Xu, G.-C., Zhang, L.-L., and Ni, Y. (2016). Enzymatic preparation of d-phenyllactic acid at high space-time yield with a novel phenylpyruvate reductase identified from *Lactobacillus s*p. CGMCC 9967. *J. Biotechnol.* 222, 29–37. doi: 10.1016/j.jbiotec.2015.12.011

Zhang, J., and Li, X. (2018). Novel strategy for phenyllactic acid biosynthesis from phenylalanine by whole cell recombinant *Escherichia coli* coexpressing L-phenylalanine oxidase and L-lactate dehydrogenase. *Biotechnol. Lett.* 40, 165–171. doi: 10.1007/s10529-017-2456-5

Zhang, X., Zhang, S., Shi, Y., Shen, F., and Wang, H. (2014a). A new high phenyl lactic acid-yielding *Lactobacillus plantarum* IMAU10124 and a comparative analysis of lactate dehydrogenase gene. *FEMS Microb. Lett.* 356, 89–96. doi: 10.1111/1574-6968.12483

Zhang, Y. F., Liu, S. Y., Du, Y. H., Feng, W. J., Liu, J. H., and Qiao, J. J. (2014b). Genome shuffling of *Lactococcus lactis* subspecies *lactis* YF11 for improving nisin Z production and comparative analysis. *J. Dairy Sci.* 97, 2528–2541. doi: 10.3168/jds.2013-7238

Zhou, Q., Gu, R., Li, P., Lu, Y., Chen, L., and Gu, Q. (2020). Anti-*Salmonella* mode of action of natural L-phenyl lactic acid purified from *Lactobacillus plantarum* ZJ316. *Appl. Microbiol. Biotechnol.* 104, 5283–5292. doi: 10.1007/s00253-020-10503-4

Conflict of Interest: The authors declare that the research was conducted in the absence of any commercial or financial relationships that could be construed as a potential conflict of interest.

frontiers in Bioengineering and Biotechnology

ORIGINAL RESEARCH
published: 03 March 2021
doi: 10.3389/fbioe.2021.622835

Gene-Trait Matching and Prevalence of Nisin Tolerance Systems in *Lactococcus lactis*

*Lieke A. van Gijtenbeek†, Thomas H. Eckhardt†‡, Lucía Herrera-Domínguez†, Elke Brockmann, Kristian Jensen, Asger Geppel, Kristian Fog Nielsen, Jannik Vindeloev, Ana Rute Neves‡ and Gunnar Oregaard**

R&D, Chr. Hansen A/S, Hørsholm, Denmark

Lactococcus lactis cheese starter cultures typically contain a mix of many strains and may include variants that produce and/or tolerate the antimicrobial bacteriocin nisin. Nisin is well-established as an effective agent against several undesirable Gram-positive bacteria in cheese and various other foods. In the current study, we have examined the effect of nisin on 710 individual *L. lactis* strains during milk fermentations. Changes in milk acidification profiles with and without nisin exposure, ranging from unaltered acidification to loss of acidification, could be largely explained by the type(s) and variants of nisin immunity and nisin degradation genes present, but surprisingly, also by genotypic lineage (*L. lactis* ssp. *cremoris* vs. ssp. *lactis*). Importantly, we identify that nisin degradation by NSR is frequent among *L. lactis* and therefore likely the main mechanism by which dairy-associated *L. lactis* strains tolerate nisin. Insights from this study on the strain-specific effect of nisin tolerance and degradation during milk acidification is expected to aid in the design of nisin-compatible cheese starter cultures.

Keywords: high-throughput screening, milk acidification, nisin degradation, nisin tolerance, nisin biosynthesis, NSR, *Lactococcus lactis,* gene-trait matching

OPEN ACCESS

Edited by:
Jian-Ming Liu, Technical University of Denmark, Denmark

Reviewed by:
Per Erik Joakim Saris, University of Helsinki, Finland
Jiaheng Liu, Tianjin University, China
Helge Holo, Norwegian University of Life Sciences, Norway

***Correspondence:**
Gunnar Oregaard
dkgor@chr-hansen.com

†These authors have contributed equally to this work

‡Present address:
Thomas H. Eckhardt, DSM Food Specialties, Wageningen, Netherlands
Ana Rute Neves, Arla Foods Ingredients P/S, Videbaek, Denmark

Specialty section:
This article was submitted to Synthetic Biology, a section of the journal Frontiers in Bioengineering and Biotechnology

Received: *29 October 2020*
Accepted: *22 January 2021*
Published: *03 March 2021*

Citation:
van Gijtenbeek LA, Eckhardt TH, Herrera-Domínguez L, Brockmann E, Jensen K, Geppel A, Nielsen KF, Vindeloev J, Neves AR and Oregaard G (2021) Gene-Trait Matching and Prevalence of Nisin Tolerance Systems in Lactococcus lactis. Front. Bioeng. Biotechnol. 9:622835. doi: 10.3389/fbioe.2021.622835

INTRODUCTION

Lactococcus lactis is a lactic acid bacterium widely used in the dairy industry for milk fermentation. Some *L. lactis* strains produce the Class I bacteriocin nisin, a 34 amino-acid-long peptide that shows potent antimicrobial activity against a broad range of Gram-positive bacteria (Mattick and Hirsch, 1947; Gross and Morell, 1971). Nisin is heat-resistant and acid-tolerant, largely because of a set of stable post-translational modifications (Delves-Broughton, 1996). Nisin in powder format was first introduced to the market in the 1950's as a natural product to contribute to shelf-life extensions of cheese by preventing growth of food spoilage organisms including *Clostridi*a, *Propionibacteria* and *Listeria* (Hirsch, 1951; Delves-Broughton, 1996; Molloy et al., 2011). Nisin-producing strains can be added or are naturally present in cheese starter cultures (Delves-Broughton, 1996; de Arauz et al., 2009; Ávila et al., 2014).

To match the increasing demands of the dairy industry, new starter cultures are constantly being developed by either blending traditional undefined cultures or targeted culture design (Ayad et al., 2001). Starter cultures for semi-hard cheeses like Gouda or Edam are typically composed of a mixture of lactococcal strains, including *Lactococcus lactis* ssp. *lactis* and *Lactococcus lactis* ssp. *cremoris,* and *Leuconostoc* strains (Erkus et al., 2013; Düsterhöft et al., 2017). Differences in strain

composition and diversity of the starter culture impact robustness toward phage attack, acidification, eye-formation, flavor development, and rheological properties of the cheese. Hence, it is crucial to understand how the starter culture composition and subsequently the cheese quality is affected by different factors. *L. lactis* strains devoid of nisin immunity or degradation machineries are highly susceptible to nisin. We therefore hypothesized that presence of nisin may inhibit *L. lactis* cheese culture strains to different extents depending on the genetic blueprint of the strains, e.g., presence of nisin immunity and/or nisin degradation genes in each strain.

Nisin exerts multiple modes of action against bacteria. Small amounts of nisin can be sufficient to hinder cell division by binding to and subsequent displacement of lipid II molecules, which are essential precursors required for bacterial cell wall synthesis (Brötz et al., 1998; Breukink et al., 1999; Wiedemann et al., 2001; Hasper et al., 2006). When nisin concentrations increase, it assembles together with lipid II into membrane pore-forming entities (Hasper et al., 2004). At even higher concentrations, nisin molecules are also known to self-assemble into pores without the requirement for lipid II (Sahl et al., 1987; Breukink et al., 1999). Pore formation results in the dissipation of proton motive force, cytoplasm leakage including the release of autolysins, and eventually cell death (Bierbaum and Sahl, 1985; Breukink et al., 1999; MartÃnezCuesta et al., 2000). Nisin also prevents the outgrowth of bacterial spores, presumably by lipid II binding and pore formation (Egan et al., 2016 and references therein). Since nisin targets any bacterial cytoplasmic membrane including that of *L. lactis* itself, nisin-producing *L. lactis* strains co-express proteins that confer nisin autoimmunity. These are NisI, a membrane associated lipoprotein, and NisFEG, an ABC transporter (Kuipers et al., 1993; Engelke et al., 1994; Qiao et al., 1995; Siegers and Entian, 1995). Extracellular NisI binds nisin thereby abolishing pore formation (Takala et al., 2004; AlKhatib et al., 2014a; Hacker et al., 2015). Recently, it was shown that NisI also functions in cell aggregation thereby reducing accessibility to lipid II even more (AlKhatib et al., 2014a). NisFEG forms an efflux pump that translocates nisin from the membrane into the extracellular space (Stein et al., 2003). NisI and NisFEG have a synergistic effect and enable *L. lactis* cells to tolerate high levels of nisin (up to 700 nM, ∼2.35 mg L^{-1}), which drops to 10–30% when expressed separate from each other (Kuipers et al., 1993; Qiao et al., 1995; Duan et al., 1996; Ra et al., 1996, 1999; Stein et al., 2003; AlKhatib et al., 2014a,b).

Nisin production and immunity by *L. lactis* strains are established by a conserved biosynthesis gene cassette consisting of four transcriptional units, *nisABTCIPRK, nisI, nisRK,* and *nisFEG* (Kuipers et al., 1993; Ra and Saris, 1995; de Ruyter et al., 1996; Ra et al., 1996; Li and O'Sullivan, 2006; Trmčić et al., 2011) The *nisA* gene encodes the nisin bacteriocin of which several variants have been reported (A, Z, F, and Q) in *L. lactis* (Mulders et al., 1991; De Kwaadsteniet et al., 2008; Fukao et al., 2008). The transcription of the nisin biosynthesis and autoimmunity operons (*nisABTCIPRK* and *nisFEG*) is activated through a nisin-mediated positive feedback loop conducted by the two-component system NisRK (Kuipers et al., 1995; de Ruyter et al., 1996; Kleerebezem et al., 1997). Due to this positive autoregulation, strains that carry the complete nisin biosynthesis cassette are locked in a nisin-producing state. The two other transcriptional units, *nisI* and *nisRK,* are driven by a weak and a relatively strong constitutive promoter, respectively, that function in the absence of nisin (de Ruyter et al., 1996; Li and O'Sullivan, 2006). However, both are believed to be trivial in nisin-producing strains as transcription from the *nisA* promoter overrules the effect of the internal operator sites.

In addition to *nisI* and *nisFEG*, a third nisin resistance determinant (*nsr*) was mapped to certain plasmids in non-nisin producing lactococci (McKay and Baldwin, 1984; Froseth and McKay, 1991; Liu et al., 1997). Already in 1984, it was suggested that the product of this gene might function as a nisinase, a nisin degrading enzyme previously discovered in *Streptococcus thermophilus* (Alifax and Chevalier, 1962). Over a quarter of a century later, it was confirmed that NSR is a tail-specific membrane-bound protease that cleaves nisin Z after the 28th position (Sun et al., 2009). This renders the remaining peptide close to inactive through a significant reduction in membrane affinity and pore-forming capacity (Sun et al., 2009). Over the years, similar membrane-associated proteases have been identified in Gram-positive species (Khosa et al., 2013; Draper et al., 2015). One of these is the well-characterized *Streptococcus agalactiae* nisin resistance protein SaNSR of which its structure has been resolved (Khosa et al., 2015). While the IC_{50} of a nisin-sensitive *L. lactis* strain overexpressing NisI is 5-to-10-fold greater than the wild type, SaNSR overexpression in the same cells enabled cells to withstand up to 18-to-20-fold more nisin (Khosa et al., 2013).

To investigate the potential effect of nisin on *L. lactis* strains, we initiated a study directed at evaluating the effect of nisin on the individual acidification profiles of 710 individual *L. lactis* strains, from which many are derived or used in common starter cultures. By genome sequencing and PCR, we correlated the observed acidification profiles with the presence or absence of nisin immunity and degradation genes, concurrently giving insights in the collection-wide distribution of such elements. Furthermore, nisin production and degradation was measured using a newly developed high-throughput HPLC-MS/MS method, which enabled us to elucidate the nisin degradation capacity of each strain during milk fermentations.

MATERIALS AND METHODS

Strains and Growth Conditions

A total of 710 proprietary *L. lactis* strains originating from the Chr. Hansen Culture Collection were used in this study, for details see **Supplementary Table 1**. The strains were routinely grown as standing cultures in Oxoid M17 (Thermo Fisher Scientific, Waltham, MA, USA) with glucose 0.5% (w/v) (GM17) or a mixture of 1% (w/v) glucose and 1% (w/v) lactose (GLM17) at 30°C for 18 h.

Genome Sequencing and Analyses

All 710 strains were subjected to whole-genome sequencing on an Illumina MiSeq, yielding reads of 250 bases. The reads were assembled into contigs using CLC Genomics Workbench

(Qiagen, Århus, Denmark). Contigs with a mean depth of coverage <0.25 of the total mean depth of coverage were discarded as contaminants. A gene search was conducted in all 710 genomes to map the presence of genes encoding nisin-related proteins. The query sequences used in the gene search can be found in **Supplementary Table 2**. The genomes were searched using blastn and tblastn for nucleotide sequence and protein sequence queries, respectively, with an *E*-value cut-off of 0.01. A gene was considered present in a genome if a hit with more than 90% query coverage and 80% identity was found. After observing nisin degradation in strains where no *nsr* gene was detected, it was found that some strains had shorter versions of *nsr*. To identify such variants, we repeated the tblastn search for the *nsr* protein sequence while reducing the query coverage threshold to 20% (Schliep, 2011). Whole genome k-mer trees [K-mer length: 16, prefix: AT, distance function: Feature Frequency Profile *via* Jensen-Shannon divergences (FFP)] of the 710 draft genomes and 219 RefSeq genomes were calculated using the Microbial Genomics module of the CLC Genomics workbench. A newly developed MLST scheme was employed including the household genes *dnaK*, *fusA*, *groEL*, *gyrA*, *gyrB*, *ileS*, *lep*, *pheS*, *recA*, *rpoA*, *rpoB*, and *rpoC* (see **Supplementary File 1** for sequences of indicated genes for all strains). Concatenated sequences of the twelve genes were used to calculate a maximum likelihood tree with the Phangorn package I (Schliep, 2011) in R software. Due to quality requirements, a total of 206 instead of 219 *L. lactis* RefSeq genomes were taken along in the MLST analysis. Both k-mer and MLST trees were plotted with iTOLv5.5 (Letunic and Bork, 2019).

Milk Acidification Profiles With and Without Nisin

Cell-free supernatants (CFS) with or without nisin were obtained from 500 mL GLM17 cultures of *L. lactis* well-studied strains ATCC11454 or Wg2, respectively, by centrifugation for 5 min at 5,000×*g*. Collected supernatant was adjusted to pH 6.0 by the addition of 0.25 M NaOH, filter-sterilized using a Minisart® 0.22 μm filter (Sartorius, Göttingen, Germany) and stored at −80°C in 10 mL aliquots. CFS of Wg2 yielded 0.0 μg ml^{-1} nisin A, whereas CFS of ATCC 11454 yielded 6.1 ± 0.8 μg ml^{-1} nisin A, as measured using the HPLC-MS/MS method detailed below. The two CFS types were subsequently used to evaluate the milk acidification profiles of the 710 *Lactococcus* strains as follows. A volume of 20 μl fresh overnight culture of each *L. lactis* strain grown in GLM17 in a 96-wells microtiter plate was used to inoculate 1,980 μl prewarmed (30°C) pasteurized semi-skimmed milk supplemented with 0.2% (w/v) yeast extract and 5% (v/v) pH indicator solution (1 g L^{-1} Bromocresol Purple sodium salt (Sigma Aldrich, St. Louis, MS, United States); 1 g L^{-1} Bromocresol Green sodium salt (Sigma Aldrich), pH 7.0, filtered-sterilized). One hundred and fifty microliter of each of the 710 inoculated milk samples were then mixed with 50 μl of one of the two CFS types described above, resulting in a final nisin A concentration of 0.0 or 1.5 μg ml^{-1}, and incubated for 18 h at 30°C on flatbed scanners (HP ScanJet G4010) to obtain HUE-values every 6 min. Acidification profiles were obtained by converting HUE-values into pH values as described previously (Poulsen et al., 2019). Experiments with CFS from Wg2 and ATCC 11454 were always run in parallel and the experiments were performed in triplicates: one technical and two biological replicates.

Analysis of Milk Acidification Profiles

As mentioned above, inoculation material for the milk acidifications originated from overnight cultures with different biomass and pH, which caused small changes in both initial and end pH, as well as the time for the acidification to start. Therefore, in order to define robust thresholds for phenotypic classification, the acidification curves were first normalized to the same maximum (initial) pH of 6.4. The pH values were re-scaled by setting the minimum and maximum pH for each pair of curves per strain to 0 and 1, respectively. Next, curves were also normalized in time so that starting timepoint of each pair of acidification curves was the same across replicates. The starting time was calculated per replicate using the milk acidification curve that had no nisin. This starting point was then subtracted across all timepoints from each pair of curves. Finally, absolute change in pH, area under the curve and starting timepoint for each curve and condition were calculated and averaged across replicates. These parameters were used to define the four different phenotypes. For detailed description on the data processing steps see **Supplementary Table 3**. Data and statistical analyses were performed using the computing environment R. Raincloud plots were made according to Allen et al. (2019). The central matrix layout was used using the UpSet package (Gu et al., 2016).

Detection of Nisin A and Nisin$^{1-28}$ by HPLC-MS/MS in Culture CFS

To set up a detection method for full-length and NSR-degraded nisin A, CFS was collected from *L. lactis* strains CH-1 (*nisA*–, *nsr*+) and ATCC 11454 (*nisA*+, *nsr*–) grown in GM17 spiked with 0.9 μg ml^{-1} nisin A (Chrisin®, Chr. Hansen A/S, Denmark). Chrisin® was shown to be 2.26% pure when compared to nisin A from Sigma-Aldrich (defined as 2.5% by FAO, 2013). Sterile GM17 spiked with 0.9 μg/ml nisin A was taken along as a blank control sample. A 30 μL sample from each CFS was then mixed in 1.5 mL Eppendorf tubes with 870 μL extraction buffer to which nisin Q was introduced as an internal standard (IS) to improve the precision of the assay. Nisin Q was chosen to get: (i) an as similar molecule to nisin A as possible; (ii) an IS not interfering with nisin A measurements; and (iii) an IS also susceptible to NSR degradation. The extraction buffer containing nisin Q was made as follows: CFS collected from a culture of the nisin Q-producing CH-5 strain grown in GM17 was quenched by adding 3% (v/v) acetonitrile (ACN) and 1% (v/v) formic acid (FA). 1.5 ml of this extract was then added to 100 ml of extraction buffer consisting of 100 mg/L Bovine Serum Albumin (BSA; A-2153, Sigma), 20% (v/v) ACN and 0.5% (v/v) FA dissolved in MilliQ water. The extracts were transferred to polypropylene HPLC vials, and nisin A, nisin Q, and nisin$^{1-28}$ (nisin A degraded by NSR) levels were analyzed on a binary ACQUITY UPLC system (Waters, Milford, MA, USA) equipped with a sample organizer (held at 8°C) and connected to a Xevo

TQ-XS Triple Quadrupole Mass Spectrometry (MS) instrument (Waters) equipped with an Electrospray source operated in positive mode. One microliter subsamples were injected onto a PLRP-S 300 Å, 2.1 × 150 mm, 3 μm HPLC column (Agilent Technologies, Waldbronn, Germany) held at 60°C and eluted using a linear gradient of 25–40% (v/v) ACN with 0.1% (v/v) FA using a flow rate of 0.5 mL min^{-1}. The following MS conditions were applied: Capillary voltage: 3 kV, collision gas (Ar), desolvation temperature: 550°C, desolvation gas flow: 1,100 L/h, cone flow: 150 L/h, nebulizer: 6 bar. For all analytes the cone was held at 40 V and a fragmentation energy of 16 eV. Waters TargetLynx Software was used for data analysis and peak integration. The following multiple reaction monitoring (MRM) fragmentations, with a dwell time of 20 ms, were used for detection: (1) the $[M+5H]^{5+}$ ion of nisin A from *m/z* 671.7 to 811.2, (2) the $[M+5H]^{5+}$ ion of nisin Q from *m/z* 666.2 to 804.4, and (3) the $[M+4H]^{4+}$ ion of $nisin^{1-28}$ *m/z* 680.55–869.7). $Nisin^{1-28}$ eluted ∼0.35 min later than nisin A but 0.29 min earlier than nisin Q. From calibrants with constant nisin Q and variable nisin A concentrations, the nisin A peak areas, divided by the peak area of the nisin Q peak area, was used to determine the nisin A concentrations. From a degradation of nisin A with cell free NSR culture extract, the response factor difference between nisin A and $nisin^{1-28}$ was estimated to approximate $nisin^{1-28}$ concentrations in ATCC 11454 and CH-1 CFS. This method was also used to obtain the nisin A concentrations in the CFS of ATCC 11454 and Wg2 added during the milk acidification experiment.

High-Throughput Detection of Nisin Degradation and Nisin A Production by *L. lactis* Strains

Nisin degradation and nisin A production by each of the 710 *L. lactis* strains was assessed by measuring the decrease or increase of nisin in samples spiked with known concentrations of nisin, using a high-throughput HPLC-MS/MS as follows. Two milliliter of skimmed milk supplemented with 0.9 μg ml^{-1} nisin A and 0.2% (w/v) yeast extract was inoculated with 20 μl of a *L. lactis* GLM17 overnight culture and incubated in 2.5 mL deep well plates for 18 h at 30°C and stored at −20°C until further analysis. As a control, non-inoculated skimmed milk samples, to which 0.9 μg ml^{-1} nisin A was added, were taken along. Thirty microliter from each of the thawed samples was extracted with 870 μL extraction buffer in a 1 mL microtiter deep well plate. The plates were shaken for 1 h on an orbital mixing table, left overnight at 5°C and centrifuged at 6,000×*g* for 30 min, after which the samples were loaded for HPLC-MS/MS as described in the method above, except that a MRM for nisin Z was also included at *m/z* 667.2–739. Due to variations in the control samples from plate to plate, nisin concentrations in control samples were set to 1 AU mL^{-1} and nisin concentrations in fermented milk samples were converted to ratios of this arbitrary control value. Since we added a known concentration of nisin A, a decrease or increase of nisin A levels was used as a proxy for degradation and production, respectively. Degradation of nisin was confirmed in a subset of samples by measuring the accumulation of the NSR degradation product with the method described in the section above (**Supplementary Table 1**).

Re-evaluation of Strains With a Genotype/Phenotype Discrepancy

Strains with a *nsr*– genotype that displayed a nisin degrading phenotype, as well as strains where the *nsr* gene was found on the edge of a contig, were individually examined for the presence of the *nsr* gene using a colony PCR approach with REDTaq DNA polymerase Master Mix (VWR, Radnor, PA, USA) and primers annealing to two conserved regions within the *nsr gene* of *L. lactis* strains (oLIGI021 and oLIGI022), ranging from nucleotide 112–901 of the 958-nts long *nsr* gene. A total of 46 strains were tested by colony PCR using oLIGI021 and oLIGI022 to confirm the presence of a copy of the *nsr* gene. Of the 15 strains in which the *nsr* gene was detected at the edge of a contig in the genome sequence, 14 strains resulted in a PCR product validating the presence of *nsr,* while one strain contained an estimated insertion of roughly 6 kB in its *nsr* gene. The 31 remaining strains, corresponding to those in which the *nsr* gene could not be detected in the genome sequence but that showed signs of nisin degradation, 25 were confirmed to carry the *nsr* gene. Primer sets to confirm several genotypes were oLIGI023/24 for *nisA*, oLIGI043/44 for *nisI*, oLIGI045/46 for *nisF*. An overview of primers used in this study can be found in **Supplementary Table 4**.

nisA and *nsr* Mutant Generation

For targeted gene deletions in strain CH-2, the pCS1966/*oroP* system was employed (Solem et al., 2008). Standard molecular cloning techniques were performed essentially as described (Sambrook et al., 1989). Flanking regions of either *nisA* or *nsr* gene were amplified using Q5 DNA polymerase (NEB, Ipswich, MA, USA) from CH-2 chromosomal DNA with primer pairs oLIGI003/oLIGI004 and oLIGI005/oLIGI006 or primer pairs oLIGI014/oLIGI015 and oLIGI016/oLIGI017, respectively. The backbone of pCS1966 was amplified using oLIGI001 and oLIGI002. Fragments were assembled using NEBuilder® HiFi DNA Assembly Master Mix (NEB) and transformed into competent *E. coli* DH5α cells (NEB), yielding pLIGI001 and pLIGI003. Purification of DNA fragments was done using the Monarch® PCR & DNA Cleanup and DNA Gel Extraction Kits (NEB) and plasmids were isolated using the NucleoSpin® Plasmid kit (Macherey-Nagel, Düren, Germany). pLIGI001 was then used to delete *nisA*, whereas pLIGI003 was used to delete *nsr*, both as described previously (Solem et al., 2008). Electrocompetent *L. lactis* cells were transformed using electroporation with a Bio-Rad Gene Pulser (Bio-Rad Laboratories, Richmond, CA). PCR amplification on colonies with REDTaq DNA Polymerase Master Mix (VWR) was used for routine checks for correct DNA constructs.

Well Diffusion Assays

For well diffusion assays, strains ATCC 11454, CH-1, CH-2, CH-3, CH-4, mutant strains CH-2 Δ*nisA* and CH-2 Δ*nsr*, and the nisin-sensitive MG1363 strain were grown to stationary phase in 16 h from single colonies in GM17. CFS of all strains

except MG1363 was collected by centrifugation for 10 min at 4,000×g and subsequent filter-sterilization of the supernatant. The MG1363 culture was diluted 1,000 times in fresh GM17 broth, mixed 1:1 with GM17 agar and poured as a soft agar layer while leaving out 10 mm holes that were filled with 200 μL of the collected CFS samples. The assay was incubated at room temperature until halos were visible. For measurements of nisin A and the nisin$^{1-28}$ fragment in GM17, the cultures were grown as described above and stored for 24 h at −80°C before CFS was collected using 0.22 μm 96w filter plates (Acroprep, Pall laboratory, Ann Arbor, MI). These samples were then subjected to HPLC-MS/MS analysis using the extraction and analysis procedure as described above.

RESULTS

Effect of Nisin on Milk Acidification by Individual *L. lactis* Strains

A total of 710 *L. lactis* strains were monitored, in a time-resolved fashion, to evaluate their ability to acidify milk in the presence of nisin (CFS collected from the nisin producing *L. lactis* strain ATCC 11454, CFS_{nisin}) or in absence of nisin (CFS collected from the non-nisin producing *L. lactis* strain Wg2, $CFS_{control}$). Without nisin, all strains were able to acidify milk in <18 h: the majority (88%) of the strains were able to acidify milk from a start pH of 6.4 down to a pH value below 5.0, while the remaining strains acidified milk to an end pH between 5.0 and 6.0 instead (**Supplementary Table 1**). The addition of CFS_{nisin} (final concentration of nisin A in milk of 1.5 μg ml^{-1}), led to a wide variation of acidification profiles, ranging from unaltered acidification to loss of acidification. In order to get an impartial comparison of the obtained milk acidification profiles in the presence or absence of nisin for each separate strain, the start and end pH were normalized to correspond to values 1 and 0, respectively, and the curves were synchronized so that the control curves would start acidifying at the same timepoint. From each normalized acidification curve the absolute change in pH (ΔpH) was derived, and the difference in area under the curve (ΔAUC) and acidification starting time points ($\Delta time_0$) between CFS_{nisin} and $CFS_{control}$ treated conditions for every strain were calculated. After multiple attempts for classification, we noticed that ΔAUC alone could not allow for a clear separation of the phenotypes. Instead, combining these three parameters (ΔpH, ΔAUC, $\Delta time_0$) allowed us to classify strains into four distinct phenotypic groups (rules are described in **Supplementary Table 3**). We define the resulting phenotypic groups as (A) loss of acidification (**LA**), (B) highly delayed acidification (**HDA**), (C) mildly delayed acidification (**MDA**), and (D) unaltered acidification (**UA**) (**Figure 1** and **Supplementary Figure 1**).

When milk fermentations were carried out in the presence of CFS_{nisin}, 279 *L. lactis* strains clustered to the LA phenotype, indicating that these strains are sensitive to nisin (**Figure 1A**). A total of 101 *L. lactis* strains grouped to the UA phenotype, for which both the acidification rate and depth remained mostly unchanged upon the addition of CFS_{nisin} compared to addition of $CFS_{control}$ (**Figure 1D**). For the remaining strains, the effect of nisin resulted in a range of delays in the onset of acidification. Of these, 121 strains clustered to the HDA and 209 to the MDA phenotypes (**Figures 1B,C**). We identified a small set of strains that did not show a delay but a change in acidification depth as a result of nisin addition, which therefore also clustered to the mild (MDA) phenotypic group, see also **Supplementary Figure 2A**.

Diversity of the *L. lactis* Strain Collection

In order to assess the genotypic diversity, the strains in the collection were whole-genome sequenced and their genomic relatedness assessed by a k-mer-based and a MLST-based tree construction (**Figure 2** and **Supplementary Figure 3**). From this analysis, 64% of the strains (n = 457) belong to *L. lactis* ssp. *lactis* and the remaining 36% (n = 253) of the strains belong to *L. lactis* ssp. *cremoris*. We compared our genomes to 206 unique lactococcal assemblies publicly available (July 2020) in NCBI (National Center for Biotechnology Information) RefSeq database of which 73% and 26% map to *L. lactis* ssp. *lactis* and ssp*cremoris*, respectively (**Figure 2** and **Supplementary Figure 3**). Furthermore, the comparison shows that our strain collection spans the full spectrum of genomic diversity represented by the publicly available *L. lactis* genomes with some smaller lineages exclusively represented in our collection and to a lesser extent vice versa. We subsequently searched the genome sequences of our collection for orthologous groups of protein sequences (OGs) to capture ssp. *cremoris* with a reversed phenotype e.g., strains that display a ssp. *lactis* phenotype while having a ssp. *cremoris* genotype, as previously reported (Kelleher et al., 2017; Wels et al., 2019). This analysis showed that 25% of the ssp. *cremoris* strains in our collection carry sequences corresponding to OGs specific for ssp. *cremoris* strains with a ssp. *lactis* phenotype (**Figure 2**). Accordingly, these strains cluster in one of the two ssp. *cremoris* lineages, together with previously identified ssp. *cremoris* strains with a ssp. *lactis* phenotype such as KW2, N41, V4, MG1363, and NCDO763 (Wels et al., 2019).

Effect of *nsr*, *nisFEG*, and *nisI* on Milk Acidification in the Presence of Nisin

To better understand how the presence of genes for nisin biosynthesis, nisin immunity and/or nisin degradation correlate to the observed variability in milk acidification upon addition of nisin, we performed gene-trait matching of nisin-related genes to observed acidification phenotypes. The distribution of genes encoding key proteins involved in nisin biosynthesis (a nisin structural gene: *nisA*; the nisin biosynthetic machinery: *nisB*, *nisT*, *nisC*, and *nisP; nis* gene regulation: *nisR* and *nisK*), nisin immunity (*nisI* and *nisFEG*) and nisin degradation (*nsr*) within the 710 strains along with the milk acidification phenotypes (LA, HDA, MDA, UA) are visualized in **Figure 2** and **Supplementary Figure 1**. It is apparent that most ssp. *cremoris* have the LA phenotype, whereas the ssp. *lactis* have more variable phenotypes, with many strains belonging to UA, MDA, and HDA.

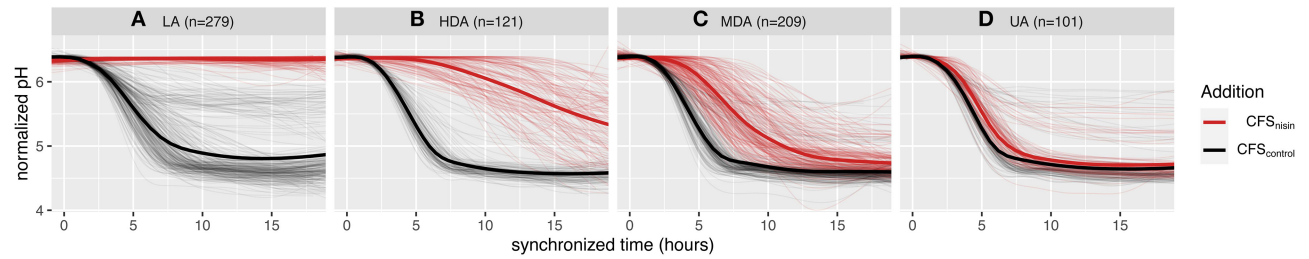

FIGURE 1 | Effect of nisin on milk acidification profiles and phenotypic classification of 710 *L. lactis* strains. Milk acidification curves of strains grown at 30°C without nisin (CFS$_{control}$) and with 1.5 μg ml^{-1} nisin addition (CFS$_{nisin}$) The thin lines depict the averaged milk acidification data of three replicates while the thicker line depicts the averaged curves per group. The nisin-containing milk phenotypes are classified to four groups; **(A)** LA, loss of acidification; **(B)** HDA, highly delayed acidification; **(C)** MDA, mildly delayed acidification; and **(D)** UA, unaltered acidification. All acidification curves are synchronized based on acidification onset of each respective CFS$_{control}$ profile and normalized to a start pH of 6.4.

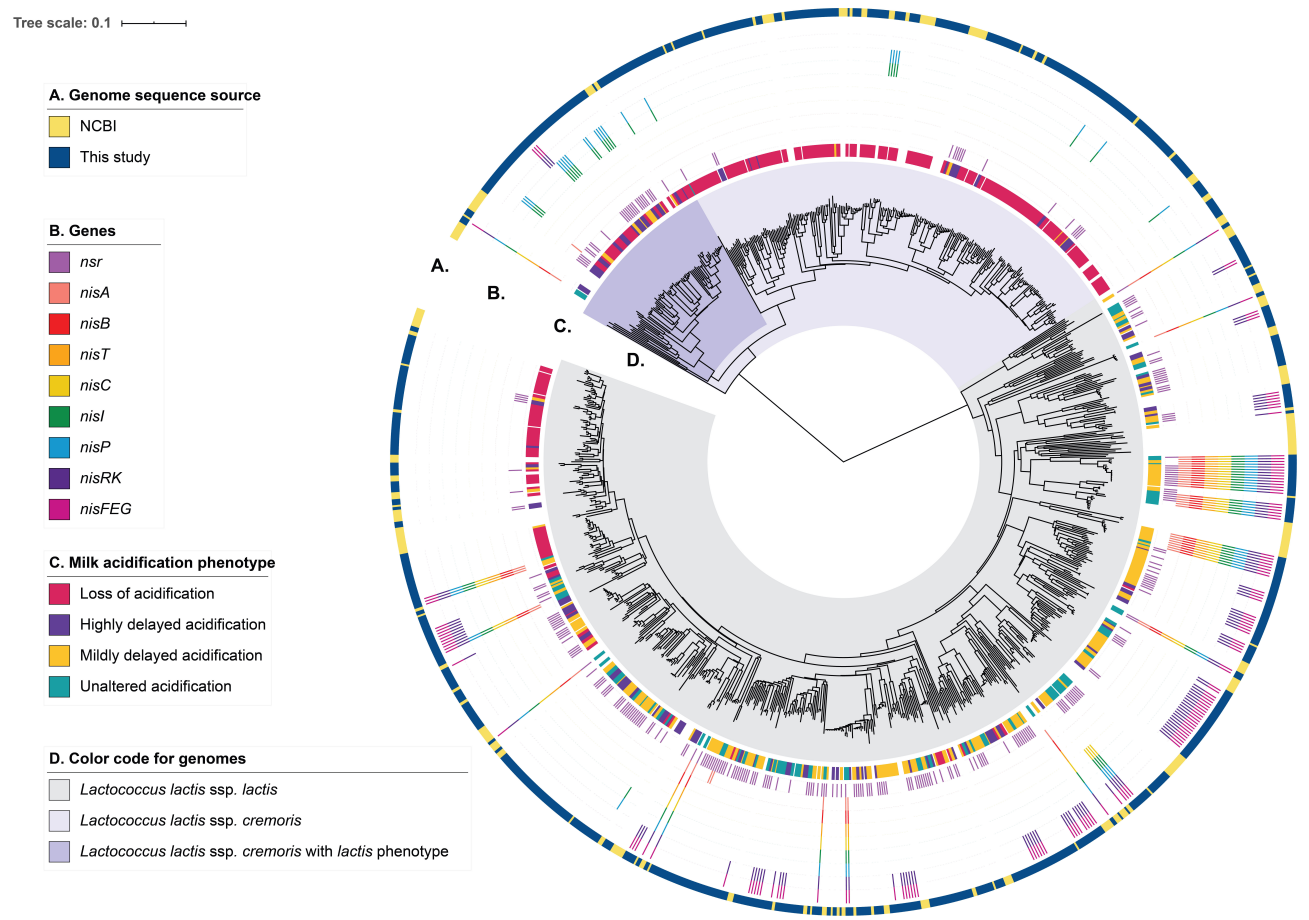

FIGURE 2 | Genotypic diversity of the *L. lactis* strains. A *k*-mer tree depicting the genotypic relatedness of 929 *L. lactis* ssp. *cremoris* and ssp. *lactis* strains. Indicated from outer to inner ring are: **(A)** Strain-specific genome sequence origin, obtained either from the 710 draft genomes from this study or the publicly available 219 *L. lactis* RefSeq genomes. **(B)** Strain-specific presence of nisin-related genes or gene clusters. **(C)** Strain-specific milk acidification phenotypes. **(D)** Subspecies clusters of *L. lactis* ssp. *lactis* and *L. lactis* ssp. *cremoris.* The latter is further divided into whether ssp. *cremoris* strain is predicted to have a *cremoris* or a *lactis* phenotype.

Complete Nisin Gene Cassette vs. Acidification

A total of 45 strains (6.3%) contain the full nisin gene cluster required for nisin biosynthesis (*nisABTCIPRK-FEG*). In fact, 24 of these strains acidified milk without any delay in the presence of CFS$_{nisin}$, and were classified to the UA phenotypic group, while 21 do so with only a mild delay or higher end pH and therefore classified to the MDA phenotypic group (**Figure 3** and **Supplementary Figure 2**). Out of 45 strains, 44 belong to the

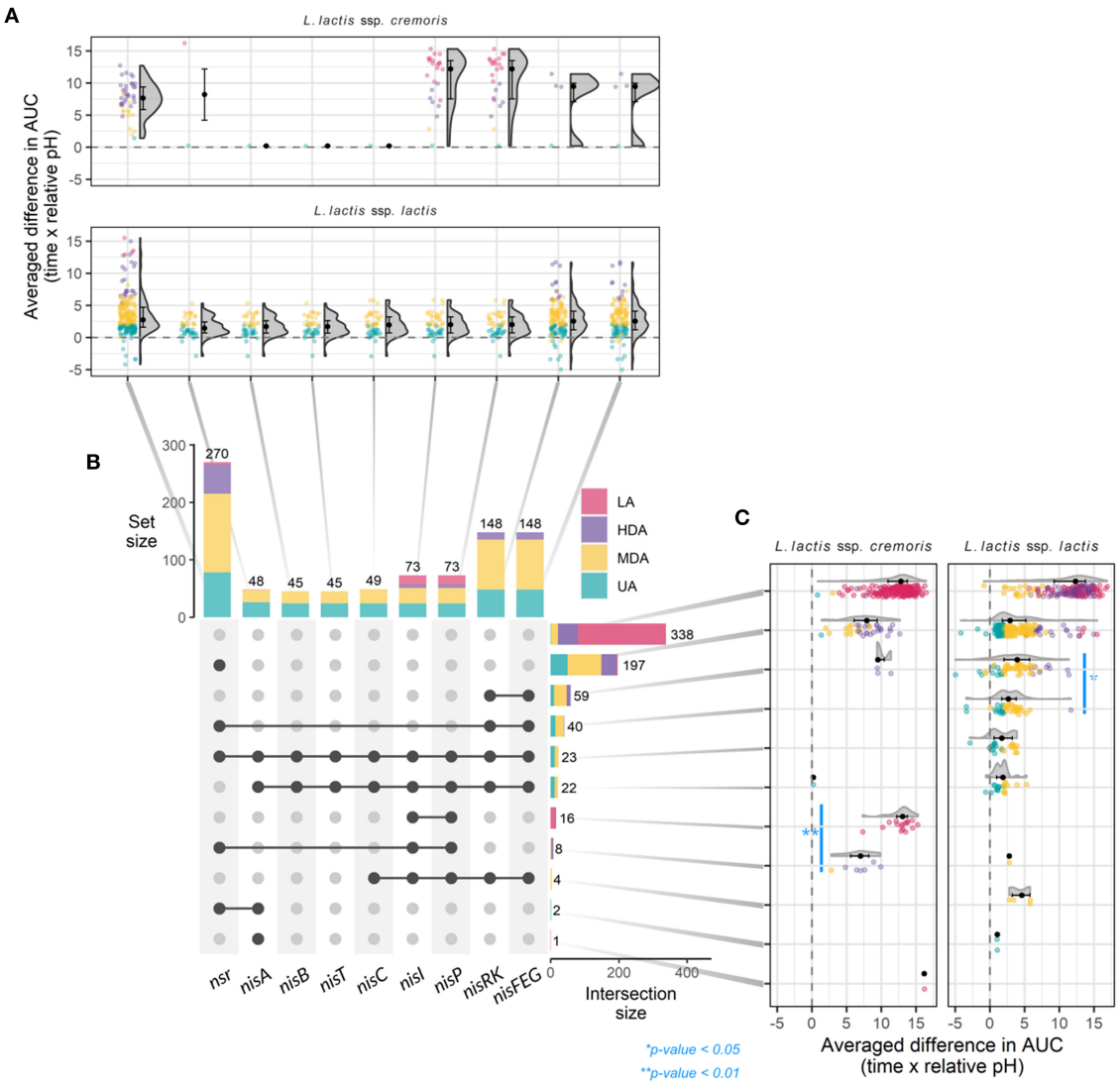

FIGURE 3 | Gene-trait matching of nisin tolerance genotypes with milk acidification patterns. **(A)** Raincloud plots depicting the averaged ΔAUC of every strain for milk acidification curves with and without nisin, grouped by individual nisin-related gene and subspecies. **(B)** Matrix layout showing individual presence (vertical) and overlap in (horizontal) nisin-related genes in 710 *L. lactis* strain and the respective distributions of phenotypes and total number of strains that contain the indicated gene or set of genes. Dark dots connected with solid lines indicate genes present in a group, while gray dots indicate gene absence. **(C)** Raincloud plots depicting ΔAUC values as in **(A)**, but now grouped by genotype for nisin-related genes and subspecies. For all raincloud plots, black dots represent the median values whereas black lines mark the boundaries for the center 50% of the distribution. *P*-values were calculated using the Mann-Whitney-Wilcoxon test.

ssp. *lactis* group. The single ssp. *cremoris* strain that contains the nisin gene cassette groups to the genotype *cremoris*/phenotype *lactis* clade and is one out of only three ssp. *cremoris* strains that are not affected by the addition of nisin (Wels et al., 2019) (see also **Figure 2**).

Interestingly, of all strains that contain a full nisin biosynthesis gene cluster, 23 also contain *nsr* (**Figure 3** and **Supplementary Figure 1**). We therefore wondered if the presence of both *nsr* and immunity genes would allow for faster acidification than that of only the immunity genes. We found a bimodal distribution in the acidification delays for the former group of strains indicating that two subgroups exist, one containing strains that acidify better than the strains with just immunity and a second, less tolerant group (**Figure 3**). Interestingly, the two subgroups appeared to have different variations of the *nsr* sequence (variant 25 for the UA group and variant 17 for the MDA group), putatively yielding proteases with different activities (**Supplementary Table 1** and **Supplementary Figure 6D**).

To summarize, the current data confirms previous reports that the presence of nisin immunity genes *nisI* and *nisFEG* together constitute a strong mechanism in establishing nisin tolerance. Moreover, we find that the full nisin gene cluster is a feature mainly present in ssp. *lactis*.

Partial Nisin Gene Cassette vs. Acidification

Many strains exist that do not possess the full subset of genes for nisin biosynthesis and immunity but, instead, only contain one nisin immunity component (*nisI* and/or *nisFEG*) (**Figure 3** and **Supplementary Figure 1**) (Wels et al., 2019). Four ssp. *lactis* were identified that contain genes for full nisin immunity (*nisIP-RK-FEG*) but have lost the corresponding synthesis genes. All show an MDA phenotype. A total of 59 strains contain *nisRK-FEG* without the rest of the nisin gene cassette. Like reported previously, we find that *nisFEG* genes always co-occur with *nisRK* (Wels et al., 2019). The three ssp. *cremoris* strains that possess unaccompanied *nisRK-FEG* display a HDA phenotype, while the 56 ssp. *lactis* strains appear divided over HDA (9), MDA (37), and UA (10) phenotypes (**Figure 3** and **Supplementary Figure 1**). This again indicates that ssp. *lactis* strains with only *nisRK-FEG* are coping better with nisin than ssp. *cremoris* strains with the same set of immunity genes. Furthermore, *nisRK-FEG* genes are more prevalent in ssp. *lactis* than in ssp. *cremoris*. As reported previously, the *nisI* gene, when found without the remainder of the nisin biosynthesis cassette, typically still co-occurs with *nisP* (Tarazanova et al., 2016; Wels et al., 2019). In our collection, *nisIP* is uniquely present in 16 ssp. *cremoris*, all displaying LA (**Figure 3**). In contrast to these findings, NisI was previously reported to deliver substantial, but not full immunity against nisin in the absence of NisFEG (AlKhatib et al., 2014a; Tarazanova et al., 2016). NisI is believed to interact in an equimolar stoichiometry with nisin molecules (Hacker et al., 2015). This could lead to a significant surplus of nisin molecules under the tested conditions here in which a high concentration of nisin was employed. In order to test if NisI alone has the capacity to protect the cells against nisin, albeit at lower levels, the acidification experiments were repeated for these strains in the presence of 0.2 μg ml^{-1} nisin (**Supplementary Figure 4**). We did not detect an improvement in all but one of the acidification profiles in the presence of lower levels of nisin.

In short, strains with NisFEG alone are mostly ssp. *lactis* and can cope relatively well in the presence of nisin, whereas strains that only possess NisI are uniquely ssp. *cremoris* and do not. Interestingly, the average difference in AUC is slightly less in *nsr*+ strains compared to *nisFEG*+ strains, and even more so in *nsr*+/*nisFEG*+ strains, indicating that the presence of the *nsr* gene confers better tolerance toward nisin, and that NSR thus is a stronger protective force than the individual immunity systems from the nisin gene cassette (**Figure 3**).

nsr+ Genotype vs. Acidification

A striking 270 *L. lactis* strains (38%) possess a gene encoding the nisin protease NSR (**Figure 3**) of which the majority (98%) were able to acidify milk, albeit with a wide window of delays (UA: 78, MDA: 137, and HDA: 51 and LA: 4). Of these, 197 of the strains (73%) contain only *nsr* and none of the immunity genes (**Figure 3**). The fact that 149 strains with *nsr*+ genotype and no nisin immunity genes display a UA or MDA phenotype clearly demonstrates the importance of NSR for nisin tolerance. The milk acidification profiles of the strains that only have the *nsr*+ genotype differ greatly between ssp. *lactis* and ssp. *cremoris* strains, with the former showing generally better acidification in the presence of nisin (**Figure 3C** and **Supplementary Figure 5**). In summary, it is evident that there is large phenotypic variation between *nsr*+ strains in terms of nisin tolerance. The general trend is that strains with only *nsr* are able to acidify milk in the presence of nisin, albeit with different delays in the onset of acidification. It could be that the underlying differences in genetic make-up and/or post-transcriptional regulation between ssp. *cremoris* and ssp. *lactis* play an important role in further determining nisin tolerance.

Strains Without Nisin Immunity or *nsr* Genes vs. Acidification

A total of 338 strains did neither contain *nsr, nisI* nor *nisFEG*. As expected, the majority of these strains (258; 76%) did not acidify milk in the presence of nisin. However, 1, 21, and 58 strains mapped to the UA, MDA, and HDA phenotypic group, respectively (**Figure 3** and **Supplementary Table 1**). As these phenotypes deviate from the predicted LA phenotype of a strain with a *nsr- nisI- nisFEG-* genotype, we confirmed the absence of nisin immunity and degradation genes using a colony PCR. Therefore, the reason behind the UA, MDA, and HDA phenotypes of these strains remains elusive.

Effect of *nsr*+ Strains on Nisin Degradation

Since a high fraction of *nsr*+ strains were tolerant to nisin in milk, we were interested to find out to what extent nisin can be degraded by distinct *nsr*+ strains. To study the impact of each strain on nisin degradation in more detail, we first validated the role of lactococcal NSR in nisin A degradation. To accurately measure nisin A and detect its NSR degradation product, an assay based on high resolution mass spectrometry was developed. It was previously shown that nisin Z is cleaved after position 28 by the NSR enzyme thereby creating a large and a small fragment, which for nisin A should result in two fragments with monoisotopic masses of 2718.1854 Da (nisin$^{1-28}$) and 869.3752 Da (nisin$^{29-34}$), respectively (Sun et al., 2009). We initially identified nisin$^{1-28}$ in CFS of CH-1(*nis*–, *nsr*+) incubated with nisin A by high resolution mass spectrometry on a HPLC-QTOF instrument (data not shown). Using a HPLC-MS/MS Triple Quadrupole Mass spectrometer, MS/MS fragmentation of CFS eluates collected from ATCC 11454 (*nisA*+, *nsr*–) and CH-1 (*nsr*–, *nsr*+) strains grown in the presence of nisin A and later on spiked with nisin Q as an internal standard led to the identification of quantification ions specific for nisin A, nisin Q, and nisin$^{1-28}$ (**Figure 4**). In CFS of ATCC 11454, an increase in nisin A can be detected over the nisin A-spiked control sample. In contrast, no nisin A could be detected in the CFS derived from the *nsr*+ strain CH-1. However, in the latter, a fragment corresponding to the large NSR degradation product nisin$^{1-28}$ could be accurately detected. This confirms that the lactococcal NSR is able to degrade nisin A. This was then used to measure nisin A and detect its NSR degradation in all further samples.

We next aimed to study how much nisin A is broken down into nisin$^{1-28}$ in a co-culture containing both a nisin-degrading and a nisin-producing strain. To do so, we employed ATCC 11454 and CH-1 as control as well as three different *nisA*+ *nsr*+

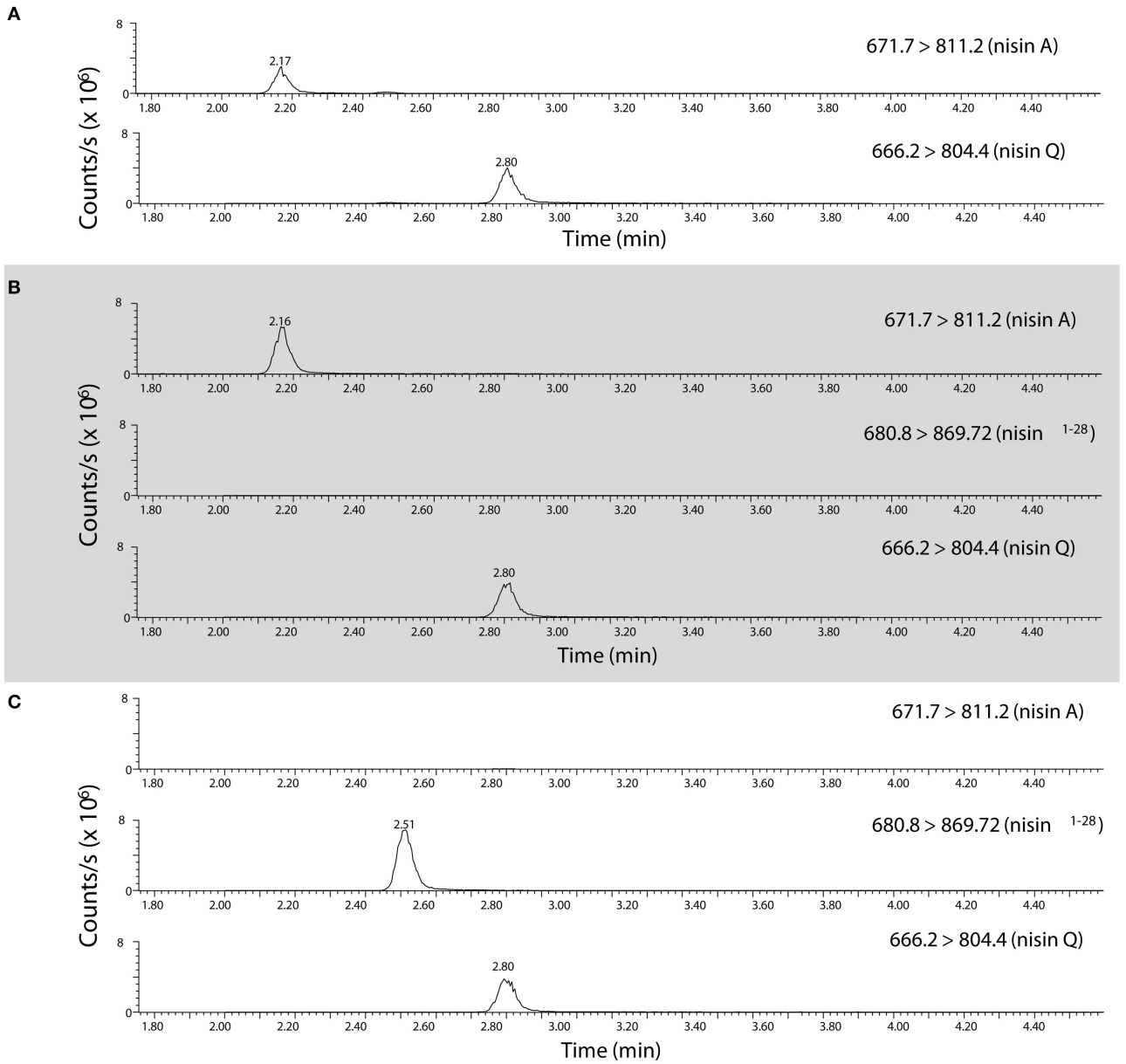

FIGURE 4 | Identification of nisin A, nisin Q, and nisin$^{1-28}$ in CFS using high resolution mass spectrometry. HPLC-MS/MS MRM transitions of quantification ions for nisin A [the $[M+5H]^{5+}$ ion from *m/z* 671.7 to 811.2], nisin Q [the $[M+5H]^{5+}$ ion of nisin Q from *m/z* 666.2 to 804.4,] and nisin$^{1-28}$ [the $[M+4H]^{4+}$ ion from *m/z* 680.55 to 869.7] as detected in **(A)** a control mix of nisin A and nisin Q, **(B)** CFS collected from CHCC 11454 (*nisA+, nsr-*) and **(C)**, CFS collected from CH-1 (*nsr–, nsr+*). Note that the parent isolation window of the $[M+4H]^{4+}$ ion of nisin$^{1-28}$ (*m/z* 680.55) was moved *m/z* 0.25 as the A+1 isotopomer was the most abundant, creating the MRM transition 680.8 → 869.7.

strains. CH-2 (*nisA+ nsr+*) has the same genetic make-up as CH-1 but has received the sucrose-nisin transposable element from ATCC 11454 *via* conjugation. CH-3 (*nisA+ nsr+*) also possesses an intact *nsr* gene, while CH-4 was found to naturally contain a point mutation in the *nsr* gene, introducing a stop codon at amino acid position 58 yielding a truncated NSR protein. To validate that the possession of *nisA* or *nsr* alone is responsible for nisin synthesis or nisin degradation, a clean deletion of either *nisA* or *nsr* was generated in CH-2, resulting in strains CH-2Δ*nisA* and CH-2Δ*nsr*, respectively. CFS of the seven *L. lactis* strains grown to stationary phase in a rich nutrient broth (GM17) was collected and tested for antibacterial activity by means of well diffusion assays using a nisin-sensitive *L. lactis* strain as indicator. In addition, the presence of nisin A and nisin$^{1-28}$ was assessed using the HPLC-MS/MS method described above. As expected, CFS of strains producing both nisin and NSR displayed a reduced

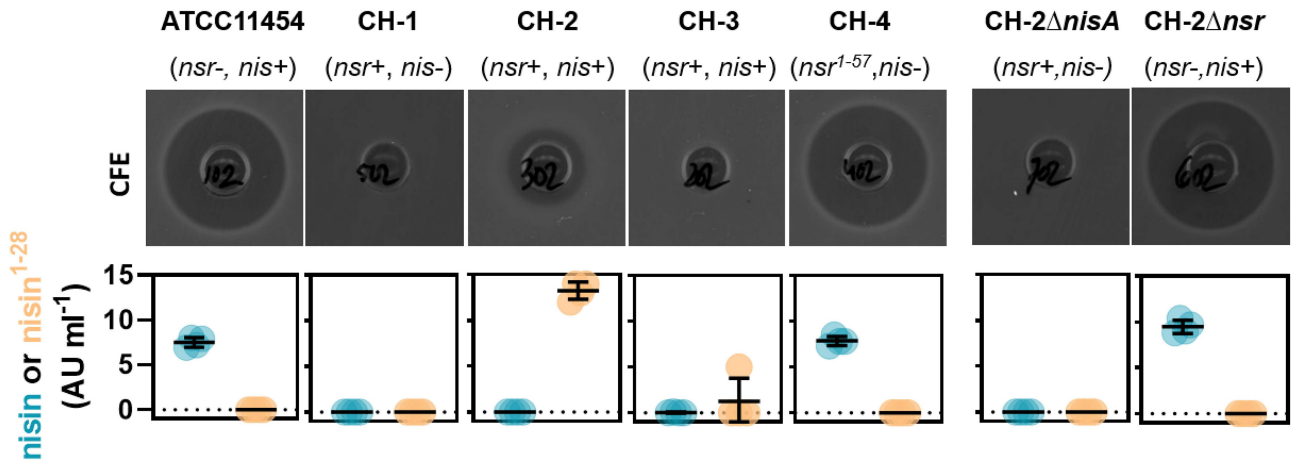

FIGURE 5 | Impact of *nsr* genotype on bactericidal activity and nisin production. Top row: Well diffusion assays showing the antibacterial activity of CFS collected from indicated strains grown in GM17 for 16 h against the nisin-sensitive *L. lactis* strain Wg2. Bottom row: Graphs displaying nisin A and nisin$^{1-28}$ concentrations in CFS collected from indicated strains grown in GM17 for 24 h as measured using HPLC-MS/MS.

activity against the nisin-sensitive indicator strain (**Figure 5**). In agreement, large amount of nisin$^{1-28}$ degradation products and no full-length nisin peptides were detected in the CFS of CH-2 and CH-3 (**Figure 5**). CFS of CH-4 (*nisA*+ *nsr*$^{1-57}$) showed the same level of inhibition as ATCC 11454 (**Figure 5**). In addition, nisin$^{1-28}$ could not be detected by HPLC-MS/MS, confirming the loss in function of truncated NSR$^{1-57}$. Deleting *nisA* in CH-2 effectively ceased the production of nisin A and thereby also any degraded nisin$^{1-28}$, while deleting *nsr* in CH-2 abolished the presence of nisin$^{1-28}$ in the CFS (**Figure 5**). However, nisin levels were similar to those detected for ATCC 11454 in CH-2Δ*nsr*, confirming that NSR breaks down nisin produced by *nisA*+ *nsr*+ strains. Together, this data confirms that full-length NSR suffices for nisin degradation.

Screening of *L. lactis* Strains for Nisin Degradation

After establishing that functional NSR is responsible for nisin degradation, we spiked milk with 0.9 μg mL^{-1} nisin A and determined changes in its concentration after fermentation for 18 h with each of the 710 *L. lactis* strains. This allowed us to map the impact of each strain on nisin: Either nisin concentrations increased, remained unaltered or decreased. We used this information to further divide the established phenotypic groups based on acidification profiles into a 3-by-4 phenotypic matrix (**Figure 6**). In addition, we plotted nisin degradation per variation of the NSR protein sequence to screen for possible inactive variants (**Supplementary Figure 6**).

The top row of the matrix displayed in **Figure 6** shows those strains that led to an increase in nisin A levels above the initial nisin A concentration. As expected, all 16 strains in this group contain the complete nisin A biosynthesis gene cassette and have either an UA or an MDA phenotype (**Figure 6**). Interestingly, we observe a >5-fold increase in the levels of nisin A of the eight *nsr*+ strains with a nisin biosynthesis cassette, indicating that the nisin production rate by these strains is higher than their nisin degradation rate (**Figure 6**). It should be noted that, out of 45 strains that contain a full nisin biosynthesis cassette, 29 encode versions other than nisin A that are not detected in the employed HPLC-MS/MS method. As a consequence, these will show up in the middle or bottom row instead.

In the middle row of **Figure 6**, the largest number of strains can be found. In milk fermentations carried out with these strains, the nisin A concentration remained stable. These largely correspond to strains that do not have the *nsr* gene (430 out of 444). Note that strains mapping to the LA phenotype typically fail to degrade nisin A (**Figure 6**). Fourteen *nsr*+ strains did not show nisin-degrading activity. Further examination of the NSR protein sequences of these strains revealed 13 different NSR variants (**Supplementary Figure 6**). Six of these variants were also present in strains with degradation activity, while strains possessing the remaining seven variants showed no indication of nisin degradation. The NSR protein sequences of these seven strains were compared to variant 25, the most abundant form in strains that degrade nisin (also present in CH-1) and a homolog of *S. aureus* NSR of which the structure has been resolved (Khosa et al., 2016) (**Supplementary Figure 6**). One strain had a N-terminal truncated NSR (variant 21), which likely renders the protease incapable of being transported out of the cell where nisin degradation takes place. For the remaining variants, we found several amino acid substitutions in domains that we speculate abolishes NSR activity (**Supplementary Figure 6C**) (Khosa et al., 2016).

Strains that map to the bottom row in **Figure 6** cause a decline in nisin A, indicative of nisin degradation. Almost all of the 250 milk fermentations (99%) in which a decrease in nisin was observed were carried out by *nsr*+ strains, further strengthening the view that NSR is the fundamental contributor to nisin degradation and hence allows strains to grow and acidify milk in the presence of nisin (**Figure 6**). We noted in the acidification experiments that strains containing *nsr* as well as nisin immunity showed a bimodal distribution with respect

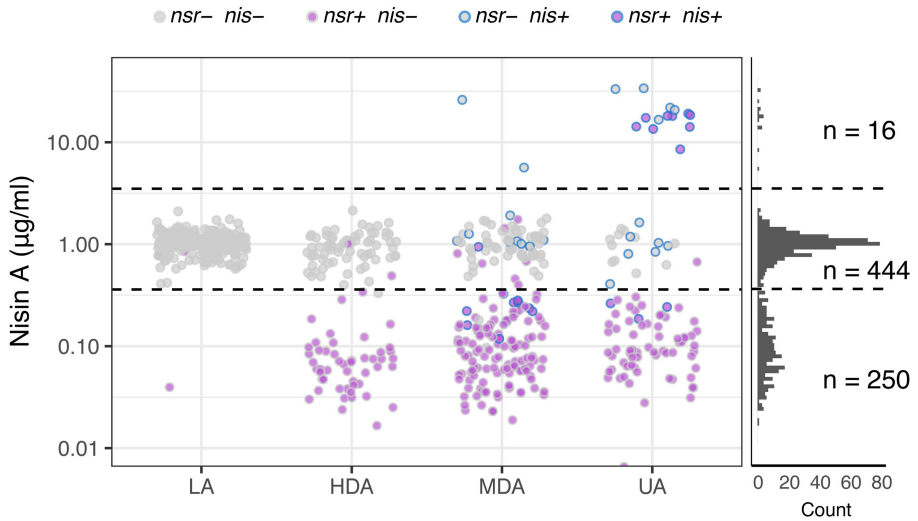

FIGURE 6 | Nisin degradation by individual *L. lactis* strains. Dot plots depicting nisin A concentrations as quantified with HPLC-MS/MS after incubating 0.9 μg ml^{-1} of nisin A in milk inoculated with *L. lactis* strains belonging to one of the four phenotypic groups LA, HDA, MDA and UA. Dots are further color-coded to indicate the presence or absence of *nsr* and/or nisin biosynthesis genes (*nis*) in the tested strain. The right panel displays the distribution of resultant nisin A concentrations derived from the complete set of tested strains ($n = 710$). Horizontal dashed lines are drawn to indicate the boundaries between observations showing an increase of nisin A (16 datapoints above 3.5—upper dashed line), an unchanged nisin A concentration (444 datapoints between dashed lines) or a decreased nisin concentration (250 datapoints below 0.36—lower dashed line).

to delay in acidification (**Figure 3C**). Because NSR variant 17 or 25 were overrepresented in the subgroups with either more or less delay in acidification, respectively, we evaluated their respective nisin degradation capacities when situated in non-nisin producers and found that variant 25 reduced nisin A levels more than variant 17 (**Supplementary Figure 6D**).

In summary, it is evident from these nisin measurements that nisin degradation by NSR is very common and a mechanism utilized by *L. lactis* strains to protect against nisin.

DISCUSSION

Nisin-producing strains are added to milk fermentations for cheese production, but how genetic variation in *L. lactis* strains contributes to differences regarding milk acidification remains largely unexplored. We therefore investigated the effect of nisin on milk fermentations from 710 individual *L. lactis* strains. We found that changes in milk acidification by nisin can largely be explained by the presence or absence of nisin immunity (*nisI*, *nisFEG*) or degradation (*nsr*) genes, in a subspecies dependent manner. Still, within each group a range of strain-specific acidification profiles occurs, which reveal nuances that are easily overlooked in single strain studies focusing on the singular or combinatorial contribution of nisin degradation and/or immunity to nisin tolerance.

Nisin Degradation Is a Common Trait in Lactococci

Our study identifies nisin degradation by NSR as a very common feature present in 38% of the *L. lactis* strain collection examined (710 strains). In view of these results, nisin degradation *via* NSR appears to be the main mechanism by which lactococci tolerate nisin. Based on this prevalence, we find it likely that one or more *nsr*+ *L. lactis* strains would occur both in natural milk fermentations and undefined starter cultures. In agreement, we have found NSR-specific breakdown products in milk fermented with *L. lactis*-based starter cultures, and in cheese (data not shown). The immunity factors NisFEG and NisI only deliver self-protection, while NSR offers a community-level nisin resistance, cross-protecting also nisin-sensitive strains through the degradation of nisin in the environment. Importantly, the data shows that ssp. *lactis nsr*+ strains are better equipped to degrade nisin in milk than ssp. *cremoris nsr*+ strains.

We believe that NSR activity in a given starter culture is an important determinant for the level by which nisin impacts mixed-strain milk fermentations. On the one hand, NSR presents an advantage by protecting the nisin-sensitive members of the starter culture. On the other hand, a reduction of nisin levels might allow for the growth of undesirable organisms, such as *Clostridia,* which will compete for nutrients and may lead to spoilage of the cheese (Meijer et al., 1998; Sallami et al., 2004). These antitheses pose an important challenge on starter culture design.

Distribution and Prevalence of Nisin Immunity Genes Vary Between Subspecies

Nisin production and autoimmunity is a trait naturally encountered in strains isolated from raw milk and natural bulk starter cultures (Alegría et al., 2010; Cosentino et al., 2012). Of the *L. lactis* strains examined, 6.3% of the strains contain a full nisin biosynthesis cassette. Thus, this trait is significantly less common than the *nsr* genotype. Nisin synthesis is a property typically assigned to ssp. *lactis* strains, which is further supported by our dataset in which all but one of the nisin-producing strains belong

to ssp. *lactis* (De Vuyst, 1994; Alegría et al., 2010; Virolainen et al., 2012). Strikingly, we have identified several nisin producers that also carry the *nsr* gene. At this stage we are unable to put forward an explanation for the role of NSR in nisin-producing strains and we question whether it has a different function that confers a competitive advantage under the right conditions.

Tolerance to nisin can be achieved *via* two mechanisms: degradation with proteases or activity of the immunity proteins NisI and NisFEG. A close inspection of the *L. lactis* collection revealed that about 9% of the strains possessed *nisRK-FEG*, but no synthesis genes. In general, these strains show mild delays in the onset of acidification. The expression of *nisFEG* genes is dependent on nisin-induced activation of NisRK (de Ruyter et al., 1996; Ra et al., 1996). Since *nisRK-FEG* strains do not produce nisin, it is likely that NisFEG proteins are absent in cells of pre-cultures but build up after inoculation in nisin-containing milk. The time that elapses before a sufficient amount of NisFEG is produced for cells to effectively remove nisin from the membrane and resume growth might dictate the severity of the milk acidification lag phase of *nisRK-FEG* strains. Interestingly, *nisRK-FEG* is almost uniquely found in ssp. *lactis* and only present in three ssp. *cremoris* strains. In fact, the unaccompanied *nisIP* operon is the only nisin element specific for ssp. *cremoris* strains. This plasmid-localized operon was shown to confer protection against 20 ng ml^{-1} nisin in ssp. *cremoris* NCDO712 (Tarazanova et al., 2016; Wels et al., 2019). However, the results presented in the current study do not support that NisI alone gives nisin immunity under application-relevant conditions in which nisin concentrations typically range from 1.25 to 7.5 μg ml^{-1} (Davies et al., 1997; Sallami et al., 2004; Aly et al., 2012). Because *nisIP* is only expressed at a low constitutive rate in the absence of nisin-induced *nisABTCIPRK* transcription (Kuipers et al., 1995; de Ruyter et al., 1996; Li and O'Sullivan, 2006; Trmčić et al., 2011), NisI levels are likely to remain lower in *nisIP* strains than in those with the full nisin cassette. NisI quantity directly impacts nisin tolerance due to the fixed 1:1 molar stoichiometry with which it interacts with nisin molecules (Takala et al., 2004; Hacker et al., 2015; Jeong and Ha, 2018). Once nisin outnumbers NisI proteins exposed on the cell surface, the latter can no longer protect nisin from reaching lipid II (AlKhatib et al., 2014a). Taken together, NisI in *nisIP* strains seems to constitute a functional defense mechanism only against low levels of nisin, for instance, when NSR is produced by the same or another strain in the culture. NisFEG in *nisRK-FEG* strains, on the other hand, allows cells to grow in the presence of higher levels of nisin. Like strains that have the full set of immunity genes in combination with NSR, NisFEG or NisI with NSR generally results in an additive effect in nisin tolerance. Given the lack of correlation between the presence of *nisIP* and tolerance to nisin in ssp. *cremoris*, it is reasonable to speculate that NisIP plays a different role in this subspecies.

Subspecies Are Differently Affected by Nisin During Milk Acidification

Unlike ssp. *lactis,* nisin-tolerant ssp. *cremoris* strains appear to be rare, as substantiated by the following observations derived from our dataset. First, effective nisin immunity and/or resistance seem to be less prevalent in ssp. *cremoris*. Second, ssp. *cremoris* strains that contain *nisFEG* and/or *nsr* generally acidify nisin-containing milk with more delay than ssp. *lactis* of the same genotype. Third, those ssp. *cremoris* strains capable of acidifying milk with a delay have genotypes corresponding to a *lactis* phenotype (Kelleher et al., 2017; Wels et al., 2019). *L. lactis* ssp. *cremoris* strains are used for flavor development of specific cheeses such as cheddar (Broadbent et al., 1998; Børsting et al., 2015). This has been attributed to their ability to lyse, a process that can be accelerated by bacteriocins, thereby releasing intracellular enzymes like peptidases contributing to the flavor during ripening (Morgan et al., 1997). It can thus be argued that the nisin sensitivity of ssp. *cremoris* is desirable and might even have been selected for during its domestication. In general, ssp. *cremoris* are less tolerant than ssp. *lactis* to stress such as elevated temperature, low pH, salt and reactive oxygen species (Kim et al., 1999; Sanders et al., 1999; Dijkstra et al., 2014, 2016). Based on our results, we find that ssp. *cremoris* strains are also less tolerant to nisin.

Nisin Tolerance Besides Immunity and Degradation

We identified 20 ssp. *lactis* and two ssp. *cremoris* strains that are tolerant (UA or MDA) to nisin, but do not encode any obvious nisin immunity or degradation machineries. We performed a search for homologs of multidrug transporters such as the CprABC-type and BceAB-type systems that are known to confer resistance to nisin in other Gram-positive bacteria, including pathogens and spoilers (Clemens et al., 2018 and references therein), but the results were inconclusive (data not shown). At this stage, we cannot put forward an explanation to why nisin failed to impair acidification of milk by *L. lactis* strains devoid of nisin immunity and degradation pathways. It is well-known that Gram-positive bacteria can adapt to tolerate more nisin (Kramer et al., 2004, 2006, 2008; Giaouris et al., 2008; Bergholz et al., 2013). For instance, adaptive laboratory evolution yielded a ssp. *lactis* strain that could withstand over 75-fold more nisin than its mother strain through temporary transcriptomic alterations (Kramer et al., 2006). Changes in expression were mapped to genes involved in cell wall and phospholipid composition, drug transport and the cell envelope stress response (Kramer et al., 2006; Giaouris et al., 2008). Similar transcriptional responses were also observed in *Staphylococcus aureus, Streptococcus pneumoniae*, *Listeria monocytogenes*, and *Bacillus subtilis* challenged with nisin (Ming and Daeschel, 1995; Mazzotta and Montville, 1997; Peschel et al., 1999; Hansen et al., 2009; Collins et al., 2010a,b, 2012; Majchrzykiewicz et al., 2010). Moreover, *L. lactis* cells treated with nisin showed overlapping physiological responses to cells challenged with other membrane-perturbing compounds such as Lcn972, another lipid II-binding bacteriocin produced by *L. lactis*, c2 lytic phages, and lysozyme, or by the recombinant production of heterologous membrane proteins (Kramer et al., 2006; Martínez et al., 2007; Veiga et al., 2007; Fallico et al., 2011; Pinto et al., 2011; Roces et al., 2012a,b). In many cases, pre-activating expression of the identified genes improved tolerance toward membrane perturbing compounds including nisin. In order to pinpoint factors involved in the observed subspecies-dependent deviations in innate nisin tolerance, it would be of importance to study nisin-induced changes in gene expression profiles of ssp. *lactis*

and ssp. *cremoris* strains that do not have any immunity or degradation machineries in place.

In conclusion, we have characterized a large set of *L. lactis* strains for which we mapped the contribution of nisin immunity and/or degradation genes to nisin tolerance and degradation during milk fermentations. The prevalence of *nsr* and associated nisin degradation is a more common trait than previously reported, albeit the degree of protection established by NSR seems to be highly variable. Full immunity (*nisI* plus *nisFEG*), especially in combination with *nsr*, conferred the best protection. Unlike *nisFEG*, *nisI* alone hardly delivered immunity under application-relevant conditions. Particularly, nisin impacts ssp. *cremoris* milk acidification more than ssp. *lactis*. Strains that do not produce nisin but have immunity are of great interest for the design of nisin-compatible starter cultures as these would circumvent the requirement for NSR to protect starter culture composition. Such strains have been identified previously and are also found in the current study (Tarazanova et al., 2016; Wels et al., 2019). We believe that the generated dataset lays a new foundation toward understanding how nisin influences cheese fermentation processes that typically involve starter cultures containing multiple nisin-related genotypic variants. Furthermore, the knowledge of how individual strains react to nisin is highly relevant for the design of compatible culture compositions to help fermentation deliver the desired flavor and characteristic properties together with a strong bioprotective effect in the cheese.

DATA AVAILABILITY STATEMENT

All data is available, except the whole genome sequences, because these are proprietary strains.

AUTHOR CONTRIBUTIONS

Experiments were designed by TE, JV, GO, LG, and KN. Experiments were performed by TE, LG, LH-D, AG, and KN. Data was analyzed by LH-D, LG, KN, KJ, EB, TE, AN, and GO. All authors contributed to the first draft with main contributions by LG and TE. Editing and finalization of manuscript was done by LG, LH-D, TE, AN, and GO.

FUNDING

The authors declare that this study was funded entirely by Chr. Hansen A/S. The funder was not involved in the study design, collection, analysis, interpretation of data, the writing of this article or the decision to submit it for publication.

ACKNOWLEDGMENTS

We acknowledge the input and effort made by Martin Karkov Kristensen to study the effect of nisin degrading strains in complex cultures and for inspirational scientific discussions. The large amount of data made available in this work could only be composed after a great effort done by Birgit Albrecht Svendsen, Elahe Ghanei Moghadam, Rikke Dollerup Bech, Helle Simonsen and our Chr. Hansen NGS team.

SUPPLEMENTARY MATERIAL

The Supplementary Material for this article can be found online at: https://www.frontiersin.org/articles/10.3389/fbioe.2021.622835/full#supplementary-material

Supplementary Figure 1 | Effect of nisin on milk acidification profiles by 710 *L. lactis* strains co-plotted according to subspecies, phenotypic classification, and genetic make-up of nisin-related gene sets. Milk acidification curves at 30°C of **(A)** *L. lactis* ssp. *lactis* strains and **(B)** *L. lactis* ssp. *cremoris* strains, in the absence ($CFS_{control}$) or presence of 1.5 μg ml^{-1} nisin (CFS_{nisin}) and further grouped according to acidification phenotype (rows) and presence or absence of genes for nisin immunity, synthesis, and/or degradation (columns). Thin lines depict averaged milk acidification data of three replicates while thick lines depict the averaged curves per group. The nisin-containing milk phenotypes are: LA, loss of acidification; HDA, highly delayed acidification; MDA, mildly delayed acidification; and UA, unaltered acidification. All acidification curves are synchronized based on acidification onset of each respective $CFS_{control}$ profile and normalized to a start pH of 6.4.

Supplementary Figure 2 | Effect of nisin on milk acidification of strains containing a full nisin biosynthesis gene cassette. Graphs depicting milk acidification at 30°C in the absence ($CFS_{control}$) or presence of 1.5 μg ml^{-1} nisin (CFS_{nisin}) by strains with *nisABTCIPRK-FEG* genotypes mapping to the **(A)** MDA or **(B)** UA phenotypic group. Each graph depicts the averaged curve of three replicates. Strain IDs as further described in **Supplementary Table 1** and subspecies (*lactis* or *cremoris*) are indicated above each pair of curves. All acidification curves are synchronized based on acidification onset of each respective $CFS_{control}$ profile and normalized to a start pH of 6.4.

Supplementary Figure 3 | Genotypic diversity of the *L. lactis* strains as revealed by a MLST tree. A MLST-tree depicting the genotypic relatedness of 916 *L. lactis* ssp. *cremoris* and ssp. *lactis* strains. Indicated from outer to inner ring are: **(A)** Strain-specific genome sequence origin, obtained either from the 710 draft genomes from this study or the publicly available 206 *L. lactis* RefSeq genomes. **(B)** Strain-specific presence of nisin-related genes or gene clusters. **(C)** Strain-specific milk acidification phenotypes. **(D)** Subspecies clusters of *L. lactis* ssp. *lactis* and *L. lactis* ssp. *cremoris*.

Supplementary Figure 4 | The presence of *nisI* as the sole nisin tolerance factor is not sufficient to deliver protection of ssp. *cremoris* strains to dairy-relevant nisin concentrations. Single replicates of milk acidification profiles of *L. lactis* ssp. *cremoris* strains with *nsr- nisIP+ nisFEG-* genotypes in the absence ($CFS_{control}$), presence of 0.2 μg ml^{-1} nisin or presence of 1.5 μg ml^{-1} ($CFS_{control}$). All acidification curves are synchronized based on acidification onset of each respective $CFS_{control}$ profile and normalized to a start pH of 6.4.

Supplementary Figure 5 | The presence of *nsr* leads to greater nisin tolerance in ssp. *lactis* strains than in ssp. *cremoris* strains. Upper panels: Milk acidification profiles of ssp. *cremoris* and ssp. *lactis nsr+* strains in the absence ($CFS_{control}$) or presence (CFS_{nisin}) of 1.5 μg ml^{-1} nisin. Thin lines depict the averaged curve between replicates of the same strains while thick lines depict the averaged acidification of each genotypic group. All acidification curves are synchronized based on acidification onset of each respective $CFS_{control}$ profile and normalized to a start pH of 6.4. Lower panels: Subspecific distributions of *nsr+* strains over acidification phenotypes LA, HDA, MDA, and UA per subspecies.

Supplementary Figure 6 | Nisin A levels by NSR variant and subspecies show different protection efficiency. Dot plots depicting resultant nisin A concentrations as quantified with HPLC-MS/MS after incubating 0.9 μg ml^{-1} of nisin A in milk inoculated with **(A)** *L. lactis* ssp. *cremoris* or **(B)** *L. lactis* ssp. *lactis*, as a function of the NSR variant detected in each strain. Dots are further coded according to the phenotypic group (LA, HDA, MDA, and UA) each strain belongs (colors) and if the *nsr* gene is present alone or accompanied by nisin biosynthesis genes

(shapes). NSR variants highlighted in green or blue/red indicate most common or non-nisin-degrading NSR variants, respectively. **(C)** Protein sequence alignments of the second-most common NSR variant 17 and non-degrading NSR variants with the most common and functional NSR variant 25 from CH-2. Color-shaded regions of the query sequence of NSR variant 25 indicate domains important for NSR catalytic activity and/or nisin binding reported for the structure function of NSR from *S. agalactiae* (Khosa et al., 2016). **(D)** Box and raincloud plot depicting the difference in resultant nisin A levels in milk fermentations performed with non-nisin A producing strains containing either NSR variant 17 or 25 (Mann-Whitney U, $P < 0.01$).

Supplementary Table 1 | List of strains, their genotypes and milk acidification phenotypes, used in this study.

Supplementary Table 2 | Query sequences used for gene blasts to identify nisin biosynthesis, immunity and degradation genes.

Supplementary Table 3 | Details on data processing steps.

Supplementary Table 4 | Primers used in this study.

Supplementary Table 5 | Separate milk acidification profiles for all 710 *L. lactis* strains in the presence and absence of nisin.

Supplementary File 1 | Sequences of the 12 conserved genes (*dnaK*, *fusA*, *groEL*, *gyrA*, *gyrB*, *ileS*, *lep*, *pheS*, *recA*, *rpoA*, *rpoB*, and *rpoC*) for each of the 710 *L. lactis* strains, used for the MLST tree presented in **Supplementary Figure 3**.

REFERENCES

Alegría, Á., Delgado, S., Roces, C., López, B., and Mayo, B. (2010). Bacteriocins produced by wild *Lactococcus lactis* strains isolated from traditional, starter-free cheeses made of raw milk. *Int. J. Food Microbiol.* 143, 61–66. doi: 10.1016/j.ijfoodmicro.2010.07.029

Alifax, P. R., and Chevalier, R. (1962). Etude de la nisinase produite par *Streptococcus thermophilus*. *J. Dairy Res.* 29, 233–240. doi: 10.1017/S0022029900011043

AlKhatib, Z., Lagedroste, M., Fey, I., Kleinschrodt, D., Abts, A., and Smits, S. H. J. (2014a). Lantibiotic immunity: inhibition of nisin mediated pore formation by NisI. *PLoS ONE* 9:e102246. doi: 10.1371/journal.pone.0102246

AlKhatib, Z., Lagedroste, M., Zaschke, J., Wagner, M., Abts, A., Fey, I., et al. (2014b). The C-terminus of nisin is important for the ABC transporter NisFEG to confer immunity in *Lactococcus lactis*. *Microbiol. Open* 3, 752–763. doi: 10.1002/mbo3.205

Allen, M., Poggiali, D., Whitaker, K., Marshall, T. R., and Kievit, R. A. (2019). Raincloud plots: a multi-platform tool for robust data visualization. *Wellcome Open Res.* 4:63. doi: 10.12688/wellcomeopenres.15191.1

Aly, S., Floury, J., Piot, M., Lortal, S., and Jeanson, S. (2012). The efficacy of nisin can drastically vary when produced *in situ* in model cheeses. *Food Microbiol.* 32, 185–190. doi: 10.1016/j.fm.2012.06.001

Ávila, M., Gómez-Torres, N., Hernández, M., and Garde, S. (2014). Inhibitory activity of reuterin, nisin, lysozyme and nitrite against vegetative cells and spores of dairy-related *Clostridium* species. *Int. J. Food Microbiol.* 172, 70–75. doi: 10.1016/j.ijfoodmicro.2013.12.002

Ayad, E. H. E., Verheul, A., Wouters, J. T. M., and Smit, G. (2001). Population dynamics of lactococci from industrial, artisanal and non-dairy origins in defined strain starters for Gouda-type cheese. *Int. Dairy J.* 11, 51–61. doi: 10.1016/S0958-6946(01)00041-3

Bergholz, T. M., Tang, S., Wiedmann, M., and Boor, K. J. (2013). Nisin resistance of *Listeria monocytogenes* is increased by exposure to salt stress and is mediated via LiaR. *Appl. Environ. Microbiol.* 79, 5682–5688. doi: 10.1128/AEM.01797-13

Bierbaum, G., and Sahl, H.-G. (1985). Induction of autolysis of staphylococci by the basic peptide antibiotics Pep 5 and nisin and their influence on the activity of autolytic enzymes. *Arch. Microbiol.* 141, 249–254. doi: 10.1007/BF00408067

Børsting, M. W., Stallknecht, M. K., Vogensen, F. K., and Ardö, Y. (2015). Influence of proteolytic *Lactococcus lactis* subsp. *cremoris* on ripening of reduced-fat Cheddar cheese made with camel chymosin. *Int. Dairy J.* 41, 38–45. doi: 10.1016/j.idairyj.2014.09.002

Breukink, E., Wiedemann, I., van Kraaij, C., Kuipers, O. P., Sahl, H. G., and de Kruijff, B. (1999). Use of the cell wall precursor lipid II by a pore-forming peptide antibiotic. *Science* 286, 2361–2364. doi: 10.1126/science.286.5448.2361

Broadbent, J. R., Strickland, M., Weimer, B. C., Johnson, M. E., and Steele, J. L. (1998). Peptide accumulation and bitterness in Cheddar cheese made using single-strain *Lactococcus lactis* starters with distinct proteinase specificities. *J. Dairy Sci.* 81, 327–337. doi: 10.3168/jds.S0022-0302(98)75581-X

Brötz, H., Josten, M., Wiedemann, I., Schneider, U., Götz, F., Bierbaum, G., et al. (1998). Role of lipid-bound peptidoglycan precursors in the formation of pores by nisin, epidermin and other lantibiotics. *Mol. Microbiol.* 30, 317–327. doi: 10.1046/j.1365-2958.1998.01065.x

Clemens, R., Zaschke-Kriesche, J., Khosa, S., and Smits, S. H. J. (2018). Insight into two ABC transporter families involved in lantibiotic resistance. *Front. Mol. Biosci.* 4:91. doi: 10.3389/fmolb.2017.00091

Collins, B., Curtis, N., Cotter, P. D., Hill, C., and Ross, R. P. (2010a). The ABC transporter AnrAB contributes to the innate resistance of *Listeria monocytogenes* to nisin, bacitracin, and various β-lactam antibiotics. *Antimicrob. Agents Chemother.* 54, 4416–4423. doi: 10.1128/AAC.00503-10

Collins, B., Guinane, C. M., Cotter, P. D., Hill, C., and Paul Ross, R. (2012). Assessing the contributions of the LiaS histidine kinase to the innate resistance of Listeria monocytogenes to nisin, cephalosporins, and disinfectants. *Appl. Environ. Microbiol.* 78, 2923–2929. doi: 10.1128/AEM.07402-11

Collins, B., Joyce, S., Hill, C., Cotter, P. D., and Ross, R. P. (2010b). TelA contributes to the innate resistance of *Listeria monocytogenes* to nisin and other cell wall-acting antibiotics. *Antimicrob. Agents Chemother.* 54, 4658–4663. doi: 10.1128/AAC.00290-10

Cosentino, S., Fadda, M. E., Deplano, M., Melis, R., Pomata, R., and Pisano, M. B. (2012). Antilisterial activity of nisin-like bacteriocin-producing *Lactococcus lactis* subsp. *lactis* isolated from traditional Sardinian dairy products. *J. Biomed. Biotechnol.* 2012:376428. doi: 10.1155/2012/376428

Davies, E. A., Bevis, H. E., and Delves-Broughton, J. (1997). The use of the bacteriocin, nisin, as a preservative in ricotta-type cheeses to control the food-borne pathogen *Listeria monocytogenes*. *Lett. Appl. Microbiol.* 24, 343–346. doi: 10.1046/j.1472-765X.1997.00145.x

de Arauz, L. J., Jozala, A. F., Mazzola, P. G., and Vessoni Penna, T. C. (2009). Nisin biotechnological production and application: a review. *Trends Food Sci. Technol.* 20, 146–154. doi: 10.1016/j.tifs.2009.01.056

De Kwaadsteniet, M., Ten Doeschate, K., and Dicks, L. M. T. (2008). Characterization of the structural gene encoding nisin F, a new lantibiotic produced by a *Lactococcus lactis* subsp. *lactis* isolate from freshwater catfish (*Clarias gariepinus*). *Appl. Environ. Microbiol.* 74, 547–549. doi: 10.1128/AEM.01862-07

de Ruyter, P. G., Kuipers, O. P., Beerthuyzen, M. M., van Alen-Boerrigter, I., and de Vos, W. M. (1996). Functional analysis of promoters in the nisin gene cluster of *Lactococcus lactis*. *J. Bacteriol.* 178, 3434–3439. doi: 10.1128/JB.178.12.3434-3439.1996

De Vuyst, L. (1994). Nisin production variability between natural *Lactococcus lactis* subsp. *lactis* strains. *Biotechnol. Lett.* 16, 287–292. doi: 10.1007/BF00134627

Delves-Broughton, J. (1996). Applications of the bacteriocin, nisin. *Antonie van Leeuwenhoek* 69, 193–202. doi: 10.1007/BF00399424

Dijkstra, A. R., Alkema, W., Starrenburg, M. J. C., Hugenholtz, J., Van Hijum, S. A. F. T., and Bron, P. A. (2016). Strain-dependent transcriptome signatures for robustness in *Lactococcus lactis*. *PLoS ONE* 11:e0167944. doi: 10.1371/journal.pone.0167944

Dijkstra, A. R., Setyawati, M. C., Bayjanov, J. R., Alkema, W., Van Hijum, S. A. F. T., Bron, P. A., et al. (2014). Diversity in robustness of *Lactococcus lactis* strains during heat stress, oxidative stress, and spray drying stress. *Appl. Environ. Microbiol.* 80, 603–611. doi: 10.1128/AEM.03434-13

Draper, L. A., Cotter, P. D., Hill, C., and Ross, R. P. (2015). Lantibiotic resistance. *Microbiol. Mol. Biol. Rev.* 79, 171–191. doi: 10.1128/MMBR.00051-14

Duan, K., Harvey, M. L., Liu, C.-Q., and Dunn, N. W. (1996). Identification and characterization of a mobilizing plasmid, pND300, in *Lactococcus lactis* M189

and its encoded nisin resistance determinant. *J. Appl. Bacteriol.* 81, 493–500. doi: 10.1111/j.1365-2672.1996.tb03538.x

Düsterhöft, E. M., Engels, W., and Huppertz, T. (2017). "Chapter 34: gouda and related cheeses," in *Cheese, 4th Edn*, eds P. L. H. McSweeney, P. F. Fox, P. D. Cotter, and D. W. Everett (San Diego, CA: Academic Press), 865–888. doi: 10.1016/B978-0-12-417012-4.00034-X

Egan, K., Field, D., Rea, M. C., Ross, R. P., Hill, C., and Cotter, P. D. (2016). Bacteriocins: Novel solutions to age old spore-related problems? *Front. Microbiol.* 7:461. doi: 10.3389/fmicb.2016.00461

Engelke, G., Gutowski-Eckel, Z., Kiesau, P., Siegers, K., Hammelmann, M., and Entian, K. D. (1994). Regulation of nisin biosynthesis and immunity in Lactococcus lactis 6F3. *Appl. Environ. Microbiol.* 60, 814–825. doi: 10.1128/AEM.60.3.814-825.1994

Erkus, O., De Jager, V. C. L., Spus, M., Van Alen-Boerrigter, I. J., Van Rijswijck, I. M. H., Hazelwood, L., et al. (2013). Multifactorial diversity sustains microbial community stability. *ISME J.* 7, 2126–2136. doi: 10.1038/ismej.2013.108

Fallico, V., Ross, R. P., Fitzgerald, G. F., and McAuliffe, O. (2011). Genetic response to bacteriophage infection in *Lactococcus lactis* reveals a four-strand approach involving induction of membrane stress proteins, D-alanylation of the cell wall, maintenance of proton motive force, and energy conservation. *J. Virol.* 85, 12032–12042. doi: 10.1128/JVI.00275-11

FAO (2013). *Compendium of Food Additive Specifications. Joint FAO/WHO Expert Committee on Food Additives (JECFA), 77th Meeting 2013. FAO JECFA Monographs 14.* Available online at: http://www.fao.org/3/a-at879e.pdf

Froseth, B. R., and McKay, L. L. (1991). Molecular characterization of the nisin resistance region of *Lactococcus lactis* subsp. *lactis biovar diacetylactis* DRC3. *Appl. Environ. Microbiol.* 57, 804–811. doi: 10.1128/AEM.57.3.804-811.1991

Fukao, M., Obita, T., Yoneyama, F., Kohda, D., Zendo, T., Nakayama, J., et al. (2008). Complete covalent structure of nisin Q, new natural nisin variant, containing post-translationally modified amino acids. *Biosci. Biotechnol. Biochem.* 72, 1750–1755. doi: 10.1271/bbb.80066

Giaouris, E., Briandet, R., Meyrand, M., Courtin, P., and Chapot-Chartier, M. P. (2008). Variations in the degree of D-alanylation of teichoic acids in *Lactococcus lactis* alter resistance to cationic antimicrobials but have no effect on bacterial surface hydrophobicity and charge. *Appl. Environ. Microbiol.* 74, 4764–4767. doi: 10.1128/AEM.00078-08

Gross, E., and Morell, J. L. (1971). The structure of nisin. *J. Am. Chem. Soc.* 93, 4634–4635. doi: 10.1021/ja00747a073

Gu, Z., Eils, R., and Schlesner, M. (2016). Complex heatmaps reveal patterns and correlations in multidimensional genomic data. *Bioinformatics* 32, 2847–2849. doi: 10.1093/bioinformatics/btw313

Hacker, C., Christ, N. A., Duchardt-Ferner, E., Korn, S., Göbl, C., Berninger, L., et al. (2015). The solution structure of the lantibiotic immunity protein NisI and its interactions with nisin. *J. Biol. Chem.* 290, 28869–28886. doi: 10.1074/jbc.M115.679969

Hansen, M. E., Wangari, R., Hansen, E. B., Mijakovic, I., and Jensen, P. R. (2009). Engineering of *Bacillus subtilis* 168 for increased nisin resistance. *Appl. Environ. Microbiol.* 75, 6688–6695. doi: 10.1128/AEM.00943-09

Hasper, H. E., De Kruijff, B., and Breukink, E. (2004). Assembly and stability of nisin-Lipid II pores. *Biochemistry* 43, 11567–11575. doi: 10.1021/bi049476b

Hasper, H. E., Kramer, N. E., Smith, J. L., Hillman, J. D., Zachariah, C., Kuipers, O. P., et al. (2006). An alternative bactericidal mechanism of action for lantibiotic peptides that target lipid II. *Science* 313, 1636–1637. doi: 10.1126/science.1129818

Hirsch, A. (1951). Growth and nisin production of a strain of *Streptococcus lactis*. *J. Gen. Microbiol.* 5, 208–221. doi: 10.1099/00221287-5-1-208

Jeong, J. H., and Ha, S. C. (2018). Crystal structure of NisI in a lipid-free form, the nisin immunity protein, from *Lactococcus lactis*. *Antimicrob. Agents Chemother.* 62. doi: 10.1128/AAC.01966-17

Kelleher, P., Bottacini, F., Mahony, J., Kilcawley, K. N., and van Sinderen, D. (2017). Comparative and functional genomics of the *Lactococcus lactis* taxon; insights into evolution and niche adaptation. *BMC Genomics* 18:267. doi: 10.1186/s12864-017-3650-5

Khosa, S., AlKhatib, Z., and Smits, S. H. J. (2013). NSR from *Streptococcus agalactiae* confers resistance against nisin and is encoded by a conserved *nsr* operon. *Biol. Chem.* 394, 1543–1549. doi: 10.1515/hsz-2013-0167

Khosa, S., Frieg, B., Mulnaes, D., Kleinschrodt, D., Hoeppner, A., Gohlke, H., et al. (2016). Structural basis of lantibiotic recognition by the nisin resistance protein from *Streptococcus agalactiae*. *Sci. Rep.* 6:18679. doi: 10.1038/srep18679

Khosa, S., Hoeppner, A., Kleinschrodt, D., and Smits, S. H. J. (2015). Overexpression, purification, crystallization and preliminary X-ray diffraction of the nisin resistance protein from *Streptococcus agalactiae*. *Acta Crystallogr. Sect. FStructural Biol. Commun.* 71(Pt 6), 671–675. doi: 10.1107/S2053230X15006226

Kim, W. S., Ren, J., and Dunn, N. W. (1999). Differentiation of *Lactococcus lactis* subspecies *lactis* and subspecies *cremoris* strains by their adaptive response to stresses. *FEMS Microbiol. Lett.* 171, 57–65. doi: 10.1111/j.1574-6968.1999.tb13412.x

Kleerebezem, M., Quadri, L. E. N., Kuipers, O. P., and De Vos, W. M. (1997). Quorum sensing by peptide pheromones and two-component signal-transduction systems in Gram-positive bacteria. *Mol. Microbiol.* 24, 895–904. doi: 10.1046/j.1365-2958.1997.4251782.x

Kramer, N. E., Hasper, H. E., van den Bogaard, P. T. C., Morath, S., de Kruijff, B., Hartung, T., et al. (2008). Increased D-alanylation of lipoteichoic and a thickened septum are main determinants in the nisin resistance mechanism of *Lactococcus lactis*. *Microbiology* 154, 1755–1762. doi: 10.1099/mic.0.2007/015412-0

Kramer, N. E., Smid, E. J., Kok, J., De Kruijff, B., Kuipers, O. P., and Breukink, E. (2004). Resistance of Gram-positive bacteria to nisin is not determined by Lipid II levels. *FEMS Microbiol. Lett.* 239, 157–161. doi: 10.1016/j.femsle.2004.08.033

Kramer, N. E., Van Hijum, S. A. F. T., Knol, J., Kok, J., and Kuipers, O. P. (2006). Transcriptome analysis reveals mechanisms by which *Lactococcus lactis* acquires nisin resistance. *Antimicrob. Agents Chemother.* 50, 1753–1761. doi: 10.1128/AAC.50.5.1753-1761.2006

Kuipers, O. P., Beerthuyzen, M. M., De Ruyter, P. G. G. A., Luesink, E. J., and De Vos, W. M. (1995). Autoregulation of nisin biosynthesis in *Lactococcus lactis* by signal transduction. *J. Biol. Chem.* 270, 27299–27304. doi: 10.1074/jbc.270.45.27299

Kuipers, O. P., Beerthuyzen, M. M., Siezen, R. J., and De Vos, W. M. (1993). Characterization of the nisin gene cluster *nisABTCIPR* of *Lactococcus lactis*: requirement of expression of the *nisA* and *nisI* genes for development of immunity. *Eur. J. Biochem.* 216, 281–291. doi: 10.1111/j.1432-1033.1993.tb18143.x

Letunic, I., and Bork, P. (2019). Interactive Tree Of Life (iTOL) v4: recent updates and new developments. *Nucleic Acids Res.* 47, W256–W259. doi: 10.1093/nar/gkz239

Li, H., and O'Sullivan, D. J. (2006). Identification of a *nisI* promoter within the *nisABCTIP* operon that may enable establishment of nisin immunity prior to induction of the operon via signal transduction. *J. Bacteriol.* 188, 8496–8503. doi: 10.1128/JB.00946-06

Liu, C. Q., Harvey, M. L., and Dunn, N. W. (1997). Cloning of a gene encoding nisin resistance from *Lactococcus lactis* subsp. *lactis* M189 which is transcribed from an extended−10 promoter. *J. Gen. Appl. Microbiol.* 43, 67–73. doi: 10.2323/jgam.43.67

Majchrzykiewicz, J. A., Kuipers, O. P., and Bijlsma, J. J. E. (2010). Generic and specific adaptive responses of *Streptococcus pneumoniae* to challenge with three distinct antimicrobial peptides, bacitracin, LL-37, and nisin. *Antimicrob. Agents Chemother.* 54, 440–451. doi: 10.1128/AAC.00769-09

MartÃnezCuesta, M. C., Kok, J., Herranz, E., PelÃ¡ez, C., Requena, T., and Buist, G. (2000). Requirement of autolytic activity for bacteriocin-induced lysis. *Appl. Environ. Microbiol.* 66, 3174–3179. doi: 10.1128/AEM.66.8.3174-3179.2000

Martínez, B., Zomer, A. L., Rodríguez, A., Kok, J., and Kuipers, O. P. (2007). Cell envelope stress induced by the bacteriocin Lcn972 is sensed by the lactococcal two-component system CesSR. *Mol. Microbiol.* 64, 473–486. doi: 10.1111/j.1365-2958.2007.05668.x

Mattick, A. T., and Hirsch, A. (1947). Further observations on an inhibitory substance (nisin) from lactic streptococci. *Lancet* 2, 5–8. doi: 10.1016/s0140-6736(47)90004-4

Mazzotta, A. S., and Montville, T. J. (1997). Nisin induces changes in membrane fatty acid composition of *Listeria monocytogenes* nisin-resistant strains at 10°C and 30°C. *J. Appl. Microbiol.* 82, 32–38. doi: 10.1111/j.1365-2672.1997.tb03294.x

McKay, L. L., and Baldwin, K. A. (1984). Conjugative 40-megadalton plasmid in *Streptococcus lactis* subsp. *diacetylactis* DRC3 is associated with

resistance to nisin and bacteriophage. *Appl. Environ. Microbiol.* 47, 68–74. doi: 10.1128/AEM.47.1.68-74.1984

Meijer, W., van de Bunt, B., Twigt, M., de Jonge, B., Smit, G., and Hugenholtz, J. (1998). Lysis of *Lactococcus lactis* subsp. *cremoris* SK110 and its nisin-immune transconjugant in relation to flavor development in cheese. *Appl. Environ. Microbiol.* 64, 1950–1953. doi: 10.1128/AEM.64.5.1950-1953.1998

Ming, X., and Daeschel, M. A. (1995). Correlation of cellular phospholipid content with nisin resistance of *Listeria monocytogenes* Scott A. *J. Food Prot.* 58, 416–420. doi: 10.4315/0362-028X-58.4.416

Molloy, E. M., Hill, C., Cotter, P. D., and Ross, R. P. (2011). "Bacteriocins," in *Encyclopedia of Dairy Sciences*, 2nd Edn, eds J. W. Fuquay, P. F. Fox, and P. L. H. McSweeney (London: Elsevier Inc; Academic Press), 420–429. doi: 10.1016/B978-0-12-374407-4.00049-2

Morgan, S., Ross, R. P., and Hill, C. (1997). Increasing starter cell lysis in Cheddar cheese using a bacteriocin-producing adjunct. *J. Dairy Sci.* 80, 1–10. doi: 10.3168/jds.S0022-0302(97)75906-X

Mulders, J. W. M., Boerrigter, I. J., Rollema, H. S., Siezen, R. J., and de Vos, W. M. (1991). Identification and characterization of the lantibiotic nisin Z, a natural nisin variant. *Eur. J. Biochem.* 201, 581–584. doi: 10.1111/j.1432-1033.1991.tb16317.x

Peschel, A., Otto, M., Jack, R. W., Kalbacher, H., Jung, G., and Götz, F. (1999). Inactivation of the dlt operon in *Staphylococcus aureus* confers sensitivity to defensins, protegrins, and other antimicrobial peptides. *J. Biol. Chem.* 274, 8405–8410. doi: 10.1074/jbc.274.13.8405

Pinto, J. P. C., Kuipers, O. P., Marreddy, R. K. R., Poolman, B., and Kok, J. (2011). Efficient overproduction of membrane proteins in *Lactococcus lactis* requires the cell envelope stress sensor/regulator couple CesSR. *PLoS ONE* 6:e21873. doi: 10.1371/journal.pone.0021873

Poulsen, V. K., Derkx, P., and Oregaard, G. (2019). High-throughput screening for texturing *Lactococcus strains*. *FEMS Microbiol. Lett.* 366. doi: 10.1093/femsle/fnz001

Qiao, M., Immonen, T., Koponen, O., and Saris, P. E. J. (1995). The cellular location and effect on nisin immunity of the NisI protein from *Lactococcus lactis* N8 expressed in *Escherichia coli and L. lactis*. *FEMS Microbiol. Lett*. 131, 75–80. doi: 10.1111/j.1574-6968.1995.tb07757.x

Ra, R., Beerthuyzen, M. M., De Vos, W. M., Saris, P. E. J., and Kuipers, O. P. (1999). Effects of gene disruptions in the nisin gene cluster of *Lactococcus lactis* on nisin production and producer immunity. *Microbiology* 145, 1227–1233. doi: 10.1099/13500872-145-5-1227

Ra, R. S., and Saris, P. E. J. (1995). Characterization of prokaryotic mRNAs by RT-PCR. *Biotechniques* 18, 792–795.

Ra, S. R., Qiao, M., Immonen, T., Pujana, I., and Saris, P. E. J. (1996). Genes responsible for nisin synthesis, regulation and immunity form a regulon of two operons and are induced by nisin in *Lactoccocus lactis* N8. *Microbiology* 142, 1281–1288. doi: 10.1099/13500872-142-5-1281

Roces, C., Courtin, P., Kulakauskas, S., Rodríguez, A., Chapot-Chartier, M. P., and Martínez, B. (2012a). Isolation of *Lactococcus lactis* mutants simultaneously resistant to the cell wall-active bacteriocin Lcn972, lysozyme, nisin, and bacteriophage c2. *Appl. Environ. Microbiol.* 78, 4157–4163. doi: 10.1128/AEM.00795-12

Roces, C., Pérez, V., Campelo, A. B., Blanco, D., Kok, J., Kuipers, O. P., et al. (2012b). The putative lactococcal extracytoplasmic function anti-sigma factor Llmg2447 determines resistance to the cell wall-active bacteriocin Lcn972. *Antimicrob. Agents Chemother.* 56, 5520–5527. doi: 10.1128/AAC.01206-12

Sahl, H. G., Kordel, M., and Benz, R. (1987). Voltage-dependent depolarization of bacterial membranes and artificial lipid bilayers by the peptide antibiotic nisin. *Arch. Microbiol.* 149, 120–124. doi: 10.1007/BF00425076

Sallami, L., Kheadr, E. E., Fliss, and Vuillemard, J. C. (2004). Impact of autolytic, proteolytic, and nisin-producing adjunct cultures on biochemical and textural properties of cheddar cheese. *J. Dairy Sci.* 87, 1585–1594. doi: 10.3168/jds.S0022-0302(04)73312-3

Sambrook, J., Fritsch, E. F., and Maniatis, T. (1989). *Molecular Cloning: A Laboratory Manual*. Cold Spring Harbour, NY: Cold Spring Harbor Laboratory Press.

Sanders, J. W., Venema, G., and Kok, J. (1999). Environmental stress responses in *Lactococcus lactis*. *FEMS Microbiol. Rev.* 23, 483–501. doi: 10.1111/j.1574-6976.1999.tb00409.x

Schliep, K. P. (2011). phangorn: phylogenetic analysis in R. *Bioinformatics* 27, 592–593. doi: 10.1093/bioinformatics/btq706

Siegers, K., and Entian, K. D. (1995). Genes involved in immunity to the lantibiotic nisin produced by*Lactococcus lactis* 6F3. *Appl. Environ. Microbiol.* 61:1082. doi: 10.1128/AEM.61.3.1082-1089.1995

Solem, C., Defoor, E., Jensen, P. R., and Martinussen, J. (2008). Plasmid pCS1966, a new selection/counterselection tool for lactic acid bacterium strain construction based on the *oroP* gene, encoding an orotate transporter from *Lactococcus lactis*. *Appl. Environ. Microbiol.* 74, 4772–4775. doi: 10.1128/AEM.00134-08

Stein, T., Heinzmann, S., Solovieva, I., and Entian, K. D. (2003). Function of *Lactococcus lactis* nisin immunity genes *nisI* and *nisFEG* after coordinated expression in the surrogate host *Bacillus subtilis*. *J. Biol. Chem.* 278, 89–94. doi: 10.1074/jbc.M207237200

Sun, Z., Zhong, J., Liang, X., Liu, J., Chen, X., and Huan, L. (2009). Novel mechanism for nisin resistance via proteolytic degradation of nisin by the nisin resistance protein NSR. *Antimicrob. Agents Chemother.* 53, 1964–1973. doi: 10.1128/AAC.01382-08

Takala, T. M., Koponen, O., Qiao, M., and Saris, P. E. J. (2004). Lipid-free NisI: interaction with nisin and contribution to nisin immunity via secretion. *FEMS Microbiol. Lett.* 237, 171–177. doi: 10.1111/j.1574-6968.2004.tb09693.x

Tarazanova, M., Beerthuyzen, M., Siezen, R., Fernandez-Gutierrez, M. M., de Jong, A., van der Meulen, S., et al. (2016). Plasmid complement of *Lactococcus lactis* NCDO712 reveals a novel pilus gene cluster. *PLoS ONE* 11:e0167970. doi: 10.1371/journal.pone.0167970

Trmčić, A., Monnet, C., Rogelj, I., and Bogovič Matijašić, B. (2011). Expression of nisin genes in cheese: a quantitative real-time polymerase chain reaction approach. *J. Dairy Sci.* 94, 77–85. doi: 10.3168/jds.2010-3677

Veiga, P., Bulbarela-Sampieri, C., Furlan, S., Maisons, A., Chapot-Chartier, M. P., Erkelenz, M., et al. (2007). SpxB regulates O-acetylation-dependent resistance of *Lactococcus lactis* peptidoglycan to hydrolysis. *J. Biol. Chem.* 282, 19342–19354. doi: 10.1074/jbc.M611308200

Virolainen, N., Guglielmetti, S., Arioli, S., and Karp, M. (2012). Bioluminescence-based identification of nisin producers - a rapid and simple screening method for nisinogenic bacteria in food samples. *Int. J. Food Microbiol.* 158, 126–132. doi: 10.1016/j.ijfoodmicro.2012.07.007

Wels, M., Siezen, R., Van Hijum, S., Kelly, W. J., and Bachmann, H. (2019). Comparative genome analysis of *Lactococcus lactis* indicates niche adaptation and resolves genotype/phenotype disparity. *Front. Microbiol.* 10:4. doi: 10.3389/fmicb.2019.00004

Wiedemann, I., Breukink, E., van Kraaij, C., Kuipers, O. P., Bierbaum, G., de Kruijff, B., et al. (2001). Specific binding of nisin to the peptidoglycan precursor lipid II combines pore formation and inhibition of cell wall biosynthesis for potent antibiotic activity. *J. Biol. Chem.* 276, 1772–1779. doi: 10.1074/jbc.M006770200

Conflict of Interest: All authors were employed by CHR HANSEN A/S during the work presented here. CHR HANSEN A/S is a company that develops and commercializes dairy starter cultures.

frontiers in Bioengineering and Biotechnology

REVIEW
published: 12 May 2021
doi: 10.3389/fbioe.2021.612285

Metabolism Characteristics of Lactic Acid Bacteria and the Expanding Applications in Food Industry

Yaqi Wang[1], Jiangtao Wu[1], Mengxin Lv[1], Zhen Shao[1], Meluleki Hungwe[1], Jinju Wang[1], Xiaojia Bai[1], Jingli Xie[2], Yanping Wang[1] and Weitao Geng[1]**

[1] State Key Laboratory of Food Nutrition and Safety, College of Food Science and Engineering, Tianjin University of Science and Technology, Tianjin, China, [2] State Key Laboratory of Bioreactor Engineering, East China University of Science and Technology, Shanghai, China

OPEN ACCESS

Edited by:
Mingfeng Cao, University of Illinois at Urbana-Champaign, United States

Reviewed by:
Sastia Prama Putri, Osaka University, Japan
Michael Gänzle, University of Alberta, Canada
Shaohua Wang, Wake Forest School of Medicine, United States
Zhongtian Zhang, North Carolina State University, United States, in collaboration with reviewer SW

***Correspondence:**
Yanping Wang
ypwang40@163.com
Weitao Geng
gengwt@tust.edu.cn

Specialty section:
This article was submitted to Synthetic Biology, a section of the journal Frontiers in Bioengineering and Biotechnology

Received: *30 September 2020*
Accepted: *16 April 2021*
Published: *12 May 2021*

Citation:
Wang Y, Wu J, Lv M, Shao Z, Hungwe M, Wang J, Bai X, Xie J, Wang Y and Geng W (2021) Metabolism Characteristics of Lactic Acid Bacteria and the Expanding Applications in Food Industry. Front. Bioeng. Biotechnol. 9:612285. doi: 10.3389/fbioe.2021.612285

Lactic acid bacteria are a kind of microorganisms that can ferment carbohydrates to produce lactic acid, and are currently widely used in the fermented food industry. In recent years, with the excellent role of lactic acid bacteria in the food industry and probiotic functions, their microbial metabolic characteristics have also attracted more attention. Lactic acid bacteria can decompose macromolecular substances in food, including degradation of indigestible polysaccharides and transformation of undesirable flavor substances. Meanwhile, they can also produce a variety of products including short-chain fatty acids, amines, bacteriocins, vitamins and exopolysaccharides during metabolism. Based on the above-mentioned metabolic characteristics, lactic acid bacteria have shown a variety of expanded applications in the food industry. On the one hand, they are used to improve the flavor of fermented foods, increase the nutrition of foods, reduce harmful substances, increase shelf life, and so on. On the other hand, they can be used as probiotics to promote health in the body. This article reviews and prospects the important metabolites in the expanded application of lactic acid bacteria from the perspective of bioengineering and biotechnology.

Keywords: lactic acid bacteria, degradation, products, metabolism characteristics, expanding applications

INTRODUCTION

In recent years, more and more attention has been paid to the metabolism of lactic acid bacteria. Lactic acid bacteria (LAB) are a type of gram-positive bacteria that use carbohydrates as the only or main carbon source (George et al., 2018). Lactic acid bacteria are generally cocci or rods, and have strong tolerance to low pH. Although lactic acid bacteria include more than 60 genera, the frequently genera occur in food fermentation generally include *Lactobacillus*, *Lactococcus*, *Leuconostoc*, *Pediococcus*, *Streptococcus*, *Enterococcus*, *Weissella*, etc. (Mokoena, 2017). But it has recently been proposed to merge *Lactobacillaceae* and *Leuconostocaceae* in one family *Lactobacillaceae*. The genus *Lactobacillus* was also reclassified into 25 genera (Zheng et al., 2020). For the taxonomy of the genus *Lactobacillus* was recently revised, the current nomenclature are used throughout this review.

As a fermentation strain, lactic acid bacteria should have several important metabolism characteristics, such as the ability to produce acid and aroma, the ability to hydrolyze protein, the ability to produce viscous exopolysaccharides and the ability to inhibit bacteria. In this review, the

metabolic characteristics of lactic acid bacteria and its application in food industry were reviewed from the aspects of degradation (**Table 1**) and biosynthesis (**Table 2**) metabolism of lactic acid bacteria. We hope to summarize the new development trends and promote the contribution of lactic acid bacteria related metabolic engineering and food biotechnology to the food industry.

DEGRADATION OF MACROMOLECULES

Degradation of Indigestible Polysaccharides

Polysaccharides are polymers composed of more than ten identical or different monosaccharide units linked by α - or β - glycosidic bonds (Gerwig, 2019). In plants, polysaccharides include starch, cellulose, fructan, hemicellulose and so on. The degradation of polysaccharides by lactic acid bacteria depends on various hydrolases. In fermented food, the decomposition of polysaccharides can provide energy for lactic acid bacteria and provide a variety of beneficial substances for human beings. Different kinds of lactic acid bacteria can metabolize different polysaccharides, which determines the different application prospects of related strains in food industry (Velikova et al., 2016).

In fermented food processing, the degradation of polysaccharides by lactic acid bacteria can produce monosaccharides or lactic acid, etc., which can improve the quality of food. For example, the ability of lactic acid bacteria to degrade polysaccharides has be used in beverage processing to replace the use of the enzymes from molds that decompose polysaccharides. In addition, some genera of lactic acid bacteria are generally regarded as probiotics in the intestine, include *Lactobacillus*, *Enterococcus*, *S*treptococcus, Pediococcus, Leuconostoc (Fijan, 2014). The growth of the probiotics can be promoted by some kinds of polysaccharides, which be defined as prebiotics. In recent years, with the in-depth study of intestinal microbial ecology, research on commercial prebiotic oligosaccharides has increased greatly. The nature of lactic acid bacteria in degrading polysaccharides has attracted more and more attention, not only in the food and fermentation industries, but even in the medical and health-related industries.

In the past, it was thought that lactic acid bacteria made a greater contribution to fermented dairy products, and had a weak ability to hydrolyze sugars and proteins in grains. But it was found that there is a corresponding starch metabolism pathway through the analysis of the KEGG metabolic pathway of lactic acid bacteria. It is also been proved that starch can be hydrolyzed by extracellular enzymes secreted by lactic acid bacteria (Gänzle and Follador, 2012). Due to the important role played by the starch and other polysaccharides hydrolysis ability in starch-rich sourdough, this part will focus on the metabolic properties of lactic acid bacteria on starch. Starch includes amylose composed of α-(1→4) glucose chain and amylopectin composed of α-(1→4) glucose main chain and α-(1→6) glucose side chain (van der Maarel et al., 2002). According to the different types of glycosidic bonds in amylose and amylopectin, their hydrolysis require amylase (both alpha and beta type) and amylopullulanase, respectively. Lactic acid bacteria also play an important role in the fermentation of sourdough. Common bacterial species for starch hydrolysis include *Lactiplantibacillus plantarum* and *Levilactobacillus brevis* (Gänzle and Zheng, 2019). *Lactiplantibacillus plantarum* can produce amylase to hydrolyze starch into dextrin, and finally into glucose (Oguntoyinbo and Narbad, 2012). There is a potential gene encoding maltogenic amylase in the *Weissella* genome, which is used to hydrolyze starch in sourdough (Falasconi et al., 2020).

Degradation of Proteins

During food processing, the degradation of macromolecular proteins is an important process that affects food quality, food safety and food nutrition. Dairy fermentations are only food fermentation where protein hydrolysis by lactic acid bacteria is relevant, in all others, proteases from other organisms or the substrate are much more important. Proteolysis in lactic acid bacteria can be divided into several steps, including protein degradation, peptide transport, peptide degradation and amino acid catabolism (Kunji et al., 1996; Christensen et al., 1999). **Figure 1** shows the metabolic pathway of lactic acid bacteria to degrade casein in milk. Proteolysis in lactic acid bacteria is initiated by cell envelope proteinase (CEP), which degrades proteins into oligopeptides. The second stage of protein degradation is the transfer of dipeptides, tripeptides, and oligopeptides into cells. Three transport systems have been found in lactic acid bacteria, namely oligopeptide, dipeptide and tripeptide transport systems (Opp, DtpP, and DtpT, respectively) (Hagting et al., 1994; Sanz et al., 2003). Peptides are degraded in cells to amino acid by a variety of peptidases, which include endopeptidases, aminopeptidases, dipeptides, tripeptidases and proline specific peptidases (Vesanto et al., 1996).

In the food industry, the degradation of proteins by lactic acid bacteria can eliminate protein allergens in food. Especially in the fermentation process of dairy products, lactic acid bacteria can degrade casein, thereby reducing the allergenicity of dairy products (Iwamoto et al., 2019). For example, certain strains of *Enterococcus faecium* isolated from fermented milk and cheese can express metalloproteases or cell envelope proteinase (CEP) (Genay et al., 2009), etc., which can effectively hydrolyze casein in milk (Biscola et al., 2018; Kordesedehi et al., 2018; Worsztynowicz et al., 2019). Lactic acid bacteria have made significant contributions not only in dairy products, but also in other fermented foods, such as fermented fruit and vegetable products and fermented grain products. For example, some strains of lactic acid bacteria isolated from sourdough can hydrolyse some of the proteins in wheat including albumins, globulins and gliadins (Stefańska et al., 2016). A strain of *Lacticaseibacillus casei* from sourdough can metabolize all the immunotoxic 33-mer peptide (97.5 ppm) derived from α2-gliadin (Alvarez-Sieiro et al., 2016a). Another study found that some lactic acid bacteria can hydrolyze the IgE binding epitopes of the protein allergens in wheat, thereby reducing the allergenicity of wheat sourdough (Stefańska et al., 2016). Therefore, it has become a new challenge to obtain strains for removing allergens in fermented foods through natural screening or metabolic engineering methods.

Lactic acid bacteria could produce a variety of substances that are beneficial to humans when hydrolyze proteins in the surrounding environment for their own growth needs (Savijoki et al., 2006). Lactic acid bacteria can improve the digestibility of protein in food and enhance the nutritional value of food protein. In the fermentation of dairy products, the lactic acid bacteria could help the human intestinal tract to absorb the amino acids in dairy products (Meisel and Bockelmann, 1999). Fermentation of faba bean flour by a strain of *Lactiplantibacillus plantarum* VTT E-133328 can improve the *in vitro* digestibility of its protein, especially the content of essential amino acids and free amino acids (Coda et al., 2015). For the by-products of pigmented wheat varieties, hull-less barley and emmer, after lactic acid bacteria fermentation combined with xylanase treatment, the protein digestibility *in vitro* can be as high as 87%, and the product has high free radical scavenging activity and high concentration of peptides and free amino acids (Pontonio et al., 2020). Lactic acid bacteria can decompose the protein in food to produce a variety of small molecule peptides or free amino acids. For example, the main group of lactobacilli in the kefir culture has a strong decomposing effect on milk protein in milk (Dallas et al., 2016). Lactic acid bacteria such as *Lactobacillus delbrueckii*, *Lactococcus lactis*, *Lentilactobacillus kefiri*, *Streptococcus thermophilus*, *Lactobacillus acidophilus*, *Lacticaseibacillus casei*, and *Lactobacillus helveticus* can produce angiotensin converting enzyme (ACE) inhibitory peptides (Fuglsang et al., 2003; Ramchandran and Shah, 2008; Rai et al., 2017; Daliri et al., 2018; Wu et al., 2019; Rubak et al., 2020). In addition, in *Lactococcus lactis*, starter lactocepin specificity type may have an important influence on the level of bitterness in low salt-in-moisture cheeses (Pillidge et al., 2003).

Catabolism of Amino Acids

Lactic acid bacteria can also metabolize amino acids in food, and its products include not only a variety of flavor substances, but also substances that people do not want to appear in fermented foods such as biogenic amines (BA). In lactic acid bacteria, the metabolism of amino acids includes deamination and decarboxylation (Gardini et al., 2016; Barbieri et al., 2019). The deamination reaction produces various α-carboxylic acids, which are involved in various metabolisms in lactic acid bacteria cells. Amino acids can generate a variety of biogenic amines under the action of lactic acid bacteria decarboxylase. For example, after decarboxylation, lysine, tryptophan, tyrosine, histidine and ornithine can generate cadaverine, tryptamine, tyramine, histamine, putrescine (Barbieri et al., 2019), etc., respectively, as shown in **Figure 1**.

Biogenic amines in food may be beneficial to the survival of lactic acid bacteria, but foods containing a large number of biogenic amines are toxic to humans (Lonvaud-Funel, 2001). The amines in fermented foods can be converted by monoamine oxidase. In cheese, *Lactobacillus* and *Enterococcus* will convert tyrosine to tyramine through the action of decarboxylase and transporter TyrP (Komprda et al., 2008). In aged cheese, *Pediococcus pentosaceus* can produce histamine in cheese (Møller et al., 2020). In view of food safety, some unfavorable metabolic activities of lactic acid bacteria under certain environmental conditions cannot be ignored. Therefore, how to balance the contribution of lactic acid bacteria to the quality of food and the accompanying potential safety issues need to be studied in the future development of lactic acid bacteria species resources and food processing (Diaz et al., 2020).

In addition, the metabolism of amino acids is of great significance for lactic acid bacteria in order to adapt to the environment (Even et al., 2002). Amino acid (especially glutamine, glutamic acid and arginine) metabolism plays an important role in the adaptation of lactic acid bacteria to the acid environment. The synthesized NH_3 during amino acids deamination can increase the pH value inside and outside the cell, thereby protecting the cell from acid stress (Papadimitriou et al., 2016). In *Lentilactobacillus hilgardii*, the decarboxylation reaction of histidine and tyrosine also contributes to the acid resistance of the bacteria (Lamberti et al., 2011). *Levilactobacillus brevis*, *Latilactobacillus curvatus,*

TABLE 1 | The degradation of macromolecular substances in food by lactic acid bacteria.

Substance	Metabolic Engineering works	Expanding applications in the food industry	Lactic acid bacteria strains (References)
Polysaccharides	Hydrolyze polysaccharides with α-(1→4) glycosidic bonds	Hydrolyze starch or fructan in sourdough	*Weissella* (Falasconi et al., 2020) *Lactiplantibacillus plantarum* (Oguntoyinbo and Narbad, 2012)
Proteins and related Amino acids	Heterologous expression of *prtB* gene encoding the protease	Effectively hydrolyze protein in milk	*Enterococcus faecium* (Biscola et al., 2018; Kordesedehi et al., 2018; Worsztynowicz et al., 2019)
	Different bioactive peptides and the bioactivity diversity can be increased by editing the proteolytic system of *Lactococcus lactis*	Improve the *in vitro* digestibility of protein of cereal products	*Lactiplantibacillus plantarum* VTT E-133328 (Coda et al., 2015)
Other non-nutritive and harmful substances		Produce urethanase-promoted EC degradation in alcohol fermentation	*Oenococcus oeni*, *Levilactobacillus brevis*, and *Lactiplantibacillus plantarum* (Fang et al., 2019)
		Decompose phytic acid in the fermentation process of yam-based foods	*Leuconostoc lactis* CCMA 0415, *Lactiplantibacillus plantarum* CCMA 0744 (Batista et al., 2019)
		Hydrolyze bitter peptides in cheese production	*Lactobacillus helveticus* (Komprda et al., 2008)

TABLE 2 | Substances synthesized in food by lactic acid bacteria.

Substance	Metabolic Engineering works	Expanding applications in the food industry	Lactic acid bacteria strains (References)
Lactic acid	Heterologous expression of gene encoding short-chain dehydrogenase for higher yield of D-lactic acid	Use dairy industry waste as a substrate to reduce costs	*Pediococcus acidilactici* (Qiu et al., 2020), *Lacticaseibacillus rhamnosus* B103 (Bernardo et al., 2016) *Lacticaseibacillus casei*, *Lactiplantibacillus pentosus* and *Lactobacillus sp.* (Shirai et al., 2001) *Enterococcus faecalis* (Deibel and Niven, 1964)
	Improve the yield of lactic acid by adding different nutrients such as the substrate glucose or vitamin B compounds or adopting pH control strategies	Fermentation strategies and metabolic engineering are often used to improve the yield and purity of lactic acid	*Lacticaseibacillus rhamnosus* HN001 (Wang et al., 2019), *Pediococcus acidilactici* ZY271 (Han et al., 2019) *Lactiplantibacillus pentosus* CECT4023T (Cubas-Cano et al., 2019)
Other organic acids	The organic acid (formic acid, acetic acid, propionic acid, butyric acid, and succinic acid) production of lactic acid bacteria in fish infusion broth	Detection of organic acids produced by lactic acid bacteria and improvement of food quality and safety	*Lactobacillus lactis subsp. Lactis* (Sezen et al., 2016)
	3-Hydroxypropionic acid produced through glycerol metabolism	3-Hydroxypropionic acid is an important platform chemical	*Limosilactobacillus reuteri* (Kumar et al., 2013)
	The production of lactic acid, propionic acid was and succinic acid in fermented silages	The production of organic acids in fermented fish silages replaces the need of the addition of chemical additives for acidification	*Levilactobacillus brevis, Lactiplantibacillus plantarum, Pediococcus acidilactici,* and *Streptococcus spp.*
	Heterologous expression of mvaES gene of *Enterococcus faecalis*	Synthesize mevalonate	*Enterococcus faecalis* (Wada et al., 2017)
Bacteriocin		Inhibit the growth of *Listeria monocytogenes* in raw minced beef and gilthead sea bream	*Lactiplantibacillus plantarum* TN8 (Trabelsi et al., 2019), *Latilactobacillus sakei* CTC494 (Costa et al., 2019)
	Gasserins has antibacterial activity against *Listeria monocytogenes* or *Bacillus cereus*	Gassericin A can be an important tool for food preservation	*Lactobacillus gasseri* (Pandey et al., 2013)
	Sakacin P has antibacterial activity against *Listeria monocytogenes* or *Bacillus cereus*	Sakacin P exerts its antibacterial effect in fermented sausage	*Latilactobacillus sakei* (Chen et al., 2012)
Vitamins	Add passion fruit by-product and oligofructose to soy milk can produce folic acid	Synthesize folic acid in dairy products	*Streptococcus*, *Lactobacillus* and *Lactococcus* (Khalili et al., 2020), *Lactococcus lactis* NZ9000 (Wegkamp et al., 2007),
	Insert a 1059-bp DNA fragment into the upstream regulatory region of the rib operon of *Lactiplantibacillus plantarum*	Induce the overexpression of riboflavin biosynthesis	*Lactiplantibacillus plantarum* (Ge et al., 2020)
	Purine biosynthesis can trigger riboflavin secretion more effectively in *Lactococcus lactis*		*Lactococcus lactis* JC017 (Chen et al., 2017)
Extracellular polysaccharides	Synthesize glucan using sucrose	Synthesize isomalto-/malto-polysaccharides by using different substrate	*Leuconostoc mesenteroides* (Yan et al., 2018) *Lactobacillus crispatus* (Hidalgo-Cantabrana et al., 2019) *Limosilactobacillus reuteri* 35-5 (Bai et al., 2016)
		Increase the extracellular polysaccharide content of yogurt	*Streptococcus thermophilus* zlw TM11 and *Lactobacillus delbrueckii subsp. bulgaricus* 34.5 (Han et al., 2016)
		Has strong inhibitory activity with a variety of pathogenic bacteria	*Lactococcus lactis* F-mou (Nehal et al., 2019), *Lactiplantibacillus plantarum* BR2 (Sasikumar et al., 2017)
	Two glycosyltransferases participate in the formation of glucan	Exploration of a new way of glucan biosynthesis	*Lactobacillus johnsonii* (Mayer et al., 2020)
	Glucan will extend to the crumb porosity of bread	Improvement of bread texture	*Limosilactobacillus reuteri* (Leemhuis et al., 2014)

(Continued)

TABLE 2 | Continued

Substance	Metabolic Engineering works	Expanding applications in the food industry	Lactic acid bacteria strains (References)
γ-aminobutyric acid	Mutations in the GadA or *gadR* gene facilitate the conversion of L-monosodium glutamate (MSG) to GABA	Increase the GABA content in fermented cereals	*Levilactobacillus brevis* (Lyu et al., 2019) *Levilactobacillus brevis* D17 (Gong et al., 2019)
	GadC transports L-glutamate into the cell		*Lactococcus lactis* (Small and Waterman, 1998)
	Glutamate decarboxylase and pyridoxal-5′-phosphate participate in the decarboxylation reaction of L-glutamate		*Lactococcus lactis* (Cui et al., 2020)
	The cell immobilization technology increase GABA production		*Levilactobacillus brevis* RK03 (Hsueh et al., 2017) *Levilactobacillus brevis* (Shi et al., 2017)
Flavor substances	SHMT gene encodes a serine hydroxymethyltransferase with threonine aldolase activity	Produce flavor substances (2,3-butanedione and 2,3-pentanedione, etc.) in wine, vinegar, bread, sourdough and cheese	*Streptococcus thermophilus* (Chaves et al., 2002), (Bancalari et al., 2017)
	Heterologous expression of thl, hbd, and crt which encode thiolase, β-hydroxybutyryl-CoA dehydrogenase, and crotonase, and the Treponema denticola for higher yield of N-butanol		*Levilactobacillus brevis* (Li et al., 2020), *Lacticaseibacillus casei*, *Lacticaseibacillus rhamnosus* and *Streptococcus thermophilus* (Bancalari et al., 2017), *Streptococcus thermophilus* and *Lacticaseibacillus casei* (Chammas et al., 2006)
Antioxidant substances	*Lactiplantibacillus plantarum* fermentation significantly enhanced the ability to scavenge free radical's DPPH when the fermenting conditions were optimized by the method of responsive surface design in fermenting sheep bone	Produce antioxidant substances (active phenol metabolites, chlorogenic acid glucoside, sulforaphane) have a variety of beneficial effects on the human body	*Lactiplantibacillus plantarum* (Ge et al., 2019; Mu et al., 2019; Ryu et al., 2019), *Lacticaseibacillus rhamnosus*, *Lactobacillus acidophilus* (Kêska and Stadnik, 2018), *Leuconostoc mesenteroides* (Nam et al., 2017)
	Metabolize phenolic acid by decarboxylase and reductase	Reduce the damage of phenolic substances to the plasma membrane and cell wall of lactic acid bacteria	*Levilactobacillus brevis*, *Limosilactobacillus fermentum* and *Lactiplantibacillus plantarum* (Filannino et al., 2018)
	Hydroxycinnamic acid (*P*-coumaric, ferulic acid and caffeic acid) can be degraded.		*Lactiplantibacillus plantarum* NC8 (Barthelmebs et al., 2000)
	Hydroxybenzoic acid (gallic acid and protocatechuic acid) can be degraded.		*Lactiplantibacillus plantarum* CECT 748T (Rodriguez et al., 2008) *Lactiplantibacillus plantarum* (Whiting and Coggins, 1971)
	Convert oxidized glutathione taken from the environment into reduced glutathione	Promotion of glutathione synthesis in industry	*Limosilactobacillus fermentum CECT* 5716 (Surya et al., 2018) *Streptococcus thermophilus* (Qiao et al., 2018)
	Mutant strain *Fructilactobacillus sanfranciscensis* DSM20451 Δ*gshR* lacking the glutathione reductase gene	Increase dough rheology; promote the hydrolysis of egg white protein; improve the acid resistance of lactic acid bacteria	*Latilactobacillus sakei* and *Fructilactobacillus sanfranciscensis* (Loponen et al., 2008) *Fructilactobacillus sanfranciscensis* (Xu et al., 2018) *Ligilactobacillus salivarius* (Lee et al., 2010)

Enterococcus faecalis, *Lactococcus lactis* can hydrolyze agmatine into putrescine, NH_3, CO_2 and ATP through the AgDI pathway, which increases the pH of the cytoplasm (Papadimitriou et al., 2016). In *Streptococcus thermophilus*, the metabolism of arginine relieves the decrease of intracellular pH by consuming protons and generating NH_3 (Huang et al., 2016).

Conversion of Other Non-nutritive and Harmful Substances in Food

In the food and fermentation industry, lactic acid bacteria can't only degrade the main nutritional macromolecular substances such as polysaccharides and proteins, but also can degrade some other undesirable substances. Fist of all, lactic acid bacteria can be used to inhibit the accumulation of mycotoxins during the preservation of cereal products. After artificially infected almonds with *Aspergillus flavus*, the inoculation of *Lentilactobacillus kefiri* FR7 can greatly reduce the accumulation of aflatoxin B1 and aflatoxin B2 (Ben Taheur et al., 2019). Lactic acid bacteria can also decompose harmful substances that may be produced in alcohol fermentation. For example, three lactic acid bacteria (*Oenococcus oeni*, *Levilactobacillus brevis*, and *Lactiplantibacillus plantarum*) produce urethanase-promoted EC degradation during co-cultivation with *Saccharomyces cerevisiae* to break down the potential carcinogenic ethyl carbamate (Fang et al., 2019). Lactic acid bacteria can also decompose the phytic

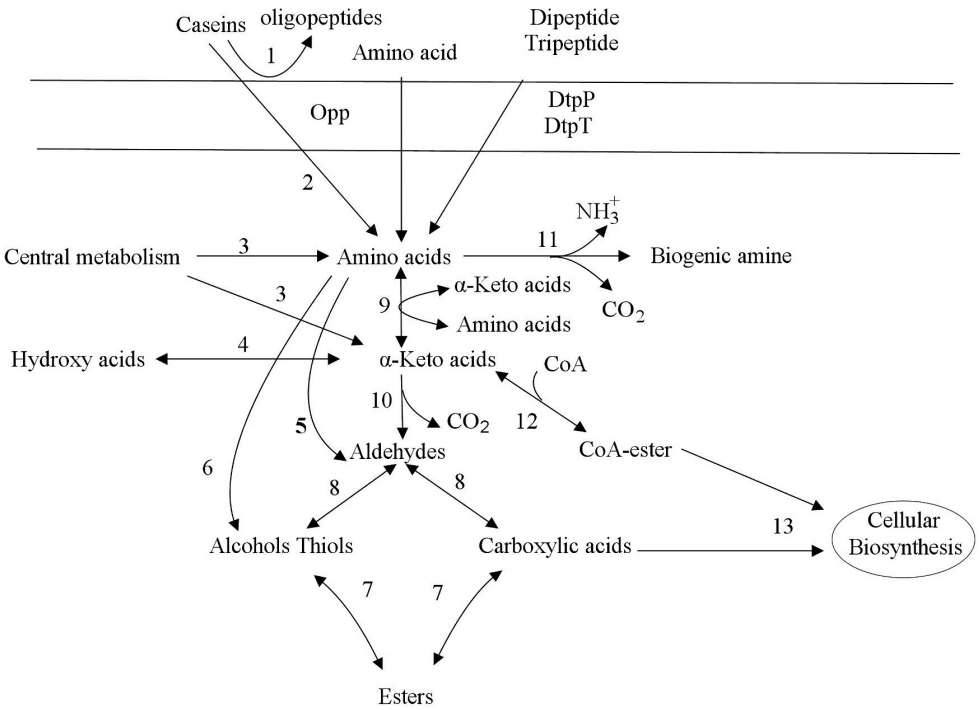

FIGURE 1 | Decomposition of protein and metabolism of amino acids (Smit et al., 2005). Proteolysis in lactic acid bacteria is initiated by cell envelope proteinase (CEP), which degrades proteins into oligopeptides. The second stage of protein degradation is the transfer of dipeptides, tripeptides, and oligopeptides into cells. Three transport systems have been found in lactic acid bacteria, namely oligopeptide, dipeptide and tripeptide transport systems (Opp, DtpP, and DtpT, respectively). Finally, the Pep family hydrolyzes dipeptides, tripeptides, and oligopeptides into amino acids. The metabolism of amino acids includes deamination and decarboxylation. The deamination reaction produces various α-carboxylic acids, which are involved in various metabolisms in lactic acid bacteria cells. The amino acid decarboxylation reaction produces biogenic amines, which mainly includes the transport of amino acids into the cell, decarboxylation, and transport outside the cell after being converted into biogenic amines. Transamination of amino acids leads to the formation of alpha-keto acids. Alpha-keto acids can be converted to aldehydes by decarboxylation. Aldehydes are converted to alcohols or carboxylic acids by dehydrogenation. The direct dehydrogenation of alpha-keto acids leads to the formation of hydroxy acids. 1: cell envelope proteinase, 2: peptidases, 3: biosynthetic enzymes, 4: dehydrogenase, 5: aldolases, 6: lyases, 7: acyltransferases esterases, 8: dehydrogenase, 9: aminotransferases, 10: decarboxylase, 11: deiminases decarboxylase, 12: dehydrogenase complex, 13: biosynthetic enzymes.

acid that affects the taste of food and is difficult to digest. For example, in the fermentation process of yam-based foods, phytase produced by *Leuconostoc lactis* CCMA 0415, *Lactiplantibacillus plantarum* CCMA 0744 and *Limosilactobacillus fermentum* CCMA 0745 can decompose phytic acid (Batista et al., 2019). The addition of lactic acid bacteria will also reduce the possible undesirable flavors in fermented foods. For example, based on the properties of lactic acid bacteria to produce acid and aroma, the undesirable flavor caused by the fermentation of *Bacillus* can be improved through fermentation of mixed strains (Ben-Harb et al., 2019). *Lactobacillus helveticus* can be used as an auxiliary starter to hydrolyze bitter peptides in cheese production (Komprda et al., 2008). In addition, *Oxalobacter* and *Lactobacillus* species exist symbiotically in the human gut can prevent the formation of stones by producing specific enzymes that help oxalate salts degradation (Sadaf et al., 2017). Although lactic acid bacteria have shown a variety of degradation effects, because lactic acid bacteria are not traditionally considered microorganisms with strong degrading ability, the specific degradation mechanism of most harmful substances in foods still needs extensive and far-reaching research. Moreover, this degradation has limitations in efficiency, effectiveness and environmental conditions. Therefore, the use of lactic acid bacteria to achieve efficient conversion of unwanted substances in food still has certain challenges (Perczak et al., 2018).

PRODUCTS SYNTHESIZED BY LACTIC ACID BACTERIA

Organic Acids

In the metabolism of lactic acid bacteria, certain metabolic processes such as lactic acid fermentation can synthesize a variety of organic acids including lactic acid. Lactic acid is an important bio-based platform compound, which can be divided into D-lactic acid and L-lactic acid according to its optical rotation. It is widely used in agriculture, food, medicine, chemical industry and environmental protection. In view of the importance of lactic acid as an important industrial raw material, related synthesis research has continued to be a hot spot in recent decades. And this part will mainly discuss the application of lactic acid synthesis in the food industry and related metabolic engineering research.

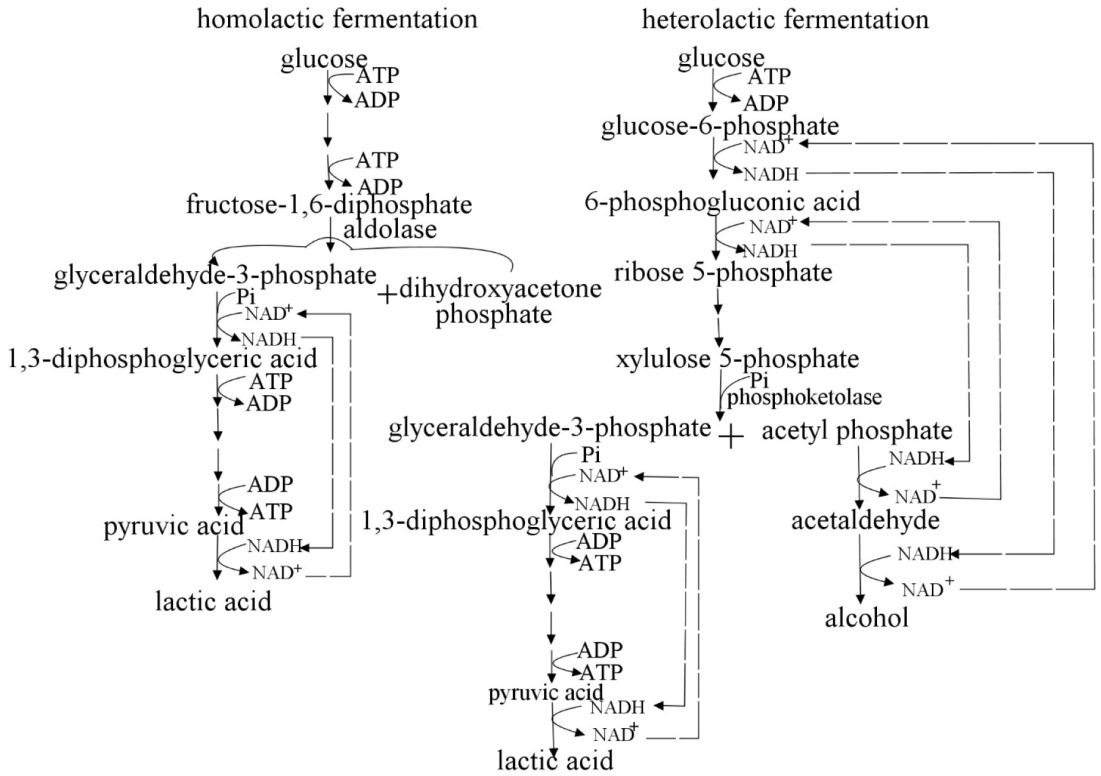

FIGURE 2 | Homolactic fermentation and heterolactic fermentation. *Lactococcus spp.* performs homolactic fermentation, while *Lactobacillus* and *Leuconostoc spp.* perform heterolactic fermentation. (1) In the process of pure lactic acid fermentation, lactic acid bacteria use glucose as a carbon source to produce pyruvate through glycolysis, and then produce lactic acid under the action of lactate dehydrogenase. In theory, 1 mole of glucose produces 2 moles of lactic acid. (2) In lactic acid bacteria of the heterolactic fermentation type, glucose can be decomposed into lactic acid, ethanol, CO_2 (in *Leuconostoc*, etc.) through the phosphoketolase (PK) pathway. In theory, 1 mole of glucose produces 1 mole of lactic acid. (3) Through the pentose phosphate (PP) pathway, glucose 6-phosphate was converted into carbon dioxide, ribulose 5-phosphate and NADPH (Eiteman and Ramalingam, 2015; Stincone et al., 2015).

According to whether aldolase is used in the process of producing lactic acid, lactic acid bacteria can be divided into homolactic fermentation and heterolactic fermentation (**Figure 2**). *Lactococcus* and *Lactobacillus* perform homolactic fermentation, while *Leuconostoc, Weissella* and *Oenococcus* perform heterolactic fermentation (Sridhar et al., 2005; Zaunmüller et al., 2006). (1) In the process of pure lactic acid fermentation, lactic acid bacteria use glucose as a carbon source to produce pyruvate through glycolysis, and then produce lactic acid under the action of lactate dehydrogenase (Eiteman and Ramalingam, 2015). In theory, 1 mole of glucose produces 2 moles of lactic acid. (2) In lactic acid bacteria of the heterolactic fermentation type, glucose can be decomposed into lactic acid, ethanol, CO_2 (in *Leuconostoc*, etc.) through the phosphoketolase (PK) pathway. In theory, 1 mole of glucose produces 1 mole of lactic acid (Eiteman and Ramalingam, 2015). (3) Through the pentose phosphate (PP) pathway, glucose 6-phosphate was converted into carbon dioxide, ribulose 5-phosphate and NADPH (Eiteman and Ramalingam, 2015; Stincone et al., 2015). Lactate dehydrogenase is a key enzyme for lactic acid bacteria to transform pyruvate into lactic acid, and its stereospecificity determines the configuration of lactic acid. D-lactic acid and L-lactic acid are catalyzed by D-lactate dehydrogenase and L-lactate dehydrogenase, respectively. The optical type of lactic acid synthesized by microorganisms depends on the expression levels of D-lactate and L-lactate dehydrogenase in the strain (Kim et al., 2020).

In the food industry, there are many studies on how to improve the yield and optical purity of lactic acid during food processing (Zhang et al., 2016), and a variety of methods provide ideas from different approaches. In currently industrial production, fermentation strategies are often used to improve the yield and purity of lactic acid. These fermentation strategies include adding different nutrients such as the substrate glucose or vitamin B compounds during the fermentation process (Han et al., 2019; Wang et al., 2019), adopting pH control strategies (Cubas-Cano et al., 2019), and using dairy industry waste as a substrate to reduce costs (Bernardo et al., 2016), etc. Among them, strategies such as simultaneous saccharification fermentation (SSF) and both separate hydrolysis and fermentation (SHF) are used for the production of lactic acid to obtain products with high optical purity (>99.9%) and reduce the amount of residual sugar (Xu et al., 2016; Müller et al., 2017).

In addition to mainly producing lactic acid, lactic acid bacteria also produce acetate, propionate, 3-hydroxypropionate, formate and succinate. For example, when shrimp waste silage

is used as a substrate, *Lactiplantibacillus pentosus* can also produce acetic acid (Shirai et al., 2001). *Lactobacillus* and *Limosilactobacillus reuteri* produce 3-hydroxypropionic acid through glycerol metabolism pathway (Kumar et al., 2013). Succinic acid produced by lactic acid bacteria fermentation is also one of the final fermentation products of anaerobic metabolism (Kuley et al., 2020). The organic acids usually be as a part of the flavor substances. However, due to the complexity of the types of flavor substances, we will discuss them in the following content. In general, the synthetic pathways of organic acids mainly include hetero-lactic fermentation pathways and amino acid metabolism. Firstly, the hetero-lactic fermentation will synthesize other organic acids besides lactic acid. For example, in addition to being decomposed into lactic acid, pyruvic acid can also be decomposed into acetic acid, formic acid, and ethanol under certain conditions, or decomposed into acetic acid and carbon dioxide. In addition, the α-acetolactate is formed by the conversion of excess pyruvate by α-acetolactate synthase (ALS) under aerobic conditions (Dorau et al., 2019). Secondly, some organic acids are produced in amino acid metabolism. For example, in *Lactococcus lactis*, *Lactiplantibacillus plantarum*, *Levilactobacillus brevis*, *Leuconostoc mesenteroides* and some other lactic acid strains, leucine can generate 2-ketoisocaproic acid (KICA) after transamination, and 2-ketoisocaproic acid (KICA) can be reduced to 2-hydroxyisocaproic acid (HICA). Therefore, adding the above lactic acid bacteria can increase the HICA content in fermented foods (Park et al., 2017). In *Lactiplantibacillus plantarum* LY-78, phenyllactic acid (PLA) can be accumulated as a by-product of phenylalanine catabolism (Sun et al., 2019).

Lactic acid bacteria may metabolize in the intestine to produce organic acids, which is also an important metabolic feature of probiotics. At the same time, the study of the interaction between probiotics and the intestine found that the synthesis of a variety of organic acids is affected by many environmental factors (Liao et al., 2016). Moreover, the synthesis process of a certain product is often complicated, and multiple key genes may play a synergistic role (Ali et al., 2019). Therefore, research on the synthesis of organic acids from lactic acid bacteria in the context of food or intestines, and clarifying the molecular basis of lactic acid bacteria as probiotics, are also challenging tasks in the future.

Bacteriocin

Bacteriocins are primary metabolites of polypeptides, proteins or protein complexes synthesized by bacteria using ribosomes with antibacterial activity (Diep and Nes, 2002). Bacteriocins can inhibit the growth and reproduction of a variety of bacteria. After years of research and development, people have clear reports on the molecular composition and antibacterial mechanism of bacteriocins. The bacteriocin will interact with the cell surface to increase the permeability of the cell; inhibit the production of cell wall; inhibit the synthesis of nucleic acid; inhibit the synthesis of protein (Kumariya et al., 2019). Bacteriocins may be divided into two categories: Category I is lantibiotics containing lanthionine (such as nisin, epidermin, streptin, etc.; Deegan et al., 2006). Nisin secreted by *Lactococcus lactis* is the first lanthiococin to be identified (Mattick and Hirsch, 1947). Nisin's mechanism of action is to cause small pores to form in the plasma membrane of gram-positive bacteria, thereby causing cell damage (Montville and Chen, 1998). The second category is bacteriocins without lanthionine (Cotter et al., 2005). And there are also a type III bacteriocins, such as helveticin M produced by *Lactobacillus crispatus* and helveticin J produced by *Lactobacillus helveticus*. The bacteriocins with biologically must be secreted out of the cell (Nes et al., 1996; Fimland et al., 2000). For example, the secretion mechanism of bacteriocins (such as class II bacteriocins) generally uses the double glycine guide sequence transport system, and some are signal-dependent, which are processed and transported by the secretory pathway transfer membrane protein (GSP) system. In addition, most of the type I and type II bacteriocins are transferred to the outside of the cell through a specific ABC transporter system (Rincé et al., 1997).

Because of its safety to the human body, some bacteriocins have been used in the food industry as bacteriostats and preservatives (Mulet-Powell et al., 1998; Cotter et al., 2005; Alvarez-Sieiro et al., 2016b). Gasserins produced by *Lactobacillus gasseri*, bacteriocin produced by *Lactococcus lactis*, and Sakacin P produced by *Latilactobacillus sakei* have antibacterial activity against *Listeria monocytogenes* or *Bacillus cereus* (Chen et al., 2012; Pandey et al., 2013; Azhar et al., 2017). *Lactiplantibacillus plantarum* TN8 can inhibit spoilage microorganisms in raw minced beef and extend the shelf life of these products (Trabelsi et al., 2019). *Latilactobacillus sakei* CTC494 can inhibit the growth of *Listeria monocytogenes* in gilthead sea bream (*Sparus aurata*), thereby improving the safety of the food (Costa et al., 2019). The bacteriocin yield of *Enterococcus mundtii* LP17 can reach 1280 AU/ml, and it has a strong inhibitory ability against *Listeria monocytogenes* (Iseppi et al., 2019). In addition to inhibiting some food contaminated strains, it has been reported that nisin may also inhibit the growth of *Latilactobacillus sakei* in ham production (Kalschne et al., 2014).

The synthesis of bacteriocins is also very important for lactic acid bacteria to perform the function of probiotics in the intestine. For example, *Levilactobacillus brevis* B50 Biocenol (CCM 8618) can significantly increase the proportion of lactic acid bacteria in the intestinal microbiota of bees, and enhance the resistance of bees to infectious diseases and harsh environments (Maruščáková et al., 2020). However, how to make lactic acid bacteria synthesize bacteriocins in a controlled dose, and efficiently and stably play the functions of antibacterial, food preservation, and intestinal health promotion in food is the future development direction of bacteriocin synthesis in the food industry.

Vitamins

Many studies now show that lactic acid bacteria can synthesize a variety of vitamins, such as folic acid, riboflavin, vitamin C, pyridoxal (Capozzi et al., 2012), cobalamine (Taranto et al., 2003) and so on. In the food industry, the vitamins synthesized during the fermentation of lactic acid bacteria can be considered as nutritional fortification of food. This nutritional fortification expands the application of lactic acid bacteria to formulate

fermented foods rich in certain vitamins for special populations (Wu et al., 2017).

Folic acid is a water-soluble vitamin B composed of three parts, purine, p-aminobenzoic acid and polyglutamic acid. As a coenzyme, it participates in the transfer of one carbon unit, thereby playing a role in the biosynthesis of nucleotides and proteins. Because humans and other mammals lack genes related to folic acid synthesis, they can only absorb folic acid in food or synthesized by intestinal flora. Most of the reported strains that can synthesize folic acid belong to the genus *Streptococcus*, *Lactobacillus*, and *Lactococcus* (Khalili et al., 2020). The folic acid synthesis pathways of lactic acid bacteria include the Pterin branches and the pABA branches, and only when these two branches function at the same time can they synthesize folic acid (Wegkamp et al., 2007). Therefore *Lactobacillus* strains can only metabolize and produce folic acid after adding p-Aminobenzoic acid (pABA) to the culture medium. Lactic acid bacteria can use a variety of substrates to synthesize or convert vitamins, such as dairy products and cereals. For example, *Streptococcus thermophilus* ST-M6 and TH-4 to add passion fruit by-product and oligofructose to soy milk can produce folic acid. Among them, passion fruit by-product as a growth factor can stimulate the synthesis of folic acid in lactic acid bacteria (Albuquerque et al., 2017).

Riboflavin can be produced by many microorganisms including fungi (such as yeast) and bacteria. In lactic acid bacteria, riboflavin synthase coding genes are clustered on a *rib* operon, and its products (RibC, RibB, RibA, and RibH) can catalyze the conversion of GTP and 5-phosphate ribose into riboflavin. In the study of constructing genetically engineered strains with high production of riboflavin, it was found that certain changes in DNA regions related to regulation will affect the synthesis of riboflavin in lactic acid bacteria. For example, by inserting a 1059-bp DNA fragment into the upstream regulatory region of the rib operon of *Lactiplantibacillus plantarum*, the amount of riboflavin produced by the mutant strain will be higher than that of the wild type (Ge et al., 2020). Another study found that in the *Lactococcus lactis* JC017 mutant, purine starvation induced the overexpression of riboflavin biosynthesis cluster *ribABGH*, indicating that mutations that inhibit purine biosynthesis can trigger riboflavin secretion more effectively (Chen et al., 2017).

In addition to folic acid and riboflavin, lactic acid bacteria can also produce other types of vitamins. For example, the aerobic fermentation of *Lactococcus lactis* subsp. *cremoris* MG1363 with fructose or trehalose as a carbon source can synthesize vitamin K2 (Liu et al., 2019). A strain of *Latilactobacillus sakei* UONUMA promotes the content of vitamin B2 (riboflavin), B3 (nicotinic acid and nicotinamide), and B6 (pyridoxine) in the traditional sweet Japanese beverage (koji amazake) (Oguro et al., 2017). *Limosilactobacillus reuteri* CRL 1098 and *Lactobacillus coryniformis* CRL 1001 are well-known cobalamin producing strains (Torres et al., 2018).

Exopolysaccharides

Polysaccharides are macromolecular substances produced by the polymerization of multiple monosaccharides or their derivatives. In recent years, exopolysaccharides have been favored because of their excellent physical properties and probiotic functions (Salazar et al., 2016). A variety of lactic acid bacteria can synthesize different kinds of exopolysaccharides, such as *Streptococcus thermophilus*, *Limosilactobacillus reuteri, Lacticaseibacillus casei*, *Lactiplantibacillus plantarum* and so on. The exopolysaccharides of lactic acid bacteria are not only related to the adhesion of lactic acid bacteria, but also give new characteristics to fermented foods (Majee et al., 2017). Many review articles discussed the important influence of exopolysaccharides on the physiological function of lactic acid bacteria (Ruas-Madiedo and de los Reyes-Gavilán, 2005; Górska et al., 2007; Patel et al., 2012; Caggianiello et al., 2016; Rahbar Saadat et al., 2019; Zhou et al., 2019; Wu et al., 2021). In view of the potential applications of the physical, chemical and biological properties of exopolysaccharides in fermented foods, this section introduces exopolysaccharides and their synthetic strains.

The genome of lactic acid bacteria contains one or more clusters of exopolysaccharides gene synthesis (Cerning, 1990). A typical polysaccharide synthesis gene cluster generally includes genes related to sugar nucleotide synthesis, glycosyltransferase genes, and polysaccharide synthesis regulatory genes (Boels et al., 2001). Take the hetero-exopolysaccharide (HepS) as an example, the synthesis pathway (**Figure 3**) mainly includes the synthesis of precursor nucleotide sugars, the initiation and extension of repeating units, the inversion and polymerization of repeating units, and the output of polysaccharides. In the synthesis of exopolysaccharides, sugars are first transported to the cytoplasm and sugar-1-phosphate is synthesized. Phosphoenolpyruvate transport system can transfer phosphate groups to sugar during sugar transport (Boels et al., 2001). It is subsequently activated into sugar-nucleotide structural units (such as UDP-glucose, GDP-mannose, UDP-galactose, dTDP-rhamnose, etc.) and then polymerized in a certain order, and finally secreted and exported to form exopolysaccharides. In addition to the monosaccharide structural units mentioned above, the monosaccharide components of exopolysaccharide of lactic acid bacteria also include: fructose, glucuronic acid, fucose, N-acetylglucosamine, and N-acetylgalactosamine (Boels et al., 2001).

Exopolysaccharides (EPS) can be used as an additive in the food industry, especially in the fermented dairy industry. For example, glucan can be used as a gelling agent, stabilizer, thickener and emulsifier in the production of food and cosmetics. Similarly, its production strains can also be used in the processing of fermented foods. For example, some starters that can synthesize EPS (such as *Streptococcus thermophilus* zlw TM11 and *Lactobacillus delbrueckii subsp. bulgaricus* 34.5) can increase the exopolysaccharides content of yogurt and improve the syneresis, texture and sensory of yogurt (Han et al., 2016). A new type of EPS produced by a strain of *Lactococcus lactis* F-mou (LT898177.1), showing good water and oil holding capacities, high antioxidant efficiency and excellent anti-clotting activity, and has strong inhibitory activity with a variety of pathogenic bacteria (Nehal et al., 2019). The high molecular weight EPS synthesized by *Lactiplantibacillus plantarum* BR2 has strong antioxidant activity, radical scavenging activity, and no

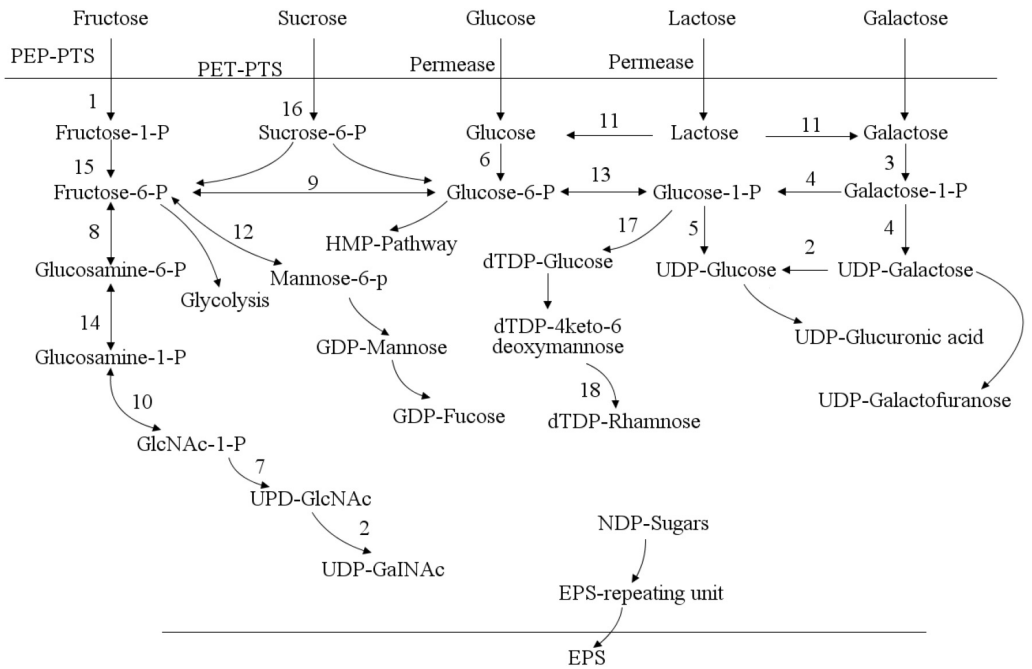

FIGURE 3 | Pathways of sugar metabolism and exopolysaccharides (EPS) biosynthesis in *Streptococcus thermophilus* (Laws et al., 2001). In *Streptococcus thermophilus*, exopolysaccharides is synthesized through a series of complex intracellular enzyme interactions. It is exported to the extracellular environment in the form of macromolecules through a special lipid carrier. The biosynthetic pathway of exopolysaccharides includes sugar entry into the cytoplasm, sugar-1-phosphate synthesis, polysaccharide synthesis and exopolysaccharides export. 1: fructokinase; 2: UDP-galactose-4-epimerase; 3: galactokinase; 4: galactose-1-phosphate uridylyltransferase; 5: UDP-glucose pyrophosphorylase; 6: glucokinase; 7: N-acetylglucosamine-1-phosphate uridyltransferase; 8: glucosamine-6-phosphate deaminase; 9: glucose-6-phosphate isomerase; 10: glucosamine-1-phosphate N-acetyltransferase; 11: β-glalactosidase; 12: mannose-6 phosphate isomerase; 13: α-phosphoglucomutase; 14: phosphoglucosamine mutase; 15: phosphomutase; 16: sucrose-6-phosphate hydrolase; 17: dTDP-glucose pyrophosphorylase; 18: UDP-glucose 6-dehydrogenase.

cytotoxicity (Sasikumar et al., 2017). Adding sucrose to the dough can promote the production of glucan, and the special effect of the glucan structure may extend to the pores of the crumbs, thereby improving the texture of the bread (Chen et al., 2016). In short, exopolysaccharides and their production strains have important potential applications in the food industry, but due to the complex structure of exopolysaccharides, the relationship between the synthesis mechanism and functional properties of exopolysaccharides is also the focus of future research.

Gamma-Aminobutyric Acid

Gamma-aminobutyric acid (γ-aminobutyric acid, GABA) is a non-protein natural amino acid that is widely found in nature. GABA is an important neurotransmitter in the central nervous system, and its concentration in the human brain is related to many diseases. L-Glu decarboxylation reaction is the main manner of intracellular GABA synthesis. Glutamate decarboxylase (GAD) is the key rate-limiting enzyme that catalyzes the production of GABA. GAD (Glutamate decarboxylase) and pyridoxal-5'-phosphate participate in the decarboxylation reaction of L-glutamate to generate γ-aminobutyric acid (Small and Waterman, 1998). Several important genes that regulate GABA synthesis have been discovered. For example, in *Levilactobacillus brevis*, mutations in the GadA gene facilitate the conversion of L-monosodium glutamate (MSG) to GABA (Lyu et al., 2019). In addition, in the high GABA production *Levilactobacillus brevis* D17, the potential transcriptional regulator gene *gadR* can control the synthesis of GABA and the acid resistance of the strain, and the inactivation of *gadR* completely eliminates the synthesis of GABA (Gong et al., 2019).

At present, in the fermentation industry, *Levilactobacillus brevis* is generally used to produce GABA alone or in combination with other strains. Among them, *Levilactobacillus brevis* TCCC 13007 can convert the substrates L-glutamic acid and monosodium glutamate into GABA, and the final titer reaches 201.18 g/L, and the molar bioconversion ratio is 99.4% (Shi et al., 2017). In addition, the cell immobilization technology also plays an important role in the optimization of GABA production (Hsueh et al., 2017). In the food industry, some microorganisms with high safety that can produce GABA can be used in the production of functional health food ingredients. For example, some lactic acid bacteria can increase the GABA content in fermented cereals. Cheese, yogurt and fermented milk produced by fermentation of lactic acid bacteria can also become GABA-enriched products (Yunes et al., 2016). In traditional Chinese fermented soybean (Sufu), *Levilactobacillus brevis* and *Bacillus subtilis* can be inoculated together to increase the concentration of GABA in the product and reduce the concentration of harmful substances (histamine and serotonin)

(Bao et al., 2020). In addition, in traditional Korean soybean paste, the co-fermentation of *Levilactobacillus brevis* GABA100 and *Aspergillus oryzae* KACC 40250 accelerates the conversion of monosodium glutamate and soybean isoflavone glycosides to GABA and soybean isoflavone aglycones (Li et al., 2017).

Flavor Substances

The initial recognition of lactic acid bacteria may be due to its great contribution to humans, that is, to transform perishable milk into flavored yogurt with extended shelf life (Ibarra et al., 2012). Although yogurt has become very common in daily life, the important message brought by yogurt is that lactic acid bacteria have the potential to transform food ingredients into flavor substances. The flavor substances produced by lactic acid bacteria include organic acids, alcohols, ketones and esters (Coolbear et al., 2011). There are generally four ways of formation of flavor substances in food, biosynthesis, enzymatic action (Smit et al., 2005), oxidative decomposition and pyrolysis. In fermented foods (such as fermented dairy products, kimchi, vinegar, and fermented dough) (Azam et al., 2017), lactic acid bacteria either act as the dominant bacteria or work in concert with other dominant bacteria to produce acetaldehyde, diacetyl and other flavor substances through biosynthesis and enzymatic action. The biosynthesis of flavor substances mainly depends on two types of metabolic pathways, one is the citric acid metabolism pathway, and the other is the amino acid metabolism pathway.

The Metabolism of Citric Acid Produces Flavor Compounds

Lactic acid bacteria can produce diacetyl, acetoin, butanediol and other substances in the process of metabolizing citrate, and the secretion of related substances does not require specific transporters. In citric acid metabolism (**Figure 4**), extracellular citric acid is transported to the cell through membrane-associated permease, such as 2-hydroxycarboxylate transporter (2-HCT) (Bandell et al., 1997). After citrate enters the cell, it is converted into acetate and oxaloacetate under the catalysis of citric acid lyase complex. Then, oxaloacetate is decarboxylated by oxaloacetate decarboxylase (OAD) to produce pyruvate and carbon dioxide. Subsequently, pyruvate can be metabolized in lactic acid bacteria to produce different end products, including lactate, formate, acetate and ethanol (Sarantinopoulos et al., 2001), as well as important aromatic compounds diacetyl, acetoin and butanediol (**Figure 4**). Some strains of lactic acid bacteria cannot convert citric acid to pyruvate, but use citrate transporter to generate succinic acid through malic acid and fumaric acid (Torino et al., 2005). Acetaldehyde can be directly catalyzed by pyruvate decarboxylase or pyruvate oxidase, or it can be produced indirectly by the intermediate product acetyl-CoA catalyzed by pyruvate dehydrogenase (Bekal et al., 1998). Diacetyl is produced by the metabolic intermediate α-acetolactate through oxidative decarboxylation (Drinan et al., 1976), and at the same time, α-acetolactate can also be catalyzed by α-acetolactate decarboxylase or through non-oxidative decarboxylation to produce acetoin. When α-acetolactate decarboxylase is inactivated and NADH-oxidase is overexpressed, α-acetolactate can be efficiently converted into diacetyl (Hugenholtz et al., 2000).

In addition, lactic acid bacteria can synthesize sugar alcohols in some processes of sugar metabolism. Sugar alcohols are also called polyols and can be used as thickeners, softeners, stabilizers, etc. Certain lactic acid bacteria (such as *Levilactobacillus brevis* and *Leuconostoc*) can directly reduce fructose to mannitol (Jeske et al., 2018), which can be incorporated into food as a sweetener to exert a variety of beneficial effects. Other hetero-fermentative lactic acid bacteria can synthesize erythritol under certain culture conditions, such as *Oenococcus alcohol, Leuconostoc mesenteroides, and Fructilactobacillus sanfranciscensis* (Ortiz et al., 2013).

The Metabolism of Amino Acids Produces Flavor Substances in Fermented Foods

In addition to the above pathways, there are other ways to synthesize acetaldehyde. Deoxynucleic acid aldolase catalyzes the decomposition of thymine to acetaldehyde and glyceraldehyde phosphate. In addition, several amino acids can be converted into the intermediate metabolite pyruvate and finally acetaldehyde, or directly into acetaldehyde (**Figure 3**). For example, *Streptococcus thermophilus* commonly used in the yogurt industry contains the SHMT gene, which encodes a serine hydroxymethyltransferase (SHMT) with threonine aldolase (TA) activity, which catalyzes the decomposition of threonine into glycine and acetaldehyde (Chaves et al., 2002). In addition, the serine hydroxymethyltransferase encoded by the *glyA* gene can also catalyze the specific reaction of acetaldehyde formation.

In addition, some strains of *Lactiplantibacillus plantarum* can promote the production of aspartic acid related flavor compounds. In *Lacticaseibacillus paracasei*, aspartic acid may be decomposed into diacetyl, acetoin and 1,3-butanediol under the catalysis of aminotransferase (Thage et al., 2005). Some strains of *Lacticaseibacillus casei*, *Lacticaseibacillus rhamnosus*, and *Streptococcus thermophilus* contribute to the production of branched chain amino acid derivatives and aromatic amino acid derivatives (Bancalari et al., 2017). *Streptococcus thermophilus* and *Lacticaseibacillus casei* metabolize to produce 2,3-butanedione and 2,3-pentanedione during milk "laban" fermentation (Chammas et al., 2006).

Contribution of Lactic Acid Bacteria in Fermented Food in Synthesizing Flavor Substances

Acetaldehyde, diacetyl, acetoin and butanediol are typical aroma compounds of many fermented dairy products. A variety of lactic acid bacteria play a role in cheese processing. For example, *Lacticaseibacillus paracasei* 4341 can produce aroma and sour substances in Italian long ripened cheeses (Bancalari et al., 2017). *Limosilactobacillus reuteri* INIA P572 enhances the formation of 12 volatile compounds in cheese, but reduces the formation of 5 other volatile compounds (Gómez-Torres et al., 2016). A strain of in Stilton cheese can produce high concentrations of alcohol, organic acids and acetone (Mugampoza et al., 2019). In addition, during the fermentation

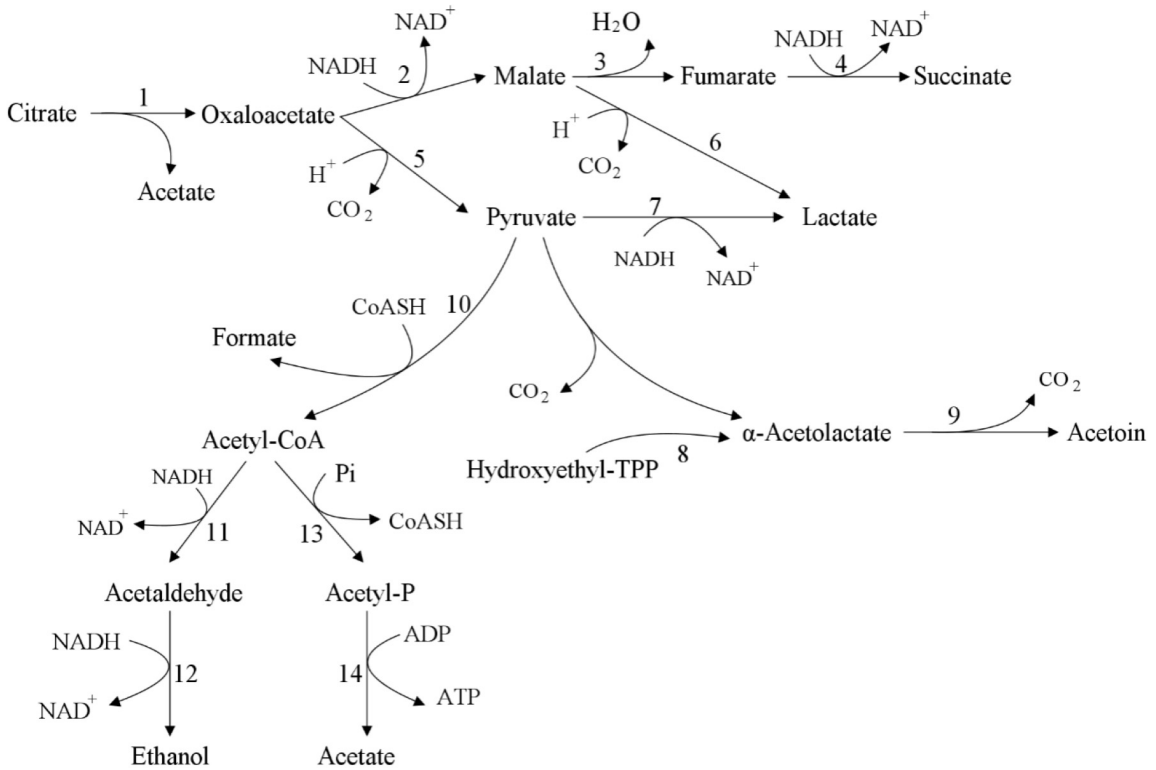

FIGURE 4 | Citric acid metabolism (Gänzle, 2015). The citric acid in lactic acid bacteria is converted into succinate, lactate, acetate, and ethanol or acetylacetone through the intermediate metabolite oxaloacetate. 1: citrate lyase; 2: malate dehydrogenase; 3: fumarate hydratase; 4: succinate dehydrogenase; 5: oxaloacetate decarboxylase; 6: malolactic enzyme; 7: lactate dehydrogenase; 8: acetolactate synthase; 9: acetolactate decarboxylase; 10: pyruvate formate lyase; 11: acetaldehyde dehydrogenase; 12: alcohol dehydrogenase; 13: phosphotransacetylase; 14: acetate kinase.

of cheese, with the participation of *Lacticaseibacillus paracasei* strains, the metabolism of cysteine and methionine will form a sulfuric flavor (Wüthrich et al., 2018). Therefore, the research on the enzymes expressed by lactic acid bacteria will help to screen out suitable strains or combinations of strains to improve or increase the flavor of cheese (Peralta et al., 2016).

In fermented sourdough, lactic acid bacteria also play a role in the formation of flavor substances. For example, during the fermentation of bread sourdough, the combined use of lactic acid bacteria (*Lactiplantibacillus plantarum*, *Lactiplantibacillus plantarum, Furfurilactobacillus rossiae*, and *Lacticaseibacillus casei*) and yeast produces compounds related to the sour aromas of bread, and contributes to the aroma characteristics of bread (Winters et al., 2019). *Lactiplantibacillus plantarum* may promote the production of more C_4-C_6 alcohols in sourdough (Liu et al., 2020). In the fermentation of alcoholic beverages, lactic acid bacteria also affect the production of flavor substances. In wine fermentation, lactic acid bacteria can perform malic acid-lactic acid fermentation (MLF), that is, directly produce lactic acid by decarboxylation of L-malic acid. Lactic acid bacteria also affect the production of esters in wine. Some substances have outstanding influence and contribution to fermented products, for example, esters play an important role in the aroma of wine (Cappello et al., 2017). In Bordeaux red wines, lactic acid bacteria are the only bacteria that strongly influence the content of branched hydroxylated esters (ethyl 2-hydroxy-3-methylbutanoate and ethyl 2-hydroxy-4-methylpentanoate) (Gammacurta et al., 2018). The synergistic effect of lactic acid bacteria contributes to the production of flavor substances in vinegar. Some *Lactobacillus* strains, such as *Lentilactobacillus buchneri*, *Limosilactobacillus reuteri*, *Limosilactobacillus fermentum,* and *Levilactobacillus brevis*, may convert 2-acetolactate into acetoin, play important roles in the formation of flavor substances in Zhenjiang aromatic vinegar (Lu et al., 2016).

Based on the above analysis, many lactic acid bacteria will give fermented food a variety of flavor substances. However, due to the variety of lactic acid bacteria, fermentation substrates and flavors produced, it is difficult to fully describe. Therefore, in-depth research on the types of metabolism that produce flavor substances has become critical, which helps to find general strategies for regulating flavor substances. Although the whole genomics, transcriptomics (Liu et al., 2020) and metabonomics (Zhao et al., 2016), and metabolomics are currently developing rapidly, there are still many functional proteins and metabolic pathways that are still unknown. In addition, although the technology for qualitative and quantitative analysis of flavor

substances in fermented products has been greatly developed, the effect of the synergy between multiple flavors is still difficult to evaluate. At the same time, since the stability of the fermentation strain is easily affected by many factors, there may still be changes in flavor substances of different product batches. Therefore, the above-mentioned problems constitute the challenges for the in-depth application of the characteristics of lactic acid bacteria to synthesize flavor substances in the food industry in the future.

Antioxidant Substances

In fermented foods, lactic acid bacteria produce antioxidant substances that are highly safe, and can have a variety of beneficial effects on the human body through food. In recent years, there have been many reports on the synthesis of antioxidant metabolites by lactic acid bacteria. Antioxidant substances have excellent ability to scavenge free radicals and are closely related to human health. Many substances (such as vitamins and polysaccharides) involved in the previous sections have antioxidant capacity, so this section only involves the synthesis of some substances that are mainly used to reflect the antioxidant function of lactic acid bacteria in food. The antioxidant part mainly introduces the metabolism of some phenolic substances by lactic acid bacteria and the limited ability of lactic acid bacteria to synthesize glutathione.

Some lactic acid bacteria (such as *Levilactobacillus brevis*, *Limosilactobacillus fermentum* and *Lactiplantibacillus plantarum*) can metabolize phenolic acid through decarboxylase and reductase (Filannino et al., 2015). Through the decarboxylation and reduction reaction of phenolic acid, hydroxycinnamic acid (*p*-coumaric acid, caffeic acid, ferulic acid and *m*-coumaric acid) and some hydroxybenzoic acid (gallic acid and protocatechuic acid) can be degraded (Rodriguez et al., 2008). For example, after fermentation of blueberries by *Lactiplantibacillus plantarum*, the polyphenols in blueberries can be converted into active phenol metabolites with strong antioxidant and antiproliferative activities (Ryu et al., 2019). The dextransucrase expressed by *Leuconostoc mesenteroides* can convert sucrose into chlorogenic acid glucoside, which increases the water solubility of chlorogenic acid and has better browning resistance (Nam et al., 2017). The fermentation of lactic acid bacteria increases the content of sulforaphane in broccoli puree (Cai et al., 2020). *Lacticaseibacillus rhamnosus*, *Lactobacillus acidophilus* improves the anti-free radical activity of protein extracts from cured meats (Kêska and Stadnik, 2018). *Lactiplantibacillus plantarum* significantly reduces the protein carbonyl content and protein surface hydrophobicity in fermented sausages, and increases the content of total sulfhydryl contents (Ge et al., 2019).

As a natural antioxidant, glutathione is a tripeptide composed of glutamic acid, cysteine and glycine (Wu et al., 2004). Two enzymes are important enzymes involved in glutathione metabolism. Glutathione peroxidase catalyzes the conversion of reduced glutathione to its oxidized form, and glutathione reductase regenerates reduced glutathione (Qiao et al., 2018). Glutathione is rare in Gram-positive bacteria, but it can also be produced in some lactic acid bacteria, such as *Streptococcus thermophilus*, *Enterococcus faecalis*, *Lacticaseibacillus casei*, *Lacticaseibacillus rhamnosus*, *Lactiplantibacillus plantarum*, *Latilactobacillus sakei* and *Ligilactobacillus ruminis*, etc. (Pophaly et al., 2012). Although *Limosilactobacillus fermentum* CECT 5716 cannot synthesize glutathione, it can convert oxidized glutathione taken from the environment into reduced glutathione. This also promotes the release of glutathione to the environment (Surya et al., 2018). As an additive, glutathione makes outstanding contributions to increase dough rheology (Loponen et al., 2008) and promote the hydrolysis of egg white protein (Loponen et al., 2008). For example, the glutathione reductase of *Fructilactobacillus sanfranciscensis* affects the volume of bread by affecting the thiol content in wheat dough and the polymerization and aggregation of gluten (Xu et al., 2018). In addition, glutathione also improves the acid resistance of lactic acid bacteria (Xu et al., 2018).

Numerous studies have shown that antioxidants, as a class of metabolites of great concern, have also played an important supplementary role in explaining the mechanism of lactic acid bacteria as probiotics. For example, *Lactiplantibacillus plantarum* Y44 plays an antioxidant role by free radical scavenging ability and activating the Nrf2 signaling pathway. In injury-induced Caco-2 cells, it can down-regulate the expression of inflammatory-related cytokines IL-8 and tumor necrosis factor-α, and at the same time enhance the expression of intracellular tight junction proteins β-catenin and E-cadherin (Mu et al., 2019). Therefore, in-depth study of its metabolic pathways has an important guiding role for the promotion of lactic acid bacteria in human health, or the discovery of more efficient antioxidant substances used in food.

METABOLIC ENGINEERING STRATEGIES APPLICATION IN LAB

Metabolic engineering refers to the use of synthetic biology and systems biology methods to improve the utilization of existing or create new biosynthetic metabolic pathways. In the food industry, the main purpose of applying metabolic engineering strategies in lactic acid bacteria is to increase the production of certain metabolites of lactic acid bacteria (such as exopolysaccharides, sugar alcohol compounds, vitamins and bacteriostatic peptides, etc.).

For example, using central carbon metabolism pathways (including glycolysis, gluconeogenesis, pentose pathway and citric acid cycle, etc.) as the target, the output of a certain target product can be increased by changing the metabolic flux. The research methods mainly include expanding existing metabolic pathways and constructing novel metabolic pathways. (1) Expanding existing pathways means overexpression of rate-limiting enzyme genes in related biosynthetic pathways on the basis of existing metabolic pathways, and inhibiting competitive metabolism. For example, pyruvate is a key substance in the central carbon metabolism pathway, and its content is very important for the synthesis of organic acids such as lactic acid, α-acetolactate, acetic acid, and formic acid. Therefore, in the

production of lactic acid, methods such as adjusting the metabolic flow of pyruvate and enhancing the expression of lactate dehydrogenase can be used to achieve high yields. In addition, the use of metabolic engineering can also effectively optimize the ability of lactic acid bacteria to degrade proteins, which in turn helps to control protein hydrolysis and help obtain the most optimized food processing technology. (2) The construction of a novel metabolic pathway refers to the expression of multiple genes encoding a pathway-specific enzyme in a non-natural host to construct a new pathway. This is generally due to the fact that although all possible genetic manipulation procedures and metabolic engineering strategies are used in natural strains, sometimes the production titer of the required metabolites is still very low or does not meet the requirements. For example, by integrating the gene of the short-chain dehydrogenase encoded by *Corynebacterium glutamicum* into *Pediococcus acidilactici*, the resulting genetically engineered strain synthesizes higher yield of D-lactic acid (Qiu et al., 2020).

In short, with the development of the CRISPR-Cas9 system and other gene editing systems (Hidalgo-Cantabrana et al., 2019), a variety of metabolic engineering strategies can be used to meet the growing demand for microbial metabolites in industrial production.

CONCLUSION AND PERSPECTIVES

Although the lactic acid bacteria had been used in fermentation products for a long time. The lactic acid bacteria work in a vast array of ways that its functional characteristics are quite different. In the food industry, a variety of bacteria's can ferment a variety of substrates into products or produce a variety of industrial raw materials during the fermentation process. Due to the limited output of its products, despite some of the products being valuable, some lactic acid bacteria may not be enough to be used as industrial-grade bacteria. Therefore, the use of synthetic biology technology to carry out targeted transformation of strains can help synthesize certain products in high yield. The constructed lactic acid bacteria engineering strain can be used to increase the production of organic acids such as γ-aminobutyric acid and lactic acid, exopolysaccharides, vitamins and other products, and can also be used to express enzymes that decompose proteins and polysaccharides. Among them, *Levilactobacillus brevis*, *Lactococcus lactis*, *Lactiplantibacillus plantarum* and other lactic acid strains have carried out excellent metabolic engineering work. In addition, the use of industrial wastes such as whey as production substrates is also an important way to alleviate the current situation of resource shortages. However, in some cases, when the inherent flora structure in the human intestine encounters excessive intake of certain lactic acid bacteria, it may cause the original flora structure to become unbalanced and cause human discomfort. Therefore, the understanding of strain metabolism can avoid some damage to human health.

In addition, the development of modern biotechnology such as multi-omics technology and gene editing technology and its application in lactic acid bacteria have also strongly promoted in-depth research on the metabolism of lactic acid bacteria. The research on the metabolic pathways and metabolic characteristics of lactic acid bacteria will help further guide the application of lactic acid bacteria in the food industry and human health industry.

AUTHOR CONTRIBUTIONS

All authors listed have made a substantial, direct and intellectual contribution to the work.

FUNDING

This work was supported by the National Natural Science Foundation of China (31801514).

ACKNOWLEDGMENTS

This research was also supported by Open Funding Project of the State Key Laboratory of Bioreactor Engineering and the Innovative Research Team of Tianjin Municipal Education Commission (TD13-5015).

REFERENCES

Albuquerque, M., Bedani, R., LeBlanc, J., and Saad, S. (2017). Passion fruit by-product and fructooligosaccharides stimulate the growth and folate production by starter and probiotic cultures in fermented soymilk. *Int. J. Food Microbiol.* 261, 35–41. doi: 10.1016/j.ijfoodmicro.2017.09.001

Ali, N., Gong, H., Giwa, A., Yuan, Q., and Wang, K. (2019). Metagenomic analysis and characterization of acidogenic microbiome and effect of pH on organic acid production. *Arc. Microbiol.* 201, 1163–1171. doi: 10.1007/s00203-019-01676-2

Alvarez-Sieiro, P., Montalbán-López, M., Mu, D., and Kuipers. (2016a). Bacteriocins of lactic acid bacteria: extending the family. *Appl. Microbiol. Biot.* 100, 2939–2951. doi: 10.1007/s00253-016-7343-9

Alvarez-Sieiro, P., Redruello, B., Ladero, V., Martín, M. C., Fernández, M., and Alvarez, M. A. (2016b). Screening sourdough samples for gliadin-degrading activity revealed *Lactobacillus casei* strains able to individually metabolize the coeliac-disease-related 33-mer peptide. *Can. J. Microbiol.* 62, 422–430. doi: 10.1139/cjm-2015-0796

Azam, M., Mohsin, M., Ijaz, H., Tulain, U. R., Ashraf, M. A., Fayyaz, A., et al. (2017). Review-Lactic acid bacteria in traditional fermented Asian foods. *Pak. J. Pharm. Sci.* 30, 1803–1814.

Azhar, N., Md Zin, N., and Hamid, T. (2017). Lactococcus lactis strain a5 producing nisin-like bacteriocin active against gram positive and negative bacteria. *Tro. Life. Sci. Res.* 28, 107–118. doi: 10.21315/tlsr2017.28.2.8

Bai, Y., Dobruchowska, J., Gerwig, G., and Dijkhuizen, L. (2016). Structural basis for the roles of starch and sucrose in homo-exopolysaccharide formation by *Lactobacillus reuteri* 35-5. *Carbohyd. Polym.* 151, 29–39. doi: 10.1016/j.carbpol.2016.05.048

Bancalari, E., Savo Sardaro, M., Levante, A., Marseglia, A., Caligiani, A., Lazzi, C., et al. (2017). An integrated strategy to discover *Lactobacillus casei* group strains for their potential use as aromatic starters. *Food Res. Int.* 100, 682–690. doi: 10.1016/j.foodres.2017.07.066

Bandell, M., Ansanay, V., Rachidi, N., Dequin, S., and Lolkema, J. (1997). Membrane potential-generating malate and citrate transporters of lactic

acid bacteria are homologous proteins. Substrate specificity of the 2-hydroxycarboxylate transporter family. *J. Biol. Chem.* 272, 18140–18146. doi: 10.1074/jbc.272.29.18140

Bao, W., Huang, X., Liu, J., Han, B., and Chen, J. (2020). Influence of *Lactobacillus brevis* on metabolite changes in bacteria-fermented sufu. *J. Food Sci.* 85, 165–172. doi: 10.1111/1750-3841.14968

Barbieri, F., Montanari, C., Gardini, F., and Tabanelli, G. (2019). Biogenic amine production by lactic acid bacteria: a review. *Foods* 8:17. doi: 10.3390/foods8010017

Barthelmebs, L., Divies, C., and Cavin, J. (2000). Knockout of the p-coumarate decarboxylase gene from *Lactobacillus plantarum* reveals the existence of two other inducible enzymatic activities involved in phenolic acid metabolism. *Appl. Environ. Microb* 66, 3368–3375. doi: 10.1128/aem.66.8.3368-3375.2000

Batista, N., Ramos, C. L., de Figueiredo Vilela, L., Dias, D. R., and Schwan, R. F. (2019). Fermentation of yam by indigenous phytase-producing lactic acid bacteria strains. *Braz. J. Microbiol.* 50, 507–514. doi: 10.1007/s42770-019-00059-5

Bekal, S., Van Beeumen, J., Samyn, B., Garmyn, D., Henini, S., Diviès, C., et al. (1998). Purification of *Leuconostoc mesenteroides* citrate lyase and cloning and characterization of the cit CDEFG gene cluster. *J. Bacteriol.* 180, 647–654. doi: 10.1128/JB.180.3.647-654.1998

Ben Taheur, F., Mansour, C., Kouidhi, B., and Chaieb, K. (2019). Use of lactic acid bacteria for the inhibition of *Aspergillus flavus* and *Aspergillus carbonarius* growth and mycotoxin production. *Toxicon* 166, 15–23. doi: 10.1016/j.toxicon.2019.05.004

Ben-Harb, S., Saint-Eve, A., Panouillé, M., Souchon, I., Bonnarme, P., Dugat-Bony, E., et al. (2019). Design of microbial consortia for the fermentation of pea-protein-enriched emulsions. *Int. J. Food Microbiol.* 293, 124–136. doi: 10.1016/j.ijfoodmicro.2019.01.012

Bernardo, M., Coelho, L., Sass, D., and Contiero, J. (2016). l-(+)-Lactic acid production by *Lactobacillus rhamnosus* B103 from dairy industry waste. *Braz. J. Microbiol.* 47, 640–646. doi: 10.1016/j.bjm.2015.12.001

Biscola, V., Choiset, Y., Rabesona, H., Chobert, J., Haertlé, T., and Franco, B. (2018). Brazilian artisanal ripened cheeses as sources of proteolytic lactic acid bacteria capable of reducing cow milk allergy. *J. Appl. Microbiol.* 125, 564–574. doi: 10.1111/jam.13779

Boels, I., Kranenburg, R., Hugenholtz, J., Kleerebezem, M., and Vos, W. (2001). Sugar catabolism and its impact on the biosynthesis and engineering of exopolysaccharide production in lactic acid bacteria. *Int. Dairy. J.* 11, 723–732.

Caggianiello, G., Kleerebezem, M., and Spano, G. (2016). Exopolysaccharides produced by lactic acid bacteria: from health-promoting benefits to stress tolerance mechanisms. *Appl. Microbiol. Biotechnol.* 100, 3877–3886. doi: 10.1007/s00253-016-7471-2

Cai, Y., Augustin, M. A., Jegasothy, H., Wang, J., and Terefe, N. (2020). Mild heat combined with lactic acid fermentation: a novel approach for enhancing sulforaphane yield in broccoli puree. *Food Funct.* 11, 779–786. doi: 10.1039/c9fo02089f

Capozzi, V., Russo, P., Dueñas, M. T., López, P., and Spano, G. (2012). Lactic acid bacteria producing B-group vitamins: a great potential for functional cereals products. *Appl. Microbiol. Biot.* 96, 1383–1394. doi: 10.1007/s00253-012-4440-2

Cappello, M., Zapparoli, G., Logrieco, A., and Bartowsky, E. (2017). Linking wine lactic acid bacteria diversity with wine aroma and flavour. *Int. J. Food Microbiol.* 243, 16–27. doi: 10.1016/j.ijfoodmicro.2016.11.025

Cerning, J. (1990). Exocellular polysaccharides produced by lactic acid bacteria. *FEMS Microbiol. Rev.* 7, 113–130. doi: 10.1111/j.1574-6968.1990.tb04883.x

Chammas, G., Saliba, R., Corrieu, G., and Béal, C. (2006). Characterisation of lactic acid bacteria isolated from fermented milk "laban". *Int. J. Food Microbiol.* 110, 52–61. doi: 10.1016/j.ijfoodmicro.2006.01.043

Chaves, A., Fernandez, M., Lerayer, A., Mierau, I., Kleerebezem, M., and Hugenholtz, J. (2002). Metabolic engineering of acetaldehyde production by *Streptococcus thermophilus*. *Appl. Environ. Microb* 68, 5656–5662. doi: 10.1128/aem.68.11.5656-5662.2002

Chen, H., Tian, F., Li, S., Xie, Y., Zhang, H., and Chen, W. (2012). Cloning and heterologous expression of a bacteriocin sakacin P from *Lactobacillus sakei* in *Escherichia coli*. *Appl. Microbiol. Biot.* 94, 1061–1068. doi: 10.1007/s00253-012-3872-z

Chen, J., Vestergaard, M., Jensen, T., Shen, J., Dufva, M., Solem, C., et al. (2017). Finding the needle in the haystack-the use of microfluidic droplet technology to identify vitamin-secreting lactic acid bacteria. *mBio* 8:e00526-17. doi: 10.1128/mBio.00526-17

Chen, X., Levy, C., and Gänzle, M. (2016). Structure-function relationships of bacterial and enzymatically produced reuterans and dextran in sourdough bread baking application. *Int. J. Food Microbiol.* 239, 95–102. doi: 10.1016/j.ijfoodmicro.2016.06.010

Christensen, J., Dudley, E., Pederson, J., and Steele, J. (1999). Peptidases and amino acid catabolism in lactic acid bacteria. *Anton. Leeuw* 76, 217–246.

Coda, R., Melama, L., Rizzello, C., Curiel, J., Sibakov, J., Holopainen, U., et al. (2015). Effect of air classification and fermentation by *Lactobacillus plantarum* VTT E-133328 on faba bean flour nutritional properties. *Int. J. Food Microbiol.* 193, 34–42. doi: 10.1016/j.ijfoodmicro.2014.10.012

Coolbear, T., Weimer, B., and Wilkinson, M. G. (2011). Lactic acid bacteria | lactic acid bacteria in flavor development. Encyclopedia. *Dairy Scis* 73, 160–165.

Costa, J., Bover-Cid, S., Bolívar, A., Zurera, G., and Pérez-Rodríguez, F. (2019). Modelling the interaction of the sakacin-producing *Lactobacillus sakei* CTC494 and Listeria monocytogenes in filleted gilthead sea bream under modified atmosphere packaging at isothermal and non-isothermal conditions. *Int. J. Food Microbiol.* 297, 72–84. doi: 10.1016/j.ijfoodmicro.2019.03.002

Cotter, P., Hill, C., and Ross, R. (2005). Bacteriocins: developing innate immunity for food. *Nat. Rev. Microbiol.* 3, 777–788. doi: 10.1038/nrmicro1273

Cubas-Cano, E., González-Fernández, C., and Tomás-Pejó, E. (2019). Evolutionary engineering of *Lactobacillus pentosus* improves lactic acid productivity from xylose-rich media at low pH. *Bioresource Technol.* 288:121540. doi: 10.1016/j.biortech.2019.121540

Cui, Y., Miao, K., Niyaphorn, S., and Qu, X. (2020). Production of gamma-aminobutyric acid from lactic acid bacteria: a systematic review. *Int. J. Mol Sci.* 21:995. doi: 10.3390/ijms21030995

Daliri, E., Lee, B., Park, B., Kim, S., and Oh, D. H. (2018). Antihypertensive peptides from whey proteins fermented by lactic acid bacteria. *Food Sci. Biotechnol.* 27, 1781–1789. doi: 10.1007/s10068-018-0423-0

Dallas, D., Citerne, F., Tian, T., Silva, V., Kalanetra, K., Frese, S., et al. (2016). Peptidomic analysis reveals proteolytic activity of kefir microorganisms on bovine milk proteins. *Food Chem.* 197, 273–284. doi: 10.1016/j.foodchem.2015.10.116

Deegan, L., Cotter, P., Hill, C., and Ross, P. (2006). Bacteriocins: biological tools for bio-preservation and shelf-life extension. *Int. Dairy J.* 16, 1058–1071.

Deibel, R. H., and Niven, C. F. Jr. (1964). Pyruvate fermentation by *Streptococcus faecalis*. *J. Bacteriol.* 88, 4–10. doi: 10.1128/JB.88.1.4-10.1964

Diaz, M., Del Rio, B., Ladero, V., Redruello, B., Fernández, M., Martin, M. C., et al. (2020). Histamine production in *Lactobacillus vaginalis* improves cell survival at low pH by counteracting the acidification of the cytosol. *Int. J. Food. Microbiol.* 321:108548. doi: 10.1016/j.ijfoodmicro.2020.108548

Diep, D., and Nes, I. F. (2002). Ribosomally synthesized antibacterial peptides in Gram positive bacteria. *Curr. Drug Targets* 3, 107–122. doi: 10.2174/1389450024605409

Dorau, R., Chen, L., Liu, J., Jensen, P., and Solem, C. (2019). Efficient production of α-acetolactate by whole cell catalytic transformation of fermentation-derived pyruvate. *Microb. Cell Fact.* 18:217. doi: 10.1186/s12934-019-1271-1

Drinan, D., Robin, S., and Cogan, T. (1976). Citric acid metabolism in hetero- and homofermentative lactic acid bacteria. *Appl. Environ. Microb* 31, 481–486. doi: 10.1128/AEM.31.4.481-486.1976

Eiteman, M., and Ramalingam, S. (2015). Microbial production of lactic acid. *Biotechnol. Lett.* 37, 955–972. doi: 10.1007/s10529-015-1769-5

Even, S., Lindley, N., Loubière, P., and Cocaign-Bousquet, M. (2002). Dynamic response of catabolic pathways to autoacidification in *Lactococcus lactis*: transcript profiling and stability in relation to metabolic and energetic constraints. *Mol. Microbiol.* 45, 1143–1152. doi: 10.1046/j.1365-2958.2002.03086.x

Falasconi, I., Fontana, A., Patrone, V., Rebecchi, A., Duserm Garrido, G., Principato, L., et al. (2020). Genome-assisted characterization of Lactobacillus fermentum, weissella cibaria, and weissella confusa strains isolated from sorghum as starters for sourdough fermentation. *Microorganisms* 8:1388. doi: 10.3390/microorganisms8091388

Fang, R., Zhou, W., and Chen, Q. (2019). Ethyl carbamate regulation and genomic expression of *Saccharomyces cerevisiae* during mixed-culture yellow rice wine

fermentation with *Lactobacillus sp*. *Food Chem.* 292, 90–97. doi: 10.1016/j.foodchem.2019.04.014

Fijan, S. (2014). Microorganisms with claimed probiotic properties: an overview of recent literature. *Int. J. Environ. Res. Public. Health* 11, 4745–4767. doi: 10.3390/ijerph110504745

Filannino, P., Bai, Y., Di Cagno, R., Gobbetti, M., and Gänzle, M. (2015). Metabolism of phenolic compounds by *Lactobacillus spp*. during fermentation of cherry juice and broccoli puree. *Food Microbiol.* 46, 272–279. doi: 10.1016/j.fm.2014.08.018

Filannino, P., Di Cagno, R., and Gobbetti, M. (2018). Metabolic and functional paths of lactic acid bacteria in plant foods: get out of the labyrinth. *Curr. Opin. Biotech.* 49, 64–72. doi: 10.1016/j.copbio.2017.07.016

Fimland, G., Johnsen, L., Axelsson, L., Brurberg, M., Nes, I., Eijsink, V., et al. (2000). A C-terminal disulfide bridge in pediocin-like bacteriocins renders bacteriocin activity less temperature dependent and is a major determinant of the antimicrobial spectrum. *J. Bacteriol.* 182, 2643–2648. doi: 10.1128/jb.182.9.2643-2648.2000

Fuglsang, A., Rattray, F., Nilsson, D., and Nyborg, N. (2003). Lactic acid bacteria: inhibition of angiotensin converting enzyme in vitro and in vivo. *Anton. Leeuw* 83, 27–34. doi: 10.1023/a:1022993905778

Gammacurta, M., Lytra, G., Marchal, A., Marchand, S., Christophe Barbe, J., Moine, V., et al. (2018). Influence of lactic acid bacteria strains on ester concentrations in red wines: specific impact on branched hydroxylated compounds. *Food Chem.* 239, 252–259. doi: 10.1016/j.foodchem.2017.06.123

Gänzle, M., and Follador, R. (2012). Metabolism of oligosaccharides and starch in lactobacilli: a review. *Front. Microbiol.* 3:340. doi: 10.3389/fmicb.2012.00340

Gänzle, M., and Zheng, J. (2019). Lifestyles of sourdough lactobacilli - do they matter for microbial ecology and bread quality? *Int. J. Food. Microbiol.* 302, 15–23. doi: 10.1016/j.ijfoodmicro.2018.08.019

Gänzle, M. G. (2015). Lactic metabolism revisited: metabolism of lactic acid bacteria in food fermentations and food spoilage. *Curr. Opin. Food Sci.* 2, 106–117.

Gardini, F., Özogul, Y., Suzzi, G., Tabanelli, G., and Özogul, F. (2016). Technological factors affecting biogenic amine content in foods: a review. *Front. Microbiol.* 7:1218. doi: 10.3389/fmicb.2016.01218

Ge, Q., Chen, S., Liu, R., Chen, L., Yang, B., Yu, H., et al. (2019). Effects of *Lactobacillus plantarum* NJAU-01 on the protein oxidation of fermented sausage. *Food Chem.* 295, 361–367. doi: 10.1016/j.foodchem.2019.05.154

Ge, Y., Zhang, J., Corke, H., and Gan, R. (2020). Screening and spontaneous mutation of pickle-derived Lactobacillus plantarum with overproduction of riboflavin, related mechanism, and food application. *Foods* 9:88. doi: 10.3390/foods9010088

Genay, M., Sadat, L., Gagnaire, V., and Lortal, S. (2009). prtH2, not prtH, is the ubiquitous cell wall proteinase gene in *Lactobacillus helveticus*. *Appl. Environ. Microb* 75, 3238–3249. doi: 10.1128/AEM.02395-08

George, F., Daniel, C., Thomas, M., Singer, E., Guilbaud, A., Tessier, F., et al. (2018). Occurrence and dynamism of lactic acid bacteria in distinct ecological niches: a multifaceted functional health perspective. *Front. Microbiol.* 9:2899. doi: 10.3389/fmicb.2018.02899

Gerwig, G. (2019). Structural analysis of exopolysaccharides from lactic acid bacteria. *Methods Mole. Biol.* 1887, 67–84. doi: 10.1007/978-1-4939-8907-2_7

Gómez-Torres, N., ávila, M., Delgado, D., and Garde, S. (2016). Effect of reuterin-producing *Lactobacillus reuteri* coupled with glycerol on the volatile fraction, odour and aroma of semi-hard ewe milk cheese. *Int. J. Food Microbiol.* 232, 103–110. doi: 10.1016/j.ijfoodmicro.2016.05.031

Gong, L., Ren, C., and Xu, Y. (2019). Deciphering the crucial roles of transcriptional regulator GadR on gamma-aminobutyric acid production and acid resistance in *Lactobacillus brevis*. *Microb. Cell Fact.* 18:108. doi: 10.1186/s12934-019-1157-2

Górska, S., Grycko, P., Rybka, J., and Gamian, A. (2007). Egzopolisacharydy bakterii kwasu mlekowego - biosynteza i struktura [Exopolysaccharides of lactic acid bacteria: structure and biosynthesis]. *Postepy. Hig. Med. Dosw.* 61, 805–818.

Hagting, A., Kunji, E., Leenhouts, K., Poolman, B., and Konings, W. (1994). The di- and tripeptide transport protein of *Lactococcus lactis*. a new type of bacterial peptide transporter. *J. Biol. Chem.* 269, 11391–11399.

Han, X., Li, L., Wei, C., Zhang, J., and Bao, J. (2019). Facilitation of l-lactic acid fermentation by lignocellulose biomass rich in vitamin b compounds. *J. Agr. Food Chem.* 67, 7082–7086. doi: 10.1021/acs.jafc.9b02297

Han, X., Yang, Z., Jing, X., Yu, P., Zhang, Y., Yi, H., et al. (2016). Improvement of the texture of yogurt by use of exopolysaccharide producing lactic acid bacteria. *BioMed. Res. Int.* 2016:7945675. doi: 10.1155/2016/7945675

Hidalgo-Cantabrana, C., Goh, Y., Pan, M., Sanozky-Dawes, R., and Barrangou, R. (2019). Genome editing using the endogenous type I CRISPR-cas system in *Lactobacillus crispatus*. *Proc. Natl. Acad. Sci. U S A.* 116, 15774–15783. doi: 10.1073/pnas.1905421116

Hsueh, Y., Liaw, W., Kuo, J., Deng, C., and Wu, C. (2017). Hydrogel Film-Immobilized *Lactobacillus brevis* RK03 for γ-aminobutyric acid production. *Int. J. Mol. Sci.* 18:2324. doi: 10.3390/ijms18112324

Huang, S., Ai, Z., Sun, X., Liu, G., Zhai, S., Zhang, M., et al. (2016). Influence of arginine on the growth, arginine metabolism and amino acid consumption profiles of *Streptococcus thermophilus* T1C2 in controlled pH batch fermentations. *J. Appl. Microbiol.* 121, 746–756. doi: 10.1111/jam.13221

Hugenholtz, J., Kleerebezem, M., Starrenburg, M., Delcour, J., de Vos, W., and Hols, P. (2000). *Lactococcus lactis* as a cell factory for high-level diacetyl production. *Appl. Environ. Microb* 66, 4112–4114. doi: 10.1128/aem.66.9.4112-4114.2000

Ibarra, A., Acha, R., Calleja, M., Chiralt-Boix, A., and Wittig, E. (2012). Optimization and shelf life of a low-lactose yogurt with *Lactobacillus rhamnosus* HN001. *J. Dairy Sci.* 95, 3536–3548. doi: 10.3168/jds.2011-5050

Iseppi, R., Stefani, S., de Niederhausern, S., Bondi, M., Sabia, C., and Messi, P. (2019). Characterization of Anti-Listeria monocytogenes properties of two bacteriocin-producing *Enterococcus mundtii* isolated from fresh fish and seafood. *Curr. Microbiol.* 76, 1010–1019. doi: 10.1007/s00284-019-01716-6

Iwamoto, H., Matsubara, T., Okamoto, T., Matsumoto, T., Yoshikawa, M., and Takeda, Y. (2019). Ingestion of casein hydrolysate induces oral tolerance and suppresses subsequent epicutaneous sensitization and development of anaphylaxis reaction to casein in mice. *Int. Arch. Allergy Imm.* 179, 221–230. doi: 10.1159/000497410

Jeske, S., Zannini, E., Lynch, K., Coffey, A., and Arendt, E. (2018). Polyol-producing lactic acid bacteria isolated from sourdough and their application to reduce sugar in a quinoa-based milk substitute. *Int. J. Food Microbiol.* 286, 31–36. doi: 10.1016/j.ijfoodmicro.2018.07.013

Kalschne, D., Geitenes, S., Veit, M., Sarmento, C., and Colla, E. (2014). Growth inhibition of lactic acid bacteria in ham by nisin: a model approach. *Meat. Sci.* 98, 744–752. doi: 10.1016/j.meatsci.2014.07.002

Kêska, P., and Stadnik, J. (2018). Stability of antiradical activity of protein extracts and hydrolysates from dry-cured pork loins with probiotic strains of LAB. *Nutrients* 10:521. doi: 10.3390/nu10040521

Khalili, M., Rad, A., Khosroushahi, A., Khosravi, H., and Jafarzadeh, S. (2020). Application of probiotics in folate bio-fortification of yoghurt. *Probiotics. Antimicro* 12, 756–763. doi: 10.1007/s12602-019-09560-9567

Kim, K., Chun, B., Baek, J., Roh, S., Lee, S., and Jeon, C. (2020). Genomic and metabolic features of *Lactobacillus sakei* as revealed by its pan-genome and the metatranscriptome of kimchi fermentation. *Food Microbiol.* 86:103341. doi: 10.1016/j.fm.2019.103341

Komprda, T., Burdychová, R., Dohnal, V., Cwiková, O., Sládková, P., and Dvorácková, H. (2008). Tyramine production in dutch-type semi-hard cheese from two different producers. *Food Microbiol.* 25, 219–227. doi: 10.1016/j.fm.2007.11.006

Kordesedehi, R., Taheri-Kafrani, A., Rabbani-Khorasgani, M., Kazemi, R., Mutangadura, D., and Haertle, T. (2018). Modification of IgE binding to αS1-casein by proteolytic activity of *Enterococcus faecium* isolated from Iranian camel milk samples. *J. Biotechnol.* 27, 10–14.

Kuley, E., Özyurt, G., Özogul, I., Boga, M., Akyol, I., Rocha, J. M., et al. (2020). The role of selected lactic acid bacteria on organic acid accumulation during wet and spray-dried fish-based silages. *Microorganisms* 8:172. doi: 10.3390/microorganisms8020172

Kumar, V., Ashok, S., and Park, S. (2013). Recent advances in biological production of 3-hydroxypropionic acid. *Biotechnol. Adv.* 31, 945–961. doi: 10.1016/j.biotechadv.2013.02.008

Kumariya, R., Garsa, A., Rajput, Y., Sood, S., Akhtar, N., and Patel, S. (2019). Bacteriocins: classification, synthesis, mechanism of action and resistance development in food spoilage causing bacteria. *Microbial. Pathogenesis* 128, 171–177. doi: 10.1016/j.micpath.2019.01.002

Kunji, E., Mierau, I., Hagting, A., Poolman, B., and Konings, W. (1996). The proteolytic systems of lactic acid bacteria. *Anton. Leeuw* 70, 187–221. doi: 10.1007/BF00395933

Lamberti, C., Purrotti, M., Mazzoli, R., Fattori, P., Barello, C., Coïsson, J., et al. (2011). ADI pathway and histidine decarboxylation are reciprocally regulated in *Lactobacillus hilgardii* ISE 5211: proteomic evidence. *Amino. Acids* 41, 517–527. doi: 10.1007/s00726-010-0781-2

Laws, A., Gu, Y., and Marshall, V. (2001). Biosynthesis, characterisation, and design of bacterial exopolysaccharides from lactic acid bacteria. *Biotechnol. Adv.* 19, 597–625. doi: 10.1016/s0734-9750(01)00084-2

Lee, K., Pi, K., Kim, E., Rho, B., Kang, S., Lee, H., et al. (2010). Glutathione-mediated response to acid stress in the probiotic bacterium, *Lactobacillus salivarius*. *Biotechnol. Lett.* 32, 969–972. doi: 10.1007/s10529-010-0244-6

Leemhuis, H., Dobruchowska, J., Ebbelaar, M., Faber, F., Buwalda, P., van der Maarel, M., et al. (2014). Isomalto/malto-polysaccharide, a novel soluble dietary fiber made via enzymatic conversion of starch. *J. Agr. Food Chem.* 62, 12034–12044. doi: 10.1021/jf503970a

Li, Q., Loponen, J., and Gänzle, M. G. (2020). Characterization of the extracellular fructanase frua in *Lactobacillus crispatus* and its contribution to fructan hydrolysis in breadmaking. *J. Agr. Food Chem.* 68, 8637–8647. doi: 10.1021/acs.jafc.0c02313

Li, Y., Ku, S., Park, M., Li, Z., and Ji, G. (2017). Acceleration of aglycone isoflavone and γ-aminobutyric acid production from doenjang using whole-cell biocatalysis accompanied by protease treatment. *J. Microb. Biotech.* 27, 1952–1960. doi: 10.4014/jmb.1705.05052

Liao, X., Guo, L., Ye, Z., Qiu, L., Gu, F., and Lin, J. (2016). Use of autochthonous lactic acid bacteria starters to ferment mango juice for promoting its probiotic roles. *Prep. Biochem. Biotechnol.* 46, 399–405. doi: 10.1080/10826068.2015.1045615

Liu, T., Li, Y., Yang, Y., Yi, H., Zhang, L., and He, G. (2020). The influence of different lactic acid bacteria on sourdough flavor and a deep insight into sourdough fermentation through RNA sequencing. *Food Chem.* 307:125529. doi: 10.1016/j.foodchem.2019.125529

Liu, Y., van Bennekom, E., Zhang, Y., Abee, T., and Smid, E. (2019). Long-chain vitamin K2 production in *Lactococcus lactis* is influenced by temperature, carbon source, aeration and mode of energy metabolism. *Microb. Cell. Fact* 18:129. doi: 10.1186/s12934-019-1179-9

Lonvaud-Funel, A. (2001). Biogenic amines in wines: role of lactic acid bacteria. *FEMS Microbiol. Lett.* 199, 9–13. doi: 10.1111/j.1574-6968.2001.tb10643.x

Loponen, J., König, K., Wu, J., and Gänzle, M. G. (2008). Influence of thiol metabolism of lactobacilli on egg white proteins in wheat sourdoughs. *J. Agr. Food Chem.* 56, 3357–3362. doi: 10.1021/jf703600t

Lu, Z., Liu, N., Wang, L., Wu, L., Gong, J., Yu, Y., et al. (2016). Elucidating and regulating the acetoin production role of microbial functional groups in multispecies acetic acid fermentation. *Appl. Environ. Microb* 82, 5860–5868. doi: 10.1128/AEM.01331-16

Lyu, C., Liu, L., Huang, J., Zhao, W., Hu, S., Mei, L., et al. (2019). Biosynthesis of γ-aminobutyrate by engineered Lactobacillus brevis cells immobilized in gellan gum gel beads. *J. Biosci. Bioeng.* 128, 123–128. doi: 10.1016/j.jbiosc.2019.01.010

Majee, S., Avlani, D., Gopa, R., and Biswas, G. (2017). Rheological behaviour and pharmaceutical applications of bacterial exopolysaccharides. *J. App. Pharm. Sci.* 7, 224–232.

Maruščáková, I., Schusterová, P., Bielik, B., Toporčák, J., Bíliková, K., and Mudroňová, D. (2020). Effect of application of probiotic pollen suspension on immune response and gut microbiota of honey bees. *Probiotics Antimicro* 12, 929–936. doi: 10.1007/s12602-019-09626-6

Mattick, A., and Hirsch, A. (1947). Further observations on an inhibitory substance (nisin) from *Lactic streptococci*. *Lancet* 2, 5–8. doi: 10.1016/s0140-6736(47)90004-4

Mayer, M., D'Amato, A., Colquhoun, I., Le Gall, G., and Narbad, A. (2020). Identification of genes required for glucan exopolysaccharide production in *Lactobacillus johnsonii* suggests a novel biosynthesis mechanism. *Appl. Environ. Microb* 86, e2808–e2819. doi: 10.1128/AEM.02808-19

Meisel, H., and Bockelmann, W. (1999). Bioactive peptides encrypted in milk proteins: proteolytic activation and thropho-functional properties. *Anton. Leeuw* 76, 207–215.

Mokoena, M. (2017). Lactic acid bacteria and their bacteriocins: classification, biosynthesis and applications against uropathogens: a mini-review. *Molecules* 22:1255. doi: 10.3390/molecules22081255

Møller, C., Ücok, E., and Rattray, F. (2020). Histamine forming behaviour of bacterial isolates from aged cheese. *Food Res. Int.* 128:108719. doi: 10.1016/j.foodres.2019.108719

Montville, T., and Chen, Y. (1998). Mechanistic action of pediocin and nisin: recent progress and unresolved questions. *Appl. Microbiol. Biot.* 50, 511–519. doi: 10.1007/s002530051328

Mu, G., Li, H., Tuo, Y., Gao, Y., and Zhang, Y. (2019). Antioxidative effect of *Lactobacillus plantarum* Y44 on 2,2'-azobis(2-methylpropionamidine) dihydrochloride (ABAP)-damaged Caco-2 cells. *J. Dairy. Sci.* 102, 6863–6875. doi: 10.3168/jds.2019-16447

Mugampoza, D., Gkatzionis, K., Linforth, R., and Dodd, C. (2019). Acid production, growth kinetics and aroma profiles of *Lactobacillus flora* from stilton cheese. *Food Chem.* 287, 222–231. doi: 10.1016/j.foodchem.2019.02.082

Mulet-Powell, N., Lacoste-Armynot, A., Viñas, M., Simeon, and de Buochberg, M. (1998). Interactions between pairs of bacteriocins from lactic bacteria. *J. Food Protect.* 61, 1210–1212. doi: 10.4315/0362-028x-61.9.1210

Müller, G., Kalyani, D., and Horn, S. (2017). LPMOs in cellulase mixtures affect fermentation strategies for lactic acid production from lignocellulosic biomass. *Biotechnol. Bioeng.* 114, 552–559. doi: 10.1002/bit.26091

Nam, S., Ko, J., Jun, W., Wee, Y., Walsh, M., Yang, K., et al. (2017). Enzymatic synthesis of chlorogenic acid glucoside using dextransucrase and its physical and functional properties. *Enzyme. Microb Tech.* 107, 15–21. doi: 10.1016/j.enzmictec.2017.07.011

Nehal, F., Sahnoun, M., Smaoui, S., Jaouadi, B., Bejar, S., and Mohammed, S. (2019). Characterization, high production and antimicrobial activity of exopolysaccharides from *Lactococcus lactis* F-mou. *Microb. Pathogenesis* 132, 10–19. doi: 10.1016/j.micpath.2019.04.018

Nes, I., Diep, D., Håvarstein, L., Brurberg, M., Eijsink, V., and Holo, H. (1996). Biosynthesis of bacteriocins in lactic acid bacteria. *Anton. Leeuw* 70, 113–128. doi: 10.1007/BF00395929

Oguntoyinbo, F., and Narbad, A. (2012). Molecular characterization of lactic acid bacteria and in situ amylase expression during traditional fermentation of cereal foods. *Food Microbiol.* 31, 254–262. doi: 10.1016/j.fm.2012.03.004

Oguro, Y., Nishiwaki, T., Shinada, R., Kobayashi, K., and Kurahashi, A. (2017). Metabolite profile of koji amazake and its lactic acid fermentation product by *Lactobacillus sakei* UONUMA. *J. Biosci. Bioeng.* 124, 178–183. doi: 10.1016/j.jbiosc.2017.03.011

Ortiz, M., Bleckwedel, J., Raya, R., and Mozzi, F. (2013). Biotechnological and in situ food production of polyols by lactic acid bacteria. *Appl. Microbiol. Biot.* 97, 4713–4726. doi: 10.1007/s00253-013-4884-z

Pandey, N., Malik, R., Kaushik, J., and Singroha, G. (2013). Gassericin A: a circular bacteriocin produced by lactic acid bacteria *Lactobacillus gasseri*. *World J. Microb. Biot.* 29, 1977–1987. doi: 10.1007/s11274-013-1368-3

Papadimitriou, K., Alegría, Á, Bron, P., de Angelis, M., Gobbetti, M., Kleerebezem, M., et al. (2016). Stress physiology of lactic acid bacteria. *Microbiol. Mol. Biol. R: MMBR* 80, 837–890. doi: 10.1128/MMBR.00076-15

Park, B., Hwang, H., Chang, J., Hong, S., Lee, S., Jung, M., et al. (2017). Identification of 2-hydroxyisocaproic acid production in lactic acid bacteria and evaluation of microbial dynamics during kimchi ripening. *Sci. Rep-UK* 7:10904. doi: 10.1038/s41598-017-10948-0

Patel, S., Majumder, A., and Goyal, A. (2012). Potentials of exopolysaccharides from lactic acid bacteria. *Indian. J. Microbiol.* 52, 3–12. doi: 10.1007/s12088-011-0148-8

Peralta, G., Bergamini, C., and Hynes, E. (2016). Aminotransferase and glutamate dehydrogenase activities in lactobacilli and streptococci. *Braz. J. Microbiol.* 47, 741–748. doi: 10.1016/j.bjm.2016.04.005

Perczak, A., Goliński, P., Bryła, M., and Waśkiewicz, A. (2018). The efficiency of lactic acid bacteria against pathogenic fungi and mycotoxins. *Arh. Hig. Rada. Toksiko* 69, 32–45. doi: 10.2478/aiht-2018-69-3051

Pillidge, C., Crow, V., Coolbear, T., and Reid, J. (2003). Exchanging lactocepin plasmids in lactococcal starters to study bitterness development in Gouda cheese: a preliminary investigation. *Int. Dairy. J.* 13, 345–354.

Pontonio, E., Dingeo, C., Di Cagno, R., Blandino, M., Gobbetti, M., and Rizzello, C. G. (2020). Brans from hull-less barley, emmer and pigmented wheat

varieties: from by-products to bread nutritional improvers using selected lactic acid bacteria and xylanase. *Int. J. Food Microbiol.* 313:108384. doi: 10.1016/j.ijfoodmicro.2019.108384

Pophaly, S., Singh, R., Pophaly, S., Kaushik, J., and Tomar, S. (2012). Current status and emerging role of glutathione in food grade lactic acid bacteria. *Microbial. Cell Fact* 11:114. doi: 10.1186/1475-2859-11-114

Qiao, Y., Liu, G., Leng, C., Zhang, Y., Lv, X., Chen, H., et al. (2018). Metabolic profiles of cysteine, methionine, glutamate, glutamine, arginine, aspartate, asparagine, alanine and glutathione in *Streptococcus thermophilus* during pH-controlled batch fermentations. *Sci. Rep.* 8:12441. doi: 10.1038/s41598-018-30272-5

Qiu, Z., Fang, C., Gao, Q., and Bao, J. (2020). A short-chain dehydrogenase plays a key role in cellulosic D-lactic acid fermentability of Pediococcus acidilactici. *Bioresource Technol.* 297:122473. doi: 10.1016/j.biortech.2019.122473

Rahbar Saadat, Y., Yari Khosroushahi, A., and Pourghassem Gargari, B. (2019). A comprehensive review of anticancer, immunomodulatory and health beneficial effects of the lactic acid bacteria exopolysaccharides. *Carbohy. Polym.* 217, 79–89. doi: 10.1016/j.carbpol.2019.04.025

Rai, A., Sanjukta, S., and Jeyaram, K. (2017). Production of angiotensin I converting enzyme inhibitory (ACE-I) peptides during milk fermentation and their role in reducing hypertension. *Crit. Rev. Food Sci.* 57, 2789–2800. doi: 10.1080/10408398.2015.1068736

Ramchandran, L., and Shah, N. (2008). Proteolytic profiles and angiotensin-I converting enzyme and alpha-glucosidase inhibitory activities of selected lactic acid bacteria. *J. Food Sci.* 73, M75–M81. doi: 10.1111/j.1750-3841.2007.00643.x

Rincé, A., Dufour, A., Uguen, P., Le Pennec, J., and Haras, D. (1997). Characterization of the lacticin 481 operon: the *Lactococcus lactis* genes lctF, lctE, and lctG encode a putative ABC transporter involved in bacteriocin immunity. *Appl. Environ. Microb* 63, 4252–4260. doi: 10.1128/AEM.63.11.4252-4260.1997

Rodriguez, H., Landret, J., De Las Rivas, B., and Munoz, R. (2008). Metabolism of food phenolic acids by *Lactobacillus plantarum* CECT 748T. *Food Chem.* 107, 1393–1398.

Ruas-Madiedo, P., and de los Reyes-Gavilán, C. (2005). Invited review: methods for the screening, isolation, and characterization of exopolysaccharides produced by lactic acid bacteria. *J. Dairy Sci.* 88, 843–856. doi: 10.3168/jds.S0022-0302(05)72750-8

Rubak, Y., Nuraida, L., Iswantini, D., and Prangdimurti, E. (2020). Angiotensin-I-converting enzyme inhibitory peptides in milk fermented by indigenous lactic acid bacteria. *Veterinary World* 13, 345–353. doi: 10.14202/vetworld.2020.345-353

Ryu, J., Kang, H., and Cho, S. (2019). Changes over the fermentation period in phenolic compounds and antioxidant and anticancer activities of blueberries fermented by *Lactobacillus plantarum*. *J. Food Sci.* 84, 2347–2356. doi: 10.1111/1750-3841.14731

Sadaf, H., Raza, S., and Hassan, S. (2017). Role of gut microbiota against calcium oxalate. *Microb. Pathogenesis* 109, 287–291. doi: 10.1016/j.micpath.2017.06.009

Salazar, N., Gueimonde, M., de Los Reyes-Gavilán, C., and Ruas-Madiedo, P. (2016). Exopolysaccharides produced by lactic acid bacteria and bifidobacteria as fermentable substrates by the intestinal microbiota. *Crit. Rev. Food Sci.* 56, 1440–1453. doi: 10.1080/10408398.2013.770728

Sanz, Y., Toldrá, F., Renault, P., and Poolman, B. (2003). Specificity of the second binding protein of the peptide ABC-transporter (Dpp) of *Lactococcus lactis* IL1403. *FEMS Microbiol. Lett.* 227, 33–38. doi: 10.1016/S0378-1097(03)00662-1

Sarantinopoulos, P., Kalantzopoulos, G., and Tsakalidou, E. (2001). Citrate metabolism by *Enterococcus faecalis* FAIR-E 229. *Appl. Environ. Microb* 67, 5482–5487. doi: 10.1128/AEM.67.12.5482-5487.2001

Sasikumar, K., Kozhummal Vaikkath, D., Devendra, L., and Nampoothiri, K. (2017). An exopolysaccharide (EPS) from a Lactobacillus plantarum BR2 with potential benefits for making functional foods. *Bioresource Technol.* 241, 1152–1156. doi: 10.1016/j.biortech.2017.05.075

Savijoki, K., Ingmer, H., and Varmanen, P. (2006). Proteolytic systems of lactic acid bacteria. *Appl. Microbiol. Biot.* 71, 394–406. doi: 10.1007/s00253-006-0427-1

Sezen, Ö, Esmeray, K., and Fatih, Ö (2016). Formation of lactic, acetic, succinic, propionic, formic and butyric acid by lactic acid bacteria. *LWT* 73, 536–542. doi: 10.1016/j.lwt.2016.06.066

Shi, X., Chang, C., Ma, S., Cheng, Y., Zhang, J., and Gao, Q. (2017). Efficient bioconversion of L-glutamate to γ-aminobutyric acid by *Lactobacillus brevis* resting cells. *J. Ind. Microbiol. Biot.* 44, 697–704. doi: 10.1007/s10295-016-1777-z

Shirai, K., Guerrero, I., Huerta, S., Saucedo, G., Castillo, A., Obdulia Gonzalez, R., et al. (2001). Effect of initial glucose concentration and inoculation level of lactic acid bacteria in shrimp waste ensilation. *Enzyme. Microb. Tech.* 28, 446–452. doi: 10.1016/s0141-0229(00)00338-0

Small, P., and Waterman, S. (1998). Acid stress, anaerobiosis and gadCB: lessons from *Lactococcus lactis* and *Escherichia coli*. *Trends. Microbiol.* 6, 214–216. doi: 10.1016/s0966-842x(98)01285-2

Smit, G., Smit, B., and Engels, W. (2005). Flavour formation by lactic acid bacteria and biochemical flavour profiling of cheese products. *FEMS Microbiol. Rev.* 29, 591–610. doi: 10.1016/j.femsre.2005.04.002

Sridhar, V., Hughes, J., Welker, D., Broadbent, J., and Steele, L. (2005). Identification of endopeptidase genes from the genomic sequence of *Lactobacillus helveticus* CNRZ32 and the role of these genes in hydrolysis of model bitter peptides. *Appl. Environ. Microb* 71, 3025–3032. doi: 10.1128/AEM.71.6.3025-3032.2005

Stefańska, I., Piasecka-Jóźwiak, K., Kotyrba, D., Kolenda, M., and Stecka, K. M. (2016). Selection of lactic acid bacteria strains for the hydrolysis of allergenic proteins of wheat flour. *J. Sci. Food. Agr.* 96, 3897–3905. doi: 10.1002/jsfa.7588

Stincone, A., Prigione, A., Cramer, T., Wamelink, M., Campbell, K., Cheung, E., et al. (2015). The return of metabolism: biochemistry and physiology of the pentose phosphate pathway. *Bioll. Rev. Camb. Philos Soc.* 90, 927–963. doi: 10.1111/brv.12140

Sun, D., Li, H., Song, D., Zhang, L., Zhao, X., and Xu, X. (2019). Genome, transcriptome and fermentation analyses of *Lactobacillus plantarum* LY-78 provide new insights into the mechanism of phenyllactate biosynthesis in lactic acid bacteria. *Biochem. Bioph. Res. Co* 519, 351–357. doi: 10.1016/j.bbrc.2019.09.011

Surya, A., Liu, X., and Miller, M. J. (2018). Glutathione utilization in *Lactobacillus fermentum* CECT 5716. *J. Agr. Food Chem.* 66, 12651–12656. doi: 10.1021/acs.jafc.8b06136

Taranto, M., Vera, J., Hugenholtz, J., De Valdez, G., and Sesma, F. (2003). *Lactobacillus reuteri* CRL1098 produces cobalamin. *J. Bacteriol.* 185, 5643–5647. doi: 10.1128/jb.185.18.5643-5647.2003

Thage, B., Broe, M., Petersen, M., Petersen, M., Bennedsen, M., and Ard, Y. (2005). Aroma development in semi-hard reduced-fat cheese inoculated with *Lactobacillus paracasei* strains with different aminotransferase profiles. *Int. Dairy J.* 15, 795–805.

Torino, M., Taranto, M., Font, and de Valdez, G. (2005). Citrate catabolism and production of acetate and succinate by *Lactobacillus helveticus* ATCC 15807. *Appl. Microbiol. Biot.* 69, 79–85. doi: 10.1007/s00253-005-1949-7

Torres, A., Vannini, V., Font, G., Saavedra, L., and Taranto, M. (2018). Novel pathway for corrinoid compounds production in *Lactobacillus*. *Front. Microbiol.* 9:2256. doi: 10.3389/fmicb.2018.02256

Trabelsi, I., Ben Slima, S., Ktari, N., Triki, M., Abdehedi, R., Abaza, W., et al. (2019). Incorporation of probiotic strain in raw minced beef meat: study of textural modification, lipid and protein oxidation and color parameters during refrigerated storage. *Meat. Sci.* 154, 29–36. doi: 10.1016/j.meatsci.2019.04.005

van der Maarel, M., van der Veen, B., Uitdehaag, J., Leemhuis, H., and Dijkhuizen, L. (2002). Properties and applications of starch-converting enzymes of the alpha-amylase family. *J. Biotechnol.* 94, 137–155. doi: 10.1016/s0168-1656(01)00407-2

Velikova, P., Stoyanov, A., Blagoeva, G., Popova, L., Petrov, K., Gotcheva, V., et al. (2016). New findings from institute of microbiology update understanding of lactates (Starch utilization routes in lactic acid bacteria: new insight by gene expression assay). *Environ. Conserv.* 68, 953–960.

Vesanto, E., Peltoniemi, K., Purtsi, T., Steele, J., and Palva, A. (1996). Molecular characterization, over-expression and purification of a novel dipeptidase from *Lactobacillus helveticus*. *Appl. Microbiol. Biot.* 45, 638–645. doi: 10.1007/s002530050741

Wada, K., Toya, Y., Banno, S., Yoshikawa, K., Matsuda, F., and Shimizu, H. (2017). 13C-metabolic flux analysis for mevalonate-producing strain of *Escherichia coli*. *J. Biosci. Bioeng.* 123, 177–182. doi: 10.1016/j.jbiosc.2016.08.001

Wang, C., Sun, J., Lassabliere, B., Yu, B., Zhao, F., Zhao, F., et al. (2019). Potential of lactic acid bacteria to modulate coffee volatiles and effect of glucose

supplementation: fermentation of green coffee beans and impact of coffee roasting. *J. Sci. Food Agr.* 99, 409–420. doi: 10.1002/jsfa.9202

Wegkamp, A., van Oorschot, W., de Vos, W., and Smid, E. (2007). Characterization of the role of para-aminobenzoic acid biosynthesis in folate production by *Lactococcus lactis*. *Appl. Environ. Microb* 73, 2673–2681. doi: 10.1128/AEM.02174-2176

Whiting, G., and Coggins, R. (1971). The role of quinate and shikimate in the metabolism of *Lactobacilli*. *Anton. Leeuw* 3, 33–49. doi: 10.1007/BF02218465

Winters, M., Panayotides, D., Bayrak, M., Rémont, G., Viejo, C., Liu, D., et al. (2019). Defined co-cultures of yeast and bacteria modify the aroma, crumb and sensory properties of bread. *J. Appl. Microbiol.* 127, 778–793. doi: 10.1111/jam.14349

Worsztynowicz, P., Schmidt, A., Białas, W., and Grajek, W. (2019). Identification and partial characterization of proteolytic activity of *Enterococcus faecalis* relevant to their application in dairy industry. *Acta. Biochim. Pol.* 66, 61–69. doi: 10.18388/abp.2018_2714

Wu, G., Fang, Y., Yang, S., Lupton, J., and Turner, N. D. (2004). Glutathione metabolism and its implications for health. *J. Nutr.* 134, 489–492. doi: 10.1093/jn/134.3.489

Wu, J., Zhang, Y., Ye, L., and Wang, C. (2021). The anti-cancer effects and mechanisms of lactic acid bacteria exopolysaccharides in vitro: a review. *Carbohyd. Polym.* 253:117308. doi: 10.1016/j.carbpol.2020.117308

Wu, N., Xu, W., Liu, K., Xia, Y., and Shuangquan. (2019). Angiotensin-converting enzyme inhibitory peptides from *Lactobacillus delbrueckii* QS306 fermented milk. *J. Dairy. Sci.* 102, 5913–5921. doi: 10.3168/jds.2018-15901

Wu, Z., Wu, J., Cao, P., Jin, Y., Pan, D., Zeng, X., et al. (2017). Characterization of probiotic bacteria involved in fermented milk processing enriched with folic acid. *J. Dairy Sci.* 100, 4223–4229. doi: 10.3168/jds.2017-12640

Wüthrich, D., Wenzel, C., Bavan, T., Bruggmann, R., Berthoud, H., and Irmler, S. (2018). Transcriptional regulation of cysteine and methionine metabolism in *Lactobacillus paracasei* FAM18149. *Front. Microbiol.* 9:1261. doi: 10.3389/fmicb.2018.01261

Xu, D., Tang, K., Hu, Y., Xu, X., and Gänzle, M. G. (2018). Effect of glutathione dehydrogenase of *Lactobacillus sanfranciscensis* on gluten properties and bread volume in type I wheat sourdough bread. *J. Agr. Food Chem.* 66, 9770–9776. doi: 10.1021/acs.jafc.8b03298

Xu, Q., Zang, Y., Zhou, J., Liu, P., Li, X., Yong, Q., et al. (2016). Highly efficient production of D-lactic acid from chicory-derived inulin by *Lactobacillus bulgaricus*. *Bioproc. Biosyst. Eng.* 39, 1749–1757. doi: 10.1007/s00449-016-1650-5

Yan, M., Wang, B., Xu, X., Chang, P., Hang, F., Wu, Z., et al. (2018). Molecular and functional study of a branching sucrase-like glucansucrase reveals an evolutionary intermediate between two subfamilies of the GH70 enzymes. *Appl. Environ. Microb* 84, e2810–e2817. doi: 10.1128/AEM.02810-2817

Yunes, R., Poluektova, E., Dyachkova, M., Klimina, K., Kovtun, A., Averina, O., et al. (2016). GABA production and structure of gadB/gadC genes in *Lactobacillus* and bifidobacterium strains from human microbiota. *Anaerobe* 42, 197–204. doi: 10.1016/j.anaerobe.2016.10.011

Zaunmüller, T., Eichert, M., Richter, H., and Unden, G. (2006). Variations in the energy metabolism of biotechnologically relevant heterofermentative lactic acid bacteria during growth on sugars and organic acids. *Appl. Microbiol. Biot* 72, 421–429. doi: 10.1007/s00253-006-0514-3

Zhang, Y., Vadlani, P., Kumar, A., Hardwidge, P., Govind, R., Tanaka, T., et al. (2016). Enhanced D-lactic acid production from renewable resources using engineered *Lactobacillus plantarum*. *Appl. Microbiol. Biot* 100, 279–288. doi: 10.1007/s00253-015-7016-0

Zhao, N., Zhang, C., Yang, Q., Guo, Z., Yang, B., Lu, W., et al. (2016). Selection of taste markers related to lactic acid bacteria microflora metabolism for Chinese traditional paocai: a gas chromatography-mass spectrometry-based metabolomics approach. *J. Agr. Food Chem.* 64, 2415–2422. doi: 10.1021/acs.jafc.5b05332

Zheng, J., Wittouck, S., Salvetti, E., Franz, C., Harris, H., Mattarelli, P., et al. (2020). A taxonomic note on the genus *Lactobacillus*: description of 23 novel genera, emended description of the genus *Lactobacillus beijerinck* 1901, and union of Lactobacillaceae and Leuconostocaceae. *Int. J. Syst. Evol. Microbiol.* 70, 2782–2858. doi: 10.1099/ijsem.0.004107

Zhou, Y., Cui, Y., and Qu, X. (2019). Exopolysaccharides of lactic acid bacteria: structure, bioactivity and associations: a review. *Carbohyd. Polym.* 207, 317–332. doi: 10.1016/j.carbpol.2018.11.093

Conflict of Interest: The authors declare that the research was conducted in the absence of any commercial or financial relationships that could be construed as a potential conflict of interest.

Advantages of publishing in Frontiers

OPEN ACCESS
Articles are free to read for greatest visibility and readership

FAST PUBLICATION
Around 90 days from submission to decision

HIGH QUALITY PEER-REVIEW
Rigorous, collaborative, and constructive peer-review

TRANSPARENT PEER-REVIEW
Editors and reviewers acknowledged by name on published articles

Frontiers
Avenue du Tribunal-Fédéral 34
1005 Lausanne | Switzerland

Visit us: www.frontiersin.org
Contact us: frontiersin.org/about/contact

REPRODUCIBILITY OF RESEARCH
Support open data and methods to enhance research reproducibility

DIGITAL PUBLISHING
Articles designed for optimal readership across devices

FOLLOW US
@frontiersin

IMPACT METRICS
Advanced article metrics track visibility across digital media

EXTENSIVE PROMOTION
Marketing and promotion of impactful research

LOOP RESEARCH NETWORK
Our network increases your article's readership